

Use of *Bacteroides thetaiotaomicron* derived
extracellular vesicles as vaccine delivery
vehicles for mucosal vaccines against
respiratory pathogens

Ariadna Miquel Clopés

Submitted for the degree of Doctor of Philosophy
University of East Anglia
Quadram Institute

May 2023

This copy of the thesis has been supplied on condition that anyone who consults it is understood to recognise that its copyright rests with the author and that use of any information derived therefrom must be in accordance with current UK Copyright Law. In addition, any quotation or extract must include full attribution.

Abstract

Most infectious pathogens enter the body via mucosal sites, yet very few mucosal vaccines have been licensed. Major hurdles in mucosal vaccine development, such as stability, mucosal barriers and immune tolerance, hinder delivery of antigens to mucosa-immune cells. New vaccine delivery systems are therefore needed to provide broad and long-term protection against respiratory viruses. To address these issues *Bacteroides thetaiotaomicron* (Bt), a human commensal gut bacterium, has been engineered to export into their bacterial extracellular vesicles (BEVs) *Yersinia pestis*, influenza virus (IV), or SARS-CoV-2 antigens. In addition, two means of decorating Bt BEVs with antigens have also been explored, using highly expressed vitamin B12 receptors and chemical conjugation. Pre-clinical studies using non-human primates (*Y. pestis*) or murine models (IAV and SARS-CoV-2) were used to determine the immunogenicity of Bt BEV vaccines and their ability to induce protective immune responses.

Native Bt BEVs displayed inherent adjuvanticity after intranasal administration, as shown by their ability to elicit mobilisation of immune cells and the development of organised lymphoid structures in the upper and lower respiratory tract. BEV vaccines were safe with no signs of any adverse effects in immunised animals. Bt BEVs vaccine formulations induced antigen-specific local and systemic humoral (IgA/IgG) and cellular (IFN- γ and/or TNF- α producing CD4/8 T cells) immune responses. For *Y. pestis* BEV vaccines correlates of protection were obtained from serum antibody mediated neutralisation and cytotoxicity assays using live plague bacteria. BEV-IAV vaccines provided heterotypic protection against a lethal dose of H1N1 IAV. Initial pre-clinical studies of SARS-CoV-2 BEV vaccines showed them to be capable of inducing low levels of antigen-specific mucosal and systemic IgA and IgG antibodies. Additional studies to optimise antigen expression, dose and frequency refinements are needed. The results obtained showed that Bt BEV could be used as a platform to produce mucosal vaccines against respiratory pathogens.

Access Condition and Agreement

Each deposit in UEA Digital Repository is protected by copyright and other intellectual property rights, and duplication or sale of all or part of any of the Data Collections is not permitted, except that material may be duplicated by you for your research use or for educational purposes in electronic or print form. You must obtain permission from the copyright holder, usually the author, for any other use. Exceptions only apply where a deposit may be explicitly provided under a stated licence, such as a Creative Commons licence or Open Government licence.

Electronic or print copies may not be offered, whether for sale or otherwise to anyone, unless explicitly stated under a Creative Commons or Open Government license. Unauthorised reproduction, editing or reformatting for resale purposes is explicitly prohibited (except where approved by the copyright holder themselves) and UEA reserves the right to take immediate 'take down' action on behalf of the copyright and/or rights holder if this Access condition of the UEA Digital Repository is breached. Any material in this database has been supplied on the understanding that it is copyright material and that no quotation from the material may be published without proper acknowledgement.

Acknowledgments

I would first like to express my deepest appreciation to my primary supervisor, Professor Simon Carding, for his warm welcome from day one, his sense of humour, his trust in me, and the continued encouragement, guidance, and support throughout my PhD journey. My gratitude also extends to my other supervisors, Professor Tom Wileman, Professor James Stewart, and Dr Regis Stentz, for their valuable feedback and encouragement.

I am extremely grateful to the UKRI-BBSRC Norwich Research Park Biosciences Doctoral Training Partnership for funding my project. I would also like to thank Dr Penny Powell and Dr Robin Flynn in advance for their time and effort in reading and examining this thesis.

My sincere thanks go to all the collaborators who have contributed to making this project a reality. First, I want to thank Professor James Stewart and Eleanor Bentley for their invaluable advice and contribution to intranasal mice experiments at the University of Liverpool. Many thanks to Professor Mark Smales and Dr David Beal at the University of Kent for their helpful advice and work on chemical conjugations. I am also grateful to Public Health England (PHE), especially Dr Simon Funnell, and Defence Science and Technology Laboratory (DSTL) for their work related to the plague vaccine. I also wish to thank Drs Sonia Fonseca, Aimee Parker, and Emily Jones for their belief in my abilities and their invaluable contribution to mice work. Thanks also to Dr Rokas Juodeikis for his practical suggestions and work on BEV conjugation.

I am forever grateful to my lab colleagues Adnan, Aimee, Amisha, Anne, Emily, Fiona, Katharine, Rik, Rokas, Steve, Udo, and especially Sonia and Regis for their support, motivation, and friendship. A special thanks to Ana Carvalho for always giving opportunities to students, making me love working in the lab and encouraging me to start the PhD.

My thanks also go to ssDNAfrica, Santie, Rose, Cheryl, Jacob and all the students who participated in the workshops in the University of Kilifi in Kenya for an amazing PIPS placement. Big thanks to my YES21 team, Maria, Gloria and Federico and everyone who helped us reach the finals for all the valuable learning process.

I would also like to express my gratitude to everyone who motivated me to move to the UK for my Erasmus+ training, those who encouraged me to stay, and those who have supported me throughout my PhD. To my hometown friends for supporting me from afar,

my "familia Norwichena," and all my fellow friends and colleagues at the NRP with whom I shared so much, especially Annalisa, Dani, Iliana, Jacob, Jennifer, Katharine, Lluís, Maria, Martina, Petros, Rik and Victor.

Above all, to all my family, particularly my mother, father, and sister -Enriqueta, Joan, and Meritxell- for their consistent encouragement, countless visits, and unconditional love. And my partner Javi for unwavering support.

Contribution Statement

Some of the work and data described in chapter 2, 3 and 4 is an adaptation of published work and appear with permission (1-3).

Chapter 3 features collaborative research involving Public Health England (PHE) and Defence Science and Technology Laboratory (DSTL), which was funded by Innovate UK. PHE managed the NHP, analysed histology samples and performed bactericidal assays, while DSTL produced recombinant proteins and antibodies and developed and performed the competitive ELISA. Drs Ana Carvalho and Emily Jones from QIB performed the bead-based multiplex assay, and Andrea Telatin analysed and created the taxonomic profile data generated by Animal and Plant Health Agency Scientific. In addition, Dr Udo Wegmann produced the plasmid constructs.

Chapter 4 showcases collaborative work with the University of Liverpool, where Professor James Stewart and Eleanor Bentley conducted and analysed the intranasal delivery data.

In Chapter 5, the first intranasal delivery was performed by Professor James Stewart at the University of Liverpool, and the others were performed at the Disease Modelling Unit (DMU) at the University of East Anglia by Drs Sonia Fonseca, Aimee Parker, and Emily Jones. Additionally, Dr Rokas Juodeikis produced the BEVs decorated with vitamin B12, while the chemical conjugation was carried out by Professor Mark Smales and Dr David Beal at the University of Kent.

List of contents

CHAPTER 1	INTRODUCTION	18
1.1	Respiratory infections and the importance of mucosal vaccines	18
1.2	Immunity in the respiratory tract	20
1.3	Types of vaccines	23
1.3.1	Attenuated vaccines	23
1.3.2	Inactivated vaccines	24
1.3.3	Subunit vaccines	24
1.4	Licensed intranasal vaccines	25
1.5	Challenges for developing intranasal vaccines	26
1.6	Adjuvants	27
1.6.1	Immunostimulatory molecules	27
1.6.2	Delivery system	28
1.7	Bacterial extracellular vesicles	33
1.8	Using BEVs in mucosal vaccine formulations	35
1.9	BEVs as a vaccine	37
1.10	Bacteroides thetaiotaomicron-derived BEVs	40
1.11	Aims and objectives	42
CHAPTER 2	MATERIALS AND METHODS	43
2.1	Bacterial strains and growth conditions	43
2.1.1	BDM recipe	44
2.2.	Production of bacterial stocks	45
2.3.	Cloning	46
2.3.1	Synthetic gene design	46
2.3.2	Restriction Digests	46
2.3.3	Plasmids used	46
2.3.4	Plasmid and DNA isolation and purification	46
2.3.5	DNA ligation	46
2.3.6	Transformation of competent cells	47
2.3.7	Screening of transformed colonies	47
2.3.8	Agarose gel electrophoresis	47
2.3.9	DNA sequencing	48
2.3.10	Triparental mating procedure	48

2.4.	Assessing protein expression	48
2.4.1	Culture of Bt transconjugants	48
2.4.2	Preparation of cell extracts	49
2.4.3	Analysis of total protein	49
2.5.	BEV isolation	49
2.5.1	Supernatant collection	49
2.5.2	BEV concentration	49
2.5.3	BEVs purification	51
2.5.4	Size and concentration BEV analysis	51
2.6.	SDS-PAGE and immunoblot	52
2.7.	Dot blot	53
2.8.	Antigen quantification	53
2.9.	Proteinase K accessibility/protection assay	53
2.10.	NiNTA protein purification	54
2.11.	Animal models	54
2.11.1	Mice	54
2.11.2	Macaques, Ethics statement	55
2.12.	Immunisation	55
2.13.	Saliva and BAL extraction	51
2.14.	ELISA	55
2.15.	Antibodies used	56
2.16.	Recombinant proteins used	58
2.17.	T cells analysis	58
2.17.1	Splenocytes isolation and culture	58
2.17.2	Flow cytometry	59
2.18.	DNA extraction from stool samples and nasal swabs	61
2.19.	Storage of BEVs	62
2.20.	TEM imaging	62
2.21.	Statistical analysis	63
CHAPTER 3	USE OF BIOENGINEERED BT BEVS AS A PLAGUE VACCINE	64
3.1	Introduction	64
3.2	Results	67
3.2.1	Construction of <i>Y. pestis</i> F1 and V antigen expression vectors	67
3.2.2	Expression of <i>Y. pestis</i> vaccine antigens in Bt BEVs	68

3.2.3 BEV immunisation	72
3.2.4 Host response to recombinant F1 and V antigens	73
3.2.5 Host response to F1-BEV plague vaccine	74
3.2.6 Host response to V-BEV plague vaccine	77
3.2.7 Host response to combined V-BEV and F1-BEV vaccines	80
3.2.8 Cell-mediated immune responses	84
3.2.9 Reactogenicity of F1-BEVs and V-BEVs vaccines.	86
3.2.10 Functionality of BEVs-elicited IgG antibodies	92
3.3 Discussion	94
CHAPTER 4 USE OF BIOENGINEERED BT BEV AS AN INFLUENZA VACCINE	99
4.1 Introduction	99
4.2 Results	103
4.2.1 Adjuvanticity of Bt BEVs	103
4.2.2 Construction of IV H5F and NP antigen expression vectors	105
4.2.3 Expression of H5F vaccine antigen in Bt BEVs	105
4.2.4 Generating recombinant H5F protein	106
4.2.5 H5F-BEVs immunisations	109
4.2.6 Host response to H5F-BEVs	110
4.2.7 Bt Growth Media Optimisation	113
4.2.8 Expression of NP vaccine antigen in Bt BEV	116
4.2.9 Optimisation of T cell flow cytometric assay	119
4.2.10 NP-BEV Immunisations	121
4.2.11 Host response to NP-BEVs	122
4.3 Discussion	129
CHAPTER 5 USE OF BIOENGINEERED BT BEVS AS A COVID-19 VACCINE	132
5.1 Introduction	132
5.2 Results	135
5.2.1 Complexing S to Bt BEVs	135
5.2.2 B12.S-BEVs immunisation	137
5.2.3 Construction of SARS-CoV-2 NC antigen expression vector	141
5.2.4 Expression of SARS-CoV-2 NC antigen in Bt BEVs	142
5.2.5 B12.S-NC-BEV preparation	144
5.2.6 B12.S-NC-BEVs immunisation	144
5.2.7 S complexed to BEVs using chemical conjugation	149

5.2.8 c.S-NC-BEVs immunisation	151
5.3 Discussion	163
CHAPTER 6 STABILITY OF BT BEVS	167
6.1 Introduction	167
6.2 Results	169
6.2.1 Thermostability of V-BEVs	169
6.2.2 Stability of NP-BEVs	170
6.3 Discussion	176
CHAPTER 7 DISCUSSION	178
REFERENCES	183
APPENDIX-PUBLICATIONS	208

List of Figures

Figure 1.1 Representation of the respiratory immune system NALT	22
Figure 1.2 Biogenesis of BEVs	33
Figure 1.3 Composition of OMV	34
Figure 1.4 Overall study plan	42
Figure 2.1 Isolation module system	51
Figure 2.2 Example of gating strategy used to analyse cytokine production on CD4+ and CD8+ T cells in splenocytes	61
Figure 3.1 Overview of bioengineered Bt BEVs as plague vaccine study design	67
Figure 3.2 Detection of V in V-BEVs by immunoblotting	68
Figure 3.3 Detection of F1 in F1-BEVs by immuno-dot-blot	69
Figure 3.4 Quantification of hydrodynamic particle size of WT-BEVs, F1-BEVs and V-BEVs by NTA	71
Figure 3.5 Overview of animal studies to determine immune response to of V-BEV and F1-BEV vaccinations	73
Figure 3.6 Quantification of serum IgG antibodies to recombinant V or F1 by ELISA	74
Figure 3.7 Quantification of systemic antibodies to F1-BEV vaccine	75
Figure 3.8 Quantification of mucosal antibodies to F1-BEV vaccine by ELISA	76
Figure 3.9 Quantification of systemic antibodies to V-BEV by ELISA	78
Figure 3.10 Quantification of mucosal antibodies to V-BEV by ELISA	79
Figure 3.11 Quantification of systemic antibodies to F1 and V by ELISA	81
Figure 3.12 Quantification of saliva antibodies to F1 and V by ELISA	83
Figure 3.13 Quantification of BAL and salivary glands antibodies to F1 and V by ELISA	84
Figure 3.14 Quantification of cytokine expressed in stimulated PMBCs from NHPs immunised with F1-BEV + V-BEV by flow cytometry	86
Figure 3.15 Histopathological sections of immunised NHPs	87

Figure 3.16 Comparison of DNA extracted from faecal samples, rectal and nasal swab	89
Figure 3.17 Bubble chart from 16S rRNA sequences (V4-V5) obtained from animals immunised with V-BEV	90
Figure 3.18 Functionality of immune sera from V-BEVs immunised animals analysed by competitive ELISA	93
Figure 4.1 Diagram of IV indicating major protein components	101
Figure 4.2 Overview of bioengineered Bt BEV as influenza vaccine study design	103
Figure 4.3 Adjuvanticity of Bt BEVs by immunohistology	104
Figure 4.4 Quantification of hydrodynamic particle size of WT-BEVs and H5F-BEVs by NTA	106
Figure 4.5 Production of recombinant H5F	108
Figure 4.6 Animal study to determine flu protection from H5F-BEVs vaccination	110
Figure 4.7 Quantification of antibodies to IAV and H5 by ELISA	110
Figure 4.8 Host response to H5F-BEV vaccine	113
Figure 4.9 Growth curves of Bt cultured in BHIH, BDM, or BDM+ media	115
Figure 4.10 Activation of NF-KB by BEVs isolated from BHIH and BDM+ media using THP1-Blue cells	116
Figure 4.11 Detection of NP in NP-BEV by immunoblotting	117
Figure 4.12 Quantification of hydrodynamic particle size of WT-BEVs and NP-BEVs by NTA	118
Figure 4.13 Concatenated data of splenocytes against different concentration of antibodies and SI analysis by flow cytometry	120
Figure 4.14 Animal studies to determine immune response of NP-BEVs vaccination	121
Figure 4.15 Quantification of antibodies to NP by ELISA	123
Figure 4.16 Frequency of CD4+ and CD8+ T cells expressing TNF- and/or IFN- from splenocytes from first NP-BEVs experiment by flow cytometry	125
Figure 4.17 Percentage of live cells from splenocytes stained with live/dead NIR from the second NP-BEVs experiment by flow cytometry	126

Figure 4.18 Frequency of CD4+ and CD8+ T cells expressing TNF- α and/or IFN- γ from splenocytes from the second NP-BEVs experiment by flow cytometry	128
Figure 5.1 Overview of bioengineered Bt BEVs as Covid-19 vaccine study design	135
Figure 5.2 Representation of S linked to Bt BEVs using vitamin B12 and B12 receptor	136
Figure 5.3 Quantification of hydrodynamic particle size of B12.S-BEVs by NTA	137
Figure 5.4 Animal study to determine optimal dose of B12.S-BEV vaccination	137
Figure 5.5 Quantification of serum IgG antibodies to B12.S in response of B12.S-BEV dose study by ELISA	138
Figure 5.6 Animal study to determine covid-19 protection from B12.S-BEVs vaccination	139
Figure 5.7 Quantification of serum IgG antibodies to B12.S in response of B12.S-BEV protection study by ELISA	140
Figure 5.8 Host response to B12.S-BEV vaccine	141
Figure 5.9 Detection of NC in NC-BEV by immunoblotting	142
Figure 5.10 Quantification of hydrodynamic particle size of B12.S-NC-BEV by NTA	143
Figure 5.11 Detection of B12.S in B12.S-NC-BEV before and after SEC by immunoblotting	144
Figure 5.12 Animal study to determine cellular immunity to B12.S-NC-BEV vaccination .	145
Figure 5.13 Quantification of serum IgG antibodies to NC and B12.S in response of B12.S-NC-BEV by ELISA	146
Figure 5.14 Quantification of cytokines expressed in splenocytes from mice immunised with B12.S-NC-BEV by flow cytometry	148
Figure 5.15 Representation of S linked to Bt BEVs using chemical conjugation	149
Figure 5.16 Quantification of hydrodynamic particle size of c.S-NC-BEV by NTA	150
Figure 5.17 Animal study to determine dose response to c.S-NC-BEV vaccination	151
Figure 5.18 Quantification of serum IgG antibodies to NC and c.S in response of c.S-NC-BEV dose study by ELISA	152
Figure 5.19 Quantification of cytokines expressed in splenocytes from mice immunised with c.S-NC-BEV by flow cytometry	153

Figure 5.20 Quantification of cytokines expressed in stimulated splenocytes from mice immunised with c.S-NC-BEV by flow cytometry	154
Figure 5.21 Quantification of cytokines expressed in stimulated splenocytes from mice immunised with c.S-NC-BEV by ELISA	156
Figure 5.22 Animal study to determine mucosal immune response to c.S-NC-BEV vaccination	157
Figure 5.23 Quantification of serum IgG antibodies to NC and c.S in response of intranasal c.S-NC-BEV study by ELISA	158
Figure 5.24 Quantification of mucosal antibodies to NC and c.S in response of intranasal c.S-NC-BEV study by ELISA	159
Figure 5.25 Quantification of cytokines expressed in splenocytes from mice immunised IN with c.S-NC-BEV by flow cytometry	160
Figure 5.26 Quantification of cytokines expressed in stimulated splenocytes from mice immunised IN with c.S-NC-BEV by flow cytometry	161
Figure 5.27 Quantification of cytokines expressed in BAL cells from mice immunised IN with c.S-NC-BEV by flow cytometry	162
Figure 6.1 Thermostability of V-BEVs by immunoblot	170
Figure 6.2 Storage conditions of NP-BEVs to assess stability	171
Figure 6.3 Stability of NP-BEV upon different storage conditions	173
Figure 6.4 TEM images of NP-BEV upon different storage conditions	174
Figure 6.5 Thermostability of NP-BEVs by immunoblot	175

List of Tables

Table 1.1 Mucosal Covid-19 vaccines in use	25
Table 1.2 Mucosal vaccine delivery systems	28
Table 2.1 List of bacterial strains used in this study	43
Table 2.2 BDM media	44
Table 2.3 List of DNA primers used for colony PCR and sequencing	47
Table 2.4 List of primary antibodies used	57
Table 2.5 Secondary antibodies used linked to HRP	57
Table 2.6 Recombinant proteins used	58
Table 2.7 List of antibodies used for Flow cytometry	60
Table 3.1 Detection of F1 in F1-BEV by proteomics	69
Table 3.2 Summary of serum antibody bactericidal assay outputs	94
Table 4.1 Detection of H5F in H5F-BEVs by proteomics.	105
Table 4.2 Characteristics of BEV vaccines used for IAV lethal challenge experiment.	110
Table 4.3 Detection of NP in NP-BEV by proteomics	117
Table 4.4 Characteristics of BEV vaccines used for NP-BEVs experiments	122
Table 5.1 Characteristics of optimal dose of B12.S-BEVs	138
Table 5.2 Characteristics of intranasally administered B12.S-BEVs	139
Table 5.3 Detection of NC in NC-BEV by proteomics	143
Table 5.4 Characteristics of cellular immunity to B12.S-NC-BEV experiment	145
Table 5.5 Peptides used for restimulation of splenocytes	147
Table 5.6 Detection of S chemically attached to NC-BEV by proteomics	150
Table 5.7 Characteristics of dose response to c.S-NC-BEV experiment.	151
Table 5.8 Characteristics of intranasal c.S-NC-BEV experiment	157
Table 5.9 Comparison of all SARS-CoV-2 Bt BEVs vaccine experiments	163

Table 6.1 N. meningitidis OMV vaccine excipients 168

Table 7.1 Correlation of Bt BEVs with TPP for plague, IV and SARS-Cov-2 vaccines 178

List of non-standard abbreviations

APC	Antigen presenting cells
B12	Vitamin B12
B12.S	Vitamin B12 conjugated to Spike
BAL	Bronchoalveolar lavage
BALT	Bronchus-associated lymphoid
BDM	Bacteroides defined media
BEV	Bacterial extracellular vesicles
BFA	Brefeldin A
BHI	Brain heart infusion with Hemin
BSA	Bovine serum albumin
c.S	Chemically conjugated Spike
CAC	Cell activation cocktail
CMV	cytoplasmic membrane vesicles
CT	Cholera toxin
CTB	Cholera toxin subunit B
DC	Dendritic cells
ELISA	Enzyme-linked immunosorbent assay
EOMV	Explosive outer membrane vesicles
EV	Extracellular vesicles
F1	<i>Yersinia pestis</i> Fractin 1 antigen
H5F	Hemagglutinin fraction from H5N1
HA	Hemagglutinin
IAV	Influenza A virus
IFN	Interferon
IN	intranasal
IP	Intraperitoneal
IV	Influenza virus

LAIV	Live attenuated Influenza vaccines
LB	Luria-Bertani Media
LC-MS	liquid chromatography-mass spectrometry
LOS	Lipooligosaccharide
LPS	Lipopolysaccharide
LT	Heat-labile enterotoxin
M	Microfold cell
MW	Molecular weight
NALT	nasal-associated lymphoid tissue
NC	SARS-CoV-2 Nucleocapsid
Ni-NTA	Nickel-Nitrilotriacetic Acid
NK	Natural Killer
NOD	Nucleotide oligomerization domain
NP	Influenza Nucleoprotein
NTA	Nanoparticle tracking analysis
NW	Nasal wash
OD600	Optical density at 600 nm
OG	Oral gavage
OIMV	Outer inner membrane vesicles
Omp	Outer membrane protein
OMV	Outer membrane protein
PAMP	pathogen-associated molecular pattern
PBS	Phosphate buffered saline
PCR	Polymerase chain reaction
PES	Polyethersulfone
PMSF	Phenylmethylsulfonyl fluoride
PRR	pattern recognition receptors
PVDF	Polyvinylidene difluoride
r	Recombinant
RBD	receptor binding domain
S	Spike
SD	Standard deviation (of the mean)
SDS	Sodium dodecyl sulphate
SDS-PAGE	Sodium Dodecyl Sulfate Polyacrylamide Gel Electrophoresis

SEC	Size exclusion chromatography
Th	Helper T cell
TLR	Toll-like receptor
TNF	Tumour Necrosis Factor
TPP	Target product profile
TRM	Tissue-resident memory T cells
V	<i>Yersinia pestis</i> low- calcium response V antigen
VLP	Virus like particle
VOC	Variants of concern
WT	Wild type

Chapter 1 Introduction

1.1 Respiratory infections and the importance of mucosal vaccines

Respiratory infections are a prominent cause of worldwide mortality. In 2019, lower respiratory infections were the fourth leading cause of death globally, causing 2.6 million deaths (4). Global mortality due to respiratory infections has become more relevant since the SARS-CoV-2 pandemic, making it the third most common cause of death in the USA (5), and the leading cause in England in 2020 (6). Besides SARS-CoV-2, Influenza (IV) and *Streptococcus pneumoniae* are common causative agents of both upper (nasal mucosa) and lower (lungs) respiratory tract infections (7, 8).

Respiratory viruses are amongst the 80% of human pathogens that enter the body and replicate in mucosal surfaces, which include the ocular site, gastrointestinal tract, urogenital tract, and respiratory tract (9). However, most vaccines against mucosal pathogens are administered parenterally and usually intramuscularly. Intramuscular vaccines elicit circulating antigen-specific B and T cells, but are less effective at eliciting responses in mucosa-associated lymphocytes (10). Intramuscular vaccines are effective at preventing severe infections that can require hospitalisation, but they do not always prevent pathogen replication or transmission (11).

The induction of strong adaptive immunity at mucosal sites has the capacity to prevent pathogen binding and uptake across epithelial surfaces. It also has the capacity to block pathogen transmission, essential to control the spread of disease. Mucosal vaccines are therefore needed to enhance broad protection and block pathogen invasion and infection. To induce mucosal immune responses, vaccines need to be administered to inductive sites in mucosal tissues, for example via oral or intranasal delivery. Intranasal vaccines are needle-free, and can be self-administered, making them better suited to mass vaccination.

The different architectures and composition of lymphoid tissue in different mucosal tissues are important factors in determining the effectiveness of vaccine-elicited immune responses, in terms of their potency and longevity. Moreover, mucosal immunisation can also benefit from shared mucosal immunity in which the induction of immune response in one mucosal site leads to responses in other mucosal sites. For

example, intranasal immunisation can induce immunity in the urogenital tract, with oral administration inducing immune responses in mammary tissue and salivary glands (12). In most cases, mucosal vaccination is also effective in priming antigen-specific systemic immune responses, including serum antibodies with neutralising properties (13), reflecting the crosstalk between the mucosal and systemic immune systems.

1.2 Immunity in the respiratory tract

The immune system of the respiratory tract includes both innate and adaptive immunological defences. The first layer of defence is the mucus covering the luminal surface. It is produced by secretory epithelial cells and contain mucins, antimicrobial peptides, lysozyme, cytokines, and secretory IgA (14). By mucus entrapment and mucociliary clearance particles and pathogens can be removed (14). Furthermore, the respiratory tract contains organised structures made up of B and T cells, named nasal-associated lymphoid tissue (NALT) which also includes cervical lymph nodes in the upper respiratory tract (Fig. 1.1). The lower respiratory tract contains bronchial/tracheal-associated lymphoid tissue (BALT) and mediastinal lymph nodes.

After crossing the mucus barrier, highly conserved pathogen-associated molecular patterns (PAMPs) expressed by viruses and bacteria are recognised by pattern recognition receptors (PRRs) (e.g., Toll-like receptors (TLRs) and nucleotide oligomerization domain (NOD)) on epithelial and resident immune cells (e.g., macrophages) leading to induction of innate immune responses (15). Viral PAMPs (e.g., glycoproteins, DNA, RNA) can trigger the production of pro-inflammatory mediators including the cytokines IFN, IL1 β , TNF- α , IL6, IL12, IL8, MCP1, and inflammasome responses. Similarly, bacterial PAMPs such as lipopolysaccharide (LPS), peptidoglycan, and lipoproteins activate NF- κ B signalling pathway leading to IL6, IL8, IL18, TNF α , and inflammasome response (15). Resident B and T cells and peripheral innate immune cells, such as neutrophils, monocytes, eosinophils and natural killer (NK), are then recruited to the sites of infection to contain and clear the pathogen.

Antigen presenting cells (APC), specifically dendritic cells (DC), capture antigens directly or indirectly via presentation by epithelial cells and microfold (M) cells and migrate to local lymph nodes. M cells are cells within the epithelium specialised in taking up luminal antigens and pathogens, and transporting them to the underlying lymphoid tissue

(16), typically found on NALT but not in BALT (17). In lymph nodes, antigens are presented to naïve lymphocytes and CD8⁺ (cytotoxic) and CD4⁺ (helper (Th)) T cells to undergo clonal expansion (18). Cytotoxic T cells are important for killing viral infected cells or cancerous cells. Helper T cells coordinate immune responses and mobilise other immune cells including CD8⁺, B cells and macrophages (19). Antigen-specific immune cells can re-circulate to the original mucosal site of infection using tissue-specific homing receptors, including integrin $\alpha 4\beta 7$ and chemokine receptor CCR9, which is integral to the common mucosal immune network (20). The homing receptors bind ligands on peripheral tissue vasculature, guiding immune cells to the original sites of infection. Activated cells can also travel to the bloodstream to participate in systemic immune responses.

In draining lymph nodes, CD4⁺ Th cells induce B cell activation that proliferate and differentiate into low-affinity IgG or IgA producing plasma cells (21). These cells can then traffic to sites of infection or enter germinal centres where B cells differentiate into high-affinity long-lived memory B cells which then traffic to sites of infection. At the site of infection, plasma cells produce dimeric antigen-specific IgA and IgG antibodies. Antibodies can attach to pathogens via their Fab region, resulting in a process called antibody opsonisation. This coating of pathogens with antibodies enhances their susceptibility to ingestion by phagocytes such as macrophages. The Fc region of the antibody, on the other hand, is recognised by Fc receptors in macrophages and monocytes and trigger the engulfment of antibody-coated bacteria. T cells can also be induced and expanded in the bone marrow and spleen during intermediate and late stages of a respiratory infection. After subsequent re-exposure to a pathogen, memory T and B cells recognise prior exposed antigens and rapidly respond to clear the pathogen infection.

The main immunoglobulin produced by the mucosal immune system is IgA. IgA has a role in mediating the adaptive humoral response at mucosal surfaces. There are two types of IgA in humans, IgA1 produced in bone marrow plasma cells, predominantly monomeric and present in serum, and IgA2, polymeric, mainly dimer, and found in mucosal tissues (22). Dimeric IgA can also be secreted across epithelium as secretory IgA. The main function of secretory IgA antibodies is to limit access of pathogens to the mucosal surfaces. Secretory IgA forms large antigen-antibody complexes that inhibit bacterial and viral adhesion to epithelial cells and facilitates their removal by mucociliary clearance (23). IgA production avoids induction of inflammatory response by not acting as an opsonin or activating the classical pathway of complement. However, the efficacy of

secretory IgA in combating virus infections can be compromised by mutations of viral surface glycoproteins as seen for IV and SARS-CoV-2 viruses (24).

Tissue-resident T cells are also a key element in mucosal immune responses. After antigen encounter, they become tissue-resident memory T cells TRMs which proliferate *in situ*, acting as a first line of defence by blocking spread of infection. After induction, CD4+ and CD8+ TRM in the nasal cavity are stored for long term, but CD8+ TRM in the lungs are generally short lived (25). Repeated antigen exposure can however improve longevity (25). To generate resident nasal and pulmonary TRM, vaccines need to be delivered into the airways (26) with TRM being pivotal for limiting IV and SARS-CoV-2 virus spread (25).

While the innate immune response is triggered within minutes to hours after antigen detection, antigen-specific adaptive immune response takes several days to weeks to develop. Vaccines need to induce both the innate and adaptive immune response to provide protection.

The respiratory and gastrointestinal tracts have mechanism in place to prevent the immune system from mounting inflammatory responses to harmless antigens. They do this by inducing immune tolerance, which trains the immune system to recognise harmless antigens and not react to them with an inflammatory response (27). Immune tolerance is the lack of immune response to a substance that could otherwise induce an immune response. In the lungs, immune tolerance is mainly mediated by regulatory T cells that limit proliferation of other T cells and produce immunosuppressive cytokines, leading to B, T and APC inactivation (e.g., anergy) and/or cell death (27, 28). Commensal bacteria send signals to the immune system that assist in identifying and tolerating them as harmless and beneficial to the host. For example *Bacteroides fragilis* capsular polysaccharide (PSA) that induces regulatory T cells and anti-inflammatory cytokines (29).

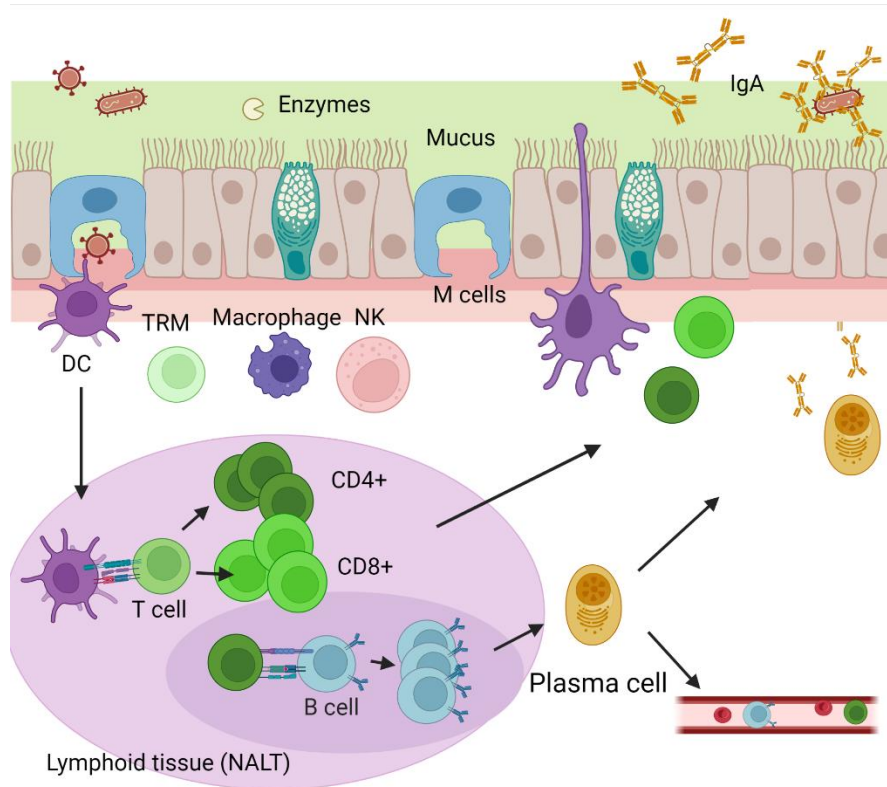


Figure 1.1 Representation of the respiratory immune system NALT. Created in Biorender.com.

1.3 Types of vaccines

Vaccines can be divided into three main types, attenuated, inactivated and subunit.

1.3.1 Attenuated vaccines

Attenuated vaccines contain weakened whole bacteria or viruses. They are still immunogenic and replicative but lose ability to cause disease. The attenuation can be done by repeated culturing of a pathogen in unnatural host or condition (e.g., cold-adapted conditions for IV), that generate gene alterations which lead to attenuation, or by genetically modification (30). Attenuated vaccines elicit strong immune responses which are unsuitable for young children, the elderly or immunocompromised individuals with co-morbidities. Such populations have weakened immune systems which fight infections less efficiently than most people and are more likely to get infections. In this case, delivering attenuated vaccines to populations with weakened immune system can lead to secondary effects, or cause illness, as their ability to limit the replication of the attenuated pathogen is compromised (31).

Examples of live attenuated vaccines include oral poliovirus vaccine (OPV), live attenuate influenza vaccine (LAIV), and measles, mumps, and rubella vaccine (MMRV). The OPV is the most successful mucosal vaccine to date, blocking transmission of the virus with the number of polio cases being reduced by more than 99% since 1980 (32). However, there are still disease outbreaks of vaccine-associated paralytic polio (VAPP) that arise due to small genetic changes occurring in the attenuated poliovirus after vaccination (33).

1.3.2 Inactivated vaccines

Inactivated vaccines contain killed or altered whole bacteria or viruses, whose genetic material has been destroyed, typically using heat or chemicals such as formaldehyde or formalin so that they cannot infect cells (30). Inactive vaccines are safer than attenuated vaccines as they are non-replicative. However, inactivation may destroy antigens, reducing their immunogenicity and thus requiring multiple doses and the addition of adjuvants to induce the immune system (34). Some examples are hepatitis A vaccine (commercial names e.g., Havrix and Vaqta), rabies vaccines (commercial names e.g., KEDRAB, HyperRab and Imogam) and inactivated polio vaccine (IPV).

1.3.3 Subunit vaccines

Subunit vaccines contain purified parts of the pathogen (e.g., polysaccharides, proteins antigens, RNA). Similar to inactivated vaccines, they are non-infectious but lack immunogenicity and depend on multiple doses or adjuvants. Subunit vaccines can be classified according to their makeup:

Protein/ polysaccharide subunit vaccines include proteins or polysaccharides from the pathogen. For example, hepatitis B vaccine (commercial names e.g., Engerix-B, Heplisav-B, and Recombivax HB) contains surface antigen HBsAg (35), and Pneumococcal vaccine (Pneumovax 23) contains polysaccharides from 23 serotypes (36).

Toxoid vaccines include toxins from the pathogen that are inactivated by heat or chemicals (37). For example, Tetanus vaccine contains inactivated tetanus toxin produced by *Clostridium tetani*, and Diphtheria vaccine contains diphtheria toxin produced by *Corynebacterium diphtheriae* (37).

Nucleic acid vaccines incorporate RNA encoding viral or bacterial antigens. Once the RNA is inside the host cells and translated into proteins, antigens are recognised by the immune system. RNA vaccines normally use mRNA inside a lipid membrane. The

Covid-19 vaccines Pfizer/BioNTech and Moderna are examples which use mRNA encoding Spike protein.

Viral vector vaccines utilise modified harmless viruses, usually non-replicative, as vectors. Viral vectors can carry antigens or genetic material to produce antigens from a pathogen when taken up by host cells. The intramuscular Oxford-AstraZeneca Covid-19 vaccine uses a modified non-replicable chimpanzee adenovirus that protects the DNA sequence of Spike protein (38).

Virus-like particles are particles that mimic the conformation of viruses but are non-infectious. For example, human papillomavirus vaccine (HPV) is obtained by expressing the surface capsid protein of human papillomavirus (39).

Bacterial extracellular vesicles (BEVs) are non-replicative lipid bilayer vesicles, naturally produced by bacteria. Bexsero *Neisseria meningitidis* vaccine contains BEVs in its formulation. More information about BEVs is discussed in section 1.7.

1.4 Licensed intranasal vaccines

The first licensed intranasal vaccine was Fluenz (UK and EU)/ FluMist (USA), against IV. Since the licensing of this vaccine, similar intranasal vaccines against IV have been licensed including, Ultravac (Russia), Nasovac (India) and Ganwu (China). All of them are LAIV consisting of four cold-adapted weakened IV strains. The virus can replicate efficiently at 25°C, which is the temperature found in the nasal cavity, but fails to replicate at higher temperatures elsewhere in the body, including lungs (40). LAIV retain IV immunogenicity and produce similar lung CD4+ and CD8+ TRM to those produced after IV infections (26). Although LAIVs have been licensed and widely used in children, their use is restricted to healthy and non-pregnant individuals from 2 to 49 years of age for safety reasons. Similar to intramuscular vaccines, intranasal LAIVs efficacy varies every year (27% to 65% in the UK, between 2015 and 2020) due to the rapid evolution of the virus (41).

Four respiratory mucosal vaccines against SARS-CoV-2 have been approved for emergency use in some countries by their health authorities, although none have received WHO prequalification (as of November 2022) (42, 43) (Table 1.1). These vaccines are inactivated or subunit vaccines containing adjuvants or viral vectors used as carriers and adjuvants.

Table 1.1 Mucosal Covid-19 vaccines in use

Developer (location)	Name	Vaccine type	Adjuvants used	Ref
Bharat Biotech (India)	COVAXIN	Inactivated	Aluminium hydroxide and TLR 7 /8 agonist (imidazoquinolinone)	(44)
Razi Vaccine and Serum Research Institute (Iran)	RAZI-COV PARS	Protein subunit	RAS-01 (oil-in-water emulsion)	(45)
CanSino Biologics (China)	Convidecia Air	Viral vector (Ad5-nCoV)		(46)
Gamaleya Research Institute of Epidemiology and Microbiology (Russia)	Gam-COVID- Vac	Viral vector (Ad5-nCoV)		(47)

Table adapted from Waltz et al. (47).

1.5 Challenges for developing intranasal vaccines

Mucosal surfaces are constantly exposed to foreign antigens. Immune tolerance predominates in mucosal sites to prevent induction of inflammatory responses to harmless antigens and avoid unnecessary tissue damage (27). Immune tolerance is the lack of immune response to a substance that could otherwise induce an immune response. Therefore, vaccine candidates with weak immunogenicity require adjuvants to overcome immune tolerance to the vaccine.

Additionally, the presence of enzymes such as proteases within the mucus barrier, secreted from the respiratory epithelium, can degrade vaccines and affect their stability (48). The renewal of mucus and mucociliary clearance also dilute and aid elimination of the vaccine (49). Antigens can also be physically excluded by the epithelial barrier, hindering their uptake and presentation by APCs.

1.6 Adjuvants

Adjuvants are excipients added to vaccine formulations to boost potency, breadth, and longevity of immune response. They are used to compensate for weak or low immunogenicity of inactivated or subunit vaccines.

Adjuvants for intramuscular or parenteral vaccines are well known, and their effectiveness and safety are well established (50). These include aluminium salts, oil-in-water emulsions, and lipid nanoparticles. The most widely used adjuvant is aluminium hydroxide, an aluminium salt, collectively called “alum”. Alum was licensed in the 1930s and has long been used in hepatitis B, diphtheria, tetanus, pertussis, and human papillomavirus vaccines (50). Alum with adsorbed antigens increases antigen uptake and induces humoral immunity, but has low ability to induce CD8+ T cell responses essential for killing viral infected cells (51). Furthermore, alum can also stimulate the release of damage-associated molecular patterns (DAMPs) and elicit IgA after intranasal administration (52).

Unique and different characteristics of mucosal versus systemic vaccine target sites (mucus barrier, pH, lymphoid cell makeup and organisation) can make intramuscular or parenteral adjuvants less effective in mucosal sites (53). Adjuvants used in intranasal Covid-19 vaccines are the first ones used for intranasal delivery (alum and imidazoquinolinone in Covaxin, and RAS-01, oil-in-water emulsion, in the RAZI-COV PARS vaccine; Table 1.1) and have been approved for emergency use only (44, 45). Mucosal adjuvants should aim to have mucolytic, mucopenetrative or mucoadhesive properties to allow penetration of mucus, ensure stability of the vaccine, promote antigen uptake by M cells, epithelial cells or APC and ideally, stimulate humoral and cellular immunity memory (54).

Adjuvants can be classified into immunostimulatory molecules and delivery systems.

1.6.1 Immunostimulatory molecules

Immunostimulatory molecules improve immune responses to vaccine antigens. An example is toxoid adjuvant, which includes derivatives of *E. coli* heat-labile enterotoxin (LT) and cholera toxin (CT). However, the use of these two toxins in intranasal vaccines has resulted in cases of Bell's palsy (55, 56). Other modified enterotoxins or synthetic

derivatives, such as double mutant LT or multiple-mutated CT, are examples of detoxified endotoxins currently being used in oral or intranasal delivery adjuvants in pre-clinical studies (57-59). Recombinant cholera toxin subunit B (CTB) is the only adjuvant accepted for oral use in the Dukoral vaccine against *Vibrio cholera* bacteria. However, CTB is now recognised as a subunit antigen and not an adjuvant due to the presence of residual cholera toxin and LPS in CTB preparations, and their role in inducing cholera toxin-specific antibodies to eliminate cholera (10).

Other immunostimulatory molecules include sodium alginate or cell-penetrating peptides that promote uptake of antigens (60), production of cytokines (61) and act as TLR agonists to promote non-specific immune response (62). Chitosan is another well studied mucosal adjuvant. It attaches to mucus membranes and reduces cilia clearance of antigens (63). Chitosan can also be used to create nanoparticles as a delivery system (64).

1.6.2 Delivery system

Delivery systems confer protection and enhance stability of antigens while inducing effective antigen presentation and activation of immune system. Delivery systems can be coated or modified with immunostimulants molecules. Delivery systems used for mucosal vaccines are compared in Table 1.2.

Table 1.2 Mucosal vaccine delivery systems

Delivery system	Structure	Advantages	Limitations	Ref.
Viral vector (e.g., Adenovirus)	Replication-deficient virus expressing antigens of interest	<ul style="list-style-type: none"> • Highly immunogenic • Elicit antibody and cellular responses • Can be genetically modified to reduce reactogenicity 	<ul style="list-style-type: none"> • Previous exposure can reduce immunogenicity 	(65)
Liposomes	Spherical phospholipid bilayer entrapping an aqueous solution core	<ul style="list-style-type: none"> • Ease of incorporating distinct types of antigens • Adaptable physicochemical properties • Self-adjuvanticity 	<ul style="list-style-type: none"> • Relatively low intrinsic stability for storage and after administration • Potent toxicity of cationic lipids (dose-dependent) • Non-specific interaction 	(66)
Lipid nanoparticles	Spherical phospholipid layer entrapping a non-aqueous core	<ul style="list-style-type: none"> • Sustained drug released • Simple formulation 	<ul style="list-style-type: none"> • Non-specific uptake • Poor physicochemical and microbiological stability • Poor drug loading capacity • Highly inflammatory in intranasal delivery 	(67)

ISCOM, ISCOMATRIX	Cage-like structure comprised of cholesterol, phospholipids and saponin	<ul style="list-style-type: none"> • Composition, size, and surface structure like virus • Self-adjuvantcity • Ease of antigen loading 	<ul style="list-style-type: none"> • Difficulty in including hydrophobic antigens 	(68)
Bacterial extracellular vesicles (BEV)	BEVs from Gram negative bacteria containing MAMPs and membrane proteins.	<ul style="list-style-type: none"> • Self-adjuvantcity • Easy of manufacture • Protect antigens from degradation 	<ul style="list-style-type: none"> • Chemical detoxification required for pathogenic derived BEVs– reduced adjuvantcity • Variable efficacy 	(69)
Virus like particles (VLP)	Particles that mimic virus without carrying genetic material	<ul style="list-style-type: none"> • Highly immunogenic • Stable 	<ul style="list-style-type: none"> • Purification can be a challenge and expensive • May have poor quality and consistency • Contamination by host materials 	(70)
Emulsions Water in oil/ oil in water	Nanosized droplets	<ul style="list-style-type: none"> • Slow release of immunogen • Ease of manufacture • Self-adjuvantcity 	<ul style="list-style-type: none"> • Reactogenicity • Limited stability after administration • Low preservation of antigen structure 	(71)

Synthetic polymeric nanoparticles (e.g., Polylactide (PLA) and poly lactic-co-glycolic acid (PLGA))	PLA or PLGA based nano- and micro particles. FDA approved agents	<ul style="list-style-type: none"> • Controlled release of antigens • Biodegradable and biocompatible biopolymer 	<ul style="list-style-type: none"> • Sensitivity to harsh gastric environment • Low loading capacity 	(64)
Natural polymeric nanoparticles (e.g., chitosan)	Chitosan based nano and micro particles.	<ul style="list-style-type: none"> • Mucoadhesive • Self-adjuvantivity 	<ul style="list-style-type: none"> • Irregular distribution • Low physical stability 	(72, 73)
Nanogel (e.g., cationic cholesterol-bearing pullulan nanogel (cCHP))	cCHP self-assembles with water due to their amphiphilic polysaccharides.	<ul style="list-style-type: none"> • Prolonged binding to nasal epithelium. • Ability to function as an artificial chaperone that transcytoses antigens into the subepithelial mucosa 	<ul style="list-style-type: none"> • Optimization of biodistribution and degradation mechanism • Component toxicity 	(74, 75)
Lactic acid bacteria (LAB)	Live recombinant LAB expressing antigens. Generally recognized as safe (GRAS).	<ul style="list-style-type: none"> • Easy and safe production and storage • Survives gastric environment • Self-adjuvantivity 	<ul style="list-style-type: none"> • Safety concerns using genetically modified organisms as they can survive if released in the natural environment 	(76)

Chemically processed pollen grains	Resistant bilayer pollen grain shell.	<ul style="list-style-type: none"> • Self-adjuvantivity Protected from harsh environment 	<ul style="list-style-type: none"> • Chemical treatment methods required to eliminate allergens from pollen grain 	(77)
Terrestrial plants and algae	Plant or algae cells with an antigen created by gene modification.	<ul style="list-style-type: none"> • Highly resilient cell wall • Easy manufacturing process and scale up • Suitable for mass vaccination • No cold chain requirement 	<ul style="list-style-type: none"> • Use of transgenic plants and regulatory body approvals 	(78)
Bilosomes	Bile salt stabilized vesicles.	<ul style="list-style-type: none"> • Stable in gastric environment • High stability 	<ul style="list-style-type: none"> • Relatively low antigen dose 	(79, 80)

Modified table also published in Miquel-Clopes et al. 2019. (81)

Adenovirus-based intranasal vaccines have been recently developed for SARS-CoV-2 vaccines by CanSino Biologics (46). Intranasal CanSino vaccine uses a replication-defective human adenovirus type-5 vector-based vaccine expressing spike S protein from SARS-CoV-2 (46). Adenovirus vectors are highly immunogenic, however, pre-existing immunity to adenovirus reduces immune stimulation as the vaccine can be neutralised by antibodies formed in previous infections (82).

Liposomes are stable bilayer vesicles, that can be modified by chitosan, cholesterol or Polyethelene Glycol (PEG) to increase particle permeability and stability or decrease toxicity (83). Liposomes have one ring of lipid bilayer surrounding an aqueous lumen. Contrarily, lipid nanoparticles contain a single phospholipid outer layer. Lipid nanoparticles have been used in intramuscular Covid-19 vaccines (Moderna and Pfizer/BioNTech) to encapsulate mRNA encoding the SARS-CoV-2 Spike protein but resulted in strong inflammatory responses when administered intranasally (84).

Another delivery vehicle that has gained interest recently for their role in crosstalk between microbes and host immune system are BEVs. Advantages and challenges of BEVs are described more extensively in the next section.

1.7 Bacterial extracellular vesicles

All living organisms release extracellular vesicles (EV) (85), with those produced by bacteria termed bacterial extracellular vesicles (BEVs). BEVs are produced naturally and continuously throughout their growth cycle. They are non-replicative structures and can contribute to inter- and cross-kingdom interactions with other bacteria and with their host, respectively (86). Their functions, composition and size are diverse (87).

Based on the origin of BEVs, they can be classified into four different types of vesicle (88) (Fig. 1.1). First, Gram positive bacteria produce cytoplasmic membrane vesicles (CMVs) that carry membrane and cytoplasmic components. Second, gram negative bacteria produce outer membrane vesicles (OMVs) that have a single bilayer membrane and are produced by the blebbing of the outer membrane. Gram negative bacteria also produce vesicles after explosive cell lysis; to produce thirdly, explosive outer membrane vesicles (EOMVs) and fourthly, outer-inner membrane vesicles (OIMVs), which have two membrane bilayers that derive from the inner and outer membranes.

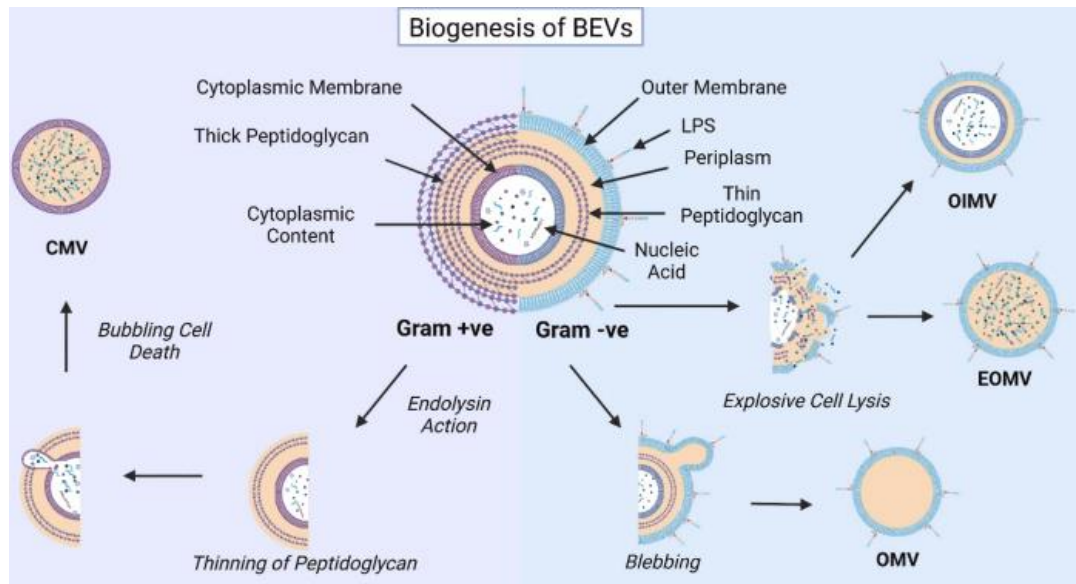


Figure 1.2 Biogenesis of BEVs. BEVs from gram positive bacteria after bubbling form cytoplasmic membrane vesicles (CMVs). In gram negative bacteria BEVs can be formed during explosive cell lysis resulting in outer-inner membrane vesicles (OIMVs) and explosive outer membrane vesicles (EOMVs). Or by blebbing which form outer membrane vesicles (OMVs). Image from Suri et al. 2022 (89).

BEVs of different origin have a similar size, this hinders their individual isolation and can lead to making general assumptions regarding their characteristics (87). Most literature use the term OMVs to describe extracellular vesicles made by gram-negative bacteria. However, due to the inability to separate different BEVs, preparations of OMVs are heterogeneous, containing a mixture of BEVs. Throughout the thesis I will use the term OMVs when talking specifically about literature results, but BEVs when talking about general characteristics and my work.

BEVs are isolated from a bacterial growth by a combination of centrifugation and ultracentrifugation and/or ultrafiltration. BEVs can be further purified by size fractionation to eliminate contaminating material and sterile filtered (Fig.1.4) (90, 91).

BEVs composition reflects the structure of the outer membrane of parental cells and contains immunostimulatory components such as outer membrane proteins (OMPs), LPS, lipoproteins and glycoproteins that confer self-adjuvanticity to BEVs (92). Periplasmic proteins, peptidoglycan and RNA/DNA can also be found in BEVs (93). However, BEV cargo and production is variable according to the bacterial strain, growth conditions, and environment (94). For example, *Helicobacter pylori* derived OMVs extracted from different growth stages are different in size, shape and protein composition (95). Also, different

growth media supplements modify the cargo of the *H. pylori* OMVs that can produce different impacts on macrophages (96).

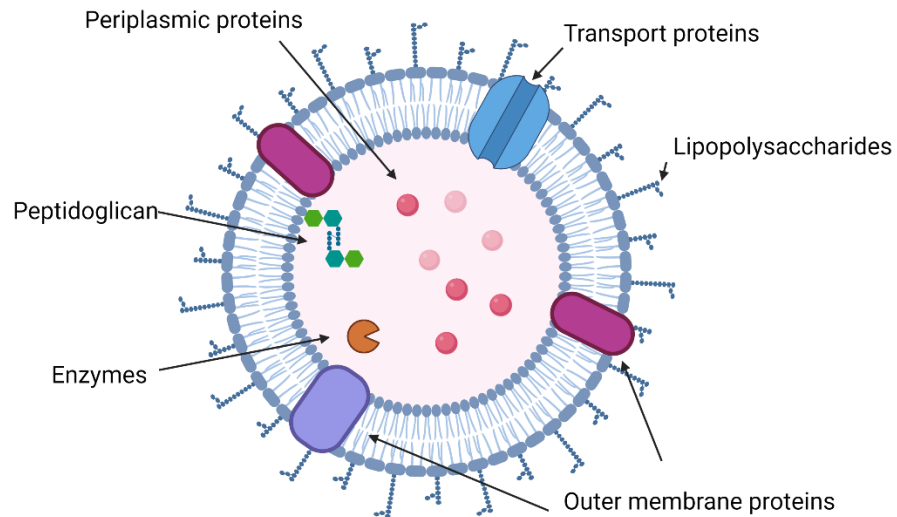


Figure 1.3 Composition of OMV. Created in Biorender.com.

The complex composition of BEVs and different cargo is related to the multiple functions of BEVs. The roles and functions of BEVs differ from bacteria and environmental factors and same BEV can have multiple roles simultaneously.

One of the major roles of BEVs is their capacity to modulate host immune cell function. Commensal bacteria derived BEVs generally promote homeostatic responses (29, 97, 98). For example, commensal bacteria *Bacteroides fragilis* BEVs contain capsular polysaccharide (PSA) that induces regulatory T cells and anti-inflammatory cytokines (29). Likewise, BEVs from *Lactobacillus rhamnosus* (98) and *Bacteroides thetaiotaomicron* (97) enhance regulatory IL-10 production in gastrointestinal tract.

BEVs derived from pathogenic bacteria secrete toxins and other virulence factors that promote colonisation and inducement of pro-inflammatory immune responses (99-101). For example, *Pseudomonas aeruginosa* derived BEVs deliver multiple virulence factors such as hemolytic phospholipase C, alkaline phosphatase, and Cif, to the host cells that cause cellular death (99). Enterohemorrhagic *E. coli* (EHEC) BEVs contain Shiga toxin, EHEC hemolysin and cytolethal distending toxin V, induce DNA damage to host cells inducing cell death (100). Also, *P. aeruginosa* BEVs containing short RNA sequences,

reduce host innate immune response by attenuating neutrophil infiltration and cytokine secretion (101).

BEVs can also help bacteria to protect against antimicrobial agents. For example, β -lactam antibiotic resistant *E.coli* can incorporate proteins involved in degrading β -lactam antibiotics, and help survive other antibiotic susceptible bacteria (102). BEVs can also carry antibiotic-resistant genes as seen with *K. pneumoniae* BEVs transferring β -lactamase gene to other bacteria through their BEVs (103). Or act as decoy, as *Acinetobacter baumannii* negatively-charged vesicles BEVs trapped positively-charged antibiotic polymyxin B benefiting microbial community (104).

In contrast, BEVs can also contain antibiotics, inducing bacteria mortality in competing bacteria. For example, *P. aeruginosa* BEVs contain quinolones demonstrated to inhibit growth of *Staphylococcus epidermidis* (105).

Moreover, BEVs contribute to acquire nutrients. For example, *Bacteroides thetaiotaomicron* (Bt) BEVs bind to B12, an essential dietary nutrient and deliver it to parental bacterium and host cells (106). And *B. pertussis* delivers iron to parental bacterium in iron-limiting conditions (107). Other BEV roles include detoxification of bacteria by elimination of misfolded proteins (108), adhesion and biofilm formation. For example, *V. cholerae* BEVs containing DegP protein induce secretion of matrix components (RmbA, RmbB, Bap1) that promote biofilm formation (109).

1.8 Using BEVs in mucosal vaccine formulations

Crossing the mucosal barrier (mucus and epithelial cells) is a major challenge for mucosal vaccines. However, BEVs can diffuse through the mucus layer and access underlying epithelial cells (110, 111). Particles bigger than 200nm have a greater probability of being trapped and removed by mucociliary clearance (112). BEVs of 50-200nm in size, which is the average size of respiratory viruses, can cross the mucus barrier (113, 114). In the gastrointestinal tract, BEVs also can permeate the mucus barrier and be acquired by epithelial cells via endocytic pathways including micropinocytosis, clathrin-mediated endocytosis, or caveolin-mediated endocytosis (115). BEVs can also be internalised by respiratory epithelial cells (116) but the exact mechanisms are not known.

BEVs possess innate adjuvant properties and PAMPs that can be recognised by dendritic cells, M cells and macrophages, thereby stimulating innate immune responses

(117). For example, the lipid A site of LPS binds TLR4 (118), and lipoproteins and polysaccharides bind TLR2 (119, 120), leading to activation of NF- κ B. Peptidoglycans present in BEVs can also bind the cytosolic NOD-1 and NOD-2 (121). Thus, BEVs represent an attractive platform to induce humoral and cell-mediated immune responses.

Moreover, BEVs can carry multiple antigens that retain their native conformation with the lipid bilayer protecting antigens from dilution and physical, chemical, or proteolytic degradation (122).

Additionally, BEVs that are naturally released from bacteria in complex or defined growth media are straightforward to purify and cost-effective compared to conventional vaccine production costs. The licensed BEV-based vaccine Bexero also demonstrates scale-up feasibility.

There are limitations to the use of BEVs in vaccine formulations. A major concern in using pathogen derived BEVs is unintended toxicity. LPS and lipooligosaccharides (LOS) potent stimulant of pro-inflammatory responses and are expressed in BEVs. LOS and LPS are both composed of lipid A and core oligosaccharide, and LPS have additional extended polysaccharide chain (123). The degree of acylation, which refers to the process of adding an acyl group to the lipid-A component of LPS, is directly related to its affinity for binding TLR4 receptor. This affinity affects the degree of immune response that is triggered by the LPS molecule. Hexa-acylated LPS are the most potent activators of TLR4-mediated signalling that can result in an acute inflammatory response (124). On the contrary, penta-acylated LPS or LOS molecules, such as those found in Bt BEVs, have a low ability to induce TLR4 signals, resulting in a weaker inflammatory response. BEVs from bacteria producing hexa-acylated LPS like *N. meningitidis* and *E. coli*, need to be detoxified before they can be used as vaccine components (125). A common method to detoxify BEVs, used in Bexsero, is using detergent, which lowers the LPS content and increases vesicle formation. The use of detergents not only makes the isolation process more prolonged and expensive, but also compromises vesicle stability, increases cytoplasmic proteins and the loss of important protective antigens (126).

The toxicity of lipid A can also be removed or modified by engineering the parental bacterium (126). However, the difficulty in assessing pathogenicity genes for mutation can result in BEVs which are still toxic due to limited screening or unwanted secondary mutations (127).

The limited production of BEVs can be another limitation. This can however be overcome by inducing hypervesiculation. Stress conditions such as iron or oxygen limitation, pH, temperature or exposure to antibiotics increases vesicle production (128). Bacteria can also be genetically modified to increase blebbing by different mechanisms such as changes in peptidoglycan dynamics (129), accumulation of misfolded proteins (130), or phospholipid accumulation in the outer membrane that leads to the formation of OIMV (131). However, the induction of hypervesiculation can affect size, structure, and cargo of the vesicles (129-131). Continuous production of *N. meningitidis* OMV has also been investigated to increase the yield, showing its feasibility and promise by increasing volumetric productivity and reducing costs (132).

Other limitations of using BEVs as a vaccine include the heterogeneity of BEVs during production and difficulty of standardising composition and efficacy. This can be overcome with more studies observing BEVs variation over different conditions and by implementing extensive quality controls assessments. Another limitation can be low expression levels of protective antigens which can be improved by genetic engineering of BEV-producing strains.

1.9 BEVs as a vaccine

BEVs are highly versatile and can be used in a variety of ways in vaccine formulations. There are three main approaches to utilizing BEVs: homologous, heterologous expressed, and heterologous decorated BEVs. Homologous BEVs are produced by bacteria that express their own antigens, while heterologous expressed BEVs are generated by genetically modifying bacteria to express different antigens in their BEVs. Lastly, heterologous decorated BEVs are produced by bacteria and then decorated with various antigens on their surface after production.

The Bexsero meningococcal vaccine is the only currently licensed vaccine that contains BEVs. *N. meningitidis* enters the body through respiratory airways and infects the lining of the brain and spinal cord, leading to meningococcal disease. The vaccine is administered intramuscularly and comprises OMVs isolated from *N. meningitidis* group B strains, together with recombinant proteins adsorbed on aluminium hydroxide (133). The protective effect of meningococcus B OMV is mainly mediated by PorA P1.4, which is highly variable between strains (134). However, other PAMPs (fHbp and NHBA antigens)

in the OMVs also induce immune responses and confer protection (135). Previous vaccines using only homologous *N. meningitidis* OMV were strain-specific and recombinant proteins were later added to the vaccine to promote heterotypic protection (136).

Other homologous BEVs vaccines for intranasal delivery have been studied preclinically. Mixtures of OMVs from *H. influenzae* strain administered to mice resulted in robust mucosal humoral responses (137). Also, *Bordetella pertussis* OMVs induced humoral and CD4+ T cells induction and prevented colonisation in mice after intranasal immunisation (138). Indeed, studies have demonstrated that homologous BEVs vaccines are effective but confer low cross-protection against different strains (136-138).

Most pre-clinical studies examining BEVs have focused on engineering pathogenic bacteria to reduce toxicity of LPS and to express other pathogen antigens in their BEVs. For example, OMVs from genetically detoxified *V. cholerae* modified to express *E. coli* antigens induced mucosal immune response after intranasal delivery in mice (139). Similarly, *Salmonella enterica* serovar Typhimurium, engineered to express pneumococcal antigens in the lumen of its OMVs, induced antibody responses after intranasal immunisation of mice (140). Likewise, genetically detoxified *Vibrio cholerae* and *E. coli*, expressing the receptor-binding domain (RBD) of Spike from SARS-CoV-2 in their OMVs, induced mucosal humoral response in mice after intranasal immunised (141).

Expression of heterologous antigens can be directed and incorporated into BEVs by different mechanisms. In detoxified OMVs of *Vibrio cholerae* and *E. coli* expressing SARS-CoV-2 Spike RBD, the receptor binding domain was fused N-terminally to a sequence consisting of N-terminal signal sequence with 9 amino acids of the major outer membrane lipoprotein (Lpp), together with 110 amino acids of outer membrane protein A (OmpA) (Transmembrane porin protein abundantly expressed in bacteria and BEVs (142)). The Lpp directs the fusion protein to the membrane region of OmpA, which contains five membrane spanning segments that leads to the presence of RBD at the surface of the OMV (141). Other techniques include fusing the antigen of interest to the secretion system of OmpA to bring the protein to the periplasm (142-144). Also proteins known to be secreted in OMVs such as β -lactamase secretion system (140), or Cytolysin A (*E. coli* pore-forming toxin)(145, 146), are used to transport antigens to the periplasmic space.

Decorating BEVs externally has the advantage of conjugating native antigens with post-translational modifications (glycosylation or disulphide bonds) that bacteria cannot do. This strategy has been used for SARS-COV-2 vaccines as Spike antigen undergoes

extensive post-translational modifications. Different decorating methods have been used including, SpyTag-SpyCatcher. In this case, BEVs are engineered to express SpyCatcher and SpyTag is conjugated to the antigen of interest. When SpyTag and SpyCatcher are combined, they form a spontaneous and stable covalent amide bond (147), enabling the conjugation of antigens to the membrane of BEVs. This method has been applied for *Salmonella enterica* serovar Typhimurium-derived OMVs decorated with SARS-CoV-2 spike antigen, which induced both mucosal and systemic humoral response, resulting in less severe lung pathology after a SARS-CoV2 infection in hamsters immunised intranasally (148). Another method used is mCRAMP, a short amphipathic peptide that has affinity for the negative phosphate group in LPS. This was used for the Intravacc 10 vaccine against SARS-CoV-2, now in phase I clinical trials (149). The vaccine consists of Spike antigen from SARS-CoV-2 fused to mCRAMP that bound to LPS of genetically detoxified *N. meningitidis* derived OMVs (150).

From a manufacturing point of view, expression and purification of antigens and posterior conjugation to BEVs adds extra steps to the vaccine production process increasing the difficulty and cost. Expressed heterologous BEVs, which can be used directly after isolation with no further manipulations, have a simpler production process and are more cost-effective.

Recently, commercial companies are becoming interested in using BEVs as a vaccine vehicle including GSK and other relatively new and BEV related companies Intravacc, Versatope and Biomvis targeting multiple disease. These companies use pathogenic bacteria (*N. meningitidis* and *E. coli*) that are genetically modified to reduce toxicity and overexpress antigens or decorate BEVs with antigens.

1.10 Bacteroides thetaiotaomicron-derived BEVs

To overcome the issue of toxicity in the use of pathogen derived BEVs our group has used BEVs from a human commensal gut bacterium Bt (151), as a source of BEVs for use in vaccine formulations. Bt has been extensively used to study host immune-microbiota interactions and plays important roles in maintaining homeostasis and gut health (97, 152). Bt can restore disrupted epithelial tight junction barrier (152) and promote anti-inflammatory activity (153). Lyophilised Bt is also being used in clinical trials as a live biotherapeutic in patients with Crohn's disease (154).

Naturally produced BEVs from Bt (155) can mediate and replicate the functions of Bt. For example, Bt BEVs can process dietary nutrients (106, 156) and contribute to microbiota and immune homeostasis (97, 120). Bt BEVs also contain mucin-degrading enzymes such as sulfatases and glycosidase hydrolases that degrade mucin glycoproteins and facilitate crossing the mucus barrier (157, 158) and accessing intestinal epithelial cells (111). Bt BEVs can also transmigrate epithelial cells via paracellular or transcellular routes and reach the lamina propria (120). Bt BEVs can interact with and activate immune cells, in particular APCs via TLR-2 and NF- κ B activation, leading to the induction of innate immune responses (120). Bt BEVs then induce mucosal and systemic immunoregulatory responses characterised by the production of protective IL-6 and regulatory IL-10 (97). IL-10 is important in the development of T regulatory cells that can contribute to maintaining immune homeostasis and microbial tolerance (159). Interestingly, this immunoregulatory IL-10 response of immune cells to Bt BEVs is diminished or absent in inflammatory bowel disease patients, characterised by leaky gut, inflammation, and inappropriate response to constituents of the intestinal microbiota (97).

Bt BEVs can also have a role in interspecies interactions as they can modulate the virulence of *Shigella flexneri*, *ex vivo*, by repressing expression of virulent genes (160); extracted lipids from Bt BEVs had the same effect as that of intact Bt BEVs (160). Bt BEVs present penta-acylated lipooligosaccharides (LOS) which function as immunological adjuvants without the cytotoxicity associated with hexa-acylated LPS (161). Relevant to this thesis, Bt LOS have been defined as adjuvants for antigen-specific immune responses by Chilton et al. (162), who showed that *in vivo* mice administration of Bt LOS induces specific humoral immunity and CD4⁺ T cells.

Bt BEVs are therefore able to interact and modify both the innate and adaptive immune system and they are also a versatile and stable mucosal delivery systems. After oral administration to mice, Bt BEVs have been detected in various tissues, including the gastrointestinal tract and liver, which illustrates their wide biodistribution and ability to interact with immune cells throughout the body (111). Moreover, Bt BEVs have been shown to be an effective means of delivering therapeutic proteins to the gastrointestinal tract, with oral administration of Bt BEVs containing human keratinocyte growth factor-2, being effective at treating acute colitis in mice and promoting intestinal epithelial repair and recovery (3, 120).

1.11 Aims and objectives

The aim was to evaluate the use of Bt BEVs as a mucosal vaccine delivery system to generate protective immunity to respiratory pathogens. BEVs from genetically engineered Bt were used to develop vaccine formulation against *Yersinia pestis*, Influenza virus and SARS-CoV-2. The vaccine candidates were tested in different animal models collecting blood and tissue samples to assess their ability to elicit humoral and cellular mucosal and systemic immune responses and confer protection.

The overall study plan is depicted in Fig. 1.4.

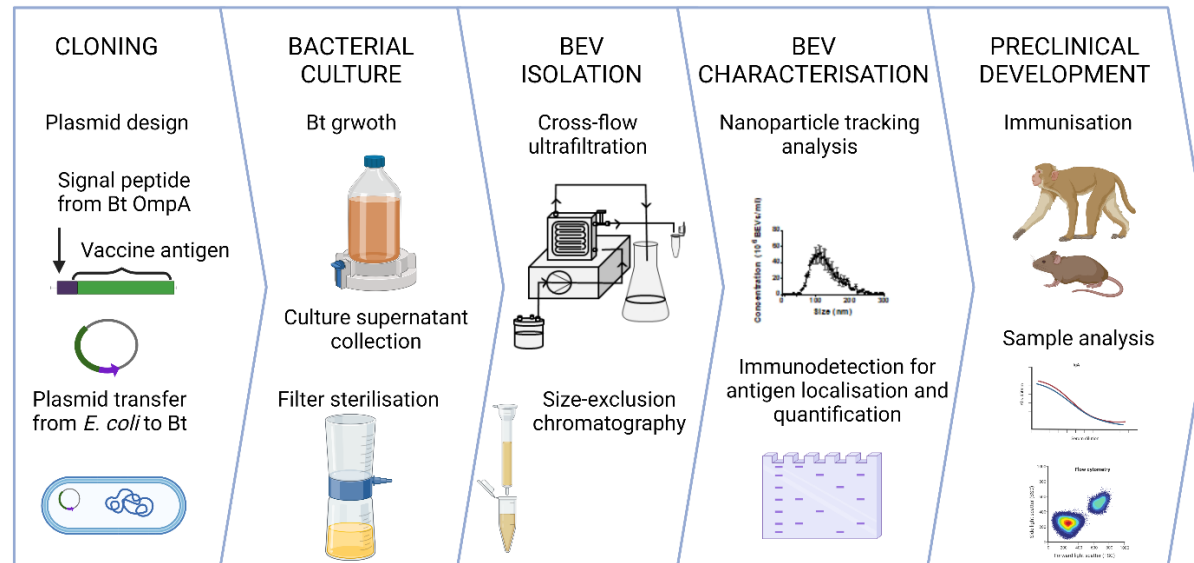


Figure 1.4 Overall study plan. The main steps include fusing antigens of interest N-terminally to the signal peptide of Bt OmpA, bacterial culture and BEVs isolation, BEVs characterisation, antigen detection, immunisation of animal models and sample analysis.

Chapter 2 Materials and Methods

2.1 Bacterial strains and growth conditions

Strains of bacteria used in this thesis are presented in Table 2.1. Bt strains were grown under anaerobic conditions at 37°C in Brain heart infusion (BHI) medium (Oxoid) supplemented with 0.001% haemin (BHIH) or Bacteroides Defined Media (BDM). Antibiotic-resistance markers in Bt were selected using Erythromycin 5µg/ml. *E. coli* strains were grown in Luria-Bertani (LB) medium at 37°C with Ampicillin 100µg/ml.

For small-scale bacterial culture, 20ml of BHIH or BDM was inoculated with a working stock for 16h. For a medium-scale, 0.5ml of a pre-inoculum (small-scale bacterial culture) was added to 500ml of BHIH or BDM (starting OD₆₀₀ ~0.005) for 16h with mild stirring.

To quantify bacterial density, absorbance at 600nm (OD₆₀₀) was determined using a spectrophotometer (Eppendorf 6131 BioPhotometer Spectrophotometer) Dilutions of the culture in growth medium (BHIH or BDM) were prepared to accurately determine absorbance.

Table 2.1 List of bacterial strains and plasmids used in this study

Species	Strain	Plasmid	Protein expressed	Antibiotic selection	Reference
Bt	VPI-5482	N/A	N/A	N/A	DMSZ
	GH490	pGH090	N/A	Ery	(163)
	GH487	pGH179	<i>Y. pestis</i> V	Ery	This study / (2)
	GH488	pGH180	<i>Y. pestis</i> F1	Ery	This study / (2)
	GH503	pGH184	IAV H5F	Ery	This study / (3)
	GH539	pGH215	IAV NP	Ery	This study
	GH536	pGH212	SARS-Cov-2-NP	Ery	This study
	GH359	pGH117	N/A	Ery	(164)
	<i>E. coli</i>	NEB 5-alpha	N/A	N/A	Tet
GH537		pGH213	IAV H5F	Amp, Cm	This study
J53/R751		N/A	Helper strain	Trim	(165)

Ery: erythromycin, Amp: ampicillin, Cm: Chloramphenicol, Tet: tetracycline, Trim: Trimethoprim, DMSZ: German Collection of Microorganisms and Cell Cultures. N/A not applicable.

2.1.1 BDM recipe

Two different BDM media were used; BDM and BDM+.

Table 2.2 BDM media

Compound	Concentration BDM	Concentration BDM+
H ₂ O	N/A	N/A
KH ₂ PO ₄	100mM (pH7.4)	30.4mM
K ₂ HPO ₄ * 3H ₂ O	N/A	69.6mM
NaCl	15mM	15mM
(NH ₄) ₂ SO ₄	8.5mM	8.5mM
Vitamin B12	3.7 10 ⁻⁷ mM	N/A
Hemin	0.0019mM	N/A
Protoporphyrin IX	N/A	2μM
Glucose	30mM	30mM
L-Histidine	0.2mM	0.2mM
L-Methionine	N/A	200μM
Vitamin K3 (Menadione)	N/A	6μM
MgCl ₂	0.1mM	0.1mM
CaCl ₂	50μM	50μM
FeSO ₄ * 7 H ₂ O	N/A	1.4μM
L-Cysteine * HCl	4mM	4mM

N/A not applicable

To prepare the supplement L-cysteine HCl the stock was dissolved in anaerobic water and filtrated in the anaerobic cabinet. Stock solutions of FeSO₄ 7*H₂O stock, MgCl₂ and CaCl₂ were kept in the anaerobic cabinet. To prepare BDM media, KH₂PO₄ was dissolved in water and then NaCl, (NH₄)₂SO₄, MgCl₂, CaCl₂ were added. The media was kept in the anaerobic cabinet for a minimum of 4 days after autoclaving. To prepare BDM+, first the KH₂PO₄ and K₂HPO₄ * 3H₂O were added together with NaCl and (NH₄)₂SO₄. The

pH was adjusted to 7.4 using 5M NaOH. Media was autoclaved and kept in the anaerobic cabinet for minimum of 24h. In both medias the rest of the supplements were added the day of the inoculation. Protoporphyrin IX was prepared fresh each time dissolving 2.2508mg Protoporphyrin IX in 1 mL 0.1 M NaOH and adding 1ml EtOH after.

2.2. Production of bacterial stocks

To produce long term stocks of Bt, the bacteria was grown in 20ml of BHIH or BDM with Erythromycin (5µg/ml). After 16h, bacterial culture was collected at OD₆₀₀ ~2 in a 15ml corning tube. The culture was separated by centrifugation at 12,000g for 15 minutes at 4°C and the pellet resuspended in 200µl of 40% glycerol. The culture was then added into a sterile cryotube containing beads and stored at -70°C.

To produce long term stocks of *E. coli*, the bacteria was grown in 10ml of LB with Ampicillin (10mg/ml) at 37°C shaking at 250rpm. After 16h, two aliquots of 1.5ml were harvested and separated by centrifugation at 12,000g for 15 minutes at 20°C. Pellets were resuspended in 100µl of 40% glycerol, added into a sterile cryotube containing cryopreservation beads and stored at -70°C.

To create working stocks of Bt, a single cryopreservation bead from the long-term stock was aseptically picked and added to 10ml of either BHIH or BDM media. After ~24h, the culture was distributed into 1.5ml Eppendorf and separated by centrifugation at 12,000g for 10 minutes at 20°C. The pellet was resuspended with 100µl of glycerol 40% and stored at -70°C. Working stocks were prepared from an original long-term stock to prevent possible mutations in the strains.

To prepare *E. coli* working stocks, 10 mL of LB culture was grown for 16 hours at 37°C and shaken at 250 rpm. The resulting culture was divided into 13 Eppendorf tubes, to which 270 µL of 99% glycerol was added to 730 µL of the culture. The tubes were then stored at -70°C for future use.

2.3. Cloning

2.3.1 Synthetic gene design

The DNA sequence of the antigen of interest was fused in frame N-terminally to the signal peptide of Bt OmpA (Bt_3852); MKKILMLLAFAGVASVASA. Starting and terminal codon were added together with flanking restriction sites. The codon usage was optimised for expression in Bt and the correct cleavage site of the chimeric protein was tested using SignalIP (<http://www.cbs.dtu.dk/services/SignalP/>). The Designed DNA sequence was synthesised de novo using commercial gene synthesis services (Eurofins).

2.3.2 Restriction Digests

New England Biolabs (NEB) restrictions enzymes were used with the appropriate buffers following manufacturer's instructions.

2.3.3 Plasmids used

The synthetic genes were cloned into the Eurofins pEX-K168 vector, which confers Kanamycin resistance. Shuttle expression vector pGH090(163) was used to express antigens of interest in Bt with Erythromycin resistance. Additionally, the pGH117 expression vector containing a mannan-inducible promoter region was used for the same purpose (164). For the production of recombinant proteins in E. coli, the pET15b plasmid, containing an N-terminal His-Tag sequence, was utilized.

2.3.4 Plasmid and DNA isolation and purification

The QIAprepR Spin Miniprep Kit (Qiagen) was used to isolate plasmids from bacteria. SureClean plus (Bioline) was used for nucleic-acid purification after PCR reactions or enzymatic digestions. The kits were used according to the manufacturer's instructions. Purified DNA samples were stored at -20 °C.

2.3.5 DNA ligation

Fast-Link™ DNA ligation Kit (Lucigen) was used to ligate inserts into plasmids using a molar ratio of 3:1. DNA quantification was done using NanoDrop™.

2.3.6 Transformation of competent cells

Between 1 and 5µl of ligation mixture were added to an ice-thawed vial of high efficiency transformation NEB 5-alpha competent cells (Biolab). The cells were left on ice for 30 minutes, heat-shock at 42°C for 30s and incubated on ice for an additional 5 minutes. 950µl of SOC Medium was then added and incubated at 37°C with agitation (250 rpm). After 1h, 100µl bacterial suspension was plated onto agar plates containing ampicillin and incubated for 16-18h at 37°C.

2.3.7 Screening of transformed colonies

Single colonies from the transformation agar plates were picked with a toothpick or pipette tip and put into 10µl sterile H₂O; using the same pipette tip the colony was plated onto a new agar plate. Colony PCR of each colony was done using GoTaq® Green Master Mix (Fisher scientific) following manufacturer's instructions. The list of primers used can be found below.

Table 2.3 List of DNA primers used for colony PCR and sequencing

Name	Sequence (5' to 3')	Tm (°C)
Reverse Universal	AGCGGATAACAATTTACACAGGA	57
BglII_pUK linker_3'	GGATCTTAAAGACATTACACAA	57
rH5F_Fwr_pET15b	TGACCCATGGATGGGCAGCAGCCACCATCATCATCAC CATTG	59
rH5F_Rev_pET15b	TGACGGATCCTTAAAGAAAC	59
NPcv_125med_up	GTAATCATGACTGACAACGGTCCGCAGAAC	65
NPcv_125med_rev	GTACAGGCCTAGCCTGAGTAGAGTCAGCAG	65

2.3.8 Agarose gel electrophoresis

Agarose gels were used to analyse restriction fragments, ligations, and PCR products. Gels had 1% (w/v) agarose dissolved in Tris-borate-EDTA buffer, Midori Green Xtra (Nippon Genetics) was used to stain the gel. Gel Loading Dye, Purple (6x) (New England Biolabs) and 2 Log DNA Ladder (New England Biolabs) were used as a DNA loading buffer and ladder.

2.3.9 DNA sequencing

BigDye™ Terminator v3.1 Cycle Sequencing Kit (Thermo Fisher) was used to prepare DNA for following sequencing carried out by Eurofins Genomics.

2.3.10 Triparental mating procedure

The plasmids were mobilized from *E. coli* strains to Bt through a triparental mating procedure together with helper *E. coli* J53 (pR751). All three strains were grown for 16h. *E. coli* donor strain was grown with 100µg/ml ampicillin and *E. coli* helper with 200µg/ml trimethoprim in 10ml of LB at 37°C under agitation. Bt recipient strain was grown in the anaerobic cabinet in BHIH at 37°C. 10ml of LB was inoculated with 100µl of *E. coli* donor and helper strain without antibiotics for 2h at 37°C with agitation. In parallel, 800µl of Bt culture were inoculated into 30ml of BHIH in a 50ml falcon tube for 2h in the anaerobic cabinet. Donor and helper cultures were mixed with the Bt in the falcon tube and after a brief mixing with the vortex, the cultures were separated by centrifugation at 2000g for 15 minutes at 20°C. Supernatant was removed, and pellet resuspended in 100µl of BHIH. Cells were then transferred to the surface of a sterile 0.45µm pore size filter disc (MF-Millipore) placed on a BHIH agar plate and incubated aerobically for 16h at 37°C. Filter was transferred into a sterile wide-necked universal bottle and 1ml of BHIH was added to resuspend with the help of the vortex the bacterial conjugation mixture. Serial dilutions of the cell suspension were plated onto BHIH agar plates containing gentamicin (200µg/ml) to remove *E. coli* and erythromycin (5mg/ml) to select for Bt transconjugants.

2.4. Assessing protein expression

2.4.1 Culture of Bt transconjugants

For assessing protein expression, 1 to 4 colonies were picked from agar plates with transconjugants. Colonies were re-streaked each one on separate BHIH agar plates containing gentamicin and erythromycin and incubated anaerobically for 48h at 37°C. 20ml BHIH bottles were inoculated with each colony and incubated anaerobically at 37°C. After 48h, the cell culture was separated by centrifugation in 50ml tubes at 6,000g for 15 minutes at 4°C. Supernatant was filter-sterilised with 0.22µm syringe filter to posterior

BEV isolation and cell pellet was stored at -20°C prior to analysis for a minimum of 30 minutes.

2.4.2 Preparation of cell extracts

Thawed cell pellets were resuspended in 250µl of 0.2M Tris-HCl (pH 7.2). Cells were disrupted via sonication using eight 10-second pulses (amplitude, 6µm) with 30-second pauses on ice between each pulse. After, the cells were separated by centrifugation at 14,000g for 30 minutes at 4°C and the supernatant was collected.

2.4.3 Analysis of total protein

Total protein concentration of bacterial culture or BEVs was done either using Bradford protein assay (Bio-Rad), or BCA protein assay kit for low protein concentrations (Abcam) according to manufacturer's instructions. Standard curves for both kits were done with Bovine serum albumin (BSA).

2.5. BEV isolation

2.5.1 Supernatant collection

For small-scale, bacterial cultures were separated by centrifugation in 50ml corning tubes at 12,000g for 15 minutes at 4°C. Supernatant was filter-sterilised with 0.22µm pore-size polyether sulfone (PES) membrane (Sartorius).

For medium-scale, bacterial cultures were decanted into two Nalgene PPCO Centrifuge Bottles and separated by centrifugation at 6037g for 45 minutes at 4°C. Supernatant was filter-sterilised with 0.22µm bottle top filter unit and the filtrate transferred into a sterile 500ml bottle. Samples were stored at 4°C for up to 24h if the BEVs isolation was not done immediately.

2.5.2 BEV concentration

For a small-scale bacterial cultures, the filter sterilised supernatant was concentrated by ultrafiltration using 100kDa molecular weight cut-off Vivaspin 20 (Sartorius). The retentate was rinsed once with 20ml of PBS (pH 7.4) and concentrated to a final volume of 250µl.

For medium-scale bacterial cultures, the supernatant was concentrated by ultrafiltration using 100kDa molecular weight cut-off, Hydrostat model VF05H4 molecular weight cut-off Vivaflow 50R (Sartorius). Retentate was rinsed with 500ml of PBS (pH 7.4) and concentrated to 1mL. BEV isolation was carried out at ~20°C.

In more detail, the system was set up as illustrated in Figure 2.1 Option 2 and the module was rinsed with 400ml of deionised water. The speed setting was set up at 4–5 (200–300 mL/minutes) until there was ~5ml left in the system that the speed was reduced to 1–2 (20–40 mL/minutes) to avoid foaming. Once the system had been rinsed and checked for any leaks it was set up as illustrated in Figure 2.1 Option 1 and the reservoir was filled with 500ml of filtrate. When ~5ml were left in the system 500ml of PBS was added to the reservoir. To collect the concentrated sample, the system was set up as illustrated in Figure 2.1 Option 3 and the sample was collected in either a 15ml tube or Eppendorf. Additionally, 0.5-1ml of PBS was added to help flush remaining BEVs. Collected BEVs suspensions were then filter sterilised with 0.22µm PES syringe filters and stored at 4°C.

For decontamination and washing, the system was set up as illustrated in Figure 2.1 Option 2 and 400ml of deionised water was added. When water was filtrated, the system was set up as Option 1 and 25ml of decontamination solution (250ml 0.5M NaOH) was added, followed by another 400ml of deionised water and 250ml of 10% EtOH. The system module was dismantled, and the cassette membrane stored with 10% EtOH inside to avoid any contamination at 4°C.

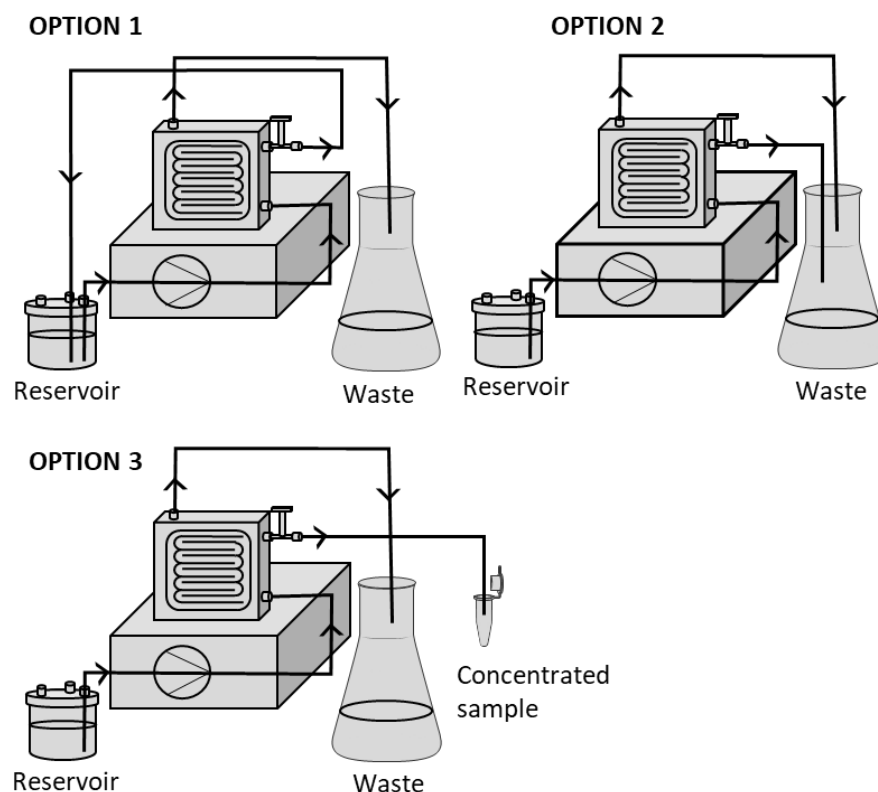


Figure 2.1 Isolation module system. Option 1. Sample concentration. Option 2. Module rinsing/decontamination. Option 3. Collection of concentrated samples. Image also published in Stentz et al. 2021 (1).

2.5.3 BEVs purification

Contaminants such as proteins or protoporphyrin IX of BEVs were removed by size exclusion chromatography (SEC) using qEVoriginal or qEVsingle 35nm (Izon Science) columns according to manufacturer's instructions. Briefly, the column, PBS and BEVs preparations were brought to 20°C. The column was secured into the automatic fraction collector, 1.5X column volume of PBS was added followed by 0.5ml of BEVs suspension, after 2.75ml of void volume was discarded, 10 fractions of 0.5ml were collected into 1.5ml Eppendorf. For cleaning and storing, the columns were flushed with 1.5X column volume of PBS and stored with 20% Ethanol at 4°C.

2.5.4 Size and concentration BEV analysis

Size and concentration of isolated BEVs was determined by nanoparticle tracking analysis (NTA), a method to measure particles in suspension based on the analysis of Brownian motion using ZetaView PMX-220 TWIN instrument from Particle Metrix GmbH.

The instrument was set up according to the manufacturer's instructions and 100nm polystyrene standard bead suspension was used to perform the focus auto-alignment. Size distribution video was acquired using the following settings: temperature: 25°C; frames: 60; duration: 2 seconds; cycles: 2; positions: 11; camera sensitivity: 80 and shutter value: 100. Data was analysed using ZetaView NTA software (version 8.05.12) with the following post acquisition settings: minimum brightness: 20; maximum area: 2000; minimum area: 5 and trace length: 30. Samples were diluted with H₂O at an optimal concentration for the instrument to operate.

The size distribution obtained from ZetaView is not the core diameter of the particle but the hydrodynamic particle size. This is calculated from the behaviour of the particle to diffuse in a liquid and the result includes the diameter of the particle together with the hydration layer surrounding it.

2.6. SDS-PAGE and immunoblot

Samples were prepared using NuPAGE Sample Reducing Agent 10X (ThermoFisher) and NuPAGE LDS sample buffer (4X) and denatured by boiling the sample on a heating block for 10 minutes at 90°C. Pre-stained PageRuler Prestained Protein Ladder and samples were loaded onto 12% precast NuPAGE Bis-Tris pre-cast gels and separated by electrophoresis at 200 volts for 40 minutes using NuPAGE MES SDS Running Buffer and NuPAGE Antioxidant.

For protein visualisation gels were stained with InstantBlue® Coomassie Protein Stain (Abcam) and gels imaged using BioRad ChemDoc XRS+.

For immunoblotting, proteins were transferred onto a 0.45µm pore size polyvinylidene difluoride (PVDF) membrane (Invitrogen) at 30volts for 1h in a solution containing NuPAGE transfer buffer with 10% methanol and NuPAGE Antioxidant. Membranes were subsequently blocked with 10% BSA or 5% Non-fat Dry Milk (NFDM) in TBS-Tween (TBS [50mM Tris-HCl; 150 mM NaCl; pH 7.5] with 0.05% Tween) by shaking for 30 minutes at 20°C. Blocking solution was then discarded, and membrane incubated for 16–18h at 4°C in TBS-Tween with 5% BSA or 1.5% NFDM containing primary antibody. After washing 3 times with TBS-Tween, membranes were incubated in 5% BSA or 1.5% NFDM in TBS-Tween containing HRP-conjugated secondary antibody for 1h at 20°C. After

3 washes with TBS-Tween, Clarity Western ECL Substrate (Bio-Rad) was used to develop the blot.

2.7. Dot blot

Serial twofold dilution of vesicles in a final volume of 10 μ l were spotted into nitrocellulose membranes and air-dried. The membranes were processed as described for immunoblotting (above). First, membranes were blocked for 30 minutes at 20°C with 5% NFD in TBS-Tween. Then, membranes were incubated with primary antibody for 16–18h at 4°C in TBS-Tween with 1.5% NFD. After washing the membrane 3 times with TBS-Tween, membranes were incubated with HRP-conjugated secondary antibody for 1h at 20°C in TBS-Tween with 1.5% NFD. After 3 more washes, SuperSignal West Pico chemiluminescent Substrate (Thermo Fisher) was used to detect bound antibody.

2.8. Antigen quantification

Quantity tool of Image Lab Software (Bio-Rad) was used to determine the amount of antigen expressed in BEVs. For this, an immunoblot with serial dilutions of known concentration of recombinant proteins was used to compare the bands intensity.

2.9. Proteinase K accessibility/protection assay

Proteinase K accessibility/protection assay was done to establish if heterologous proteins were expressed in the lumen or at the surface of BEVs. Proteinase K digests proteins exposed in the surface of the BEVs but not in the lumen. SDS-treated vesicles were used as a control as SDS breaks the BEVs and makes the luminal content accessible to proteinase K.

A suspension of 10¹¹ BEVs/mL or solubilised (in 1% SDS) BEVs were incubated for 1h at 37°C in the presence of 100mg/L proteinase K (Sigma-Aldrich). After proteinase K was deactivated with 1mM phenylmethanesulfonyl fluoride (PMSF; Sigma-Aldrich) samples were analysed by immunoblotting as described above.

2.10. NiNTA protein purification

E coli strains were grown in 10ml of LB for 16h at 36°C with agitation at 250rpm. In a 1l flask 200ml of LB was inoculated with the preculture at a starting OD₆₀₀ 0.1 with 100µg/ml ampicillin. The culture was induced with 1Mm IPTG at OD₆₀₀ 0.5 and cells were harvested after 5h at 37°C or 16h at 20°C. Cells were separated by centrifugation at 6000rpm for 30 minutes at 4°C, and pellet kept at -20°C for at least 30 minutes. Thawed pellets were resuspended in 10ml of native lysis buffer (50mM NaH₂PO₄; 300mM NaCl; 10mM imidazole; pH 8) or denature lysis buffer (7M urea; 0.1M NaH₂PO₄; 0.01M Tris-Cl; pH 8) with 10mg of lysozyme and 1µl of Benzonase for 30 minutes on ice. Cells were sonicated using eight 10-second pulses (amplitude, 6µm) with 30-second pauses on ice between each pulse and separated by centrifugation at 14,000g 30 minutes at 4°C. In the meantime, Ni-NTA Superflow column (Qiagen) was rinsed with 10ml H₂O, and 1ml of Ni-NTA resin was added and allowed to settle. Next, supernatant was added to the column, followed by two washes of 4ml native wash buffer (50mM NaH₂PO₄; 300mM NaCl; 20mM imidazole; pH 8) or denature wash buffer (8M urea; 0.1M NaH₂PO₄; 0.01M Tris-Cl; pH 6.3). The protein of interest was eluted into a new tube with the addition of twice 1ml of native elution buffer (50mM NaH₂PO₄; 300mM NaCl; 250mM imidazole, pH 8) or denature elution buffer (8M urea; 0.1M NaH₂PO₄; 0.01M Tris-Cl; pH 4.5).

2.11. Animal models

2.11.1 Mice

C57BL/6 or C57BL/6-K18-hACE2 transgenic male mice of 6-8 weeks of age were maintained in the Disease Modelling Unit (DMU) at the University of East Anglia or the University of Liverpool. Mice were housed in individually ventilated cages and exposed to 12h light/dark cycle with free access to drinking water and standard chow diet. Animal experiments were conducted in full accordance with the Animal Scientific Procedures Act 1986 under UK Home Office (HMO) approval and HMO project license 70/8232 (UEA) and 70/8599 (University of Liverpool).

2.11.2 Macaques, Ethics statement

Cynomolgus macaques (*Macaca fascicularis*) were housed and managed by PHE (UKHSA), Porton. Animals were housed in compatible social groups, in accordance with the Home Office (UK) Code of Practice for the Housing and Care of Animals Bred, Supplied or Used for Scientific Purposes, December 2014, and the National Committee for Refinement, Reduction and Replacement (NC3Rs), Guidelines on Primate Accommodation, Care and Use, August 2006. All animals were aged between 3 and 5 years and none of the animals had been used previously for experimental procedures, were free of herpes B-virus, tuberculosis (TB), simian immunodeficiency virus (SIV) and simian T-cell leukaemia virus (STLV) and were inspected by the named veterinary surgeon prior to entry into the study. All animal procedures and study design were approved by the Public Health England, Porton Down Animal Welfare and Ethical Review Committee, and authorized under an appropriate UK Home Office project licence (30/2993 and P76404B45) (2).

2.12. Immunisation

Macaques or mice received a primary immunisation of filtered sterilised BEVs via intraperitoneal, intranasal, or oral route with or without a booster immunisation 4-10 days later. Some experiments followed with infectious challenge after further 7-10 days. At necropsy body fluids and tissues were harvested for downstream analysis.

2.13. Saliva and BAL extraction

Saliva was taken from sedated NHP by gentle insertion of a 1ml syringe (without needle) into the oral cavity. At necropsy the lungs were removed to leave the full length of the trachea intact (from larynx down) and to avoid any blood contamination. The BAL was performed using a 3mm flexible catheter to infuse PBS in two aliquot volumes of 10ml. The diluent was collected by inversion of the lung set and gentle massage to encourage removal of fluid into a receiving vessel.

BAL obtained from scarified mice was isolated by opening the ribcage to near the clavicle, isolated the trachea using forceps, clamping it, and inserting a needle with sterile 0.8ml PBS to inflate and withdraw BAL from the lungs.

2.14. ELISA

96 well Nunc MaxiSorp plates (Thermo Fisher) were coated with 50µl of target antigens in 0.1M NaHCO₃ and incubated for 16h at 4°C. Recombinant proteins used for coating the plate were *Y. pestis* V and F protein provided by DSTL and used at 15µg/ml; IAV H5 HA (P5060, 2B Scientific Ltd) used at 10µg/ml, IAV NP from Sino Biological used at 1µg/ml, S and NC provided by University of Kent used at 10µg/ml. After washing three times with 100µl of ELISA Wash buffer (PBS supplemented with 0.05% Tween 20 (PBST)), plates were blocked with 100µl of ELISA blocking buffer (PBST with 2% BSA) at 20°C with gentle agitation. After 3h, buffer was flicked out and diluted samples with PBST 2% BSA were added to the plate wells and incubated for 16h at 4°C. Serum samples were diluted 1:10 prior to serial 1:4 dilutions and saliva, salivary glands, bronchoalveolar lavage and nasal wash samples were added in the plate in 1:2 serial dilutions. Plates were then washed six times with PBST and incubated with blocking buffer containing secondary HRP-antibody for 1h at 20°C with gentle agitation. Plates were washed six times with PBST and then incubated in darkness with 100µl TMB high Sensitivity substrate solution (BioLegend) for 15 minutes at 20°C. The reaction was stopped by adding 50µl of 2N H₂SO₄ and the optical density was measured at 450nm using a TECAN infinite f50 spectrophotometer (Männedorf, Switzerland).

For quantification of absolute amounts of IgG and IgA a modified ELISA incorporating a range of concentration of purified monkey IgG (Bio Rad) and IgA (Life Diagnostics, Inc., West Chester, PA, USA) were used to generate standard curves from which IgG and IgA concentrations of individual animals were determined.

TNF-α and IFN-γ secretion from splenocytes was measured using the Invitrogen TNF-α or IFN-γ mouse ELISAs (Thermo Fisher) according to manufacturer's protocols.

2.15. Antibodies used

All antibodies used are listed in Tables 2.4 and 2.5.

Table 2.4 List of primary antibodies used

Antigen detected	Clone	Assay	Origin	Supplier	Dilution used
V protein of <i>Yersinia pestis</i>	Polyclonal	WB, ELISA	Rabbit	DSTL	1:1000
F protein of <i>Yersinia pestis</i>	Polyclonal	Dot blot, ELISA	Rabbit	DSTL	1:1000
Influenza Nucleoprotein	Monoclonal	WB, ELISA	Mouse	Abcam	(1:300 – 1:1000)
SARS-CoV-2 Spike S1	Monoclonal	WB, ELISA	Human	Abcam	1:1000
SARS-CoV-2 Nucleocapsid	Polyclonal	WB, ELISA	Rabbit	Thermo fisher	1:2000
Hexa-His tag	Monoclonal	WB	Mouse	Sigma-Aldrich	1:3000
Multiple	Polyclonal	ELISA	Monkey IgA	Bio Rad	1:200 - 1:20000
Multiple	Polyclonal	ELISA	Monkey IgG	Life Diagnostics	1:200 - 1:20000

Table 2.5 Secondary antibodies used linked to HRP

Antigen detected	Assay	Origin	Supplier	Dilution used
Anti-rabbit IgG	WB, ELISA	Goat	Thermo fisher	1:3000
Anti-macaque IgG	ELISA	Goat	Sigma	1:10000
Anti-macaque IgA	ELISA	Goat	Sigma	1:10000
Anti-mouse IgG	WB, ELISA	Goat	Abcam	1:10000
Anti-mouse IgG	WB, ELISA	Goat	Thermo fisher	1:2000
Anti-mouse IgA	ELISA	Goat	Thermo fisher	1:2000
Anti-Human IgG H&L	WB, ELISA	Goat	Abcam	ELISA 1:1000 WB 1:100

2.16. Recombinant proteins used

All recombinant proteins used are listed in Table 2.6.

Table 2.6 Recombinant proteins used

Protein	Strain	Supplier
V	<i>Y. pestis</i> CO92	DSTL
F1	<i>Y. pestis</i> CO92	DSTL
HA	A/Hong Kong/483/1997 (H5N1)	2B Scientific Ltd
NP	A/Puerto Rico/8/34/Mount Sinai (H1N1)	Sino Biological
S	B.1 SARS-CoV-2	University of Kent
B12.S	B.1 SARS-CoV-2	University of Kent
NC	B.1 SARS-CoV-2	University of Kent

2.17. T cells analysis

2.17.1 Splenocytes isolation and culture

Mice spleens were removed and collected into a falcon containing ice cold PBS. With the help of a 5ml syringe plunger, spleens capsules were disrupted by pressing the tissue through 100µm cell strainer (Fisher scientific). 10ml of PBS was used to wash the cells into a 50ml falcon tube and were kept on ice prior to further processing. Cells were pelleted after 5 minutes at 13,000rpm centrifugation at 15°C. Supernatant was discarded and cells resuspended in 3ml ACK lysis buffer (Gibco). Cells Medium was prepared adding 100U/ml of Penicillin-Streptomycin (Gibco) into TexMACS Medium (MACS Media). After 5 minutes at 20°C 5ml of Cells Medium was added to inactivate the lysis buffer. After another centrifugation 13,00rpm for 5 minutes 15°C. cells were resuspended in 2ml Cells Medium and counted by Countess Automated cell counting (Invitrogen). 10^6 cells were aliquoted in 100µl of TexMACS Medium into individual wells of Corning U-bottom 96-well polystyrene plate. Plates were incubated at 37°C with 5% CO₂ for 30 minutes. Later, 80µl of peptides or BEVs were added to a final concentration of 5µg/ml in a final volume of 200µl, or 300 BEVs/cell plated. TexMACS™ Medium alone was used as a negative control

and 1X Cell Activation Cocktail (CAC) containing PMA + ionomycin (Biolegend) as a positive control. 10µl of IL-2 was also added for a final concentration of 0.05µg/ml. Plates were then incubated for 1h at 37°C with 5% CO₂. 10µl of 20X Protein inhibitor Brefeldin A (BFA) solution (Biolegend) was then added to all wells to block the cytokine transport through the secretory pathway. Plates were incubated for another 5h.

2.17.2 Flow cytometry

Cells were washed with 100µl PBS and separated by centrifugation at 350g for 5 minutes. All wash steps were carried out at the same speed and duration. The buffer was decanted from the plates and 100µl of Zombie NIR at dilution 1:500 was added. Cells were incubated at 20°C, in the dark for 30 minutes. Cells were washed with 200µl of Cell Staining Buffer (PBS+ 4% Fetal calf serum (FCS) (Gibco)). Dilutions of antibodies used to detect extracellular markers (Table 2.7) were prepared in advance, fluorescence minus one (FMO) control, isotype controls, full cocktail and singles for compensation as listed in table 2.7. 100µl of the previously prepared antibodies were added to each well and incubated on ice for 30 minutes in the dark. Cells were washed with 200µl of Cell Staining Buffer (Biolegend). For cell fixation and membrane permeabilization 100µl of Cyto-Fast Fix/Perm Buffer (Biolegend) was added to each well, mixed and incubated for 30 minutes at 20°C. After a cell wash with 100µl of Cell Staining Buffer, cells were resuspended and washed with 100µl of 1X Cyto-Fast Perm Wash (Biolegend) solution priorly diluted with deionized water. Cells were resuspended in residual volume after plates were flicked out and volume adjusted to 50µl with 1x Cyto-Fast Perm Wash solution. Moreover, 2.5µl of normal mouse/rat serum was added to each well for blocking unspecific binding and incubated at 20°C for 15 minutes. Without washing, 50µl of previously prepared intracellular antibodies diluted in 1x Cyto-Fast Perm wash solution were added and incubated for 10h in the dark at 4°C. Cells were washed first with 100µl 1x Cyto-Fast Perm Wash solution and secondly with 200µl of Cell Staining Buffer. Samples were acquired on BD LSRFortessa Flow cytometer.

Spectral overlap between channels was automatically compensated in FlowJo software Version 10, after measurement of single-stained compensation controls prepared using either a mix of splenocytes for extracellular markers or using AbC™ Total Antibody Compensation Bead Kit (Thermofisher) for intracellular markers. The gating strategy used to visualise and enumerate TNF-α and/or IFN-γ producing CD8+ and CD4+ T cells is shown in Figure 2.2 using FlowJo software Version 10.8.

Table 2.7 List of antibodies used for Flow cytometry

Antigen detected	Clone	Conjugated	Amount used $\mu\text{g/ml}$	Isotype	Supplier
CD45	30-F11	PerCP-Cy5	0.4	Rat IgG2b, κ	Biolegend
CD3 ϵ	145-2C11	APC	2	Armenian Hamster IgG	Biolegend
CD4	GK1.5	Alexa 488	0.6	Rat IgG2b, κ	Biolegend
CD8	53-6.7	BV605	1	Rat IgG2a, κ	Biolegend
IFN - γ	XMG1.2	PE-Cy7	2	Rat IgG1, κ	Biolegend
TNF - α	MP6-XT22	PE	0.4	Rat IgG1, κ	Biolegend
Rat IgG2b κ	RTK4530	Alexa 488	0.6	Rat IgG2b, κ	Biolegend
Isotype Ctrl					
Rat IgG1, κ	G0114F7	PE-Cy7	2	Rat IgG1, κ	Biolegend
Isotype Ctrl					

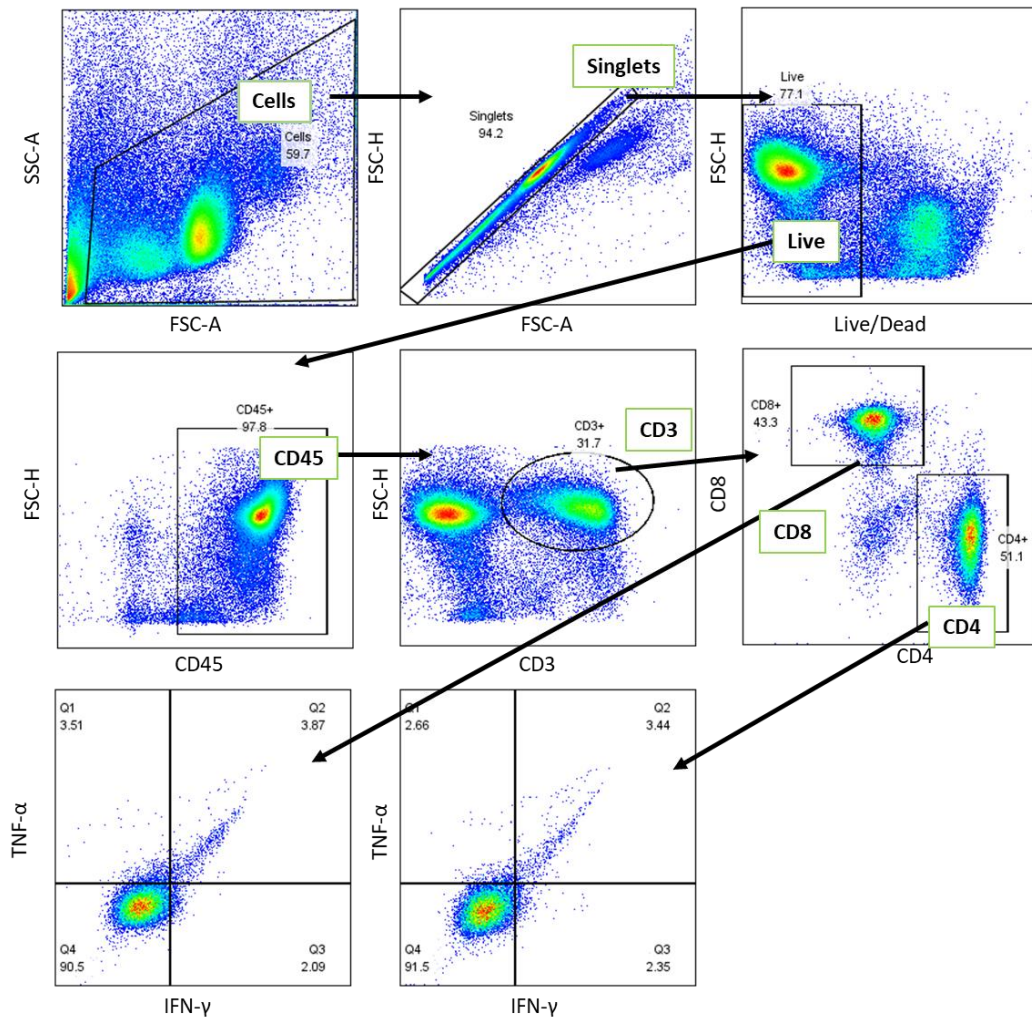


Figure 2.2 Example of gating strategy used to analyse cytokine production on CD4+ and CD8+ T cells in splenocytes. After debris and doublets exclusion live cells were selected and subsequently gated as CD45+ and CD3+. CD8+ and CD4+ cells were further selected and plotted against TNF- α IFN- γ .

2.18. DNA extraction from stool samples and nasal swabs

Stool samples were collected using the OMNIgene–GUT microbial collection and stabilisation kit (DNAgenotek # OMR–200). Samples were stored and shipped from PHE to QIB at ambient temperature. 250 μ l of sample was transferred using a tip with the end cut to the bead tube of QIAamp PowerFecal DNA Isolation Kit (Qiagen) and extraction followed the manufacturer instructions.

Nasal swabs. Two FLOQSwabs[®] 516C (Copan) were used and tips snapped off and dropped into OMNIgene-GUT tubes (from which the ball–bearing was previously removed). Samples were stored and shipped from PHE to QI at room temperature. Swabs

were added to a Lysing Matrix E, 2ml tube (MP Biomedicals) containing 1.4mm ceramic spheres, 0.1 mm silica spheres, and one 4mm glass bead. And extraction was done using QIAamp PowerFecal DNA Isolation Kit (Qiagen) following manufacturer instructions with using the bead beater, two times for 40 seconds at speed 6, instead of 10 minutes Vortex horizontally.

Taxonomic profiles were analysed by 16S rRNA amplicon sequencing of V4-V5 regions using U515F (5'-GTGYCAGCMGCCGCGGTA) and U927R (5'-CCCGYCAATTCMTTTRAGT) primers were analysed by Animal and Plant Health Agency Scientific (APHA) based on Illumina MiSeq using v3 Chemistry obtaining >100k reads per sample. Analysis of data and bubble chart was created with MEGAN Community Edition by Dr Andrea Telatin (QIB).

2.19. Storage of BEVs

After isolation BEVs were stored at 4°C for no longer than 1 month. For *in vivo* studies BEVs were used within 7 days of isolation.

For stability experiments (Chapter 6), BEVs samples were stored in 10mM Histidine + 3% sucrose or 10mM Tris-HCl + 3% sucrose buffer. Aliquots of 250µl of each sample were kept in LoBind tubes (Fisher Scientific). For lyophilisation, samples were snap frozen with dry ice and then dried for 16h using ModulyoD Freeze Dryer.

2.20. TEM imaging

BEV samples were visualized using negative staining with TEM performed by Dr Catherine Booth (QIB). Briefly, carbon coated 400Cu TEM grid (EM Solutions) were glow-discharged and 10µl OMV suspension applied for 1 minute. The sample was removed by wicking the edge of the grid with Whatman filter paper and this was followed directly by a 1 minute incubation with 2% Uranyl Acetate solution (BDH 10288). UA was removed by wicking and grids were air-dried before analysis using a FEI Talos F200C electron microscope with a Gatan Oneview digital camera.

2.21. Statistical analysis

Statistical comparisons were made using one-way analysis of variance (ANOVA) using either Dunnett's or Bonferroni for multiple comparison test or two-way ANOVA with Bonferroni post-test for grouped analysis. The statistical methods Bonferroni and Dunnett's were chosen specifically to analyse groups that have unequal variances and to handle experiments with a low number of samples. All statistical analysis was conducted on GraphPad Prism 5.04. P values of less than 0.05 were considered significant. *P < 0.05, **P < 0.01, ***P < 0.001, ****P < 0.0001.

Chapter 3 Use of Bioengineered Bt BEVs as a plague vaccine

3.1 Introduction

Yersinia pestis is the causative of plague disease and has been responsible for devastating pandemics, including the Black Death during the fourteenth century, which caused over 50 million deaths in Europe (166). This zoonotic disease continues to cause outbreaks in various parts of the world; with the Democratic Republic of Congo, Peru and Madagascar being the three most endemic countries (166). The last outbreak reported was in 2017 in Madagascar, with 2417 confirmed cases and 209 deaths (167).

Plague can manifest in three different ways: bubonic, septicaemic, and pneumonic. Bubonic plague is the most common and is transmitted from rodent reservoirs to humans by the bite of an infected flea (166, 168). After transmission, *Y. pestis* disseminates to the nearest lymph node where it proliferates and causes flu-like symptoms. Untreated infected lymph nodes can become necrotic and cause haemorrhages leading to death in approximately 50-60% of cases (166, 168). Survival rates increase significantly if treatment is initiated within 24 hours of first symptoms appearing. Septicaemic plague is caused by flea bites, direct contact with infected materials or in the advanced stages of bubonic plague. In septicaemic plague, *Y. pestis* enters the bloodstream and multiplies, releasing endotoxins that induce intravascular coagulation that can lead to gangrene of extremities. Untreated infections are usually fatal, yet treatments can increase patient survival (166, 168). Pneumonic plague arises when *Y. pestis* infects the lungs through the transmission of contaminated airborne droplets and is usually fatal (168).

Today, most registered cases are bubonic and with rapid diagnostic and antibiotic treatment, most infected people survive. Pest control and good sanitation are also key in helping prevent plague pandemics (169). Still, with the rise of multi-drug resistant strains, treatment has become more complicated (170, 171). Furthermore, due to the nature of

Y. pestis, this pathogen could be used as a biological weapon if distributed in aerosol and cause a pneumonic epidemic. Hence *Y. pestis* is described to have high risk to the public and national security (172).

Overall, due to the rapid course of the disease, high mortality, and the potential application as a bioweapon, effective plague vaccines are needed.

Since the mid-1930s, a live attenuated vaccine against *Y. pestis* (EV76) has been used in Russia, Mongolia, and China. The vaccine can be administered in three different ways: percutaneously (skin scarification), intradermally or via aerosol (173, 174). However, the vaccine is associated with several adverse effects, short duration of immunity and concerns about risk of reversion to fully virulence. Therefore, the vaccine is only recommended in endemic areas, and it is not licensed in other countries (175-177).

Another vaccine derived from a highly virulent formalin-killed *Y. pestis* strain named USP was used for American military personnel during the Vietnam war. The vaccine helped ameliorate bubonic disease but was ineffective against pneumonic plague (178, 179). The vaccine was discontinued due to questionable efficacy and reactogenicity and failed to provide long-term protection against bubonic plague (176, 177).

Subunit vaccines are safer and recent efforts have focused on developing new vaccines using mainly two antigens, the capsular antigen fraction 1 (F1) and the low calcium response protein (V) (180, 181). Other antigens less frequently used are YscF antigen and pesticin coagulase (182). F1 is encoded by the *caf1* operon comprising transcriptional factor regulator Caf1R, chaperone Caf1M and outer membrane protein Caf1A (183, 184). F1 forms fibres of a single subunit that creates a capsule-like envelope and has significant antiphagocytic activity (185). Although F1 is immunogenic, natural occurring strains without F1 proteins are still virulent (186). V is a structural component of the type three secretion system (T3SS) that is used to bind *Y. pestis* with a host cell to inject toxins and other proteins into host cells (Fig. 3.1).

F1 and V, have been used in vaccines as a mixed cocktail or fusion formats showing protection against bubonic and pneumonic plague in different animal models (187-191). Furthermore, two different subunit vaccines using F1 and V are currently in clinical trials (192, 193). However, these vaccines have some limitations, for example: they need adjuvants to increase their immunogenicity, require several doses to confer protective immunity or they induce weak or no protection at mucosal sites (187-191, 194). As pneumonic plague is the most serious form of disease and can be spread from person

to person, according to the WHO target product profile (TPP) for plague vaccines (169), pneumonic plague vaccines should be delivered either orally (OG) or intranasally (IN) to induce mucosal immune response at the entry site of *Y. pestis*.

The aims of this chapter are to:

- Engineer commensal Bt to express conformationally correct *Y. pestis* antigens F1 and V
- Assess the capacity of BEVs containing F1 and V antigens to activate systemic and mucosal immune response in mucosal vaccinated macaques.
- Determine the optimal dose and immunisation route for the BEV vaccine, orally or intranasally.

The goal is to determine the safety and suitability of F1-BEV and V-BEV vaccines as a plague vaccine.

To do this, Bt was engineered to produce either the V or the F1 antigen from *Y. pestis*. The BEVs containing the antigen were isolated and characterised followed by intranasal or oral immunisation to macaques (non-human primates (NHP)). Samples were collected and analysed to quantify antibody levels by ELISAs, cytokine levels by flow cytometry, histology, microbiome relative abundance and bactericidal assay (Fig. 3.1).

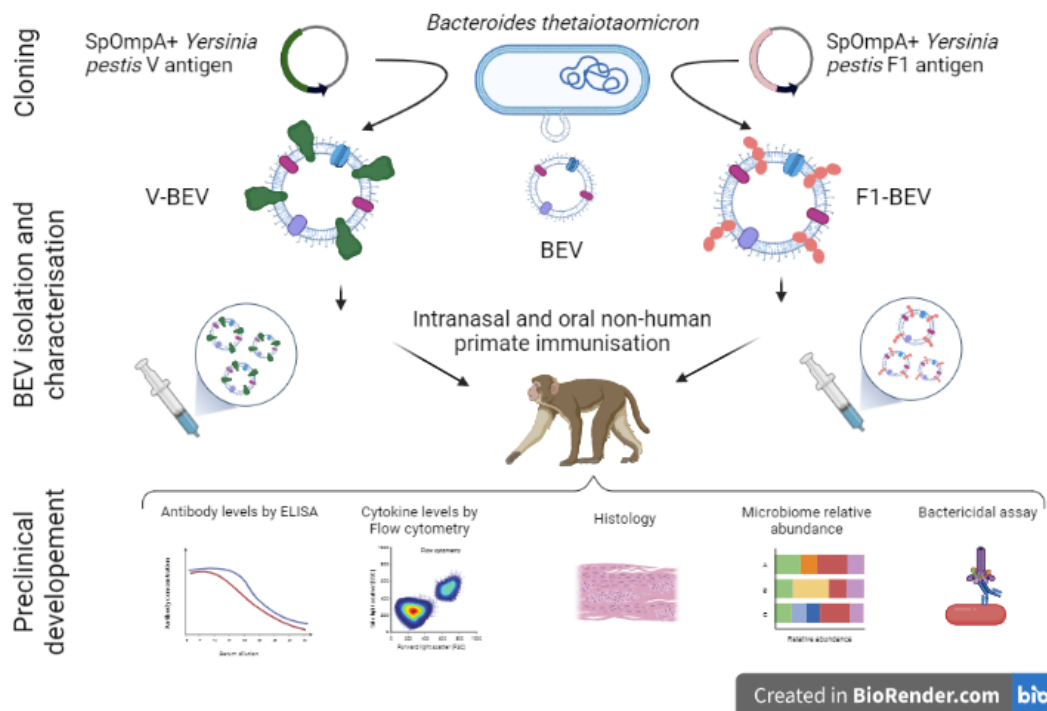


Figure 3.1 Overview of bioengineered Bt BEVs as plague vaccine study design. Created in BioRender.com

3.2 Results

3.2.1 Construction of *Y. pestis* F1 and V antigen expression vectors

To express F1 protein Drs Udo Wegmann and Regis Stentz designed a synthetic construct consisting of caf1M followed by caf1A and caf1 with the OmpA signal peptide (SPompA) fused to the N-terminal. For the V antigen, the 986 base pairs that encode for V were also fused to the SPompA N-terminal. BspHI and EcoRI restriction enzyme sites were added to both gene sequences at their 5' and 3' ends and synthesised *de novo*. The resulting gene cassettes for F1 and V were cloned into *Escherichia coli* plasmids pEX-K4 and pEX-A2 (Eurofins, Hamburg, Germany), respectively. The genes encoding F1 or V were excised from the pEX-K4 and pEX-A2 using BspHI and EcoRI and ligated into the NcoI/EcoRI-restricted pGH090 expression vector (163), resulting in pGH180 and pGH179, respectively. Sequences integrities of the cloned fragments were verified through sequencing.

3.2.2 Expression of *Y. pestis* vaccine antigens in Bt BEVs

Genes encoding the F1 and V were cloned and expressed in Bt BEVs. Approximately 8µg of V-BEV and WT-BEV produced in BDM media together with 20ng of recombinant V (rV) were loaded on to SDS gels and immunoblotted with rabbit polyclonal antibody anti-V to confirm expression of V antigen in V-BEVs. Based on the intensity of the antibody-reactive bands, there were 15µg of V protein in 600ug V-BEVs total protein (Fig. 3.2.a). The appearance of higher bands in Fig. 3.2.a could be due to non-specific binding resulting from the use of high quantity of antibody, or potentially to poor quality of the antibody.

Luminal versus outer membrane distribution of V in V-BEVs was established using a proteinase K protection assay. Proteinase K or PBS was added to V-BEVs and rV and analysed by immunoblotting. rV protein was degraded when proteinase K was added but V protein in V-BEVs was not. As proteinase K cannot degrade luminal proteins, it was assumed that V protein in V-BEVs was expressed within the lumen of V-BEVs (Fig. 3.2.b).

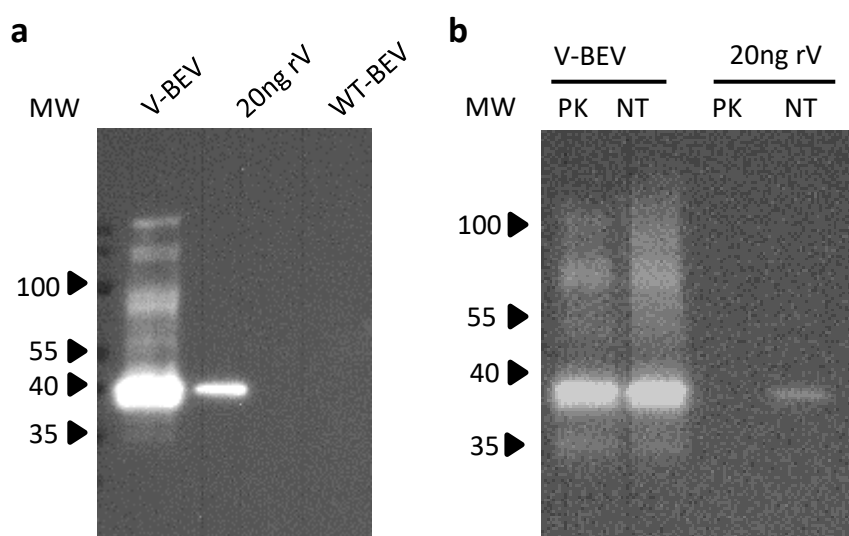


Figure 3.2 Detection of V in V-BEVs by immunoblotting . WT-Bt and V-Bt strains were grown in BDM media and BEVs isolated following a method described at materials and methods chapter. (a) Immunoblot of V-BEVs using recombinant V (rV) and wild-type BEV (WT-BEV) as controls. (b) Localization of V in V-BEVs after treatment with proteinase K (PK) or not treated (NT). Molecular weight (MW) expressed in kDa.

Expression of F1 protein in F1-BEV could not be confirmed by immunoblotting and instead relied on proteomics analysis of F1-BEVs carried out by the Proteomics Facility at the University of Bristol using liquid chromatography-mass spectrometry (LC-MS) (Table

3.1). Other proteins found in abundance in the samples were uncharacterised proteins, outer membrane proteins, and OmpA. Additionally, periplasmic proteins were identified such as a peptidoglycan hydrolase and a lipocalin-like domain-containing protein. Peptidoglycan hydrolases are enzymes responsible for cleaving the bonds in peptidoglycan chain (195), while bacterial lipocalin proteins work mainly as transport and carrier of proteins (196).

An immuno-dot-blot assay also confirmed F1 protein expression in F1-BEV (Fig 3.3). Approximately 6µg of F1-BEV and WT-BEVs in their natural, intact, state and 120ng of recombinant F1 (rF1) were serially diluted (1:2) and spotted into nitrocellulose membranes. Since F1-BEV samples showed a more intense signal than WT-BEV dots, it was assumed that F1 protein was expressed in F1-BEVs and that it was expressed on the surface of BEVs. Based on the intensity of the dots, it was calculated that there were 10µg of F1 in ~600µg total protein of F1-BEVs (Fig. 3.3).

Table 3.1 Detection of F1 in F1-BEV by proteomics

Name	Media	Coverage	Relative abundance
F1	BDM	55.7%	131/1228

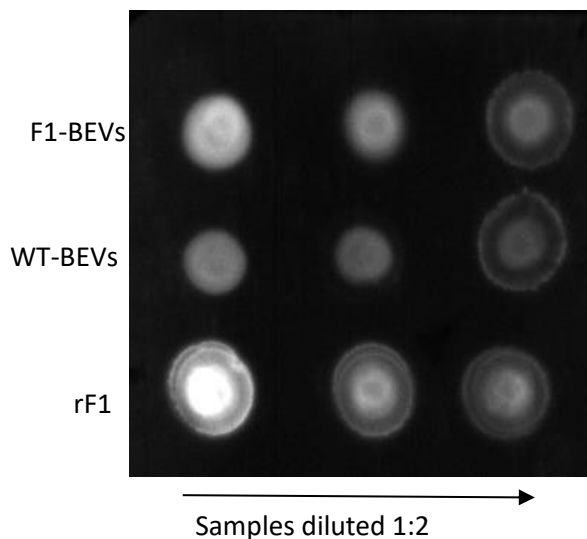


Figure 3.3 Detection of F1 in F1-BEVs by immuno-dot-blot. Bt strains were grown in BDM media and BEVs isolated following a method described at materials and methods chapter. Samples of intact F1-BEVs, wild-type BEVs (WT-BEVs) or recombinant F1 (rF1) were serially diluted 1:2, added

to the nitrocellulose membrane, and analysed using anti-rabbit IgG to detect the binding of rabbit anti-F1 IgG.

BEVs were analysed by ZetaView producing hydrodynamic particle size distribution curves. The size of BEVs ranged from 50-200nm, with an average hydrodynamic peak size \pm SD of 112.7nm \pm 3.4 for WT-BEVs, 118nm \pm 9.5 for F1-BEVs and 115.9nm \pm 6.4 for V-BEVs (Fig. 3.4).

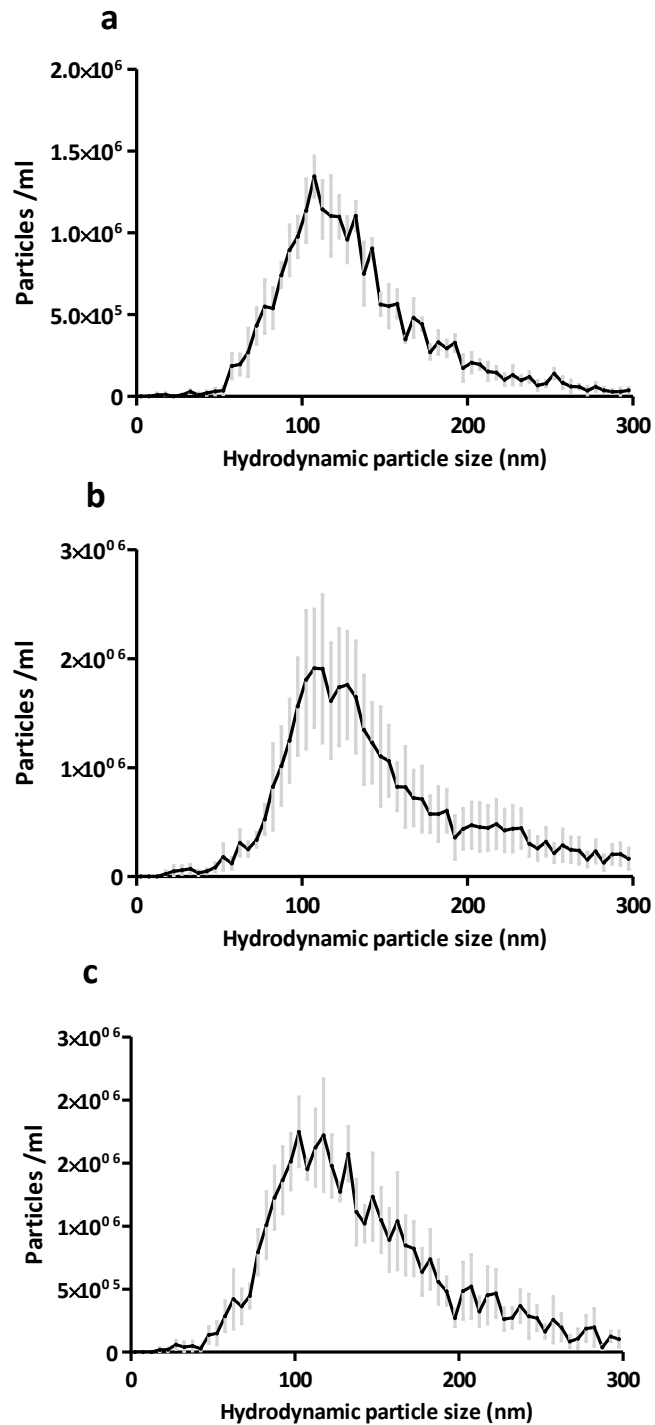


Figure 3.4 Quantification of hydrodynamic particle size of WT-BEVs, F1-BEVs and V-BEVs by NTA. WT-Bt, F1-Bt and V-Bt were grown in BDM media, BEVs isolated and (a) WT-BEVs, (b) F1-BEVs and (c) V-BEVs analysed using Zetaview PMX-220 TWIN instrument (Particle Metrix GmbH). Data is represented by the mean value for each value \pm standard deviation from 3 different isolations.

3.2.3 BEV immunisation

Cynomolgus macaques (*Macaca fascicularis*) were used as an animal model for these experiments to better understand Bt BEV efficacy and safety in humans. The NHP were housed and used at Public Health England (now UK Health Security Agency), UK.

To evaluate the immune response to the recombinant antigens and refine the experimental protocols, two NHP received 50µg of rF1 with 20% (v/v) alum adjuvant, while two others received 50µg of rV with 20% (v/v) alum adjuvant. All animals were given a booster shot 28 days after the initial injection to enhance their immune response. Serum was collected on day 42 and analysed by ELISA. Stool, rectal and nasal swabs were also taken to optimise DNA extraction protocol.

The aim of the following experiments was to evaluate the safety and effectiveness of the BEV vaccines in inducing an immune response through oral gavage or intranasal administration (Fig. 3.5). These experiments were conducted on four NHP that had not been used in previous studies. To identify the optimal vaccination route, both local and systemic F1 and V-specific IgG and IgA antibodies were measured. A dose of 50µg of F1 or V antigen was used orally gavage, as similar doses have been previously used and are equivalent to the dose used in humans (197-199). The same dose was used for intranasal administration in addition to 12.5µg and 25µg to determine the lowest dose required to induce an immune response. The vaccines formulations consisted of BEV isolated from BDM media and rinsed with PBS. A concentrated bulk batch was produced for each immunisation and vaccines concentrations were adjusted using PBS. Total protein of the batch was calculated by Bradford protein assay kit and the three different vaccines doses were adjusted using the previously calculated antigen concentration in BEVs, so that a dose of 1ml contained either 12.5µg, 25µg or 50µg of F1 or V.

Vaccinations consisted of a prime-boost regimen. Blood, saliva, nasal swabs, salivary glands, bronchoalveolar lavage (BAL) and stool were collected on two pre-immunisation days, -14 and 0, and three post immunisation days, 28, 42 and 56. Each animal served as their own control for evaluating vaccine responses (Fig. 3.5). Antibody titres were determined using an in-house developed ELISA using commercial sources of capture and detection antibodies and in-house generated recombinant protein antigens.

V/F1-OMV or V-OMV + F1-OMV
IN (12.5, 25, 25 μ g) or OG (50 μ g)

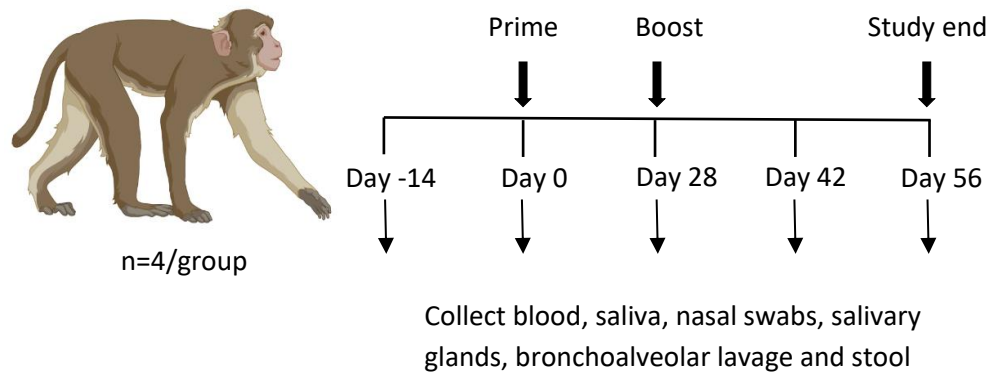


Figure 3.5 Overview of animal studies to determine immune response to of V-BEV and F1-BEV vaccinations. NHPs were immunised with either V-BEV, F1-BEV or V-BEV with F1-BEV intranasally or orally gavage containing either 12.5, 25 or 50 μ g of V or F1 antigen in PBS. NHPs were primed and boosted within 28 days and study ended at day 56. From day -14 until endpoint, blood, saliva, nasal swabs, salivary glands, BAL and stool were collected. Health and body weight were also closely monitored.

3.2.4 Host response to recombinant F1 and V antigens

NHPs immunised with rF1 or rV intramuscularly with alum adjuvant showed three times higher levels of specific serum anti-F1 or anti-V IgG at log reciprocal serum dilution 3.4 compared to the other group (Fig. 3.6). Values from saturated reactions that formed dark precipitates in the wells of the ELISA were discarded.

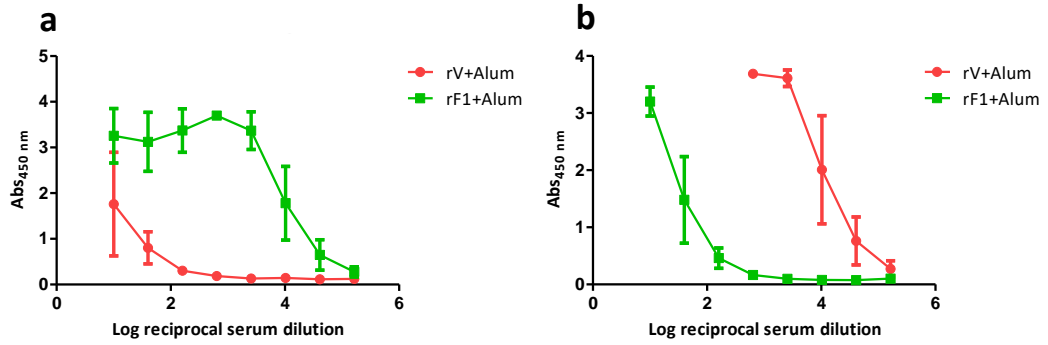


Figure 3.6 Quantification of serum IgG antibodies to recombinant V or F1 by ELISA. NHPs were immunised with 50 μ g of recombinant F1 or V with 20% (v/v) alum and boosted 28 days later. Blood was collected on day 56 and analysed to detect antibodies anti-F1 (a) and anti-V (b). Data is represented by the mean value for each group $n=2 \pm$ standard deviation.

3.2.5 Host response to F1-BEV plague vaccine

F1-BEV vaccine immune response was evaluated by measuring antigen-specific IgG levels in serum (Fig. 3.7) and IgA in mucosal secretions (Fig 3.8) of immunised animals by ELISAs. In F1-BEV vaccinated animals, serum anti-F1 IgG levels reached $\sim 1.5\mu$ g/ml at day 42 and decreased thereafter to $\sim 1\mu$ g/ml at day 56. There was no clear evidence for an effect of antigen dose nor for administration route as all groups showed similar levels of IgG. It was not possible to detect F1-specific IgA in saliva samples. By contrast, NHPs that received the lower dose showed double level of F1-specific BAL and salivary glands IgG than NHPs immunised orally.

The mean concentration of serum IgG in rhesus macaques is around 20mg/ml (200), while the concentration of IgA in saliva is 0.6mg/ml (201). Although the proportion of increased antibodies after vaccination is low, it is important to note that there is no universally defined good or optimal IgG or IgA level that guarantees protection.

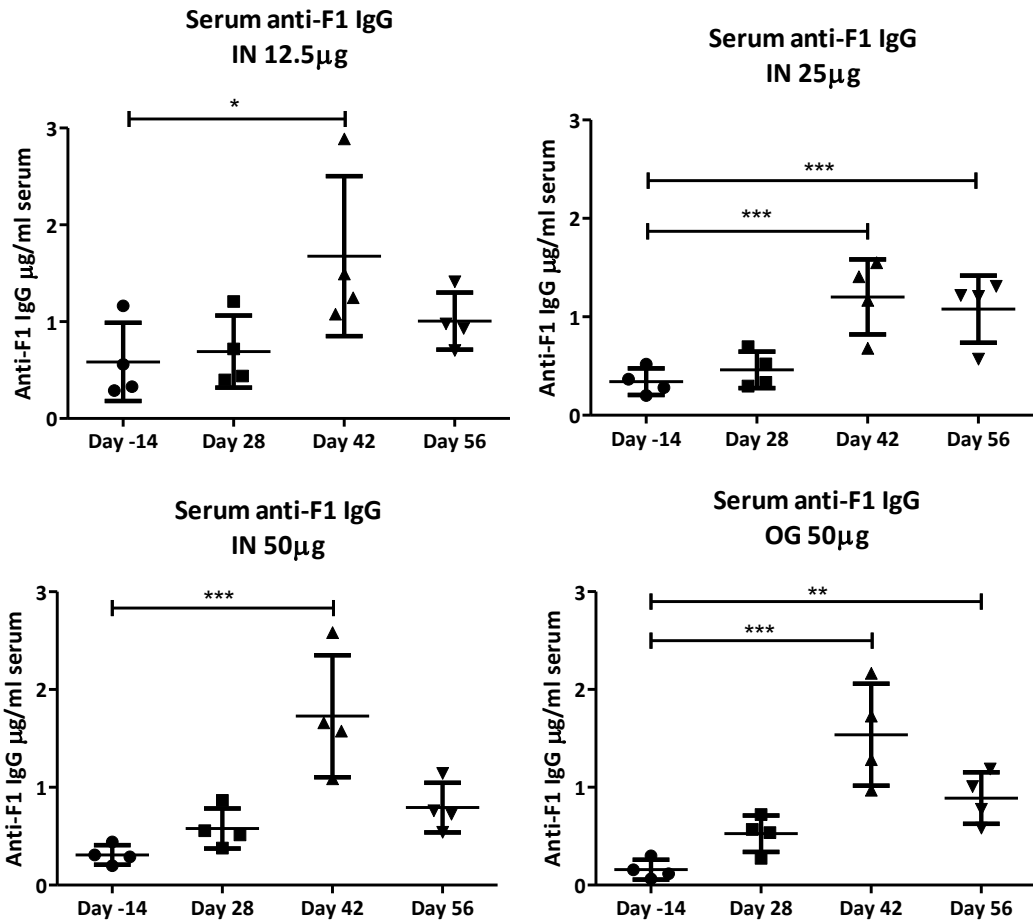


Figure 3.7 Quantification of systemic antibodies to F1-BEV vaccine. NHPs were immunised with F1-BEV isolated from BDM media culture containing either 12.5 or 25µg of V intranasally or 50µg intranasally and orally. Blood was collected and analysed on day -14, 28, 42 and end point day 56. Data represented by the mean value for each group n=4 ± standard deviation. Statistical analysis was performed using one-way ANOVA with Dunnett test. *<0.05; **<0.01; ***<0.001.

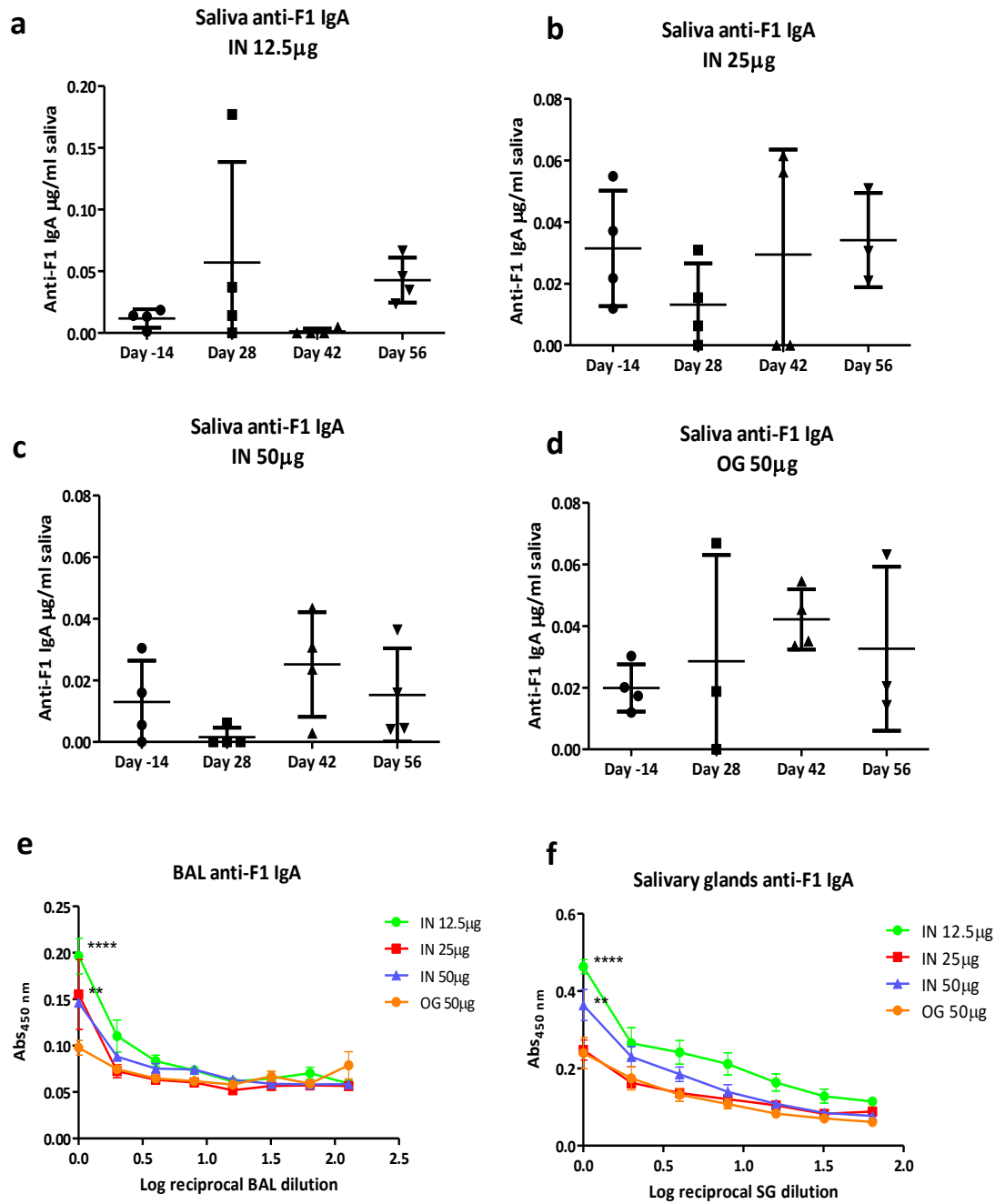


Figure 3.8 Quantification of mucosal antibodies to F1-BEV vaccine by ELISA. NHPs were immunised with F1-BEV isolated from BDM media culture containing either 12.5 or 25 μ g of V intranasally or 50 μ g intranasally and orally. (a, b, c, d) IgA from saliva collected and analysed on day -14, 28, 42 and 56. (e) BAL and (f) salivary glands specific anti F1 IgA titre. Data represented by the mean value for each group $n=4 \pm$ standard deviation. Statistical analysis was performed using one-way ANOVA with Dunnett test (a,b,c,d) and two-way ANOVA with Bonferroni post-test (e,f). * < 0.05; ** < 0.01; *** < 0.001.

3.2.6 Host response to V-BEV plague vaccine

V-BEV vaccine administered intranasally generated higher titres of V-specific IgG in serum than in orally vaccinated animals ($p < 0.001$) (Fig. 3.9). The highest levels of V-specific IgG ($\sim 25 \mu\text{g/ml}$, with one NHP reaching $42 \mu\text{g/ml}$) at the study endpoint were in animals intranasally vaccinated with the $25 \mu\text{g}$ dose. Titres of anti-V IgG increased from $\sim 8 \mu\text{g/ml}$ to $\sim 20\text{-}25 \mu\text{g/ml}$ over the study period in animals immunised with either the 12.5 or $25 \mu\text{g}$ dose. Two animals immunised with $50 \mu\text{g}$ showed higher levels of IgG ($30\text{-}60 \mu\text{g/ml}$) at both pre-immunisation time points (day -14 and 0) than the other two in the group. Levels of IgG in oral immunised animals remained at $5\text{-}8 \mu\text{g/ml}$ over time.

Low levels between $0\text{-}0.1 \mu\text{g/ml}$ of V-specific IgA were recorded at mucosal sites at all time points (Fig. 3.10). Consistent with the superior performance of the $25 \mu\text{g}$ dose in serum levels of antibodies, $0.15 \mu\text{g/ml}$ of V-specific IgA were recorded in NHPs immunised with the $25 \mu\text{g}$ dose with one NHP reaching $0.2 \mu\text{g/ml}$ at day 42. Comparable to systemic IgG levels, V-specific IgA reached $0.29 \mu\text{g/ml}$ at a pre-vaccination time point (day -14) in NHPs immunised with $50 \mu\text{g}$ intranasally.

Similar to the antibody response generated by F1-BEVs, V-BEVs administered orally showed almost half the levels of mucosal antibodies in BAL and salivary glands compared to intranasally delivered vaccine. The $50 \mu\text{g}$ dose of orally administered V-BEVs achieved the highest titres of V-specific IgA in BAL ($p < 0.001$), compared to oral administered vaccine. There was no evidence of dose-dependent response in salivary glands as each dose elicited similar levels of V-specific IgA.

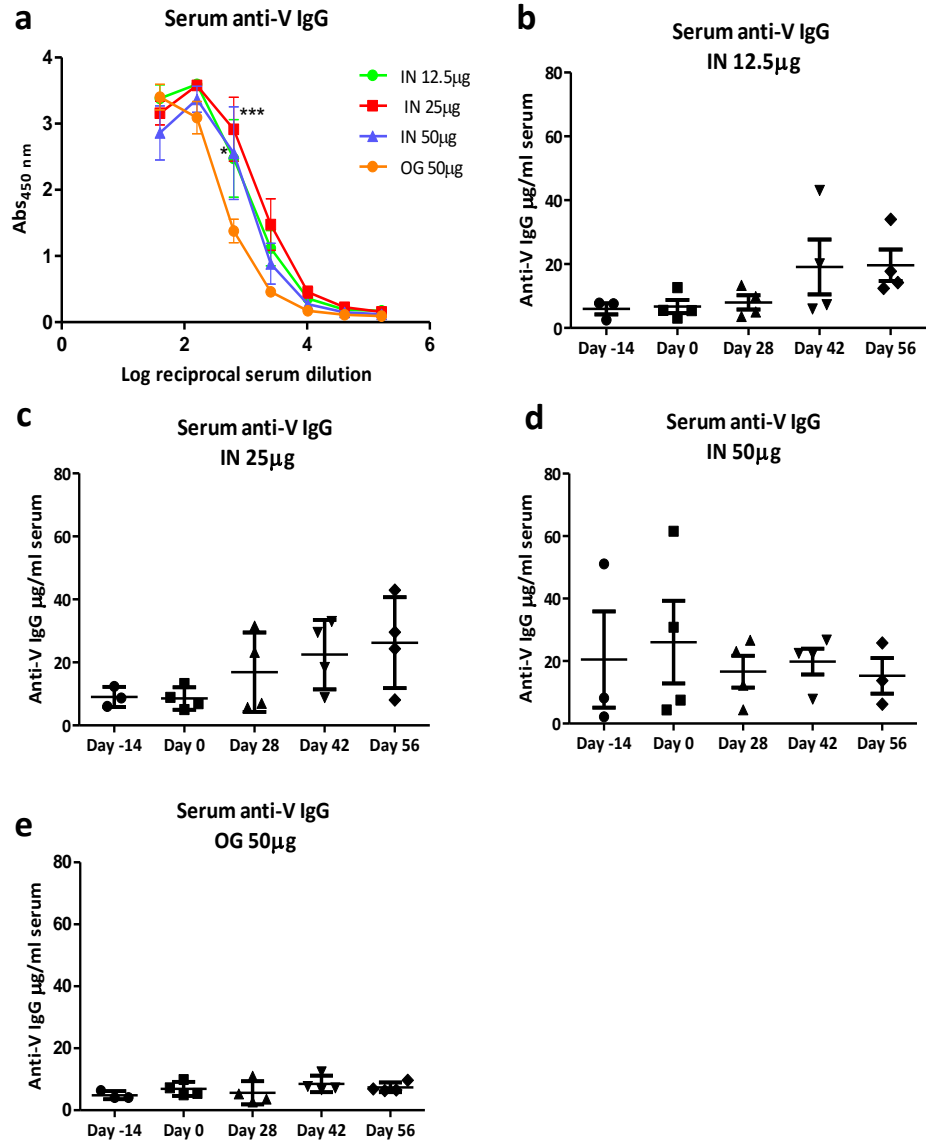


Figure 3.9 Quantification of systemic antibodies to V-BEV by ELISA. NHPs were immunised with V-BEV isolated from BDM media culture containing either 12.5 or 25µg of V intranasally or 50µg intranasally and orally. Blood was collected and analysed on day -14, 0, 28, 42 and end point day 56. (a) Titre of V-specific IgG at endpoint. (b, c, d, e) Quantification of V-antigen specific IgG over time. Data represented by the mean value for each group $n=4 \pm$ standard deviation. Statistical analysis was performed using two-way ANOVA with Bonferroni post-test (a), or one-way ANOVA with Dunnett test (b, c, d, e). * <0.05 ; ** <0.01 ; *** <0.001 .

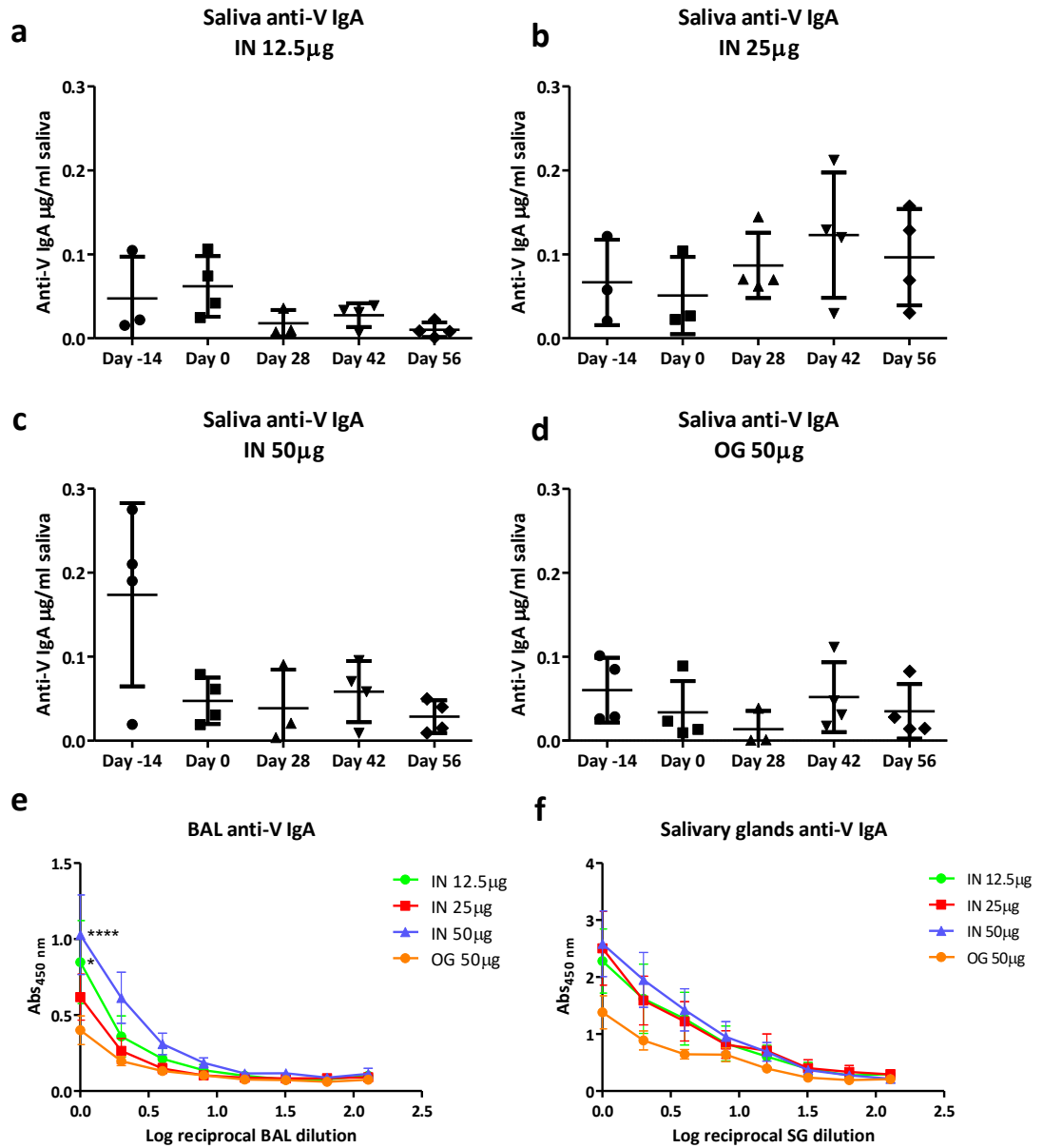


Figure 3.10 Quantification of mucosal antibodies to V-BEV by ELISA. NHPs were immunised with V-BEVs isolated from BDM media culture containing either 12.5 or 25 μ g of V intranasally or 50 μ g intranasally and orally. (a, b, c, d) IgA from saliva collected and analysed on day -14, 0, 28, 42 and 56. (e) BAL and (f) salivary glands specific anti-V IgA titre. Data represented by the mean value for each group $n=4 \pm$ standard deviation. Statistical analysis was performed using one-way ANOVA with Dunnett test (a,b,c,d) and two-way ANOVA with Bonferroni post-test (e,f). * <0.05 ; ** <0.01 ; *** <0.001 .

3.2.7 Host response to combined V-BEV and F1-BEV vaccines

The immune response to a combined F1-BEV and V-BEV vaccine was evaluated by measuring antigen-specific IgG levels in serum (Fig. 3.11) and IgA in mucosal secretions (Fig 3.12 and Fig. 3.13) using ELISA.

NHPs that received V-BEVs and F1-BEVs together did not show an increase of serum F1-specific IgG over time compared to NHPs immunised with F1-BEVs alone (Fig. 3.11). Specific anti-V IgG reached 20µg/ml in intranasally vaccinated NHPs at day 28 or 42 post-vaccination and decreased thereafter to 10µg/ml. Differently to some NHPs immunised with only V-BEVs that reached 40µg/ml after the boost.

In mucosal samples, low titres of F1 and V-specific IgA in saliva were recorded in all groups (Fig. 3.12). Only one NHP that received the 50µg dose intranasally showed 0.13µg/ml of anti-V IgA at day 56, compared to the 0-0.05µg/ml the other groups showed. Consistent with the superior performance of intranasally delivered F1-BEVs and V-BEVs for generating IgA antibodies, levels of V-specific IgA were recorded to be double in the BAL and salivary glands, of animals immunised intranasally with the combined vaccines, compared to those immunised orally (Fig. 3.13). Similar levels of anti-F1 IgA were analysed in all the immunisation groups immunised with the combined vaccine.

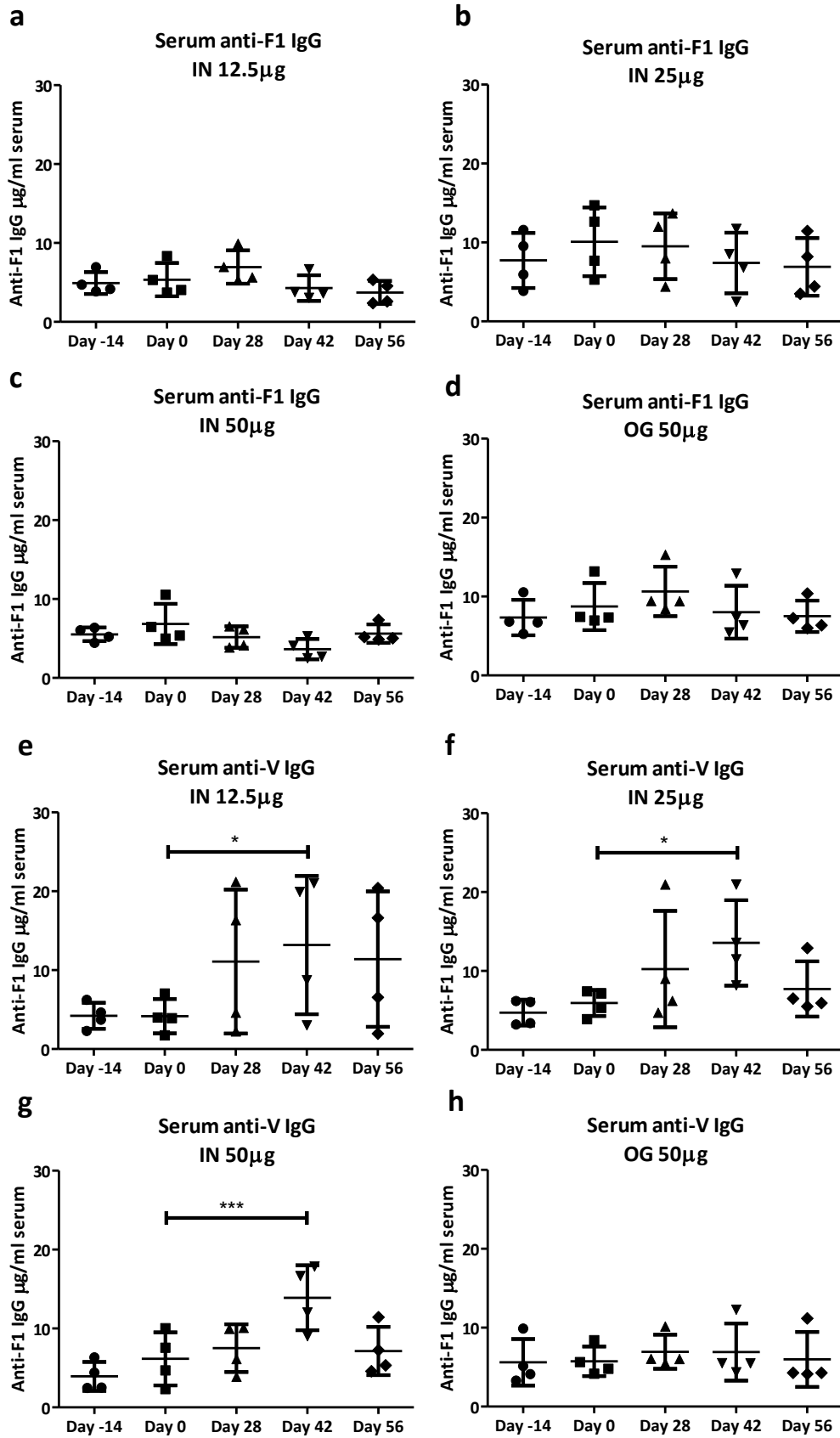


Figure 3.11 Quantification of systemic antibodies to F1 and V by ELISA. Humoral systemic immune response to combined V-BEVs and F1-BEVs vaccines. NHPs were immunised with V-BEVs and F1-

BEVs isolated from BDM media culture either 12.5 or 25µg of V intranasally or 50µg intranasally and orally. Blood was collected and analysed on day -14, 0, 28, 42 and end point. (a, b, c, d) Quantification of F1-antigen or (e, f, g, h) V-specific IgG over time. Data represented by the mean value for each group $n=4 \pm$ standard deviation. Statistical analysis was performed using one-way ANOVA with Dunnett test. * <0.05 ; ** <0.01 ; *** <0.001 .

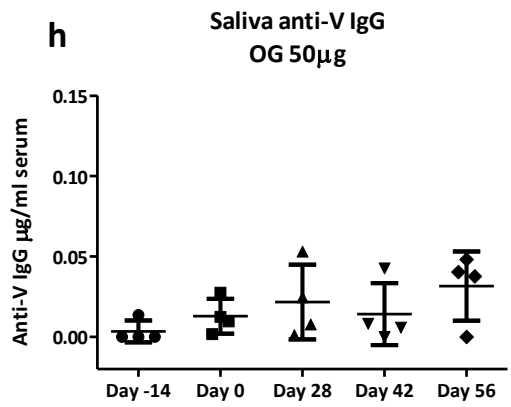
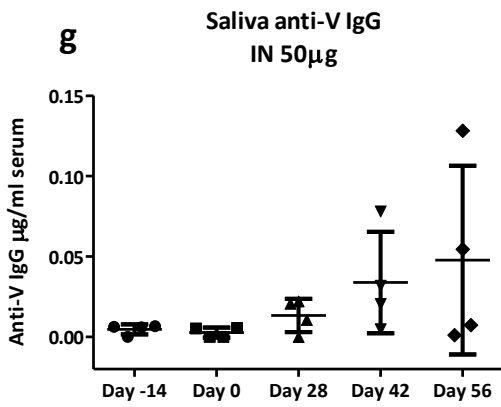
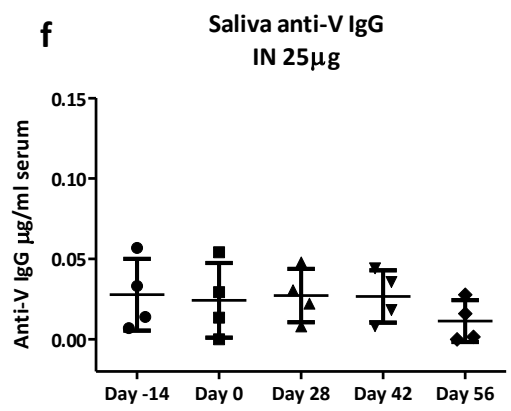
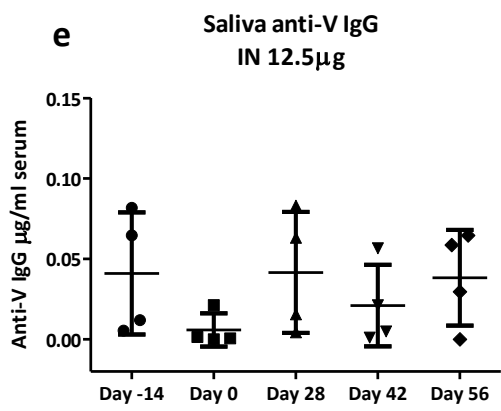
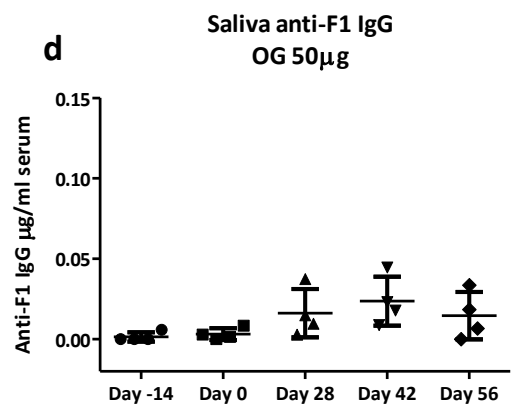
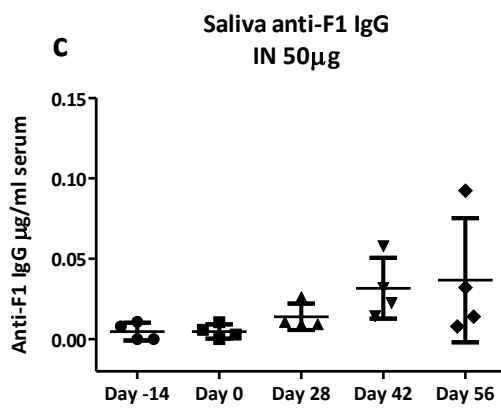
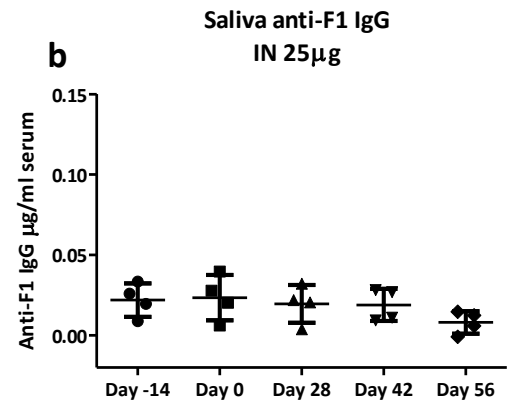
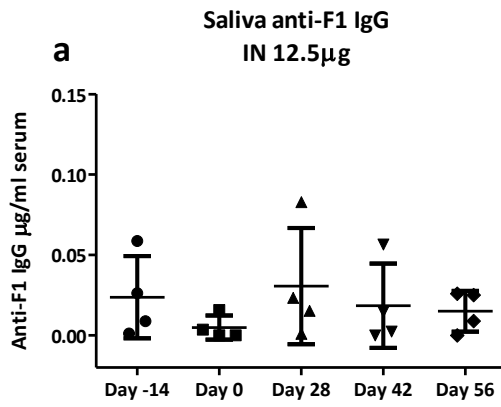


Figure 3.12 Quantification of saliva antibodies to F1 and V by ELISA. NHPs were immunised with V-BEVs and F1-BEVs isolated from BDM media culture containing either 12.5 or 25µg of V intranasally or 50µg intranasally and orally. Saliva was collected on day -14, 0, 28 42 and analysed by ELISA. (a, b, c, d) Quantification of V-antigen and (e, f, g, h) F1-specific IgA in saliva. Data represented by the mean value for each group $n=4 \pm$ standard deviation. Statistical analysis was performed using one-way ANOVA with Dunnett test.

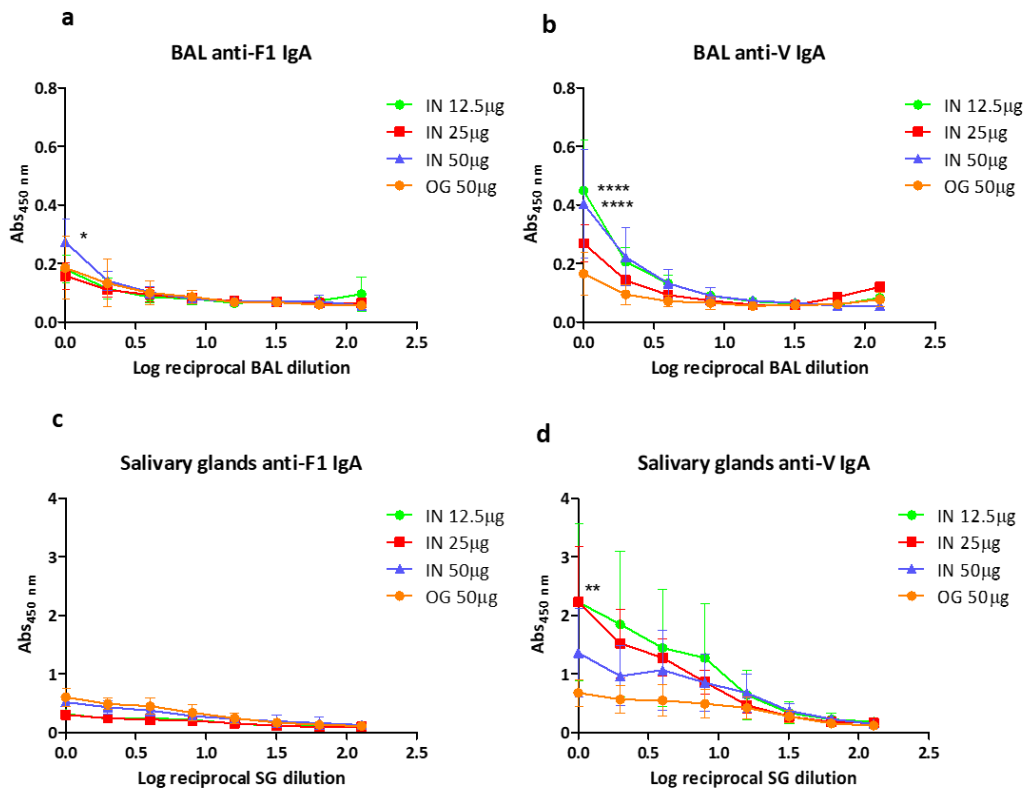


Figure 3.13 Quantification of BAL and salivary glands antibodies to F1 and V by ELISA. NHPs were immunised with V-BEVs and F1-BEVs isolated from BDM media culture containing either 12.5 or 25µg of V intranasally or 50µg intranasally and orally. BAL and salivary glands were collected on day 56 and analysed by ELISA. (a, b) Quantification of F1 and V-specific IgA in BAL and (c, d) in salivary glands. Data represented by the mean value for each group $n=4 \pm$ standard deviation. Statistical analysis was performed using two-way ANOVA with Bonferroni post-test. * <0.05 ; ** <0.01 ; *** <0.001 .

3.2.8 Cell-mediated immune responses

Cytokine production from restimulated peripheral blood lymphocytes (PBMC), analysed by Drs Ana Carvalho and Emily Jones (QIB), was used as an indicator of cell-mediated immune responses. PBMC from animals immunised intranasally or orally with F1-BEVs and V-BEVs were restimulated with either PBS, rF1, or rV antigen in vitro for 72h

and cytokine content of supernatants determined using a bead-based multiplex assay (LEGENDplex Human Inflammation Panel 1 (13-plex)) and BD LSRFortessa flow cytometer. The detailed protocol can be found in Carvalho et al. 2019a (2).

Stimulation with rV or rF1 increased levels of IL-6 in all the immunisation groups with the higher values seen in the NHPs immunised with the 12.5µg dose reaching 2000pg/ml of IL-6 compared to the other groups that had ~1000-1500pg/ml (Fig. 3.14). The vaccine also significantly increased MCP-1 ($p<0.0001$ and $p<0.01$), IL-8 ($p<0.001$ and ns) and IL-23 ($p<0.05$ and $p<0.05$) in PBMC restimulated with rF1 and rV compared to PBS from NHPs immunised with the lowest dose of the combined vaccine. IL-6, MCP-1, IL-8 and IL-23 are inflammatory cytokines. IL-6 induces proliferation and differentiation of T and B cells. MCP-1 attracts monocytes and regulates their migration to sites of inflammation. IL-8 is responsible for recruiting neutrophils to the site of infection, and IL-23 promotes proliferation of T helper 17 cells (202). Other cytokines including TNF- α , IL-12, IL-18, IFN- γ , IL-10, INF- α and IL-17A were also analysed but were below the assay detection limit ($\leq 1\text{pg/ml}$).

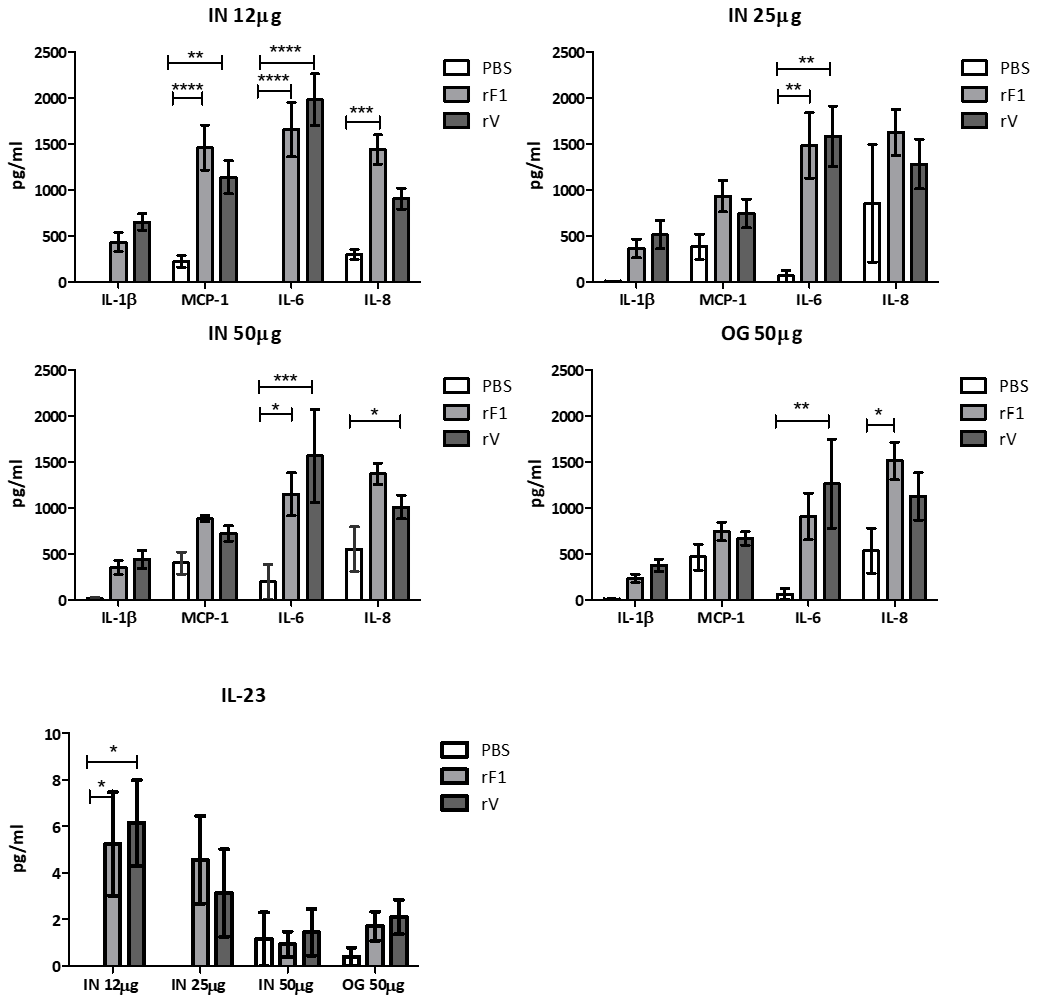


Figure 3.14 Quantification of cytokine expressed in stimulated PMBCs from NHPs immunised with F1-BEV + V-BEV by flow cytometry. PMBC were cultured with either rF1, rV or PBS for 72h and supernatant analysed for cytokine content using multiplex bead assay and flow cytometry. Data represent quantified cytokines levels in pg/ml, represented by the mean value for each group n=4 ± standard error of the mean. Statistical analysis was performed using one-way ANOVA using a Bonferroni post-test. *<0.05; **<0.01; ***<0.001; ****<0.0001.

3.2.9 Reactogenicity of F1-BEVs and V-BEVs vaccines.

All animals immunised with F1-BEVs, V-BEVs or a combination of the two had no reported adverse reactions (PHE veterinary surgeon reported observations). Additionally, screening tests were clear of high-consequence pathogens such as tuberculosis, measles, simian immunodeficiency virus, Salmonella, Campylobacter, Giardia. However, a routine rectal swab identified *Pseudomonas aeruginosa* in a single NHP that received the 50µg V-BEV dose intranasally.

Histology of the lungs, lymph nodes, brain, heart, liver, spleen, kidney, and regions of the gastrointestinal tract was carried out by PHE using haematoxylin and eosin staining and light microscopy. The results revealed no macroscopic signs of pathogenic infection or pathology consistent with the biosafety of F1-BEVs and V-BEVs vaccines.

In three out of four NHPs from all immunisation groups showed evidence of an ongoing or recent immune response as evidenced by histopathology of spleen and lymph nodes. The immune response was characterised by the presence of scattered secondary follicles with mitotic figures and apoptotic cells within splenic white pulp (Fig. 3.15.a) and cortex of the lymph nodes (Fig. 3.15.b). NHPs also had a mild to moderate infiltration of lymphoplasmacytic cells in the mucosa of the duodenum (Fig 3.15.c), stomach, jejunum (Fig 3.15.d), ileum (Fig 3.15.e), caecum and colon. This was noted by the veterinary surgeon as a common finding in NHPs in the PHE facility, that might reflect a low-grade gastritis/enteritis/colitis. Although a noteworthy difference between groups was not observed, NHPs immunised with V-BEVs, dose 25µg and 50µg, showed increased prominence of bronchus-associated lymphoid tissue, without any presence of pathogens within the parenchyma (Fig. 3.15.f), suggestive of a recent, mild inflammatory immune response. The remaining tissues (kidney, liver, brain, heart) were normal.

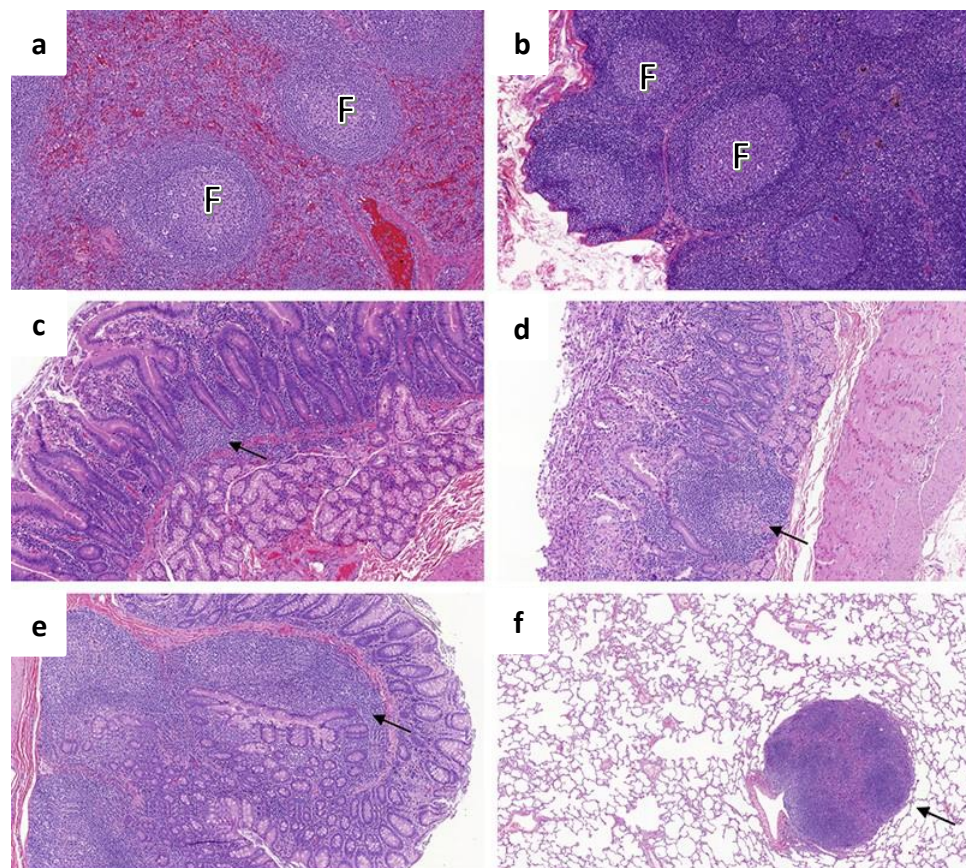


Figure 3.15 Histopathological sections of immunised NHPs. Haematoxylin and eosin-stained sections are from NHPs that received the highest dose of either F1-BEVs (a, b) or V-BEVs (c, d, e, f) collected on day 56. (a) Spleen with splenic follicles (F); (b) Lymph node; (c) Duodenum with lymphoplasmacytic infiltration (black arrow). (d) Jejunum with proliferated lymphoid follicle like structures (black arrow); (e) Ileum with activated Peyer Patches. (arrow); (f) Lung with focal proliferation of bronchus-associated lymphoid tissue (black arrow).

The taxonomic profile of the gastrointestinal tract and respiratory microbiota was also evaluated as part of assessing the biosafety of BEVs vaccines. This is because the immune response to a vaccine can impact the gut or respiratory microbiome by altering conditions such as pH, nutrient availability, potentially leading to temporary changes in the microbial composition for example overgrown of a specific strain (203). By assessing the taxonomic profile before and after vaccination can help understand how BEVs vaccine impact the microbiome and identify potential risks and benefits associated. DNA extraction from faecal samples and nasal swabs was optimised prior to sequencing. The DNA from the samples was first isolated using OMNIgene® GUT microbial DNA purification protocol using MoBio® PowerFecal® DNA Isolation Kit. Genomic DNA was amplified by PCR with primers targeting the hypervariable V1-V9 region of the 16S rRNA gene and analysed with 1% (w/v) agarose gel to assess the integrity of DNA. The concentration extracted using this method quantified by NanoDrop™ was 50ng/μl for stool DNA and 3.3ng/μl and 0.4ng/μl for rectal and nasal swabs respectively. The protocol was optimised by using two Neonatal FLUOswabs per sample instead of one and adding them to a Lysing Matrix E (MP Biomedicals) used to lyse cells from a wide variety of starting materials. The isolation kit was also changed to the QIAamp PowerFecal DNA Isolation Kit (Qiagen), and the vortex step was substituted by the beat beater to increase cell lysis (Fig. 3.16). After optimisation, an average yield of 100ng/μl DNA was obtained from faecal samples, nasal and rectal swabs.

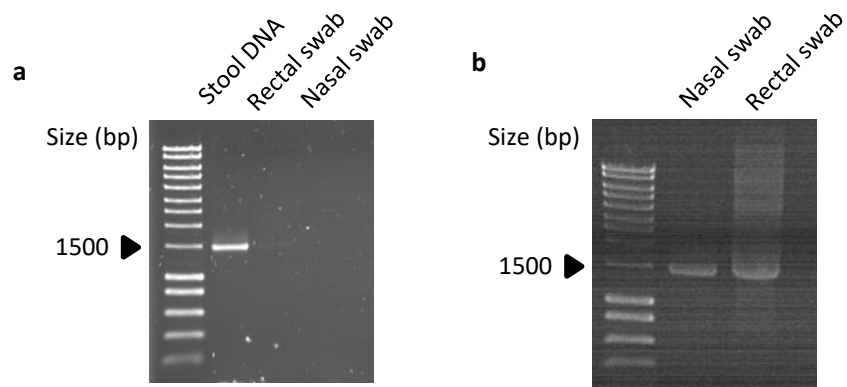
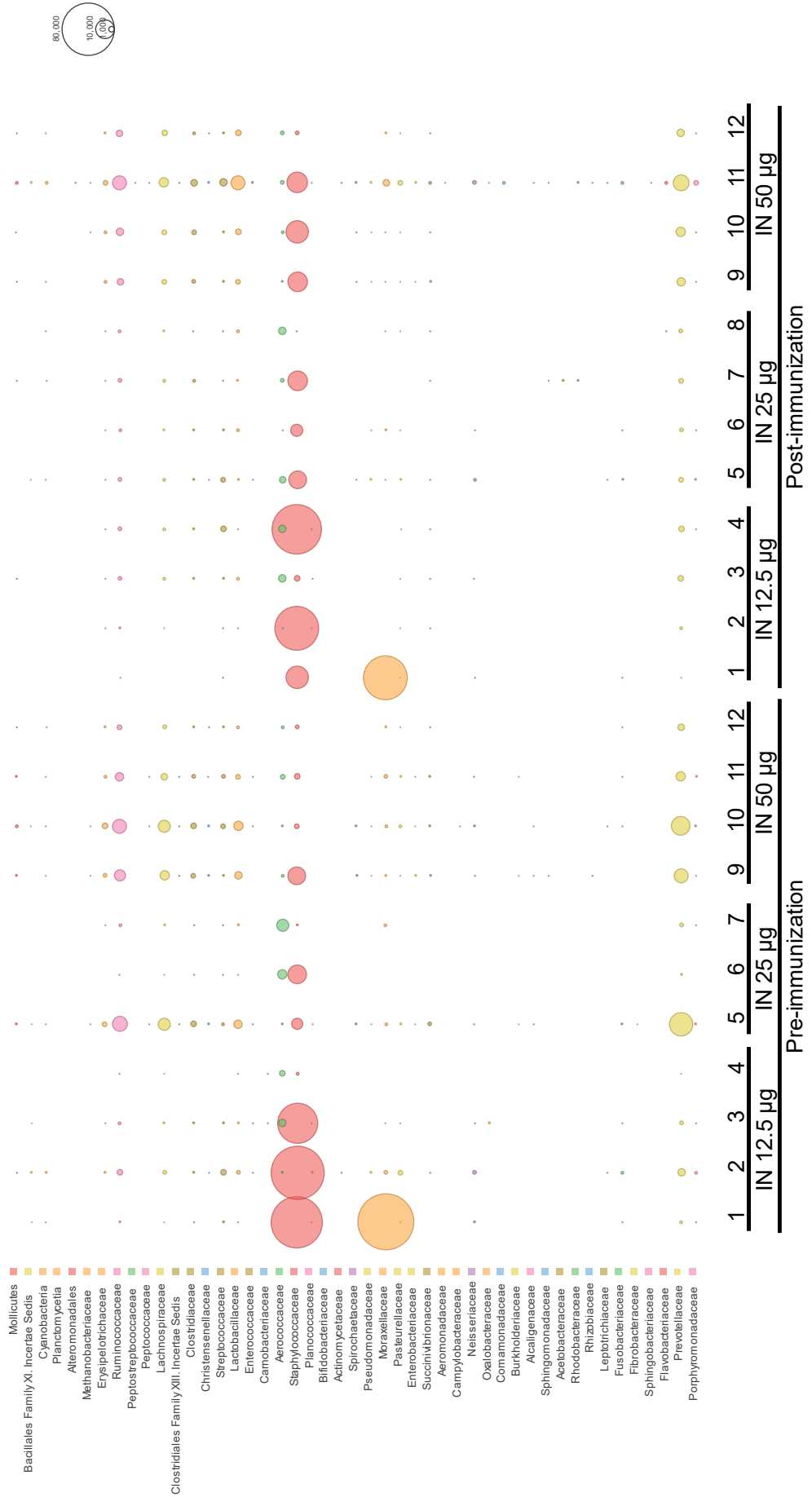


Figure 3.16 Comparison of DNA extracted from faecal samples, rectal and nasal swab. 1% (w/v) agarose gel of genomic DNA amplified by PCR with primers targeting V1-V9 region of 16S to assess integrity of DNA. Stool DNA: 50ng/ μ l. Rectal swab: 3.3ng/ μ l. Nasal swab: 0.4ng/ μ l. (a) DNA extracted using OMNIgene GUT microbial DNA purification protocol using MoBio® PowerFecal® DNA Isolation Kit. (b) DNA extracted using Lysing Matrix E, 2ml tube (MP Biomedicals) with QIAamp PowerFecal DNA Isolation Kit (Qiagen). Nasal swab: 117.8ng/ μ l. Rectal swab: 120.2ng/ μ l.

Due to budgetary and time considerations only stool and nasal swabs from V-BEV vaccinated animals were sequenced. 16S rRNA community profiling revealed considerable interindividual variation in nasal microbiota of NHPs in pre-immunisation samples (Fig. 3.17.a). Vaccination did not noticeably alter nasal microbiota profile at any dose. V-BEVs orally immunised animals produced small changes in the faecal microbiota (Fig. 3.17.b). This included an increase in the prevalence of Prevotellaceae from 30% at pre-immunisation to 44% after immunisation and a decrease in the prevalence of Succinivibrionaceae from 9 to 0.4%. Collectively this analysis suggests that V-BEVs have only a minor impact on the faecal microbiota.

a



b

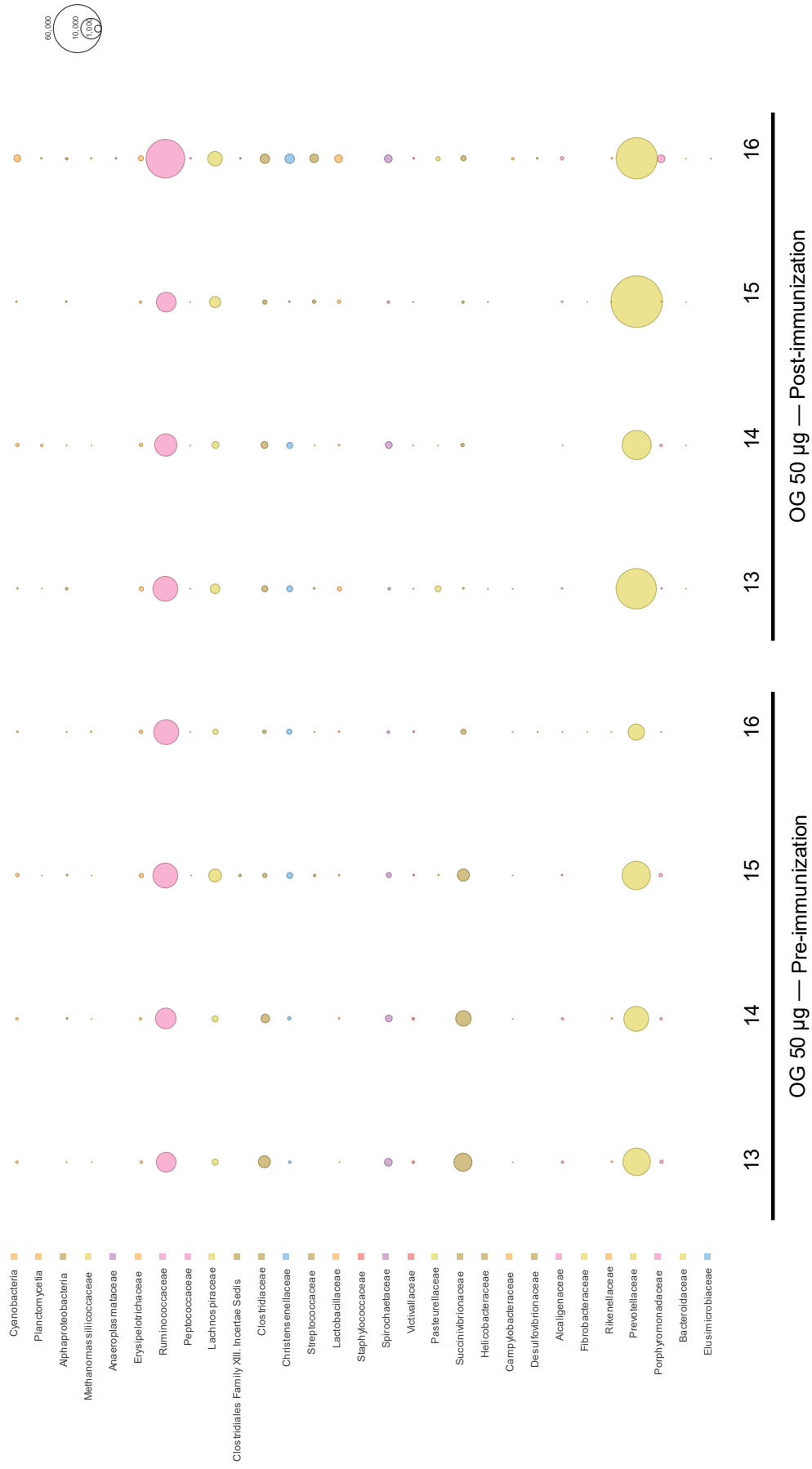


Figure 3.17 Bubble chart from 16S rRNA sequences (V4-V5) obtained from animals immunised with V-BEV. Size of bubble is proportional to the number of sequences. Number 1-16 represent individual animals. (a) Nasal microbiota pre- and post-immunisation from animals immunised intranasally. (b) Faecal microbiota from pre and post immunisation of animals immunised orally gavage. Figure created with MEGAN Community Edition by A. Telatin (QIB).

3.2.10 Functionality of BEVs-elicited IgG antibodies

A common way to assess functionality of activated immune response after vaccination is by infection challenge. Due to biosafety, containment concerns and use of high-cost biosafety level 3 facilities, we used *in vitro* correlates of plague protection using a competitive ELISA (developed and performed at DSTL) and a bactericidal assay (developed and performed at PHE/UKHSA).

The competitive ELISA quantified the ability of vaccine-generated IgG to compete with a monoclonal antibody (mAb 7.3), that confers protection in mice against *Y. pestis* infection (204), for the binding to rV. The data represent the loss of binding of mAb 7.3 to rV with increasing concentration of pulled serum samples. Serum from NHPs immunised with rV and alum was used as a reference. Non-specific activity was corrected by subtracting values from serum from non-immunised animals. The detailed protocol can be found in Carvalho et al. 2019a (2).

Serum from animals intranasally immunised with 25µg or 50µg of antigen in V-BEVs inhibited the binding of mAb 7.3 at dilution 1:100 similar to the reference serum with an absorbance value of 0.2. In contrast, serum from NHPs immunised with the lowest dose orally showed an absorbance of 0.8 for all the dilutions of serum from the NHPs showing no binding to the rV (Fig. 3.18).

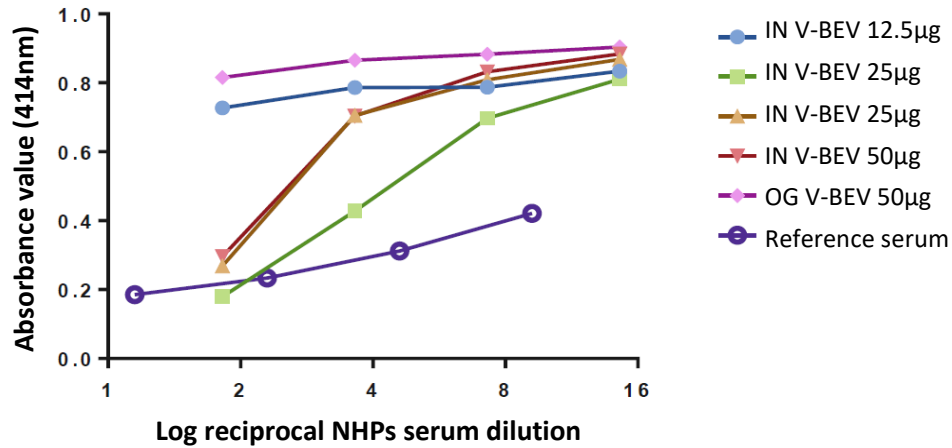


Figure 3.18 Functionality of immune sera from V-BEVs immunised animals analysed by competitive ELISA. Pooled serum from V-BEVs immunised animals were serially diluted and tested for their ability to displace a monoclonal V antibody bound to rV antigen. Reference immune serum was from NHPs immunised intramuscularly with rF1 and rV antigen plus alum adjuvant.

The bactericidal assay assessed the level of antibody in serum samples able to kill *Y. pestis* in the presence of exogenous complement. The assay simulates the natural response that would take place against an infection with *Y. pestis*. Serum samples from animals immunised with F1-BEVs or V-BEVs were pooled and compared to a reference serum generated by immunising NHPs intramuscularly with rF1 and rV with alum adjuvant. The detailed protocol can be found in Carvalho et al. 2019a (2).

The immune response induced by 25µg dose of V-BEVs or F-BEVs administered intranasally provided similar or higher bactericidal cytotoxic antibody titres than that generated by recombinant proteins with alum ~10% (Table 3.2). However, serum from NHPs immunised with 25µg or 50µg either with F1-BEVs or V-BEVs showed high background reactivity at day 0 (0.6-12%) (Table 3.2). Intranasal administration induced higher serum bactericidal response (from 0.6 to >45%) than oral administration (>45%). On day 28 or 42, all groups (except the lowest intranasally dose for both vaccines) demonstrated functional immunity to *Y. pestis*, while at day 56, the activity in some groups was weakened.

Table 3.2 Summary of serum antibody bactericidal assay outputs. ED50 in units of % serum †. Results are shown in percentages of serum necessary to be able to kill 50% of *Y. pestis*. The lower the number, the higher their ability to kill *Y. pestis*.

Vaccine	Dose (µg)	Route	Day 0	Day 28	Day 42	Day 56
F1-BEV	12.5	IN	>45	21.6	>45	39.2
V-BEV	12.5	IN	>45	>45	20.9	22.5
F1-BEV	25	IN	1.4	1.6	1.5	6.2
V-BEV	25	IN	1.9	0.5	15.3	13.7
F1-BEV	50	IN	12.1	36.2	14.9	>45
V-BEV	50	IN	0.6	5.5	0.8	14.9
F1-BEV	50	OG	>45	17.0	13.0	> 45
V-BEV	50	OG	>45	1.8	6.3	>45
rF1+rV Alum	50	IM	–	–	–	10.7*

† The initial dilution of antibody in the assay was 45%, hence the limit of the assay was nominally set at 45%. 50% Effective dose (ED₅₀), Alhydrogel (Alum), * Average of six determinations, – Not included in the study design. Sera with an ED₅₀ below the limit of detection were assigned an ED₅₀ of > 45%.

3.3 Discussion

Y. pestis still causes outbreaks of disease in various parts of the world today (166, 168). Due to their high mortality, rapid spread, and potential use as a bioweapon, effective vaccines are needed (169). In this study, I have shown that engineered BEVs from the commensal gut Bt expressing F1 and V proteins induce humoral response in NHPs which supports the potential use of Bt engineered BEVs as a vaccine technology for plague.

The use of parenteral BEVs vaccines (Bexsero) has been demonstrated to be safe and effective in preventing *Neisseria meningitidis* infections in adults and children (205). Their use as intranasal vaccines was studied in 1998 in humans but did not progress further because of lack of immune stimulation (206). This study therefore represents one of the

first to explore the efficiency and safety of BEVs delivered orally and intranasally in a NHP model.

Bt engineered BEV vaccines were shown to be safe. Animals immunised intranasally or orally with Bt engineered BEVs displayed no adverse clinical reaction and post-mortem tissue histology showed evidence of immune activation and formation of organised lymphoid follicles in the absence of any pathology. Gastrointestinal tract and respiratory tract microbiota profiles were not significantly altered post-vaccination. These findings are consistent with Bt engineered BEV vaccines being safe and able to induce an immune response in NHPs.

Bt can be engineered to express both antigens, F1 and V in their native immunogenic form in BEVs. The difficulties in identifying F1 protein in BEVs by immunoblotting might be attributable to the antibody used which is reactive with the native F1 protein and may therefore lack sufficient reactivity to denatured F1 in immunoblotting assays for detection. Consistent with this interpretation is the ability to detect F1 protein with this antibody in an immune-dot-blot assay which incorporates native and not denatured protein.

Both vaccine formulations F1-BEVs and V-BEVs induce some degree of systemic and mucosal humoral response when administered separately. However, F1-BEVs did not induce specific antibodies when co-administered with V-BEVs. Vesicles were quantified before immunisation and the total protein and vaccine antigen content were equivalent in the single and combined formulations. It is possible therefore that different BEV characteristics occur when combined producing different responses. For example, co-administration of different BEVs could interfere with their uptake by host APC although there is no evidence of this from *in vitro* studies (207). More detailed analysis of BEV formulations may help determine how, and under what conditions, BEV-elicited immune response occur. This could include assessing lipid content and composition, additional purification steps, and biological activity using indicator immune cells lines (e.g., the human monocytic cell line THP1 with activation reporter genes; THP-1 Blue cells) to increase batch-to-batch consistency.

Systemic antibody responses from F1-BEVs, V-BEVs immunised animals increased over time, reflecting the importance of the booster immunisation, although antibody titres decreased by day 56. Over time, immunity generated by vaccines fades and the objective is to keep them high for as long as possible and at least one year (169). The live

attenuated vaccine used in endemic areas maintain high serum antibody levels for around 8 months and is therefore administered yearly (173). The waning of antibody levels is also observed in the clinical trial of a vaccine from the Lanzhou Institute of Biological Products consisting of rF1 with rV and alum administered intramuscularly (198). The vaccine induces high levels of IgG that peak at day 56 post immunisation but decrease after 6 months (198). It is also important to note that antibody levels may not be a direct correlate of protection (208) with low levels of high affinity antigen-specific antibodies being as or more protective than high levels of low affinity antibodies

In this study, a second booster may increase the strength and duration of the immune response generated by the BEV vaccines. The latest *Neisseria meningitidis*-based BEV vaccine formulation, Bexsero, relies on two or three intramuscular immunisation regimens to protect against Meningitidis B disease (209). Moreover, two plague vaccines undergoing clinical trials require two (University of Oxford) (192) or three (Lanzhou Institute of Biological Products) intramuscular injections (193). Although one dose is the preferred option, adding an extra boost could be feasible and acceptable for mucosal BEV vaccines as they are non-invasive, easy to administer and are more acceptable than repeated injections.

The most effective route of mucosal BEV vaccine administration is intranasal, as shown by the production of antigen-specific IgA and neutralising and cytotoxic serum IgG antibodies. Moreover, intranasal administration also elicits cellular immune responses as indicated by proinflammatory cytokine production by *in vivo* primed PBMC cells after re-stimulation with F1 and V antigens. The weaker immunogenicity of BEVs delivered orally might be due to the harsh conditions of the GI tract including low pH, digestive enzymes, dilution, and the mucus barrier impacting on their uptake and acquisition by cells in inductive immune sites in the intestinal mucosa. The ability of Bt WT-BEVs to transmigrate the intestinal epithelial barrier after oral administration (210) and activation of mucosal APC has been demonstrated (97), although this remains to be determined for BEVs expressing vaccine antigens.

Although there is no clear evidence of one dose being superior, an intermediate dose of 25µg F1 or V generally performed as well as, if not better, than a two-fold higher dose in terms of B cell (antibody) and T cell (cytokine) responses. Similarly, African green monkeys vaccinated intramuscularly with flagellin-F1-V showed that a dose of 25µg and 100µg had comparable results in the animals (211). Moreover, the Lanzhou vaccine undergoing clinical trials phase IIb, is based on a 30µg of F1 and 30µg V dose (193).

Different vaccination routes may require different doses to generate effective immune responses. The doses used in this study are compared with intramuscular doses for recombinant protein-based vaccines as no mucosal vaccination study has been performed in NHPs or humans.

Identifying *Pseudomonas aeruginosa* in one of the NHPs immunised with 50µg V-BEVs may be related to the high response that some NHPs had on pre-vaccination days as shown in ELISA and bactericidal assays. *P. aeruginosa* together with, *Vibrio* spp., and *Aeromonas* spp. encode homologs of *Y. pestis* V antigen (212, 213). Antibodies generated against these homologs through natural infection by *P. aeruginosa* or against a related commensal bacteria may cross-react with V antigen (214). Although *P. aeruginosa* was only found in one animal, the bacteria could have also infected other animals without being detected, as it could have been eliminated earlier by their immune system. Similarly, in a human study, (198) participants have been shown to have serum anti-V antibodies, without any known infection with *Y. pestis*, before vaccination. The authors of the study suggest that participants may have prior exposure to *Yersinia pseudotuberculosis* or *Yersinia enterocolitica* that have significant homology to *Y. pestis* antigens (215). Extra caution in identifying infections from strains with homology to *Y. pestis* should therefore be considered in future experiments. With extensive test, participants or animal models should be removed from the studies, if positively identified with any homologues of *Y. pestis*, to avoid misinterpretation of any immune based assays.

Although interpretation of the bactericidal assay was complicated due to the suggestive cross-protection, together with the competitive ELISA, both assays identified *Y. pestis* neutralising antibodies in BEV vaccinated animals. Antibodies binding V antigen that are cytotoxic for *Y. pestis* are good correlates and indicators of protection induced by the vaccine. Ideally, this would be confirmed in a lethal infectious challenge experiment, which was not possible due to logistical issues, including cost and biosafety containment considerations.

Neutralising antibodies are needed to protect against plague, but cell-mediated immunity is also essential. Cellular immunity against plague has been difficult to analyse as cytokines levels are not detected in active or recovering pneumonic plague patients (except for IL-6) (216, 217). However, the important role of cellular immunity has been proven in animal models where T cells, in the absence of antibody, confer protection to *Y. pestis* infection (218-220). Also, animals transfused with CD4+ and CD8+ from immune animals are protected against infection (221).

The relative importance of individual cytokines in protecting against *Y. pestis* infection is unclear. Live attenuated plague vaccine in humans induce IL-17 producing CD4 T helper cells (Th17) after many rounds of vaccination with no differences in IFN- γ , IL-10 and TNF- α seen between vaccinated and non-vaccinated individuals (222). Contrary to this, mouse studies show that IFN- γ , TNF- α , and NOS2, are key elements of cellular immunity to protect against *Y. pestis* infection (223). Furthermore, two independent studies of subunit intramuscular vaccines in NHPs identified increases in IL-2 and IFN- γ (224, 225) together with TNF- α , IL-4, IL-5 and IL-6. (225). Additionally, in a clinical trial using live *Yersinia pseudotuberculosis* as a plague vaccine, IFN- γ levels are associated with protection, however some immunised individuals produced no detectable IFN- γ (226). This suggest that there is no clear correlation between cytokines and protection as multiple mechanisms and multiple cytokines might be involved in plague protection.

In this study, BEV vaccines induced the proinflammatory of IL-6, IL-1b, IL-23, MCP-1 and IL-8 cytokines that can activate an immune response to protect against plague infection. Of note, F1-BEVs and V-BEVs induced high levels of IL-6 that promotes B cell and CD4 differentiation and was the only cytokine that distinguishes between pneumonic plague patients and healthy individuals (216). It is interesting to note that the lowest dose of the F1-BEVs and V-BEVs vaccine produce more cytokines than higher doses. Although the reasons for this are unclear, the higher doses of F1-BEVs + V-BEVs may elicit a tolerogenic immune response. The inclusion of additional control groups, such as animals immunised with WT-BEVs and PBS in infectious challenge experiments, would help confirm these findings. By using larger groups of animals would also help to understand the significance of any changes in cytokine production in conferring protection.

In summary, Bt BEVs have been engineered to produce F1 and V antigens. These BEVs have shown to be capable of eliciting antigen-specific mucosal and systemic humoral responses able to kill plague bacteria, primarily when a dose of 25 μ g of V or F1 in BEVs were delivered intranasally. No adverse effects were seen in immunised animals and therefore, the findings suggests that the engineered BEVs could be used for developing safe and effective plague vaccines.

Chapter 4 Use of bioengineered Bt BEV as an Influenza vaccine

4.1 Introduction

Flu is a contagious acute respiratory infection caused by IV that spreads by air through contaminated droplets, and it infects the nose, the throat and sometimes the lungs. Illness range from mild to severe and even death (227). WHO estimates that IV is responsible for 3 to 5 million cases of severe illness and between 290,000 and 650,000 deaths annually worldwide (227). During the emergence of the Covid-19 pandemic, the number of cases declined but rose again during the 2021-2022 influenza season (228).

The rapid evolution of IV can make a significant proportion of the population, particularly immunocompromised, young children, and elderly individuals, vulnerable to infection by new strains resulting in high morbidity. The rapid changes of the virus are mainly mediated through minor but gradual mutations occurring in the viral RNA called antigenic drift (229). This happens when Influenza error-prone polymerase replicates the viral genome and introduces errors that cannot be corrected afterwards. Antigenic drift creates new virus strains able to evade the immune recognition and cause influenza epidemics (230). Moreover, major genetic changes, called antigenic shift, occurs when different strains of IV swap gene segments when they infect the same cell. The segmented viral genome of IV and the diversity of infected hosts facilitate this reassortment which can create new pandemic subtypes (229).

Although influenza affects humans, their reservoirs are animals, mainly wild aquatic birds (231). There are 4 types of IV: A, B, C and D. Each type of IV has different pathogenicity and hosts. IV A (IAV) has been responsible for recent pandemics and epidemics and has a broad host distribution. IV B also causes yearly epidemics with IV C and D very rarely causing infections in humans (227). IV B are separated into two main lineages Victoria and Yamagata. IAVs are classified into subtypes based on the surface glycoproteins hemagglutinin (HA) and Neuraminidase (NA). There are 18 HA and 11 NP

subtypes (232). The most prevalent subtypes currently circulating globally are H1N1 and H3N2 in humans and H5N1 and H9N2 in poultry (233-235). Each subtype of IAV can be divided into further clades and sub-clades.

Following the international naming of IV published by WHO in 1980 (236), each IV is named by first the antigenic type (A, B, C, D), followed by the host of origin if it is an animal, geographical origin (e.g., Vietnam, Sydney), strain number, year of collection and virus subtype in case of IAV. The two strains used in this thesis are A/Vietnam/1203/2004(H5N1) and A/Puerto Rico/8/1934(H1N1).

Although influenza vaccines are available and are the best line of defence against the disease, their efficacy ranges from 40% to 60% (237). There are two main types of licensed vaccines against IV, attenuated and inactivated vaccines. These vaccines contain attenuated or inactivated strains of IV that are selected 6 months ahead of vaccine distribution based on surveillance. They induce strain-specific immunity that is ineffective if the strains used do not match the circulating strains. As the virus change rapidly, new vaccines are offered every year that contain the expected strains to cause the next seasonal flu epidemic (238). These vaccines also offer little or no protection against emerging pandemics or new zoonotic IV subtypes (238).

Most licensed vaccines are administered via the parenteral route and therefore, produce weak or no mucosal immune responses needed to provide protection at the initial site of infection (239). There are currently 4 intranasal licensed LAIV vaccines, FluMist (USA), which is Fluenz in the UK and EU, Ultravac (EU), Nasovac (India) and Ganwu (China). All contain three or four attenuated IV strains that generate cross-strain protection via the induction of mucosal IgA and lung-localised T cells (26, 240, 241). However, the vaccine is only suitable for ages 2 to 49 years old, and is not recommended for immunocompromised people, pregnant women, asthmatics, or people with other underlying medical conditions. This is because the attenuated strain can lead to secondary effects in these population that have weakened immune system (240, 242, 243). Moreover the efficacy of LAIV vaccines has varied every year ranging from 27% to 65%, between 2015 and 2020, in the UK (41).

Improved or new mucosal influenza vaccines are therefore needed to generate long-lasting protection against multiple IV subtypes, including newly emerging strains and subtypes. Recently, vaccine development has focused on recombinant vaccines using conserved epitopes (244).

The most utilised antigen for vaccines is HA, which generates antibodies that neutralise the virus. HA is formed by a trimer of the variable globular head domain (HA1) and a more conserved stem or stalk domain (HA2) (Fig. 4.1) (245). The head domain mediates binding to sialic acid residues of cell surface glycoproteins expressed by host cells. The stalk domain fuses the viral and endosomal membranes to allow the release of the IV genome into the cytosol. However, due to evolutionary selection pressure, most mutations accumulate in antigenic sites on the globular head domain (246). Vaccines based on the head domain of HA become ineffective when the glycoprotein change (230). Recent studies use the stalk domain to produce cross-protective antibodies that block viral fusion and entry of the viral genome (247-249). Stalk domain antibodies can also inhibit NA by binding close to the enzymatic active site or close to the sialic acid preventing its cleavage (250).

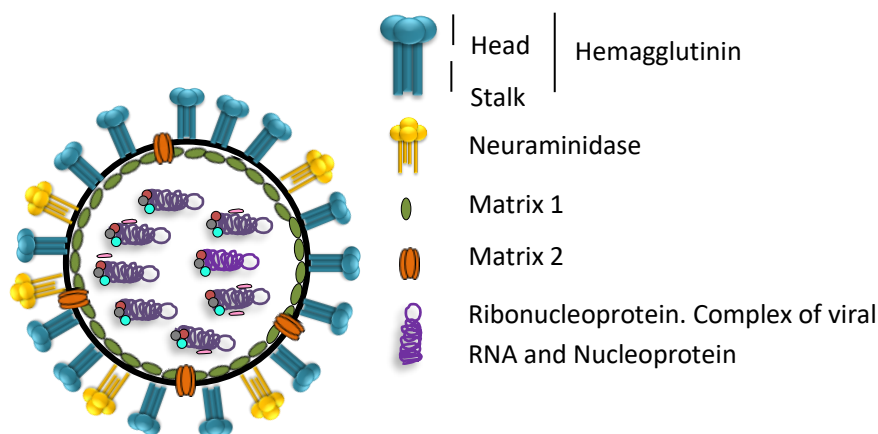


Figure 4.1 Diagram of IV indicating major protein components. The IV genome consists of single-stranded RNA negative-sense genome divided into 8 segments and is surrounded by a lipid envelope. Hemagglutinin, neuraminidase, nucleoprotein, matrix 1, and matrix 2 are the main target antigens proposed for universal vaccines.

Conserved regions of the virus can be used for generating broad-spectrum immunity against different viral strains. The common epitopes can be recognised by the same antibodies and T cells, and therefore an individual who has developed immune responses against one strain may also be able to attack other strains that share epitopes. Hence, by focusing on conserved regions of the virus, it is possible to generate immune responses that can target a broad range of viral strains.

Apart from the stalk or stem domain of the HA, the ectodomain of the ion channel M2 (M2e), the matrix protein (M1) and the Nucleoprotein (NP) are also highly conserved

cross-reactive antigens of IV (251). Amino acids sequences of NP are 90% identical across different strains (252), with their heterosubtypic immunity been attributed to T cells (253). While the stem domain of HA and M2e are accessible to antibodies, the internal proteins of the virus, M1 and NP are mainly targeted by CD4+ T cells and cytotoxic T cells (254-256). CD4+ T cells promote effective antibody responses and cytotoxic CD8+ lymphocytes limit viral replication and shedding by eliminating infected cells. Both cells secrete a variety of inflammatory cytokines such as TNF- α and IFN- γ that promote inflammatory and anti-viral immune responses (257).

In this chapter, we used Bt BEVs as a delivery system to confer protection and enhance the immunogenicity of the conserved stem region of HA and NP from IAV H5N1. By using conserved epitopes, we aimed at generating a broad-protection vaccine that can be effective against different strains that share these conserved epitopes. Moreover, the aim was to produce a broad-protection IAV vaccine that induces both humoral and cellular immune responses at mucosal sites. H5N1 is a highly pathogenic strain for poultry and humans, and it was selected for incorporation into Bt BEVs as an IV vaccine for both hosts.

The aims of this chapter are to:

- Engineer commensal Bt to express IAV HA and NP antigens.
- Assess the capacity of BEVs containing conserved region of HA to activate systemic and mucosal humoral response.
- Assess the capacity of BEVs containing NP to activate a cellular immune response.
- Assess adjuvanticity of WT-BEVs

The goal is to determine the suitability of engineered Bt BEVs containing HA and NP as an influenza vaccine.

After assessing adjuvanticity of WT-BEVs Bt was engineered to produce either the conserved part of HA from the H5N1 subtype, called H5F, or the NP antigen (Fig. 4.2). H5F-BEVs were intranasally administered to mice followed by a challenge with heterotypic IAV H1N1 subtype. Virus titre and antibody levels were analysed. NP-BEVs were intraperitoneally administered to mice and the T cell response was analysed using flow cytometry.

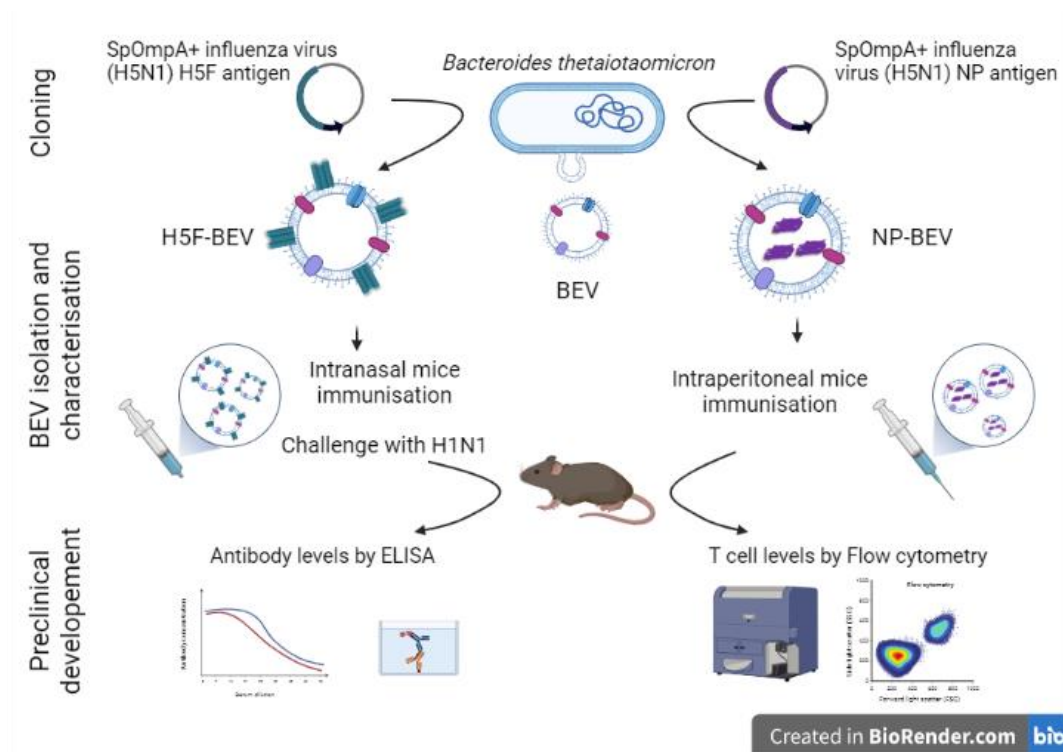


Figure 4.2 Overview of bioengineered Bt BEV as influenza vaccine study design. Created with BioRender.com.

4.2 Results

4.2.1 Adjuvanticity of Bt BEVs

The adjuvant properties of WT-BEVs were investigated by administering $\sim 10^{11}$ WT-BEVs or PBS intranasally to mice. The head and lungs were collected after 5 days and analysed by immunohistology by Dr Anja Kipar (University of Zurich).

The results show that mice receiving WT-BEVs had large organised lymphoid tissue in both the NALT (Fig. 4.3.a) and the BALT (Fig. 4.3.b). By comparison no such structures were seen in PBS administered animals. The enlarged lymphoid tissues contained mainly B cells (CD45R+; clone B220, BD Biosciences) and smaller numbers of T cells (CD3+; clone SP7; Bioscience) and macrophages/dendritic cells (Iba-1+; Wako).

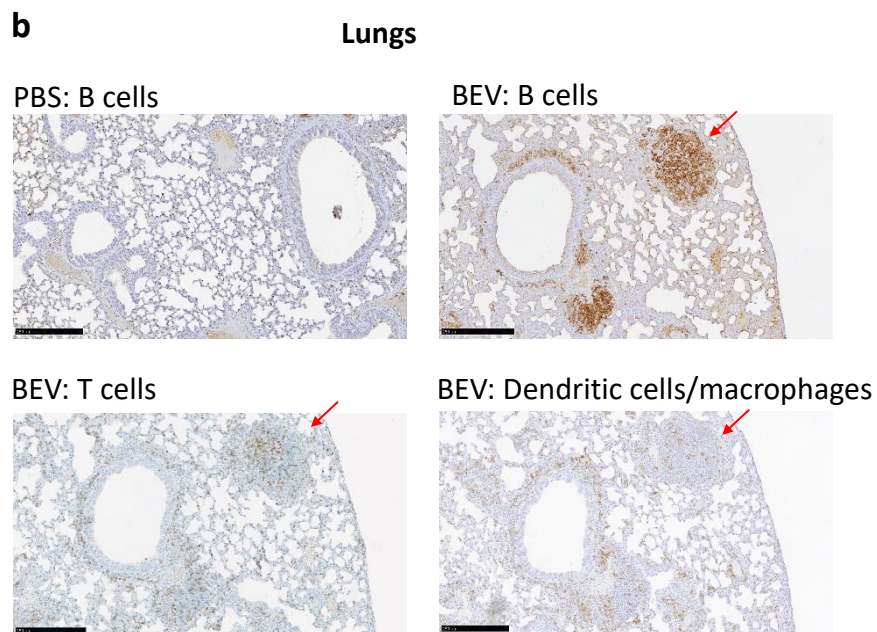
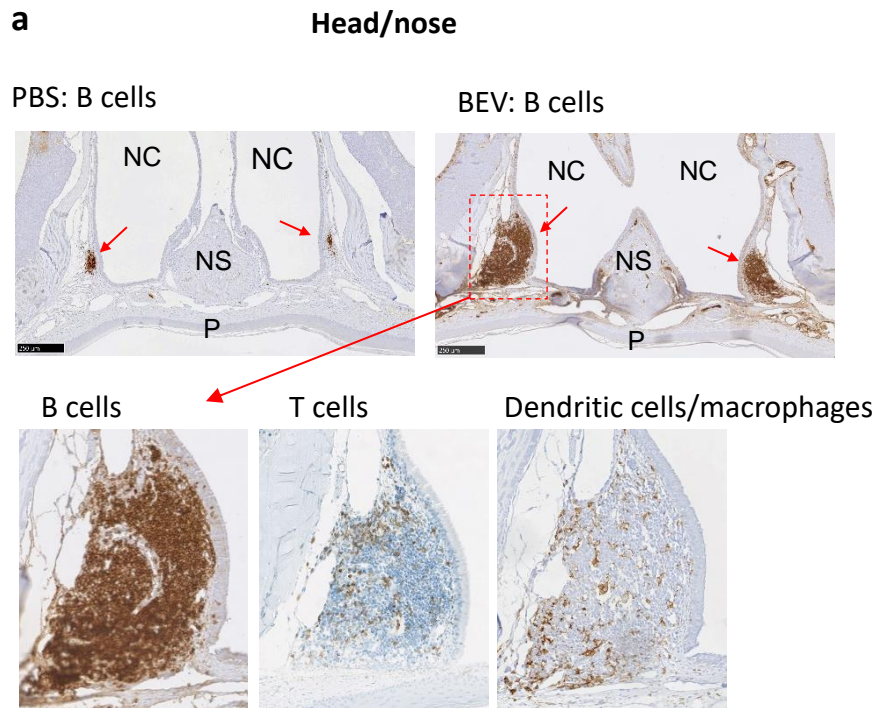


Figure 4.3 Adjuvanticity of Bt BEVs by immunohistology. Mice were intranasally administered with PBS or with 10^{11} WT-BEVs isolated from BHIH media and heads and lungs were collected 5 days later and processed for immunohistology. The tissue samples from NALT (a) and BALT (b) were stained with anti CD45R for B cells, anti CD3 for CD3+ T cells and anti-Iba-1 for macrophages and dendritic cells to visualise immune cell activation. Red arrows indicate nasal-NALT and BALT in a and b respectively. NC: nasal cavity, NS: nasal septum, P: hard palate.

4.2.2 Construction of IV H5F and NP antigen expression vectors

The sequence of the conserved region of the stem domain of HA used was design by Valkenburg et al. (258). The sequence is an epitope focused fragment of the HA of the A/Vietnam/1203/2004(H5N1) strain. The fragment is called H5F, F for fragment, it also contains a N-terminal His-tag. The synthetic genes encoding H5F and NP (Uniprot Reference: Q5EP28 · Q5EP28_9INFA) of the same strain were both fused N-terminally to the signal peptide of Bt OmpA. Furthermore, BspHI and EcoRI restriction enzyme sites were added to SPompa_IAV-H5F and SPompa_IAV-NP at its 5' and 3' ends, TAA was used as a terminal codon and ATG from the restriction enzyme as a start codon. Both sequences were obtained through gene synthesis and cloned into the *E. coli* plasmid pEX-K168 (Eurofins, Germany). SPompa_IAV-H5F and SPompa_IAV-NP were digested and ligated to NcoI/EcoRI-restricted shuttle vector pGH090 resulting in pGH184 and pGH215 respectively. The plasmid was mobilised from *E. coli* into Bt through triparental mating procedure. Finally, the sequence integrities of the cloned fragments were confirmed by DNA sequencing. Dr Udo Wegmann (QIB) produced the H5F construction expression vector, and I produced the NP construction expression vector.

4.2.3 Expression of H5F vaccine antigen in Bt BEVs

The presence of heterologous H5F protein in BEVs could not be detected by immunoblot nor immune-dot-blot using either a commercial anti-his tag antibody or an anti-HA antibody. Instead, detection of H5F was confirmed by proteomics (Proteomics Facility in John Innes Centre, Norwich) using Thermo Orbitrap Fusion LC-MS. The relative abundance position of the protein in the sample was determined using MaxQuant Software in relation to iBAQ algorithm by Gerhard Saalbach (Table 4.1).

Table 4.1 Detection of H5F in H5F-BEVs by proteomics.

Name	Media	Coverage	Relative abundance
Influenza_ H5F	BHIH	44%	223/913

Bt BEVs isolated from BHIH media were analysed by ZetaView, which produced hydrodynamic particle size distribution curves. The size of H5F-BEVs ranged from 50-

200nm, with an average hydrodynamic peak size \pm SD of $100.4\text{nm} \pm 10.8$ for WT-BEVs and $98.88\text{nm} \pm 13.83$ for H5F-BEVs (Fig. 4.4).

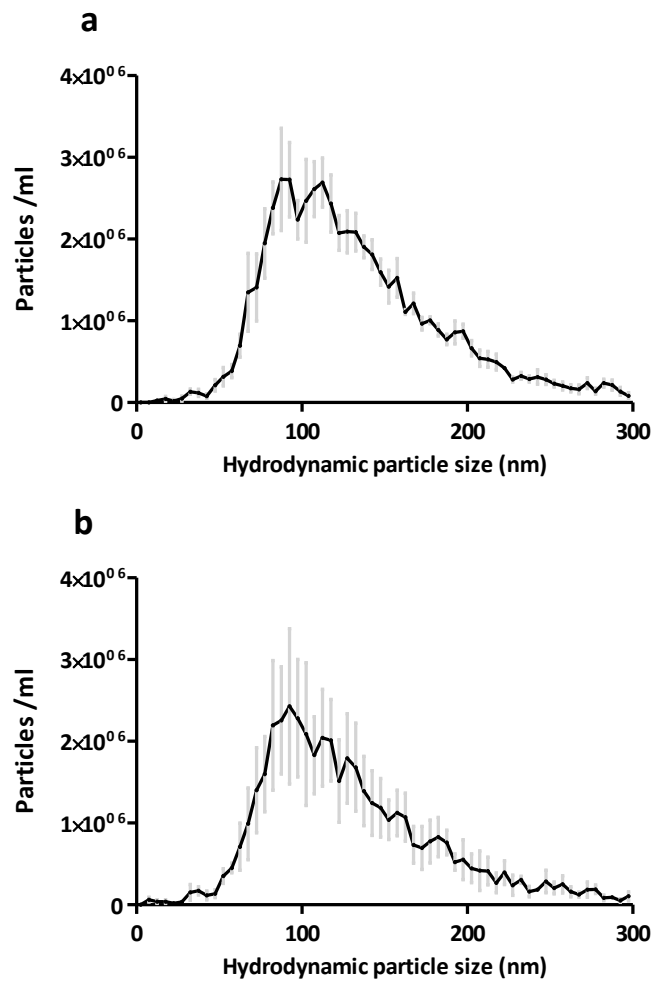


Figure 4.4 Quantification of hydrodynamic particle size of WT-BEVs and H5F-BEVs by NTA. WT-Bt and H5F-Bt were grown in BHIH media, BEVs isolated and (a) WT-BEVs and (b) H5F-BEVs analysed using Zetaview PMX-220 TWIN instrument (Particle Metrix GmbH). Data is represented by the mean value for each value \pm standard deviation from 4 different isolations.

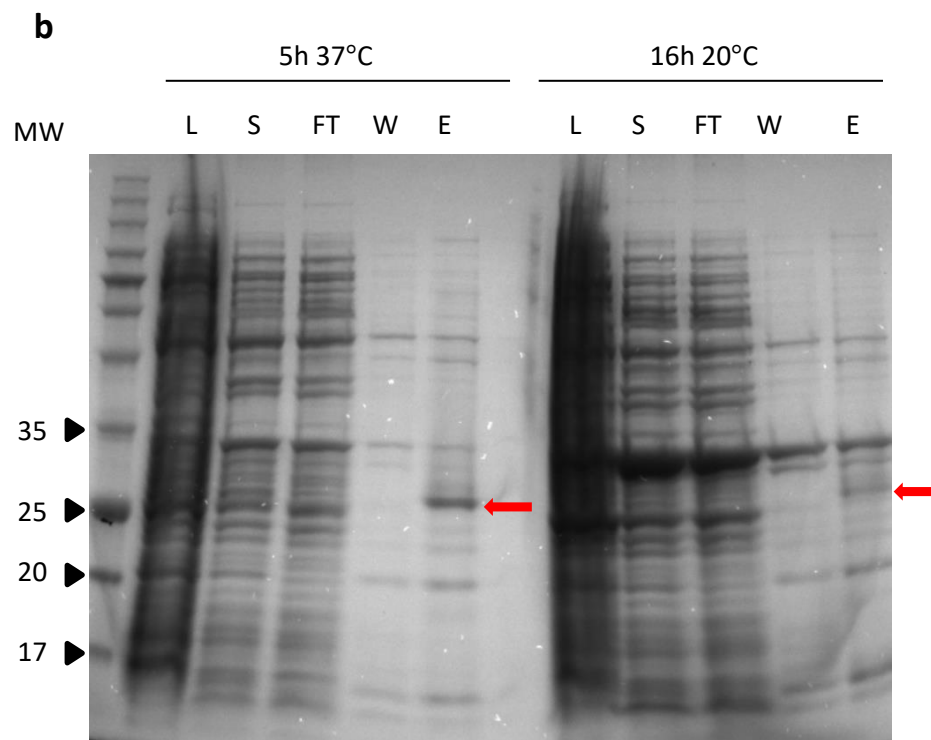
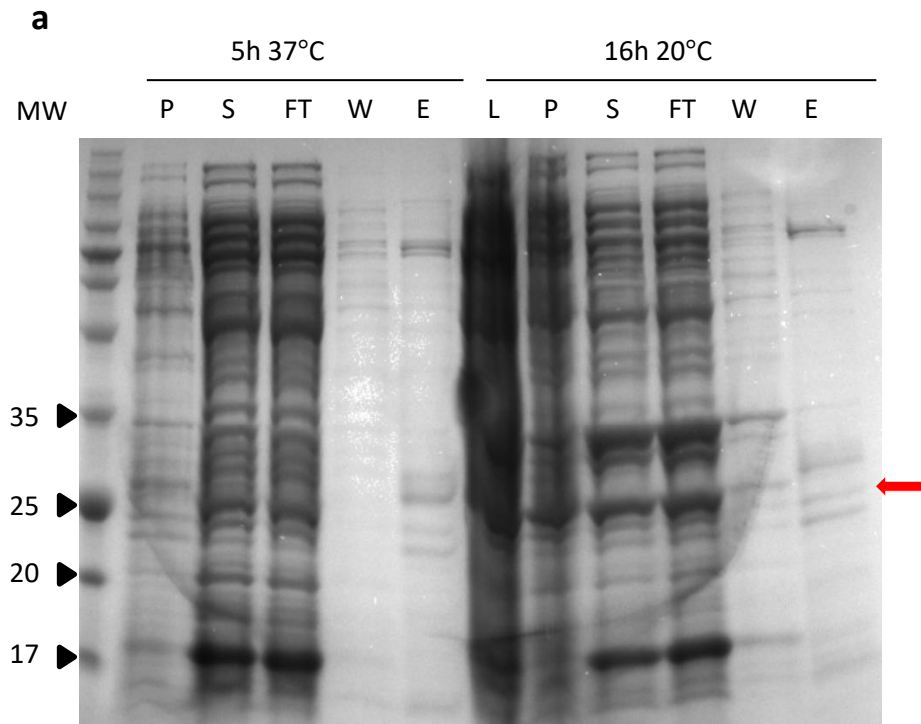
4.2.4 Generating recombinant H5F protein

E. coli was engineered to express recombinant H5F protein for use as a control in immunoblotting and serum H5F antibody detection by ELISA.

H5F cDNA was generated by PCR from SPompa_H5F-pGH090 construct using the following designed primers: -forward-TGACCCATGGATGGGCAGCAGCCACCATCATCATCACCATTC containing NcoI restriction site, MGSS amino acids used by Poon et al. (258) prior to the 6-His sequences to aid with the

solubility of the protein and -reverse- TGACGGATCCTTAAAGAAAC containing BamHI restriction site. The cDNA was cloned into the NcoI/BamHI restriction sites of pET-15b plasmid (Novagen) and transformed to high competent cells DEB DH5 α . After positive colonies were confirmed by sequencing, the plasmid was then transferred to Rosetta2 (DE3) pLysS cells which stabilise pET recombinant encoding proteins that could affect cell growth and viability.

For the H5F extraction and purification, *E. coli*-rH5F was grown in 200ml of LB media at 37°C to an OD₆₀₀ 0.1 with ampicillin and induced at OD₆₀₀ 0.5 with 1Mm IPTG. Cells were harvested either after 5h of induction at 37°C or 16h of induction at 20°C, separated by centrifugation, and kept at -20°C. Proteins from both cultures were purified using Ni-NTA columns under native conditions and eluted using imidazole gradient (Fig. 4.5.a) and under denaturing conditions using urea and eluted with pH gradient (Fig. 4.5.b). The different fractions collected were analysed by SDS gel electrophoresis (Fig. 4.5). The results show a more intense band, at the expected size 25kDa, in samples from the culture induced for 5h at 37°C and purified under denaturing conditions and these conditions were selected for the next extractions. As other proteins besides the expected H5F were observed in the elute, an extra washing step was added during purification under denaturing conditions. The extra wash successfully decreased unwanted proteins (Fig. 4.5.c). The concentration of recombinant protein isolated was 0.14mg/ml, as determined by nanodrop at 280nm, and had the expected molecular weight in immunoblots detected using a monoclonal anti-histidine antibody (Fig. 4.5.d).



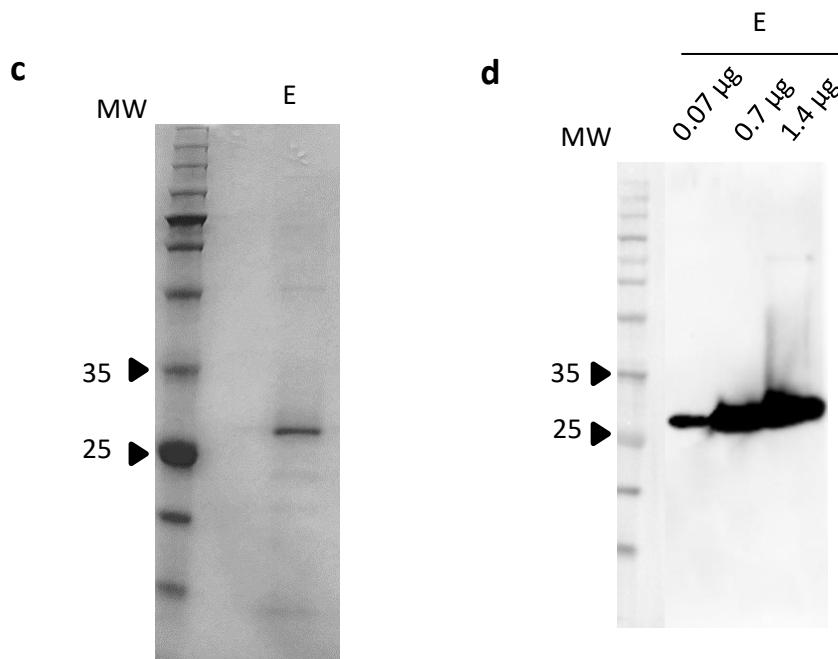


Figure 4.5 Production of recombinant H5F. SDS gel electrophoresis of recombinant H5F purified using Ni-NTA columns under native conditions (a) or denaturing conditions (b) induced for 5h at 37°C or 16h at 20°C. Elute obtained under denaturing conditions using an extra washing step (c). Immunoblot of recombinant eluted proteins using a monoclonal anti-histidine antibody (Sigma #H1029) (d). Molecular weight (MW) expressed in kDa. Red arrows indicate expected size of H5F. P: pellet, L: *E. coli* lysate S: supernatant, FT: flow through, W: wash, E: eluate.

4.2.5 H5F-BEVs immunisations

The selected animal model for this study were mice. Ferrets are the preferred animal model to study transmission and susceptibility to infection with human IV (259). However, mouse models are more convenient for preliminary vaccines studies for their relative low cost, ease of handling and the availability of reagents to assess immune responses (260). For this study, mice were kept and used at the animal facility at the University of Liverpool.

Mice were immunised intranasally with either H5F-BEVs, WT-BEVs or PBS and received a booster immunisation after 14 days (Fig. 4.6). BEVs were isolated from Bt grown with BHIH media and purified using the protocol described in the Materials and Methods section. All animals were immunised with 70µg of BEVs total protein (Bradford assay) which equated to approximately 10^{11} BEVs. On day 28, animals were challenged with a 10-fold lethal dose of a mouse adapted A/Puerto Rico/8/1934 (H1N1) strain. Animal weight

was assessed daily for 5 days after the challenge and blood, BAL and lungs were collected on day 33 (Figure 4.6).

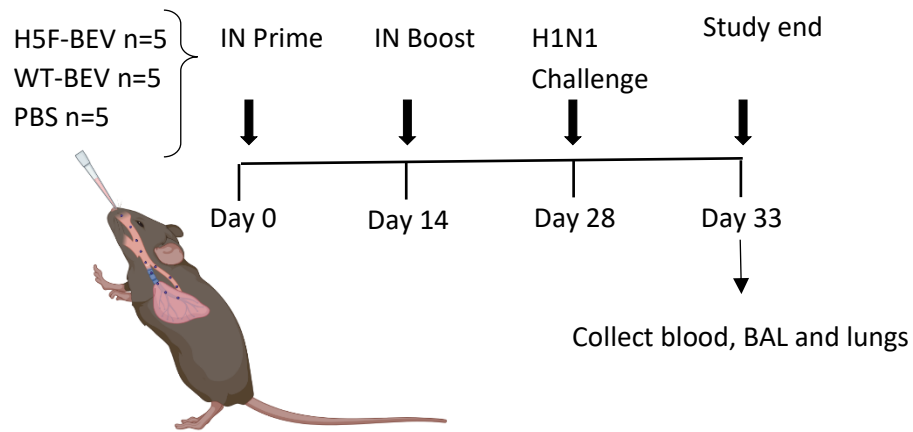


Figure 4.6 Animal study to determine flu protection from H5F-BEVs vaccination. C57BL/6 male mice were immunised intranasally with 70µg of H5F-BEVs, WT-BEVs or PBS and boosted after 14 days. On day 28th all mice were challenged with a 10-fold lethal dose of IAV strain A/Puerto Rico/8/1934 (H1N1). Mice weight were assessed daily after the challenge and at necropsy on day 33rd blood, BAL and lungs were collected.

Table 4.2 Characteristics of BEV vaccines used for IAV lethal challenge experiment.

Media	SEC	Concentration / dose	Route
BHIH	No	70µg/ ~10 ¹¹ BEVs	IN

4.2.6 Host response to H5F-BEVs

H5F-BEVs immune response was evaluated by measuring IAV-specific IgG in serum and IgA in BAL. Antibody titres, weight loss and viral titre were determined at the University of Liverpool by Prof James Stewart and Dr Eleanor Bentley using commercial sources of capture and detection antibodies and commercial protein antigen H5F or UV-treated viruses. Commercial HA protein was used as the protocol for the generation of recombinant H5F protein that I was developing was still being optimised when the experiment started. A reference serum from mice infected with H1N1 was used as a positive control.

H5F-BEVs induced higher levels of serum IAV IgG compared to PBS ($p < 0.05$) (Fig. 4.7.a). IAV-specific IgG levels in BAL were between two to four times higher in mice immunised with WT-BEVs or H5F-BEVs ($p < 0.01$) compared to mice receiving PBS (Fig. 4.7.b). In both cases, antibody levels in immunised mice were lower than those in the reference serum. Regarding mucosal antibodies, mice immunised with H5F-BEVs had levels of IgA in BAL with a mean absorbance at 450nm of 0.4, similar to the positive control and higher than the 0.2 value seen in mice immunised with WT-BEVs or 0.1 value in PBS administered mice (Fig. 4.7.c). Levels of H5-specific IgA in BAL were also higher in H5F-BEV immunised animals compared to the other groups ($p < 0.05$) (Fig. 4.7.d). In this case, the positive reference serum had a signal comparable to the one induced by PBS showing that the reference serum H1N1-infected mice had developed anti-H1 antibodies but not anti-H5 antibodies. Contrarily, H5F-BEVs induced antibodies against homologous H5 and heterotypic H1 molecules.

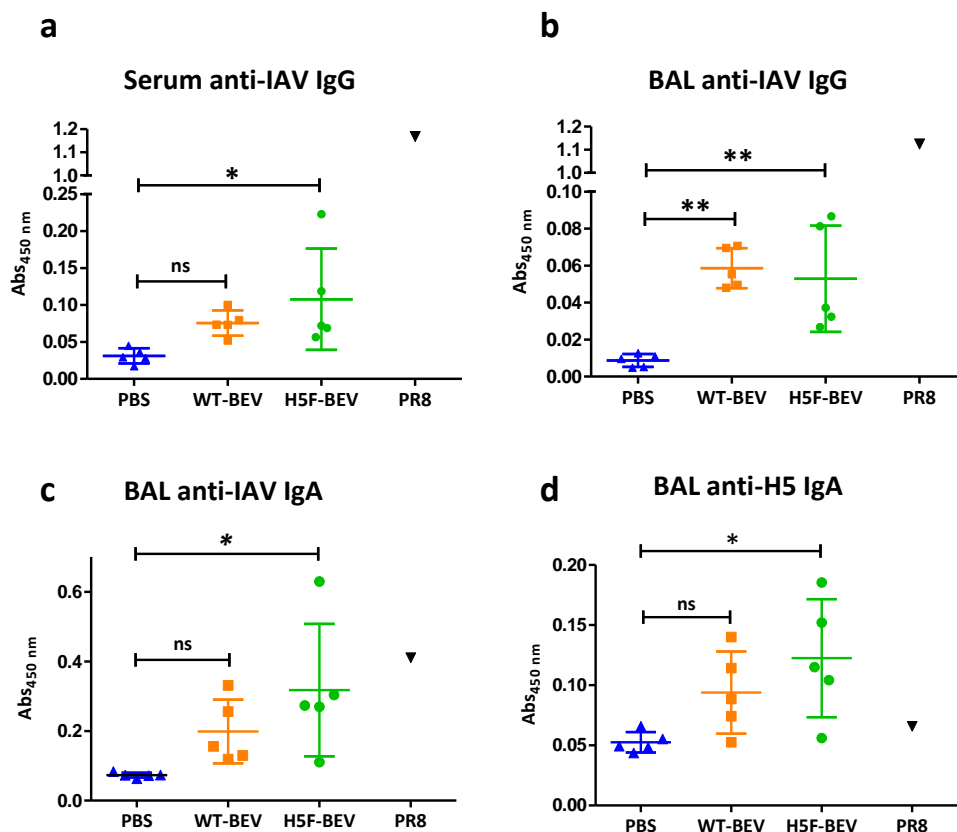


Figure 4.7 Quantification of antibodies to IAV and H5 by ELISA. Mice were intranasally immunised with H5F-BEVs, WT-BEVs or PBS, boost after 14 days and challenged on day 28th with a 10-fold dose of IAV strain A/PR/8/34 (PR8, H1N1). At the endpoint, blood (a) and BAL (b, c) were analysed by ELISA using UV-inactivated IAV PR8-H1N1 to coat the plates. BAL was also analysed for H5 HA-specific IgA by ELISA plates coated with H5 HA recombinant protein (P5060, 2B Scientific Ltd). Data

represented by the mean value of each group \pm standard deviation. Statistical analysis was performed using one-way ANOVA with Bonferroni multiple comparison post-test. * <0.05 ; ** <0.01 .

During infection, the weight loss of each mouse was recorded. The mice group that received PBS had the greatest weight loss compared to the other groups, having lost around 20% of their body weight (Fig. 4.8). Animals immunised with H5F-BEVs or WT-BEVs lost weight more gradually reaching a loss of 10% of their body weight pre-challenge. Animals immunised with the H5F-BEVs had no further decline between day 4 and day 5 post-infection (Fig. 4.8).

The viral lung titre from animals immunised with H5F-BEVs was significantly lower than the other groups being 7 to 8-fold lower in mice immunised with H5F-BEVs than those receiving PBS. The virus titre of mice immunised with WT-BEVs was comparable to mice receiving PBS, except for one mouse that had levels similar to mice receiving H5F-BEVs (Fig. 4.8).

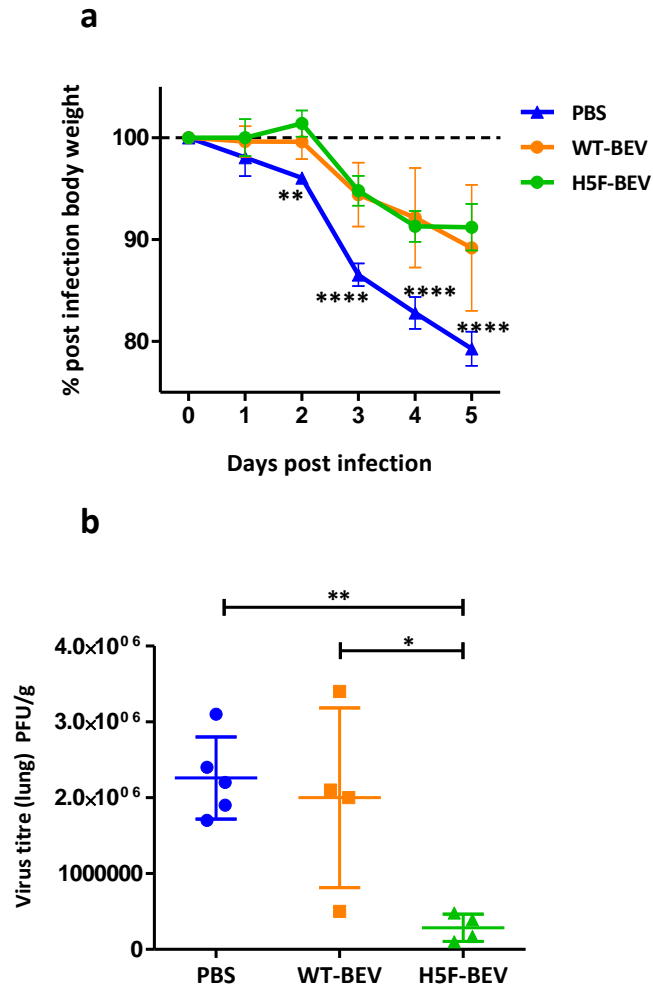


Figure 4.8 Host response to H5F-BEV vaccine. Mice were intranasally immunised with H5F-BEVs, WT-BEVs or PBS, boost after 14 days and challenge on day 28th with a 10-fold dose of IAV strain A/PR/8/34. (a) weight of animals was recorded every day after challenge. (b) viral load (PFU/g) of lung tissue was assessed in lung homogenates. Data represented by the mean value of each group \pm standard deviation. Statistical analysis was performed using two-way ANOVA with Bonferroni post-test (a) or one-way ANOVA with Bonferroni multiple comparison post-test (b). * <0.05 ; ** <0.01 ; *** <0.001 ; **** <0.0001 .

4.2.7 Bt Growth Media Optimisation

BHIH was used in the H5F-BEVs as is a rich medium that provides Bt an optimal environment for growth. However, human vaccines should not contain animal products to avoid adverse reactions and address ethical and religious considerations. BHIH was therefore replaced with chemically defined Bacteroides defined media (BDM) for producing BEVs. As the BDM that was previously used contained Hemin, which comes from bovine or porcine origin, a modified BDM, with Protoporphyrin IX instead of Hemin,

was created called BDM+. Protoporphyrin IX is the iron-free form of the heme and precursor of heme. The media was also supplemented with iron (II) sulphate heptahydrate and Vitamin K3 analogue menadione, as it enhances Bt growth (261-263). A table comparing BDM and BDM+ can be found in Table 2.2 in the materials and methods section.

Vitamin B12 replaced L-methionine at the suggestion of Dr Rokas Juodeikis. Vitamin B12 acts as a cofactor for methionine synthase, which converts homocysteine to methionine, that is essential for bacterial growth. Bt BEVs contain vitamin B12 receptors for capturing and transporting vitamin B12 (106). The use of L-methionine instead of vitamin B12 ensures that the BEVs produced and used as a vaccine do not contain any bound vitamin B12.

Other benefits of BDM+ media are that all the exact chemical ingredients are known and can be adapted and changed accordingly, unlike the BHIH, which is a complex media that can have variation batch to batch. Additionally, the chemically defined media contains minimal particle counts, contrarily to BHIH media, that contain microvesicles that can copurify with BEVs (87).

During optimisation of BDM, Bt was grown in BHIH, BDM, and BDM+ and growth curves were analysed over time (Fig. 4.9). Bt was inoculated at a starting OD_{600} of 0.05, for all three cultures. Bt reached stationary phase of OD_{600} 3 after 7h in BHIH media at which time BDM and BDM+ media cultures were still in exponential phase. In BDM+ media the lag phase was shortened compared to BDM media and the culture reached an OD_{600} of 4 at 12h while the culture in BDM had a long exponential phase reaching OD_{600} 2.7 after 18h.

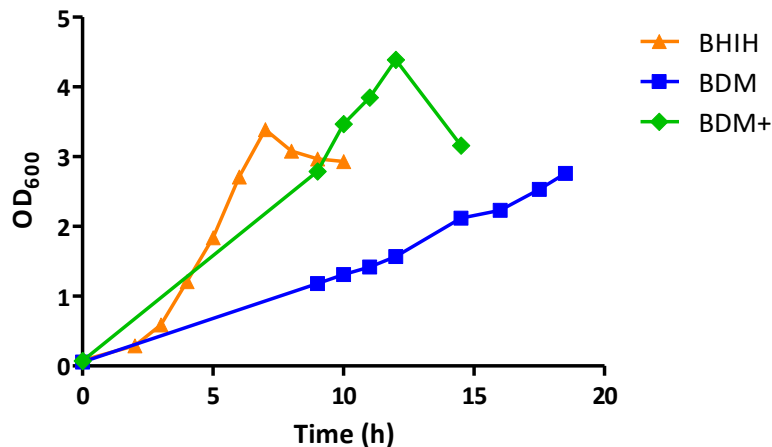


Figure 4.9 Growth curves of Bt cultured in BHIH, BDM, or BDM+ media. WT-Bt was grown in the three different media starting with an OD₆₀₀ of 0.05 and readings of OD₆₀₀ were taken at different time points.

As an indication of immune reactivity change of BEVs THP1 cells were used. THP1-Blue NF-κB cells (Invivogen) are cells used for monitoring NF-κB signal transduction pathway in modified human THP1 monocyte cell. The cells have an integrated NF-κB-inducible secreted embryonic alkaline phosphatase (SEAP) reporter construct. As a result, THP1-Blue cells allow the visualisation of NF-κB signal transduction activation, seen as the production of a chromogenic (blue) product measurable by spectrophotometer. The assay was realised by Dr Sonia Fonseca and the detailed protocol can be found in Fonseca et al. 2022 (120).

The results show no significant difference in the scores in any of the samples showing equivalent ability to activate human macrophages (Fig. 4.10).

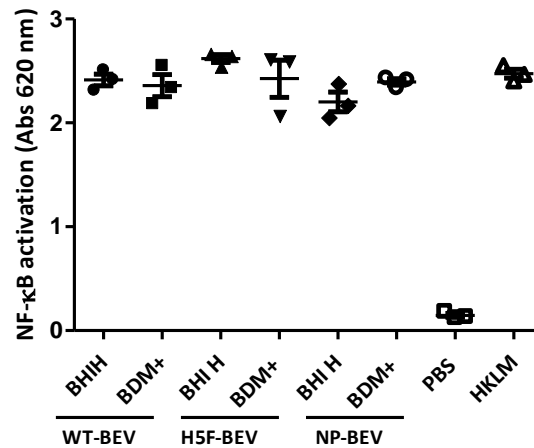


Figure 4.10 Activation of NF-κB by BEVs isolated from BHIH and BDM+ media using THP1-Blue cells. WT-BEV, H5F-BEV or NP-BEV were isolated and cultured at 20 BEV/cell with THP1-Blue NF-κB cells for 24h at 37°C and 5% CO₂. PBS and heat killed *Listeria monocytogenes* (HKLM) were used as a control.

4.2.8 Expression of NP vaccine antigen in Bt BEV

The presence of NP in BEVs isolated from either BHIH or BDM+ media was confirmed by immunoblotting (Fig. 4.11). Approximately 10^{11} NP-BEVs, 0.5μg of total protein cell extract and NP at three different concentrations were loaded onto SDS gels. Recombinant NP was detected in the gel using a mouse anti-influenza nucleoprotein antibody at the anticipated molecular weight of 58.1 KDa. NP was identified in the cell extracts of Bt-NP and in NP-BEVs isolated from both BHIH and BDM+ media but not in the WT cell extract or WT-BEVs. Additional non-specific bands were present in the immunoblot, particularly in BHIH-derived samples. Samples prepared from BDM+ media showed a higher band intensity than those prepared in BHIH. Based on the intensity of the antibody-reactive bands, it was calculated that there were approximately 275ng and 33ng of NP in 10^{11} NP-BEVs prepared in BDM+ and BHIH media, respectively.

Luminal versus outer membrane distribution of NP in NP-BEVs was established using a proteinase K protection assay. Intact NP-BEVs or NP-BEVs solubilised in 1% SDS were incubated with proteinase K prior to immunoblotting. A band corresponding to the expected size of NP was seen in BEVs incubated with proteinase K but was absent when SDS was added, consistent with NP being localised to the lumen of NP-BEVs.

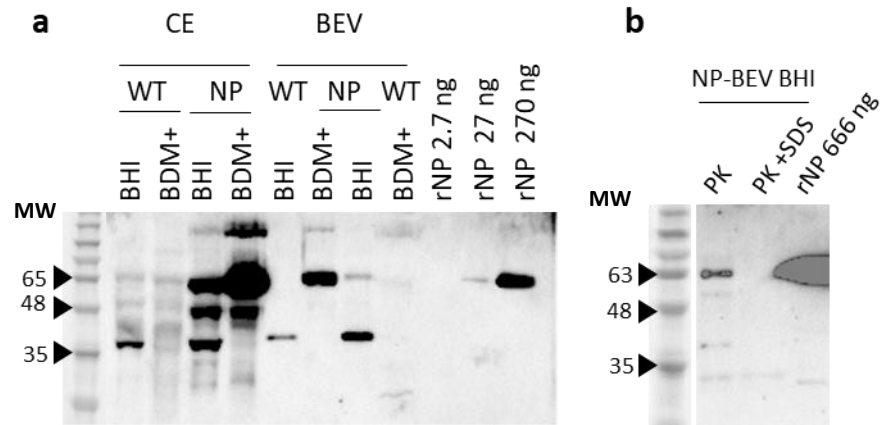


Figure 4.11 Detection of NP in NP-BEV by immunoblotting. Bt strains were grown in BHIH and BDM+ media and BEVs isolated following a method described in the materials and methods chapter. (a) Immunoblot of different samples of cell extract (CE) or BEVs from WT or Bt-NP (NP) grown in BHIH or BDM+. Recombinant NP (rNP) was used at different concentrations as a positive control. (b) Determination of protein location in BEVs by treating with proteinase K (PK) alone or with 1% SDS. Molecular weight (MW) expressed in kDa.

The presence of NP in NP-BEVs was also confirmed by proteomics (Proteomics Facility, John Innes Centre, Norwich) using Thermo Orbitrap Fusion LC-MS (Table 4.3). NP had a coverage of 69% and 66% and appeared in the 21st and 22nd position in relative abundance in NP-BEVs samples isolated from BDM+ with or without size exclusion chromatography (SEC) purification, respectively. SEC was included in the isolation and purification protocol to enhance the purity of crude BEVs extractions, remove unwanted free proteins, and increase the reproducibility of samples. The addition of SEC purification did not alter the concentration of NP expressed in NP-BEVs based on the relative abundance determined by Orbitrap mass spectrometry.

Table 4.3 Detection of NP in NP-BEV by proteomics

Name	Media	Coverage	Relative abundance
Influenza_ Nucleoprotein	BDM+	69%	21/558
Influenza_ Nucleoprotein	BDM+ with SEC	66%	22/738

The size and concentration of isolated BEVs from BDM+ media with SEC purification were determined by NTA using ZetaView PMX-220 TWIN instrument (Particle Metrix GmbH). BEVs from WT-Bt and engineered Bt expressing NP showed a similar hydrodynamic size distribution with an average peak \pm SD of 101.3nm \pm 26.3 for WT-BEVs and 105nm \pm 22.5 for NP-BEVs (Fig. 4.12).

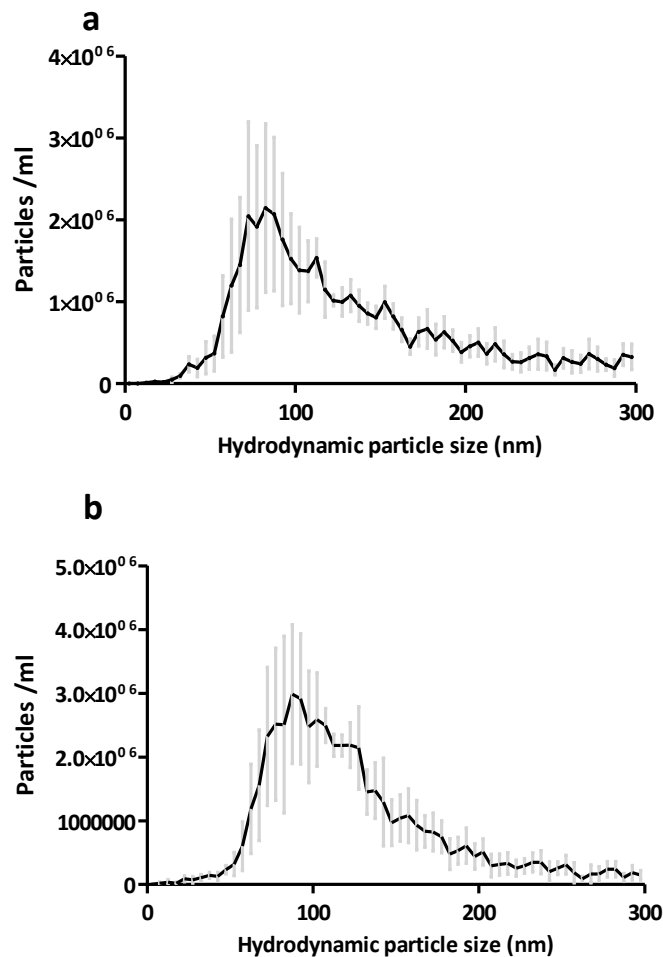


Figure 4.12 Quantification of hydrodynamic particle size of WT-BEVs and NP-BEVs by NTA. WT-Bt and NP-Bt were grown in BDM+ media, BEVs isolated, SEC purified and (a) WT-BEVs and (b) NP-BEVs analysed using Zetaview PMX-220 TWIN instrument (Particle Metrix GmbH). Data is represented by the mean value for each value \pm standard deviation from 5 different isolations.

4.2.9 Optimisation of T cell flow cytometric assay

Flow cytometry was used to analyse the T cell response against BEVs vaccines. A panel of antibodies was designed to identify live cells, CD45+, CD3+, CD4+ or CD8+ T cells expressing IFN- γ and TNF- α . Optimal concentration of antibodies was determined from antibody titration experiments and calculating the separation between the positive and the negative peak by the Separation Index (SI). The SI was calculated by the equation below, derived from the fluorescence intensity of the antibody staining using FlowJo v.10. The higher the SI value, the greater the separation between the positive and the negative populations is.

$$\text{Separation Index} = \frac{\text{MedianPositive} - \text{MedianNegative}}{84\% \text{ Negative} - \frac{\text{MedianNegative}}{0.995}}$$

Based on the results in Figure 4.13, the optimal concentration of antibody was chosen based upon a compromise between the best SI and lowest antibody usage: 0.4 μ g/ml for CD45, 2 μ g/ml for CD3, 0.6 μ g/ml for CD4, 1 μ g/ml for CD8, 2 μ g/ml for IFN- γ , 2 μ g/ml TNF- α and 1:400 dilution for NIR.

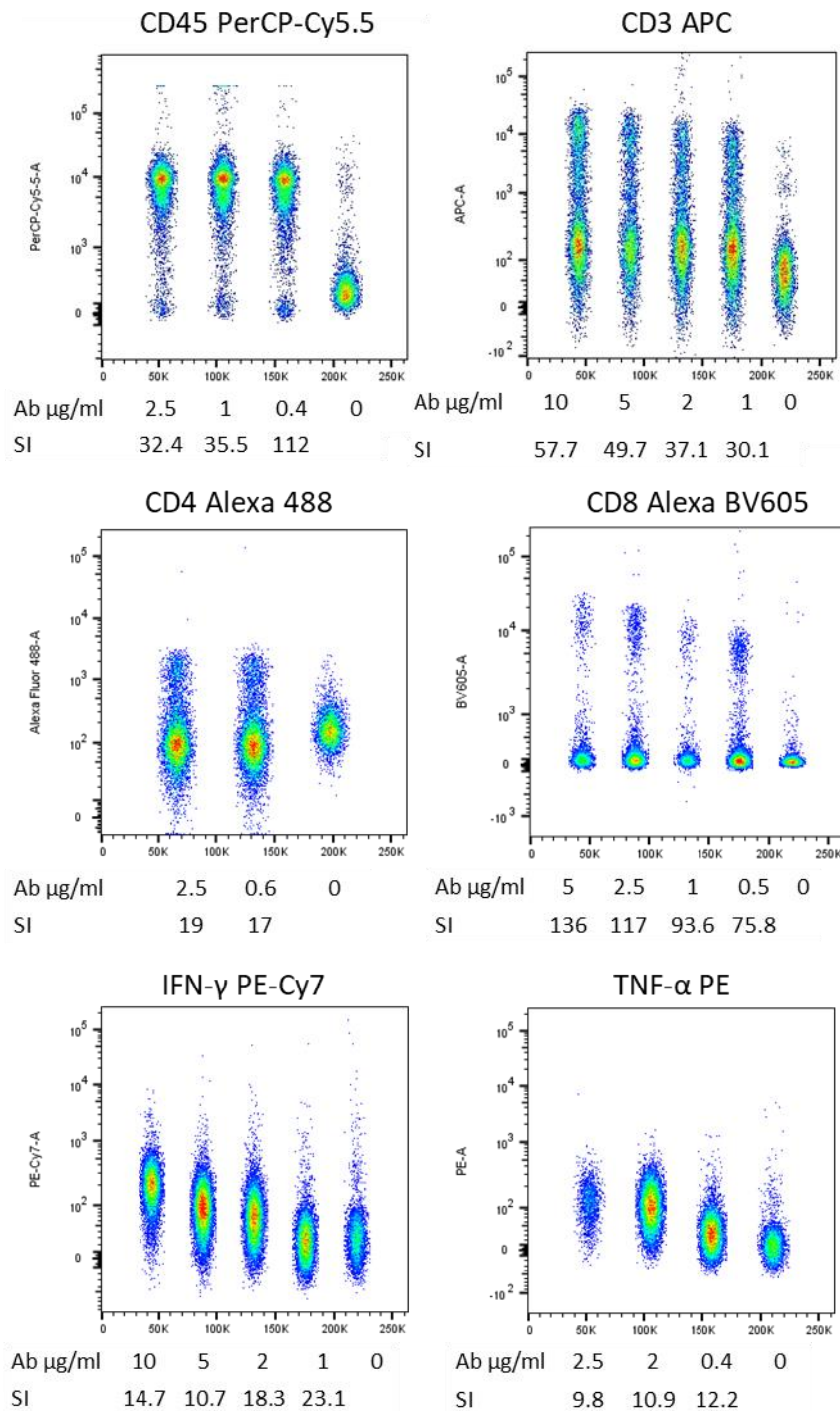


Figure 4.13 Concatenated data of splenocytes against different concentration of antibodies and SI analysis by flow cytometry. Isolated splenocytes from mice were stained with NIR and either anti-CD45 PerCP-Cy5.5, anti-CD3 APC, anti-CD4 Alexa 488, anti-CD8 Alexa BV605 for 30 minutes on ice or IFN PE-Cy7 or TNF-PE for 30 minutes after fixing and permeabilising the cells. After gating out dead cells, the positive and the negative peaks were manually selected, and the SI was analysed by FlowJo.

4.2.10 NP-BEV Immunisations

Animal experiments were done with 6 to 8 week old C57BL/6 male mice to analyse whether NP-BEVs could induce a cellular response. Mice were bred and maintained in the Disease Modelling Unit (DMU) at the University of East Anglia and vaccination and sample collections was carried out by Drs Aimee Parker and Sonia Fonseca.

Previous experiments done with Bt BEVs in an independent dose response study showed that a 10^9 dose elicited high immunogenicity. Therefore, 10^9 and 10^{10} doses of BEVs were analysed here in two different experiments. IP administration of the vaccines was done prior to IN delivery to assess the vaccine immunogenicity. In experiment one, three groups of 3-6 mice were immunised IP with 10^9 WT-BEVs, 10^9 NP-BEVs or with $1\mu\text{g}$ of recombinant NP (Fig. 4.14). In the second experiment, two groups of mice received either 10^{10} WT-BEVs or 10^{10} NP-BEVs. Both experiments consisted of a single immunisation and mice were sacrificed after 14 days to collect serum and spleens

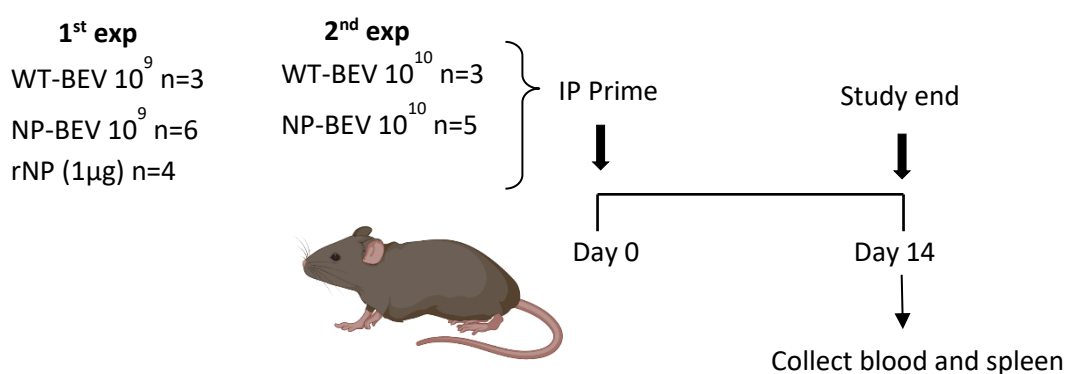


Figure 4.14 Animal studies to determine immune response of NP-BEVs vaccination. C57BL/6 male mice were immunised intraperitoneally (IP) with 10^9 WT-BEVs, 10^9 NP-BEVs or $1\mu\text{g}$ rNP in the first experiment and with 10^{10} WT-BEVs and 10^{10} NP-BEVs in the second experiment. In both experiments blood and spleen were collected after 14 days at the study end.

Table 4.4 Characteristics of BEV vaccines used for NP-BEVs experiments

Experiment	Media	SEC	BEVs dose	Route
1	BDM+	YES	10 ⁹	IP
2	BDM+	YES	10 ¹⁰	IP

4.2.11 Host response to NP-BEVs

Serum antibody responses to NP-BEVs was evaluated by measuring antigen-specific IgG levels in serum of immunised animals by ELISAs (Fig. 4.15). There were no significant differences in the levels of anti-NP IgG seen in animals immunised with NP-BEVs versus WT-BEVs or rNP in either experiment.

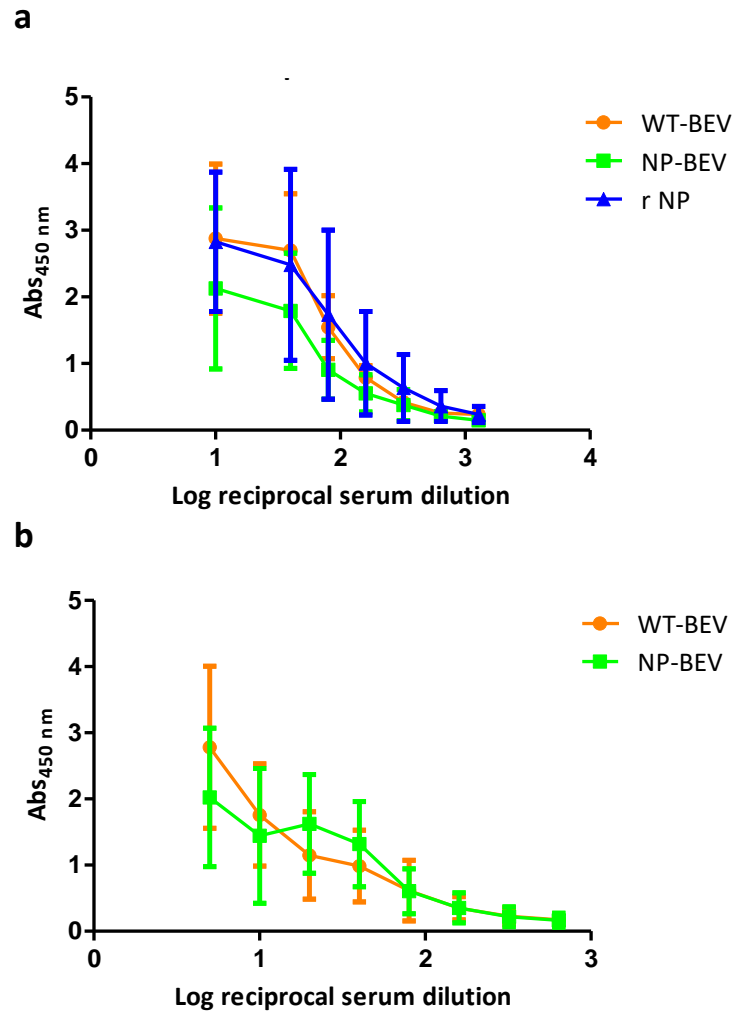


Figure 4.15 Quantification of antibodies to NP by ELISA. Mice were immunised IP with 10^9 WT-BEVs, 10^9 NP-BEVs or $1\mu\text{g}$ rNP in the first experiment (a) and with WT-BEVs 10^{10} or NP-BEVs 10^{10} on the second experiment (b). Blood was collected and analysed on day 14. Data represented by the mean value for each group $n=3-6 \pm$ standard deviation. Statistical analysis was performed using two-way ANOVA with Bonferroni post-test

BEVs vaccine induction of T-cell responses was analysed by intracellular staining for TNF- α and IFN- γ production by CD4+ and CD8+ T cells after restimulation *ex vivo* with antigens. Splenocytes from vaccinated mice were cultured *ex vivo* with either media as a negative control or media containing rNP ($5\mu\text{g}/\text{ml}$).

In the first experiment, cells were restimulated for 6h, and the Golgi transport inhibitor brefeldin A (BFA) was added after 1h of induction to accumulate intracellular cytokines in the cells. After, stimulation cells were stained, analysed, and gated as described in the Materials and Methods section. The results show that mice receiving WT-BEVs, NP-BEVs or rNP had similar levels of CD4+ and CD8+ T cells expressing TNF- α (Fig.

4.16). Mice receiving WT-BEVs had higher levels of CD8+ TNF- α compared to mice immunised with NP-BEV when restimulated with rNP ($p < 0.05$). The levels of CD4+ or CD8+ T cells expressing IFN- γ were significantly higher for mice immunised with WT-BEV compared to mice receiving rNP ($p < 0.05$ for CD4+ and $p < 0.01$ for CD8+) (Fig. 4.16.c.d). Similarly, CD4+ or CD8+ T cells expressing both TNF- α and IFN- γ from WT-BEVs immunised animals, and cultured in media alone, had double the level of cytokine expressing cells compared to the other groups (Fig. 4.16.e.f). In all three vaccinated groups, stimulation of cells by rNP had only a marginal effect on the levels of cytokine-expressing T cells (Fig. 4.16).

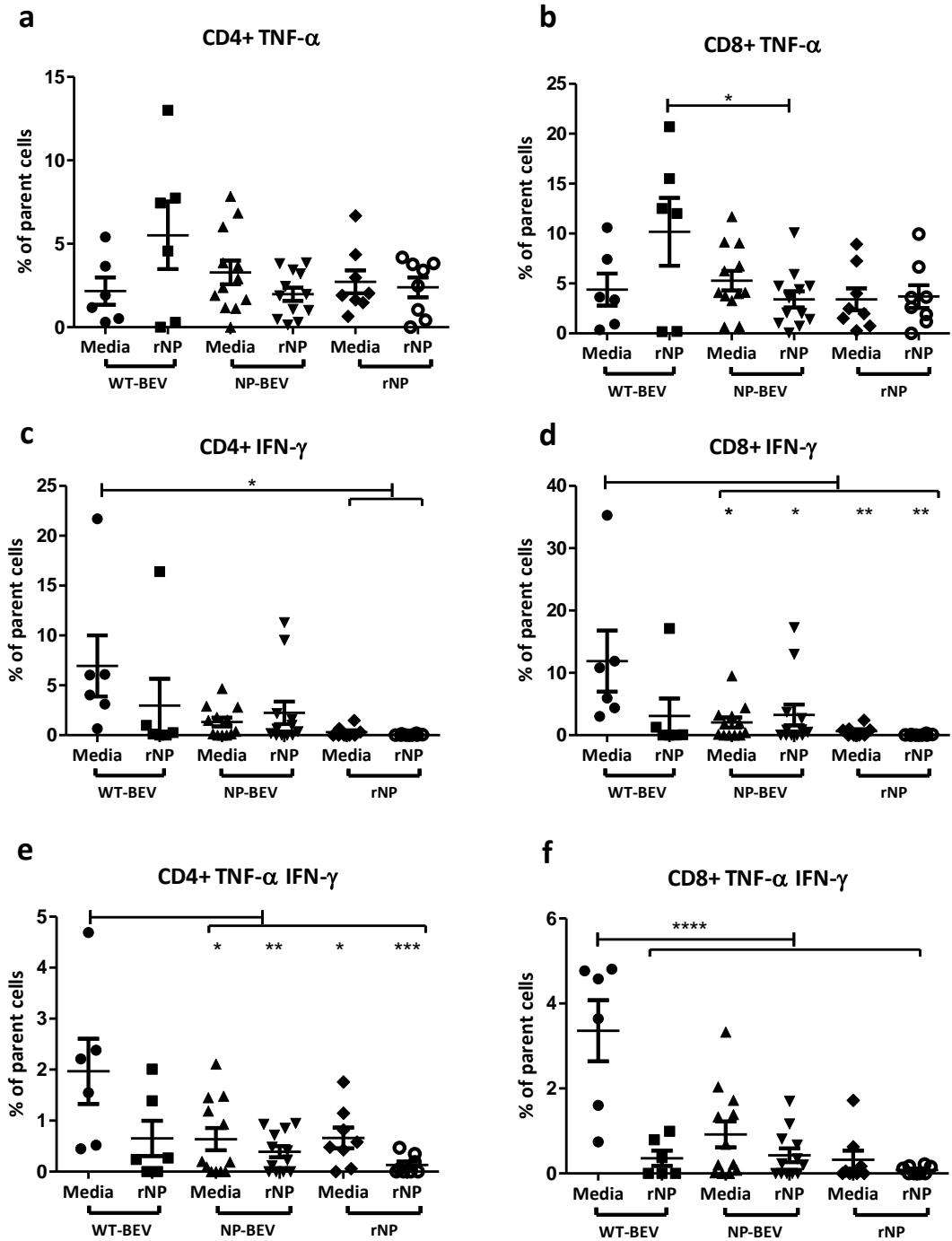


Figure 4.16 Frequency of CD4+ and CD8+ T cells expressing TNF- and/or IFN- from splenocytes from first NP-BEVs experiment by flow cytometry. Mice were immunised with WT-BEVs, NP-BEVs or rNP, splenocytes collected at day 14 and analysed following a stimulation *ex vivo* with media or rNP for 6h. Data represented by the mean value for each group $n=3-6 \pm$ standard deviation with two technical replicates. Statistical analysis was performed using one-way ANOVA with Bonferroni post-test. * <0.05 ; ** <0.01 ; *** <0.001 ; **** <0.0001 .

In the second experiment, the concentration of stimulant rNP was increased to 10µg/ml. Additionally, other stimulants (WT-BEVs and NP-BEVs (200 BEV/Cell)) were included in an attempt to optimise detection of cytokine producing T cells. The pre-stimulation period was increased to 21h with BFA added on the last 5h. Rat serum was also included in the intracellular staining protocol to reduce unspecific binding.

The increased incubation time resulted in more than 40% higher amounts of cell death and debris compared to experiment one as determined by the average percentage of cell versus debris observed by FlowJo in side scatter (SSC) against forward scatter (FSC) gating. Adding rat serum in the staining protocol decreased non-specific binding. This was observed by the reduction in signal using isotype matched control antibodies which made the gating strategy more reliable.

After the debris was gated out, cells were gated for live/dead (Materials and Methods). In splenocytes stimulated with Cell Activation Cocktail (CAC) containing PMA and ionomycin, which is the positive control used, the percentage of live cells was more than double than the negative control, which is a mix of splenocytes from both immunisation groups with media as stimulant (Fig. 4.17). Two groups that also showed a significant difference between the negative control group were cells from mice immunised with WT-BEVs and NP-BEVs stimulated with WT-BEVs, ($p < 0.05$ and $p < 0.01$, respectively). Cells stimulated with rNP or NP-BEVs had similar levels of live cells compared to groups cultured with media alone.

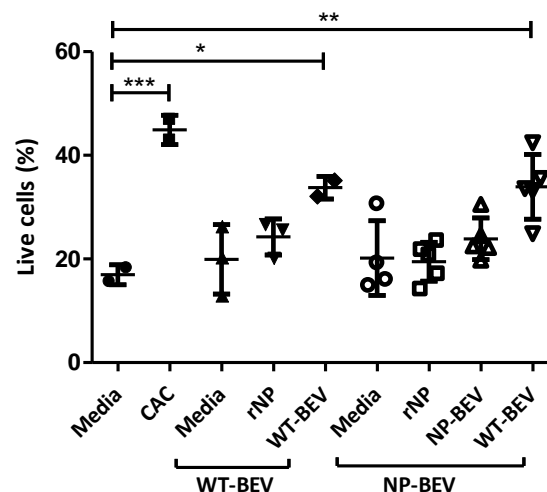


Figure 4.17 Percentage of live cells from splenocytes stained with live/dead NIR from the second NP-BEVs experiment by flow cytometry. Splenocytes from mice immunised with WT-BEVs or NP-BEVs were stimulated with media, CAC, rNP, WT-BEVs or NP-BEVs for 21h. Cells were stained with

live/dead staining and quantified by flow cytometry. Data represented by the mean value for each group $n=3-5 \pm$ standard deviation. Statistical analysis was performed using one-way ANOVA with Dunnett post-test comparing all columns versus media stimulated control group. * <0.05 ; ** <0.01 ; *** <0.001 .

The levels of CD4+ or CD8+ expressing TNF- α and/or IFN- γ were not significantly different between WT-BEVs and NP-BEVs immunisation groups (Fig. 4.18). The cytokine levels in both immunisation groups were also comparable using different cell stimulants (Media, rNP, WT-BEVs, NP-BEVs), analogous to experiment one.

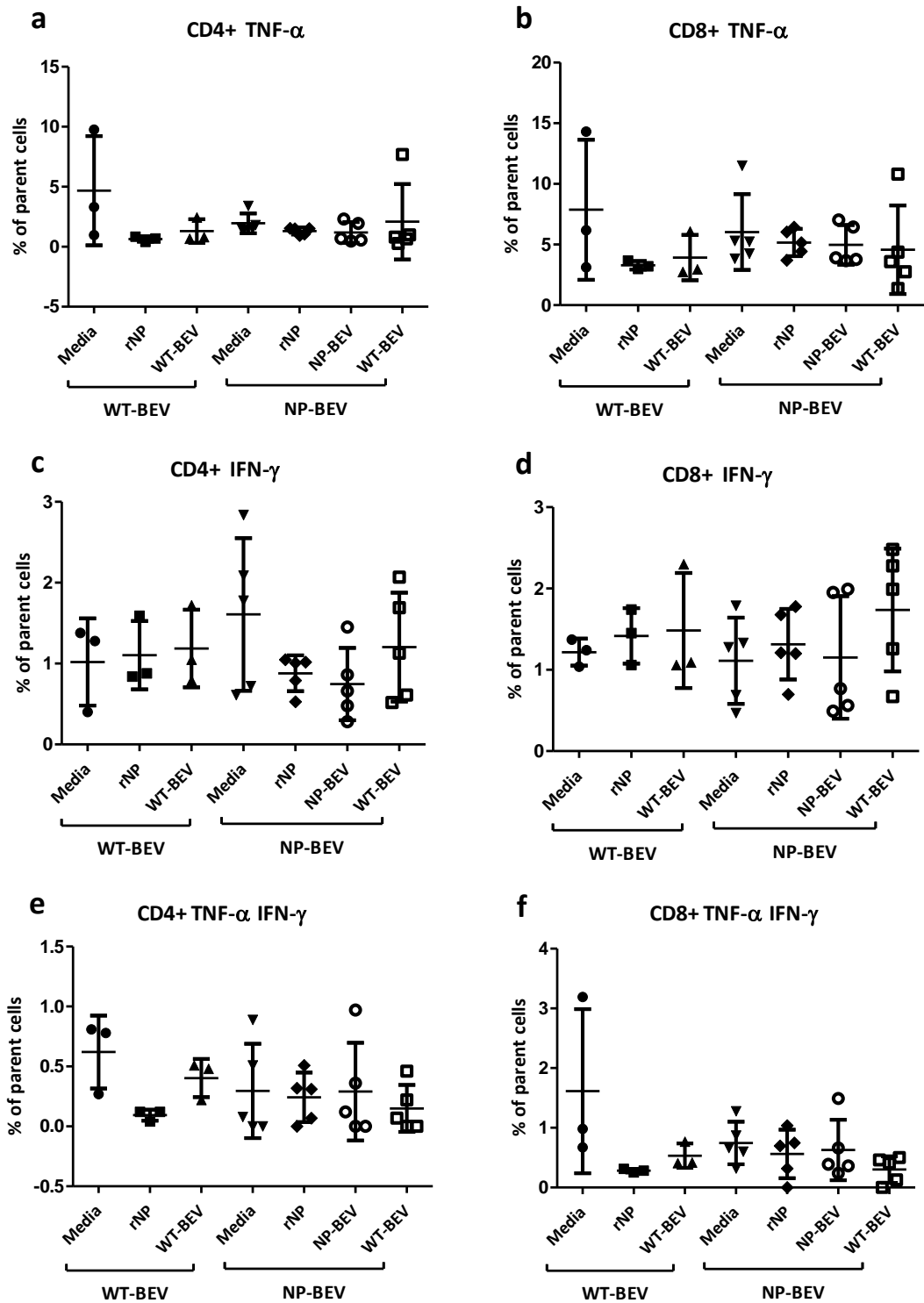


Figure 4.18 Frequency of CD4+ and CD8+ T cells expressing TNF- α and/or IFN- γ from splenocytes from the second NP-BEVs experiment by flow cytometry. Flow cytometry analysis of splenocytes from mice immunised with WT-BEVs or NP-BEVs stimulated *ex vivo* with media, rNP, WT-BEVs or NP-BEVs for 21h. Data represented by the mean value for each group n=3-6 \pm standard deviation with two technical replicates. Statistical analysis was performed using one-way ANOVA with Bonferroni post-test.

4.3 Discussion

IV evolves rapidly causing yearly epidemics and increasing the likelihood of pandemics caused by new virus strains (227). Due to their quick spread and high morbidity effective cross-protective vaccines are needed.

In this study, engineered BEVs from the commensal gut Bt expressing a conserved region of H5N1 subtype HA induce systemic and mucosal humoral response that protect mice against a heterotypic IAV strain (H1N1). Moreover, BEVs expressing NP have also been created, although demonstrating their capacity to induce T cell immune response requires further optimisation. Given that Bt BEVs possess intrinsic adjuvanticity properties, there is potential to use them as a mucosal vaccine technology for flu.

Bt was successfully engineered to express H5F antigen, and its presence was confirmed by proteomics but not by immunoblot or immune-dot-blot. For the immunoblots, two different antibodies were used (anti-his tag and anti-HA) and neither identified H5F in BEV extracts. This might be attributable to the lack of accessibility of his-tag or lack of epitopes in the H5F protein. The anti-HA antibody used (CR6261) is a monoclonal antibody that recognizes a highly conserved region in the stem of HA capable of protecting mice from a lethal challenge with H1N1 and H5N1 (264). However, in this experiment, CR6261 was unable to detect the conserved fragment of H5. The reason might be related to the concentration of H5F expressed in BEVs being below the detection limits of the immunoblot and immune-dot-blot. Consequently, the amount of H5F that mice received in each immunisation is unknown. Amounts of HA as low as 0.1µg might be enough to induce protection, given that Quan, et al. designed a vaccine using VLPs containing either 0.5µg of HA alone or 0.1µg of HA with *E. coli* mutant heat-labile enterotoxin adjuvant, both of which protected animals against IV infection (265).

The isolation and purification of recombinant H5F was done under denaturing conditions to allow the histidine residues to bind the Ni-ions on the Ni-NTA columns. Using native conditions for protein isolation, results in H5F appearing in the flow through. This suggests that the 6xHistag is inaccessible and unable to bind the Ni-NTA. High expression of recombinant protein in *E. coli* can result in partially folded or misfold proteins resulting in aggregation and formation of inclusion bodies (266). Lowering the temperature can help reduce protein aggregation, however, when the induction was carried out at 20°C for 16h, as described by Poon et al. (258), the concentration of protein in the elute was not increased. To produce rH5F *E. coli*-H5F can be grown and induced for 5h at 37°C and the

protein purified using denatured conditions. The recombinant protein can then dialyse to eliminate urea and enable the protein to revert to its native conformation for use in future experiments.

Intranasal administration of BEVs expressing H5F and WT-BEVs generated systemic IgG and mucosal IgA antibodies in the lower respiratory tract. It is perhaps not surprising to see that both WT and H5F expressing BEVs induce mucosal humoral responses as WT-BEVs alone can promote the development and enlargement of organised nasal and bronchus-associated lymphoid follicles essential for generating effective mucosal immune response. We have also observed that within 24h of mice receiving WT-BEVs intranasally, BEVs are acquired by CD103⁻ CD11b⁺ DC in the upper and lower respiratory tract mucosa and draining cervical lymph nodes (3). These DC can traffic the antigen to the lymph nodes and activate a T cell response (267). Bt BEVs possess therefore adjuvanticity properties without the need to detoxify their LOS as is required for *Neisseria meningitidis*, *E. coli* or Salmonella BEVs prior to their use in vaccine formulations (268).

BEVs expressing H5F conferred a significant level of protection against H1N1, an unrelated subtype of IAV. This is consistent with Valkenburg et al. (258) showing that H5F administered intramuscularly to mice with Addavax adjuvant protected the mice against unrelated H1N1 and H3N2 virus subtypes. H5F-BEVs are therefore a good candidate for the formation of heterologous antibodies able to neutralise multiple strains.

In future experiments, long term protection needs to be assessed after for example, challenging the mice 1, 3, 6 and 10 months after H5F-BEVs immunisation. Subtypes H3N2 or H5N1, current major health concern in the UK, could be used for the infection challenge (234, 235).

Contrary to HA, NP is known to induce antigen-specific T cells (4, 5) in addition to non-neutralising antibodies that are important to clear virus infections (269). The cellular immune response was analysed by stimulation of vaccinated mice splenocytes using flow cytometry. Despite using two different protocols for the splenocytes stimulation, the cellular response was similar in all vaccinated groups and was not induced by restimulation *ex vivo* with various combinations of antigens. To optimise the protocol, the period of *ex vivo* re-stimulation was increased to allow more time for the recombinant protein to be processed and re-activate *in vivo* primed antigen-specific T cells. The longer stimulation period, however, resulted in increased cell death while the expression levels of

intracellular cytokines remained unaltered, a relationship also observed by Kavehet, et al. (270).

Additional booster immunisations may elicit more robust and stronger immune responses. Still, the poor immunogenicity of NP and NP-BEVs might be attributable to sub-optimal amounts of NP in the BEV vaccine formulations. Other recombinant vaccines in pre-clinical stages using NP delivered either intramuscularly or intraperitoneally use amounts of rNP ranging from 30µg to 100µg per dose per mice (271-274). It is important to note, that all these vaccines also contain adjuvants or carriers. Although Bt BEVs have inherent adjuvant properties and can confer protection to the antigen, a dose of 0.27µg NP in mice immunised with 10^{11} NP-BEVs may still be insufficient. Future experiments need therefore to consider increasing the concentration of NP per dose. Options to increase NP concentration in BEVs could include changing the promoter in plasmid construct and signal peptide. Previously used signal peptides (140, 141) or secretion sequences of highly expressed proteins observed from proteomics of BEVs, could also be used. Another option is to decorate BEVs externally. Different mechanisms, such as SpyTag-SpyCatcher, could be used to bind antigens covalently to BEVs; effectively used previously in *E. coli*, *N. meningitidis* and Salmonella BEVs (148, 275-277).

Further optimisation to detect antigen-specific T cells could be considered for example, using tetramers. Tetramers are four Major Histocompatibility Complex (MHC) molecules associated with a specific peptide attached to a streptavidin-coated bead and linked to a fluorochrome (278). The tetramers bind to T cells that recognises the peptide in the MHC molecules. The use of tetramers facilitates specific, simple, and direct visualisation without the need for restimulation *ex vivo*. To this end, two tetramers (Class II I-A(b) NP 311-325 QVYSLIRPNENPAHK and Class I H-2D (b) NP 366-374 ASNENMETM) were obtained from the NHI Tetramer Core Facility (USA) for use in future experiments. These tetramers will enable the identification of NP-specific CD8+ and CD4+ T cells as done in other studies (279-281).

In response to the Covid-19 pandemic this project was halted and re-aligned to develop BEV based SARS-CoV-2 mucosal vaccine, which is described in the next chapter.

Chapter 5 Use of bioengineered Bt BEVs as a Covid-19 vaccine

5.1 Introduction

Coronavirus disease 2019 (Covid-19) is a highly transmissible illness caused by the severe acute respiratory syndrome coronavirus 2 (SARS-CoV-2). The virus emerged in late 2019, and quickly spread, evolving into a global pandemic causing more than 600M cases and 6.6 M deaths worldwide up to 18 November 2022 (282).

SARS-CoV-2 is an enveloped, non-segmented, positive-sense single-stranded RNA virus (283). Its genome encodes numerous open reading frames, including coding sequences for 4 structural proteins: Spike (S), Envelope, Membrane, and Nucleocapsid (NC) proteins (284). S protein is displayed as a trimer that covers the surface of the virus. Its function is to mediate the viral cell entry by binding to angiotensin-converting enzyme 2 (ACE2) receptors. S is heavily glycosylated with numerous mucin-type O-glycosylation sites and 22 predicted N-glycosylation consensus sites (285, 286). Except for the receptor binding domain (RBD), the glycans shield the protein from antibody recognition and help the virus to evade the human immune system (287). Despite this, S is the main protein that generates neutralising antibodies, especially against the RBD (288), and therefore, is the main targeted protein for vaccines. Per contra, antibody binding sites of S are under selective pressure, and are prone to mutate and escape the immune system. Moreover, the antibody titre against S can quickly drop shortly after SARS-CoV-2 infection or vaccination with S-focused vaccines, which can cause people to reinfect within 3 months (289). S protein also generates T cells after infection which remain functional for longer compared to antibody titres (290, 291). NC protein can also induce B and T cell responses (292), and has the highest density of epitopes recognised by CD8+ T cells from Covid-19 convalescents patients (293). T cells are less susceptible to viral mutations and play a key role in heterotypic protection (294). The CD8+ T cells are positively associated with effective viral clearance and less severe disease (295).

NC is responsible for packaging the viral genome and is less prone to mutation, probably, as their most immunogenic epitopes are not under selective pressure (296). NC triggers the fastest IgA response after a SARS-CoV-2 infection, earlier than S-specific IgA (297, 298).

Many Covid-19 infections are asymptomatic or cause mild to moderate respiratory illness, whereas more severe, chronic, infections can cause multiple organ failure and death. The incubation period is around 5-6 days but it can take up to 14 days to develop symptoms (299). The virus can quickly spread from person to person via virus-containing droplets and aerosols, and then enter the body by binding to ACE2 receptor expressed in mucosal epithelia of the lungs, eyes, and digestive system (300). The virus can also infect other organs that express ACE2 receptors such as heart, kidney and liver (300).

The evolution of SARS-CoV-2 through spontaneous mutations have allowed it to escape neutralising immune responses and increase transmissibility (301). Most mutations appear on the RBD of the spike protein, making binding to ACE2 receptors stronger (302). Ancestral B.1 SARS-CoV-2 virus evolved into different variants of concern (VOC), named using two nomenclatures, WHO labelling and Pango, some of which include: Alpha or B.1.1.7, Beta or B.1.351, Gamma or P.1, and Delta or B.1.617.2 (303). The current circulating VOC is Omicron or B.1.1.529, the most mutated strain discovered so far which is highly contagious but leads to less severe disease compared to other VOCs (304).

The first vaccines approved against Covid-19 became available within 1 year and were mRNA based. These vaccines delivered parenterally reduced the risk of disease by 94%-95% in adults within two months of vaccination and the protection decreases to 46%-66% within four to five months (305). Covid-19 mRNA vaccines consist of a messenger RNA encoding S protein that enables infected host cells to produce S protein and generate neutralising antibodies and T cells (306). Other intramuscular vaccines have since been licensed including inactivated virus, viral vector vaccines and subunit vaccines (306). However, the vast majority rely on a single protein (S). These vaccines reduce severity and mortality, but the longevity of immunity induced is relatively short and does not reduce transmission or reinfection by different strains of SARS-CoV-2 (307, 308).

Recently, four new mucosal vaccines for delivery to the respiratory mucosa against Covid-19 have been approved for use in Iran, Russia, India and China (Table 1.1) (309). These mucosal vaccines include live inactivated vaccines, vector vaccines and

recombinant subunit vaccines. Mucosal vaccination has the potential to prevent initial infection by SARSCoV-2 and suppress transmission. IgA dominates the neutralising humoral response to SARSCoV-2 in the early stages of infection (310), and is able restrict infection to the upper respiratory tract in mild or asymptomatic diseases (311).

While intranasal vaccines have the potential to prevent transmission, they are focused on S, which is susceptible to mutation. To provide a stronger and broader T cell response the inclusion of NC protein has gained interest and dual vaccines including S and NC proteins have been shown to enhance heterotypic protection in different vaccine studies (312-314).

The goal of this chapter is to determine the suitability of Bt BEVs containing the S and NC as a Covid-19 vaccine.

The aims are to:

- Produce Bt BEVs containing S
- Engineer Bt to express SARS-CoV-2 NC
- Assess the capacity of Bt BEVs containing NC and or S to generate systemic and mucosal immune responses in vaccinated mice

To adopt the correct 3D structure of the glycosylated S protein, it requires to be expressed in insect or mammalian cells capable of doing both O-glycosylation and N-glycosylation (315, 316). *E. coli* and Bt have the ability to add O-linked glycans. However, they do not naturally produce N-glycosylation proteins with mammalian-style glycans and fail to correctly fold S protein (316, 317). For this reason, S protein was produced using mammalian cells, at the University of Kent, and bound to the outer membrane of Bt BEVs. The conjugation of S with BEVs was done by two methods. The first one using highly expressed vitamin B12 receptors (ButG) present in Bt BEVs and S complexed with B12 (Dr Rokas Juodeikis). And the second, by amine-based conjugation using click chemistry (Professor Mark Smales and Dr Dave Beal, University of Kent). Bt BEVs containing S and or engineered to express NC were isolated, characterised and administered to mice via intraperitoneal or intranasal to mice models. Tissue and blood samples were collected and analysed to quantify antibody levels by ELISA and cytokine-producing T cells by flow

cytometry (Fig. 5.1). Both proteins S and NC were obtained from the B.1 parental lineage of SARS-Cov-2.

All animal experiments were conducted in the Disease Modelling Unit (DMU) at the University of East Anglia unless stated otherwise. Drs Aimee Parker (I3A8468C9) and Sonia Fonseca (I9ABE642A) performed the vaccinations and sample collections.

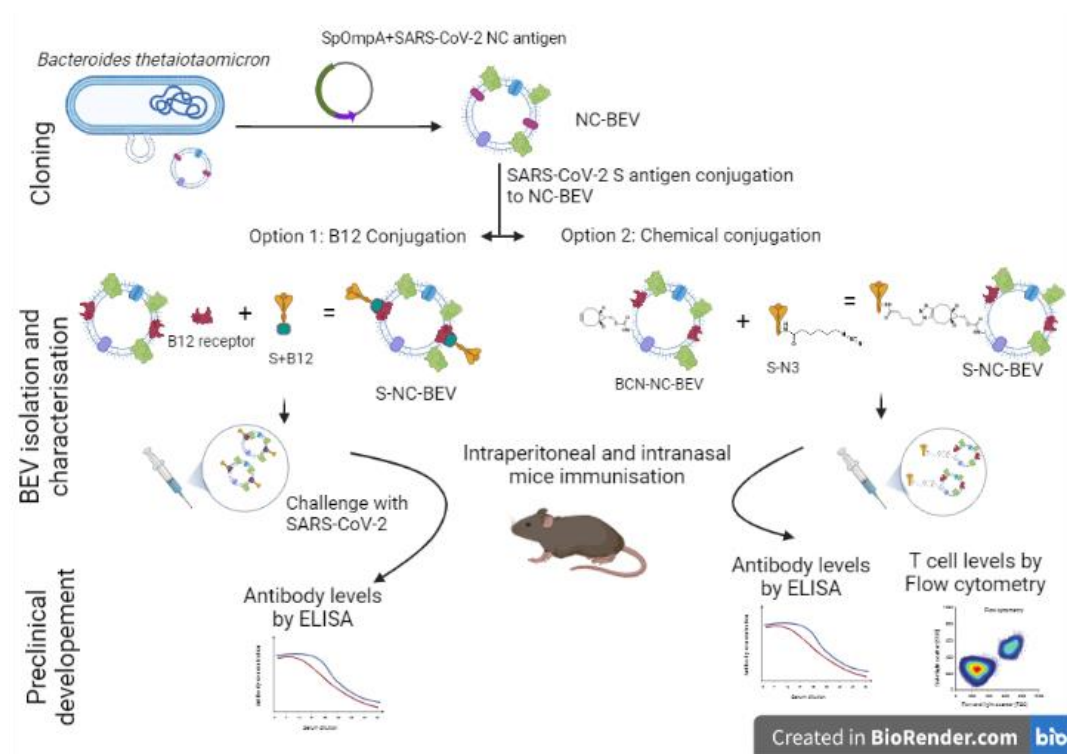


Figure 5.1 Overview of bioengineered Bt BEVs as Covid-19 vaccine study design. Created in BioRender.com.

5.2 Results

5.2.1 Complexing S to Bt BEVs

The binding of S protein to Bt BEVs was done using a novel method developed by Dr Rokas Juodeikis and Professor Simon Carding utilising vitamin B12. Bt BEVs naturally express high-affinity B12 binding receptors (BtuG) that play a role in scavenging B12 for parental bacterium or host cells (106). BEVs can bind vitamin B12 conjugated to S protein (Fig. 5.2). The conjugation of B12 to S, named B12.S, was carried out at the University of Kent. First, S protein was expressed and purified from mammalian cells. Secondly, B12-

succinate-pentafluorophenyl ester (PFP) was synthesised in a method described by Juodeikis, et al (106) and conjugated with S protein. The succinate bridge allows the amine (NH₂) of lysine residues in S to form a covalent bond with the PFP ester, resulting in an amide bond. Finally, S-succinate-B12 (B2.S), is mixed with Bt BEVs to form B12.S-BEVs (Fig. 5.2).

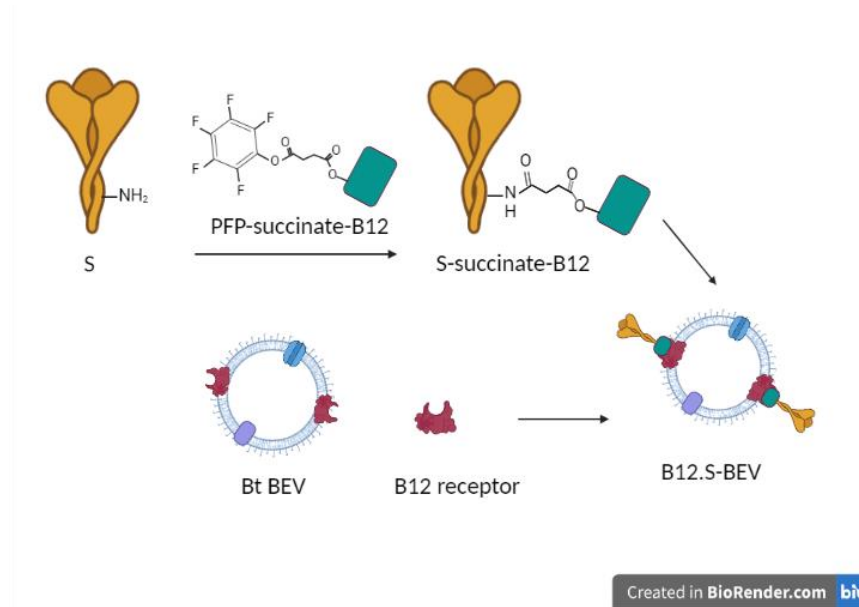


Figure 5.2 Representation of S linked to Bt BEVs using vitamin B12 and B12 receptor. Novel method to bind proteins to BEVs using naturally expressed B12 receptors with conjugated B12.S. Created in BioRender.

Initially, 10^8 BEVs were conjugated with $10\mu\text{g}$ S. Later, based on starvation and rescue culture assays performed by Dr Rokas Juodeikis, the predicted maximum amount of B12.S able to bind 10^8 BEVs was 3.6ng.

After conjugation, B12.S-BEVs were analysed by ZetaView PMX-220 TWIN instrument (Particle Metrix GmbH), which produced hydrodynamic particle size distribution curves. The size of B12.S-BEVs ranged from 50-200nm, with an average hydrodynamic peak size \pm SD of $90.3\text{nm} \pm 12.5$ (Fig. 5.3).

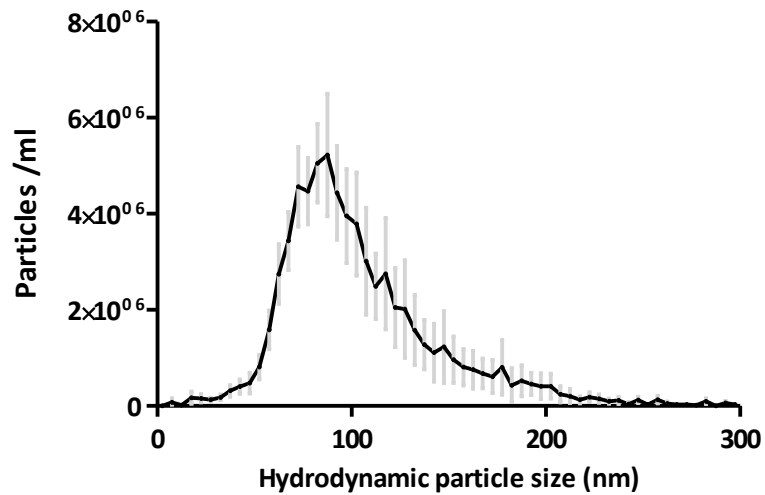


Figure 5.3 Quantification of hydrodynamic particle size of B12.S-BEVs by NTA. Bt was grown in BDM+ media and BEVs isolated, SEC purified and analysed using Zetaview PMX-220 TWIN instrument (Particle Metrix GmbH). Data is represented by the mean value for each value \pm standard deviation from 5 different isolations.

5.2.2 B12.S-BEVs immunisation

Mice were immunised intraperitoneally with 10^8 and 10^9 B12.S-BEVs or WT-BEVs. Recombinant B12.S was also administered as a control and reference (Fig. 5.4). On day 10, blood was collected for S-specific IgG antibody determination.

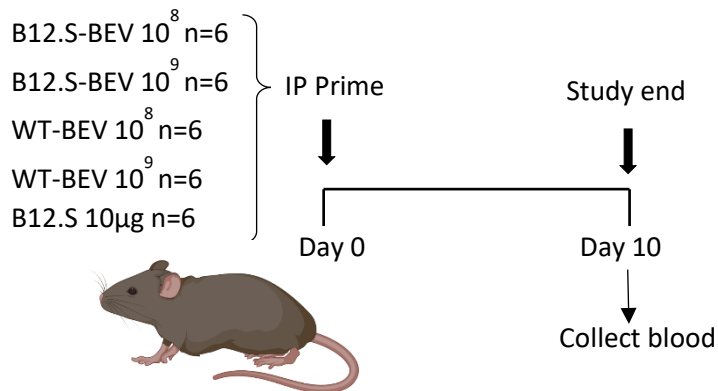


Figure 5.4 Animal study to determine optimal dose of B12.S-BEV vaccination. C57BL/6 male mice were immunised with either $10\mu\text{g}$ B12.S-BEV 10^8 , $10\mu\text{g}$ B12.S-BEV 10^9 , WT-BEV 10^8 , WT-BEV 10^9 or B12.S $10\mu\text{g}$ intraperitoneally. Blood was collected on day 10.

Table 5.1 Characteristics of optimal dose of B12.S-BEVs

Media	SEC	Spike conjugation	Spike concentration	Route
BDM+	No	B12	10µg	IP

Mice vaccinated with 10µg B12.S or B12.S-BEVs showed three times higher S-specific IgG in serum than mice immunised with 10⁹ or 10⁸ WT-BEVs (Fig. 5.5). At higher serum dilutions mice receiving the lower dose of B12.S-BEVs showed more than double amounts of antibodies than the higher dose, although the difference was not statistically significant (Fig. 5.5).

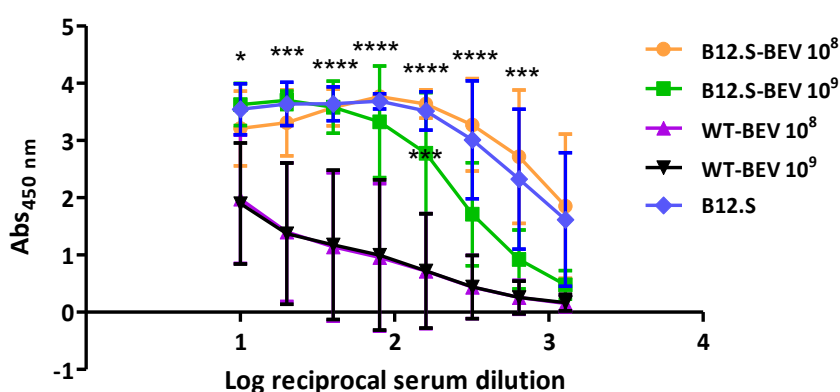


Figure 5.5 Quantification of serum IgG antibodies to B12.S in response of B12.S-BEV dose study by ELISA. Mice were immunised with either B12.S-BEV or WT-BEV at two doses 10⁸ and 10⁹ BEV or with recombinant B12.S. Blood was collected and analysed on day 10. Data is represented by the mean value for each group n=6 ± standard deviation. Statistical analysis was performed using two-way ANOVA with Bonferroni post-test. *<0.05; **<0.01; ***<0.001; ****<0.0001.

After confirming the immunogenicity of B12.S-BEVs after intraperitoneal immunisation, the vaccine was administered intranasally to K18-hACE2 transgenic mice that are susceptible to SARS-CoV-2 infection (318). Wild type mice lack ACE2 receptors and are resistant by SARS-CoV-2. For this experiment, mice were kept and managed by the University of Liverpool.

Mice were immunised with 10⁸ BEVs, selected from the previous experiment, bound to two different amounts of S, 10µg as previously used and 3.6ng as the maximum theoretical binding capacity. The two doses of B12.S were also administered alone. Also, a control group received 10⁸ WT-BEVs (Fig. 5.6). On day 30, mice were challenged with a

10-fold lethal dose of Alpha SARS-CoV-2. After 7 days, blood, BAL and lungs were collected (Fig. 5.6).

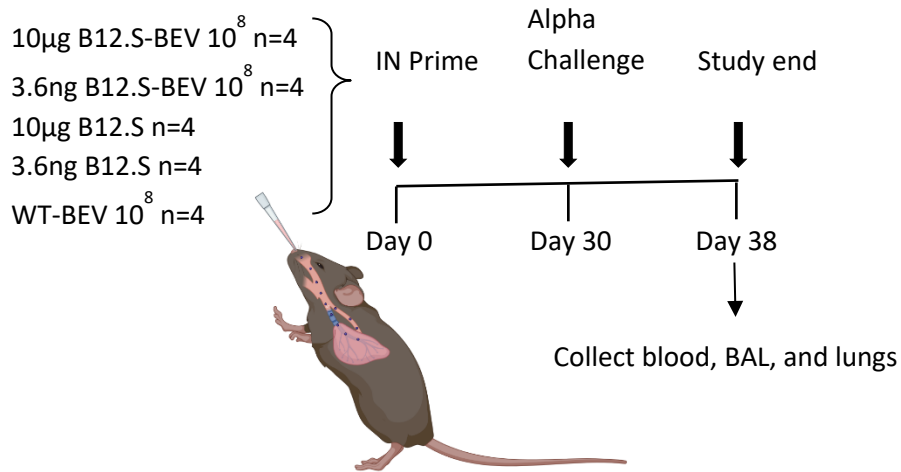


Figure 5.6 Animal study to determine covid-19 protection from B12.S-BEVs vaccination. Transgenic K18-hACE2 male mice were immunised with either 10µg B12.S-BEV 10⁸, 3.6ng B12.S-BEV 10⁸, 10µg B12.S, 3.6ng B12.S or WT-BEV 10⁸ intranasally. On day 30, mice were challenged with a 10-fold lethal dose of Alpha SARS-CoV-2. Mice weight was assessed daily after the challenge and at necropsy, on day 38, blood, BAL and lungs were collected.

Table 5.2 Characteristics of intranasally administered B12.S-BEVs

Media	SEC	Spike conjugation	Spike concentration	Route
BDM+	No	B12	10µg or 3.6ng	IN

Serum collected 8 days post challenge was analysed by ELISA to quantify specific anti-Alpha variant-derived S IgG in serum. Results show that all groups had similar levels of serum S-specific IgG (Fig. 5.7). However, mice immunised with 10µg B12.S-BEVs had approximately two-fold higher levels of antibodies at the highest serum dilutions than mice immunised with 3.6ng B12.S-BEVs.

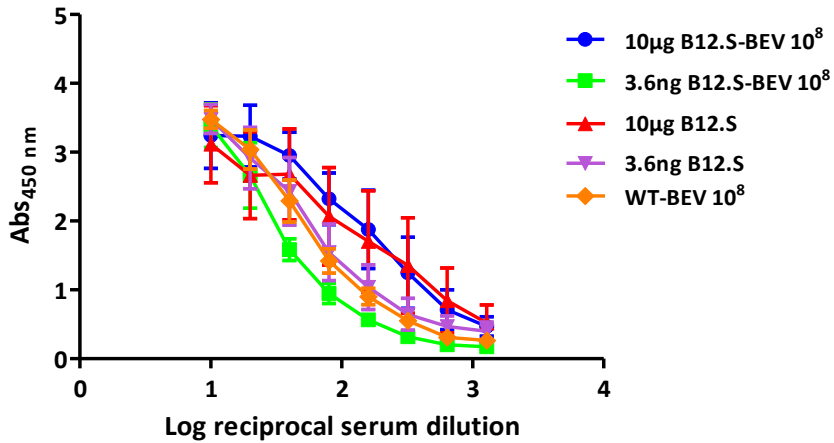


Figure 5.7 Quantification of serum IgG antibodies to B12.S in response of B12.S-BEV protection study by ELISA. Mice were immunised IN with B12.S-BEV containing either 10µg or 3.6ng of S or WT-BEVs. After 30 days mice were challenged with a 10-fold lethal dose of SARS-CoV-2 and serum was collected on day 38 and analysed by ELISA to quantify specific anti-alpha S IgG. Data is represented by the mean value for each group n=6 ± standard deviation. Statistical analysis was performed using two-way ANOVA with Bonferroni post-test.

During infection, mice receiving both doses of recombinant S protein alone and the lower dose of B12.S-BEVs had the greatest weight loss of 15% to 20% of their body weight compared to pre-challenge. Mice immunised with 10µg B12.S-BEVs and WT-BEVs had a more gradual loss reaching ~10% reduction in their initial weight (Fig. 5.8).

The viral load in the lungs of immunised mice was reduced more than 10-fold in mice receiving WT-BEVs and in 3 out of 4 mice receiving 10µg B12.S-BEVs (Fig. 5.8).

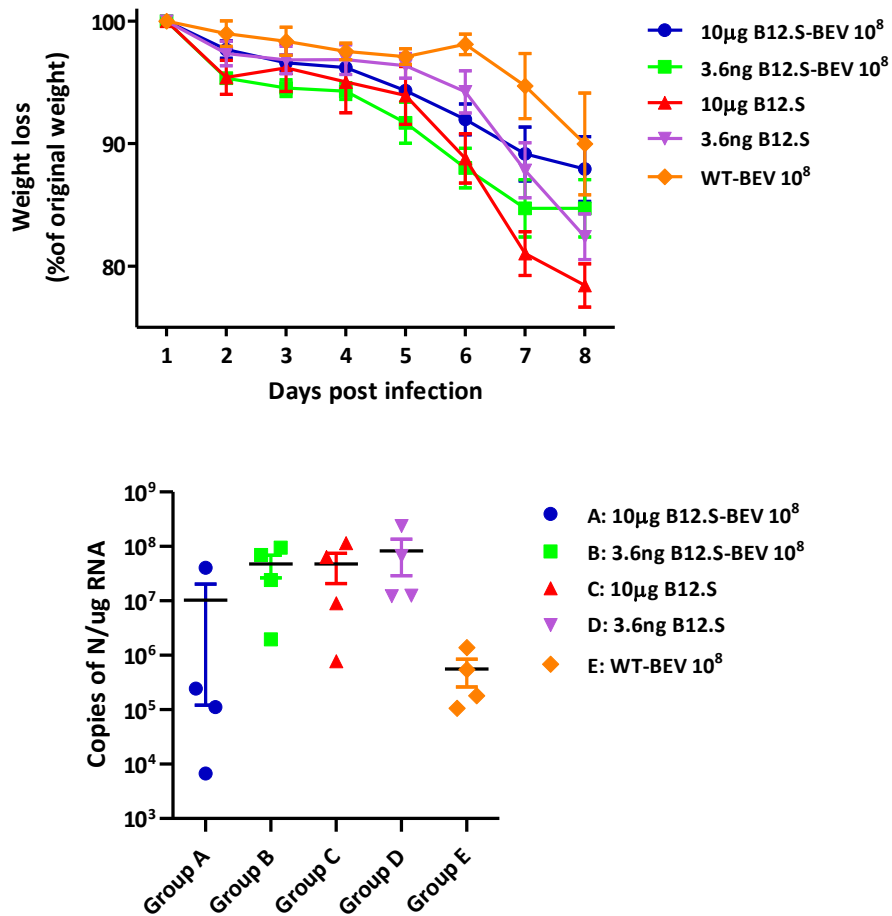


Figure 5.8 Host response to B12.S-BEV vaccine. Mice were intranasally immunised with B12.S-BEV containing either 10µg or 3.6ng of S or WT-BEVs and challenged with a lethal dose of Alpha SARS-CoV-2. (a) weight of animals recorded every day after the challenge for 7 days. (b) Virus titre in lung quantified by the number of copies of NC per µg of RNA analysed by qPCR. Data is represented by the mean value for each group n=6 ± standard deviation. Statistical analysis was performed using two-way ANOVA with Bonferroni post-test (a) or one-way ANOVA with Bonferroni multiple comparison post-test (b).

5.2.3 Construction of SARS-CoV-2 NC antigen expression vector

Two plasmids were used, pGH090 and a mannan expression vector (164). The construction of both NC expression vectors were design with Dr Regis Stentz.

The 1257bp synthetic gene encoding NC (UniProt Reference: PODTC9) was fused at its N-terminal to the OmpA signal peptide (SPompA). The gene was also fused to either *BspHI* and *EcoRI* or *NcoI* and *EcoRI* restriction enzymes sites and synthesised *de novo* (Eurofins, Germany). The resulting gene cassettes were digested and ligated to *NcoI/EcoRI*-restricted shuttle vector pGH090 or to the *NcoI* and *EcoRI*-pGH177 mannan

expression system vector. Positive transformants were sequenced to verify their identity. Bt strains containing NC gene in pGH177 plasmid were then further characterised.

5.2.4 Expression of SARS-CoV-2 NC antigen in Bt BEVs

Bt expressing NC (NC-Bt) was grown in BDM+ media using xylose instead of glucose, as glucose negatively affected the mannan promoter in the pGH177 plasmid (164). Expression was induced with mannan for either 4h or 15h. Approximately 0.5µg of cell extract protein or 10¹¹ BEVs from both WT-Bt and NC-Bt together with different amounts of recombinant NC were loaded onto SDS gels and immunoblotted with a SARS/SARS-CoV-2 NC polyclonal antibody to confirm expression (Fig. 5.9). Based on the intensity of the antibody-reactive bands 10¹¹ NC-BEVs contained approximately 200ng of NC.

Luminal versus outer membrane distribution of NC in NC-BEVs was established using a proteinase K protection assay. Proteinase K, with or without SDS, was added to NC-BEVs obtained from cultures stimulated for 15h with mannan and analysed by immunoblotting. NC was degraded when proteinase K was added, consistent with the antigen present on the outer membrane of NC-BEVs (Fig. 5.9).

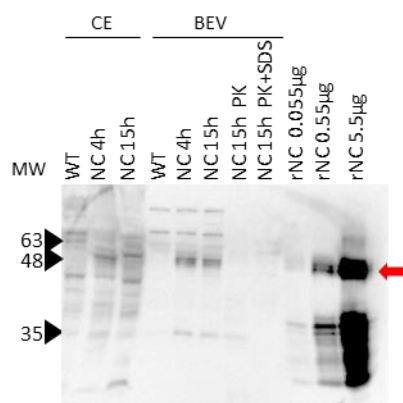


Figure 5.9 Detection of NC in NC-BEV by immunoblotting. Bt strains, (WT and Bt-NC) were grown in BDM+ media and induced with mannan for either 4h or 15h before BEV isolation and cell extraction (CE). BEVs were isolated following a method described in the materials and methods chapter. NC-BEV were treated with Proteinase K (PK) with or without SDS to identify the location of NC. The red arrow indicates the expected size of NC. Molecular weight (MW) expressed in kDa.

Expression of NC in NC-BEVs was also confirmed by LC-MS (Proteomics Facility, John Innes Centre) using Orbitrap mass spectrometry. Similar relative abundances were observed in two independent samples (Table 5.1).

Table 5.3 Detection of NC in NC-BEV by proteomics

Name	Media	SEC	Coverage	Relative abundance
SARS-CoV-2 Nucleocapsid	BDM+	NO	21%	433/741
SARS-CoV-2 Nucleocapsid	BDM+	YES	23%	832/1135

B12.S conjugated NC-BEVs (B12.S-NC-BEVs) were analysed by ZetaView PMX-220 TWIN instrument (Particle Metrix GmbH) to produce hydrodynamic particle size distribution curves. The hydrodynamic size of B12.S-NC-BEVs ranged from 50-200nm, with an average peak size \pm SD of 85nm \pm 5.4 (Fig. 5.10).

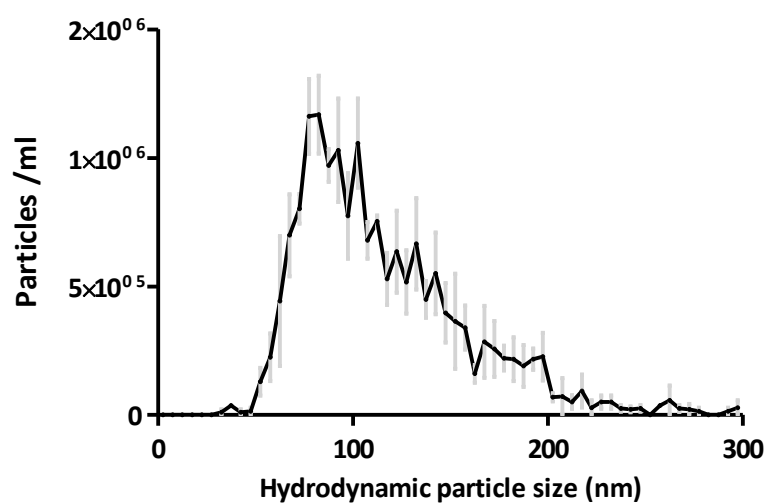


Figure 5.10 Quantification of hydrodynamic particle size of B12.S-NC-BEV by NTA. Bt was grown in BDM+ media and BEVs isolated, SEC purified and analysed using Zetaview PMX-220 TWIN instrument (Particle Metrix GmbH). Data is represented by the mean value for each value \pm standard deviation from 3 different isolations.

5.2.5 B12.S-NC-BEV preparation

10 μ g of B12.S were conjugated to 10⁸ NC-BEVs followed by SEC purification to remove non-bound S protein (Fig 5.11). The amount of B12.S bound to BEVs after SEC was undetectable by Immunoblot but was quantified in a solid phase ELISA. For the ELISA, the wells of the plate were coated with serial dilutions of a known concentration of B12.S or with B12.S-NC-BEVs and detected using a monoclonal anti-SARS-CoV-2 S glycoprotein S1 antibody and anti-human IgG-HRP. The amount of B12.S bound to NC-BEVs after SEC purification was calculated to be 0.025ng \pm 0.003 in 10⁸ B12.S-NC-BEVs.

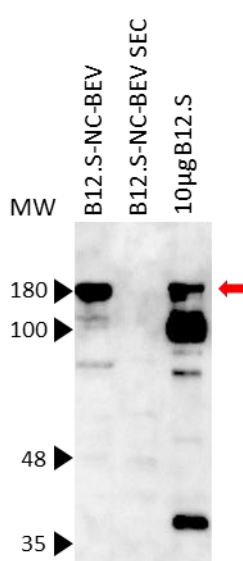


Figure 5.11 Detection of B12.S in B12.S-NC-BEV before and after SEC by immunoblotting. Bt-NC strain was grown in BDM+ media and induced with mannan for 16h before BEV isolation. Isolated BEVs were bind to B12.S for 30 minutes at room temperature and SEC purified. The red arrow indicates the expected size of S. Molecular weight (MW) expressed in kDa.

5.2.6 B12.S-NC-BEVs immunisation

To determine if SEC purified B12.S-NC-BEVs could induce a humoral or cellular immune response, mice were immunised using a two-dose regimen. Mice received either SEC purified 10⁸ B12.S-NC-BEVs, 10⁸ WT-BEVs or 1 μ g recombinant B12.S of recombinant NC with 1% Alhydrogel (Invivogen). Mice received a booster immunisation on day 10 and serum and spleens were collected on day 17 (Fig. 5.12).

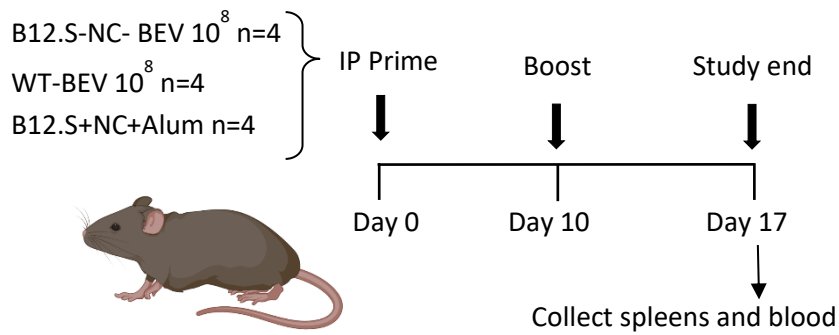


Figure 5.12 Animal study to determine cellular immunity to B12.S-NC-BEV vaccination. Overview of B12.S-NC-BEV animal study. C57BL/6 male mice were immunised with either B12.S-NC- BEV 10^8 , WT-BEV 10^8 or B12rS+NC+Alum intraperitoneally and boosted on day 10. Blood was collected at the end of the study on day 17.

Table 5.4 Characteristics of cellular immunity to B12.S-NC-BEV experiment

Media	SEC	Spike conjugation	Spike concentration	Route
BDM+	YES	B12	0.025ng	IP

Systemic antibody response against NC, in mice immunised with the recombinant S and NC with adjuvant, were approximately three times higher than in mice immunised with WT-BEVs. B12.S-NC-BEVs vaccinated animals also show higher level of NC-specific IgG than WT-BEVs, reaching levels approximately 2-fold higher in one of the serum dilutions ($p < 0.05$) (Fig. 5.13.a).

The level of anti-S IgG was approximately four times higher in mice vaccinated with recombinant S and NC than the other two groups of mice that had equivalent levels (Fig. 5.13.b).

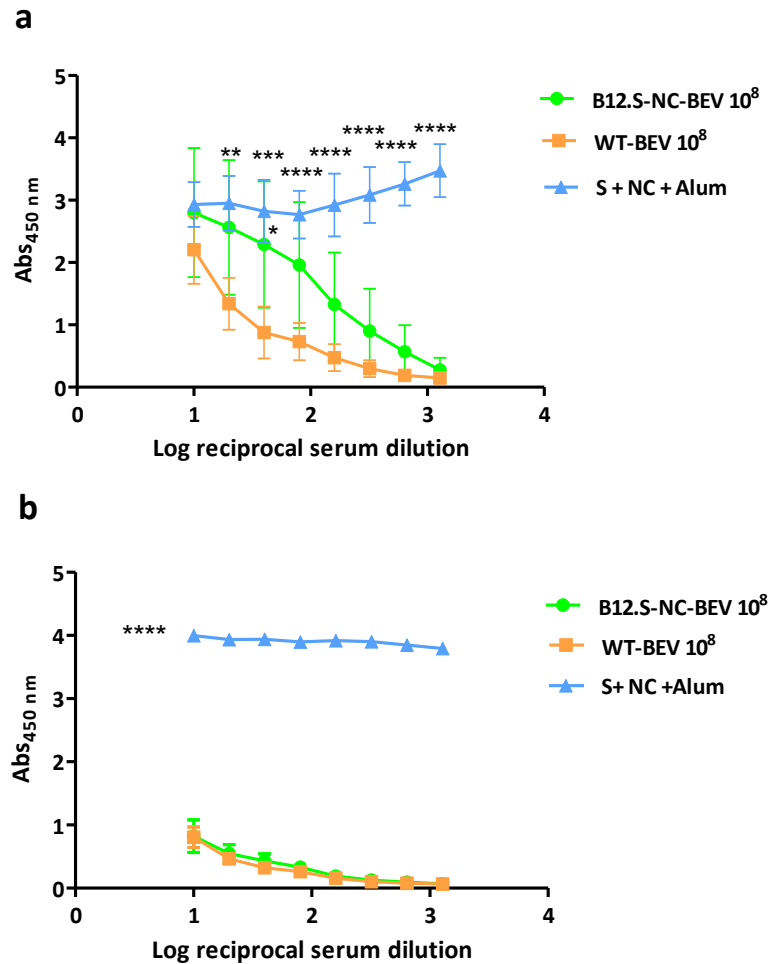


Figure 5.13 Quantification of serum IgG antibodies to NC and B12.S in response of B12.S-NC-BEV by ELISA. Mice were immunised IP with B12.S-NC-BEV, WT-BEV or recombinant B12.S with NC and Alum and boosted 10 days later. Blood was collected on day 17 and analysed by ELISA to detect specific antibodies anti-NC (a) or anti-S (b). Data is represented by the mean value for each group $n=4 \pm$ standard deviation. Statistical analysis was performed using two-way ANOVA with Bonferroni post-test. $* < 0.05$; $** < 0.01$; $*** < 0.001$; $**** < 0.0001$.

Cellular immune response induced by B12.S-NC-BEV vaccine was evaluated by *ex vivo* T cell stimulation and cytokine production using intracellular staining and flow cytometry. Splenocytes were re-stimulated with a combination of S and NC peptides or with media for 6h. The peptides were selected based on their ability to bind H-2K/Db or H-2IAb class I and II molecules expressed in C57BL/6 mice that were identified using the DTU Health Tech service (services.healthtech.dtu.dk) and protein sequences from UniProt (S: P0DTC2 and NC: P0DTC9). A list of peptides with predicted high binding were selected (Table 5.5). For Class I and Class II molecules server NetMHC-4.0 and NetMHCII-2.3 were used respectively. Peptides (Table 5.6) were generated de novo (GenScript) with a 90% purity and TFA removal and were reconstituted with DMSO upon arrival.

Table 5.5 Peptides used for restimulation of splenocytes

Class	Allele	Sequence	Length	Protein
Class I	H-2K ^b	VNFNFNGL	8	S
Class I	H-2D ^b	SAPHGVVFL	9	S
Class I	H-2D ^b	LALLLDRL	9	NC
Class I	H-2K ^b	TASWFTAL	8	NC
Class II	H-2IA ^b	PAQEKNFTTAPAICH	15	S
Class II	H-2-IA ^b	WPQIAQFAPSASAFF	15	NC

After stimulation, cells were stained, analysed, and gated as described in the Materials and Methods section.

The results show comparable levels of cytokines expressed in cells from all three vaccinated groups (Fig. 5.14). Stimulation with peptides increased IFN- γ by two-fold and decrease TNF- α production in CD4⁺ and CD8⁺ in mice immunised with B12.S-NC-BEVs. Samples from mice immunised with the recombinant proteins show levels of CD4⁺ and CD8⁺ cells expressing INF- γ around 8% compared to WT-BEVs immunised mice that had ~2.5% (Fig. 5.14. c, d).

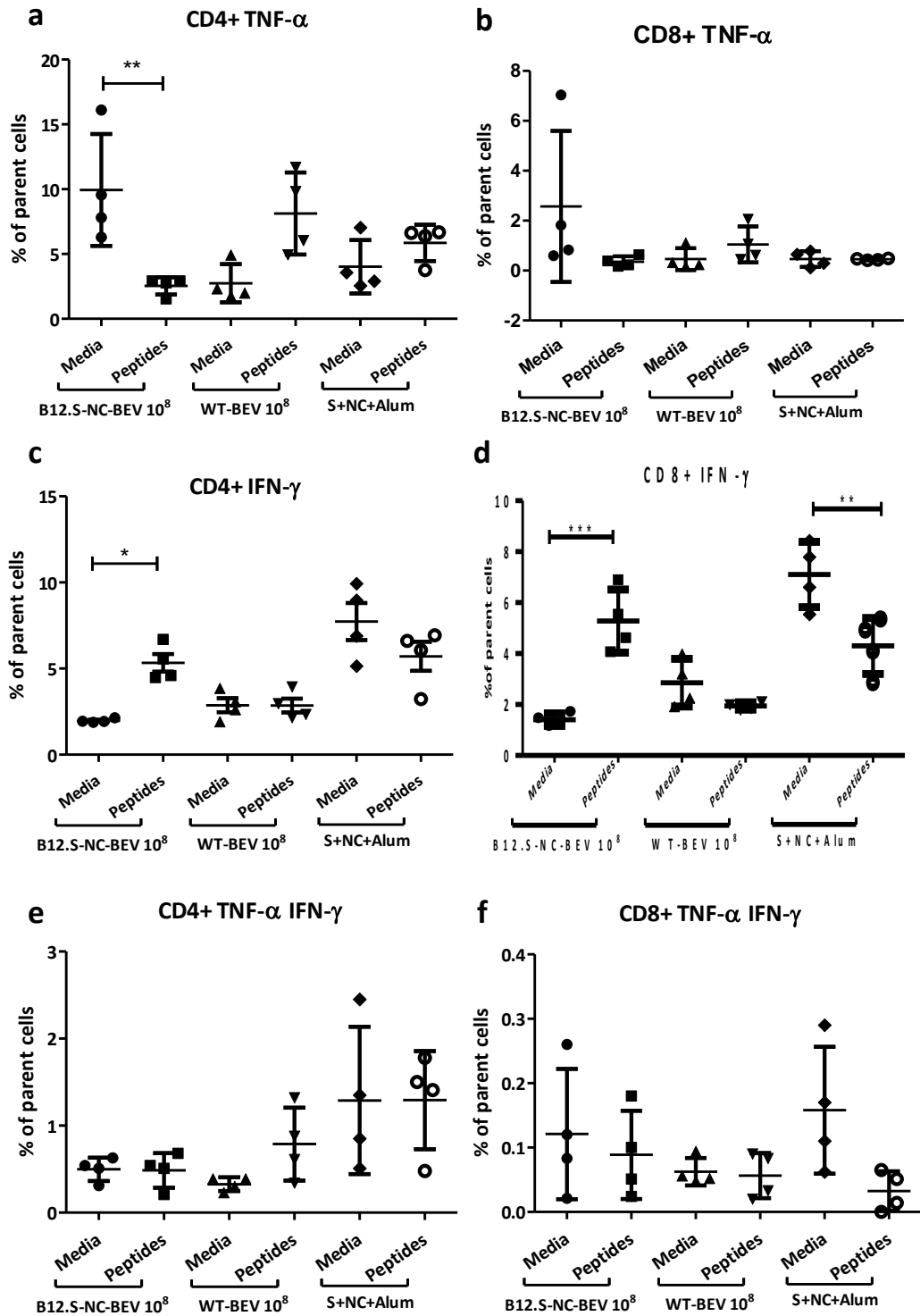


Figure 5.14 Quantification of cytokines expressed in splenocytes from mice immunised with B12.S-NC-BEV by flow cytometry. Mice were immunised IP with B12.S-NC-BEV, WT-BEV or recombinant B12.S with NC and Alum. Animals were boosted 10 days later, and spleens were harvested on day 17th. Splenocytes were cultured in complete media alone or stimulated with a combination of S and NC peptides for 6h prior to analysis. Data represented by the mean value for each group $n=4 \pm$

standard deviation. Statistical analysis was performed using one-way ANOVA with Bonferroni multiple comparison post-test. * <0.05 ; ** <0.01 ; *** <0.001 .

5.2.7 S complexed to BEVs using chemical conjugation

Dr David Beal and Professor Mark Smales, from the University of Kent, designed a novel conjugation system by amine-based conjugation chemistry, using click chemistry to link S to BEVs.

Click chemistry (319), is a spontaneous, robust and selective chemical reaction with high yields that generates minimal and non-toxic by-products. There are several types of click chemistry, the one used here is Strain-promoted azide-alkyne cycloaddition (SPAAC). The reaction use azide (N₃) to react with alkyne, in this case a cycloalkyne named Bicyclononyne (BCN), without the need of a catalyst, to form triazole.

To conjugate S to BEVs, first, amines on lysine residues in S protein were activated by N₃-Hex-CO₂PFP to produce activated S-N₃ (Fig. 5.15). The amines (NH₂) created a covalent bond with the pentafluorophenyl ester (PFP) that conjugate the S protein with azide (N₃), which is very reactive, and necessary for the click chemistry. At the same time, BEVs were activated by modifying the amines with BCN-OSu. BCN is the bicyclononyne that reacts with the Azide in S to form c.S-BEV.

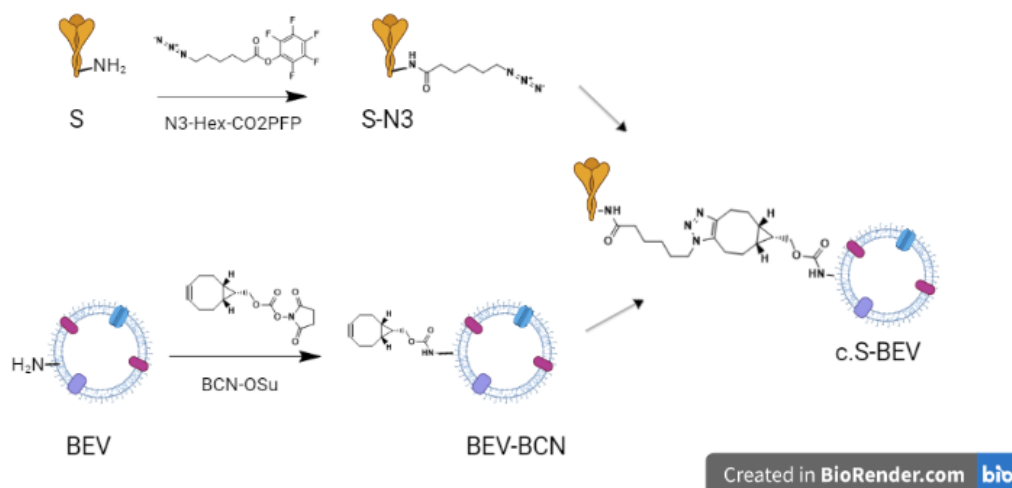


Figure 5.15 Representation of S linked to Bt BEVs using chemical conjugation. N₃-Hex-CO₂PFP linked to S create activated S-N₃. BCN-OSu is linked to BEVs to create BEV-BCN that when mixed with S-N₃ binds the S to the BEVs. Created in BioRender.

The presence of S in SEC purified c.S-BEVs was confirmed by proteomics (Proteomics Facility, John Innes Centre) using Orbitrap mass spectrometry with a coverage of 55% (Table 5.6). The presence and relative protein abundance in the sample, based on intensity and number of detected peptides, established good coverage of S protein in the sample, confirming the presence of S protein in the BEV formulations.

Table 5.6 Detection of S chemically attached to NC-BEV by proteomics

Name	Media	SEC	Coverage	Relative abundance
SARS-CoV-2 Spike	BDM+	YES	55%	112/1135

Quantification of S in c.S-BEVs, based on ELISA, indicated that 10^8 c.S-NC-BEVs contained $0.031\text{ng} \pm 0.012$ of S, comparable to the 0.025ng S in 10^8 B12.S-NC-BEV.

c.S-NC-BEVs were analysed by ZetaView PMX-220 TWIN instrument (Particle Metrix GmbH), which produced hydrodynamic particle size of 50-200nm for c.S-NC-BEVs, with an average peak size \pm SD of 93.3 ± 17.4 (Fig. 5.16).

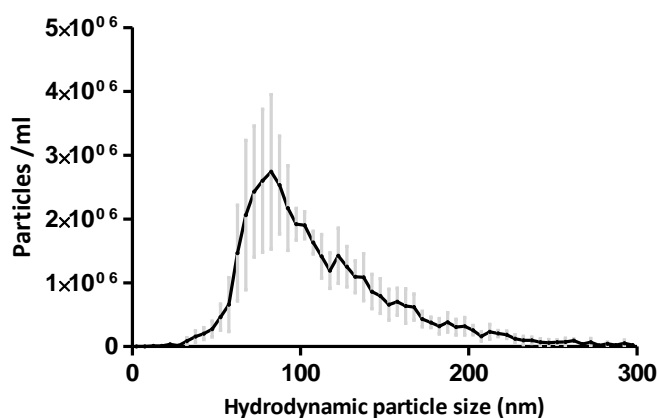


Figure 5.16 Quantification of hydrodynamic particle size of c.S-NC-BEV by NTA. Bt was grown in BDM+ media and BEVs isolated, SEC purified and analysed using Zetaview PMX-220 TWIN instrument (Particle Metrix GmbH). Data is represented by the mean value for each value \pm standard deviation from 5 different isolations.

5.2.8 c.S-NC-BEVs immunisation

The new vaccine formulation was tested in animal models increasing the concentration of BEVs to increase the amount of antigen administered.

Mice were immunised intraperitoneally with either 10^8 or 10^{11} c.S-NC-BEVs or WT-BEVs at 10^{11} and received a booster immunisation at day 10. At the study end, blood and spleens were collected for IgG antibody and T cell stimulation analysis (Fig. 5.17).

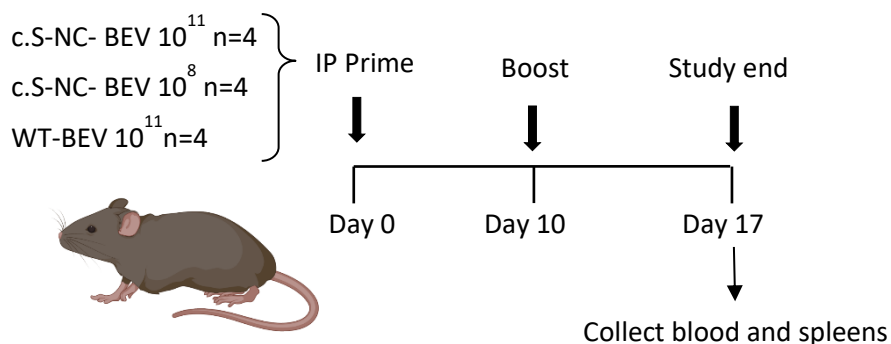


Figure 5.17 Animal study to determine dose response to c.S-NC-BEV vaccination. Overview of c.S-NC-BEV animal study. C57BL/6 male mice were immunised with either c.S-NC- BEV 10^{11} , c.S-NC- BEV 10^8 or WT-BEV 10^8 intraperitoneally and boosted on day 10. Blood and spleens were collected at the study end on day 17.

Table 5.7 Characteristics of dose response to c.S-NC-BEV experiment.

Media	SEC	Spike conjugation	Spike concentration	Route
BDM+	YES	Chemically	31ng for 10^{11} BEVs 0.031ng for 10^8 BEVs	IP

c.S-NC-BEV vaccine administered intraperitoneally generated similar titres of NC-specific IgG in serum from all three groups (Fig.5.18. a). Higher anti-S titres in mice immunised with 10^{11} c.S-NC-BEVs were generated compared to the other groups. ($p < 0.05$; $p < 0.001$) (Fig.5.18. b).

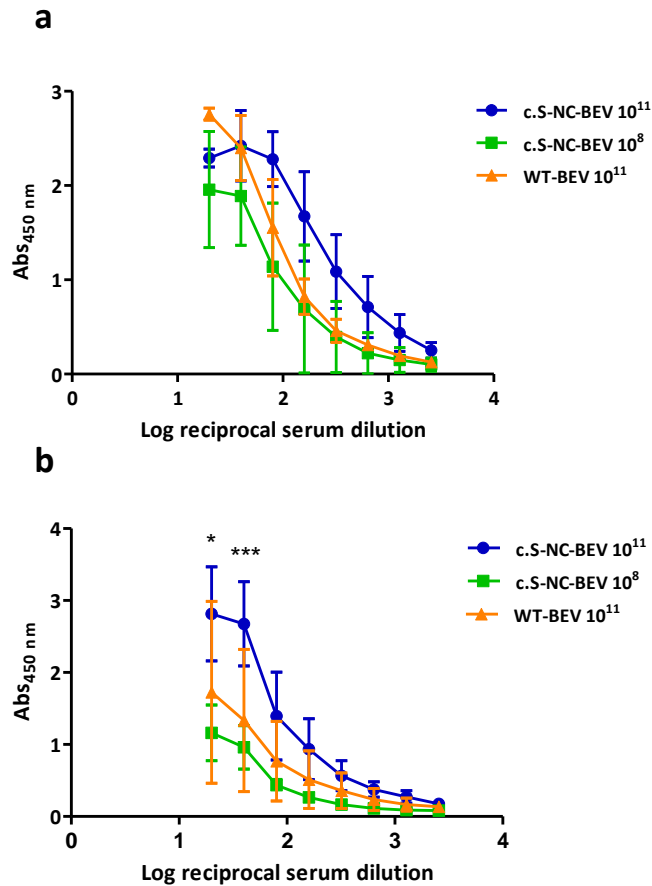


Figure 5.18 Quantification of serum IgG antibodies to NC and c.S in response of c.S-NC-BEV dose study by ELISA. Mice were immunised IP with either 10⁸ or 10¹¹ of c.S-NC-BEV or 10¹¹ WT-BEV and boosted on day 10. Blood was collected on day 17 and analysed by ELISA to detect titre of specific antibodies anti-NC (a) and anti-S (b). Data is represented by the mean value for each group n=4 ± standard deviation. Statistical analysis was performed using two-way ANOVA with Bonferroni post-test. *<0.05; ***<0.001.

The capacity of c.S-NC-BEV vaccine to induce cellular immune response was calculated using flow cytometry. Splenocytes were re-stimulated with a combination of S and NC peptides, S-NC-BEVs, WT-BEVs or with media alone for 6h. After stimulation, cells were stained, analysed, and gated as described in the Materials and Methods.

Mice receiving the higher dose of the c.S-NC-BEV expressed approximately two-fold higher frequencies of CD8+ T expressing INF- γ and TNF- α and CD4+ T cells expressing INF- γ compared to samples cultured with media alone (Fig. 5.19).

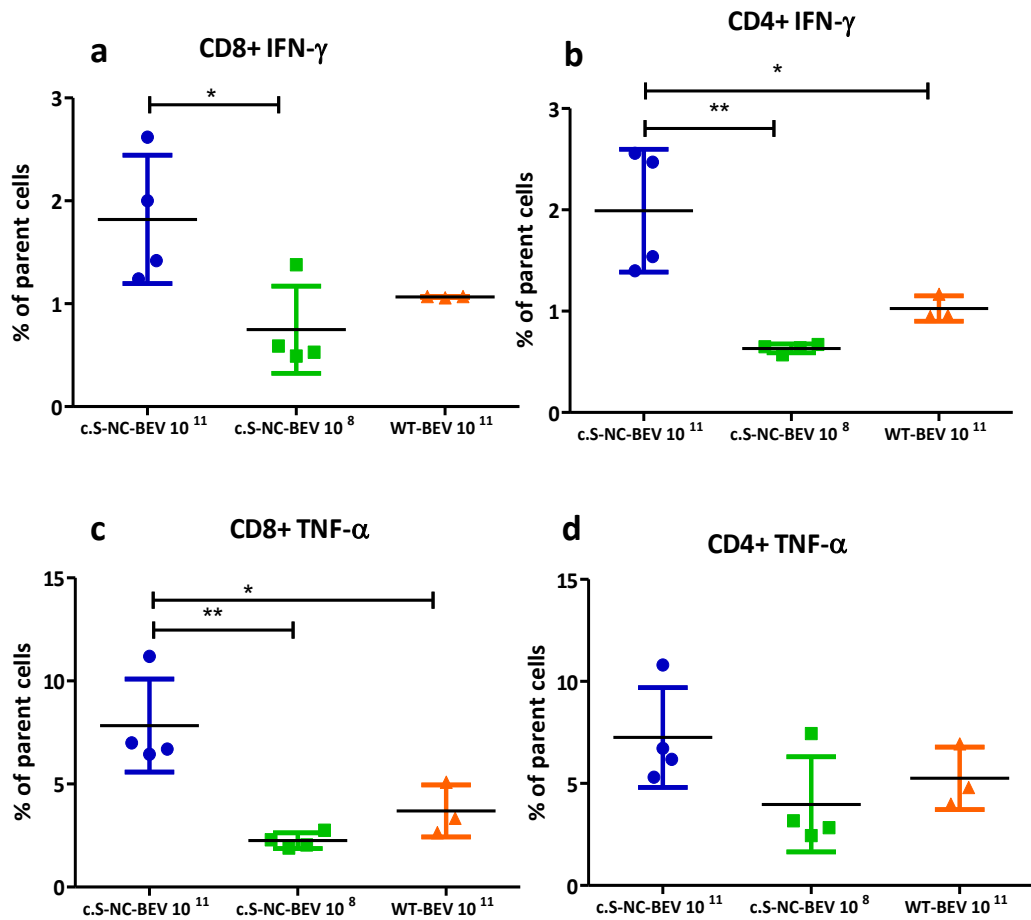


Figure 5.19 Quantification of cytokines expressed in splenocytes from mice immunised with c.S-NC-BEV by flow cytometry. Mice were immunised with c.S-NC-BEV 10^{11} , c.S-NC-BEV 10^8 or WT-BEV 10^{11} and boosted on day 10. Spleens were collected on day 17th and splenocytes were cultured in complete media alone for 6h prior to analysis. Data is represented by the mean value for each group $n=4 \pm$ standard deviation. Statistical analysis was performed using one-way ANOVA with Bonferroni multiple comparison post-test. * <0.05 ; ** <0.01 .

In splenocytes from c.S-NC-BEV 10^{11} immunised mice, levels of CD4+ and CD8+ T cells expressing INF- γ and TNF- α were increased compared to stimulation with WT-BEVs ($p<0.05$) (Fig. 20. a, b). Mice that received 10^8 S-NC-BEVs showed an increase in cytokine levels in CD8+ T cells when stimulated with S-NC-BEVs ($p<0.01$) (Fig. 20. d). Contrarily, mice immunised with WT-BEVs showed no change in levels of cytokines compared to cultures containing media alone (Fig. 20. e, f).

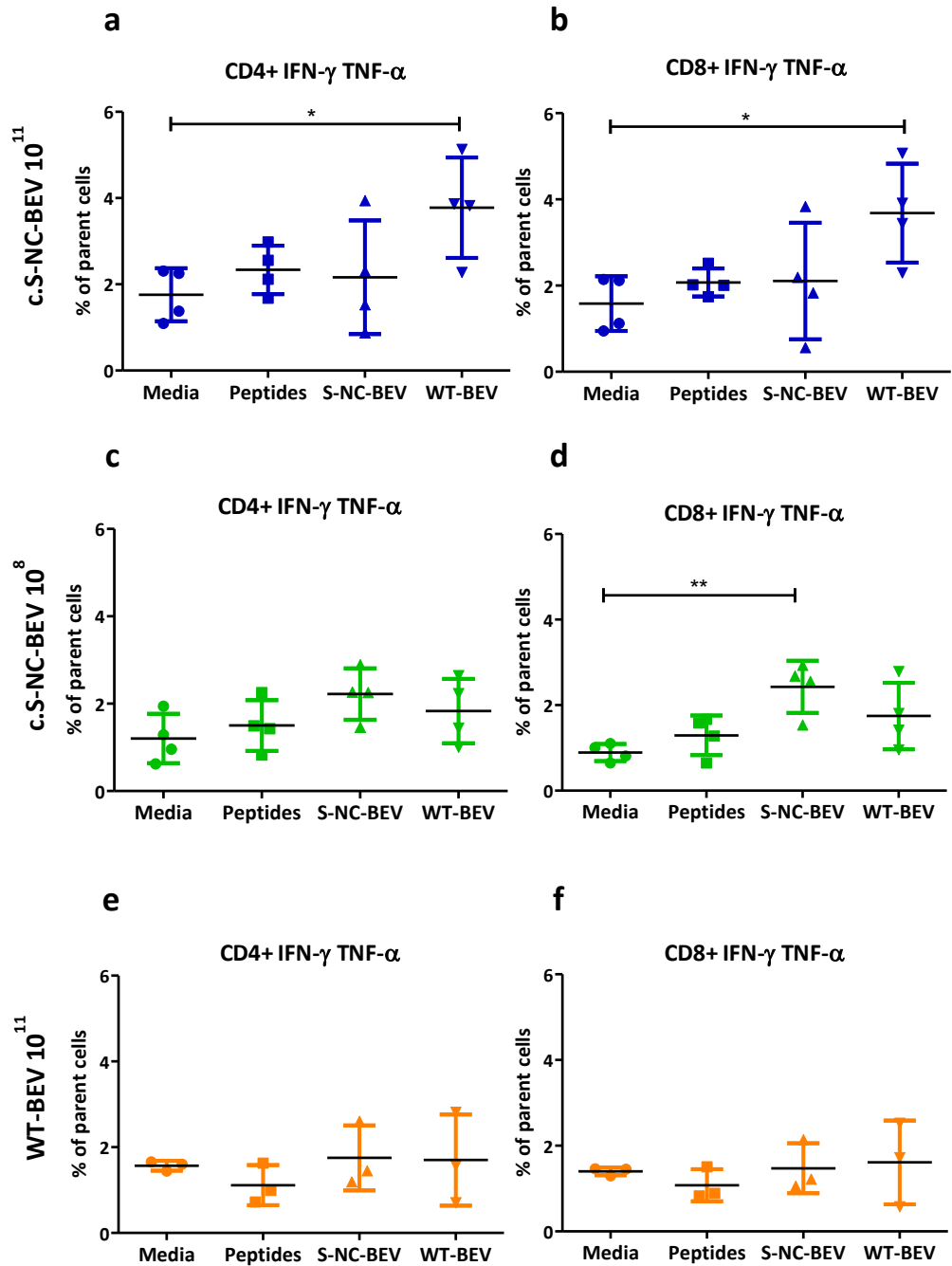


Figure 5.20 Quantification of cytokines expressed in stimulated splenocytes from mice immunised with c.S-NC-BEV by flow cytometry. Mice were immunised with c.S-NC-BEV 10^{11} (a, b), c.S-NC-BEV 10^8 (c, d) or WT-BEV 10^{11} (e, f) and boosted on day 10. Splens were collected on day 17th and splenocytes were cultured in complete media alone, stimulated with a combination of S and NC peptides, c.S-NC-BEV or WT-BEV for 6h prior to analysis. Data is represented by the mean value for each group $n=4 \pm$ standard deviation. Statistical analysis was performed using one-way ANOVA with Dunnett multiple comparison post-test. * <0.05 ; ** <0.01 .

Splenocytes were also stimulated for 72h without any BFA and analysed using an ELISA to quantify IFN- γ and TNF- α levels in cell conditioned supernatants. As seen previously, peptides had a marginal effect on cytokine stimulation. Number of cytokines expressing T cells were comparable between cells cultured in media alone or with peptides (Fig. 5.21). Contrarily, both S-NC-BEV and WT-BEV stimulated production of cytokines in all three vaccinated groups, particularly in mice immunised with c.S-NC-BEVs. Mice that received 10^{11} c.s-NC-BEV had a mean value for IFN- γ production of 328pg/ml \pm 60 and 318pg/ml \pm 148 respectively, when stimulated with S-NC-BEV and WT-BEV. While cells from 10^8 c.s-NC-BEV immunised mice produced 368pg/ml \pm 264 and 556pg/ml \pm 485 of IFN- γ . Contrarily, the levels of TNF- α produced in mice immunised with 10^{11} c.S-NC-BEVs and 10^8 were similar when stimulated with S-NC-BEV or WT-BEV (113pg/ml and 127pg/ml for 10^{11} dose and 94pg/ml and 92pg/ml for 10^8 dose) (Fig. 5.21).

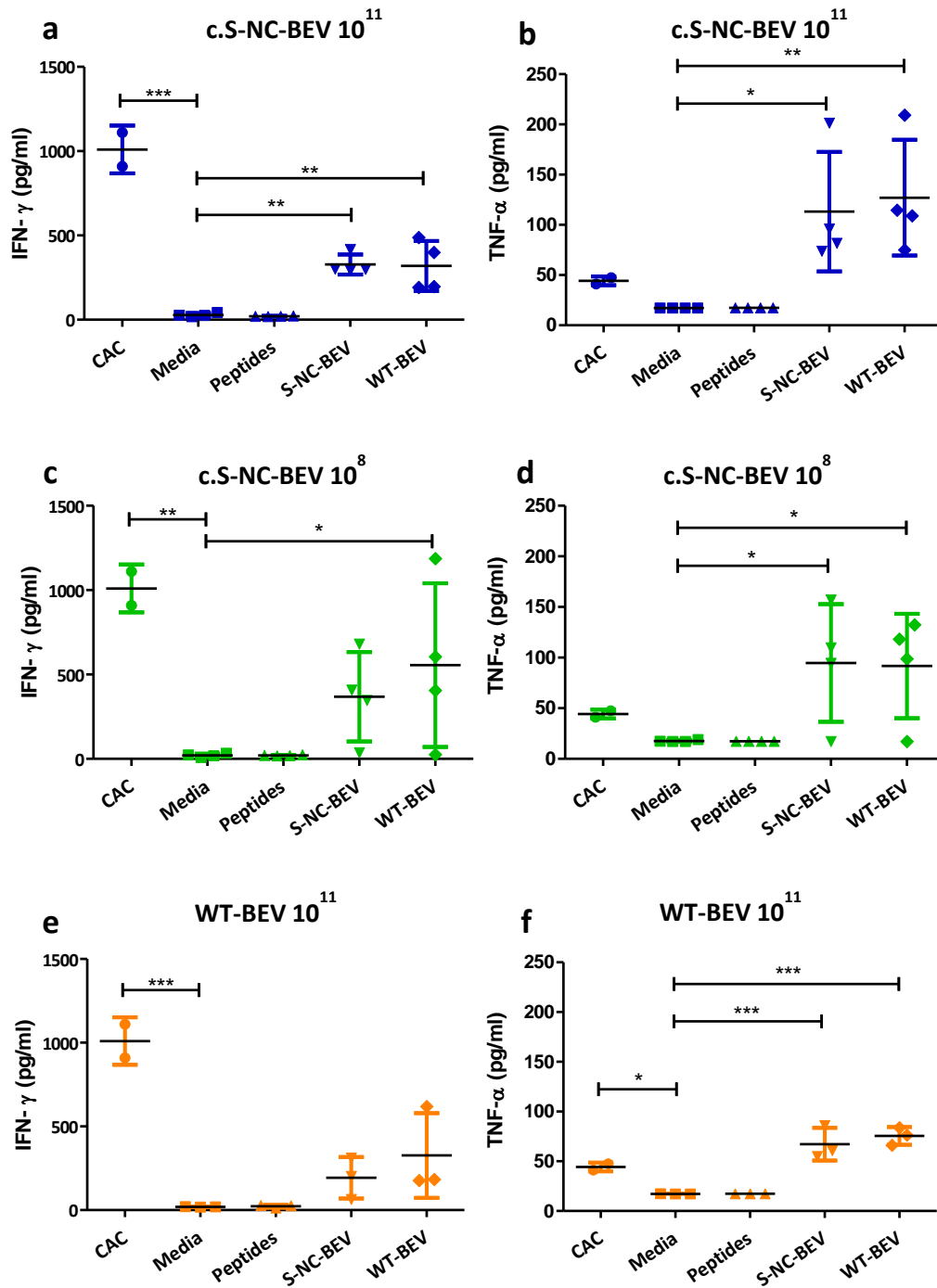


Figure 5.21 Quantification of cytokines expressed in stimulated splenocytes from mice immunised with c.S-NC-BEV by ELISA. Mice were immunised with c.S-NC-BEV 10^{11} , c.S-NC-BEV 10^8 or WT-BEV and boosted on day 10. Spleens were collected on day 17th and splenocytes were cultured in complete media alone, stimulated with Cell activation cocktail (CAC) containing PMA/ionomycin, a combination of S and NC peptides, c.S-NC-BEV or WT-BEV for 72h prior to analysis. Data is represented by the mean value for each group $n=4 \pm$ standard deviation. Statistical analysis was performed using one-way ANOVA with Dunnett multiple comparison post-test. * <0.05 ; ** <0.01 ; *** <0.001 .

Based on the previous experiment mice were vaccinated intranasally with either c.S-NC- BEVs 10^{11} , WT-BEVs 10^{11} or PBS and boosted on day 10. On day 17 blood, BAL, nasal wash (NW), and spleens were collected (Fig. 5.22).

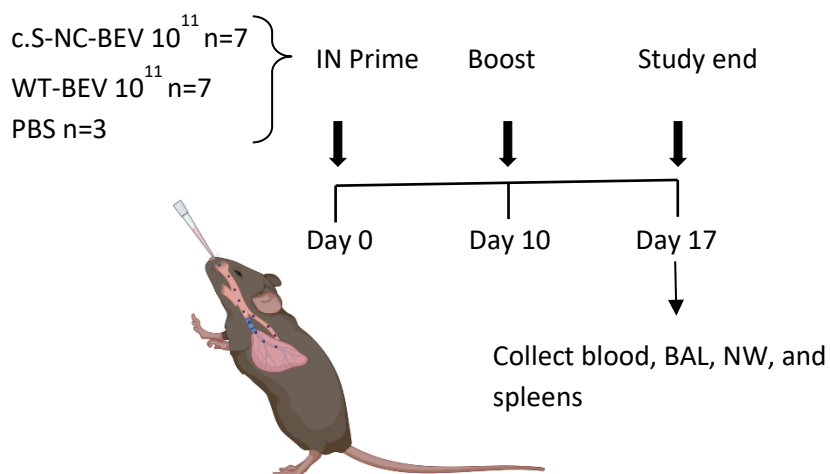


Figure 5.22 Animal study to determine mucosal immune response to c.S-NC-BEV vaccination. C57BL/6 male mice were immunised with either c.S-NC- BEV 10^{11} , WT-BEV 10^{11} or PBS intranasally and boosted on day 10. Blood, BAL, NW and spleens were collected at the end of the study on day 17.

Table 5.8 Characteristics of intranasal c.S-NC-BEV experiment

Media	SEC	Spike conjugation	Spike concentration	Route
BDM+	YES	Chemically	31ng	IN

The levels of both NC and S-specific IgG in serum collected at the end point of the study were similar in all three immunisation groups (Fig. 5.23).

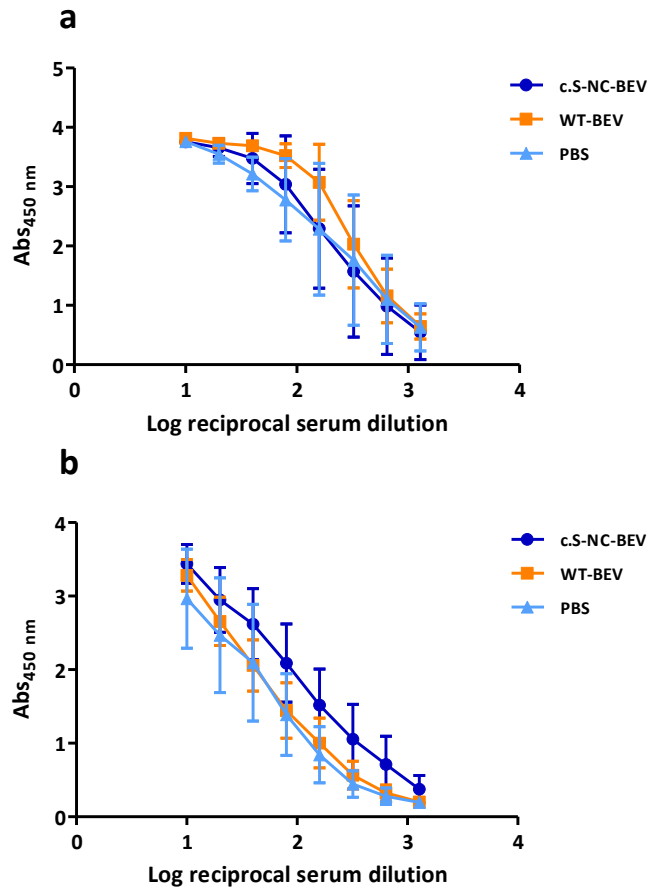


Figure 5.23 Quantification of serum IgG antibodies to NC and c.S in response of intranasal c.S-NC-BEV study by ELISA. Mice were immunised IN with c.S-NC-BEV 10^{11} , WT-BEV 10^{11} or PBS and boosted on day 10. Blood was collected on day 17 and analysed by ELISA to detect titre of specific antibody anti-NC (a) and anti-S (b). Data is represented by the mean value for each group $n=6 \pm$ standard deviation. Statistical analysis was performed using two-way ANOVA with Bonferroni post-test.

Antibodies analysed from NW also showed similar levels of anti-NC and anti-S IgA in all three groups (Fig. 5.24. a, b). In BAL samples, levels of NC-specific IgA were significantly higher in mice immunised with WT-BEVs than in mice immunised with c.S-NC-BEVs or PBS ($p<0.0001$) (Fig. 5.24.c). Contrarily, levels of S-specific IgA were higher in mice immunised with c.S-NC-BEVs than the other two groups, although not statistically significant (5.24.d).

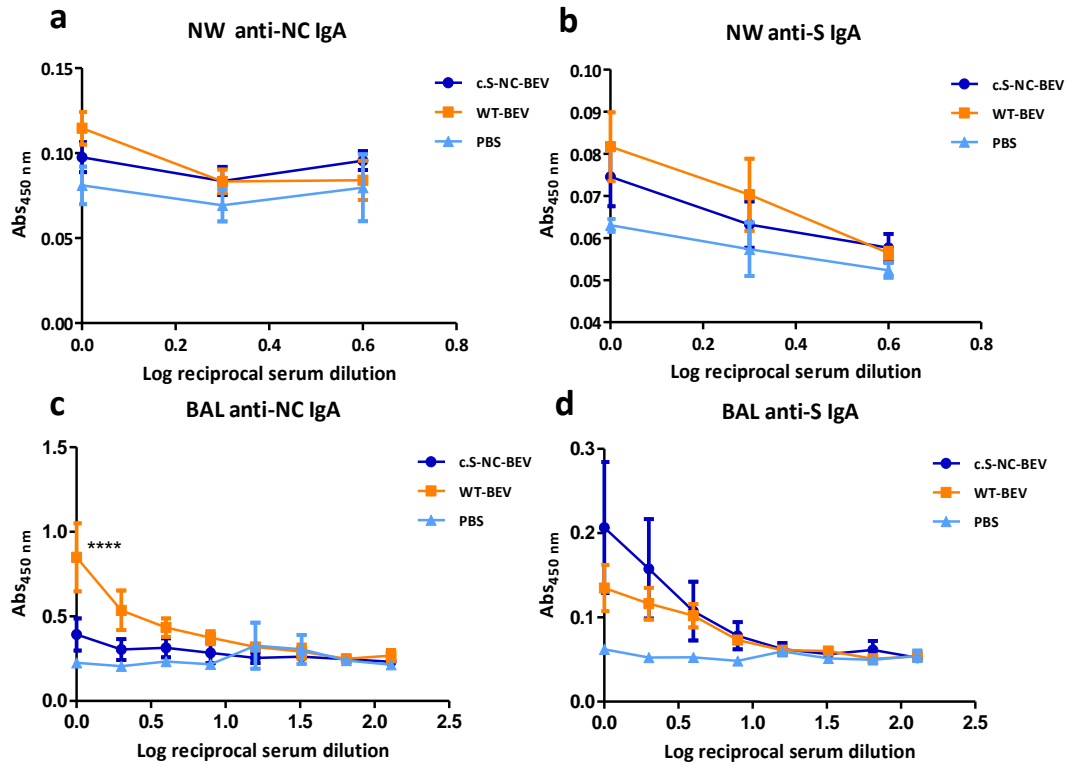


Figure 5.24 Quantification of mucosal antibodies to NC and c.S in response of intranasal c.S-NC-BEV study by ELISA. Mice were immunised IN with c.S-NC-BEV 10^{11} , WT-BEV 10^{11} or PBS and boosted on day 10. NW (a,b) and BAL (c,d) were collected on day 17 and analysed by ELISA. Data is represented by the mean value for each group $n=6 \pm$ standard deviation. Statistical analysis was performed using two-way ANOVA with Bonferroni post-test. **** <0.0001 .

Splenocytes analysed by flow cytometry showed approximately two-fold higher levels of CD4+ and CD8+ T cells expressing TNF- α or IFN- γ in mice immunised with either c.S-NC-BEVs or WT-BEVs than with PBS (Fig. 5.25). No difference was observed between samples from c.S-NC-BEVs and WT-BEVs immunised animals.

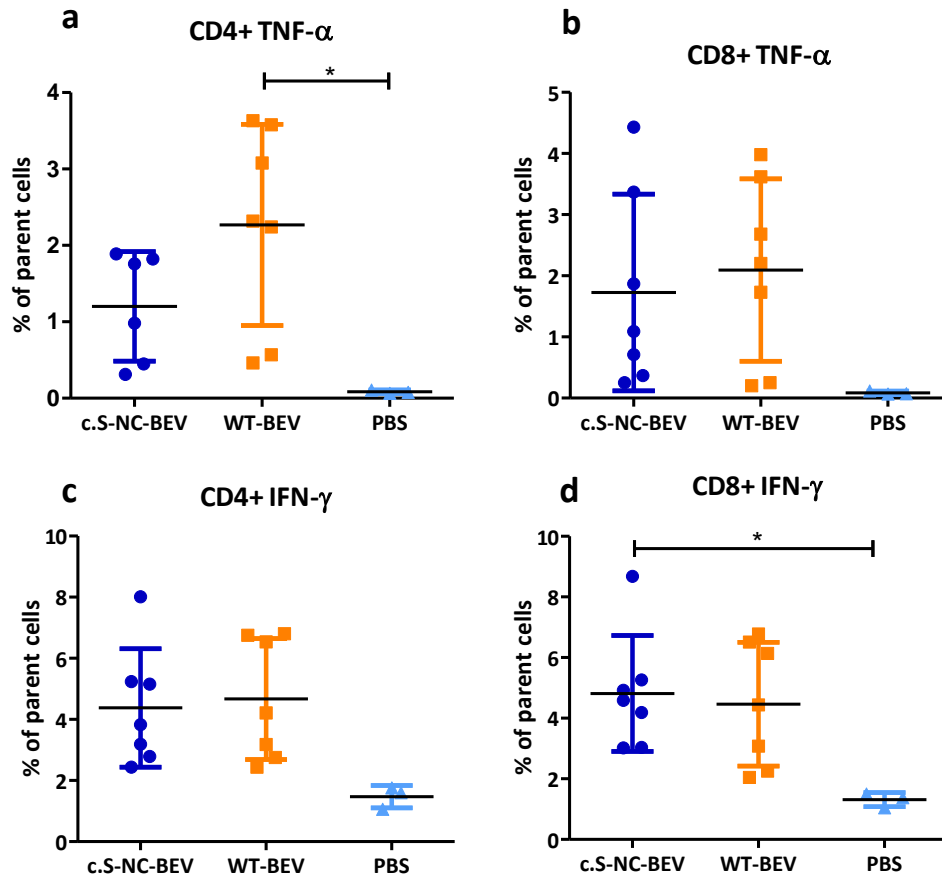


Figure 5.25 Quantification of cytokines expressed in splenocytes from mice immunised IN with c.S-NC-BEV by flow cytometry. Mice were immunised with c.S-NC-BEV, WT-BEV or PBS and boosted on day 10. Splens were collected on day 17th and splenocytes were cultured in complete media alone for 6h prior to analysis. Data is represented by the mean value for each group $n=4 \pm$ standard deviation. Statistical analysis was performed using one-way ANOVA with Bonferroni multiple comparison post-test. $* < 0.05$.

Stimulation of splenocytes did not induce production of cytokines in any of the vaccinated groups. Higher numbers of both TNF- α and IFN- γ producing CD4+ T cells were seen in mice immunised with WT-BEVs with a mean of $\sim 2\%$ compared to $\sim 1\%$ in c.S-NC-BEV group and $\sim 0.3\%$ in PBS group (Fig. 5. 26).

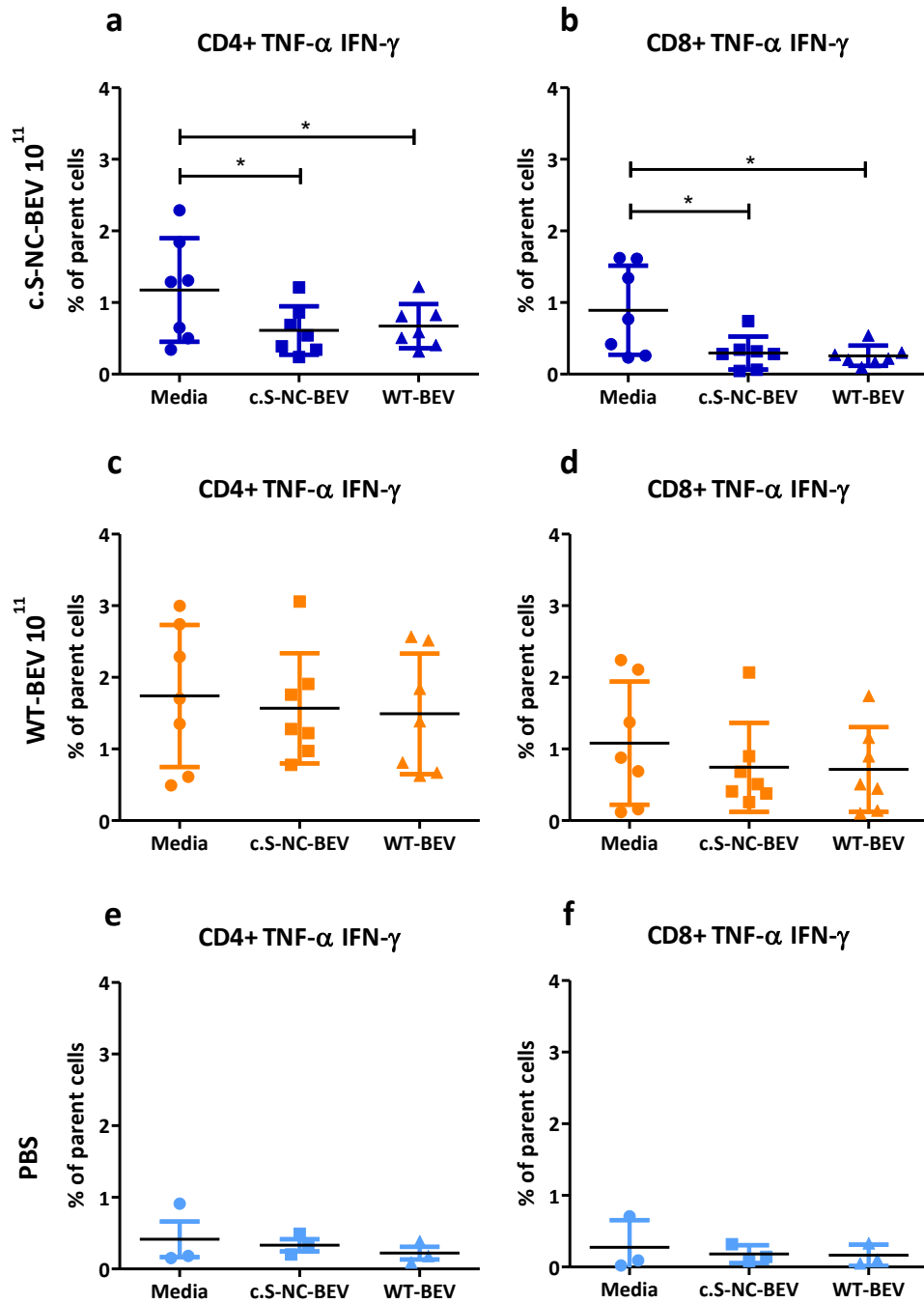


Figure 5.26 Quantification of cytokines expressed in stimulated splenocytes from mice immunised IN with c.S-NC-BEV by flow cytometry. Mice were immunised with c.S-NC-BEV, WT-BEV or PBS and boosted on day 10. Spleens were collected on day 17th and splenocytes were cultured in complete media alone, c.S-NC-BEV or WT-BEV and stimulation for 6h prior to analysis. Data is represented by the mean value for each group $n=4 \pm$ standard deviation. Statistical analysis was performed using one-way ANOVA with Bonferroni multiple comparison post-test. $* < 0.05$.

BAL collection was difficult and only one sample could be collected, from the PBS treated group. The results show that levels of cytokines in CD4+ or CD8+ T cells were equivalent in all three immunisation groups (Fig. 5.27).

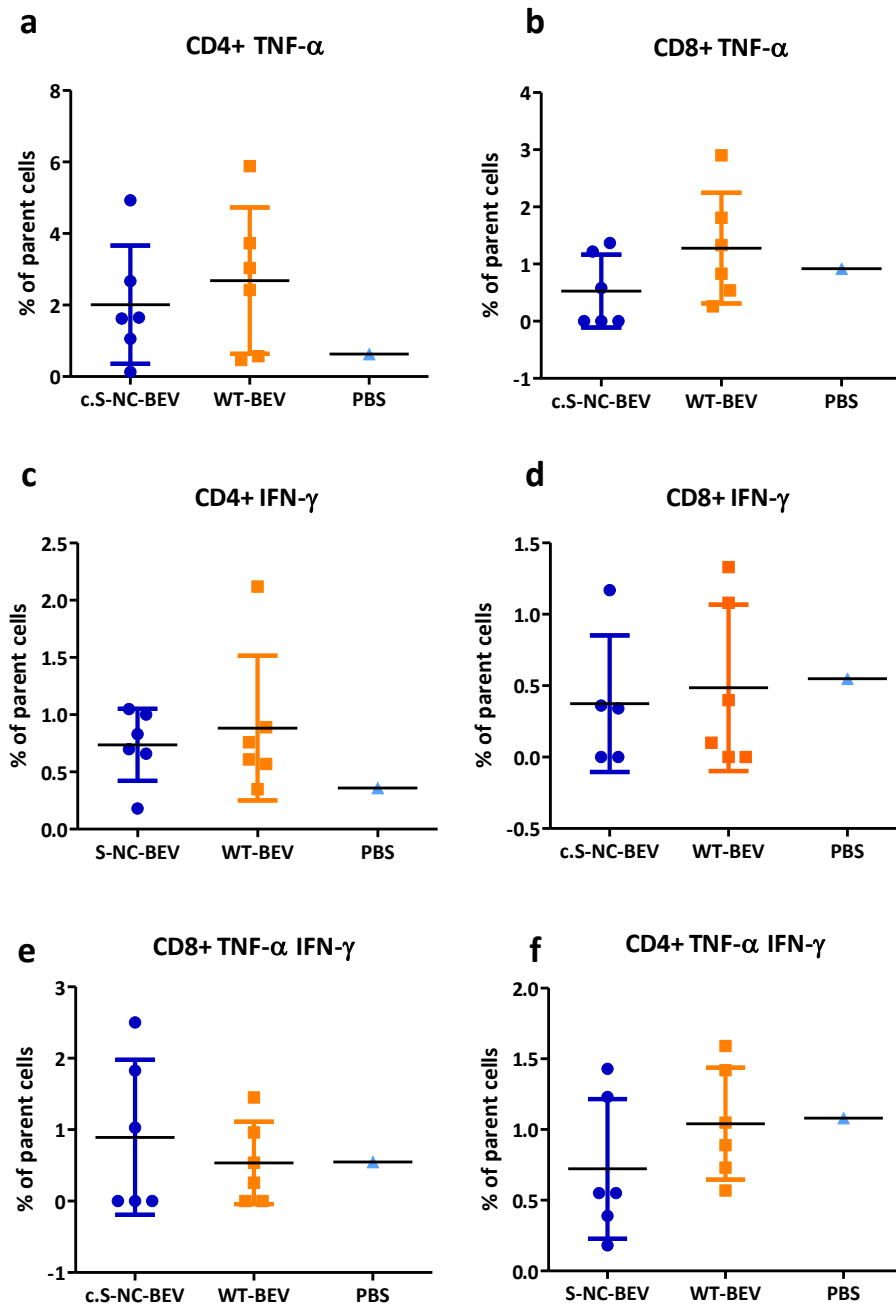


Figure 5.27 Quantification of cytokines expressed in BAL cells from mice immunised IN with c.S-NC-BEV by flow cytometry. Mice were immunised with c.S-NC-BEV, WT-BEV or PBS and boosted on day 10. BAL was collected on day 17th and cells were cultured in complete media alone for 6h prior to analysis. Data is represented by the mean value for each group $n=4 \pm$ standard deviation. Statistical analysis was performed using one-way ANOVA with Bonferroni multiple comparison post-test.

5.3 Discussion

SARS-CoV-2 virus causes life-threatening disease (Covid-19) and although vaccines have limited the spread of the virus, new vaccines are needed to provide front line, mucosal, long-term immunogenicity. In this study, I have shown that Bt BEVs may be an option for mucosal vaccine for SARS-CoV-2. Bt BEVs can be decorated with viral proteins using vitamin B12 receptors (ButG), highly expressed by Bt BEVs, and S conjugated with vitamin B12, or by amine-based conjugation using click chemistry. With the aim of generating a multi-valent vaccine, Bt has been engineered to export NC to BEVs. Different vaccine formulation containing S and NC proteins have, in initial immunisations studies, provided evidence of immunogenicity (Table 5.9). However, further optimisation of dose formulation is required to generate effective cell and humoral immune responses that can provide long-lasting mucosal and systemic immunity.

Table 5.9 Comparison of all SARS-CoV-2 Bt BEVs vaccine experiments

Experiments	1st	2nd	3rd	4th	5th
Route	IP	IN	IP	IP	IN
Formulation	B12.S-BEV	B12.S-BEV	B12.S-NC-BEV	c.S-NC-BEV	c.S-NC-BEV
Dose	10 ⁸	10 ⁸	10 ⁸	10 ¹¹	10 ¹¹
S dose	10µg	10µg	0.025ng	31ng	31ng
SEC	no	no	yes	yes	yes
Systemic Ab	++	+	++	++	-
Mucosal Ab	n. a	n. a	n. a	n. a	+
T cell	n. a	n. a	-	++	+
Protection	n. a	+	n. a	n. a	n. a

n. a: not assessed, - : no stimulation, + : weak stimulation, ++ : strong stimulation.

In the 2nd experiment, intranasally vaccinated mice were challenged with a heterotypic strain, and the vaccine formulation containing 10µg B12.S-BEV had a bigger impact on reducing viral load than the lower 3.6ng dose. This indicates that the amount of

S protein delivered, bound or unbound to Bt BEVs, is an important factor. SEC purification eliminated non-bound proteins and reduced the amount of S delivered per dose in 10^8 BEVs to 0.025ng. This could explain the weak immune responses elicited by SEC-purified BEV vaccines in experiments 3-5. Other BEV-based SARS-CoV-2 vaccines in the literature contain between 280ng to 25,000ng of S per dose (141, 148, 150) with or without additional adjuvants (320, 321). In these studies, the lowest dose of S found to be protective was $3 \cdot 10^{10}$ *Salmonella enterica* serovar Typhimurium BEVs decorated with 280ng of S delivered intranasally (148). Which is approximately ten times higher than the amount of S delivered using Bt BEVs.

Quantification of S protein attached to Bt BEVs was made difficult due to small amounts expressed that could not be reliably detected by conventional sandwich-ELISAs using available antibodies. The maximum amount of S bound to BEVs via the B12 receptor was calculated based on the amount of vitamin B12 added to BEVs that could sustain the growth of vitamin B12-dependent Bt (Dr Rokas Juodeikis). An in-house solid phase ELISA was used to verify this approach. Although this approach was able to provide an estimate of bound S, the results should be interpreted with caution. The results were based on only a small number of replicates and relied on NTA (Zetaview) to determine the concentration of BEVs. NTA can display variance in yield that contributes to the accuracy of quantification.

The two methods of decorating BEVs have similar capacity to conjugate S protein. Due to protocol and methodological differences, it was not possible to ascertain which method was superior in terms of inducing immune responses. This requires a side-by-side comparison of the same dose of BEVs obtained using the same purification method. Both methods are however highly versatile as both can be used to decorate BEVs with structurally different antigens including sugars, peptides, and proteins.

Future experiments would include optimising further the chemical conjugation by for example, using different S concentrations and binding times. More replicates and other quantification techniques could also be used to improve the accuracy of the results. For example, dyes (Cy5 or GFP) bound to S or N3 could be used to quantify S binding to BEVs using reference concentrations. Also, increasing further the expression of high affinity B12 receptors or B12 binding protein in BEVs, by engineering, could also be considered to increase the amount of B12.S conjugated to BEVs.

Quantification of NC in BEVs relied on immunoblotting, resulting in 0.2µg of NC expressed by 10^{11} NC-BEVs. Of note, NC coverage by proteomics-based analysis was ~20% which is lower than previous expressed proteins (40-70%). The coverage indicates that from 26 tryptic peptides produced by NC, six are detected (23% of the detectable size range) with the other peptides being undetectable. Detection of peptides vary as different proteins produce different numbers of detectable tryptic peptides, which bind differently to the liquid chromatography columns and ionise differently in MS electrospray. Also, in complex samples such as BEVs, the MS is not able to analyse all peptides from the proteins coming in continuously from the liquid chromatography because of time limitations. Proteomics is also not quantitative and relies on calculating relative abundance. Accurate quantification requires special targeted methods with synthetic peptide standards.

The marginal effect of NC-BEVs in generating specific immune responses compared to WT-BEVs in intranasal delivery could be related to sub-optimal amounts of NC delivered. Other vaccine formulations containing NC together with S and adjuvants parenterally deliver between 10 to 120µg of NC (322-324).

Regarding the dose of BEVs, the higher dose of 10^{11} chemically attached S-NC-BEV, when delivered parenterally, induces the highest levels of anti-S and anti-NC IgG antibodies, as well as IFN-γ and TNF-α producing CD4+ and CD8+ T cells. This is analogous to our prior study using $\sim 10^{11}$ BEVs containing Influenza H5F which induced protection against infection by a heterotypic virus. However, when the same S-NC-BEV vaccine formulation and dose was administered intranasally no significant difference was observed in humoral or T cell response compared to WT-BEVs. Different immunisation sites might need different optimal vaccine doses to elicit protection. Also, different vaccine formulations might need different doses. Future experiments should focus on doing an intranasal dose response experiment to assess the best dose for this vaccine formulation.

Levels of cytokine-expressing antigen-specific T cells induced by vaccine antigens are expected to be low (325-327) with small variations in compensation, gating or number of events recorded potentially making it difficult to reliably detect and quantify responding, antigen-specific, T cells. ELISAs were used to obtain an independent assessment of cytokine production by vaccine-elicited immune cells. The results obtained confirm the flow cytometry data and show production of IFN-γ and TNF-α by splenocytes from S-NC-BEV and WT-BEVs vaccinated mice stimulated with BEVs. The difference in

incubation time between the flow cytometry assay (6h) and ELISA (72h) made a difference in cytokine expression T cells cultured in media alone.

Higher levels of cytokines produced by cells cultured in media alone, compared to those that were re-stimulated with antigen/BEVs, in the flow cytometry assay, could indicate that T cells stimulated *in vivo* are refractory to re-stimulation (possibly anergic) *ex vivo* or, that the conditions used for re-stimulation were sub-optimal. Also of note, splenocytes from mice immunised IP with 10^{11} c.S-NC-BEVs and then cultured with WT-BEVs produced higher cytokine levels compared to those re-stimulated with c.S-NC-BEVs. Although the reasons for this are unclear, S binding to BEVs externally might hide or make PAMPs, such as LOS, recognised by APC inaccessible, modifying therefore the uptake distribution of BEVs.

Administering WT-BEVs reduces weight loss and viral titre in mice challenged with SARS-CoV-2 and increases IFN- γ and TNF- α production by CD4+ and CD8+ T cells in splenocyte cultures. Although the mechanisms of this effect are unclear it is consistent with the prior studies where WT-BEVs also improved clinical symptoms in mice challenged with IV (3). Recent work from our group has shown that BEVs are potent inducers of innate immune responses (120) and by activating APCs (97) may act to trigger or amplify T and B cell responses.

In summary, Bt BEVs engineered to express NC and decorated with S protein using two different methods can elicit modest antigen-specific responses and with further refinement and optimisation prove to be useful mucosal vaccines for SARS-CoV-2.

Chapter 6 Stability of Bt BEVs

6.1 Introduction

Stability of vaccines is an important factor that has an enormous influence on the success of immunization plans worldwide. Most vaccines are in liquid form, which are cost-effective and convenient, requiring no reconstitution or manipulation prior to use. However, most liquid vaccines are not stable at ambient temperatures and require cold or ultra-cold storage (42). Maintenance of continuous cold chain can be challenging, particularly in developing countries, and significantly increase vaccination costs. Ideally, vaccines should be stable and stored at ambient temperature with a long shelf life. However, this has been rarely achieved by current vaccines, with the vast majority needing cold, frozen, or ultra-cold storage and distribution (328). The WHO recommends vaccines to be stable and stored at +2 °C to +8 °C (329) for a minimum of 18-36 months (330).

A common approach to improve thermal stability of vaccines is lyophilisation. Freeze-drying a sample by lyophilisation involves freezing the sample followed by sublimation of water into gas in a vacuum. Lyophilisation slows degradation of molecules, hence, improving shelf life and reducing dependency on cold chain storage (331). Other benefits include reduction of product weight and reduced shipping and distribution costs. Conversely, lyophilisation adds an additional manufacturing cost and requires the extra step of reconstitution before administering the vaccine. For this reason, lyophilisation is an option for vaccines that requires freezing or ultracold storage. The licensed SARS-CoV-2 Pfizer/BioNTech vaccine is at present distributed using ultra-cold storage, with a lyophilised formulation currently being evaluated in a phase III clinical trial (332).

The lipid bilayer of BEVs confers protection of luminal content. Porin proteins in the membrane mitigate the pressure caused by temperature changes by allowing transfer of small molecules and water in and out of the BEVs (333). BEVs from *E. coli* have been used to package enzymes, which after several freeze and thaw cycles and challenging storage conditions, maintain their enzymatic activity (333, 334). BEVs are complex structures and the interaction of all their components influences their overall stability (122). As BEV cargo varies for different bacterial strains their stability will also differ (335).

Hence, stability characteristics need to be determined for each strain and vaccine formulation.

The *N. meningitidis* OMVs based vaccine, Bexero, is stored at +2 °C to +8 °C and has a shelf life of up to 4 years (133). However, three months storage of *N. meningitidis* OMVs at 37°C results in loss of immunogenicity (336). When *N. meningitidis* or *E. coli* OMVs are stored at temperatures higher than 30°C they can suffer degradation of proteins, chemical and conformational changes in LPS, and change of overall structure, or even lysis (122, 336). Some studies suggest using lyophilisation to increase the stability of BEVs at higher ambient temperatures (333, 335, 336), accepting their particle concentration may be reduced as a consequence of BEV aggregation (335, 336). *N. meningitidis* OMVs stored for three months in lyophilised form show aggregation but their immunogenicity was preserved (336). The use of cryoprotectant agents and other excipients to prevent formation of ice crystals and damage in BEVs have been used in *N. meningitidis* vaccines since 1987 (Table 6.1).

Table 6.1 *N. meningitidis* OMV vaccine excipients

Vaccine formulation	Protective agent/preservative					
	Thimerosal (preservative)	Aluminium hydroxide	Sodium chloride	Sucrose	Tris-HCl	Histidine buffer
1987 VA-MENGOC-BC (Cuba)(337)	✓	✓	✓			
2000 MonoMen (Netherlands) (338)		✓		✓	✓	
2000 MenBvac (Norway) MenZB (New Zeland) (339)		✓	✓			✓
2015 Bexsero Novartis (90)		✓	✓	✓		✓

Thimerosal was a widely used antiseptic and antifungal with aluminium hydroxide being used as an adjuvant. Sodium chloride, Tris-HCl and sucrose solutions are added to obtain an isotonic preparation and prevent pH fluctuations. Additionally, sucrose confers stability by maintaining the native state of globular proteins against chemical denaturants and temperature. Sucrose is used as stabiliser in mRNA vaccines (340), intranasal influenza vaccine (FluMist and Fluenz) (341), and oral rotavirus vaccine (342). Histidine buffers adjust pH, assure antigen adsorption to aluminium hydroxide, and reduce antigen hydrolysis to improve product stability (90). Tris and sucrose excipients are also incorporated in an OMV formulated Covid-19 vaccine now in phase I clinical trials (Intravacc 10) (150).

The goal of this chapter is to analyse the stability of Bt BEVs and determine how different storage conditions affect their biophysical characteristics.

The aims are to:

- Determine the impact of different storage conditions on the stability of antigens expressed in BEVs.
- Select the optimal buffer for stabilising Bt BEVs: PBS, Histidine buffer + sucrose or Tris-HCl + sucrose.
- Select the optimal means of long-term storage of Bt BEVs: liquid or lyophilised

6.2 Results

6.2.1 Thermostability of V-BEVs

To assess thermostability of V-BEVs expressing V antigen of *Y. pestis* (Chapter 3), duplicate aliquots were stored for 8 weeks at 4°C and 40°C prior to analysing V antigen expression by immunoblotting. The results (Figure 6.1) show that the level of V in V-BEVs in preparations stored at 4°C was equivalent to pre-storage levels (Chapter 3). However, when stored at 40°C the level of V antigen was reduced compared to pre-storage levels. To detect loss and leakage of BEVs during storage, the storage buffer was analysed in parallel to BEV lysates. It was not possible to detect V antigen in the buffer of BEVs stored at either 4°C or 40°C.

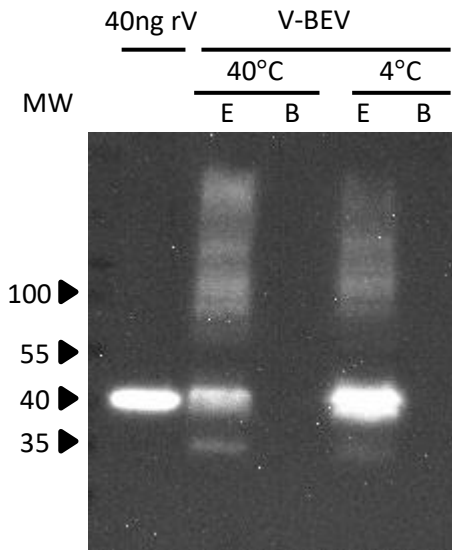


Figure 6.1 Thermostability of V-BEVs by immunoblot. V-BEVs were isolated in PBS and stored for 8 weeks at 40°C and 4°C. Stored samples were filtrated using 100K membrane ultrafiltration spin columns and both, the extracts containing BEVs (E), and the storage buffer (B) were analysed using an anti-V antibody. Molecular weight (MW) expressed in kDa.

6.2.2 Stability of NP-BEVs

The influence of different storage buffers on BEV stability was assessed using BEVs expressing Influenza antigen NP, (Chapter4). Multiple aliquots of SEC-purified NP-BEVs ($2 \cdot 10^{11}$ BEVs/ml) were stored in either PBS, 10mM Histidine + 3% sucrose, or 10mM Tris-HCl + 3% sucrose buffer at different ambient temperatures in liquid or lyophilised forms for 15 weeks (Fig. 6.2). After day 1 and week 4 and 15, total protein, THP1 cell activation, particle concentration and peak size was measured and compared to pre-storage, day zero (set to 100%).

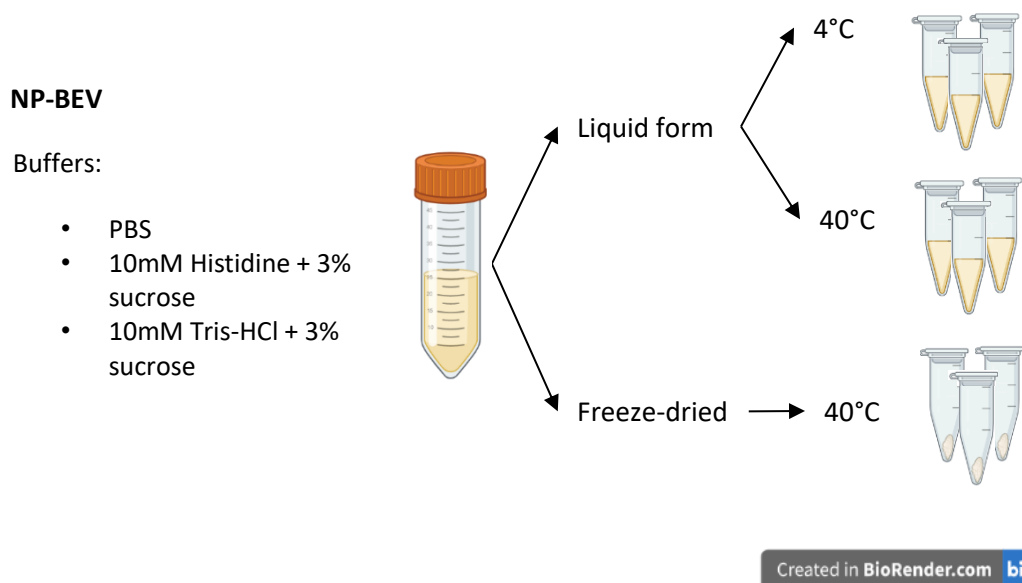


Figure 6.2 Storage conditions of NP-BEVs to assess stability. NP-BEVs were isolated, and SEC purified in either PBS, 10mM Histidine + 3% sucrose or 10mM Tris-HCl + 3% sucrose buffer. Samples were stored for 15 weeks under different conditions (liquid form at 4°C and 40°C, and in lyophilised form at 40°C) in triplicates. Figure created in BioRender.

The results (Fig. 6.3) show that total protein remained constant in PBS samples but increased by more than 5-fold in Histidine-sucrose buffer, or 10-fold in Tris-HCl-sucrose samples stored at 40°C. The activation of THP1 cells remained constant, except for samples stored at 40°C in Histidine-sucrose that displayed a reduced (by ~90%) ability to activate THP1 cells after 15 weeks. The particle concentration was reduced in all samples, with those stored in PBS at 4°C having the lower reduction compared to lyophilised samples, where the concentration decreased 70% after 15 weeks. The particle peak size of samples in PBS and Histidine-sucrose increased by day 1, which was not seen in those stored in Tris-HCl sucrose. By week 15, samples from all three buffer groups showed similar peak size than day 0.

To assess structural integrity after storage, NP-BEVs in PBS and Histidine-sucrose stored at 40°C and lyophilised samples were analysed by TEM using negative staining (Fig. 6.4). BEVs appeared heterogeneous in size having the characteristic cup shaped structure of BEVs: after drying the negative stain is retained at the outer surface of the vesicles and has a darker, deflated ball like, appearance (Fig. 6.4). Vesicles stored in PBS appeared individually disperse contrarily to NP-BEVs stored in PBS at 40°C that were aggregated. NP-BEVs in Histidine-sucrose and stored at either 40°C or lyophilised show less

aggregation than NP-BEVs in PBS stored in lyophilised form. This suggests that sucrose reduces aggregation after lyophilisation. Based on this analysis samples stored in PBS at 4°C best retained their original characteristics and appearance (97, 111).

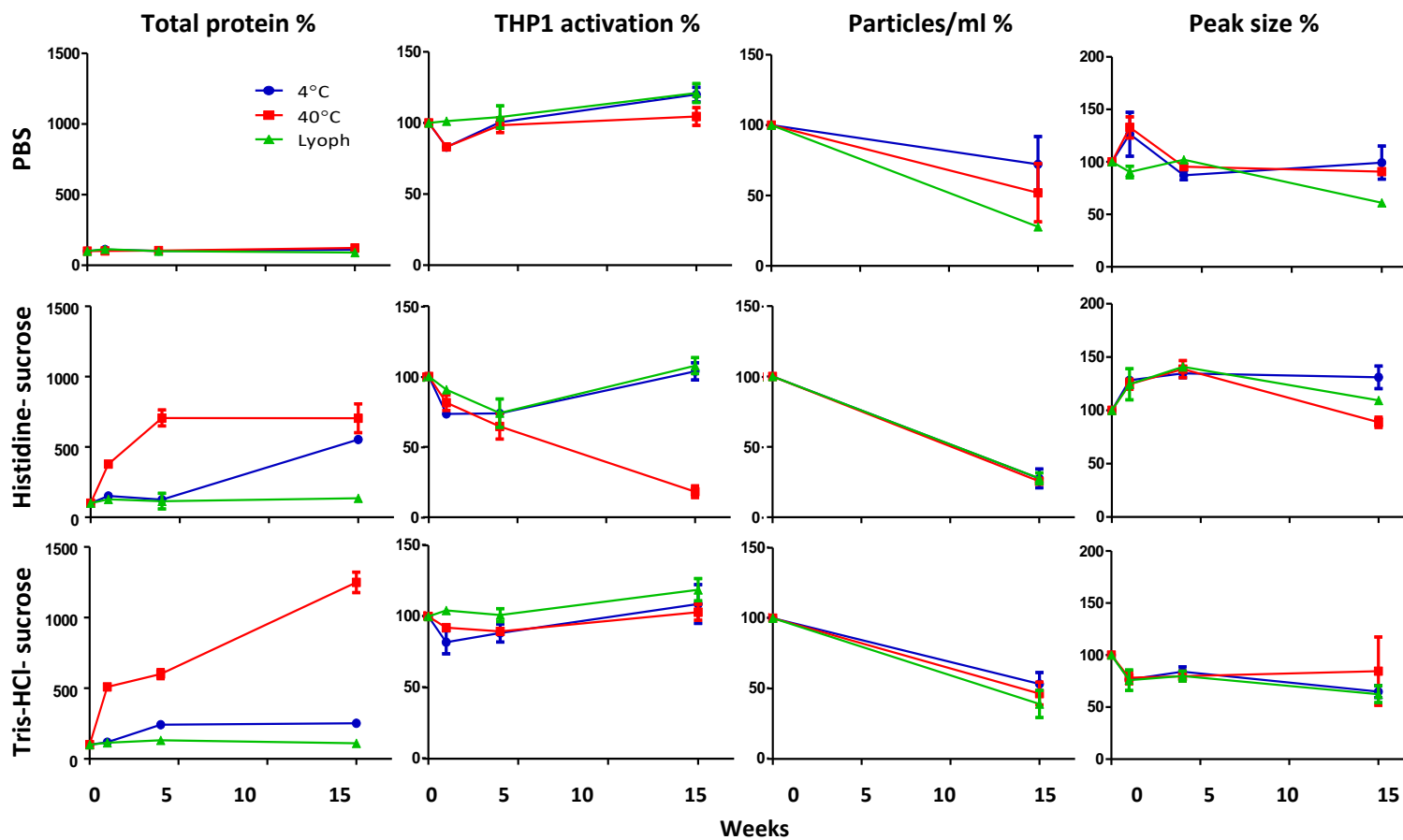


Figure 6.3 Stability of NP-BEV upon different storage conditions. NP-BEVs were isolated and purified in either PBS, 10mM Histidine + 3% sucrose or 10mM Tris-HCl + 3% sucrose buffer and stored for 15 weeks under different conditions (liquid form at 4°C and 40°C, and in lyophilised form at 40°C) in triplicates. Total protein concentration,

activation of THP1 cells, particle concentration and peak size analysed by NTA were assessed on days 0 and 1, and weeks 4 and 15 of storage. Data is represented by the mean value for each group $n=3 \pm$ standard deviation. Results expressed in 100% based on results from day 0.

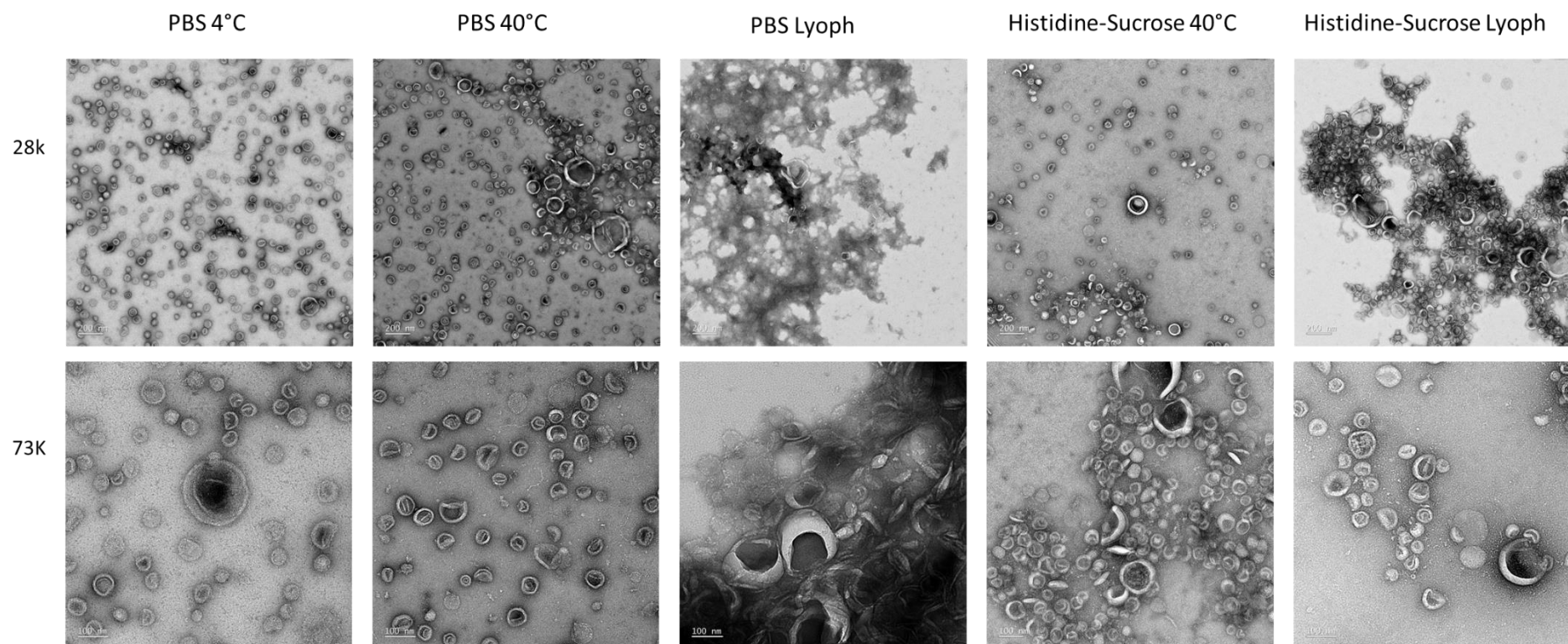


Figure 6.4 TEM images of NP-BEV upon different storage conditions. NP-BEVs were isolated and purified in either PBS or 10mM Histidine + 3% sucrose and stored for 15 weeks under different conditions (liquid form at 4°C and 40°C, and in lyophilised form at 40°C) in triplicates. After 15 weeks the triplicates were pulled together and analysed by TEM using negative staining. Images show two different magnifications, 28K and 73K, of each sample analysed.

NP-BEVs stored for 15 weeks in liquid form at 4°C and 40°C, and in lyophilised form at 40°C, were assessed by immunoblotting. Similar to BEVs expressing *Y. pestis* antigens, NP-BEVs stored at 4°C for 15 weeks exhibited high stability with minimal loss of NP. However, storage at 40°C led to a decrease in antigen detection, seen by the decrease in intensity of the antibody-reactive band compared to pre-storage levels (Chapter 4). After storage at 40°C, the lyophilised formulation showed increased antigen protection compared to the liquid formulation. No antigen was detected in the buffer storage after NP-BEVs were filtrated using 100K membrane ultrafiltration spin columns.

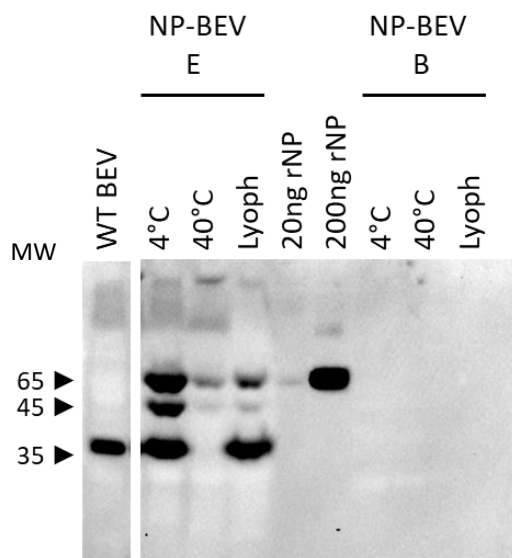


Figure 6.5 Thermostability of NP-BEVs by immunoblot. NP-BEV were isolated, and SEC purified in PBS and stored for 15 weeks at 4°C and 40°C, and in lyophilised form at 40°C. Stored samples were filtrated using 100K membrane ultrafiltration spin columns and both, the extracts containing BEVs (E) and the storage buffer (B) were analysed using an anti-NP antibody. Molecular weight (MW) expressed in kDa.

6.3 Discussion

Vaccine stability is integral to the success of global vaccination programmes. BEVs are stable structures when stored at 4°C but tend to aggregate and lose immunogenicity at higher temperatures (333, 335, 336). In this study, Bt BEVs were shown to be stable at 4°C but tended to aggregate and lose antigen at higher temperatures or after lyophilisation.

Antigen levels were reduced in V-BEVs and NP-BEVs after storage at 40°C for 8 or 15 weeks. This is analogous to denaturation of antigen followed by chemical degradation seen in *N. meningitidis* OMV after storage at 56°C for 12 weeks (336). Contrarily, substitution of PBS with Histidine-sucrose or Tris-HCl-sucrose buffer led to an apparent increase in total protein at 40°C and 4°C. The results are comparable to enrichment of proteins in storage buffer of extracellular vesicles stored at -80°C (343-345). The increase in total protein in stored EVs is defined as a result of leakage from vesicles, possible due to lysis during storage (343-345). This would mean that BCA total protein quantification only measures surface proteins and not luminal. However, when freshly isolated BEVs were supposedly lysed using 2% SDS 10 minutes at 90°C, the total protein measured using BCA method was similar, demonstrating that BCA can detect luminal and surface proteins. Sterility of samples was also confirmed by plating the sample in LB and BHIH plates stored at 37°C, 20°C and in the anaerobic cabinet and by using simple microscopy. The increase could also be consequence of an artifact created while quantifying total protein. Repeating the experiments and using other total protein methods and lysis methods could be used to understand why total protein increased in those samples.

Sucrose was effective at decreasing aggregation as seen by TEM. During lyophilisation and storage at 40°C the aggregation of BEVs is probably the result of freezing the sample which can cause crystal formation and disruption of vesicle structure, leading to aggregation after reconstitution. The presence of sucrose reduced but did not eliminate vesicle aggregation. Similarly, the addition of 3% sucrose to *N. meningitidis* OMV formulations limited but did not prevent aggregation after lyophilisation (336). On the other hand, *N. meningitidis* OMVs maintained their conformation and immunogenicity after lyophilisation (336). Lyophilisation is a good alternative for long-term storage or storage at higher temperature. The use of other cryoprotectants could be investigated such as trehalose, which has been successfully used to stabilise EV (346, 347) and could be a good alternative to sucrose.

This study has been based mainly on external changes to Bt BEVs. The ultimate way to assess immunological properties of stored Bt BEVs would be to do *in vivo* experiments and compare stored versus freshly prepared Bt BEVs vaccines. Also, more biological replicates should be used to determine reproducibility. This is also important for the TEM analysis as the staining and drying steps for the TEM sample preparation can impact on aggregation of vesicles or produce artifacts.

In conclusion the best performing storage conditions for Bt BEVs are in liquid form in PBS at 4°C which can protect BEV integrity for at least 15 weeks.

Chapter 7 Discussion

Vaccines for respiratory pathogens would ideally comprise particles that can be self-administered for example, via nasal drops or sprays, and be resistant to enzymatic or chemical degradation. Vaccines would be able to diffuse through mucus layers, avoiding entrapment and removal by mucociliary clearance, and access boundary epithelial cells and underlying APC. Moreover, vaccines should induce innate and adaptive immune responses and confer long-term protection against heterotypic strains, with a single dose, in the absence of any adverse effects. Finally, vaccines should be thermostable across a range of ambient temperatures, be straightforward to produce, and cost effective. The difficulty in meeting these essential criteria explains in large part why there are so few successful, licensed mucosal vaccines (10, 27).

The aim of this thesis was to evaluate the use of Bt BEVs as a mucosal vaccine delivery system to protect against respiratory pathogens. The work described in this thesis has demonstrated that Bt BEVs match up to many of the characteristics of an ideal vaccine and with the disease Target Product Profiles (TPP) for plague, IV and SARS-CoV-2, as defined by WHO (169, 348, 349) (Table 7.1).

Table 7.1 Correlation of Bt BEVs with TPP for plague, IV and SARS-Cov-2 vaccines

Vaccine characteristic	Preferred characteristics	Bt BEV matching
Vaccine type	Non-replicative	YES
Target population	Children, adults, and others at risk	ND
Stability	Thermostable	YES
Storage	Minimum of 2 months at 2-8°C for Covid-19 vaccine	YES
Administration route	Non-parenteral	YES
Indication for use	Protection against multiple strains	YES
Efficacy	~70% against symptomatic disease and 90% against severe disease for Covid-19	ND
Safety	Minor contraindication and reactogenicity	YES

Dose regimen	Single	ND
Durability	Protection conferred for 1 year in Covid-19 vaccines and 5 years for flu vaccines	ND

ND: Not Determined

Vaccines should be suitable for individuals across the lifespan, from infants of 6 weeks old, to the elderly, including high-risk immunocompromised individuals (169, 348, 349). Intranasal vaccines need to achieve a balance between safety and efficacy; sufficiently immunogenic to overcome immune tolerance yet avoiding eliciting aggressive immune responses that could result in tissue injury and compromise function.

This thesis has demonstrated that Bt BEVs administered intranasally to NHPs have no adverse reactions, pathology, or impact on the nasal microbiota. Also, intraperitoneal, or intranasal deliver of WT-BEVs in mice, results in no adverse impact on body weight or tissue pathology. Future experiments building on these safety evaluations would include analysis of acute toxicology, reproductive and developmental toxicity including toxicity in the offspring (350). It also could include carcinogenicity, mutagenicity and safety pharmacology assays which analyse physiological functions including the central nervous system, respiratory system and cardiovascular system (350). Bexsero vaccine is currently the only licensed vaccines containing BEVs and is administered intramuscularly to adults and children from 2 months of age (133). While this cannot be compared with the Bt BEV vaccine formulations developed and used here, it demonstrates the feasibility of BEVs being used as a safe vaccine for high-risk individuals.

In terms of stability, TPP for Covid-19 vaccines requires them to have a minimum of 2-month stability at 2-8°C. Bt BEVs maintain their biophysical characteristics after storage at 2-8°C for more than 3 months. Building on this, Bt BEVs stability for longer periods and across a wider range of ambient temperatures, particularly those associated with tropical climates could be evaluated. Additionally, other excipients such as trehalose could be assessed for further improving thermostability. More importantly, immunogenicity assays in appropriate pre-clinical models would help determine the immunological properties of stored versus freshly prepared Bt BEVs vaccines.

Needle-free delivery is the preferred means of vaccination for respiratory infections (169, 348, 349). Bt BEVs have been delivered intranasally in liquid suspensions to mice as nasal drops, which benefits mass vaccination and ensures patient compliance.

Their size (50-200nm), and biophysical and immunogenicity characteristics, enables Bt BEVs to diffuse through mucus barriers in the respiratory and gastrointestinal tracts and be taken up by mucosa-associated APCs, such as DCs, non-professional APC and epithelial cells (111, 115). Intranasal delivery of WT-BEVs in mice elicits the formation of organised lymphoid tissue in both the NALT and BALT including lymphoid structures and follicles containing DCs, B cells and T cells. NHPs also exhibit similar responses within their BALT after receiving V-BEVs intranasally. Collectively, this demonstrates that intranasally administered Bt WT-BEVs can cross the respiratory mucosal barriers and induce local and systemic immune responses.

Immunostimulant properties of Bt BEV vaccines are seen in the lower reduction of weight loss of mice challenged with IV or SARS-CoV-2, previously immunised intranasally with WT-BEVs, compared to mice that receive PBS or rS. Mice immunised with WT-BEVs and challenged with SARS-CoV-2 also show reduction in viral titre. Moreover, intranasal delivery of WT-BEVs induce mucosal and systemic antibodies which are probably polyreactive and of low affinity. Polyreactive antibodies bind to a variety of structurally unrelated antigens through their flexible antigen-binding pocket (351). These antibodies are probably activated by LOS in BEVs the same way as LPS induce polyreactive antibodies in mice by TLR4 (352). Similarly, intranasal delivery of WT-BEVs also induce T cells probably by bystander T-cell activation, where T cells respond to cytokines and TLR signalling (TLR2, TLR4) in a T-cell receptor independent manner (353). Proliferation of bystander T cells has also been observed in mice injected with LPS (353-355).

To stimulate pathogen-specific adaptive immune responses, Bt was engineered to produce BEVs containing antigens. Two immunodominant and protective antigens, able to elicit both B and T cells, were selected for each pathogen with the aim of inducing broad immune responses: *Y. pestis* BEV vaccines expressed F1 (surface) or V (lumen) antigens, IAV BEV vaccines contained H5F (not known) and NP (lumen), and SARS-CoV-2 BEV vaccine contained S (surface) or NC (surface). S protein was complexed to BEVs externally using two different systems, B12 receptors on Bt BEVs or by chemical conjugation using click chemistry. Antigen-specific antibody and T cell responses have been observed in response to antigens located in the lumen and surface of BEVs (139, 356-358). More studies are needed to determine the optimal conditions and location for antigen expression in BEVs for generating potent T and B cell responses, including comparing immune responses to BEVs expressing the same antigen on the surface versus the lumen.

Regarding recombinant BEVs, *Y. pestis* BEV vaccines induce antibodies that have properties consistent with providing protection. However, it was not possible to test this directly due to biosafety and (Biosafety level 4) containment requirements. H5F-BEV vaccines induce mucosal and systemic IgA and IgG antibodies and provide heterotypic protection in mice against a lethal challenge, suggesting it could be used as a universal IV vaccine protecting against different IAV strains. Moreover, S-NC-BEVs induce low levels of IFN- γ and/or TNF- α producing CD4/8 T cells and mucosal antibodies.

A single vaccine dose should generate protection to infection that lasts for a minimum of five years for flu or at least 1 year for Covid-19 (348, 349). For H5F-BEVs, a two-dose regimen protects mice against a heterotypic strain. A two-dose regimen also shows the highest levels of immune responses and correlates of protection for plague and Covid-19 BEV vaccines. The importance of a booster immunisation was observed with the V-BEVs and F1-BEVs in increasing antibody levels. This could be particularly important for TRM cells which need repeated antigen exposure to improve the durability of otherwise short-lived lung TRM cells (25). Yet, the number of doses in intranasal vaccines may not be a major issue due to their ease of administration and high patient compliance.

The duration of immune protection has not been studied in this thesis and needs to be analysed in future experiments. This would consist of vaccinating mice and analysing their protection ability against a lethal challenge after several time points, for example 1, 3, 6 and 10 months.

Future consideration should also be given to increasing the amount of antigen expressed in Bt BEVs to assess the dosing regimen that generates long lived protection against infection. As a starting point, the use of alternative promoters in plasmid constructs and signal peptides could increase the incorporation of antigens into BEVs. Lipoprotein export systems (359, 360) or a combination of lipoprotein export system with OmpA (141) are also options. Valguarnera et al. (361) found that lipoproteins enriched in Bt BEVs contained a lipoprotein export sequence that mediates lipoproteins translocation from the periplasm to the BEV surface, and could be used as alternative to the OmpA secretion system.

Future experiments could also improve the conjugation of external antigens to BEVs by either increasing B12 receptors by engineering Bt, or by using different S concentrations and binding times in the chemical conjugation. Alternatively, other methods such as SpyTag-SpyCatcher could be used.

Additionally, it would be beneficial to combine multiple antigens into the same BEV preparation to determine the capacity of multi-antigen BEVs to provide greater protection than single antigen containing BEVs. Multi-antigen BEVs would also reduce preparation time including isolation, quality control assessment and costs. Production of BEVs uses readily accessible manufacturing technology as demonstrated for the Bexsero vaccine. However, scale up and continuous production is needed to improve BEV yield and would reduce costs. This would involve yield quantification and comparison of BEVs characteristics (structure and composition) between batch to batch. For continuous production the dilution rate and the possible mutations in Bt should also be assessed.

Bt BEVs have many attractive features that make them good vaccines candidates. However, as highlighted throughout this section of the thesis, there is room for further improvements and refinements to improve their performance. Understanding the composition of BEVs at different phases of the growth cycle is important for reproducibility and minimising batch-to-batch variability. This would include assessing lipid and protein composition, size, structure, and yields. Accurate quantification is also integral to ensuring reproducibility. BEV quantification has relied on NTA, Bradford, and BCA-based protein content. Although NTA analysis is quick and easy, results can be variable. Protein content in *N. meningitidis* BEVs is dependent on the growth stage, while lipid content is more consistent and less variable (362). Therefore, lipid quantification would be a useful additional quantification method to use in future experiments. Lipids in BEVs have been quantified using lipophilic dyes (FM4-64) (363), phosphate assays (Malachite Green) (364), ELISA and LPS quantification (365) and by modified liquid gas chromatography (150). It is important to note that there is no universally accepted method for determining BEV yield and quantity. Future experiments should assess different techniques for lipid assays, such as phosphate assays and lipophilic dyes, in parallel with NTA and total protein. The results could be used to establish a reproducible means of reliably determining Bt BEV yield. This, together with sterility assessments and biological quality control methods including immune cell (e.g., THP-1 cells) activation would increase the reproducibility of samples.

Collectively, this thesis supports the use of Bt BEVs as a platform to produce mucosal vaccines against respiratory pathogens.

References

1. Stentz R, Miquel-Clopés A, Carding SR. 2022. Production, Isolation, and Characterization of Bioengineered Bacterial Extracellular Membrane Vesicles Derived from *Bacteroides thetaiotaomicron* and Their Use in Vaccine Development, p 171-190. In Bidmos F, Bossé J, Langford P (ed), *Bacterial Vaccines: Methods and Protocols* doi:10.1007/978-1-0716-1900-1_11. Springer US, New York, NY.
2. Carvalho AL, Miquel-Clopés A, Wegmann U, Jones E, Stentz R, Telatin A, Walker NJ, Butcher WA, Brown PJ, Holmes S, Dennis MJ, Williamson ED, Funnell SGP, Stock M, Carding SR. 2019. Use of bioengineered human commensal gut bacteria-derived microvesicles for mucosal plague vaccine delivery and immunization. *Clinical and Experimental Immunology* 196:287-304.
3. Carvalho AL, Fonseca S, Miquel-Clopés A, Cross K, Kok K-S, Wegmann U, Gil-Cardoso K, Bentley EG, Al Katy SHM, Coombes JL, Kipar A, Stentz R, Stewart JP, Carding SR. 2019. Bioengineering commensal bacteria-derived outer membrane vesicles for delivery of biologics to the gastrointestinal and respiratory tract. *Journal of Extracellular Vesicles* 8:1632100.
4. Organization WH. 2020. The top 10 causes of death. <https://www.who.int/news-room/fact-sheets/detail/the-top-10-causes-of-death>. Accessed 2022 October 10.
5. Shiels MS, Haque AT, Berrington de González A, Freedman ND. 2022. Leading Causes of Death in the US During the COVID-19 Pandemic, March 2020 to October 2021. *JAMA Internal Medicine* 182:883-886.
6. Statistics OfN. 2022. How coronavirus (COVID-19) compares with flu and pneumonia as a cause of death. <https://www.ons.gov.uk/peoplepopulationandcommunity/healthandsocialcare/conditionsanddiseases/articles/howcoronaviruscovid19compareswithfluasacauseofdeath/2022-05-23>. Accessed 2022 October 26.
7. Troeger CE, Blacker BF, Khalil IA, Zimsen SRM, Albertson SB, Abate D, Abdela J, Adhikari TB, Aghayan SA, Agrawal S, Ahmadi A, Aichour AN, Aichour I, Aichour MTE, Al-Eyadhy A, Al-Raddadi RM, Alahdab F, Alene KA, Aljunid SM, Alvis-Guzman N, Anber NH, Anjomshoa M, Antonio CAT, Aremu O, Atalay HT, Atique S, Attia EF, Avokpaho EFGA, Awasthi A, Babazadeh A, Badali H, Badawi A, Banoub JAM, Barac A, Bassat Q, Bedi N, Belachew AB, Bennett DA, Bhattacharyya K, Bhutta ZA, Bijani A, Carvalho F, Castañeda-Orjuela CA, Christopher DJ, Dandona L, Dandona R, Dang AK, Daryani A, Degefa MG, Demeke FM, et al. 2019. Mortality, morbidity, and hospitalisations due to influenza lower respiratory tract infections, 2017: an analysis for the Global Burden of Disease Study 2017. *The Lancet Respiratory Medicine* 7:69-89.
8. Sender V, Hentrich K, Henriques-Normark B. 2021. Virus-Induced Changes of the Respiratory Tract Environment Promote Secondary Infections With *Streptococcus pneumoniae*. *Frontiers in Cellular and Infection Microbiology* 11.
9. Saeed S. 2021. Mucosal Immunology, p Ch. 1. In Elena Franco R (ed), *Prebiotics and Probiotics* doi:10.5772/intechopen.98863. IntechOpen, Rijeka.
10. Lavelle EC, Ward RW. 2022. Mucosal vaccines — fortifying the frontiers. *Nature Reviews Immunology* 22:236-250.
11. Mostaghimi D, Valdez CN, Larson HT, Kalinich CC, Iwasaki A. 2022. Prevention of host-to-host transmission by SARS-CoV-2 vaccines. *Lancet Infect Dis* 22:e52-e58.
12. Kar S, Devnath P, Emran TB, Tallei TE, Mitra S, Dhama K. 2022. Oral and intranasal vaccines against SARS-CoV-2: Current progress, prospects, advantages, and challenges. *Immunity, Inflammation and Disease* 10:e604.

13. An X, Martinez-Paniagua M, Rezvan A, Sefat SR, Fathi M, Singh S, Biswas S, Pourpak M, Yee C, Liu X, Varadarajan N. 2021. Single-dose intranasal vaccination elicits systemic and mucosal immunity against SARS-CoV-2. *iScience* 24:103037.
14. Kaler L, Iverson E, Bader S, Song D, Scull MA, Duncan GA. 2022. Influenza A virus diffusion through mucus gel networks. *Communications Biology* 5:249.
15. Mettelman RC, Allen EK, Thomas PG. 2022. Mucosal immune responses to infection and vaccination in the respiratory tract. *Immunity* 55:749-780.
16. Kimura S, Mutoh M, Hisamoto M, Saito H, Takahashi S, Asakura T, Ishii M, Nakamura Y, Iida J, Hase K, Iwanaga T. 2019. Airway M Cells Arise in the Lower Airway Due to RANKL Signaling and Reside in the Bronchiolar Epithelium Associated With iBALT in Murine Models of Respiratory Disease. *Frontiers in Immunology* 10:1323.
17. Silva-Sanchez A, Randall TD. Anatomical Uniqueness of the Mucosal Immune System (GALT, NALT, iBALT) for the Induction and Regulation of Mucosal Immunity and Tolerance. *Mucosal Vaccines*. 2020:21-54. doi: 10.1016/B978-0-12-811924-2.00002-X. Epub 2019 Oct 25.
18. Worbs T, Hammerschmidt SI, Förster R. 2017. Dendritic cell migration in health and disease. *Nature Reviews Immunology* 17:30-48.
19. Luckheeram RV, Zhou R, Verma AD, Xia B. 2012. CD4⁺T cells: differentiation and functions. *Clin Dev Immunol* 2012:925135.
20. Wang Y, Lu X, Wu H, Li W. 2018. Gut-homing α 4 β 7 CD4⁺ T cells: potential key players in both acute HIV infection and HIV-associated cancers. *Cellular & Molecular Immunology* 15:190-192.
21. Eisen HN. 2014. Affinity enhancement of antibodies: how low-affinity antibodies produced early in immune responses are followed by high-affinity antibodies later and in memory B-cell responses. *Cancer Immunol Res* 2:381-92.
22. Kumar Bharathkar S, Parker BW, Malyutin AG, Haloi N, Huey-Tubman KE, Tajkhorshid E, Stadtmueller BM. 2020. The structures of secretory and dimeric immunoglobulin A. *Elife* 9.
23. Reinholdt J HS. 2013. IgA and Mucosal Homeostasis., Madame Curie Bioscience Database [Internet], Landes Bioscience.
24. Peter AS, Grüner E, Socher E, Fraedrich K, Richel E, Mueller-Schmucker S, Cordsmeier A, Ensser A, Sticht H, Überla K. 2022. Characterization of SARS-CoV-2 Escape Mutants to a Pair of Neutralizing Antibodies Targeting the RBD and the NTD. *Int J Mol Sci* 23.
25. Zheng MZM, Wakim LM. 2022. Tissue resident memory T cells in the respiratory tract. *Mucosal Immunology* 15:379-388.
26. Zens KD, Chen JK, Farber DL. 2016. Vaccine-generated lung tissue-resident memory T cells provide heterosubtypic protection to influenza infection. *JCI Insight* 1.
27. Duan W, Croft M. 2014. Control of regulatory T cells and airway tolerance by lung macrophages and dendritic cells. *Ann Am Thorac Soc* 11 Suppl 5:S306-13.
28. Traxinger BR, Richert-Spuhler LE, Lund JM. 2022. Mucosal tissue regulatory T cells are integral in balancing immunity and tolerance at portals of antigen entry. *Mucosal Immunology* 15:398-407.
29. Shen Y, Torchia Maria Letizia G, Lawson Gregory W, Karp Christopher L, Ashwell Jonathan D, Mazmanian Sarkis K. 2012. Outer Membrane Vesicles of a Human Commensal Mediate Immune Regulation and Disease Protection. *Cell Host & Microbe* 12:509-520.

30. Hajra D, Datey A, Chakravorty D. 2021. Attenuation Methods for Live Vaccines, p 331-356. *In* Pfeifer BA, Hill A (ed), Vaccine Delivery Technology: Methods and Protocols doi:10.1007/978-1-0716-0795-4_17. Springer US, New York, NY.
31. Pollard AJ, Bijker EM. 2021. A guide to vaccinology: from basic principles to new developments. *Nature Reviews Immunology* 21:83-100.
32. Anonymous. 2022. World Health Organization. Poliomyelitis. <https://www.who.int/news-room/fact-sheets/detail/poliomyelitis>. Accessed 2022 November 25.
33. Anonymous. 2022. World Health Organization. Statement – European Region 20 years polio-free: a celebratory moment but a fragile legacy. <https://www.who.int/europe/news/item/24-10-2022-statement---european-region-20-years-polio-free--a-celebratory-moment-but-a-fragile-legacy>. Accessed 2022 November 17.
34. Khoshnood S, Arshadi M, Akrami S, Koupaei M, Ghahramanpour H, Shariati A, Sadeghifard N, Heidary M. 2022. An overview on inactivated and live-attenuated SARS-CoV-2 vaccines. *Journal of Clinical Laboratory Analysis* 36:e24418.
35. Anonymous. 2022. World Health Organization. Hepatitis B. <https://www.who.int/teams/health-product-policy-and-standards/standards-and-specifications/vaccine-standardization/hep-b>. Accessed 2022 December 6.
36. Anonymous. 2021. Electronic medicines compendium. Pneumovax 23 solution for injection in pre-filled syringe. <https://www.medicines.org.uk/emc/product/9692/smpc#gref>. Accessed 2022 December 6.
37. Stratton K FA, Rusch E, . 2011. Adverse Effects of Vaccines: Evidence and Causality, National Academies Press (US).
38. Folegatti PM, Ewer KJ, Aley PK, Angus B, Becker S, Belij-Rammerstorfer S, Bellamy D, Bibi S, Bittaye M, Clutterbuck EA, Dold C, Faust SN, Finn A, Flaxman AL, Hallis B, Heath P, Jenkin D, Lazarus R, Makinson R, Minassian AM, Pollock KM, Ramasamy M, Robinson H, Snape M, Tarrant R, Voysey M, Green C, Douglas AD, Hill AVS, Lambe T, Gilbert SC, Pollard AJ. 2020. Safety and immunogenicity of the ChAdOx1 nCoV-19 vaccine against SARS-CoV-2: a preliminary report of a phase 1/2, single-blind, randomised controlled trial. *Lancet* 396:467-478.
39. Anonymous. 2021. National cancer institute NIH. Human Papillomavirus (HPV) vaccines. <https://www.cancer.gov/about-cancer/causes-prevention/risk/infectious-agents/hpv-vaccine-fact-sheet#:~:text=Three%20vaccines%20that%20prevent%20infection,used%20in%20the%20United%20States>. Accessed 2022 December 6.
40. Chen Z, Aspelund A, Kemble G, Jin H. 2008. Molecular studies of temperature-sensitive replication of the cold-adapted B/Ann Arbor/1/66, the master donor virus for live attenuated influenza FluMist® vaccines. *Virology* 380:354-362.
41. Anonymous. 2022. Vaccine Knowledge Project-University of Oxford. Nasal Flu Vaccine. <https://vk.ovg.ox.ac.uk/vk/nasal-flu-vaccine>. Accessed 2022 November 20.
42. Anonymous. 2022. World Health Organization. COVID-19 Vaccines with WHO Emergency Use Listing. <https://extranet.who.int/pqweb/vaccines/vaccinescovid-19-vaccine-eul-issued>. Accessed 2022 November 9.
43. Anonymous. 2022. World Health Organization. Status of COVID-19 Vaccines within WHO EUL/PQ evaluation process. World Health Organization
44. Anonymous. 2022. Bharat Biotech International Limited. Covaxin. SARS-CoV-2 vaccine by Bharat Biotech. Fact sheet for vaccine recipients and caregivers. Bharat Biotech International Limited,

45. Banihashemi SR, Es-haghi A, Fallah Mehrabadi MH, Nofeli M, Mokarram AR, Ranjbar A, Salman M, Hajimoradi M, Razaz SH, Taghdiri M, Bagheri M, Dadar M, Hassan ZM, Eslampanah M, Salehi Najafabadi Z, Lotfi M, Khorasani A, Rahmani F. 2022. Safety and Efficacy of Combined Intramuscular/Intranasal RAZI-COV PARS Vaccine Candidate Against SARS-CoV-2: A Preclinical Study in Several Animal Models. *Frontiers in Immunology* 13.
46. Anonymous. 2022. CanSinoBIO's Convidecia Air™ Receives Approval in China, *on* CanSinoBio. <https://www.cansinotech.com/html/1/179/180/1100.html>. Accessed 2022 November 25.
47. Waltz E. 2022. How nasal-spray vaccines could change the pandemic.
48. Meyer M, Jaspers I. 2015. Respiratory protease/antiprotease balance determines susceptibility to viral infection and can be modified by nutritional antioxidants. *Am J Physiol Lung Cell Mol Physiol* 308:L1189-201.
49. Bustamante-Marin XM, Ostrowski LE. 2017. Cilia and Mucociliary Clearance. *Cold Spring Harb Perspect Biol* 9.
50. Anonymous. 2022. Centers for Disease Control and Prevention. Adjuvants and Vaccines. <https://www.cdc.gov/vaccinesafety/concerns/adjuvants.html>. Accessed 2022 October 27.
51. Ghimire TR. 2015. The mechanisms of action of vaccines containing aluminum adjuvants: an in vitro vs in vivo paradigm. *SpringerPlus* 4:181.
52. Sasaki E, Asanuma H, Momose H, Furuhashi K, Mizukami T, Hamaguchi I. 2021. Nasal alum-adjuvanted vaccine promotes IL-33 release from alveolar epithelial cells that elicits IgA production via type 2 immune responses. *PLOS Pathogens* 17:e1009890.
53. Aoshi T. 2017. Modes of Action for Mucosal Vaccine Adjuvants. *Viral Immunol* 30:463-470.
54. Zeng L. 2016. Mucosal adjuvants: Opportunities and challenges. *Hum Vaccin Immunother* 12:2456-8.
55. Lewis DJ, Huo Z, Barnett S, Kromann I, Giemza R, Galiza E, Woodrow M, Thierry-Carstensen B, Andersen P, Novicki D, Del Giudice G, Rappuoli R. 2009. Transient facial nerve paralysis (Bell's palsy) following intranasal delivery of a genetically detoxified mutant of *Escherichia coli* heat labile toxin. *PLoS One* 4:e6999.
56. van Ginkel FW, Jackson RJ, Yuki Y, McGhee JR. 2000. Cutting edge: the mucosal adjuvant cholera toxin redirects vaccine proteins into olfactory tissues. *J Immunol* 165:4778-82.
57. Stone AE, Scheuermann SE, Haile CN, Cuny GD, Velasquez ML, Linhuber JP, Duddupudi AL, Vigliaturo JR, Pravetoni M, Kosten TA, Kosten TR, Norton EB. 2021. Fentanyl conjugate vaccine by injected or mucosal delivery with dmLT or LTA1 adjuvants implicates IgA in protection from drug challenge. *NPJ Vaccines* 6:69.
58. Heine SJ, Franco-Mahecha OL, Sears KT, Drachenberg CB, van Roosmalen ML, Leenhouts K, Picking WL, Pasetti MF. 2019. A Combined YopB and LcrV Subunit Vaccine Elicits Protective Immunity against *Yersinia* Infection in Adult and Infant Mice. *Journal of Immunology* 202:2005-2016.
59. Lebens M, Terrinoni M, Karlsson SL, Larena M, Gustafsson-Hedberg T, Källgård S, Nygren E, Holmgren J. 2016. Construction and preclinical evaluation of mmCT, a novel mutant cholera toxin adjuvant that can be efficiently produced in genetically manipulated *Vibrio cholerae*. *Vaccine* 34:2121-8.
60. Mosafer J, Sabbaghi A-H, Badiie A, Dehghan S, Tafaghodi M. 2019. Preparation, characterization and in vivo evaluation of alginate-coated chitosan and trimethylchitosan nanoparticles loaded with PR8 influenza virus for nasal immunization. *Asian Journal of Pharmaceutical Sciences* 14:216-221.

61. Kayamuro H, Yoshioka Y, Abe Y, Arita S, Katayama K, Nomura T, Yoshikawa T, Kubota-Koketsu R, Ikuta K, Okamoto S, Mori Y, Kunisawa J, Kiyono H, Itoh N, Nagano K, Kamada H, Tsutsumi Y, Tsunoda S. 2010. Interleukin-1 family cytokines as mucosal vaccine adjuvants for induction of protective immunity against influenza virus. *Journal of Virology* 84:12703-12.
62. Miller SM, Cybulski V, Whitacre M, Bess LS, Livesay MT, Walsh L, Burkhart D, Bazin HG, Evans JT. 2020. Novel Lipidated Imidazoquinoline TLR7/8 Adjuvants Elicit Influenza-Specific Th1 Immune Responses and Protect Against Heterologous H3N2 Influenza Challenge in Mice. *Frontiers in Immunology* 11.
63. Lampe AT, Farris EJ, Brown DM, Pannier AK. 2021. High- and low-molecular-weight chitosan act as adjuvants during single-dose influenza A virus protein vaccination through distinct mechanisms. *Biotechnology and Bioengineering* 118:1224-1243.
64. Al-Nemrawi NK, Darweesh RS, Al-Shriem LA, Al-Qawasmi FS, Emran SO, Khafajah AS, Abu-Dalo MA. 2022. Polymeric Nanoparticles for Inhaled Vaccines. *Polymers (Basel)* 14.
65. Travieso T, Li J, Mahesh S, Mello JDFRE, Blasi M. 2022. The use of viral vectors in vaccine development. *npj Vaccines* 7:75.
66. Corthesy B, Bioley G. 2018. Lipid-Based Particles: Versatile Delivery Systems for Mucosal Vaccination against Infection. *Front Immunol* 9:431.
67. Ghasemiyeh P, Mohammadi-Samani S. 2018. Solid lipid nanoparticles and nanostructured lipid carriers as novel drug delivery systems: applications, advantages and disadvantages. *Res Pharm Sci* 13:288-303.
68. Sun H-X, Xie Y, Ye Y-P. 2009. ISCOMs and ISCOMATRIX™. *Vaccine* 27:4388-4401.
69. Kashyap D, Panda M, Baral B, Varshney N, R S, Bhandari V, Parmar HS, Prasad A, Jha HC. 2022. Outer Membrane Vesicles: An Emerging Vaccine Platform. *Vaccines* 10:1578.
70. Di Cola E, Cantu L, Brocca P, Rondelli V, Fadda GC, Canelli E, Martelli P, Clementino A, Sonvico F, Bettini R, Del Favero E. 2019. Novel O/W nanoemulsions for nasal administration: Structural hints in the selection of performing vehicles with enhanced mucopenetration. *Colloids Surfaces B Biointerfaces* 183:110439.
71. Banihashemi SR, Es-Haghi A, Fallah Mehrabadi MH, Nofeli M, Mokarram AR, Ranjbar A, Salman M, Hajimoradi M, Razaz SH, Taghdiri M, Bagheri M, Dadar M, Hassan ZM, Eslampanah M, Salehi Najafabadi Z, Lotfi M, Khorasani A, Rahmani F. 2022. Safety and Efficacy of Combined Intramuscular/Intranasal RAZI-COV PARS Vaccine Candidate Against SARS-CoV-2: A Preclinical Study in Several Animal Models. *Frontiers in Microbiology* 13:836745.
72. Xing L, Fan Y-T, Zhou T-J, Gong J-H, Cui L-H, Cho K-H, Choi Y-J, Jiang H-L, Cho C-S. 2018. Chemical Modification of Chitosan for Efficient Vaccine Delivery. *Molecules (Basel, Switzerland)* 23:229.
73. Potaś J, Szymańska E, Winnicka K. 2020. Challenges in developing of chitosan – Based polyelectrolyte complexes as a platform for mucosal and skin drug delivery. *European Polymer Journal* 140:110020.
74. Nakahashi-Ouchida R, Uchida Y, Yuki Y, Katakai Y, Yamanoue T, Ogawa H, Munesue Y, Nakano N, Hanari K, Miyazaki T, Saito Y, Umemoto S, Sawada S-i, Mukerji R, Briles DE, Yasutomi Y, Akiyoshi K, Kiyono H. 2021. A nanogel-based trivalent PspA nasal vaccine protects macaques from intratracheal challenge with pneumococci. *Vaccine* 39:3353-3364.
75. Pinelli F, Saadati M, Zare EN, Makvandi P, Masi M, Sacchetti A, Rossi F. 2022. A perspective on the applications of functionalized nanogels: promises and challenges. *International Materials Reviews* doi:10.1080/09506608.2022.2026864:1-25.

76. Moon A, Sun Y, Wang Y, Huang J, Zafar Khan MU, Qiu H-J. 2022. Lactic Acid Bacteria as Mucosal Immunity Enhancers and Antivirals through Oral Delivery. *Applied Microbiology* 2:837-854.
77. Iravani S, Varma RS. 2021. Plant Pollen Grains: A Move Towards Green Drug and Vaccine Delivery Systems. *Nano-Micro Letters* 13:128.
78. Kurup VM, Thomas J. 2020. Edible Vaccines: Promises and Challenges. *Molecular Biotechnology* 62:79-90.
79. Shukla A, Mishra V, Kesharwani P. 2016. Bilosomes in the context of oral immunization: development, challenges and opportunities. *Drug Discovery Today* 21:888-899.
80. Gebril A, Obeid MA, Bennett EM, Pujol A, Chovel ML, Mahy T, Acevedo R, Ferro VA. 2022. Mucosal and systemic immune responses following mucosal immunisation of tetanus toxoid entrapped in lipid nanoparticles prepared by microwave reactor. *European Journal of Pharmaceutics and Biopharmaceutics* 171:11-18.
81. Miquel-Clopés A, Bentley EG, Stewart JP, Carding SR. 2019. Mucosal vaccines and technology. *Clinical and Experimental Immunology* 196:205-214.
82. Mendonça SA, Lorincz R, Boucher P, Curiel DT. 2021. Adenoviral vector vaccine platforms in the SARS-CoV-2 pandemic. *npj Vaccines* 6:97.
83. Ma S, Yu R, Mai Y, Yu N, Gao T, Yang J. 2022. Enhanced Influenza Immunity by Nasal Mucosal Administration of the TPGS-Modified Liposomal Vaccine. *AAPS PharmSciTech* 23:272.
84. Ndeupen S, Qin Z, Jacobsen S, Bouteau A, Estantbouli H, Igyártó BZ. 2021. The mRNA-LNP platform's lipid nanoparticle component used in preclinical vaccine studies is highly inflammatory. *iScience* 24:103479.
85. Woith E, Fuhrmann G, Melzig MF. 2019. Extracellular Vesicles-Connecting Kingdoms. *International Journal of Molecular Sciences* 20.
86. Roszkowiak J, Jajor P, Guła G, Gubernator J, Żak A, Drulis-Kawa Z, Augustyniak D. 2019. Interspecies Outer Membrane Vesicles (OMVs) Modulate the Sensitivity of Pathogenic Bacteria and Pathogenic Yeasts to Cationic Peptides and Serum Complement. *International Journal of Molecular Sciences* 20.
87. Juodeikis R, Carding SR. Outer Membrane Vesicles: Biogenesis, Functions, and Issues. *Microbiology and Molecular Biology Reviews* 0:e00032-22.
88. Toyofuku M, Nomura N, Eberl L. 2019. Types and origins of bacterial membrane vesicles. *Nature Reviews Microbiology* 17:13-24.
89. Suri K, D'Souza A, Huang D, Bhavsar A, Amiji M. 2023. Bacterial extracellular vesicle applications in cancer immunotherapy. *Bioact Mater* 22:551-566.
90. Anonymous. 2012. European Medicines Agency. Bexsero. Meningococcal group B Vaccine (rDNA, component, adsorbed). Assessment report., European Medicines Agency.
91. Reimer SL, Beniac DR, Hiebert SL, Booth TF, Chong PM, Westmacott GR, Zhanel GG, Bay DC. 2021. Comparative Analysis of Outer Membrane Vesicle Isolation Methods With an *Escherichia coli* tolA Mutant Reveals a Hypervesiculating Phenotype With Outer-Inner Membrane Vesicle Content. *Frontiers in Microbiology* 12.
92. Mancini F, Rossi O, Necchi F, Micoli F. 2020. OMV Vaccines and the Role of TLR Agonists in Immune Response. *International Journal of Molecular Sciences* 21:4416.
93. Pérez-Cruz C, Carrión O, Delgado L, Martínez G, López-Iglesias C, Mercade E. 2013. New type of outer membrane vesicle produced by the Gram-negative bacterium

- Shewanella vesiculosa* M7T: implications for DNA content. *Appl Environ Microbiol* 79:1874-81.
94. Stentz R, Jones E, Juodeikis R, Wegmann U, Guirro M, Goldson AJ, Brion A, Booth C, Sudhakar P, Brown IR, Korcsmáros T, Carding SR. 2022. The Proteome of Extracellular Vesicles Produced by the Human Gut Bacteria *Bacteroides thetaiotaomicron* In Vivo Is Influenced by Environmental and Host-Derived Factors. *Applied and Environmental Microbiology* 88:e00533-22.
 95. Zavan L, Bitto NJ, Johnston EL, Greening DW, Kaparakis-Liaskos M. 2019. *Helicobacter pylori* Growth Stage Determines the Size, Protein Composition, and Preferential Cargo Packaging of Outer Membrane Vesicles. *PROTEOMICS* 19:1800209.
 96. Ahmed AAQ, Zheng R, Abdalla AME, Bakadia BM, Qi F, Xiao L, Atta OM, Mao L, Yang G. 2021. Heterogeneous Populations of Outer Membrane Vesicles Released from *Helicobacter Pylori* SS1 with Distinct Biological Properties. *Engineered Science* 15:148-165.
 97. Durant L, Stentz R, Noble A, Brooks J, Gicheva N, Reddi D, O'Connor MJ, Hoyles L, McCartney AL, Man R, Pring ET, Dilke S, Hendy P, Segal JP, Lim DNF, Misra R, Hart AL, Arebi N, Carding SR, Knight SC. 2020. *Bacteroides thetaiotaomicron*-derived outer membrane vesicles promote regulatory dendritic cell responses in health but not in inflammatory bowel disease. *Microbiome* 8:88.
 98. Al-Nedawi K, Mian MF, Hossain N, Karimi K, Mao Y-K, Forsythe P, Min KK, Stanis AM, Kunze WA, Bienenstock J. 2015. Gut commensal microvesicles reproduce parent bacterial signals to host immune and enteric nervous systems. *The FASEB Journal* 29:684-695.
 99. Bomberger JM, MacEachran DP, Coutermarsh BA, Ye S, O'Toole GA, Stanton BA. 2009. Long-Distance Delivery of Bacterial Virulence Factors by *Pseudomonas aeruginosa* Outer Membrane Vesicles. *PLOS Pathogens* 5:e1000382.
 100. Bielaszewska M, Rüter C, Bauwens A, Greune L, Jarosch K-A, Steil D, Zhang W, He X, Llobes R, Fruth A, Kim KS, Schmidt MA, Dobrindt U, Mellmann A, Karch H. 2017. Host cell interactions of outer membrane vesicle-associated virulence factors of enterohemorrhagic *Escherichia coli* O157: Intracellular delivery, trafficking and mechanisms of cell injury. *PLOS Pathogens* 13:e1006159.
 101. Koeppen K, Hampton TH, Jarek M, Scharfe M, Gerber SA, Mielcarz DW, Demers EG, Dolben EL, Hammond JH, Hogan DA, Stanton BA. 2016. A Novel Mechanism of Host-Pathogen Interaction through sRNA in Bacterial Outer Membrane Vesicles. *PLOS Pathogens* 12:e1005672.
 102. Kim SW, Park SB, Im SP, Lee JS, Jung JW, Gong TW, Lazarte JMS, Kim J, Seo J-S, Kim J-H, Song J-W, Jung HS, Kim GJ, Lee YJ, Lim S-K, Jung TS. 2018. Outer membrane vesicles from β -lactam-resistant *Escherichia coli* enable the survival of β -lactam-susceptible *E. coli* in the presence of β -lactam antibiotics. *Scientific Reports* 8:5402.
 103. Dell'Annunziata F, Dell'Aversana C, Doti N, Donadio G, Dal Piaz F, Izzo V, De Filippis A, Galdiero M, Altucci L, Boccia G, Galdiero M, Folliero V, Franci G. 2021. Outer Membrane Vesicles Derived from *Klebsiella pneumoniae* Are a Driving Force for Horizontal Gene Transfer. *International Journal of Molecular Sciences* 22:8732.
 104. Park J, Kim M, Shin B, Kang M, Yang J, Lee TK, Park W. 2021. A novel decoy strategy for polymyxin resistance in *Acinetobacter baumannii*. *eLife* 10:e66988.
 105. Mashburn LM, Whiteley M. 2005. Membrane vesicles traffic signals and facilitate group activities in a prokaryote. *Nature* 437:422-425.
 106. Juodeikis R, Jones E, Deery E, Beal DM, Stentz R, Krätzler B, Carding SR, Warren MJ. 2022. Nutrient smuggling: Commensal gut bacteria-derived extracellular

- vesicles scavenge vitamin B12 and related cobamides for microbe and host acquisition. *Journal of Extracellular Biology* 1:e61.
107. Gasperini G, Arato V, Pizza M, Aricò B, Leuzzi R. 2017. Physiopathological roles of spontaneously released outer membrane vesicles of *Bordetella pertussis*. *Future Microbiol* 12:1247-1259.
 108. McBroom AJ, Kuehn MJ. 2007. Release of outer membrane vesicles by Gram-negative bacteria is a novel envelope stress response. *Mol Microbiol* 63:545-58.
 109. Altindis E, Fu Y, Mekalanos JJ. 2014. Proteomic analysis of *Vibrio cholerae* outer membrane vesicles. *Proceedings of the National Academy of Sciences* 111:E1548-56.
 110. Maerz JK, Steimle A, Lange A, Bender A, Fehrenbacher B, Frick JS. 2018. Outer membrane vesicles blebbing contributes to *B. vulgatus* mpk-mediated immune response silencing. *Gut Microbes* 9:1-12.
 111. Jones EJ, Booth C, Fonseca S, Parker A, Cross K, Miquel-Clopés A, Hautefort I, Mayer U, Wileman T, Stentz R, Carding SR. 2020. The Uptake, Trafficking, and Biodistribution of *Bacteroides thetaiotaomicron* Generated Outer Membrane Vesicles. *Frontiers in Microbiology* 11.
 112. Bandi SP, Kumbhar YS, Venuganti VVK. 2020. Effect of particle size and surface charge of nanoparticles in penetration through intestinal mucus barrier. *Journal of Nanoparticle Research* 22:62.
 113. Zhu N, Zhang D, Wang W, Li X, Yang B, Song J, Zhao X, Huang B, Shi W, Lu R, Niu P, Zhan F, Ma X, Wang D, Xu W, Wu G, Gao GF, Tan W. 2020. A Novel Coronavirus from Patients with Pneumonia in China, 2019. *New England Journal of Medicine* 382:727-733.
 114. Mosley VM, Wyckoff RW. 1946. Electron micrography of the virus of influenza. *Nature* 157:263.
 115. Stentz R, Carvalho AL, Jones EJ, Carding SR. 2018. Fantastic voyage: the journey of intestinal microbiota-derived microvesicles through the body. *Biochem Soc Trans* 46:1021-1027.
 116. Schaar V, de Vries SP, Perez Vidakovics ML, Bootsma HJ, Larsson L, Hermans PW, Bjartell A, Mörgelin M, Riesbeck K. 2011. Multicomponent *Moraxella catarrhalis* outer membrane vesicles induce an inflammatory response and are internalized by human epithelial cells. *Cell Microbiol* 13:432-49.
 117. Tarashi S, Zamani MS, Omrani MD, Fateh A, Moshiri A, Saedisomeolia A, Siadat SD, Kubow S. 2022. Commensal and Pathogenic Bacterial-Derived Extracellular Vesicles in Host-Bacterial and Interbacterial Dialogues: Two Sides of the Same Coin. *J Immunol Res* 2022:8092170.
 118. Vanaja SK, Russo AJ, Behl B, Banerjee I, Yankova M, Deshmukh SD, Rathinam VAK. 2016. Bacterial Outer Membrane Vesicles Mediate Cytosolic Localization of LPS and Caspase-11 Activation. *Cell* 165:1106-1119.
 119. Shen Y, Giardino Torchia ML, Lawson GW, Karp CL, Ashwell JD, Mazmanian SK. 2012. Outer membrane vesicles of a human commensal mediate immune regulation and disease protection. *Cell Host Microbe* 12:509-20.
 120. Fonseca S, Carvalho AL, Miquel-Clopés A, Jones EJ, Juodeikis R, Stentz R, Carding SR. 2022. Extracellular vesicles produced by the human gut commensal bacterium *Bacteroides thetaiotaomicron* elicit anti-inflammatory responses from innate immune cells. *Frontiers in Microbiology* 13.
 121. Cañas M-A, Fábrega M-J, Giménez R, Badia J, Baldomà L. 2018. Outer Membrane Vesicles From Probiotic and Commensal *Escherichia coli* Activate NOD1-Mediated Immune Responses in Intestinal Epithelial Cells. *Frontiers in Microbiology* 9.

122. Palmieri E, Arato V, Oldrini D, Ricchetti B, Aruta MG, Pansegrau W, Marchi S, Giusti F, Ferlenghi I, Rossi O, Alfini R, Giannelli C, Gasperini G, Necchi F, Micoli F. 2021. Stability of Outer Membrane Vesicles-Based Vaccines, Identifying the Most Appropriate Methods to Detect Changes in Vaccine Potency. *Vaccines (Basel)* 9.
123. Bertani B, Ruiz N. 2018. Function and Biogenesis of Lipopolysaccharides. *EcoSal Plus* 8.
124. Ciesielska A, Matyjek M, Kwiatkowska K. 2021. TLR4 and CD14 trafficking and its influence on LPS-induced pro-inflammatory signaling. *Cell Mol Life Sci* 78:1233-1261.
125. Saha S, Pupo E, Zariri A, van der Ley P. 2022. Lipid A heterogeneity and its role in the host interactions with pathogenic and commensal bacteria. *microLife* 3.
126. Zariri A, Beskers J, van de Waterbeemd B, Hamstra HJ, Bindels TH, van Riet E, van Putten JP, van der Ley P. 2016. Meningococcal Outer Membrane Vesicle Composition-Dependent Activation of the Innate Immune Response. *Infection and Immunity* 84:3024-33.
127. Gerritzen MJH, Martens DE, Wijffels RH, van der Pol L, Stork M. 2017. Bioengineering bacterial outer membrane vesicles as vaccine platform. *Biotechnology Advances* 35:565-574.
128. Hosseini Zadeh ZS, Nemati F, Sharif E, Mohit E. 2022. The effects of different thermal and chemical stresses on release of outer membrane vesicles (OMVs) by ClearColi™. *Archives of Microbiology* 204:714.
129. Schwechheimer C, Rodriguez DL, Kuehn MJ. 2015. Nlpl-mediated modulation of outer membrane vesicle production through peptidoglycan dynamics in *Escherichia coli*. *Microbiologyopen* 4:375-89.
130. Ojima Y, Sawabe T, Konami K, Azuma M. 2020. Construction of hypervesiculation *Escherichia coli* strains and application for secretory protein production. *Biotechnology and Bioengineering* 117:701-709.
131. Ojima Y, Sawabe T, Nakagawa M, Tahara YO, Miyata M, Azuma M. 2021. Aberrant Membrane Structures in Hypervesiculating *Escherichia coli* Strain Δ mlaE Δ nlpl Visualized by Electron Microscopy. *Frontiers in Microbiology* 12:706525.
132. Gerritzen MJH, Stangowez L, van de Waterbeemd B, Martens DE, Wijffels RH, Stork M. 2019. Continuous production of *Neisseria meningitidis* outer membrane vesicles. *Applied Microbiology and Biotechnology* 103:9401-9410.
133. Agency EM. 2022. Bexero: EPAR-Product Information. https://www.ema.europa.eu/en/documents/product-information/bexsero-epar-product-information_en.pdf.
134. Holst J, Martin D, Arnold R, Huergo CC, Oster P, O'Hallahan J, Rosenqvist E. 2009. Properties and clinical performance of vaccines containing outer membrane vesicles from *Neisseria meningitidis*. *Vaccine* 27 Suppl 2:B3-12.
135. Viviani V, Biolchi A, Pizza M. 2022. Synergistic activity of antibodies in the multicomponent 4CMenB vaccine. *Expert Review of Vaccines* 21:645-658.
136. Gasparini R, Amicizia D, Domnich A, Lai PL, Panatto D. 2014. *Neisseria meningitidis* B vaccines: recent advances and possible immunization policies. *Expert Rev Vaccines* 13:345-64.
137. Roier S, Leitner DR, Iwashkiw J, Schild-Prüfert K, Feldman MF, Krohne G, Reidl J, Schild S. 2012. Intranasal immunization with nontypeable *Haemophilus influenzae* outer membrane vesicles induces cross-protective immunity in mice. *PLoS One* 7:e42664.
138. Raeven RHM, Rockx-Brouwer D, Kanojia G, van der Maas L, Bindels THE, ten Have R, van Riet E, Metz B, Kersten GFA. 2020. Intranasal immunization with outer

- membrane vesicle pertussis vaccine confers broad protection through mucosal IgA and Th17 responses. *Scientific Reports* 10:7396.
139. Schild S, Nelson EJ, Bishop AL, Camilli A. 2009. Characterization of *Vibrio cholerae* outer membrane vesicles as a candidate vaccine for cholera. *Infect Immun* 77:472-84.
 140. Muralinath M, Kuehn MJ, Roland KL, Curtiss R, 3rd. 2011. Immunization with *Salmonella enterica* serovar Typhimurium-derived outer membrane vesicles delivering the pneumococcal protein PspA confers protection against challenge with *Streptococcus pneumoniae*. *Infect Immun* 79:887-94.
 141. Thapa HB, Müller AM, Camilli A, Schild S. 2021. An Intranasal Vaccine Based on Outer Membrane Vesicles Against SARS-CoV-2. *Frontiers in Immunology* 12:752739.
 142. Alves NJ, Turner KB, Walper SA. 2016. Directed Protein Packaging within Outer Membrane Vesicles from *Escherichia coli*: Design, Production and Purification. *J Vis Exp* doi:10.3791/54458.
 143. Fantappiè L, de Santis M, Chiarot E, Carboni F, Bensi G, Jousson O, Margarit I, Grandi G. 2014. Antibody-mediated immunity induced by engineered *Escherichia coli* OMVs carrying heterologous antigens in their lumen. *Journal of Extracellular Vesicles* 3:24015.
 144. Bartolini E, Ianni E, Frigimelica E, Petracca R, Galli G, Berlanda Scorza F, Norais N, Laera D, Giusti F, Pierleoni A, Donati M, Cevenini R, Finco O, Grandi G, Grifantini R. 2013. Recombinant outer membrane vesicles carrying *Chlamydia muridarum* HtrA induce antibodies that neutralize chlamydial infection in vitro. *Journal of Extracellular Vesicles* 2:20181.
 145. Huang W, Wang S, Yao Y, Xia Y, Yang X, Li K, Sun P, Liu C, Sun W, Bai H, Chu X, Li Y, Ma Y. 2016. Employing *Escherichia coli*-derived outer membrane vesicles as an antigen delivery platform elicits protective immunity against *Acinetobacter baumannii* infection. *Scientific Reports* 6:37242.
 146. Rappazzo CG, Watkins HC, Guarino CM, Chau A, Lopez JL, Delisa MP, Leifer CA, Whittaker GR, Putnam D. 2016. Recombinant M2e outer membrane vesicle vaccines protect against lethal influenza A challenge in BALB/c mice. *Vaccine* 34:1252-1258.
 147. Sutherland AR, Alam MK, Geyer CR. 2019. Post-translational Assembly of Protein Parts into Complex Devices by Using SpyTag/SpyCatcher Protein Ligase. *ChemBioChem* 20:319-328.
 148. Jiang L, Driedonks TAP, Jong WSP, Dhakal S, Bart van den Berg van Saparoea H, Sitaras I, Zhou R, Caputo C, Littlefield K, Lowman M, Chen M, Lima G, Gololobova O, Smith B, Mahairaki V, Riley Richardson M, Mulka KR, Lane AP, Klein SL, Pekosz A, Brayton C, Mankowski JL, Luirink J, Villano JS, Witwer KW. 2022. A bacterial extracellular vesicle-based intranasal vaccine against SARS-CoV-2 protects against disease and elicits neutralizing antibodies to wild-type and Delta variants. *Journal of Extracellular Vesicles* 11:e12192.
 149. Anonymous. 2022. Safety and Efficacy of Intranasal Administration of Avacc 10 Vaccine Against COVID-19 in Healthy Volunteers (ITV2002). <https://clinicaltrials.gov/ct2/show/NCT05604690?term=Avacc+10&cond=SARS+CoV+2+infection&draw=2&rank=1>. Accessed 2022 November 9.
 150. van der Ley PA, Zariri A, van Riet E, Oosterhoff D, Kruiswijk CP. 2021. An Intranasal OMV-Based Vaccine Induces High Mucosal and Systemic Protecting Immunity Against a SARS-CoV-2 Infection. *Frontiers in Immunology* 12:781280.

151. Eckburg PB, Bik EM, Bernstein CN, Purdom E, Dethlefsen L, Sargent M, Gill SR, Nelson KE, Relman DA. 2005. Diversity of the human intestinal microbial flora. *Science* 308:1635-8.
152. Pan M, Barua N, Ip M. 2022. Mucin-degrading gut commensals isolated from healthy faecal donor suppress intestinal epithelial inflammation and regulate tight junction barrier function. *Frontiers in Microbiology* 13:1021094.
153. Delday M, Mulder I, Logan ET, Grant G. 2018. *Bacteroides thetaiotaomicron* Ameliorates Colon Inflammation in Preclinical Models of Crohn's Disease. *Inflammatory Bowel Diseases* 25:85-96.
154. Hansen R, Sanderson IR, Muhammed R, Allen S, Tzivinikos C, Henderson P, Gervais L, Jeffery IB, Mullins DP, O'Herlihy EA, Weinberg JD, Kitson G, Russell RK, Wilson DC. 2020. A Double-Blind, Placebo-Controlled Trial to Assess Safety and Tolerability of (Thetanix) *Bacteroides thetaiotaomicron* in Adolescent Crohn's Disease. *Clinical and Translational Gastroenterology* 12:e00287.
155. Stentz R, Jones E, Juodeikis R, Wegmann U, Guirro M, Goldson AJ, Brion A, Booth C, Sudhakar P, Brown IR, Korcsmáros T, Carding SR. 2022. The Proteome of Extracellular Vesicles Produced by the Human Gut Bacteria *Bacteroides thetaiotaomicron* In Vivols Influenced by Environmental and Host-Derived Factors. *Applied and Environmental Microbiology* 88:e00533-22.
156. Genth J, Kaleja P, Treitz C, Schäfer K, Graspeuntner S, Rupp J, Tholey A. The intracellular proteome of the gut bacterium *Bacteroides thetaiotaomicron* is widely unaffected by a switch from glucose to sucrose as main carbohydrate source. *PROTEOMICS* n/a:2200189.
157. Hickey CA, Kuhn KA, Donermeyer DL, Porter NT, Jin C, Cameron EA, Jung H, Kaiko GE, Wegorzewska M, Malvin NP, Glowacki RW, Hansson GC, Allen PM, Martens EC, Stappenbeck TS. 2015. Colitogenic *Bacteroides thetaiotaomicron* Antigens Access Host Immune Cells in a Sulfatase-Dependent Manner via Outer Membrane Vesicles. *Cell Host Microbe* 17:672-80.
158. Luis AS, Jin C, Pereira GV, Glowacki RWP, Gugel SR, Singh S, Byrne DP, Pudlo NA, London JA, Baslé A, Reihill M, Oscarson S, Eysers PA, Czjzek M, Michel G, Barbeyron T, Yates EA, Hansson GC, Karlsson NG, Cartmell A, Martens EC. 2021. A single sulfatase is required to access colonic mucin by a gut bacterium. *Nature* 598:332-337.
159. Rocamora-Reverte L, Melzer FL, Würzner R, Weinberger B. 2021. The Complex Role of Regulatory T Cells in Immunity and Aging. *Frontiers in Immunology* 11.
160. Xerri NL, Payne SM. 2022. *Bacteroides thetaiotaomicron* Outer Membrane Vesicles Modulate Virulence of *Shigella flexneri*. *mBio* 13:e0236022.
161. Jacobson AN, Choudhury BP, Fischbach MA. 2018. The Biosynthesis of Lipooligosaccharide from *Bacteroides thetaiotaomicron*. *mBio* 9:e02289-17.
162. Chilton PM, Hadel DM, To TT, Mitchell TC, Darveau RP. 2013. Adjuvant activity of naturally occurring monophosphoryl lipopolysaccharide preparations from mucosa-associated bacteria. *Infect Immun* 81:3317-25.
163. Wegmann U, Horn N, Carding SR. 2013. Defining the bacteroides ribosomal binding site. *Appl Environ Microbiol* 79:1980-9.
164. Horn N, Carvalho AL, Overweg K, Wegmann U, Carding SR, Stentz R. 2016. A Novel Tightly Regulated Gene Expression System for the Human Intestinal Symbiont *Bacteroides thetaiotaomicron*. *Frontiers in Microbiology* 7.
165. Shoemaker NB, Getty C, Gardner JF, Salyers AA. 1986. Tn4351 transposes in *Bacteroides* spp. and mediates the integration of plasmid R751 into the *Bacteroides* chromosome. *Journal of Bacteriology* 165:929-36.

166. Anonymous. World Health Organization. Plague, on World Health Organisation. https://www.who.int/health-topics/plague#tab=tab_1. Accessed 2022 September 5.
167. Nguyen VK, Parra-Rojas C, Hernandez-Vargas EA. 2018. The 2017 plague outbreak in Madagascar: Data descriptions and epidemic modelling. *Epidemics* 25:20-25.
168. Anonymous. 2021. Centers for Disease Control and Prevention. Plague, on Centers for Disease Control and Prevention. <https://www.cdc.gov/plague/index.html>. Accessed 2022 June 26.
169. Anonymous. 2018. World Health Organization. Plague vaccine Target Product Profile (TPP). Efficacy trials of Plague Vaccines: endpoints, trial design, site selection. World Health Organisation.
170. Lei C, Kumar S. 2022. *Yersinia pestis* antibiotic resistance: a systematic review. *Osong Public Health Res Perspect* 13:24-36.
171. Guiyoule A, Gerbaud G, Buchrieser C, Galimand M, Rahalison L, Chanteau S, Courvalin P, Carniel E. 2001. Transferable plasmid-mediated resistance to streptomycin in a clinical isolate of *Yersinia pestis*. *Emerg Infect Dis* 7:43-8.
172. Prevention CfDCa. 2018. Bioterrorism Agents/Diseases : National Center for Emerging and Zoonotic Infectious Diseases (NCEZID). <https://emergency.cdc.gov/agent/agentlist-category.asp>. Accessed
173. Sagiyeu Z, Berdibekov A, Bolger T, Merekenova A, Ashirova S, Nurgozhin Z, Dalibayev Z. 2019. Human response to live plague vaccine EV, Almaty region, Kazakhstan, 2014-2015. *PLoS One* 14:e0218366.
174. Feodorova VA, Sayapina LV, Corbel MJ, Motin VL. 2014. Russian vaccines against especially dangerous bacterial pathogens. *Emerging Microbes & Infections* 3:1-17.
175. Meyer KF, Smith G, Foster L, Brookman M, Sung M. 1974. Live, attenuated *Yersinia pestis* vaccine: virulent in nonhuman primates, harmless to guinea pigs. *J Infect Dis* 129:Suppl:S85-12.
176. Russell P, Eley SM, Hibbs SE, Manchee RJ, Stagg AJ, Titball RW. 1995. A comparison of Plague vaccine, USP and EV76 vaccine induced protection against *Yersinia pestis* in a murine model. *Vaccine* 13:1551-6.
177. Meyer KF. 1970. Effectiveness of live or killed plague vaccines in man. *Bull World Health Organ* 42:653-66.
178. Moses S, Aftalion M, Mamroud E, Rotem S, Steinberger-Levy I. 2021. Reporter-Phage-Based Detection and Antibiotic Susceptibility Testing of *Yersinia pestis* for a Rapid Plague Outbreak Response. *Microorganisms* 9.
179. Cavanaugh DC, Elisberg BL, Llewellyn CH, Marshall JD, Jr., Rust JH, Jr., Williams JE, Meyer KF. 1974. Plague immunization. V. Indirect evidence for the efficacy of plague vaccine. *J Infect Dis* 129:Suppl:S37-40.
180. Rosenzweig JA, Hendrix EK, Chopra AK. 2021. Plague vaccines: new developments in an ongoing search. *Applied Microbiology and Biotechnology* 105:4931-4941.
181. Rosario-Acevedo R, Biryukov SS, Bozue JA, Cote CK. 2021. Plague Prevention and Therapy: Perspectives on Current and Future Strategies. *Biomedicine* 9.
182. Sun W, Singh AK. 2019. Plague vaccine: recent progress and prospects. *npj Vaccines* 4:11.
183. Karlyshev AV, Galyov EE, Smirnov OY, Guzayev AP, Abramov VM, Zav'yalov VP. 1992. A new gene of the f1 operon of *Y. pestis* involved in the capsule biogenesis. *FEBS Letters* 297:77-80.
184. Galyov EE, Karlyshev AV, Chernovskaya TV, Dolgikh DA, Smirnov OY, Volkovoy KI, Abramov VM, Zav'yalov VP. 1991. Expression of the envelope antigen F1 of *Yersinia pestis* is mediated by the product of caf1M gene having homology with the chaperone protein PapD of *Escherichia coli*. *FEBS Letters* 286:79-82.

185. Zavialov AV, Berglund J, Pudney AF, Fooks LJ, Ibrahim TM, MacIntyre S, Knight SD. 2003. Structure and Biogenesis of the Capsular F1 Antigen from *Yersinia pestis*: Preserved Folding Energy Drives Fiber Formation. *Cell* 113:587-596.
186. Davis KJ, Fritz DL, Pitt ML, Welkos SL, Worsham PL, Friedlander AM. 1996. Pathology of experimental pneumonic plague produced by fraction 1-positive and fraction 1-negative *Yersinia pestis* in African green monkeys (*Cercopithecus aethiops*). *Arch Pathol Lab Med* 120:156-63.
187. Chen Y-C, Chen S-J, Cheng H-F, Yeh M-K. 2020. Development of *Yersinia pestis* F1 antigen-loaded liposome vaccine against plague using microneedles as a delivery system. *Journal of Drug Delivery Science and Technology* 55:101443.
188. Zhang W, Song X, Zhai L, Guo J, Zheng X, Zhang L, Lv M, Hu L, Zhou D, Xiong X, Yang W. 2022. Complete Protection Against *Yersinia pestis* in BALB/c Mouse Model Elicited by Immunization With Inhalable Formulations of rF1-V10 Fusion Protein via Aerosolized Intratracheal Inoculation. *Frontiers in Immunology* 13.
189. Wang X, Li P, Singh AK, Zhang X, Guan Z, Curtiss R, 3rd, Sun W. 2022. Remodeling *Yersinia pseudotuberculosis* to generate a highly immunogenic outer membrane vesicle vaccine against pneumonic plague. *Proceedings of the National Academy of Sciences* 119:e2109667119.
190. Goodin JL, Nellis DF, Powell BS, Vyas VV, Enama JT, Wang LC, Clark PK, Giardina SL, Adamovicz JJ, Michiel DF. 2007. Purification and protective efficacy of monomeric and modified *Yersinia pestis* capsular F1-V antigen fusion proteins for vaccination against plague. *Protein Expr Purif* 53:63-79.
191. Heath DG, Anderson GW, Jr., Mauro JM, Welkos SL, Andrews GP, Adamovicz J, Friedlander AM. 1998. Protection against experimental bubonic and pneumonic plague by a recombinant capsular F1-V antigen fusion protein vaccine. *Vaccine* 16:1131-7.
192. Anonymous. 2021. Oxford Vaccine Group. A phase I study to assess the safety and immunogenicity of a recombinant adenovirusbased vaccine against Plague. Oxford Vaccine Group.
193. ClinicalTrials.gov. 2022. Immunogenicity and Safety of Subunit Vaccine of Plague Vaccine With Two Immunization Regimens, ClinicalTrials.gov.
194. Jones T, Adamovicz JJ, Cyr SL, Bolt CR, Bellerose N, Pitt LM, Lowell GH, Burt DS. 2006. Intranasal Protollin™/F1-V vaccine elicits respiratory and serum antibody responses and protects mice against lethal aerosolized plague infection. *Vaccine* 24:1625-1632.
195. Chen Y-C, Kalawong R, Toyofuku M, Eberl L. 2022. The role of peptidoglycan hydrolases in the formation and toxicity of *Pseudomonas aeruginosa* membrane vesicles. *microLife* 3.
196. Bishop RE. 2000. The bacterial lipocalins. *Biochim Biophys Acta* 1482:73-83.
197. Williamson ED, Packer PJ, Waters EL, Simpson AJ, Dyer D, Hartings J, Twenhafel N, Pitt ML. 2011. Recombinant (F1+V) vaccine protects cynomolgus macaques against pneumonic plague. *Vaccine* 29:4771-7.
198. Hu J, Jiao L, Hu Y, Chu K, Li J, Zhu F, Li T, Wu Z, Wei D, Meng F, Wang B. 2018. One year immunogenicity and safety of subunit plague vaccine in Chinese healthy adults: An extended open-label study. *Human vaccines & immunotherapeutics* 14:2701-2705.
199. Williamson ED, Flick-Smith HC, Lebutt C, Rowland CA, Jones SM, Waters EL, Gwyther RJ, Miller J, Packer PJ, Irving M. 2005. Human immune response to a plague vaccine comprising recombinant F1 and V antigens. *Infect Immun* 73:3598-608.

200. Lü FX, Ma Z, Rourke T, Srinivasan S, McChesney M, Miller CJ. 1999. Immunoglobulin concentrations and antigen-specific antibody levels in cervicovaginal lavages of rhesus macaques are influenced by the stage of the menstrual cycle. *Infect Immun* 67:6321-8.
201. Schäfer F, Kewenig S, Stolte N, Stahl-Hennig C, Stallmach A, Kaup FJ, Zeitz M, Schneider T. 2002. Lack of simian immunodeficiency virus (SIV) specific IgA response in the intestine of SIV infected rhesus macaques. *Gut* 50:608-14.
202. Liu C, Chu D, Kalantar-Zadeh K, George J, Young HA, Liu G. 2021. Cytokines: From Clinical Significance to Quantification. *Advanced Science* 8:2004433.
203. Zimmermann P. 2023. The immunological interplay between vaccination and the intestinal microbiota. *npj Vaccines* 8:24.
204. Williamson ED, Flick-Smith HC, Waters E, Miller J, Hodgson I, Le Butt CS, Hill J. 2007. Immunogenicity of the rF1+rV vaccine for plague with identification of potential immune correlates. *Microb Pathog* 42:11-21.
205. Saez-Llorens X, Aguilera Vaca DC, Abarca K, Maho E, Graña MG, Heijnen E, Smolenov I, Dull PM. 2015. Immunogenicity and safety of investigational vaccine formulations against meningococcal serogroups A, B, C, W, and Y in healthy adolescents. *Hum Vaccin Immunother* 11:1507-17.
206. Haneberg B, Dalseg R, Wedege E, Høiby EA, Haugen IL, Oftung F, Andersen SR, Næss LM, Aase A, Michaelsen TE, Holst J. 1998. Intranasal Administration of a Meningococcal Outer Membrane Vesicle Vaccine Induces Persistent Local Mucosal Antibodies and Serum Antibodies with Strong Bactericidal Activity in Humans. *Infection and Immunity* 66:1334-1341.
207. Irene C, Fantappiè L, Caproni E, Zerbini F, Anesi A, Tomasi M, Zanella I, Stupia S, Prete S, Valensin S, König E, Frattini L, Gagliardi A, Isaac SJ, Grandi A, Guella G, Grandi G. 2019. Bacterial outer membrane vesicles engineered with lipidated antigens as a platform for *Staphylococcus aureus* vaccine. *Proceedings of the National Academy of Sciences* 116:21780-21788.
208. Bashaw J, Norris S, Weeks S, Trevino S, Adamovicz JJ, Welkos S. 2007. Development of in vitro correlate assays of immunity to infection with *Yersinia pestis*. *Clinical and Vaccine Immunology* 14:605-16.
209. Anonymous. 2017.
- Expert opinion on the introduction of the meningococcal B (4CMenB) vaccine in the EU/EEA; European Centre for Disease Prevention and Control. ECDC.
210. Jones EJ, Booth C, Fonseca S, Parker A, Cross K, Miquel-Clopes A, Hautefort I, Mayer U, Wileman T, Stentz R, Carding SR. 2020. The Uptake, Trafficking, and Biodistribution of Bacteroides thetaiotaomicron Generated Outer Membrane Vesicles. *Front Microbiol* 11:57.
211. Mizel SB, Graff AH, Sriranganathan N, Ervin S, Lees CJ, Lively MO, Hantgan RR, Thomas MJ, Wood J, Bell B. 2009. Flagellin-F1-V fusion protein is an effective plague vaccine in mice and two species of nonhuman primates. *Clinical and Vaccine Immunology* 16:21-8.
212. Goure J, Broz P, Attree O, Cornelis GR, Attree I. 2005. Protective Anti-V Antibodies Inhibit Pseudomonas and Yersinia Translocon Assembly within Host Membranes. *The Journal of Infectious Diseases* 192:218-225.
213. Pettersson J, Holmström A, Hill J, Leary S, Frithz-Lindsten E, Von Euler-Matell A, Carlsson E, Titball R, Forsberg Å, Wolf-Watz H. 1999. The V-antigen of Yersinia is surface exposed before target cell contact and involved in virulence protein translocation. *Molecular Microbiology* 32:961-976.
214. Sawa T, Katoh H, Yasumoto H. 2014. V-antigen homologs in pathogenic gram-negative bacteria. *Microbiol Immunol* 58:267-85.

215. Roggenkamp A, Geiger AM, Leitritz L, Kessler A, Heesemann J. 1997. Passive immunity to infection with *Yersinia* spp. mediated by anti-recombinant V antigen is dependent on polymorphism of V antigen. *Infect Immun* 65:446-51.
216. Wang X, Wang Z, Guo Z, Wei B, Tian F, Yu S, Wang H, Wang H, Yang R. 2011. Serum cytokine responses in primary pneumonic plague patients. *Clinical and Vaccine Immunology* 18:184-6.
217. Li B, Du C, Zhou L, Bi Y, Wang X, Wen L, Guo Z, Song Z, Yang R. 2012. Humoral and cellular immune responses to *Yersinia pestis* infection in long-term recovered plague patients. *Clinical and Vaccine Immunology* 19:228-34.
218. Kummer LW, Szaba FM, Parent MA, Adamovicz JJ, Hill J, Johnson LL, Smiley ST. 2008. Antibodies and cytokines independently protect against pneumonic plague. *Vaccine* 26:6901-7.
219. Lin JS, Kummer LW, Szaba FM, Smiley ST. 2011. IL-17 contributes to cell-mediated defense against pulmonary *Yersinia pestis* infection. *J Immunol* 186:1675-84.
220. Parent MA, Berggren KN, Kummer LW, Wilhelm LB, Szaba FM, Mullarky IK, Smiley ST. 2005. Cell-mediated protection against pulmonary *Yersinia pestis* infection. *Infect Immun* 73:7304-10.
221. Philipovskiy AV, Smiley ST. 2007. Vaccination with live *Yersinia pestis* primes CD4 and CD8 T cells that synergistically protect against lethal pulmonary *Y. pestis* infection. *Infect Immun* 75:878-85.
222. Feodorova VA, Lyapina AM, Khizhnyakova MA, Zaitsev SS, Sayapina LV, Arseneva TE, Trukhachev AL, Lebedeva SA, Telepnev MV, Ulianova OV, Lyapina EP, Ulyanov SS, Motin VL. 2018. Humoral and cellular immune responses to *Yersinia pestis* Pla antigen in humans immunized with live plague vaccine. *PLoS Negl Trop Dis* 12:e0006511.
223. Parent MA, Wilhelm LB, Kummer LW, Szaba FM, Mullarky IK, Smiley ST. 2006. Gamma interferon, tumor necrosis factor alpha, and nitric oxide synthase 2, key elements of cellular immunity, perform critical protective functions during humoral defense against lethal pulmonary *Yersinia pestis* infection. *Infect Immun* 74:3381-6.
224. Liu L, Wei D, Qu Z, Sun L, Miao Y, Yang Y, Lu J, Du W, Wang B, Li B. 2018. A safety and immunogenicity study of a novel subunit plague vaccine in cynomolgus macaques. *Journal of Applied Toxicology* 38:408-417.
225. Zhang Q, Wang Q, Tian G, Qi Z, Zhang X, Wu X, Qiu Y, Bi Y, Yang X, Xin Y, He J, Zhou J, Zeng L, Yang R, Wang X. 2014. *Yersinia pestis* biovar *Microtus* strain 201, an avirulent strain to humans, provides protection against bubonic plague in rhesus macaques. *Hum Vaccin Immunother* 10:368-77.
226. Demeure CE, Derbise A, Guillas C, Gerke C, Cauchemez S, Carniel E, Pizarro-Cerdá J. 2019. Humoral and cellular immune correlates of protection against bubonic plague by a live *Yersinia pseudotuberculosis* vaccine. *Vaccine* 37:123-129.
227. Anonymous. 2018. World Health Organization. Influenza (Seasonal). [http://www.who.int/news-room/fact-sheets/detail/influenza-\(seasonal\)](http://www.who.int/news-room/fact-sheets/detail/influenza-(seasonal)). Accessed 2022 September 20.
228. Anonymous. World Health Organization. Global Influenza Programme (2022), on World Health Organization. <https://www.who.int/teams/global-influenza-programme/surveillance-and-monitoring/influenza-surveillance-outputs>. Accessed 2022 August 2.
229. Louten J. 2016. Essential Human Virology. .
230. Petrova VN, Russell CA. 2017. The evolution of seasonal influenza viruses. *Nature Reviews Microbiology* 16:47.

231. Anonymous. 2018. World Health Organization. Influenza (Avian and other zoonotic). [https://www.who.int/news-room/fact-sheets/detail/influenza-\(avian-and-other-zoonotic\)](https://www.who.int/news-room/fact-sheets/detail/influenza-(avian-and-other-zoonotic)). Accessed 2022 December 5.
232. Anonymous. 2022. Centers for Disease Control and Prevention. Influenza Type A Viruses. <https://www.cdc.gov/flu/avianflu/influenza-a-virus-subtypes.htm>. Accessed 2022 August 10.
233. McAuley JL, Gilbertson BP, Trifkovic S, Brown LE, McKimm-Breschkin JL. 2019. Influenza Virus Neuraminidase Structure and Functions. *Frontiers in microbiology* 10:39-39.
234. website Ug. 30.9.22 2022. Surveillance of influenza and other seasonal respiratory viruses in winter 2021 to 2022. [https://www.gov.uk/government/statistics/annual-flu-reports/surveillance-of-influenza-and-other-seasonal-respiratory-viruses-in-winter-2021-to-2022#:~:text=Influenza%20A\(H3N2\)%20was%20the,small%20proportion%20of%20subtyped%20viruses](https://www.gov.uk/government/statistics/annual-flu-reports/surveillance-of-influenza-and-other-seasonal-respiratory-viruses-in-winter-2021-to-2022#:~:text=Influenza%20A(H3N2)%20was%20the,small%20proportion%20of%20subtyped%20viruses). Accessed 2022 October 24.
235. website Ug. 23.10.22 2022. Guidance. Avian influenza (bird flu). <https://www.gov.uk/guidance/avian-influenza-bird-flu#:~:text=Since%201%20October%202022%20there,outbreak%20began%20in%20October%202021>. Accessed 2022 October 24.
236. Anonymous. 1980. World Health Organization. A revision of the system of nomenclature for influenza viruses: a WHO memorandum. *World Health Organization* 58:585-91.
237. Anonymous. 2022. Centers for Disease Control and Prevention. Vaccine Effectiveness: How Well Do Flu Vaccines Work?, on Centers for Disease Control and Prevention. <https://www.cdc.gov/flu/vaccines-work/vaccineeffect.htm>. Accessed 2022 August 5.
238. Lewnard JA, Cobey S. 2018. Immune History and Influenza Vaccine Effectiveness. *Vaccines (Basel)* 6.
239. Nelson SA, Sant AJ. 2021. Potentiating Lung Mucosal Immunity Through Intranasal Vaccination. *Frontiers in Microbiology* 12:808527.
240. Bull MB, Cohen CA, Leung NHL, Valkenburg SA. 2021. Universally Immune: How Infection Permissive Next Generation Influenza Vaccines May Affect Population Immunity and Viral Spread. *Viruses* 13.
241. Mohn KG, Smith I, Sjursen H, Cox RJ. 2018. Immune responses after live attenuated influenza vaccination. *Hum Vaccin Immunother* 14:571-578.
242. Zhou B, Meliopoulos VA, Wang W, Lin X, Stucker KM, Halpin RA, Stockwell TB, Schultz-Cherry S, Wentworth DE. 2016. Reversion of Cold-Adapted Live Attenuated Influenza Vaccine into a Pathogenic Virus. *Journal of Virology* 90:8454-8463.
243. Anonymous. 2022. Centers for Disease Control and Prevention. Live Attenuated Influenza Vaccine [LAIV] (The Nasal Spray Flu Vaccine). <https://www.cdc.gov/flu/prevent/nasalspray.htm#:~:text=Some%20people%20shoud%20not%20get,dose%20of%20any%20flu%20vaccine>. Accessed 2022 November 10.
244. Carascal MB, Pavon RDN, Rivera WL. 2022. Recent Progress in Recombinant Influenza Vaccine Development Toward Heterosubtypic Immune Response. *Frontiers in Microbiology* 13:878943.
245. Wilson IA, Skehel JJ, Wiley DC. 1981. Structure of the haemagglutinin membrane glycoprotein of influenza virus at 3 Å resolution. *Nature* 289:366-73.

246. Myers JL, Wetzel KS, Linderman SL, Li Y, Sullivan CB, Hensley SE. 2013. Compensatory hemagglutinin mutations alter antigenic properties of influenza viruses. *Journal of Virology* 87:11168-72.
247. Song Y, Zhu W, Wang Y, Deng L, Ma Y, Dong C, Gonzalez GX, Kim J, Wei L, Kang SM, Wang BZ. 2022. Layered protein nanoparticles containing influenza B HA stalk induced sustained cross-protection against viruses spanning both viral lineages. *Biomaterials* 287:121664.
248. Subbiah J, Oh J, Kim KH, Shin CH, Park BR, Bhatnagar N, Seong BL, Wang BZ, Kang SM. 2022. A chimeric thermostable M2e and H3 stalk-based universal influenza A virus vaccine. *NPJ Vaccines* 7:68.
249. Bliss CM, Freyn AW, Caniels TG, Leyva-Grado VH, Nachbagauer R, Sun W, Tan GS, Gillespie VL, McMahon M, Krammer F, Hill AVS, Palese P, Coughlan L. 2022. A single-shot adenoviral vaccine provides hemagglutinin stalk-mediated protection against heterosubtypic influenza challenge in mice. *Mol Ther* 30:2024-2047.
250. Chen Y-Q, Lan LY-L, Huang M, Henry C, Wilson PC. 2019. Hemagglutinin Stalk-Reactive Antibodies Interfere with Influenza Virus Neuraminidase Activity by Steric Hindrance. *Journal of Virology* 93:e01526-18.
251. Nachbagauer R, Krammer F. 2017. Universal influenza virus vaccines and therapeutic antibodies. *Clinical microbiology and infection : the official publication of the European Society of Clinical Microbiology and Infectious Diseases* 23:222-228.
252. ElHefnawi M, AlAidi O, Mohamed N, Kamar M, El-Azab I, Zada S, Siam R. 2011. Identification of novel conserved functional motifs across most Influenza A viral strains. *Virology Journal* 8:44.
253. Padilla-Quirarte HO, Lopez-Guerrero DV, Gutierrez-Xicotencatl L, Esquivel-Guadarrama F. 2019. Protective Antibodies Against Influenza Proteins. *Frontiers in Immunology* 10:1677.
254. Bui H-H, Peters B, Assarsson E, Mbawuike I, Sette A. 2007. Ab and T cell epitopes of influenza A virus, knowledge and opportunities. *Proceedings of the National Academy of Sciences of the United States of America* 104:246-251.
255. Del Campo J, Pizzorno A, Djebali S, Bouley J, Haller M, Perez-Vargas J, Lina B, Boivin G, Hamelin ME, Nicolas F, Le Vert A, Leverrier Y, Rosa-Calatrava M, Marvel J, Hill F. 2019. OVX836 a recombinant nucleoprotein vaccine inducing cellular responses and protective efficacy against multiple influenza A subtypes. *NPJ Vaccines* 4:4.
256. Lee SY, Kang JO, Chang J. 2019. Nucleoprotein vaccine induces cross-protective cytotoxic T lymphocytes against both lineages of influenza B virus. *Clinical and Experimental Vaccine Research* 8:54-63.
257. Clemens EB, van de Sandt C, Wong SS, Wakim LM, Valkenburg SA. 2018. Harnessing the Power of T Cells: The Promising Hope for a Universal Influenza Vaccine. *Vaccines* 6:18.
258. Valkenburg SA, Mallajosyula VV, Li OT, Chin AW, Carnell G, Temperton N, Varadarajan R, Poon LL. 2016. Stalking influenza by vaccination with pre-fusion headless HA mini-stem. *Sci Rep* 6:22666.
259. Caceres CJ, Seibert B, Cargnin Faccin F, Cardenas-Garcia S, Rajao DS, Perez DR. 2022. Influenza antivirals and animal models. *FEBS Open Bio* 12:1142-1165.
260. Thangavel RR, Bouvier NM. 2014. Animal models for influenza virus pathogenesis, transmission, and immunology. *J Immunol Methods* 410:60-79.
261. Martens EC, Chiang HC, Gordon JI. 2008. Mucosal glycan foraging enhances fitness and transmission of a saccharolytic human gut bacterial symbiont. *Cell Host Microbe* 4:447-57.

262. Rodriguez-Castaño GP, Dorris MR, Liu X, Bolling BW, Acosta-Gonzalez A, Rey FE. 2019. *Bacteroides thetaiotaomicron* Starch Utilization Promotes Quercetin Degradation and Butyrate Production by *Eubacterium ramulus*. *Frontiers in Microbiology* 10.
263. Faddin JFM. 1985. Media for Isolation-cultivation-identification-maintenance of Medical Bacteria. Williams & Wilkins.
264. Nath Neerukonda S, Vassell R, Weiss CD. 2020. Neutralizing Antibodies Targeting the Conserved Stem Region of Influenza Hemagglutinin. *Vaccines (Basel)* 8.
265. Quan FS, Yoo DG, Song JM, Clements JD, Compans RW, Kang SM. 2009. Kinetics of immune responses to influenza virus-like particles and dose-dependence of protection with a single vaccination. *Journal of Virology* 83:4489-97.
266. Chrnyk BA, Evans J, Lillquist J, Young P, Wetzel R. 1993. Inclusion body formation and protein stability in sequence variants of interleukin-1 beta. *Journal of Biological Chemistry* 268:18053-18061.
267. Ballesteros-Tato A, León B, Lund FE, Randall TD. 2010. Temporal changes in dendritic cell subsets, cross-priming and costimulation via CD70 control CD8(+) T cell responses to influenza. *Nat Immunol* 11:216-24.
268. Aytar Çelik P, Derkuş B, Erdoğan K, Barut D, Blaise Manga E, Yıldırım Y, Pecha S, Çabuk A. 2022. Bacterial membrane vesicle functions, laboratory methods, and applications. *Biotechnology Advances* 54:107869.
269. Caddy SL, Vaysburd M, Papa G, Wing M, O'Connell K, Stoycheva D, Foss S, Terje Andersen J, Oxenius A, James LC. 2021. Viral nucleoprotein antibodies activate TRIM21 and induce T cell immunity. *The EMBO Journal* 40:e106228.
270. Kaveh DA, Whelan AO, Hogarth PJ. 2012. The Duration of Antigen-Stimulation Significantly Alters the Diversity of Multifunctional CD4 T Cells Measured by Intracellular Cytokine Staining. *PLOS ONE* 7:e38926.
271. Del Campo J, Bouley J, Chevandier M, Rousset C, Haller M, Indalecio A, Guyon-Gellin D, Le Vert A, Hill F, Djebali S, Leverrier Y, Marvel J, Combadière B, Nicolas F. 2021. OVX836 Heptameric Nucleoprotein Vaccine Generates Lung Tissue-Resident Memory CD8+ T-Cells for Cross-Protection Against Influenza. *Frontiers in Microbiology* 12:678483.
272. Yin Y, Li B, Zhou L, Luo J, Liu X, Wang S, Lu Q, Tan W, Chen Z. 2020. Protein transduction domain-mediated influenza NP subunit vaccine generates a potent immune response and protection against influenza virus in mice. *Emerging Microbes & Infections* 9:1933-1942.
273. Huang B, Wang W, Li R, Wang X, Jiang T, Qi X, Gao Y, Tan W, Ruan L. 2012. Influenza A virus nucleoprotein derived from *Escherichia coli* or recombinant vaccinia (Tiantan) virus elicits robust cross-protection in mice. *Virology* 439:317-322.
274. Zheng M, Liu F, Shen Y, Wang S, Xu W, Fang F, Sun B, Xie Z, Chen Z. 2015. Cross-protection against influenza virus infection by intranasal administration of nucleoprotein-based vaccine with compound 48/80 adjuvant. *Hum Vaccin Immunother* 11:397-406.
275. Jiang L, Driedonks T, Lowman M, Jong WSP, van den Berg van Saparoea HB, Dhakal S, Zhou R, Caputo C, Littlefield K, Sitaras I, Chen M, Lima G, Gololobova O, Smith B, Lane AP, Klein SL, Pekosz A, Brayton C, Luirink J, Villano JS, Witwer KW. 2021. A bacterial extracellular vesicle-based intranasal vaccine against SARS-CoV-2. *bioRxiv* doi:10.1101/2021.06.28.450181:2021.06.28.450181.
276. Saparoea HBvdBv, Houben D, Jonge MId, Jong WSP, Luirink J. 2018. Display of Recombinant Proteins on Bacterial Outer Membrane Vesicles by Using Protein Ligation. *Applied and Environmental Microbiology* 84:e02567-17.

277. Feng R, Li GC, Jing HM, Liu C, Xue RY, Zou QM, Li HB. 2022. A "Plug-and-Display" Nanoparticle Vaccine Platform Based on Outer Membrane Vesicles Displaying SARS-CoV-2 Receptor-binding Domain. *J Vis Exp* doi:10.3791/64213.
278. Altman JD, Davis MM. 2003. MHC-Peptide Tetramers to Visualize Antigen-Specific T Cells. *Current Protocols in Immunology* 53:17.3.1-17.3.33.
279. Kingstad-Bakke B, Toy R, Lee W, Pradhan P, Vogel G, Marinaik CB, Larsen A, Gates D, Luu T, Pandey B, Kawaoka Y, Roy K, Suresh M. 2020. Polymeric Pathogen-Like Particles-Based Combination Adjuvants Elicit Potent Mucosal T Cell Immunity to Influenza A Virus. *Frontiers in Immunology* 11:559382.
280. Hartley GE, Edwards ESJ, Bosco JJ, Ojaimi S, Stirling RG, Cameron PU, Flanagan K, Plebanski M, Hogarth PM, O'Hehir RE, van Zelm MC. 2020. Influenza-specific IgG1(+) memory B-cell numbers increase upon booster vaccination in healthy adults but not in patients with predominantly antibody deficiency. *Clinical & Translational Immunology* 9:e1199.
281. Cipolla EM, Yue M, Nickolich KL, Huckestein BR, Antos D, Chen W, Alcorn JF. 2022. Heterotypic Influenza Infections Mitigate Susceptibility to Secondary Bacterial Infection. *The Journal of Immunology* 209:760-771.
282. Anonymous. 2022. World Health Organization. WHO Coronavirus (COVID-19) Dashboard. <https://covid19.who.int/>. Accessed 2022 November 20
283. Lu R, Zhao X, Li J, Niu P, Yang B, Wu H, Wang W, Song H, Huang B, Zhu N, Bi Y, Ma X, Zhan F, Wang L, Hu T, Zhou H, Hu Z, Zhou W, Zhao L, Chen J, Meng Y, Wang J, Lin Y, Yuan J, Xie Z, Ma J, Liu WJ, Wang D, Xu W, Holmes EC, Gao GF, Wu G, Chen W, Shi W, Tan W. 2020. Genomic characterisation and epidemiology of 2019 novel coronavirus: implications for virus origins and receptor binding. *The Lancet* 395:565-574.
284. Wu F, Zhao S, Yu B, Chen Y-M, Wang W, Song Z-G, Hu Y, Tao Z-W, Tian J-H, Pei Y-Y, Yuan M-L, Zhang Y-L, Dai F-H, Liu Y, Wang Q-M, Zheng J-J, Xu L, Holmes EC, Zhang Y-Z. 2020. A new coronavirus associated with human respiratory disease in China. *Nature* 579:265-269.
285. Balieu J, Jung JW, Chan P, Lomonosoff GP, Lerouge P, Bardor M. 2022. Investigation of the N-Glycosylation of the SARS-CoV-2 S Protein Contained in VLPs Produced in *Nicotiana benthamiana*. *Molecules* 27.
286. Zhang Y, Zhao W, Mao Y, Chen Y, Wang S, Zhong Y, Su T, Gong M, Du D, Lu X, Cheng J, Yang H. 2021. Site-specific N-glycosylation Characterization of Recombinant SARS-CoV-2 Spike Proteins. *Molecular & Cellular Proteomics* 20:100058.
287. Grant OC, Montgomery D, Ito K, Woods RJ. 2020. Analysis of the SARS-CoV-2 spike protein glycan shield reveals implications for immune recognition. *Scientific Reports* 10:14991.
288. Min L, Sun Q. 2021. Antibodies and Vaccines Target RBD of SARS-CoV-2. *Frontiers in Molecular Biosciences* 8.
289. Townsend JP, Hassler HB, Wang Z, Miura S, Singh J, Kumar S, Ruddle NH, Galvani AP, Dornburg A. 2021. The durability of immunity against reinfection by SARS-CoV-2: a comparative evolutionary study. *The Lancet Microbe* 2:e666-e675.
290. Agrati C, Castilletti C, Goletti D, Sacchi A, Bordoni V, Mariotti D, Notari S, Matusali G, Meschi S, Petrone L, Aiello A, Najafi Fard S, Farroni C, Colavita F, Lapa D, Leone S, Agresta A, Capobianchi M, Ippolito G, Vaia F, Puro V, Cimini E, Tartaglia E, Casetti R, Grassi G, Cristofanelli F, Capri A, Santoro A, Orchi N, Bettini A, Francalancia M, Specchiarello E, Group IC-VS. 2022. Persistent Spike-specific T cell immunity despite antibody reduction after 3 months from SARS-CoV-2 BNT162b2-mRNA vaccine. *Scientific Reports* 12:6687.

291. Terahara K, Sato T, Adachi Y, Tonouchi K, Onodera T, Moriyama S, Sun L, Takano T, Nishiyama A, Kawana-Tachikawa A, Matano T, Matsumura T, Shinkai M, Isogawa M, Takahashi Y. 2022. SARS-CoV-2-specific CD4(+) T cell longevity correlates with Th17-like phenotype. *iScience* 25:104959.
292. Agarwal A, Beck KL, Capponi S, Kunitomi M, Nayar G, Seabolt E, Mahadeshwar G, Bianco S, Mukherjee V, Kaufman JH. 2022. Predicting Epitope Candidates for SARS-CoV-2. *Viruses* 14.
293. Ferretti AP, Kula T, Wang Y, Nguyen DMV, Weinheimer A, Dunlap GS, Xu Q, Nabilsi N, Perullo CR, Cristofaro AW, Whitton HJ, Virbasius A, Olivier KJ, Jr., Buckner LR, Alistar AT, Whitman ED, Bertino SA, Chattopadhyay S, MacBeath G. 2020. Unbiased Screens Show CD8(+) T Cells of COVID-19 Patients Recognize Shared Epitopes in SARS-CoV-2 that Largely Reside outside the Spike Protein. *Immunity* 53:1095-1107.e3.
294. Mazzoni A, Vanni A, Spinicci M, Capone M, Lamacchia G, Salvati L, Coppi M, Antonelli A, Carnasciali A, Farahvachi P, Giovacchini N, Aiezza N, Malentacchi F, Zammarchi L, Liotta F, Rossolini GM, Bartoloni A, Cosmi L, Maggi L, Annunziato F. 2022. SARS-CoV-2 Spike-Specific CD4+ T Cell Response Is Conserved Against Variants of Concern, Including Omicron. *Frontiers in Immunology* 13.
295. Moss P. 2022. The T cell immune response against SARS-CoV-2. *Nature Immunology* 23:186-193.
296. Rak A, Donina S, Zabrodskaia Y, Rudenko L, Isakova-Sivak I. 2022. Cross-Reactivity of SARS-CoV-2 Nucleocapsid-Binding Antibodies and Its Implication for COVID-19 Serology Tests. *Viruses* 14:2041.
297. Kurano M, Morita Y, Nakano Y, Yokoyama R, Shimura T, Qian C, Xia F, He F, Zheng L, Ohmiya H, Kishi Y, Okada J, Yoshikawa N, Nakajima K, Nagura Y, Okazaki H, Jubishi D, Moriya K, Seto Y, Yasui F, Kohara M, Wakui M, Kawamura T, Kodama T, Yatomi Y. 2022. Response kinetics of different classes of antibodies to SARS-CoV2 infection in the Japanese population: The IgA and IgG titers increased earlier than the IgM titers. *International Immunopharmacology* 103:108491.
298. André S, Azarias da Silva M, Picard M, Alleaume-Buteau A, Kundura L, Cezar R, Soudaramourty C, André SC, Mendes-Frias A, Carvalho A, Capela C, Pedrosa J, Gil Castro A, Loubet P, Sotto A, Muller L, Lefrant JY, Roger C, Claret PG, Duvnjak S, Tran TA, Zghidi-Abouzid O, Nioche P, Silvestre R, Corbeau P, Mammano F, Estaquier J. 2022. Low quantity and quality of anti-spike humoral response is linked to CD4 T-cell apoptosis in COVID-19 patients. *Cell Death Dis* 13:741.
299. Anonymous. 2022. World Health Organization. Coronavirus disease (COVID-19). https://www.who.int/health-topics/coronavirus#tab=tab_1. Accessed 2022 September 24.
300. Wade H, Duan Q, Su Q. 2022. Interaction between Sars-CoV-2 structural proteins and host cellular receptors: From basic mechanisms to clinical perspectives. *Adv Protein Chem Struct Biol* 132:243-277.
301. Almagro JC, Mellado-Sánchez G, Pedraza-Escalona M, Pérez-Tapia SM. 2022. Evolution of Anti-SARS-CoV-2 Therapeutic Antibodies. *Int J Mol Sci* 23.
302. Lupala CS, Ye Y, Chen H, Su XD, Liu H. 2022. Mutations on RBD of SARS-CoV-2 Omicron variant result in stronger binding to human ACE2 receptor. *Biochem Biophys Res Commun* 590:34-41.
303. Anonymous. 2022. World Health Organisation. Tracking SARS-CoV-2 variants. <https://www.who.int/activities/tracking-SARS-CoV-2-variants>. Accessed 2022 October 10.
304. Bentley EG, Kirby A, Sharma P, Kipar A, Mega DF, Bramwell C, Penrice-Randal R, Prince T, Brown JC, Zhou J, Sreaton GR, Barclay WS, Owen A, Hiscox JA, Stewart

- JP. 2021. SARS-CoV-2 Omicron-B.1.1.529 Variant leads to less severe disease than Pango B and Delta variants strains in a mouse model of severe COVID-19. *bioRxiv* doi:10.1101/2021.12.26.474085:2021.12.26.474085.
305. Ferdinands JM, Rao S, Dixon BE, Mitchell PK, DeSilva MB, Irving SA, Lewis N, Natarajan K, Stenehjem E, Grannis SJ, Han J, McEvoy C, Ong TC, Naleway AL, Reese SE, Embi PJ, Dascomb K, Klein NP, Griggs EP, Liao I-C, Yang D-H, Fadel WF, Grisel N, Goddard K, Patel P, Murthy K, Birch R, Valvi NR, Arndorfer J, Zerbo O, Dickerson M, Raiyani C, Williams J, Bozio CH, Blanton L, Link-Gelles R, Barron MA, Gaglani M, Thompson MG, Fireman B. 2022. Waning of vaccine effectiveness against moderate and severe covid-19 among adults in the US from the VISION network: test negative, case-control study. *BMJ* 379:e072141.
306. Anonymous. 2022. European Medicines Agency. COVID-19 vaccines: authorised. <https://www.ema.europa.eu/en/human-regulatory/overview/public-health-threats/coronavirus-disease-covid-19/treatments-vaccines/vaccines-covid-19/covid-19-vaccines-authorised>. Accessed 2022 October 12.
307. Herzberg J, Fischer B, Becher H, Becker AK, Honarpisheh H, Guraya SY, Strate T, Knabbe C. 2022. Short-Term Drop in Antibody Titer after the Third Dose of SARS-CoV-2 BNT162b2 Vaccine in Adults. *Vaccines (Basel)* 10.
308. Hall V, Foulkes S, Insalata F, Kirwan P, Saei A, Atti A, Wellington E, Khawam J, Munro K, Cole M, Tranquillini C, Taylor-Kerr A, Hettiarachchi N, Calbraith D, Sajedi N, Milligan I, Themistocleous Y, Corrigan D, Cromey L, Price L, Stewart S, de Lacy E, Norman C, Linley E, Otter AD, Semper A, Hewson J, D'Arcangelo S, Chand M, Brown CS, Brooks T, Islam J, Charlett A, Hopkins S. 2022. Protection against SARS-CoV-2 after Covid-19 Vaccination and Previous Infection. *New England Journal of Medicine* 386:1207-1220.
309. Waltz E. 2022. China and India approve nasal COVID vaccines - are they a game changer? *Nature* 609:450.
310. Sterlin D, Mathian A, Miyara M, Mohr A, Anna F, Claër L, Quentric P, Fadlallah J, Devilliers H, Ghillani P, Gunn C, Hockett R, Mudumba S, Guihot A, Luyt C-E, Mayaux J, Beurton A, Fourati S, Bruel T, Schwartz O, Lacorte J-M, Yssel H, Parizot C, Dorgham K, Charneau P, Amoura Z, Gorochov G. 2021. IgA dominates the early neutralizing antibody response to SARS-CoV-2. *Science Translational Medicine* 13:eabd2223.
311. Russell MW, Mestecky J. 2022. Mucosal immunity: The missing link in comprehending SARS-CoV-2 infection and transmission. *Frontiers in Immunology* 13.
312. Hajnik RL, Plante JA, Liang Y, Alameh MG, Tang J, Bonam SR, Zhong C, Adam A, Scharton D, Rafael GH, Liu Y, Hazell NC, Sun J, Soong L, Shi PY, Wang T, Walker DH, Sun J, Weissman D, Weaver SC, Plante KS, Hu H. 2022. Dual spike and nucleocapsid mRNA vaccination confer protection against SARS-CoV-2 Omicron and Delta variants in preclinical models. *Sci Transl Med* 14:eabq1945.
313. Castro JT, Azevedo P, Fumagalli MJ, Hojo-Souza NS, Salazar N, Almeida GG, Oliveira LI, Faustino L, Antonelli LR, Marçal TG, Augusto M, Valiate B, Fiorini A, Rattis B, Ramos SG, Piccin M, Nonato OC, Benevides L, Magalhães R, Cassaro B, Burle G, Doro D, Kalil J, Durigon E, Salazar A, Caballero O, Santiago H, Machado A, Silva JS, da Fonseca F, Fernandes AP, Teixeira SR, Gazzinelli RT. 2022. Promotion of neutralizing antibody-independent immunity to wild-type and SARS-CoV-2 variants of concern using an RBD-Nucleocapsid fusion protein. *Nat Commun* 13:4831.
314. Rice A, Verma M, Voigt E, Battisti P, Beaver S, Reed S, Dinkins K, Mody S, Zakin L, Tanaka S, Morimoto B, Olson CA, Gabitzsch E, Safrit JT, Spilman P, Casper C, Soon-

- Shiong P. 2022. Heterologous saRNA Prime, DNA Dual-Antigen Boost SARS-CoV-2 Vaccination Elicits Robust Cellular Immunogenicity and Cross-Variant Neutralizing Antibodies. *Frontiers in Microbiology* 13:910136.
315. Li T, Zheng Q, Yu H, Wu D, Xue W, Xiong H, Huang X, Nie M, Yue M, Rong R, Zhang S, Zhang Y, Wu Y, Wang S, Zha Z, Chen T, Deng T, Wang Y, Zhang T, Chen Y, Yuan Q, Zhao Q, Zhang J, Gu Y, Li S, Xia N. 2020. SARS-CoV-2 spike produced in insect cells elicits high neutralization titres in non-human primates. *Emerging Microbes & Infections* 9:2076-2090.
 316. Maffei M, Montemiglio LC, Vitagliano G, Fedele L, Sellathurai S, Bucci F, Compagnone M, Chiarini V, Exertier C, Muzi A, Roscilli G, Vallone B, Marra E. 2021. The nuts and bolts of SARS-CoV-2 Spike Receptor Binding Domain heterologous expression. *bioRxiv* doi:10.1101/2021.09.17.460782:2021.09.17.460782.
 317. Freitas M, Cayuela C, Antoine JM, Piller F, Sapin C, Trugnan G. 2001. A heat labile soluble factor from *Bacteroides thetaiotaomicron* VPI-5482 specifically increases the galactosylation pattern of HT29-MTX cells. *Cell Microbiol* 3:289-300.
 318. Bao L, Deng W, Huang B, Gao H, Liu J, Ren L, Wei Q, Yu P, Xu Y, Qi F, Qu Y, Li F, Lv Q, Wang W, Xue J, Gong S, Liu M, Wang G, Wang S, Song Z, Zhao L, Liu P, Zhao L, Ye F, Wang H, Zhou W, Zhu N, Zhen W, Yu H, Zhang X, Guo L, Chen L, Wang C, Wang Y, Wang X, Xiao Y, Sun Q, Liu H, Zhu F, Ma C, Yan L, Yang M, Han J, Xu W, Tan W, Peng X, Jin Q, Wu G, Qin C. 2020. The pathogenicity of SARS-CoV-2 in hACE2 transgenic mice. *Nature* 583:830-833.
 319. Kolb HC, Finn MG, Sharpless KB. 2001. Click Chemistry: Diverse Chemical Function from a Few Good Reactions. *Angew Chem Int Ed Engl* 40:2004-2021.
 320. Lam JH, Shivhare D, Chia TW, Chew SL, Sinsinbar G, Aw TY, Wong S, Venkataraman S, Lim FWI, Vandepapeliere P, Nallani M. 2022. Artificial Cell Membrane Polymersome-Based Intranasal Beta Spike Formulation as a Second Generation Covid-19 Vaccine. *ACS Nano* doi:10.1021/acsnano.2c06350.
 321. Song SJ, Kim H, Jang EY, Jeon H, Diao HP, Khan MRI, Lee MS, Lee YJ, Nam JH, Kim SR, Kim YJ, Sohn EJ, Hwang I, Choi JH. 2022. SARS-CoV-2 spike trimer vaccine expressed in *Nicotiana benthamiana* adjuvanted with Alum elicits protective immune responses in mice. *Plant Biotechnol J* doi:10.1111/pbi.13908.
 322. Nazarian S, Olad G, Abdolhamidi R, Motamedi MJ, Kazemi R, Kordbacheh E, Felagari A, Olad H, Ahmadi A, Bahirae A, Farahani P, Haghghi L, Hassani F, Hajhassan V, Nadi M, Sheikhi A, Salimian J, Amani J. 2022. Preclinical study of formulated recombinant nucleocapsid protein, the receptor binding domain of the spike protein, and truncated spike (S1) protein as vaccine candidates against COVID-19 in animal models. *Mol Immunol* 149:107-118.
 323. Hevesi Z, Gerges DA, Kapps S, Freire R, Schmidt S, Pollak DD, Schmetterer K, Frey T, Lang R, Winnicki W, Schmidt A, Harkany T, Wagner L. 2022. Preclinical Establishment of a Divalent Vaccine against SARS-CoV-2. *Vaccines (Basel)* 10.
 324. Ghaemi A, Roshani Asl P, Zargarani H, Ahmadi D, Hashimi AA, Abdolalipour E, Bathaeian S, Miri SM. 2022. Recombinant COVID-19 vaccine based on recombinant RBD/Nucleoprotein and saponin adjuvant induces long-lasting neutralizing antibodies and cellular immunity. *Frontiers in Microbiology* 13:974364.
 325. Chiuppesi F, Salazar MD, Contreras H, Nguyen VH, Martinez J, Park S, Nguyen J, Kha M, Iniguez A, Zhou Q, Kaltcheva T, Levytsky R, Ebel ND, Kang TH, Wu X, Rogers T, Manuel ER, Shostak Y, Diamond DJ, Wussow F. 2020. Development of a Synthetic Poxvirus-Based SARS-CoV-2 Vaccine. *bioRxiv* doi:10.1101/2020.07.01.183236.

326. De Rosa SC, Lu FX, Yu J, Perfetto SP, Falloon J, Moser S, Evans TG, Koup R, Miller CJ, Roederer M. 2004. Vaccination in Humans Generates Broad T Cell Cytokine Responses¹. *The Journal of Immunology* 173:5372-5380.
327. Choi HG, Kwon KW, Choi S, Back YW, Park HS, Kang SM, Choi E, Shin SJ, Kim HJ. 2020. Antigen-Specific IFN- γ /IL-17-Co-Producing CD4(+) T-Cells Are the Determinants for Protective Efficacy of Tuberculosis Subunit Vaccine. *Vaccines (Basel)* 8.
328. Anonymous. 2022. Centers for Disease Control and Prevention. Vaccine Recommendations and Guidelines of the ACIP. <https://www.cdc.gov/vaccines/hcp/acip-recs/general-recs/storage.html>. Accessed 2022 November 28.
329. Anonymous. 2011. World Health Organization. Expert Committee on Biological Standardization. World Health Organization,
330. Emily P. Wen Ronald Ellies NSP. 2015. Vaccine Development and Manufacturing John Wiley & Sons, Inc., New Jersey
331. Ghaemmaghmanian Z, Zarghami R, Walker G, O'Reilly E, Ziaee A. 2022. Stabilizing vaccines via drying: Quality by design considerations. *Advanced Drug Delivery Reviews* 187:114313.
332. Anonymous. ClinicalTrials.gov. A Study to Evaluate Safety, Tolerability, & Immunogenicity of Multiple Formulations of BNT162b2 Against COVID-19 in Healthy Adults, ClinicalTrials.gov.
333. Alves NJ, Turner KB, Medintz IL, Walper SA. 2016. Protecting enzymatic function through directed packaging into bacterial outer membrane vesicles. *Scientific reports* 6:24866-24866.
334. Thakur M, Dean SN, Moore M, Spangler JR, Johnson BJ, Medintz IL, Walper SA. 2022. Packaging of Diisopropyl Fluorophosphatase (DFPase) in Bacterial Outer Membrane Vesicles Protects Its Activity at Extreme Temperature. *ACS Biomaterials Science & Engineering* 8:493-501.
335. Schulz E, Goes A, Garcia R, Panter F, Koch M, Müller R, Fuhrmann K, Fuhrmann G. 2018. Biocompatible bacteria-derived vesicles show inherent antimicrobial activity. *Journal of Controlled Release* 290:46-55.
336. Arigita C, Jiskoot W, Westdijk J, van Ingen C, Hennink WE, Crommelin DJA, Kersten GFA. 2004. Stability of mono- and trivalent meningococcal outer membrane vesicle vaccines. *Vaccine* 22:629-642.
337. Masforrol Y, Gil J, García D, Noda J, Ramos Y, Betancourt L, Guirola O, González S, Acevedo B, Besada V, Reyes O, González LJ. 2017. A deeper mining on the protein composition of VA-MENGOC-BC[®]: An OMV-based vaccine against *N. meningitidis* serogroup B and C. *Hum Vaccin Immunother* 13:2548-2560.
338. Lafeber AB vLC, Berbers GAM, Labadie J, de Kleijn ED, de Groot R, Rumke HC, van Alphen AJW. 2000. Immunogenicity and safety of monovalent RIVM meningococcal B OMP vesicle F91 vaccine administered to children that received hexavalent meningococcal B vaccine 2.5 years ago. Rijksinstituut voor Volksgezondheid en Milieu RIVM Sophia Kinderziekenhuis / Academisch Ziekenhuis Rotterdam.
339. Holmes JD, Martin D, Ramsay C, Ypma E, Oster P. 2008. Combined administration of serogroup B meningococcal vaccine and conjugated serogroup C meningococcal vaccine is safe and immunogenic in college students. *Epidemiol Infect* 136:790-9.
340. Pfizer. 2022. Pfizer-BiONTech Covid-19 Vaccine Emergency Use Authorization Fact Sheet.

341. Anonymous. 2022. Food and Drug Administration. FluMist® Quadrivalent (Influenza Vaccine Live, Intranasal). Food and Drug Administration.
342. Group OV. 2022. Vaccine ingredients. <https://vk.ovg.ox.ac.uk/vk/vaccine-ingredients>. Accessed 2022 November 23.
343. Muller L, Hong CS, Stolz DB, Watkins SC, Whiteside TL. 2014. Isolation of biologically-active exosomes from human plasma. *J Immunol Methods* 411:55-65.
344. Maroto R, Zhao Y, Jamaluddin M, Popov VL, Wang H, Kalubowilage M, Zhang Y, Luisi J, Sun H, Culbertson CT, Bossmann SH, Motamedi M, Brasier AR. 2017. Effects of storage temperature on airway exosome integrity for diagnostic and functional analyses. *Journal of Extracellular Vesicles* 6:1359478.
345. Gelibter S, Marostica G, Mandelli A, Siciliani S, Podini P, Finardi A, Furlan R. 2022. The impact of storage on extracellular vesicles: A systematic study. *Journal of Extracellular Vesicles* 11:e12162.
346. Popowski KD, Moatti A, Scull G, Silkstone D, Lutz H, López de Juan Abad B, George A, Belcher E, Zhu D, Mei X, Cheng X, Cislo M, Ghodsi A, Cai Y, Huang K, Li J, Brown AC, Greenbaum A, Dinh PC, Cheng K. 2022. Inhalable dry powder mRNA vaccines based on extracellular vesicles. *Matter* 5:2960-2974.
347. Trenkschuh E, Richter M, Heinrich E, Koch M, Fuhrmann G, Friess W. 2022. Enhancing the Stabilization Potential of Lyophilization for Extracellular Vesicles. *Adv Healthc Mater* 11:e2100538.
348. Anonymous. 2017. World Health Organization. Preferred Product Characteristics for Next-Generation Influenza Vaccines. World Health Organization.
349. Anonymous. 2022. World Health Organization. Target Product Profiles for COVID-19 Vaccines. World Health Organization.
350. Green MD, Al-Humadi NH. 2017. Preclinical Toxicology of Vaccines. *A Comprehensive Guide to Toxicology in Nonclinical Drug Development*:709-35.
351. Gunti S, Notkins AL. 2015. Polyreactive Antibodies: Function and Quantification. *J Infect Dis* 212 Suppl 1:S42-6.
352. Gunti S, Messer RJ, Xu C, Yan M, Coleman WG, Peterson KE, Hasenkrug KJ, Notkins AL. 2015. Stimulation of Toll-Like Receptors profoundly influences the titer of polyreactive antibodies in the circulation. *Scientific Reports* 5:15066.
353. Lee H-G, Cho M-Z, Choi J-M. 2020. Bystander CD4+ T cells: crossroads between innate and adaptive immunity. *Experimental & Molecular Medicine* 52:1255-1263.
354. Tough DF, Sun S, Sprent J. 1997. T cell stimulation in vivo by lipopolysaccharide (LPS). *J Exp Med* 185:2089-94.
355. Eberl G, Brawand P, MacDonald HR. 2000. Selective bystander proliferation of memory CD4+ and CD8+ T cells upon NK T or T cell activation. *J Immunol* 165:4305-11.
356. Muralinath M, Kuehn MJ, Roland KL, Curtiss R. 2011. Immunization with *Salmonella enterica* Serovar Typhimurium-Derived Outer Membrane Vesicles Delivering the Pneumococcal Protein PspA Confers Protection against Challenge with *Streptococcus pneumoniae*. *Infection and Immunity* 79:887-894.
357. Li P, Wang X, Sun X, Cimino J, Guan Z, Sun W. 2021. Recombinant Pseudomonas Bionanoparticles Induce Protection against Pneumonic *Pseudomonas aeruginosa* Infection. *Infect Immun* 89:e0039621.
358. Schetters STT, Jong WSP, Horrevorts SK, Kruijssen LJW, Engels S, Stolk D, Daleke-Schermerhorn MH, Garcia-Vallejo J, Houben D, Unger WWJ, den Haan JMM, Luirink J, van Kooyk Y. 2019. Outer membrane vesicles engineered to express membrane-bound antigen program dendritic cells for cross-presentation to CD8(+) T cells. *Acta Biomaterialia* 91:248-257.

359. Basto AP, Piedade J, Ramalho R, Alves S, Soares H, Cornelis P, Martins C, Leitão A. 2012. A new cloning system based on the OprI lipoprotein for the production of recombinant bacterial cell wall-derived immunogenic formulations. *J Biotechnol* 157:50-63.
360. Salverda MLM, Meinderts SM, Hamstra H-J, Wagemakers A, Hovius JWR, van der Ark A, Stork M, van der Ley P. 2016. Surface display of a borrelial lipoprotein on meningococcal outer membrane vesicles. *Vaccine* 34:1025-1033.
361. Valguarnera E, Scott NE, Azimzadeh P, Feldman MF. 2018. Surface Exposure and Packing of Lipoproteins into Outer Membrane Vesicles Are Coupled Processes in Bacteroides. *mSphere* 3:e00559-18.
362. Baart GJ, Willemsen M, Khatami E, de Haan A, Zomer B, Beuvery EC, Tramper J, Martens DE. 2008. Modeling *Neisseria meningitidis* B metabolism at different specific growth rates. *Biotechnol Bioeng* 101:1022-35.
363. Macdonald IA, Kuehn MJ. 2013. Stress-induced outer membrane vesicle production by *Pseudomonas aeruginosa*. *J Bacteriol* 195:2971-81.
364. Reimer SL, Beniac DR, Hiebert SL, Booth TF, Chong PM, Westmacott GR, Zhanel GG, Bay DC. 2021. Comparative Analysis of Outer Membrane Vesicle Isolation Methods With an *Escherichia coli* tolA Mutant Reveals a Hypervesiculating Phenotype With Outer-Inner Membrane Vesicle Content. *Frontiers in Microbiology* 12:628801.
365. Duperthuy M, Sjöström AE, Sabharwal D, Damghani F, Uhlin BE, Wai SN. 2013. Role of the *Vibrio cholerae* matrix protein Bap1 in cross-resistance to antimicrobial peptides. *PLoS Pathog* 9:e1003620.

Appendix - Publications

Miquel-Clopés A, Bentley EG, Stewart JP, Carding SR. 2019. Mucosal vaccines and technology. *Clinical and Experimental Immunology* 196:205-214.

Carvalho AL, Miquel-Clopés A, Wegmann U, Jones E, Stentz R, Telatin A, Walker NJ, Butcher WA, Brown PJ, Holmes S, Dennis MJ, Williamson ED, Funnell SGP, Stock M, Carding SR. 2019. Use of bioengineered human commensal gut bacteria-derived microvesicles for mucosal plague vaccine delivery and immunization. *Clinical and Experimental Immunology* 196:287-304.

Carvalho AL, Fonseca S, Miquel-Clopés A, Cross K, Kok K-S, Wegmann U, Gil-Cardoso K, Bentley EG, Al Katy SHM, Coombes JL, Kipar A, Stentz R, Stewart JP, Carding SR. 2019. Bioengineering commensal bacteria-derived outer membrane vesicles for delivery of biologics to the gastrointestinal and respiratory tract. *Journal of Extracellular Vesicles* 8:1632100.

Stentz R, Miquel-Clopés A, Carding SR. 2022. Production, Isolation, and Characterization of Bioengineered Bacterial Extracellular Membrane Vesicles Derived from *Bacteroides thetaiotaomicron* and Their Use in Vaccine Development, p 171-190. In Bidmos F, Bossé J, Langford P (ed), *Bacterial Vaccines: Methods and Protocols*. Springer US, New York.

Fonseca S, Carvalho AL, Miquel-Clopés A, Jones EJ, Juodeikis R, Stentz R, Carding SR. 2022. Extracellular vesicles produced by the human gut commensal bacterium *Bacteroides thetaiotaomicron* elicit anti-inflammatory responses from innate immune cells. *Frontiers in Microbiology* 10:3389.

Mucosal vaccines and technology

OTHER ARTICLES PUBLISHED IN THIS REVIEW SERIES

Vaccines for emerging pathogens: from research to the clinic. Clinical and Experimental Immunology 2019, 196: 155-156.
Emerging viruses and current strategies for vaccine intervention. Clinical and Experimental Immunology 2019, 196: 157-166.
HLA-E: exploiting pathogen-host interactions for vaccine development. Clinical and Experimental Immunology 2019, 196: 167-177.
Novel multi-component vaccine approaches for Burkholderia pseudomallei. Clinical and Experimental Immunology 2019, 196: 178-188.
Novel approaches for the design, delivery and administration of vaccine technologies. Clinical and Experimental Immunology 2019, 196: 189-204.
Vaccines for emerging pathogens: prospects for licensure. Clinical and Experimental Immunology 2019, doi: 10.1111/cei.13284

A. Miquel-Clopés,* E. G. Bentley,[†]
 J. P. Stewart[†] and S. R. Carding*[‡] 

*Gut Microbes and Health Research Programme, Quadram Institute Bioscience, Norwich, [†]Department of Infection Biology, University of Liverpool, Liverpool, and [‡]Norwich Medical School, University of East Anglia, Norwich, UK

Accepted for publication 14 February 2019

Correspondence: S. R. Carding, Gut Microbes and Health Research Programme, Quadram Institute Bioscience, Norwich Research Park, Norwich NR4 7UA, UK.

E-mail: Simon.Carding@Quadram.ac.uk

Introduction

Vaccination is an efficient and cost-effective form of infectious disease prevention that can lead to global eradication, as seen for smallpox (1980) and rinderpest (2011). However, there is an urgent and growing need for the development of new and improved vaccines to further reduce the global burden of infectious disease morbidity and mortality, particularly against those targeting the respiratory and gastrointestinal (GI) tract. The paucity of effective vaccines is also acute in veterinary medicine, which is compounded by increasing multi-drug and antibiotic resistance [1]. Vaccines to combat zoonoses are a particularly urgent priority, as 60% or more pathogens with the potential to harm humans originate in animals [2]. Current vaccines are delivered by injection with associated problems of safety, compliance, morbidity and the high cost of mass immunization, particularly in resource-poor developing countries. Injected vaccines also provide partial or no protection at mucosal sites. Considering that >90% of pathogens gain access to the body via mucosal sites, using mucosal vaccination to generate protective immunity at mucosal sites could overcome the limitations of current injection-based vaccines in providing front-line protection against pathogen invasion and dissemination [3]. However, only a handful of mucosal vaccines are currently licensed. This limited

Summary

There is an urgent and unmet need to develop effective vaccines to reduce the global burden of infectious disease in both animals and humans, and in particular for the majority of pathogens that infect via mucosal sites. Here we summarise the impediments to developing mucosal vaccines and review the new and emerging technologies aimed at overcoming the lack of effective vaccine delivery systems that is the major obstacle to developing new mucosal vaccines.

Keywords: bacterial, mucosal, vaccines, viral

availability of mucosal vaccines is related to the lack of effective delivery systems able to preserve vaccine antigen integrity and strong adjuvanticity, which is compounded by the intrinsic nature of the mucosal immune system to induce tolerance [4].

Mucosal immunity and vaccine responses

The majority of mucosal vaccines are administered by the oral and nasal routes with the vaginal, rectal, ocular and sublingual routes being less frequently used. However, not all routes of administration induce an equivalent immune response in terms of potency and longevity, reflecting differences in the organization and cellular make-up of lymphoid structures in different mucosal tissues [5,6]. For example, oral immunization usually stimulates immune responses in the GI tract in addition to the oral mucosa and nasal-associated lymphoid tissues (NALT) and mammary glands. Intranasal delivery effectively induces antibody production in salivary glands, the NALT and the bronchus-associated lymphoid tissue (BALT) of the lower respiratory tract, and in the urogenital tract. Rectal immunization elicits a more pronounced immune and antibody response in nasal secretions, tears and the rectal mucosa. Thus, depending on the mucosal sites targeted by different pathogens, the route of immunization needs to be carefully considered [6–8]. In most cases, mucosal vaccination

is also effective in priming systemic immune responses and generating serum antibodies with neutralizing properties, reflecting the cross-talk between the mucosal and systemic immune systems. Serum immunoglobulin (IgG) responses in vaccinated animals can be a useful correlate of protection, either alone or in combination with secretory mucosa-derived (IgA) antibodies [9].

Size is another important consideration in the design of mucosal vaccines and targeting uptake to inductive immune sites to generate T cell and/or B cell responses. Goblet cell-associated passageways allow the entry of soluble protein antigens, but not inert particles (0.02–2 µm) into the underlying lamina propria [10]. Via endocytosis, enterocytes readily take up nanosized soluble particles of 20–40 nm, whereas M cells are the major route by which larger-sized inert particles of more than 100 nm are taken up [11]. While nanoparticles lead predominantly to T cell responses, larger microparticles are more effective at inducing humoral responses [12,13]. The fate of particles delivered via the intranasal route is influenced by their size with particles smaller than 5 µm being transported across the nasal mucosa for delivery to cells of the BALT. By contrast, larger particles exceeding 10 µm are taken up by alveolar macrophages and dendritic cells (DCs) [14,15].

Current licensed mucosal vaccine formulations

Human use

The majority of currently licensed human mucosal vaccines comprise attenuated strains of pathogenic bacteria or viruses that retain their immunogenicity during transit through the upper GI tract and can target inductive immune sites in the small and large intestine or upper respiratory tract (Table 1). The oral polio vaccine, OPV, is the most successful mucosal vaccine to date [16]. A significant drawback to using attenuated pathogen-based vaccines is the risk of reactogenicity and reversion to a virulent pathogen following vaccination, usually in immunocompromised infants, elderly people or in individuals with a specific immunodeficiency. Although the use of OPV has decreased the number of polio cases by more than 99% since 1988, there are still disease outbreaks of vaccine-associated paralytic polio (VAPP) that arise due to small genetic changes occurring during OPV replication in humans [17,18]. Another concern for live attenuated vaccines is the possibility of retrograde transport to the brain after nasal or intranasal vaccination, as happened with a replication-defective adenovirus vector carrying three proteins from human immunodeficiency virus type

Table 1. Licensed mucosal vaccines

Target	Pathogen	Trade name	Delivery route (form)	Formulation (±adjuvant)
Human	<i>Vibrio cholerae</i>	Dukoral [†]	Oral (liquid)	Inactivated (recombinant cholera toxin subunit B)
		ShanChol [†] , Euvichol [†]	Oral (liquid)	Inactivated
		Vaxchora [†]	Oral (liquid)	Live attenuated
	Influenza type A and B virus	FluMist™	Intranasal (spray)	Live attenuated
			Oral (liquid)	Live attenuated
	Poliovirus	Biopolio™ B1/3, and other oral polio vaccines – OPVs	Oral (liquid)	Live attenuated
	Rotavirus	Rotarix [†] and RotaTeq [†]	Oral (liquid)	Live attenuated
	<i>Salmonella typhimurium</i>	Typhi Vivotif [†]	Oral (capsules)	Live attenuated
Adenovirus	Not trade name Approved for military	Oral (tablets)	Live attenuated	
Animal	Rabies virus	RABORAL-V-RG	Oral (bait)	Recombinant (Vaccinia virus vector)
	Bovine parainfluenza 3 bovine respiratory syncytial virus	Rispoval	Intranasal (spray)	Live attenuated
	<i>Bordetella bronchiseptica</i>	Nobivac [†]	Intranasal (drops)	Live
	Canine parainfluenza virus			
	Newcastle disease virus	Avinev NeO™	Oral, ocular or nasal (spray, drinking water or drops)	Live attenuated

1 that was found in the central nervous system of mice after intranasal delivery, which may have reached the brain via olfactory neurones [19].

Apart from live attenuated vaccines, three World Health Organization (WHO) prequalified inactivated oral vaccines are in use for cholera (Dukoral[®], Shanchol[™] and Euvichol[®]), which have been shown to provide high levels (60–95%) of long-lived (>2 years) protection in support of the concept that non-living vaccines can be effective for mucosal delivery and vaccination [20]. Although inactivated vaccines are, in general, safe, the process of inactivation (heat and/or formalin treatment) can reduce their immunogenicity and require the addition of adjuvants such as recombinant cholera toxin subunit B, which is included in the Dukoral vaccine [20].

Subunit vaccines comprising synthetic recombinant peptides and proteins, toxoids, DNA or mRNA offer significant safety advantages over attenuated and inactivated vaccines. They are inert and non-infectious, although they can suffer from weak immunogenicity and a requirement for adjuvants. To date, subunit vaccine formulations have failed to confer long-lived protective mucosal immunity in humans [21]. The weak immunogenicity of inert molecules and protein subunit antigens after delivery to mucosal sites is due in large part to their inefficient uptake by the mucosal epithelium and delivery to the delivery to the mucosa-associated lymphoid tissue (MALT) [22,23]. This reflects the significant physical, biochemical and microbial obstacles orally and nasally administered vaccines must overcome in the GI and respiratory tracts in order to access and activate mucosal immune cells. During transit through the GI tract, vaccine antigens are diluted and can be retained or trapped in mucosal secretions and by mucus and be subsequently degraded by non-specific host or microbial enzymes prior to reaching the mucosal immune system. The acidic environment of the upper GI-tract also impacts on the stability and integrity of oral vaccines [24]. In the respiratory tract, physical discharge due to high mucociliary clearance rates, or peristalsis action in the GI tract, also impact upon vaccine integrity and retention time [25].

Veterinary use

Mucosal vaccines have been more successful in the veterinary field, with spray and drinking water vaccines routinely used for mass vaccination in poultry farming. Recent introduction of edible gel-bead-based vaccine systems offer a more stable mucosal delivery, protecting live vaccines against environmental inactivation to improve bioavailability. Use of gel-beads to deliver *Eimeria* spp. oocysts to day-old chicks offers greater uptake of oocysts than water spray containing *Eimeria* spp. oocysts, and significantly higher weight gain post-challenge infection [26]. The livestock-wildlife interface consistently poses difficulties in vaccination programmes for animals. Mucosal delivery of vaccines

through baiting allows free-ranging animals to voluntarily uptake vaccines, in order to break down interspecies transmission of infectious disease between wild and domesticated animals. Arguably, the most successful bait vaccine is RABORAL V-RG[®] which, following distribution into wildlife habitats, has aided eradication of wildlife rabies from Belgium, France and Luxembourg [27]. Wildlife bait vaccination has also helped to control other pathogens, including classical swine fever in wild boar (*Sus scrofa*) in Europe [28] and plague in prairie dogs (*Cynomys* spp.) in the United States [29,30]. Currently, licensed vaccines for parenteral application could be administered orally where it may not be possible, or feasible, to trap an animal to inject them. *Mycobacterium bovis* is a causative agent of tuberculosis (TB), and remains one the most difficult diseases of livestock to control, due largely to the prevalence of a wildlife reservoir. Bacillus Calmette–Guérin (BCG) vaccines were developed to protect cattle against bovine tuberculosis with subsequent experimental and field studies, showing that they may be efficacious in the control of *M. bovis* in wild animals after mucosal administration. White-tailed deer (*Odocoileus virginianus*) vaccinated with BCG Danish strain 1331 by oral bait or oral liquid had fewer tuberculosis lesions 5 months post-*M. bovis* challenge than control deer [31]. Badger BCG is a licensed injectable vaccine for European badgers (*Meles meles*) against TB; however, capturing animals for injection is labour-intensive and stressful. Oral administration of BCG has been shown to reduce *M. bovis* lesions in badgers [32], with 75% of captured badgers in a further study testing positive for BCG vaccine markers where the vaccine was administered in bait [33]. Dispersing mucosal vaccines in baits into high-risk areas could help to reduce endemic TB in wildlife reservoirs, reducing the risks of devastating TB outbreaks in livestock. Despite promise from field trials, there is still a lack of vaccines licensed for distribution into wildlife. A major drawback is the risk of non-target species consuming the bait; however, with further research into the use of subunit or inactivated mucosal vaccines, instead of live, this threat may be withdrawn.

The need for human mucosal vaccines

Despite many trials, there are no licensed vaccines for many human mucosal-transmitted pathogens (Table 2), or the currently available vaccines generate incomplete protection.

Improving mucosal vaccines

New technologies are being developed with the aim of protecting and preserving antigen structural integrity, as well as increasing bioavailability and induction of local

Table 2. Infectious diseases in need of mucosal vaccines

Pathogen	Mortality/annum	Morbidity/annum	Ref.
Respiratory tract			
Seasonal influenza	470 000	4 million	[34]
RSV-ALRI	128 000	33.8 million	[35]
<i>Streptococcus pneumoniae</i>	1.6 million		[36]
<i>Mycobacterium tuberculosis</i>	1.6 million	10 million	[37]
Gastrointestinal tract			
Rotavirus	215 000		[38]
<i>Helicobacter pylori</i>	14 500		[39]
Enterotoxigenic <i>Escherichia coli</i> (ETEC)	400 000		[40,41]
<i>Salmonella</i>	32 000 (Africa)	1.2 million (USA)	[42,43]
<i>Shigella</i>	700 000	80 million	[44]
<i>Clostridium (difficile/perfringens)</i>	14 000	500 000	[45]
Urogenital tract			
Syphilis	205 000		[46]
Gonorrhoea		78 million	[47]
Herpes simplex virus 2		417 million	[48]
Human papillomavirus (HPV)	270 000		[49]
Hepatitis B	887 000		[50]
Hepatitis C	399 000	71 million	[51]
HIV	940 000	36.9 million	[52]

and systemic neutralizing immune responses (Table 3). All these delivery vehicles can be modified or complemented with immunostimulatory molecules or coating agents [e.g. polyethylene glycol (PEG), chitosan] to change their charge, adhesive properties, shape, size and/or pH to improve their characteristics, interactions with host cells and targeting sites of inductive immune responses. The incorporation of PEG into polyactide (PLA) nanoparticle vaccine formulations has been shown to be effective for the oral delivery of hepatitis B surface antigens in mice [53]. Chitosan is a biodegradable, biocompatible, muco-adhesive, non-toxic polymer that has been used in a similar way to protect *Escherichia coli* O157:H7 vaccine formulations during oral delivery [54].

The inclusion of alginate, polyvinyl alcohol, hyaluronan and cellulose to micro- and nanoparticle-based vaccines increases their viscosity and augments the retention time at mucosal surfaces promoting antigen uptake. Molecules that target the carrier or vaccine antigen directly to surface receptors on M cells or antigen-presenting cells [e.g. Toll-like receptors (TLRs)] have also been used [76]. The use of adjuvants includes aluminium hydroxide to facilitate antibody and T helper type 2 (Th2) CD4 T cell responses, or *Vibrio cholerae* toxin (CT) and heat-labile enterotoxin from *E. coli* to non-specifically boost cellular and humoral immune responses [77,78]. To date, recombinant cholera toxin subunit B (rCTB) is the only adjuvant accepted for inclusion in licensed mucosal vaccines (i.e. Dukoral[®] vaccine). rCTB stimulates the production of both anti-bacterial and anti-toxin antibodies without any side effects [79]. Genetically modified enterotoxins are being developed to

reduce toxicity without adversely affecting their adjuvanticity.

Plants can be used as bioreactors to produce large quantities of vaccine that are then purified from plant extracts or can be consumed directly as an edible plant vaccine. The plants of choice are rice, lettuce or maize, with an edible rice-based cholera vaccine containing rCTB (MucoRice-CTB) currently in Phase I clinical trials [80]. An experimental lettuce-based hepatitis B virus vaccine has been tested in mice and shown to be effective at inducing neutralizing antibodies after oral administration [81]. Algae are a particularly cost-effective bioreactor option for producing large quantities of recombinant vaccines, and due to their high structural integrity and resilience of their cell walls have the potential to be used intact as vaccine delivery vehicles [74]. *Chlamydomonas reinhardtii* has been used in experimental *Staphylococcus aureus* vaccine formulations [82] and *Schizochytrium* sp. have been used to develop novel zika virus vaccines [83]; in both cases, these algae-based vaccines have been shown to be effective at eliciting both mucosal and systemic humoral immune responses.

Immunostimulatory complex (ISCOM) technology has been incorporated into commercial veterinary vaccines such as Equip F[®] vaccine against equine influenza for parenteral delivery, although Ghazi *et al.* have demonstrated protection in mice immunized orally with influenza virus subunit vaccines that incorporate ISCOM [84]. Liposomes and emulsions carriers have been used in experimental vaccines for respiratory virus infections with incorporation of the soybean oil-based emulsion W805EC into influenza

Table 3. Novel mucosal vaccine delivery systems

Delivery system	Structure	Advantages	Limitations	Ref.
Liposomes	Spherical phospholipid bilayer entrapping an aqueous solution core	<ul style="list-style-type: none"> Ease of incorporating distinct types of antigens Adaptable physicochemical properties Lipidic compounds with adjuvant properties 	<ul style="list-style-type: none"> Relatively low intrinsic stability for storage and after administration Potent toxicity of cationic lipids (dose-dependent) 	[55]
Archaeosomes	Liposomes composed of Archaea-derived polar lipids	<ul style="list-style-type: none"> Stable formulations Improved immunogenicity compared with liposomes 	<ul style="list-style-type: none"> Preparation and purification of Archaea lipids Need optimization of production and formulation 	[56]
Bilosomes	Bile salt stabilized vesicles	<ul style="list-style-type: none"> Stable in gastric environment High stability 	<ul style="list-style-type: none"> Relatively low antigen dose 	[57]
ISCOM, ISCOMATRIX	Cage-like structure comprised of cholesterol, phospholipids and saponin	<ul style="list-style-type: none"> Composition, size and surface structure like virus Self-adjuvanticity due to saponin 	<ul style="list-style-type: none"> Inclusion of antigens into the ISCOM can be difficult 	[58]
Bacterial outer membrane vesicles (OMV)	OMVs from Gram-negative pathogens containing microbe-associated molecular pattern (MAMPs) and membrane proteins	<ul style="list-style-type: none"> In-built adjuvanticity High stability over a wide range of temperatures and pH Safe use in children and adults and effective in controlling disease outbreaks 	<ul style="list-style-type: none"> Chemical detoxification required – reduced adjuvanticity Variable efficacy Strain-specific – limited heterotypic strain protection 	[59,60]
Virus-like particles (VLP)	Natural virus without carrying genetic material	<ul style="list-style-type: none"> Highly immunogenic without addition of adjuvant Antigens can be chemically conjugated or genetically inserted 	<ul style="list-style-type: none"> Purification can be a challenge May have poor quality and consistency Contamination by host materials 	[61,62]
Gene gun (DNA vaccination)	DNA-coated colloidal gold particles	<ul style="list-style-type: none"> Fast and simple Efficient DNA transduction Requires small amounts of DNA (0.1 mg/dose) Can be used to deliver multiple DNAs 	<ul style="list-style-type: none"> Costly device and reagents Limited to exposed tissues Depth of penetration <i>versus</i> tissue damage Preferentially induces T helper type 2 response Multiple factors influence efficacy 	[63]
Emulsions Water-in-oil/oil-in-water	Nanosized droplets	<ul style="list-style-type: none"> Slow release of immunogen Ease of manufacture Self-adjuvanticity 	<ul style="list-style-type: none"> Reactogenicity Limited stability after administration Low preservation of antigen structure 	[64,65]
Synthetic polymer nanoparticles (e.g. PLA/PLGA)	Poly lactide (PLA) or poly lactic-co-glycolic acid (PLGA) based nano- and micro particles	<ul style="list-style-type: none"> Controlled release of antigens Biodegradable and biocompatible biopolymer 	<ul style="list-style-type: none"> Sensitivity to harsh gastric environment, low loading capacity 	[66,67]
Natural polymer nanoparticles (e.g. chitosan)	FDA-approved agents Chitosan based nano- and microparticles	<ul style="list-style-type: none"> Biocompatible, biodegradable, mucoadhesive and immunostimulating 	<ul style="list-style-type: none"> Irregular distribution, low physical stability 	[68]
Hydrogel (e.g. cCHP nanogel)	Cationic cholesterol-bearing pullulan nanogel, self-assembles with water due to their amphiphilic polysaccharides	<ul style="list-style-type: none"> Ability to function as an artificial chaperone Prolonged binding to nasal epithelium 	<ul style="list-style-type: none"> Optimization of biodistribution and degradation mechanism Component toxicity 	[69]

Table 3. (Continued)

Delivery system	Structure	Advantages	Limitations	Ref.
Lactic acid bacteria (LAB)	Live recombinant LAB expressing antigens Generally recognized as safe (GRAS)	<ul style="list-style-type: none"> • Easy and safe production and storage • Survives gastric environment • Self-adjuvantivity 	<ul style="list-style-type: none"> • Safety concerns using genetically modified organisms 	[70]
Chemically processed pollen grains (PGs)	Resistant bilayer pollen grain shell	<ul style="list-style-type: none"> • Self-adjuvanted • Protected from harsh environment 	<ul style="list-style-type: none"> • Chemical treatment methods required to eliminate allergens from pollen grain 	[71,72]
Terrestrial plants and algae	Plant or algae cells with an antigen created by gene modification	<ul style="list-style-type: none"> • Highly resilient cell wall • Easy manufacturing process and scale-up • Suitable for mass vaccination • No cold chain requirement 	<ul style="list-style-type: none"> • Use of transgenic plants and regulatory body approvals 	[73–75]

Modified from Corthesy *et al.* [54].

virus and inactivated respiratory syncytial virus (RSV) vaccines, both of which are effective at eliciting protective systemic and mucosal antibody immune responses, and RSV vaccine also induces cellular immunity after intranasal administration [85,86]. Similarly, pneumococcal surface protein A (PspA)-based subunit vaccines incorporating a cCHP-based nanogel has been shown to induce both mucosal and systemic neutralizing antibodies in cynomolgus macaques after nasal delivery [87].

Virus-like particles (VLP) are an attractive option as a vaccine delivery vehicle due to their useful properties, such as the ability to induce adaptive immune response and to induce long-term expression of non-self-proteins [88,89]. VLPs from adeno-associated viruses (AAV) have been used to develop novel influenza virus vaccines encoding camelid-derived anti-influenza antibodies transgenes that when administered intranasally protected mice against lethal influenza A and B challenge [89,90]. Other preclinical studies using AAV as a carrier include norovirus vaccine formulations containing viral protein and RNA, that have shown promise in a Phase I clinical trial [91], and a chimpanzee-derived AAV expressing hepatitis C virus antigens that is currently in Phase II clinical trials [92,93].

Gene gun bombardment is a biolistic system for mucosal DNA vaccination. This needle-free technology is based on propelling DNA-coated colloidal gold microprojectiles at exposed tissue surfaces (e.g. skin, vulva and mouth) and penetrating the cytosol and cell nucleus of cells within deeper layers of the tissue. [94] Epidermal DNA vaccines delivered via a gene gun have been shown to elicit both humoral and cell-mediated mucosal immune responses in experimental animals and cattle [63,95,96]. To improve the potency of immune responses gene to gun gene immunizations, DNA can be combined with adjuvants such as recombinant protein antigens and plasmids encoding cytokines [94,97]. However, gene

gun-mediated delivery has limited or no control over where and how effective DNA transduction is in host cells and is generally ineffective at inducing immune responses of sufficient potency to provide effective and long-lived protection.

The use of genetically modified probiotic strains of bacteria to deliver vaccine antigens has been explored for human papilloma virus (HPV) vaccines. Although a commercial HPV vaccine is available, it does not confer protection to all HPV-related cancers [49]. Generally recognized as safe (GRAS) strains of *Lactococcus lacti* engineered to express the HPV-16 E6 oncoprotein generated humoral and cellular immune response in mice after oral administration, as well being shown to have an inhibitory effect on tumour growth [98]. There are, however, biosafety and environmental contamination concerns in using genetically modified bacteria [99].

A safer alternative to using viable bacteria as vaccine delivery vehicles are non-viable nanometer-sized lipid-containing microvesicles (outer membrane vesicles; OMVs) that are naturally produced and secreted by most Gram-negative bacteria [59]. Formulations of *Neisseria meningitidis* OMVs (VA-MENGOC-BC, MenBvac, MeNZB and Bexero) have been successfully used to vaccinate both adults and children and to control outbreaks of meningococcal B infection in several countries [100,101]. OMVs from other Gram-negative pathogens are also promising vaccine candidates, including those from *Salmonella* [102], *Shigella flexneri* [103] and *V. cholerae* [104]. However, their potential for unintended toxicity due to associated toxins is a safety concern and limits their widespread use, although chemical detoxification can overcome this, but at the loss of immunogenicity and adjuvantivity [105]. In principle, these limitations could be overcome by bioengineering the parental bacterium to improve their OMV drug-delivery capability [60]. Alternatively, non-pathogenic

commensal bacteria could be used as a source of OMVs to reduce toxicity and improve safety. We are developing an OMV-based drug and biologicals delivery technology platform based on the use of OMVs produced by strains of human commensal *Bacteroides* engineered to express in their OMVs bacterial or viral vaccine antigens or human therapeutic proteins for delivery to the respiratory and GI tracts.

In summary, while mucosal vaccines represent the ideal means of protecting against the majority of infections, there are very few licensed vaccines for either humans or animals. A raft of new technologies and innovations in vaccine antigen encapsulation and delivery are being developed to overcome the obstacles of protecting and preserving antigen structural integrity as well as increasing bioavailability and induction of local and systemic neutralizing immune responses during transit to mucosal inductive immune sites, particularly in the GI tract.

Acknowledgements

This work was supported in part by the UK Biotechnology and Biological Sciences Research Council (BBSRC) under grant numbers BB/J004529/1, BB/R012490/1 and BBS/E/F000PR10355 (SRC); a Newton Institutional Links award Ref: 332228521 (JPS); a BBSRC DTP PhD studentship Ref: BB/M011216/1 (AM-C) and a University of Liverpool postgraduate studentship (EB).

Disclosures

The authors report no conflicts of interest.

References

- 1 Vaccines and vaccination. National Office of Animal Health Available at: <https://www.noah.co.uk/briefingdocument/antibiotic-resistance-2/> (accessed 26 November 2018).
- 2 Grace DMF, Ochungo P, Kruska R *et al.* Mapping of poverty and likely zoonoses hotspots. Zoonoses Project 4. Nairobi, Kenya: International Livestock Research Institute (ILRI), 2012.
- 3 Hofstetter DF, Bruscia V, Sakala IG. Optimizing vaccine development. *Cell Microbiol* 2011; **13**:934–42.
- 4 Azizi A, Kumar A, Diaz-Mitoma F, Mestecky J. Enhancing oral vaccine potency by targeting intestinal M cells. *PLOS Pathog* 2010; **6**:e1001147.
- 5 Kantele A, Häkkinen M, Moldoveanu Z *et al.* Differences in immune responses induced by oral and rectal immunizations with *Salmonella typhi* Ty21a: evidence for compartmentalization within the common mucosal immune system in humans. *Infect Immun* 1998; **66**:5630–5.
- 6 Czerkinsky C, Holmgren J. Mucosal delivery routes for optimal immunization: targeting immunity to the right tissues. In: Kozlowski PA, ed. *Mucosal vaccines: modern concepts, strategies, and challenges*. Berlin Heidelberg: Springer, 2012:1–18.
- 7 Fujikuyama Y, Tokuhara D, Kataoka K *et al.* Novel vaccine development strategies for inducing mucosal immunity. *Expert Rev Vaccines* 2012; **11**:367–79.
- 8 Saroja C, Lakshmi P, Bhaskaran S. Recent trends in vaccine delivery systems: a review. *Int J Pharm Invest* 2011; **1**:64–74.
- 9 Plotkin SA. Correlates of protection induced by vaccination. *Clin Vaccine Immunol* 2010; **17**:1055–65.
- 10 McDole JR, Wheeler LW, McDonald KG *et al.* Goblet cells deliver luminal antigen to CD103+ dendritic cells in the small intestine. *Nature* 2012; **483**:345–9.
- 11 Howe SE, Konjufca VH. Protein-coated nanoparticles are internalized by the epithelial cells of the female reproductive tract and induce systemic and mucosal immune responses. *PLOS ONE* 2014; **9**:e114601.
- 12 Ogra PL, Faden H, Welliver RC. Vaccination strategies for mucosal immune responses. *Clin Microbiol Rev* 2001; **14**:430–45.
- 13 Xiang SD, Scholzen A, Minigo G *et al.* Pathogen recognition and development of particulate vaccines: does size matter? *Methods* 2006; **40**:1–9.
- 14 Thomas C, Gupta V, Ahsan F. Particle size influences the immune response produced by hepatitis B vaccine formulated in inhalable particles. *Pharm Res* 2010; **27**:905–19.
- 15 Carvalho TC, Peters JJ, Williams RO. Influence of particle size on regional lung deposition – what evidence is there? *Int J Pharm* 2011; **406**:1–10.
- 16 Kim S-H, Jang Y-S. Antigen targeting to M cells for enhancing the efficacy of mucosal vaccines. *Exp Mol Med* 2014; **46**:e85.
- 17 World Health Organization. Polio vaccines: WHO position paper, January 2014. *Wkly Epidemiol Rec* 2014; **89**:73–92.
- 18 Jorba J, Diop OM, Iber J *et al.* Update on vaccine-derived polioviruses – worldwide, January 2017–June 2018. *Morb Mortal Wkly Rep* 2018; **67**:1189–94.
- 19 Lemiale F, Kong WP, Akyurek LM *et al.* Enhanced mucosal immunoglobulin A response of intranasal adenoviral vector human immunodeficiency virus vaccine and localization in the central nervous system. *J Virol* 2003; **77**:10078–87.
- 20 World Health Organization (L'Organisation Mondiale de la Santé). Cholera vaccines: WHO position paper – August 2017. *Wkly Epidemiol Rec* 2017; **92**:477–98.
- 21 Mitragotri S. Immunization without needles. *Nat Rev Immunol* 2005; **5**:905–16.
- 22 Lycke N. Recent progress in mucosal vaccine development: potential and limitations. *Nat Rev Immunol* 2012; **12**:592–605.
- 23 Kiyono H, Izuhara K. New trends in mucosal immunology and allergy. *Allergol Int* 2019; **68**:1–3.
- 24 Vela Ramirez JE, Sharpe LA, Peppas NA. Current state and challenges in developing oral vaccines. *Adv Drug Deliv Rev* 2017; **114**:116–31.

- 25 Suzuki H, Nagatake T, Nasu A *et al.* Impaired airway mucociliary function reduces antigen-specific IgA immune response to immunization with a claudin-4-targeting nasal vaccine in mice. *Sci Rep* 2018; **8**:2904.
- 26 Jenkins MC, Parker C, Klopp S, O'Brien C, Miska K, Fetterer R. Gel-bead delivery of *Eimeria* oocysts protects chickens against coccidiosis. *Avian Dis* 2012; **56**:306–9.
- 27 Maki J, Guiot AL, Aubert M *et al.* Oral vaccination of wildlife using a vaccinia–rabies–glycoprotein recombinant virus vaccine (RABORAL V-RG((R))): a global review. *Vet Res* 2017; **48**:57.
- 28 Rossi S, Pol F, Forot B *et al.* Preventive vaccination contributes to control classical swine fever in wild boar (*Sus scrofa* sp.). *Vet Microbiol* 2010; **142**:99–107.
- 29 Rocke TE, Tripp DW, Russell RE *et al.* Sylvatic plague vaccine partially protects prairie dogs (*Cynomys* spp.) in field trials. *EcoHealth* 2017; **14**:438–50.
- 30 Creekmore TE, Rocke TE, Hurley J. A baiting system for delivery of an oral plague vaccine to black-tailed prairie dogs. *J Wildl Dis* 2002; **38**:32–9.
- 31 Nol P, Palmer MV, Waters WR *et al.* Efficacy of oral and parenteral routes of *Mycobacterium bovis* bacille Calmette–Guérin vaccination against experimental bovine tuberculosis in white-tailed deer (*Odocoileus virginianus*): a feasibility study. *J Wildl Dis* 2008; **44**:247–59.
- 32 Gormley E, Ni Bhuachalla D, O'Keeffe J *et al.* Oral vaccination of free-living badgers (*Meles meles*) with bacille Calmette–Guérin (BCG) vaccine confers protection against tuberculosis. *PLOS ONE* 2017; **12**:e0168851.
- 33 Palphramand K, Delahay R, Robertson A *et al.* Field evaluation of candidate baits for oral delivery of BCG vaccine to European badgers, *Meles meles*. *Vaccine* 2017; **35**:4402–7.
- 34 Influenza (seasonal) World Health Organization. 2018. Available at: [http://www.who.int/news-room/fact-sheets/detail/influenza-\(seasonal\)](http://www.who.int/news-room/fact-sheets/detail/influenza-(seasonal)) (accessed 7 November 2018).
- 35 Stein RT, Bont LJ, Zar H *et al.* Respiratory syncytial virus hospitalization and mortality: systematic review and meta-analysis. *Pediatr Pulmonol* 2017; **52**:556–69.
- 36 World Health Organization. Pneumococcal disease. Available at: <http://www.who.int/ith/diseases/pneumococcal/en/> (accessed 8 October 2018).
- 37 World Health Organization. Tuberculosis. Available at: <http://www.who.int/news-room/fact-sheets/detail/tuberculosis> (accessed 8 November 2018).
- 38 Tate JE, Burton AH, Boschi-Pinto C, Parashar UD. Global, Regional, and National Estimates of Rotavirus Mortality in Children <5 Years of Age, 2000–2013. *Clin Infect Dis* 2016; **62**:S96–S105.
- 39 Kathleen R, Stratton JSD, Lawrence RS. Appendix 7. *Helicobacter pylori*. Vaccines for the 21st century: a tool for decisionmaking. Washington DC: National Academies Press, 2000.
- 40 World Health Organization. Weekly Epidemiological Record. No. 11. Geneva: World Health Organization, 2006:81, 97–04.
- 41 World Health Organization. Future directions for research on enterotoxigenic *Escherichia coli* vaccines for developing countries. Geneva: World Health Organization, 2006.
- 42 Centers for Disease Control and Prevention. Salmonella. 2018. Available at: <https://www.cdc.gov/salmonella/> (accessed 8 November 2018).
- 43 World Health Organization. WHO's first ever global estimates of foodborne diseases find children under 5 account for almost one third of deaths. Geneva: World Health Organization, 2015.
- 44 World Health Organization. Guidelines for the control of shigellosis, including epidemics due to *Shigella dysenteriae* type 1. Geneva: World Health Organization, 2005.
- 45 Lessa FC, Mu Y, Bamberg WM *et al.* Burden of *Clostridium difficile* infection in the United States. *N Engl J Med* 2015; **372**:825–34.
- 46 World Health Organization. Report on global sexually transmitted infection surveillance 2015. Geneva: World Health Organization, 2015.
- 47 World Health Organization. WHO guidelines for the treatment of *Neisseria gonorrhoeae*. Geneva: World Health Organization, 2016.
- 48 World Health Organization. Innovative approach sheds light on prevalence of STIs and bacterial vaginosis among women in sub-Saharan Africa. Geneva: World Health Organization, 2018.
- 49 World Health Organization. Human papillomavirus (HPV) and cervical cancer. Geneva: World Health Organization. 2018. Available at: [http://www.who.int/news-room/fact-sheets/detail/human-papillomavirus-\(hpv\)-and-cervical-cancer](http://www.who.int/news-room/fact-sheets/detail/human-papillomavirus-(hpv)-and-cervical-cancer) (accessed 9 November 2018).
- 50 World Health Organization. Hepatitis B. Available at: <http://www.who.int/news-room/fact-sheets/detail/hepatitis-b> (accessed 9 November 2018).
- 51 World Health Organization. Hepatitis C. Available at: <http://www.who.int/news-room/fact-sheets/detail/hepatitis-c> (accessed 9 November 2018).
- 52 World Health Organization. HIV/AIDS. Available at: <http://www.who.int/en/news-room/fact-sheets/detail/hiv-aids> (accessed 9 November 2018).
- 53 Jain AK, Goyal AK, Mishra N, Vaidya B, Mangal S, Vyas SP. PEG–PLA–PEG block copolymeric nanoparticles for oral immunization against hepatitis B. *Int J Pharm* 2010; **387**:253–62.
- 54 Doavi T, Mousavi SL, Kamali M, Amani J, Ramandi MF. Chitosan-based intranasal vaccine against *Escherichia coli* O157:H7. *Iranian Biomed J* 2016; **20**:97–108.
- 55 Corthesy B, Bioley G. Lipid-based particles: versatile delivery systems for mucosal vaccination against infection. *Front Immunol* 2018; **9**:431.
- 56 Jacobsen A-C, Jensen SM, Fricker G, Brandl M, Treusch AH. Archaeal lipids in oral delivery of therapeutic peptides. *Eur J Pharm Sci* 2017; **108**:101–10.
- 57 Shukla A, Mishra V, Kesharwani P. Bilosomes in the context of oral immunization: development, challenges and opportunities. *Drug Discov Today* 2016; **21**:888–99.

- 58 Sun H-X, Xie Y, Ye Y-P. ISCOMs and ISCOMATRIX™. *Vaccine* 2009; **27**:4388–401.
- 59 Jan AT. Outer membrane vesicles (OMVs) of Gram-negative bacteria: a perspective update. *Front Microbiol* 2017; **8**:1053.
- 60 Gerritzen MJH, Martens DE, Wijffels RH, van der Pol L, Stork M. Bioengineering bacterial outer membrane vesicles as vaccine platform. *Biotech Adv* 2017; **35**:565–74.
- 61 Minkner R, Park EY. Purification of virus-like particles (VLPs) expressed in the silkworm *Bombyx mori*. *Biotech Lett* 2018; **40**:659–66.
- 62 Steppert P, Burgstaller D, Klausberger M *et al.* Purification of HIV-1 gag virus-like particles and separation of other extracellular particles. *J Chromatogr A* 2016; **1455**:93–101.
- 63 Raska M, Turanek J. Chapter 67: DNA vaccines for the induction of immune responses in mucosal tissues. In: Mestecky J, Strober W, Russell MW, Kelsall BL, Cheroutre H, Lambrecht BN, eds. *Mucosal immunology*, 4th edn. Boston, USA: Academic Press, 2015:1307–35.
- 64 Petrovsky N. Comparative safety of vaccine adjuvants: a summary of current evidence and future needs. *Drug Saf* 2015; **38**:1059–74.
- 65 Huang C-H, Huang C-Y, Cheng C-P *et al.* Degradable emulsion as vaccine adjuvant reshapes antigen-specific immunity and thereby ameliorates vaccine efficacy. *Sci Rep* 2016; **6**:36732.
- 66 Zhang L, Yang W, Hu C, Wang Q, Wu Y. Properties and applications of nanoparticle/microparticle conveyors with adjuvant characteristics suitable for oral vaccination. *Int J Nanomed* 2018; **13**:2973–87.
- 67 Silva AL, Soema PC, Slütter B, Ossendorp F, Jiskoot W. PLGA particulate delivery systems for subunit vaccines: linking particle properties to immunogenicity. *Hum Vacc Immunother* 2016; **12**:1056–69.
- 68 Xing L, Fan Y-T, Zhou T-J *et al.* Chemical modification of chitosan for efficient vaccine delivery. *Molecules (Basel)* 2018; **23**:229.
- 69 Azegami T, Yuki Y, Nakahashi R, Itoh H, Kiyono H. Nanogel-based nasal vaccines for infectious and lifestyle-related diseases. *Mol Immunol* 2018; **98**:19–24.
- 70 Szatraj K, Szczepankowska AK, Chmielewska-Jeznach M. Lactic acid bacteria – promising vaccine vectors: possibilities, limitations, doubts. *J Appl Microbiol* 2017; **123**:325–39.
- 71 Uddin MJ, Gill HS. Ragweed pollen as an oral vaccine delivery system: mechanistic insights. *J Control Release* 2017; **268**:416–26.
- 72 Uddin MJ, Gill HS. From allergen to oral vaccine carrier: a new face of ragweed pollen. *Int J Pharm* 2018; **545**:286–94.
- 73 Concha C, Cañas R, Macuer J *et al.* Disease prevention: an opportunity to expand edible plant-based Vaccines? *Vaccines (Basel)* 2017; **5**:14.
- 74 Specht EA, Mayfield SP. Algae-based oral recombinant vaccines. *Front Microbiol* 2014; **5**:60.
- 75 Ramos-Vega A, Rosales-Mendoza S, Bañuelos-Hernández B, Angulo C. Prospects on the use of *Schizochytrium* sp. to develop oral vaccines. *Front Microbiol* 2018; **9**:2506.
- 76 Kim SH, Jang YS. The development of mucosal vaccines for both mucosal and systemic immune induction and the roles played by adjuvants. *Clin Exp Vaccine Res* 2017; **6**:15–21.
- 77 Norton EB, Lawson LB, Freytag LC, Clements JD. Characterization of a mutant *Escherichia coli* heat-labile toxin, LT(R192G/L211A), as a safe and effective oral adjuvant. *Clin Vaccine Immunol* 2011; **18**:546–51.
- 78 Lebens M, Terronni M, Karlsson SL *et al.* Construction and preclinical evaluation of mmCT, a novel mutant cholera toxin adjuvant that can be efficiently produced in genetically manipulated *Vibrio cholerae*. *Vaccine* 2016; **34**:2121–8.
- 79 European Medicines Agency. Dukoral Scientific Discussion. 2005. Available at: <https://www.ema.europa.eu/en/medicines/human/EPAR/dukoral> (accessed 14 November 2018).
- 80 Kurokawa S, Nakamura R, Mejima M *et al.* MucoRice–cholera toxin B-subunit, a rice-based oral cholera vaccine, down-regulates the expression of α -amylase/trypsin inhibitor-like protein family as major rice allergens. *J Proteome Res* 2013; **12**:3372–82.
- 81 Dobrica M-O, Lazar C, Paruch L *et al.* Oral administration of a chimeric hepatitis B Virus S/preS1 antigen produced in lettuce triggers infection neutralizing antibodies in mice. *Vaccine* 2018; **36**:5789–95.
- 82 Dreesen IAJ, Hamri GC-E, Fussenegger M. Heat-stable oral alga-based vaccine protects mice from *Staphylococcus aureus* infection. *J Biotechnol* 2010; **145**:273–80.
- 83 Márquez-Escobar VA, Bañuelos-Hernández B, Rosales-Mendoza S. Expression of a Zika virus antigen in microalgae: towards mucosal vaccine development. *J Biotechnol* 2018; **282**:86–91.
- 84 H. O. Ghazi CWP TLSaRJ. Comparative antibody responses and protection in mice immunised by oral or p ISCOMs. *J Med Microbiol* 1995; **42**:53–61.
- 85 Stanberry LR, Simon JK, Johnson C *et al.* Safety and immunogenicity of a novel nanoemulsion mucosal adjuvant W805EC combined with approved seasonal influenza antigens. *Vaccine* 2012; **30**:307–16.
- 86 O'Konek JJ, Makidon PE, Landers JJ *et al.* Intranasal nanoemulsion-based inactivated respiratory syncytial virus vaccines protect against viral challenge in cotton rats. *Hum Vaccines Immunother* 2015; **11**:2904–12.
- 87 Fukuyama Y, Yuki Y, Katakai Y *et al.* Nanogel-based pneumococcal surface protein A nasal vaccine induces microRNA-associated Th17 cell responses with neutralizing antibodies against *Streptococcus pneumoniae* in macaques. *Mucosal Immunol* 2015; **8**:1144–53.
- 88 Mohsen MO, Gomes AC, Vogel M, Bachmann MF. Interaction of viral capsid-derived virus-like particles (VLPs) with the innate immune system. *Vaccines (Basel)* 2018; **6**:37.
- 89 Nieto K, Salvetti A. AAV vectors vaccines against infectious diseases. *Front Immunol* 2014; **5**:5.
- 90 Laursen NS, Friesen RHE, Zhu X *et al.* Universal protection against influenza infection by a multidomain antibody to influenza hemagglutinin. *Science* 2018; **362**:598–602.

- 91 Kim L, Liebowitz D, Lin K *et al.* Safety and immunogenicity of an oral tablet norovirus vaccine, a phase I randomized, placebo-controlled trial. *JCI insight* 2018; **3**:e121077.
- 92 GlaxoSmithKline. Product pipeline. Available at: <https://www.gsk.com/en-gb/investors/product-pipeline/> (accessed 16 November 2018).
- 93 European Commission. Final Report Summary – PEACHI (Prevention of Hepatitis C Virus (HCV) and HIV-1 coinfections through induction of potent T cell responses using prime-boost viral vector vaccine regimens). Luxembourg: Publications Office of the European Union, 2018.
- 94 Fuller DH, Loudon P, Schmaljohn C. Preclinical and clinical progress of particle-mediated DNA vaccines for infectious diseases. *Methods* 2006; **40**:86–97.
- 95 Loudon PT, Yager EJ, Lynch DT *et al.* GM-CSF increases mucosal and systemic immunogenicity of an H1N1 influenza DNA vaccine administered into the epidermis of non-human primates. *PLOS ONE* 2010; **5**:e11021-e.
- 96 Fuller DH, Rajakumar PA, Wilson LA *et al.* Induction of mucosal protection against primary, heterologous simian immunodeficiency virus by a DNA vaccine. *J Virol* 2002; **76**:3309–17.
- 97 Trimble C, Lin CT, Hung CF *et al.* Comparison of the CD8+ T cell responses and antitumor effects generated by DNA vaccine administered through gene gun, biojector, and syringe. *Vaccine* 2003; **21**:4036–42.
- 98 Taghinezhad-S S, Mohseni AH, Keyvani H, Razavilar V. Protection against human papillomavirus type 16-induced tumors in C57BL/6 mice by mucosal vaccination with *Lactococcus lactis* NZ9000 expressing E6 oncoprotein. *Microb Pathog* 2019; **126**:149–56.
- 99 Wegmann U, Carvalho AL, Stocks M, Carding SR. Use of genetically modified bacteria for drug delivery in humans: revisiting the safety aspect. *Sci Rep* 2017; **7**:2294.
- 100 de Kleijn ED, de Groot R, Labadie J *et al.* Immunogenicity and safety of a hexavalent meningococcal outer-membrane-vesicle vaccine in children of 2–3 and 7–8 years of age. *Vaccine* 2000; **18**:1456–66.
- 101 Sandbu S, Feiring B, Oster P *et al.* Immunogenicity and safety of a combination of two serogroup B meningococcal outer membrane vesicle vaccines. *Clin Vaccine Immunol* 2007; **14**:1062–9.
- 102 Howlader DR, Koley H, Sinha R *et al.* Development of a novel *S. Typhi* and *Paratyphi A* outer membrane vesicles based bivalent vaccine against enteric fever. *PLOS ONE* 2018; **13**:e0203631-e.
- 103 Camacho AI, de Souza J, Sanchez-Gomez S, Pardo-Ros M, Irache JM, Gamazo C. Mucosal immunization with *Shigella flexneri* outer membrane vesicles induced protection in mice. *Vaccine* 2011; **29**:8222–9.
- 104 Schild S, Nelson EJ, Camilli A. Immunization with *Vibrio cholerae* outer membrane vesicles induces protective immunity in mice. *Infect Immun* 2008; **76**:4554–63.
- 105 van der Ley P, van den Dobbelen G. Next-generation outer membrane vesicle vaccines against *Neisseria meningitidis* based on nontoxic LPS mutants. *Hum Vaccin* 2011; **7**:886–90.

Use of bioengineered human commensal gut bacteria-derived microvesicles for mucosal plague vaccine delivery and immunization

A. L. Carvalho,* A. Miquel-Clopés,*
U. Wegmann,* E. Jones,*
R. Stentz,* A. Telatin,* N. J.
Walker,† W. A. Butcher,† P. J.
Brown,‡ S. Holmes,‡ M. J. Dennis,‡
E. D. Williamson ,†
S. G. P. Funnell ,‡ M. Stock§ and
S. R. Carding *¶

*Gut Microbes and Health Research Programme, Quadram Institute Bioscience, Norwich, †Defence Science and Technology Laboratory, Salisbury, ‡Public Health England, Porton, Porton, Salisbury, §Plant Biotechnology Ltd, Norwich, and ¶Norwich Medical School, University East Anglia, Norwich, UK

Accepted for publication 25 March 2019

Correspondence: S. R. Carding, Gut Microbes and Health Research Programme, Quadram Institute Bioscience, Norwich Medical School, University East Anglia, Norwich, UK.
Present address: Udo Wegmann, School of Chemistry, University East Anglia, Norwich, UK

Email: simon.carding@quadram.ac.uk

Introduction

Plague is caused by the Gram-negative bacterium, *Yersinia pestis*. It is an ancient disease, accounting for many deaths over hundreds of years, and still exists in parts of the world today. To protect against infection vaccines must be able to elicit both humoral immunity with neutralizing antibodies and cell-mediated immunity that is effective at primary mucosal sites of infection [1,2].

There are currently no licensed plague vaccines in the western world. In the past, heat-killed whole-cell vaccines

Summary

Plague caused by the Gram-negative bacterium, *Yersinia pestis*, is still endemic in parts of the world today. Protection against pneumonic plague is essential to prevent the development and spread of epidemics. Despite this, there are currently no licensed plague vaccines in the western world. Here we describe the means of delivering biologically active plague vaccine antigens directly to mucosal sites of plague infection using highly stable microvesicles (outer membrane vesicles; OMVs) that are naturally produced by the abundant and harmless human commensal gut bacterium *Bacteroides thetaiotaomicron* (Bt). Bt was engineered to express major plague protective antigens in its OMVs, specifically Fraction 1 (F1) in the outer membrane and LcrV (V antigen) in the lumen, for targeted delivery to the gastrointestinal (GI) and respiratory tracts in a non-human primate (NHP) host. Our key findings were that Bt OMVs stably expresses F1 and V plague antigens, particularly the V antigen, in the correct, immunogenic form. When delivered intranasally V-OMVs elicited substantive and specific immune and antibody responses, both in the serum [immunoglobulin (Ig)G] and in the upper and lower respiratory tract (IgA); this included the generation of serum antibodies able to kill plague bacteria. Our results also showed that Bt OMV-based vaccines had many desirable characteristics, including: biosafety and an absence of any adverse effects, pathology or gross alteration of resident microbial communities (microbiotas); high stability and thermo-tolerance; needle-free delivery; intrinsic adjuvanticity; the ability to stimulate both humoral and cell-mediated immune responses; and targeting of primary sites of plague infection.

Keywords: antibodies, gut bacteria, humoral immunity, mucosal vaccine, non-human primates, outer membrane vesicles, plague

(listed in the US Pharmacopeia) were available and provided protection against bubonic, but not pneumonic plague. However, due to unacceptable reactogenicity these vaccines were discontinued [3]. Live-attenuated vaccines have been used in countries of the former Soviet Union and China although, due to unacceptable reactogenicity and the risk of reversion to full virulence, they have not been licensed for use elsewhere, including the United States [4].

Fraction 1 (F1) and LcrV (virulence; V antigen) *Y. pestis* proteins encoded by the Fra/pMT1 and pCD1 plasmids, respectively [5], have been identified as the major protective antigens responsible for preventing

phagocytosis of *Y. pestis* (F1) and regulating type III secretion (V antigen) [6]. The present emphasis on developing F1- and V antigen-based vaccines is on recombinant protein-based subunit vaccines (rF1V) that incorporate chemical adjuvants. If a *Y. pestis* variant occurs with a mutation in the V antigen then these F1-V vaccines may not provide protection via immunity to the V component; however, immunity to the F1 component could still provide some limited protection [7,8]. In addition, the duration of protection against pneumonic infection provided by these as a subunit vaccine, in which the F1 and V antigens are presented as a fusion protein, is also uncertain [9]. Furthermore, the requirement for injection by needle to deliver these, and other current vaccines, is problematical. It is associated with: risks of cross-contamination; lack of patient compliance; the high cost of mass immunization; and a requirement for cold chain delivery and storage. Importantly, injected vaccines provide only partial or no protection at the primary mucosal site of plague infection [2,10]. Collectively, these issues constrain the use of existing plague vaccines, particularly in resource-poor low-income settings, and these restrictions are reflected in the World Health Organization (WHO)'s draft therapeutic product profile [11].

The use of nanoparticle-based platforms is a new approach to the development of more effective mucosal vaccines against pathogens such as those that cause the plague. These include virus-like particles, immune stimulating complexes, polymeric nanoparticles, inorganic nanoparticles, liposomes and emulsions – all of which have the potential to overcome the high production costs and safety concerns associated with live vaccines and the weak immunogenicity and adjuvanticity issues associated with subunit and recombinant protein-based vaccines [10]. These nanoscale carrier technologies enable conformationally correct antigens to be incorporated into highly stable nanoparticles. This allows for control over the spatial and temporal presentation of antigens to the immune system, leading to their targeted and sustained release. An overlooked component of platform nanoscale vaccines are bacterial microvesicles, and in particular, outer membrane vesicles (OMVs) of Gram-negative bacteria [12]. While many synthetic nanoparticles are capable of transferring heterologous antigens to antigen-presenting cells (APC), the ability to efficiently stimulate the immune system is often not inherent [13]. However, OMVs can combine high stability with antigen presentation and native adjuvanticity, making them an attractive vaccine platform for further development [14].

OMV production by vesiculation is a fundamental characteristic of Gram-negative bacteria that is unrelated to bacterial lysis or membrane instability that fulfils the key

requirements of a prokaryotic secretion process [15]. Nanoscale OMV proteoliposomes that contain immunogenic components derived from the bacterial outer membrane and periplasm are capable of targeting APCs [including dendritic cells (DC)] [16–18], leading to T and B cell immunity. Recent research on OMVs from pathogenic bacteria, including *Neisseria meningitidis* and *Vibrio cholerae*, supports the case for their being good vaccine candidates [19]; OMVs derived from *N. meningitidis* have been used safely and effectively as vaccine platforms for the control of serogroup B meningococcal (MenB) disease outbreaks [20,21]. OMV-based vaccines offer significant advantages over conventional vaccines because they are: non-replicating; provide needle-free delivery; target mucosal sites; have an established safety record; can elicit innate and antigen-specific adaptive immune responses; and possess self-adjuvant properties [i.e. microbe associated molecular pattern molecules (MAMPs) such as lipopolysaccharide (LPS)]. The current limitations of pathogen-derived, OMV vaccines are: the potential for unintended toxicity due to associated toxins; low expression levels of protective antigens; variable efficacy depending on source and formulation; the need for exogenous adjuvants; and only incomplete protection because of strain variation. In principle, these limitations could be overcome by using OMVs from non-pathogenic commensal bacteria, engineered to improve their application as vaccines. In support of this, it has recently been shown that OMVs produced by the common human commensal gut bacterium, *Bacteroides thetaiotaomicron* (Bt), are able to access and influence the host's intestinal epithelial and immune cells [22,23]. This identifies a means by which commensal gut bacteria can influence host cell physiology.

Here we describe the development of a novel vaccine delivery technology, based on engineering Bt, to express the V and F1 antigens of *Y. pestis* in their OMVs for targeted delivery to the gastrointestinal (GI) and respiratory tracts in a non-human primate (NHP) host. Our findings demonstrate that OMV-based plague vaccines are an effective means of eliciting both mucosal and systemic antibody responses and systemic cell-mediated responses. Delivery of OMV vaccines via the respiratory route was particularly effective at eliciting production of antigen-specific IgG antibodies that were protective in two independent surrogate assays.

Materials and methods

Bacteria, media, growth conditions and transformations

Strains of *Escherichia coli* were grown in Luria–Bertani medium at 37°C. Bt strain VPI-5482 and derivative strains

were grown under anaerobic conditions at 37°C in brain heart infusion (BHI) medium (Oxoid, Basingstoke, UK) supplemented with 0.001% haemin (BHIH) or with 0.00005% haemin for OMV preparations. Antibiotics were added as selective agents when appropriate: ampicillin 200 µg/ml and erythromycin 5 µg/ml. The *E. coli* strain J53/R751 was supplemented with trimethoprim 200 µg/ml when grown for 18 h. *E. coli* GC10 was transformed by electroporation using a Gene Pulser II (Bio-Rad, Watford, UK). Plasmids were mobilized from *E. coli* into Bt following a triparental filter mating protocol [24] using the helper strain J53/R751. The *Y. pestis* strain CO92 (biovar Orientalis, NR641; BEI Repositories) was supplied by the Biodefence and Emerging Infections (BEI) Research Repository (Bethesda, MD, USA) in accordance with International Export and Import Regulatory Requirements and used with kind permission from National Institute of Allergy and Infectious Diseases (NIAID). The organism was stored and handled in accordance with US Biological Select Agent or Toxin requirements and was grown using the conditions and methods described previously [25].

Construction of *Y. pestis* F1- and V1-antigen expression vectors

A synthetic gene construct of 1043 base pairs (bp) encoding the V antigen and a synthetic operon construct of 3826 bp encoding *caf1M*, *caf1A* and *caf1* genes of the *caf1* operon that generates the F1 protein were N-terminally fused to the OmpA signal peptide of Bt. This created *in-silico* constructs with codon usages optimized for expression in the same species. Signal peptide prediction was obtained by SignalP at <http://www.cbs.dtu.dk/services/SignalP/>. During the design of the synthetic constructs the unique *Bacteroides* ribosomal binding site [26] required for efficient expression in *Bacteroides* was accounted for. The resulting gene cassettes for V and F1 were obtained through gene synthesis and subsequently cloned into the *E. coli* plasmids pEX-A2 and pEX-K4 (Eurofins, Hamburg, Germany), respectively. The cassettes contained *Bsp*HI and *Eco*RI restriction sites at their 5' and 3' ends, respectively, allowing for the translational fusion of the encoded gene to the start codon in the *Bacteroides* expression vector pGH090 [26]. The genes encoding V1 or F1 were excised from the pEX derivatives using *Bsp*HI and *Eco*RI and ligated into the *Nco*I/*Eco*RI-restricted pGH090 expression vector, resulting in pGH179 and pGH180, respectively. Finally, the sequence integrity of the cloned fragments was verified through sequencing.

OMV isolation and characterization

OMVs were isolated following a method adapted from Stentz *et al.* [27]. Briefly, cultures of Bt (500 ml) were centrifuged at 5500 g for 45 min at 4°C and the

supernatants filtered through polyethersulphone (PES) membranes (0.22 µm pore-size) (Sartorius, Göttingen, Germany) to remove debris and cells. Supernatants were concentrated by ultrafiltration (100 kDa molecular weight cut-off, Vivaspin 50R; Sartorius), the retentate was rinsed once with 500 ml of phosphate-buffered saline (PBS) (pH 7.4) and concentrated to 1 ml (approx. 700 µg/ml total protein). The final OMV suspensions were filter-sterilized (0.22 µm pore size). The protein content of the final OMV suspensions was determined using the Bio-Rad Protein Assay.

The distribution of heterologous proteins within Bt OMVs was established in a proteinase K accessibility/protection assay [27]. Briefly, a suspension of 250 µg of OMVs in 0.1 M phosphate/1 mM ethylenediamine tetraacetic acid (EDTA) buffer (pH 7.0) was incubated for 1 h at 37°C in the presence of 100 mg/l proteinase K (Sigma-Aldrich, Poole, UK). Proteinase K activity was stopped by addition of 1 mM phenylmethanesulphonyl fluoride (PMSF) and samples analysed by immunoblotting.

Nanoparticle analysis

Videos were generated using a Nanosight nanoparticle instrument (NanoSight Ltd, Malvern, PA, USA) to count OMV numbers in each OMV sample. The mean squared displacement (X) was measured simultaneously for each OMV tracked. The particle diffusion coefficient (D_t), and hence sphere equivalent hydrodynamic radius (r_h) were determined using the Stokes–Einstein equation,

$$D_t = \frac{k_B T}{6\pi\eta r_h},$$

where k_B is Boltzmann's constant, T is temperature and η is solvent viscosity.

Immunoblotting

OMV-V extracts were added to sodium dodecyl sulphate–polyacrylamide gel electrophoresis (SDS–PAGE) loading buffer (NuPage; Invitrogen, Carlsbad, CA, USA) containing dithiothreitol (Invitrogen). Approximately 7 µg of OMV-V was loaded onto 12% precast Tris–glycine gels (Novex/ThermoFisher Scientific, Fremont, CA, USA) and separated by electrophoresis at 180 volts for 40 min. Gels were transferred onto a polyvinylidene difluoride membrane at 25 volts over 2 h in a solution containing Tris–glycine transfer buffer (Novex). The membrane was blocked with 10% bovine serum albumin (BSA) in Tris-buffered saline (TBS) (50 mM Tris-HCl, 150 mM NaCl, pH 7.5)-Tween (0.05%) for 30 min at 20°C. Blocking solution was then discarded and the membrane incubated for 16 h at 4°C in a 1 : 1000 dilution of a primary mouse anti-V antibody (Defence Science and Technology Laboratory, Porton Down, UK) in TBS-Tween with 5% BSA. After washing with TBS-Tween three times, membranes were incubated

for 1 h at 20°C in 5% BSA in TBS-Tween with a 1 : 1000 dilution of horseradish peroxidase (HRP)-conjugated goat anti-rabbit IgG (ThermoFisher). After three washes in TBS-Tween, SuperSignal West Pico chemiluminescent Substrate (ThermoFisher) was used to detect bound antibody.

The F1 content of F1-OMV formulations was determined using a dot-blot assay in which serial twofold dilutions of extracts of F1-OMVs (10 µl) were spotted onto nitrocellulose membranes and air-dried. Serial dilutions of recombinant F1 protein (rF1) and extracts of native OMVs were also applied to the membranes. The membranes were then processed as described for immunoblotting as above, using a rabbit anti-F1 anti-sera (Defence Science and Technology Laboratory) and a secondary HRP-conjugated goat anti-rabbit IgG (ThermoFisher). Localization of F1 in Bt OMV preparations was determined by liquid chromatography and mass spectrometry (LC-MS)-based proteomics (Proteomics Facility, University of Bristol, Bristol, UK).

Cytokine analysis

Frozen PBMCs obtained from whole blood by density gradient centrifugation over Ficoll-Paque Plus (Amersham Biosciences, Chalfont St Giles, UK) were thawed, washed twice with RPMI media containing 10% FBS, 2 mM glutamine and 100 U/ml penicillin/streptomycin and adjusted to a concentration of 5×10^5 cells/ml. Aliquots of 10^6 cells were plated into individual U wells of 96-well plates and incubated in triplicate with media alone or media containing 15 µg/ml rV protein for 72 h at 37°C in an incubator with 5% CO₂. Control cultures contained media only. Conditioned media was then harvested, and cytokine content determined using a bead-based multiplex assay and BD LSRFortessa flow cytometer (BD Biosciences, San Jose, CA, USA), according to the manufacturer's instructions (BioLegend, San Diego, CA, USA).

Antibody enzyme-linked immunosorbent assay (ELISA)

Nunc-Immuno Microwell 96-well plates (ThermoScientific) were coated with 15 µg/ml of *Y. pestis* V (BG032/VDJPE1) or F (BG032/FD5Pst2) recombinant proteins (Defence Science and Technology Laboratory) in ELISA coating buffer (0.1 M NaHCO₃) and incubated for 16 h at 4°C. After washing three times with ELISA wash buffer (PBS with 1 : 2000 Tween-20), plates were blocked for 3 h with blocking buffer (PBS with 2% BSA) at 20°C with gentle agitation. Serum, saliva, salivary gland and bronchoalveolar lavage (BAL) samples were added in dilutions ranging from 1 to 163 840 and the plates were incubated for 16 h at 4°C. After six washes with ELISA wash buffer, 50 µl of 1 : 10 000 goat anti-monkey immunoglobulin

(IgG) peroxidase conjugated (Sigma; A2054-1ml) or 1 : 10 000 goat anti-monkey IgA-HRP antibody (Sigma; SAB3700759) were added and plates were incubated for 1 h at 20°C with gentle agitation. Plates were then washed six times with ELISA wash buffer and incubated with 100 µl of TMB high sensitivity substrate solution (BioLegend, San Diego, CA, USA) for 20 min at 20°C in darkness. The reaction was stopped by adding 50 µl of 2 N H₂SO₄. The plates were analysed in a microplate reader at Abs_{450 nm}. Absolute amounts of IgG and IgA antibodies in serum and mucosal samples, respectively, were determined using a modified ELISA incorporating a range of concentrations of purified monkey IgG (BioRad) and IgA (Life Diagnostics, Inc., West Chester, PA, USA) and the protocol and reagents described above to generate standard curves from which IgG and IgA concentrations of individual animals were determined.

Bactericidal assay

This prototype bactericidal assay (BCA) was developed in a series of experiments which optimized incubation times, using a standard anti-rF + rV anti-serum generated in cynomolgus macaques. All activities associated with the BCA assay were performed at ACDP3 level containment within a BSL3 safety cabinet. *Y. pestis* CO92, originally sourced by Public Health England (PHE) from the BEI research repository (catalogue number: NR-641) was used to make a working stock. Working stock was propagated on Columbia blood (COH) agar for 2 days at 26°C. A bacterial suspension was then created by harvesting the bacteria from the surface of the agar and subsequent resuspension in TSB. Sterile TSB broth was then inoculated with sufficient bacterial suspension to result in an OD_{600nm} of 0.1. After 3 h incubation at 26°C, the mid-log culture was diluted to an expected *Y. pestis* concentration of 3.3×10^3 colony-forming units (CFU)/ml ready for use as the inoculum for the bactericidal assay. This process was used in all protocols.

Heat-treated (to deplete individual sample complement) primate sera were incubated with live *Y. pestis* bacteria in the presence of 25% v/v rabbit complement (Pellfreeze Biologicals, Roger, AR, USA) for 1 h with orbital agitation on a 96-well plate shaker. After this incubation, the mixture was plated onto COH agar and permitted to be absorbed into the agar at 37°C. In preliminary experiments, human volunteer and baby rabbit complement (Pellfreeze Biologicals) were found to be similar in sensitivity to antibody-directed bactericidal activity against *Y. pestis* CO92. After this incubation, the mixture was plated onto COH agar and permitted to be absorbed into the agar. The COH plates were then incubated at 37°C for 2 days before manual enumeration to determine relative viability. Incubation at 37°C only began once the

antibody, complement and bacterial mixture was created in the assay plate. This protocol simulated the natural infection process that would take place once a flea has bitten a mammalian host. No-antibody, complement-only controls were included in all assays.

The number of bacteria counted for each test serum anti-serum was used to calculate the degree of reduction in counts compared with the plate spread with the no-antibody complement control. The dose of test serum [expressed as percentage (v/v) of serum] required to kill 50% of live *Y. pestis* CO92 was calculated by interpolation of the dose response curve for each sample. Each assessment was conducted in duplicate. Bactericidal antibody assessment assays were conducted at PHE on samples taken on each of the 4 sample days with serum pools from each of the 12 vaccine groups. In all studies, the reference standard anti-rV plus anti-rF1 primate serum was also assessed as a means of comparison and measure of reproducibility. In all studies, this standard anti-serum killed *Y. pestis* in a reproducible manner. All controls (including the no-antibody, complement-only no antibody control) were assessed and performed as expected.

Competitive ELISA

A competitive ELISA (CE-ELISA) assay was used (as previously described [1]) to detect antibodies in immune sera from V-OMV immunized animals that were able to compete with a monoclonal antibody (mAb 7:3) for binding to recombinant V protein. Briefly, rV antigen was coated onto 96-well microtitre plates (Dynex, Lincoln, UK) at 5 µg/ml in 0.05 ml PBS (16–18 h, 4°C). After washing in PBS with 0.02% Tween 20, plates were blocked with 0.2 ml 5% w/v skimmed milk powder in PBS (37°C, 1 h). After further washing, 0.05 ml mAb 7:3 (1 : 32000 in 1% w/v skimmed milk powder in PBS) was added to each well (equivalent to 80 ng/well) and plates were incubated at 4°C for 16 h. Normal, non-immune NHP serum, also diluted to 1 : 32 000, was added to negative control wells (0.05 ml per well). Plates were then washed prior to adding the test serum at a dilution of 1 :10 in 1% w/v skimmed milk powder in PBS. A positive control was included comprising a reference serum created by pooling equal aliquots of sera from four macaques previously parenterally immunized with rF1 + rV antigens and prior to surviving challenge with *Y. pestis*. Test and control serum samples were assayed in duplicate. Plates were incubated (1 h, 37°C) prior to washing and addition of HRP-goat anti-mouse IgG (Serotec, Kidlington, UK; 1 : 2000 in PBS) followed by incubation (37°C, 1 h). Plates were washed prior to addition of ABTS substrate (Sigma) with subsequent reading of absorbance at 414 nm. The optical diameter (OD)_{414nm} determined for each test and the reference serum was adjusted by subtraction of

the OD_{414nm} determined for the appropriate control serum. The data were calculated from a titration curve for loss of binding of the mouse antibody, with increased concentration of human serum.

Ethics statement

All animals used in these studies were cynomolgus macaques (*Macaca fascicularis*) obtained from the characterized breeding colonies managed by PHE that have been established and maintained as closed colonies for more than 20 years. Animals were housed in compatible social groups, in accordance with the Home Office (UK) Code of Practice for the Housing and Care of Animals Bred, Supplied or Used for Scientific Purposes, December 2014, and the National Committee for Refinement, Reduction and Replacement (NC3Rs), Guidelines on Primate Accommodation, Care and Use, August 2006. All animals were aged between 3 and 5 years and none of the animals had been used previously for experimental procedures, were free of herpes B-virus, tuberculosis (TB), simian immunodeficiency virus (SIV) and simian T-cell leukemia virus (STLV) and were inspected by the named veterinary surgeon prior to entry into the study. All animal procedures and study design were approved by the Public Health England, Porton Down Animal Welfare and Ethical Review Committee, and authorized under an appropriate UK Home Office project licence (30/2993 and P76404B45).

Generation of standard NHP reference anti-sera

In order to enable development of a functional biological assay of relevance to these studies, anti-sera to F1 and V were generated by immunizing two cynomolgus macaques with either recombinant F1 (batch BG032\FD5Pst2; Defence Science and Technology Laboratory) or recombinant V (batch BG032\VDJPE1; Defence Science and Technology Laboratory) antigens produced from *E. coli* [1] and formulated into 20% (v/v) alhydrogel adjuvant. Both vaccines were prepared and supplied to PHE by Defence Science and Technology Laboratory. Two primates (one male, one female) were immunized with either vaccine on two occasions 3 weeks apart. The dose on each vaccination occasion was 50 µg injected intramuscularly in a 250 µl volume. Once an immune response was confirmed to have been induced via ELISA, subjects were anaesthetized by intramuscular injection of ketamine (15 mg/kg) and blood samples were collected from the heart prior to euthanasia by intracardiac injection of a lethal dose of anaesthetic (Dolethal, 140mg/kg; Vétoquinol UK Ltd, Towcester, UK) in order to generate the reference stock anti-sera 56 days after primary immunization. The sera were collected after centrifugation of serum separation tubes which had permitted the blood to clot. Serum aliquots were created and frozen at below -20°C until

required. Stool samples were also collected for reference purposes into OMNIgene GUT OMR-200 tubes.

OMV vaccines and vaccination

The immune status for each NHP was assessed with regard to *Y. pestis* antigens at 14 and 0 days before immunization. For OMV-V/F1 vaccine studies, animals were randomly allocated to groups of four (two males and two females per group) and were immunized with OMV-V or OMV-F1 vaccine formulations containing 12.5, 25 or 50 µg of V or F1 protein via the intranasal route or with 50 µg of V/F1 protein via the oral route in a total volume of 1 ml PBS. Nasal dosing of vaccine was conducted using a stepwise droplet method to alternate nares using a sterile flexible plastic tube (13GA plastic feeding tube; Instech Laboratories Inc., Plymouth Meeting, PA, USA) and oral administration was performed using a flexible dosing tube to ensure accurate delivery. Twenty-eight days later, all NHPs received a booster immunization via the same route of administration. Blood, stool, saliva and rectal and nasal swab samples were collected at days -14, 0, 28, 42 and at the study end-point of 56 days with body weight, temperature, axillary and inguinal lymph node scores and haemoglobin concentration determined at each sampling time-point. Animals were sedated by intramuscular (i.m.) injection with ketamine hydrochloride (Ketaset, 100 mg/ml; Fort Dodge Animal Health Ltd, Southampton, UK; 10 mg/kg) for simple procedures such as blood sampling and vaccination that required removal from their housing. At the end of the study, animals were sedated with ketamine (15 mg/kg, i.m. administration), weighed and clinical data collected. Prior to euthanasia, anaesthesia was deepened using medetomidine hydrochloride (Sedator, 1 mg/ml; Dechra Veterinary Products, Shrewsbury, UK) 50 mg/kg and a BAL was performed. BAL fluid samples were collected using a bronchoscope (Allscope XE30 4-mm flexible bronchoscope; VES, Rochford, UK). BAL consisted of three consecutive washes performed, each using 20-ml volumes of Hanks' balanced salts (Sigma-Aldrich, Poole, UK), which was instilled in the lungs and collected. Exsanguination of each animal was affected via the heart before termination by the injection of a lethal dose of anaesthetic (140 mg/kg) (Dolethal; Vétoquinol UK Ltd). At necropsy, lung, spleen, liver, heart, lymph nodes, kidney, brain, stomach and intestine were collected for histopathology and routinely processed. The tissues were stained with haematoxylin and eosin (H&E) and examined by light microscopy and evaluated subjectively by a pathologist, blinded to the treatments and groups in order to prevent any bias.

Statistical analysis

CE-ELISA data were analysed using Graph Pad Prism software version 6 and expressed as mean \pm standard

error of the mean (s.e.m.). Statistical comparisons were made using one-way analysis of variance (ANOVA) or unpaired *t*-test. The survival data were expressed as Kaplan–Meier survival curves and statistical significance was determined by log-rank test. $P < 0.05$ was considered statistically significant. Cytokine multiplex data were analysed using one-way ANOVA with Bonferroni's multiple comparison post-test to compare PBS and rV values for each cytokine.

Results

Study rationale

The aim of this immunogenicity and reactogenicity study was to determine the suitability of OMVs produced by the human commensal gut bacteria, Bt, as a delivery platform for plague vaccine antigens that could activate mucosal and systemic immune responses in an NHP host, and be capable of protecting against plague infection. Mice are a common experimental model system used in preclinical studies of human drugs and vaccines. However, the NHP model is better suited to answering key questions about Bt OMV vaccine efficacy and safety in humans. This is because the genetic relatedness of primates, and hence greater physiological and microbiological similarity to humans, requires less interpolation compared to other animal model systems [28–31]. Therefore, the use of NHPs de-risks the development pathway for Bt-OMV vaccine by providing assurance that the NHP microbiome and histological integrity of the GI tract, and other associated tissues, are not adversely affected following immunization. In addition, the use of NHP anti-sera as a surrogate to quantify bactericidal activity and protection against infection will help to pave the way for assessment of the protective effect of Bt OMV vaccination in humans.

Expression of *Y. pestis* vaccine antigens in Bt OMVs

It is possible to engineer Bt to target protein antigens to a specific location in OMVs. The antigen can be either secreted as a soluble protein in the lumen of OMVs by making a fusion with an appropriate secretory signal peptide or, alternatively, it can be targeted to the surface of OMVs by making fusions of the antigen with OMV surface proteins. Accordingly, genes encoding the V and F1 *Y. pestis* proteins were successfully cloned downstream of sequences encoding the N-terminal signal peptides of the major OMV protein OmpA (BT_3852), the products of which were contained within the lumen or outer membrane of OMVs (Fig. 1a). The constructs were generated in *E. coli* hosts and then mobilized into Bt via a triple-filter mating protocol using a helper strain. Immunoblotting

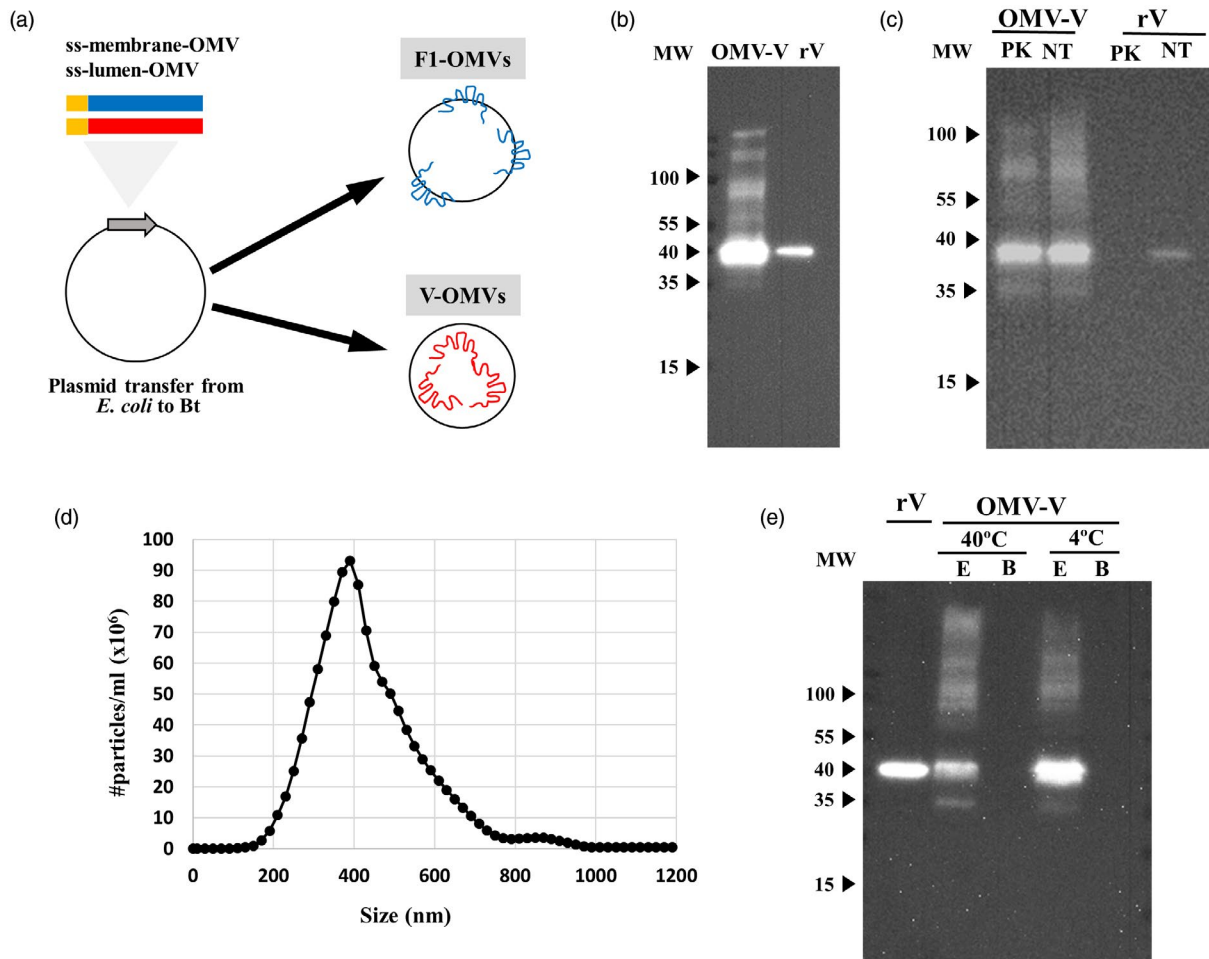


Fig. 1. *Bacteroides thetaiotaomicron* (Bt) outer membrane vesicle (OMV) plague vaccines. (a) Schematic of cloning procedure for the expression of *Yersinia* virulence proteins Fraction 1 (F1) and V antigen (V) at the surface or in the lumen, respectively, of Bt OMVs. The Bt secretion signal sequence is indicated in yellow and is fused at the N-terminus of the F1 and V genes. (b) Expression of V antigen in OMV lysates determined by immunoblotting (IB). (c) Determination of protein location after treatment with proteinase K (PK). IB of V antigen with and without pretreatment of V-OMVs or recombinant V (rV) with proteinase K. NT = not treated. (d) Size distribution of Bt V-OMVs by nanoparticle tracking analysis. The OMV suspension was diluted 100 times. (e) Thermostability of V-OMVs assessed by storing preparations at different temperatures for 8 weeks prior to analysing OMV extracts (E) or storage buffer (B) for presence of V antigen by IB. Molecular weight (MW) is expressed in kDa.

of whole cell and OMV lysates of recombinant Bt strains confirmed expression of the V antigen (approximately 15 $\mu\text{g}/\text{ml}$ of total protein) (Fig. 1b). A dot-blot assay was used to detect F1 protein in OMV lysates (approximately 10 $\mu\text{g}/\text{ml}$ of total protein) with its presence being confirmed by LC-MS proteomics of OMV lysates (data not shown). The luminal *versus* outer membrane distribution of the proteins in Bt OMVs was established using a protease protection assay. This assay demonstrated that V protein distribution was within the lumen of OMVs (Fig. 1c). The presence of F1 protein in extracts of F1-OMV was confirmed by LC-MS proteomics, with its absence in F1-OMV samples pretreated with proteinase K being consistent with its localization to the OMV outer membrane.

V and F1 containing OMVs had an average size of ~ 400 nm (Fig. 1d) and exhibited high thermostability with minimal loss of vaccine antigen content after storage for 6 weeks at either 4°C or 40°C (Fig. 1e and data not shown).

OMV immunization

OMV vaccination followed a prime and a single boost dosing regimen as depicted in Supporting information, Fig. S1, with each animal serving as their own control and reference for evaluating OMV vaccine responses. Levels of antigen-specific antibodies were assessed in serum samples obtained at two pre-immunization time-points (days -14 and 0) and at three time-points post-immunization (days 28, 42 and 56). Oral and nasal administration are

the preferred routes of vaccination to generate protective immunity at primary sites of plague infection [9]. To identify which of these routes was optimal for Bt OMV plague vaccines we measured both local and systemic antigen-specific V and F1 IgA and IgG antibodies following delivery. For oral delivery we used a dose of 50 μg of V antigen formulated in Bt OMVs, which is mid-range of the vaccine dose used previously in cynomolgus macaques [32], and is equivalent to that required for a human dose [7]. In considering the potential risks of administering agents via the intranasal route and its accessibility to the systemic circulation and the brain, we used a range of OMV vaccine antigen doses (12.5, 25 and 50 μg) to assess safety and tolerability and determined the lowest dose required to induce a strong immune response.

Host response to F1-OMV plague vaccines

F1-OMV vaccine formulations were evaluated by measuring antigen-specific IgA levels in mucosal secretions and tissues and antigen-specific IgG levels in the serum (Fig. 2 and Supporting information, Fig. S2). F1-OMVs generated antigen-specific IgG serum antibodies (~ 0.5 – 1.5 $\mu\text{g}/\text{ml}$) after both oral and intranasal immunization at day 42 and then

decreased (~ 0.5 $\mu\text{g}/\text{ml}$) at day 56. The fact that the antibody levels did not increase until day 42 reflects the importance of and requirement for a booster immunization (at day 28). There was no clear evidence for an effect of antigen dose on the levels of F1 antibodies produced, as similar levels of F1-specific IgG were recorded in animals receiving 12.5, 25 or 50 μg of F1-OMVs (Fig. 2a). There was also no clear evidence for the superiority of oral *versus* nasal delivery of F1-OMVs in terms of levels of antigen-specific IgG antibodies generated (Fig. 2a). By comparison with serum IgG antigen-specific responses, F1-OMVs elicited weak mucosal immune responses with low levels of antigen-specific IgA present in saliva (Supporting information, Fig. 2a–d) and BAL (Supporting information, Fig. S2e) samples, irrespective of the route of administration. It was not possible to detect F1-specific IgA antibodies in the salivary glands of F1-OMV immunized animals (Supporting information, Fig. S2f).

Host response to V-OMV plague vaccines

V-OMV vaccines generated strong antibody responses systemically and at mucosal sites (Fig. 3 and 4). Analysis of serum anti-V-specific IgG antibodies showed that the

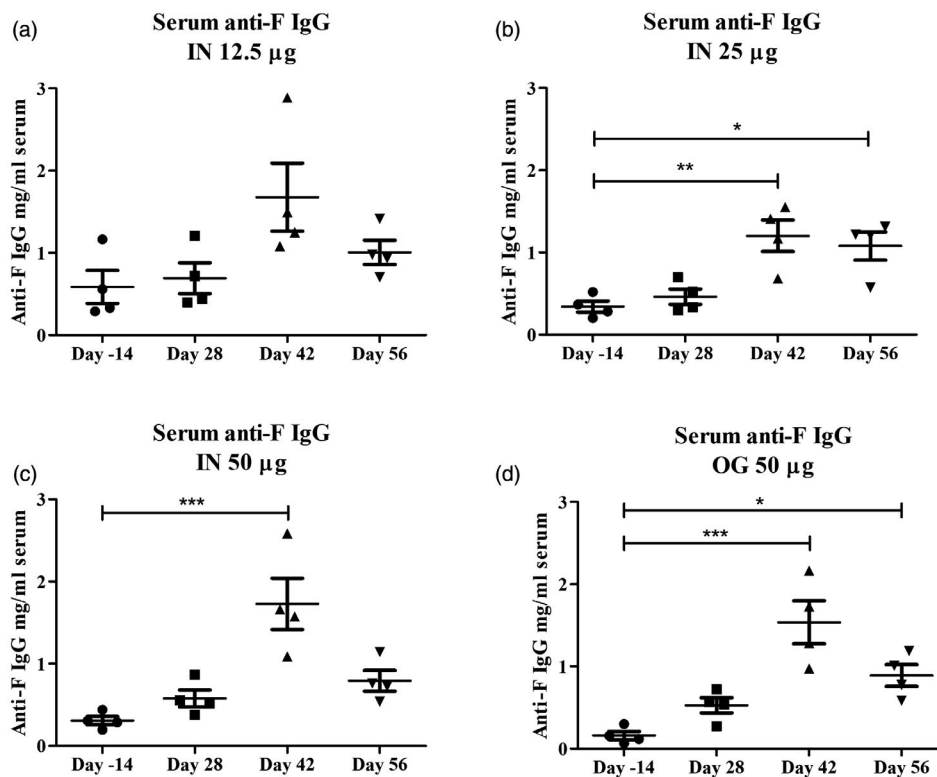


Fig. 2. Humoral systemic immune response to Fraction 1-outer membrane vesicles (F1-OMV) vaccines. The quantity and titre of F-antigen-specific immunoglobulin (IgG) in the sera of animals immunized with F1-OMVs via the intranasal or oral route was determined prior to immunization (day -14) and at three time-points post-immunization (days 28, 42 and 56) by enzyme-linked immunosorbent assay (ELISA) using an initial serum dilution of 1 : 10 prior to serial one in four dilutions. Data expressed as mean \pm standard error of the mean (s.e.m.). * < 0.05 ; ** < 0.01 ; *** < 0.001 .

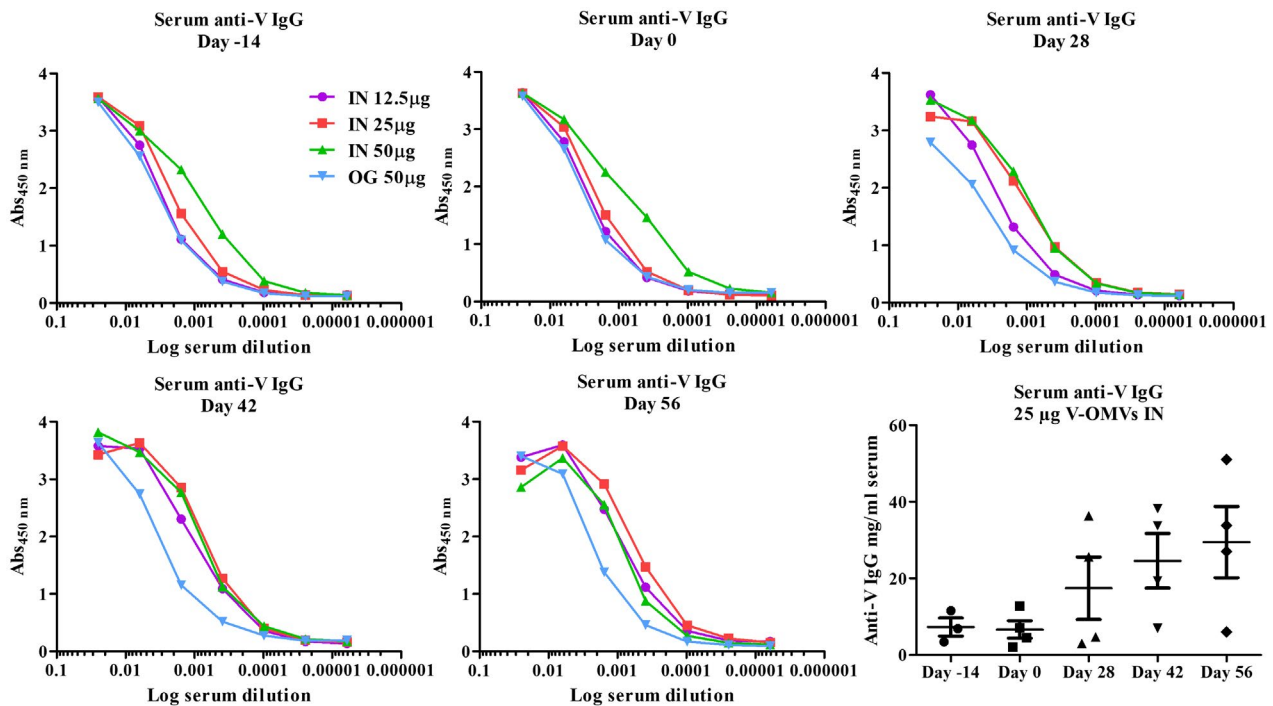


Fig. 3. Humoral systemic immune response to V antigen-outer membrane vesicles (V-OMV) vaccines. The quantity and titre of V-antigen specific immunoglobulin (Ig)G in the sera of animals immunized with V-OMVs via the intranasal or oral route was determined prior to immunization (days -14 and 0) and at three different time-points post-immunization (days 28, 42 and 56) by enzyme-linked immunosorbent assay (ELISA) using an initial serum dilution of 1 : 10 prior to serial one in four dilutions. Each line graph represents the mean value for each group ($n = 4$). The levels of V-specific IgG in individual animals immunized with 25 μ g of V-OMVs via the intranasal route is shown in the bottom right graph with the horizontal lines in each category representing the mean \pm standard error of the mean (s.e.m.).

intranasal immunization route for V-OMV immunization generated higher titres of antibodies than oral immunization (Fig. 3); in contrast, for F1-OMVs there were no differences in IgG responses between the two vaccine delivery routes (Fig. 2). The highest titres of V-specific IgG at the study end-point were in animals intranasally vaccinated with 25 μ g of V-OMV, with antibody levels increasing over the study period (Fig. 3). In mucosal samples, low titres of V-specific IgA were recorded in the saliva at all time points analysed (Fig. 4a), with the highest titres being seen at day 42 (Fig. 4b). Consistent with the superior performance of intranasally delivered V-OMVs for generating V-specific IgG antibodies, higher levels of V-specific IgA were recorded in the saliva of animals immunized intranasally compared to those immunized via the oral route (Fig. 4a,b). The 25- μ g dose of intranasally administered V-OMVs achieved the highest titres of V-specific IgA in saliva (Fig. 4a), and were similar to serum V-specific IgG antibody responses (Fig. 3). By comparison, salivary gland V-specific IgA antibody titres at day 56 were similar in animals immunized with 12.5, 25 or 50 μ g of antigen (Fig. 4c). The titre of V-specific IgA antibodies in the BAL were lower

than in either the saliva or the salivary glands, with no evidence of vaccine dose-level-dependent responses, as each dose of V-OMVs elicited similarly low levels of V-specific IgA (Fig. 4c).

As an indicator of cell-mediated immune responses to OMV vaccines, we analysed the recall response of peripheral blood lymphocytes from animals immunized intranasally or orally with V-OMVs after restimulation with rV antigen *in vitro*. PBMCs from V-OMV immunized animals constitutively produced varying levels of monocyte chemoattractant protein (MCP)-1, IL-6, IL-8 and/or IL-23 during culture in complete media alone (Fig. 5). In the presence of rV, significant increases in the levels of IL-6 ($P < 0.0001$) were seen in all PBMC samples irrespective of the immunization route or the dose of V-OMVs used. Significant increases in IL-1 β ($P < 0.001$), MCP-1 ($P < 0.0001$), IL-8 ($P < 0.001$) and IL-23 ($P < 0.0001$) were also seen in rV-stimulated PBMC samples from animals immunized intranasally with the lowest dose of V-OMV (12.5 μ g). At higher doses of intranasal or oral administered V-OMVs IL-8 was the only cytokine, in addition to IL-6, that was secreted at levels significantly higher ($P < 0.05$) after rV stimulation compared to control cultures. Other cytokines included

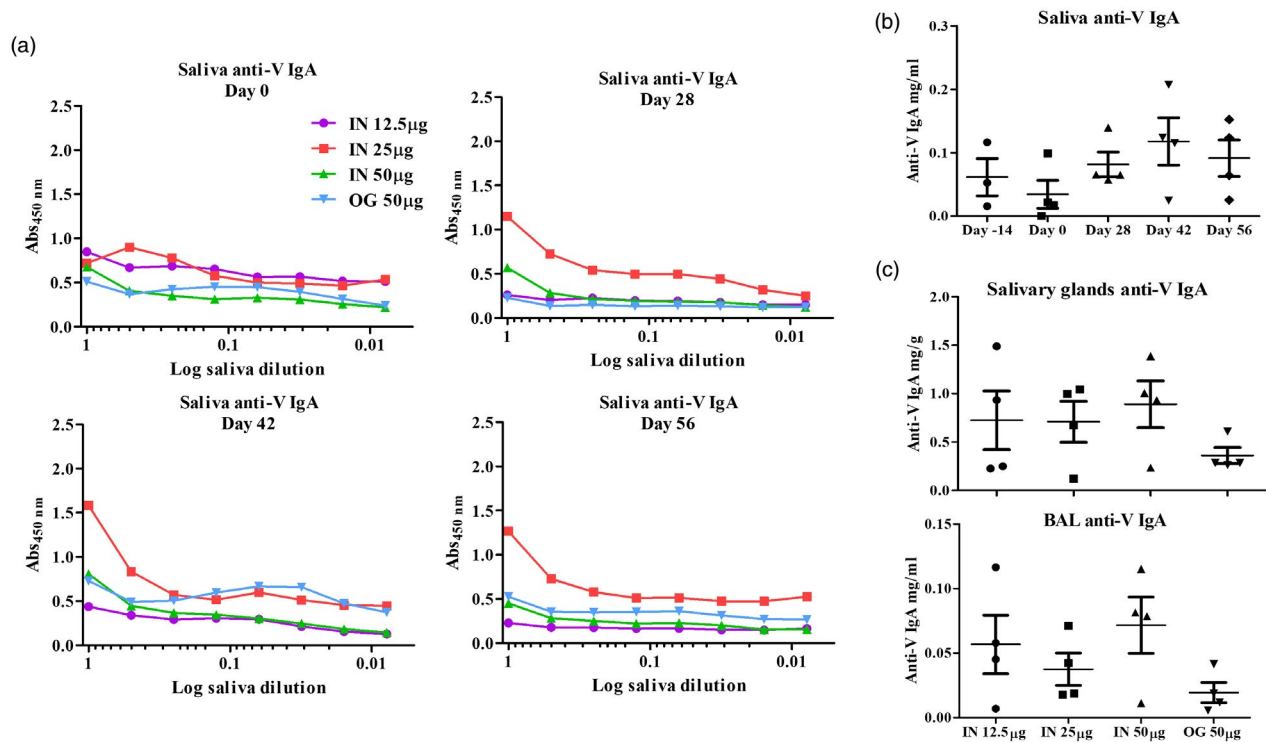


Fig. 4. Mucosal humoral immune response to V antigen-outer membrane vesicles (V-OMV) vaccines. (a) The quantity and titre of V-antigen specific immunoglobulin (IgA) in the saliva of animals immunized with V-OMVs via the intranasal or oral route was determined prior to immunization (day 0) and at three different time-points post-immunization (days 28, 42 and 56) by enzyme-linked immunosorbent assay (ELISA) using serial one in two dilutions. Each line graph represents the mean value for each group ($n = 4$). (b) Levels of V-specific IgA in saliva samples of individual animals immunized with 25 μ g of V-OMVs via the intranasal route. The horizontal lines in each category represent the mean \pm standard error of the mean (s.e.m.). (c) Levels of V-specific IgA in salivary glands and bronchoalveolar lavage (BAL) samples for animals immunized intranasally or orally with V-OMVs analysed at day 56 post-immunization.

in the analysis that were not detected in any PBMC sample or were present at levels below the detection limit of the assay (≤ 1.0 pg/ml) included IFN- γ , TNF- α , IL-10, IL-12p70, IL-17A and IL-18 (data not shown).

Reactogenicity of V-OMV vaccines

Biosafety of F-OMV and V-OMV vaccines were based on histopathology of tissue routinely recovered at necropsy (Supporting information, Fig. S3), and profiling of the resident microbial populations (microbiotas) of the GI and respiratory tracts using 16S rRNA sequence-based community profiling of faecal- and nasal swab-derived DNA samples taken pre- and post-OMV immunization (Fig. 6). Independent blinded evaluation of various tissues (lung, spleen, liver, heart, lymph nodes, kidney, brain and regions of the GI tract) at necropsy revealed no macroscopic signs of pathogenic infection or pathology.

Evidence of recent immune activation were seen in the lymphoid tissues of the spleen and lymph nodes in a proportion of animals in each group receiving F1-OMV immunization; this comprised the presence of scattered

secondary follicles with mitotic figures and apoptotic cells in the splenic white pulp (Supporting information, Fig. S3a) and cortex of the lymph nodes (Supporting information, Fig. S3b). Microscopic examination of tissues from animals receiving the highest dose of V-OMVs (50 μ g) identified regions of organized and enlarged lymphoid structures and follicles within the spleen and lungs (Supporting information, Fig. S3f) in the absence of any infection or bacteria. Lymphoplasmacytic cell infiltrates were observed with some frequency in the mucosa of all parts of the GI tract (Supporting information, Fig. S3c–e); this is a common finding in our experience with macaques, and their presence probably reflects a low-grade, chronic-active gastritis/enteritis/colitis that may or may not have been associated with clinical signs such as diarrhoea.

16S rRNA community profiling and bubble chart analysis of sequence data revealed that there was considerable interindividual variation in both the nasal (Fig. 6a) and faecal (Fig. 6b) microbiotas of NHPs at baseline. Post-immunization with V-OMVs via the intranasal routes did not noticeably alter the profiles of nasal

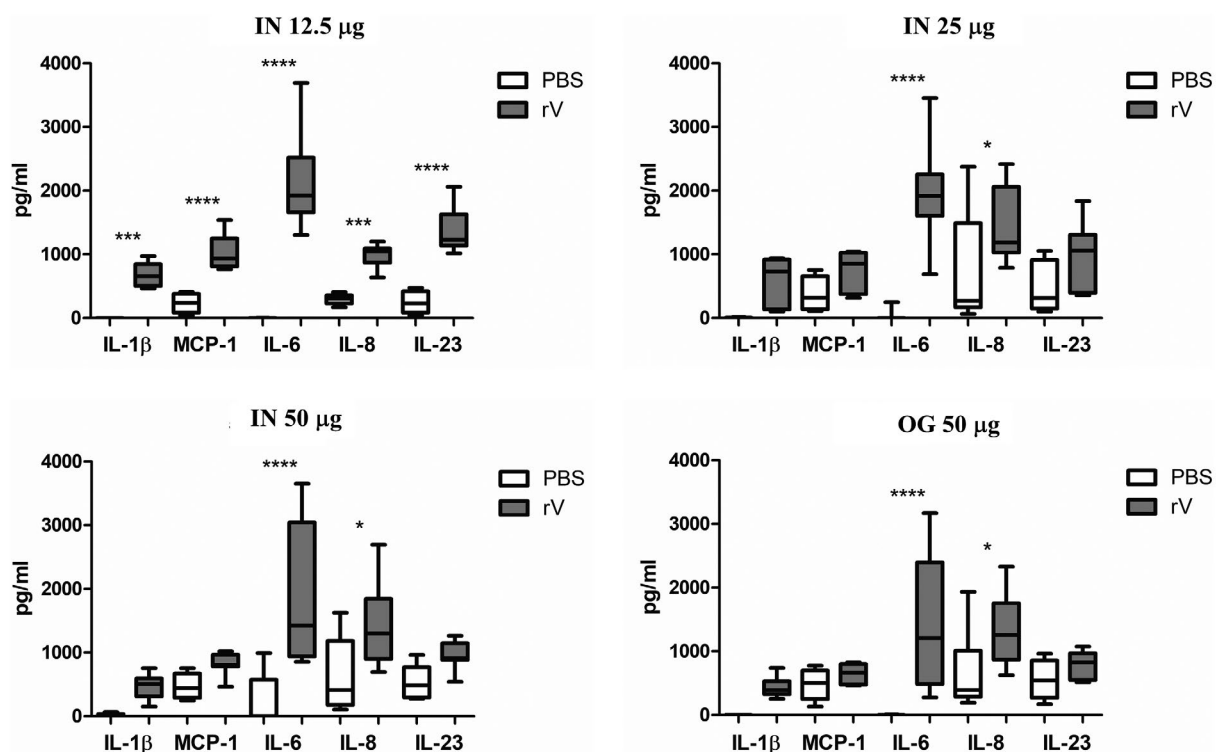


Fig. 5. Cytokine production by peripheral blood mononuclear cells (PBMCs) from V antigen-outer membrane vesicles (V-OMV)-immunized animals. PBMCs obtained from animals previously immunized with V-OMVs via the intranasal (i.n.) or oral route at day 56 post-immunization were cultured in the presence or absence [phosphate-buffered saline (PBS)] of recombinant V protein (rV) for 72 h, after which time supernatants were analysed for cytokine content using a multiplex bead assay and flow cytometry. Limit of detection for given values was interleukin (IL)-1 β < 1.11 pg/ml, MCP-1 < 1.61 pg/ml, IL-6 < 1.45 pg/ml, IL-8 < 1.02 pg/ml, IL-23 < 1.44 pg/ml. Given values represent the group mean \pm standard error of the mean (s.e.m.) of duplicate samples, $n = 4$ per group. One-way analysis of variance (ANOVA) with Bonferroni's multiple comparison post-test was used to compare PBS and rV values for each cytokine; * $P \leq 0.05$, *** $P \leq 0.001$, **** $P \leq 0.0001$.

microbiota at any vaccine dose (Fig. 6a). In faecal microbiota the bacterial composition did not significantly change, although small changes in relative abundance were noted (Fig. 6b). For example, the average prevalence of *Prevotellaceae* increased from 30% at pre-immunization to 44% after immunization. By contrast, there were decreases in the average prevalence of *Succinivibrionaceae* (from 9 to 0.4%). These findings are consistent with V-OMVs having a minor impact on resident prokaryotic communities in the upper respiratory tract.

Functionality of OMV-elicited IgG antibodies

Two independent assays were used to assess the functionality of immune sera from OMV immunized animals and to determine their usefulness as potential immune correlates for protection in humans. The first assay used was a CE-ELISA [1] that quantified the ability of immune IgG to compete for binding to the *Y. pestis* V antigen. This assay utilizes a monoclonal antibody (mAb 7.3) which

has previously been shown to protect mice fully by passive transfer against direct exposure to *Y. pestis* [33]. Alongside a passive transfer assay, we have previously demonstrated that the competitive ELISA provides a potential *in-vitro* correlate of protection for plague [1]. The second assay was a prototype BCA specifically developed for this study, which assessed the level of antibody-mediated complement killing of *Y. pestis* in serum samples using the *Y. pestis* reference strain CO92 as the target.

Serum samples collected at the study end-point from representative animals within each of the different routes of immunization and dose-level groups were assayed for their ability to displace mAb 7.3 from binding to rV *in vitro*. The data are presented as a titration line for loss of binding of the mouse monoclonal antibody with increasing concentrations of test samples (see Materials and methods) using, as a reference, macaque immune sera obtained by parenteral immunization with rF1+ rV proteins (Fig. 7). Values were also corrected for any non-specific activity by subtracting values obtained using

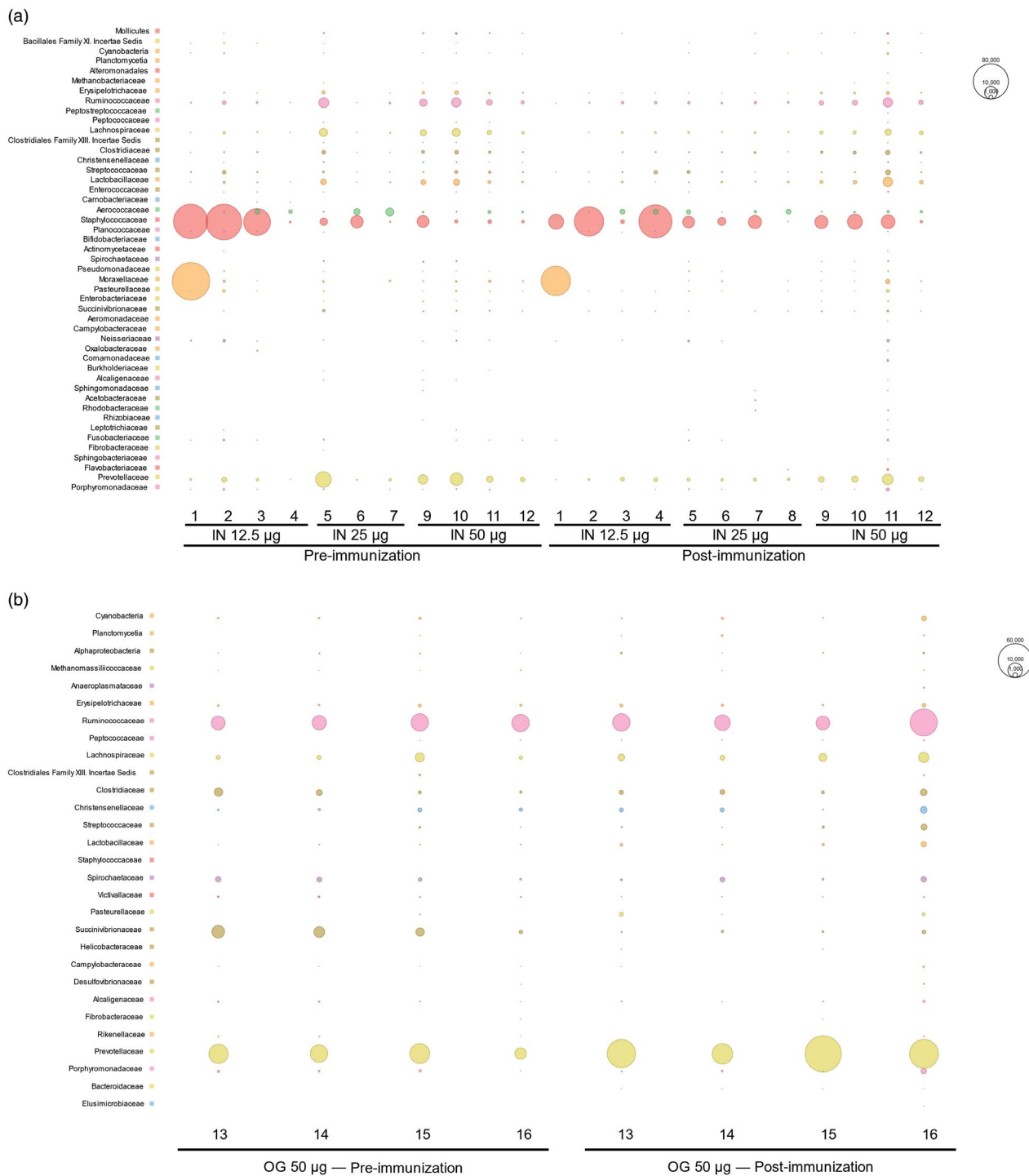


Fig. 6. Bubble charts constructed using MEGAN Community Edition for 16S rRNA sequences in which the radius of each bubble is proportional to the number of 16S rRNA sequences obtained from animals immunized with V antigen-outer membrane vesicles (V-OMV) to visualize the degree of relatedness between samples. Numbers 1–16 represent individual animals. (a) Nasal microbiota of animals pre- and post-immunization with different vaccine doses via the intranasal route. (b) Faecal microbiota of animals pre- and post-immunization with V-OMVs via the oral route.

normal, non-immune, sera. The sera from animals intranasally immunized with V-OMVs at all doses inhibited, to some extent, the binding of mAb 7-3, which at the

higher serum concentrations were comparable to the activity of the reference sera. Sera from animals immunized with 25 or 50 µg of V-OMVs had the highest titres of

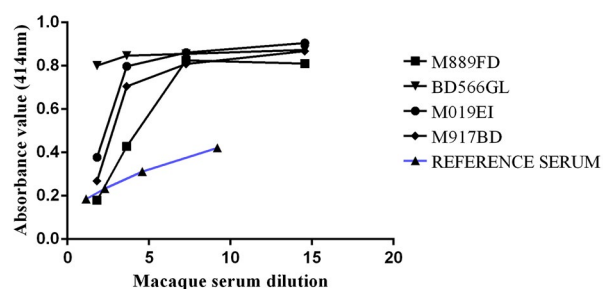


Fig. 7. A competitive enzyme-linked immunosorbent assay (ELISA) assay to assess the functionality of immune sera from V antigen-outer membrane vesicles (V-OMV)-immunized animals. Serial dilutions of sera from animals immunized with V-OMVs identified by individual code numbers shown in the key were tested for their ability to displace a monoclonal V antibody from the surface of the V antigen immobilized in microtitre plate wells. The level of competing activity of immune non-human primate (NHP) serum was determined after subtraction of the activity of non-immune serum. Reference immune serum was from NHPs immunized intramuscularly with recombinant Fraction 1 (F1) and V antigen plus adjuvant.

competitive antibodies (Fig. 7). In contrast, sera from animals immunized orally with V-OMVs had low levels, or no antibodies, capable of competing with mAb 7-3 for binding to V antigen.

The BCA provided a functional activity assessment of the different test groups of samples taken from the immunized NHPs. Throughout the assays conducted, the reference anti-sera (generated by immunizing macaques with recombinant rF1 and rV) provided consistent dose-response BCA behaviour (Table 1).

There was, however, a high background BCA reactivity in many of the macaques at day 0 which was not specific to a particular housing group. Assessment of the health records of the study subjects did not uncover any unreported health conditions and no veterinary adverse health observations were made. Although screened and found to be clear of all known high-consequence pathogens in primates, a routine rectal swab was able to identify *P. aeurugenosa* in one study participant. Although this organism was not causing disease or inducing any observable clinical sign of illness, it is possible that natural background immunity to such a commensal could cross-react with the type three secretion system (TTSS) components of *Y. pestis*. Conservation of the TTSS has been discussed and demonstrated in other studies [34–37]. Thus, it is postulated that the high background BCA observed in some study animals is due to immunity to TTSS elements of commensal bacteria present in the colony. This hypothesis was further supported by ELISA, which confirmed that there was pre-existing immunity in some primates which cross-reacted with *Y. pestis* recombinant V antigen at day 0 (Fig. 3). This immunity was also confirmed in the CE-ELISA (Fig. 7).

Intranasal administration appeared to result in higher serum bactericidal responses for both OMV-antigens. All groups immunized with V-OMVs showed bactericidal activity during the study, with the best response seen at day 42 post-immunization in the group immunized with 50 µg OMV-V intranasally. For F1-OMVs the data also suggested that an intranasal immunization dose of 25 µg was optimal. While day 56 BCA data (Table 1) suggested that there was some waning of immune functional activity in some groups, at day 42 almost all groups (except the lowest intranasally dosed F1-OMV group) appeared to demonstrate functional immunity to *Y. pestis*.

Discussion

Using bacterial OMVs generated by the bioengineering of the major human commensal bacterium, Bt, we have successfully developed formulations of plague vaccine antigens suitable for direct delivery to mucosal sites including the respiratory tract, the site of pneumonic plague infection. Bt OMVs incorporating the V antigen generated robust humoral and cell-mediated immune responses in both the upper and lower respiratory tracts, and/or in the systemic circulation. Using two independent surrogate assays to measure levels of protection, V-OMV elicited properties in the sera that were important in immune protection, including the ability to kill *Y. pestis*.

Protection against pneumonic plague is essential to prevent epidemic spread. An outbreak in Madagascar in 2017 resulted in more than 2400 confirmed cases of plague (confirmed, probable and suspected) and more than 200 deaths; the majority (~77%) of reported cases were clinically classified as pneumonic plague [38]. Foremost among the virulence factors secreted by *Y. pestis* are the F1 and V proteins that are pivotal in preventing phagocytosis (F1) and regulating type III secretion (V) by *Y. pestis*. When secreted by *Y. pestis*, V and other *Yersinia* outer proteins (Yops), also play roles in inhibiting cytokine production, platelet aggregation and apoptosis of macrophages in addition to immune suppression [39]. When combined as purified recombinant proteins, V and F1 represent a powerful candidate vaccine that is amenable to alternative formulations other than typical liquid suspension with alum [40] or alhydrogel [3]; this allows for mucosal or dual route [41] delivery.

Using a prime and single boost oral or nasal immunization protocol, V-OMVs effectively induced antigen-specific IgA in mucosal sites and IgG in the blood; intranasal delivery was the most effective route of administration, particularly for the induction of mucosal IgA responses. Intranasally delivered V-OMVs were also able to elicit cell-mediated immune responses, as evidenced by strong recall responses of PBMCs from immunized animals and

Table 1. Summary of serum antibody bactericidal assay outputs (ED₅₀ in units of % serum[†])

Vaccine	Dose (µg)	Route	Day 0	Day 28	Day 42	Day 56
OMV-F1	50	i.n.	12.1	36.2	14.9	>45
OMV-V	50	i.n.	0.6	5.5	0.8	14.9
OMV-F1	25	i.n.	1.4	1.6	1.5	6.2
OMV-V	25	i.n.	1.9	0.5	15.3	13.7
OMV-F1	12.5	i.n.	>45	21.6	>45	39.2
OMV-V	12.5	i.n.	>45	>45	20.9	22.5
OMV-F1	50	OG	>45	17.0	13.0	> 45
OMV-V	50	OG	>45	1.8	6.3	>45
rF1+rV Alhydrogel	50	i.n.	–	–	–	10.7*

OG = orogastric administration; i.n. = intranasal administration; i.m. = intramuscular administration; OMV = outer membrane vesicles; OMV-V = *Bt* OMVs containing *Y. pestis* V antigen; OMV-F1 = *Bt* OMVs containing *Y. pestis* Fraction 1 (F1) antigen; r = recombinant protein produced in *Escherichia coli*; ED₅₀ = 50% effective dose.

*Average of six determinations; – = not included in the study design.

[†]the initial dilution of antibody in the assay was 45%, hence the limit of the assay was nominally set at 45%. Sera found to have an ED₅₀ below the limit of detection were assigned an ED₅₀ of > 45%.

the production of proinflammatory cytokines. The weaker immunogenicity of V-OMVs delivered via the oral route may reflect the more hostile environment of the GI tract compared with the nasal mucosa, and the need to overcome significant physical (mechanical digestion), chemical (acidic/alkaline pH), biological (enzymes) and microbiological (the microbiota) barriers prior to accessing inductive immune sites in the lower GI tract. However, despite these obstacles, orally delivered V-OMVs were still effective in generating functional antibodies, albeit at lower titres than that in animals immunized nasally with V-OMVs. At the earliest time-point of serological analysis (28 days post-immunization), systemic and mucosal antibody responses were established and increased over time. In comparison with recombinant protein-based vaccines [41], OMV vaccine formulations may, therefore, be less effective at inducing rapid-onset immune responses (i.e. within 14 days). However, it is possible that more intensive boosting using multiple doses could be used to accelerate the onset of immunity and increase the strength and duration of immune responses (i.e. within 14 days); this is feasible for OMV vaccines that are non-invasive and more user-friendly than injected recombinant protein vaccines for which repeated injections would be a problem. Formulations of *N. meningitidis*-based OMV vaccine formulations (MenBvac, VA-Mengoc-BC, PorA P1.6-24 and MeNZB) rely on a three- or four-dose immunization regimen to provide effective protection in children and adults and control of outbreaks of MenB disease [42]. The option to increase the concentration of V antigen in OMV vaccine formulations is not supported by our data; in terms of generating high titres of both mucosal and systemic antibodies intermediate dose of antigen (25 µg) delivered intranasally performed as well as, if not better than, a twofold higher dose.

The assessment of host immune responses in NHPs was complicated by a level of pre-existing immunity in some individuals prior to OMV immunization. This 'background' immunity was confirmed in three independent serum antibody assays conducted at three different laboratories and sites. The health records of the study subjects in question did not show any health conditions and no veterinary health observations were made. More extensive investigations identified that *Pseudomonas aeruginosa* was present in some sample swabs (S.F., unpublished observations). This, however, was not accompanied by symptomatic infection and no veterinary interventions were required. Antibodies to the TTSS and the V antigen of *Y. pestis* are known to cross-react with that of other pathogenic Gram-negative bacteria, including *P. aeruginosa*, *Vibrio* species and *Aeromonas* species that encode homologues of the *Yersinia* V antigen [34]. While the presence of these bacterial species could not be confirmed in samples collected during the study, it is possible that they had infected these animals at some time prior to this study and were subsequently eliminated by the immune response they invoked; it is also possible that V-OMV vaccines may have been assisted by such pre-existing cross-reactive immunity. It is noteworthy that this phenomenon of 'background' immunity was not seen in every animal.

An important immune correlate for protection by a candidate vaccine is the ability to generate neutralizing antibodies that inhibit the killing of host target cells by bacteria and/or are cytotoxic and can actively kill the bacteria [3]. We used two assays to demonstrate the generation of neutralizing antibodies in OMV-immunized animals. The first was a competitive ELISA in which immune sera from V-OMV immunized animals was able to compete for binding to the protective epitope in the V antigen with a monoclonal antibody (mAb 7-3), which

has previously been shown to protect mice fully by passive transfer against direct exposure to *Y. pestis* [1]. The second assay is a novel *Y. pestis* BCA developed specifically for this study, in which immune sera from F1- and V-OMV immunized NHPs were shown to kill bacteria via antibody-dependent complement-mediated killing (ADCC). Intranasally administered V-OMVs were particularly effective at generating high titres of bactericidal antibodies. Interpretation of the BCA data is complicated by the suggestion of pre-existing cross-reactive immunity in some of the macaques which existed before immunization. This is evident in Fig. 3, where the group which eventually received intranasal vaccination with 50 µg of OMV-V vaccine had detectable anti-V immunity 14 days before vaccination and at day 0. This does not, however, account for all the prevaccination BCA activity. Future studies involving the use of mutants might be helpful in differentiating any cross-reactive immunity. The bactericidal activity of sera from F1-OMV immunized animals was perhaps surprising, in view of their weaker immunogenicity and the low levels of antigen-specific antibodies they generated compared with V-OMV vaccines (Fig. 2). The low levels of F1 expression in Bt, which required sensitive LC-MS techniques to detect, may be a consequence of inherent differences in the translational machinery and requirements for efficient synthesis and/or in secretion sequences that were used to target newly synthesized proteins to the periplasm and OMVs in *Yersinia versus Bacteroides* species. In addition, the inability of Bt to efficiently synthesize proteins encoded within the *cafI* operon, such as *cafIM* (which encodes the CafM1 protein that acts as a chaperone for F1 with a role in its post-translational folding and secretion [43,44]), could also compromise Bt expression of F1. The inability to detect F1 in F1-OMV lysates using various antibodies in immunoblotting protocols may also be indicative of low levels of expression. Alternatively, it could be that the protein was not being expressed in its native form, or that expression of altered structural determinants resulted in the loss of immune epitopes following expression in Bt and OMVs. In summary, the results from the two independent assays provide compelling evidence for the development of a protective immune response in OMV-immunized NHPs.

Studies performed with various animal species (including NHPs [45]) indicate that, although neutralizing antibodies provide protection against exposure, the development of cell-mediated immunity is essential for protection and clearance of bacteria from the host. Studies using mice with targeted mutations that disrupt T helper type 1 (Th1) or Th2 CD4 T cells responses have shown that Th1-driven cell-mediated immune responses are particularly important in protecting against plague [46]. The

ability of the V protein to up-regulate IL-10 production, which down-regulates the generation of proinflammatory cytokines such as TNF- α and IFN- γ , is a key mechanism for virulence and immunosuppression; this contributes to the disruption of a balanced Th1/Th2 response which, alongside specific antibodies, appears to be optimal for protection [3]. In this context the recall response of lymphocytes from V-OMV immunized animals, which is characterized by the secretion of various proinflammatory cytokines, is significant and of predicted benefit to the mobilizing (MCP-1, IL-8) and activating (IL-1 β , IL-6, IL-23) components of cell-mediated immune responses in response to plague infection in immunized animals. Of note, the lowest dose (12.5 µg) of intranasally administered V-OMVs was particularly effective at eliciting cytokine secretion by PBMCs (Fig. 5). The reasons for this phenomenon are unclear, but it is possible that higher doses of V-OMVs may have elicited qualitatively different (tolerogenic) immune responses similar to that described for other nanoparticle-based vaccine delivery systems [47].

In summary, the key findings from our study were that Bt OMVs could express plague antigens, and in particular the V antigen, in a stable and correct immunogenic form. These engineered OMV vaccine formulations elicited specific immune and antibody responses both in the serum and at mucosal surfaces, including the generation of antibodies able to kill plague bacteria. Our results also highlight the key advantages our Bt OMV vaccine technology offers over available plague vaccines in terms of technology and approach. First, OMV vaccine delivery via oral or nasal administration allows for needle-free, multi-dose delivery that would enable mass vaccination programmes in challenging environments and at relatively low cost. Advantageously, this route of immunization also specifically targets the primary sites of mucosal infection which injectable whole-cell vaccines or subunit vaccines do not. Secondly, compared with subunit or whole cell vaccines, the manufacture and reformulation of OMV vaccines is quicker, and can be achieved using readily accessible and relatively inexpensive technology that has been commercially validated in the production of licensed MenB OMV vaccines which are in current use [48]. Thirdly, patient acceptance is expected to be high, and unlike injection-based vaccines only require out-of-clinic management. Fourthly, OMVs have intrinsic adjuvanticity and the ability to activate both the innate and adaptive arms of the immune system [22,23] compared with the requirement for chemical adjuvants such as alum to improve immunogenicity of subunit vaccines. Fifthly, OMV vaccines are acellular and non-infectious, making them safer than live attenuated or killed whole cell vaccines. Finally, OMVs are stable for ultra-long periods in liquid and lyophilized form [49], and for several weeks in solution form across

a wide range of temperatures including 40°C. This allows distribution to the point of need without cold chain or cold storage, which is particularly important in tropical and low-income settings. These properties enable Bt-OMV vaccines to align well with the WHO Blueprint therapeutic product profile [11].

Acknowledgements

This work was supported by SBRI/Innovate UK under the award 971525 (to S. R. C.) and by the UK Biotechnology and Biological Sciences Research Council (BBSRC) under grant numbers BB/L004291/1 and BB/J004529/1 (S. R. C.). The funders had no role in study design, data collection and interpretation nor the decision to submit the work for publication. The authors would like to thank Laura Hunter and Javier Salguero and the PHE Histology unit for their extensive tissue processing and analysis. The authors also acknowledge the support provided by Dr Phil Nugent, Kerry Godwin, Dr Andrew Gorringer, Dr Steven Taylor, Steve Thomas, Dr Francis Alexander, Dr Caroline Cruttwell and Dr Julia Vipond for technical and operational aspects of the PHE elements of the study, as well as the various staff involved in the humane treatment and husbandry of all animals used in the project. The authors also thank the National Institutes of Allergy and Infectious Disease for permission to use *Y. pestis* strain CO92, and Dr Judith Pell for proof reading and editing the manuscript.

Author contributions

Conceptualization: S. R. C., S. F., E. D. W., M. S.; investigation: A. C., A. M. C., R. S., U. W., E. J., N. J. W., S. H., M. D.; formal analysis: A. C., A. M. C., A. T., N. J. W., P. B., S. F., E. D. W., S. H., M. D.; funding acquisition: S. R. C., M. S.; project administration: M. S.; writing, original draft preparation: S. R.C.; writing, review and editing: A. M. C., R. S., E. J., S. F., E. D. W.

Disclosures

The authors declare no financial or commercial conflicts of interest.

References

- Williamson ED, Flick-Smith HC, Waters E *et al.* Immunogenicity of the rF1+rV vaccine for plague with identification of potential immune correlates. *Micro Pathogen* 2007; **42**:11–21.
- Smiley ST. Cell-mediated defense against *Yersinia pestis* infection. *Adv Exp Med Biol* 2007; **603**:376–86.
- Williamson ED. Plague. *Vaccine* 2009; **27**(Suppl 4):D56–60.
- Meyer KF, Cavanaugh DC, Bartelloni PJ, Marshall JD Jr. Plague immunization. I. Past and present trends. *J Infect Dis* 1974; **129**:S13–S18.
- Parkhill J, Wren BW, Thomson NR *et al.* Genome sequence of *Yersinia pestis*, the causative agent of plague. *Nature* 2001; **413**:523–7.
- Quenee LE, Schneewind O. Plague vaccines and the molecular basis of immunity against *Yersinia pestis*. *Hum Vaccin* 2009; **5**:817–23.
- Williamson ED, Flick-Smith HC, Lebutt C *et al.* Human immune response to a plague vaccine comprising recombinant F1 and V antigens. *Infect Immun* 2005; **73**:3598–608.
- Oyston PC, Williamson ED. Prophylaxis and therapy of plague. *Expert Rev Anti Infect Ther* 2013; **11**:817–29.
- Feodorova VA, Corbel MJ. Prospects for new plague vaccines. *Expert Rev Vaccines* 2009; **8**:1721–38.
- Saroja C, Lakshmi P, Bhaskaran S. Recent trends in vaccine delivery systems: A review. *Int J Pharm Invest* 2011; **1**:64–74.
- World Health Organization (WHO). WHO Target Product Profile for Plague Vaccines. Geneva: WHO, 2018.
- Zhao L, Seth A, Wibowo N *et al.* Nanoparticle vaccines. *Vaccine* 2014; **32**:327–37.
- Singh M, Chakrapani A, O'Hagan D. Nanoparticles and microparticles as vaccine-delivery systems. *Expert Rev Vaccines* 2007; **6**:797–808.
- Gerritzen MJH, Martens DE, Wijffels RH, van der Pol L, Stork M. Bioengineering bacterial outer membrane vesicles as vaccine platform. *Biotechnol Adv* 2017; **35**:565–74.
- McBroom AJ, Kuehn MJ. Release of outer membrane vesicles by Gram-negative bacteria is a novel envelope stress response. *Mol Microbiol* 2007; **63**:545–58.
- Jeannin P, Magistrelli G, Goetsch L *et al.* Outer membrane protein A (OmpA): a new pathogen-associated molecular pattern that interacts with antigen presenting cells-impact on vaccine strategies. *Vaccine* 2002; **20**:A23–A27.
- Alaniz RC, Deatherage BL, Lara JC, Cookson BT. Membrane vesicles are immunogenic facsimiles of *Salmonella typhimurium* that potently activate dendritic cells, prime B and T cell responses, and stimulate protective immunity in vivo. *J Immunol* 2007; **179**:7692–701.
- Stephens DS, Edwards KM, Morris F, Mcgee ZA. Pili and outer-membrane appendages on *Neisseria meningitidis* in the cerebrospinal fluid of an infant. *J Infect Dis* 1982; **146**:568–75.
- Collins BS. Gram-negative outer membrane vesicles in vaccine development. *Discov Med* 2011; **62**:7–15.
- de Kleijn ED, de Groot R, Labadie J *et al.* Immunogenicity and safety of a hexavalent meningococcal outer-membrane-vesicle vaccine in children of 2–3 and 7–8 years of age. *Vaccine* 2000; **18**:1456–66.
- Sandhu S, Feiring B, Oster P *et al.* Immunogenicity and safety of a combination of two serogroup B meningococcal outer membrane vesicle vaccines. *Clin Vaccine Immunol* 2007; **14**:1062–9.

- 22 Kaparakis-Liaskos M, Ferrero RL. Immune modulation by bacterial outer membrane vesicles. *Nat Rev Immunol* 2015; **15**:375–87.
- 23 Hickey CA, Kuhn KA, Donermeyer DL *et al.* Colitogenic *Bacteroides thetaiotaomicron* antigens access host immune cells in a sulfatase-dependent manner via outer membrane vesicles. *Cell Host Microbe* 2015; **17**:672–80.
- 24 Shoemaker NB, Getty C, Gardner JF, Salyers AA. Tn4351 Transposons in *Bacteroides* spp. and mediates the integration of plasmid R751 into the *Bacteroides* chromosome. *J Bacteriol* 1986; **165**:929–36.
- 25 Graham VA, Hatch GJ, Bewley KR *et al.* Efficacy of primate humoral passive transfer in a murine model of pneumonic plague is mouse strain-dependent. *J Immunol Res* 2014; **2014**:807564.
- 26 Wegmann U, Horn N, Carding SR. Defining the *Bacteroides* ribosomal binding site. *Appl Environ Microbiol* 2013; **79**:1980–9.
- 27 Stentz R, Horn N, Cross K *et al.* Cephalosporinases associated with outer membrane vesicles released by *Bacteroides* spp. protect gut pathogens and commensals against beta-lactam antibiotics. *J Antimicrob Chemother* 2015; **70**:701–9.
- 28 Chen Z, Yeoh YK, Hui M *et al.* Diversity of macaque microbiota compared to the human counterparts. *Sci Rep* 2018; **8**:15573.
- 29 McKenna P, Hoffmann C, Minkah N *et al.* The macaque gut microbiome in health, lentiviral infection, and chronic enterocolitis. *PLOS Pathog* 2008; **4**:e20.
- 30 Ochman H, Worobey M, Kuo CH *et al.* Evolutionary relationships of wild hominids recapitulated by gut microbial communities. *PLOS Biol* 2010; **8**:e1000546.
- 31 Moeller AH, Caro-Quintero A, Mjungu D *et al.* Cospeciation of gut microbiota with hominids. *Science* 2016; **353**:380–2.
- 32 Williamson ED, Packer PJ, Waters EL *et al.* Recombinant (F1+V) vaccine protects cynomolgus macaques against pneumonic plague. *Vaccine* 2011; **29**:4771–7.
- 33 Hill J, Leary S, Smither S *et al.* N255 is a key residue for recognition by a monoclonal antibody which protects against *Yersinia pestis* infection. *Vaccine* 2009; **27**:7073–9.
- 34 Sawa T, Katoh H, Yasumoto H. V-antigen homologs in pathogenic gram-negative bacteria. *Microbiol Immunol* 2014; **58**:267–85.
- 35 Frank DW, Vallis A, Wiener-Kronish JP *et al.* Generation and characterization of a protective monoclonal antibody to *Pseudomonas aeruginosa* PcrV. *J Infect Dis* 2002; **186**:64–73.
- 36 Goure J, Broz P, Attree O, Cornelis GR, Attree I. Protective anti-V antibodies inhibit *Pseudomonas* and *Yersinia* translocon assembly within host membranes. *J Infect Dis* 2005; **192**:218–25.
- 37 Sawa T, Ito E, Nguyen VH, Haight M. Anti-PcrV antibody strategies against virulent *Pseudomonas aeruginosa*. *Hum Vaccin Immunother* 2014; **10**:2843–52.
- 38 World Health Organization Regional Office for Africa. Plague Outbreak Madagascar. External Situation Report. WHO, 2017. Available at: <https://www.afro.who.int/health-topics/plague/plague-outbreak-situation-reports> (accessed 11 August 2018).
- 39 Pouliot K, Pan N, Wang S, Lu S, Lien E, Goguen JD. Evaluation of the role of LcrV-Toll-like receptor 2-mediated immunomodulation in the virulence of *Yersinia pestis*. *Infect Immun* 2007; **75**:3571–80.
- 40 Heath DG, Anderson GW Jr, Mauro JM *et al.* Protection against experimental bubonic and pneumonic plague by a recombinant capsular F1-V antigen fusion protein vaccine. *Vaccine* 1998; **16**:1131–7.
- 41 Moore BD, New RRC, Butcher W *et al.* Dual route vaccination for plague with emergency use applications. *Vaccine* 2018.
- 42 Bai X, Findlow J, Borrow R. Recombinant protein meningococcal serogroup B vaccine combined with outer membrane vesicles. *Expert Opin Biol Ther* 2011; **11**:969–85.
- 43 Zav'yalov VP, Chernovskaya TV, Navolotskaya EV *et al.* Specific high affinity binding of human interleukin 1 beta by Caf1A usher protein of *Yersinia pestis*. *FEBS Lett* 1995; **371**:65–8.
- 44 Galyov EE, Karlish AV, Chernovskaya TV *et al.* Expression of the envelope antigen F1 of *Yersinia pestis* is mediated by the product of caf1M gene having homology with the chaperone protein PapD of *Escherichia coli*. *FEBS Lett* 1991; **286**:79–82.
- 45 Williamson ED, Oyston PC. The natural history and incidence of *Yersinia pestis* and prospects for vaccination. *J Med Microbiol* 2012; **61**:911–8.
- 46 Elvin SJ, Williamson ED. Stat 4 but not Stat 6 mediated immune mechanisms are essential in protection against plague. *Microb Pathog* 2004; **37**:177–84.
- 47 Cappellano G, Comi C, Chiochetti A, Dianzani U. Exploiting PLGA-based biocompatible nanoparticles for next-generation tolerogenic vaccines against autoimmune disease. *Int J Mol Sci* 2019; **20**.
- 48 Christodoulides M, Heckels J. Novel approaches to *Neisseria meningitidis* vaccine design. *Pathog Dis* 2017; **75**.
- 49 Alves NJ, Turner KB, Medintz IL, Walper SA. Protecting enzymatic function through directed packaging into bacterial outer membrane vesicles. *Sci Rep* 2016; **6**:24866.

Supporting Information

Additional supporting information may be found in the online version of this article at the publisher's web site:

Fig. S1. Schematic of OMV plague vaccine NHP immunisations via the intranasal (IN) or oral route and analyses.

Fig. S2. Mucosal humoral immune response to F OMV vaccine (a–d). Bronchoalveolar lavage fluid (BAL) (e) and salivary gland homogenates (f) were analysed for antigen specific IgA at the study end point. The data shown represents mean \pm SEM values.

Fig. S3. Histopathological sections of immunised macaques receiving 50 ug dose stained with H.E. A. Spleen showing

activated splenic follicles (f) within the white pulp. B. Lymph node showing active lymphoid follicles(f) within the cortex. C. Duodenum. Lympho plasmacytic infiltration within the mucosa and submucosa (arrow). D. Jejunum. Lympho plasmacytic infiltration within the mucosa and submucosa,

showing proliferation of lymphoid follicle like structures (arrow). E. Ileum. Lympho plasmacytic infiltration within the mucosa and submucosa adjacent to activated Peyer Patches (arrow). F. Lung. Focal proliferation of the BALT without any presence of pathogen within the organ parenchyma

RESEARCH ARTICLE



Bioengineering commensal bacteria-derived outer membrane vesicles for delivery of biologics to the gastrointestinal and respiratory tract

Ana L. Carvalho^a, Sonia Fonseca^a, Ariadna Miquel-Clopés^a, Kathryn Cross^b, Khoon-S. Kok^{a,c}, Udo Wegmann^a, Katherine Gil-Cordoso^{a,d}, Eleanor G. Bentley^e, Sanaria H.M. Al Katy^{*e}, Janine L. Coombes^e, Anja Kipar^f, Regis Stentz^a, James P. Stewart^e and Simon R. Carding^{a,c}

^aGut Microbes and Health Research Programme, Quadram Institute Bioscience, Norwich, UK; ^bCore Science Resources, Quadram Institute Bioscience, Norwich, UK; ^cNorwich Medical School, University of East Anglia, Norwich, UK; ^dDepartment of Biochemistry and Biotechnology, Universitat Rovira i Virgili, Tarragona, Spain; ^eDepartment of Infection Biology, University of Liverpool, Liverpool, UK; ^fInstitute of Veterinary Pathology, Vetsuisse Faculty, University of Zurich, Zurich, Switzerland

ABSTRACT

Gram-negative bacteria naturally produce and secrete nanosized outer membrane vesicles (OMVs). In the human gastrointestinal tract, OMVs produced by commensal Gram-negative bacteria can mediate interactions amongst host cells (including between epithelial cells and immune cells) and maintain microbial homeostasis. This OMV-mediated pathway for host-microbe interactions could be exploited to deliver biologically active proteins to the body. To test this we engineered the Gram-negative bacterium *Bacteroides thetaiotaomicron* (Bt), a prominent member of the intestinal microbiota of all animals, to incorporate bacteria-, virus- and human-derived proteins into its OMVs. We then used the engineered Bt OMVs to deliver these proteins to the respiratory and gastrointestinal (GI)-tract to protect against infection, tissue inflammation and injury. Our findings demonstrate the ability to express and package both *Salmonella enterica* ser. Typhimurium-derived vaccine antigens and influenza A virus (IAV)-derived vaccine antigens within or on the outer membrane of Bt OMVs. These antigens were in a form capable of eliciting antigen-specific immune and antibody responses in both mucosal tissues and systemically. Furthermore, immunisation with OMVs containing the core stalk region of the IAV H5 hemagglutinin from an H5N1 strain induced heterotypic protection in mice to a 10-fold lethal dose of an unrelated subtype (H1N1) of IAV. We also showed that OMVs could express the human therapeutic protein, keratinocyte growth factor-2 (KGF-2), in a stable form that, when delivered orally, reduced disease severity and promoted intestinal epithelial repair and recovery in animals administered colitis-inducing dextran sodium sulfate. Collectively, our data demonstrates the utility and effectiveness of using Bt OMVs as a mucosal biologics and drug delivery platform technology.

ARTICLE HISTORY

Received 20 November 2018
Revised 16 May 2019
Accepted 10 June 2019

KEYWORDS

Commensal bacteria; bacterial microvesicles; outer membrane vesicles; mucosal drug delivery; mucosal vaccines; therapeutic proteins

Introduction

Described over 50 years ago by Bishop and Work (1965) as “extracellular glycolipids” produced by *Escherichia coli*, outer membrane vesicles (OMVs) are now considered to be naturally produced and secreted by most Gram-negative bacteria. Analyses of these 20–400 nm bilayered lipid membrane spherical structures have shown that they contain major components of the outer membrane such as lipopolysaccharide (LPS) in addition to the periplasmic contents of their ‘parent’ bacterium [1,2].

Historically, OMVs have been associated with pathogenesis and the storage and transportation of virulence factors produced by enteric Gram-negative pathogens including *Helicobacter pylori* (VacA), *Shigella dysenteriae*

(Shiga toxin) and enterohemorrhagic *Escherichia coli* (ClyA) [3–5]. Recently, this paradigm for OMV function has been questioned due to new evidence demonstrating a non-pathogenic, mutualistic role for the OMVs produced by commensal gut bacteria. Members of the genus *Bacteroides* exclusively package carbohydrate and protein hydrolases in OMVs that perform a ‘social function’ by providing substrates for utilization by other bacteria and contributing to microbiota homeostasis [6,7]. We [8,9] and others [10] have extended these observations providing evidence for a broader role of OMVs in gastrointestinal (GI)-tract homeostasis and the ability of *Bacteroides*-derived OMVs to influence host immune and epithelial cell responses.

CONTACT Simon R. Carding  Simon.Carding@Quadram.ac.uk  Gut Microbes and Health Research Programme, Quadram Institute Bioscience, Norwich Research Park, Norwich NR4 7UA, UK

*Present affiliation for Sanaria H. M. Al Katy is Department of Pathology and Poultry Diseases, College of Veterinary Medicine, University of Mosul, Mosul, Iraq

 Supplemental data for this article can be accessed [here](#).

OMVs can contain adhesins, sulfatases and proteases which facilitate their interaction with host epithelial cells, allowing them to enter these cells through numerous routes, including micropinocytosis, lipid raft- and clathrin-dependent endocytosis [11–13]. *Bacillus fragilis* OMVs containing polysaccharide A are detected by dendritic cells via Toll Like Receptor (TLR) 2 leading to enhanced T regulatory cell activity and production of anti-inflammatory cytokines (IL-10) that protect the host from experimental colitis [10]. We have demonstrated that OMVs produced by the human commensal bacterium *B. thetaiotaomicron* (Bt) can activate mammalian intestinal epithelial cell (IEC) intracellular Ca²⁺ signalling [8]. This host cell Ca²⁺ signalling response was dependent on Minpp, a novel constituent of these OMVs. Minpp is a homologue of a mammalian inositol phosphate polyphosphatase cell-signalling enzyme. Collectively, these findings demonstrate a non-pathogenic and beneficial role for OMVs produced by commensal *Bacteroides* species and are consistent with the concept that packaging of bioactive macromolecules in OMVs enables members of the intestinal microbiota to influence host cell physiology and establish bacteria-host mutualism [13].

It is feasible that this OMV-mediated pathway for host-microbe interaction could be exploited and used to deliver biologically active proteins to the body. Delivery to mucosal sites such as the GI- and respiratory tracts would be particularly valuable as they are vulnerable to injury and disease as a result of exposure to noxious environmental chemicals and pathogens [13,14]. Indeed, OMVs from *Neisseria meningitidis* and *Vibrio cholera* have been incorporated into licensed vaccine formulations [15]; those derived from *N. meningitidis* have been successfully used to immunise both children and adults and effectively control serogroup B meningococcal (MenB) disease outbreaks [16,17]. However, there are several limitations to using non-commensal, pathogen-derived OMVs as drug and vaccine delivery systems, particularly: their potential for unintended toxicity due to associated toxins; low expression levels of the heterologous antigens; variable efficacy depending on source and formulation; and the need for

exogenous adjuvants in some applications. In principal, these limitations could be overcome by bioengineering the OMVs to improve their drug delivery capability [18]. Alternatively, non-pathogenic commensal bacteria could be used as a source of OMVs to reduce toxicity and improve safety.

To test this strategy we undertook a proof-of-principle study to determine the suitability of using OMVs produced by Bt to deliver bacteria-, virus- and human-derived proteins to the respiratory and GI-tract of mouse models (for respiratory influenza A virus infection and acute intestinal colitis) to protect them against infection, tissue inflammation and injury. Our findings, presented here provide evidence for the utility and effectiveness of using Bt OMVs as a mucosal biologics and drug delivery platform technology.

Material and methods

Bacteria strains, media and culture

Bt and its derivative strains (Table 1) were grown under anaerobic conditions at 37°C in an anaerobic cabinet. Bacterial starter-cultures were grown overnight in 20 ml “Brain Heart Infusion” (BHI) medium (Oxoid) supplemented with 15 µM haemin (Sigma-Aldrich) (BHIH). For OMV preparations, Bt cultures were inoculated with 0.5 ml of the starter-culture in a total volume of 500 ml BHI supplemented with 0.75 µM haemin. Cells were harvested after 16 h at an approximate OD_{600 nm} of 4.0, which corresponds to early stationary phase. Antibiotic-resistance markers in Bt were selected using erythromycin (5 µg/ml) and tetracycline (1µg/ml). *Escherichia coli* strains were grown in Luria-Bertani (LB) medium at 37°C with ampicillin 100 µg/ml (or 200 µg/ml trimethoprim for strain J53 [pR751]). *Lactococcus lactis* strain UKLc10 and its derivative strains were grown in M17 medium (Oxoid) supplemented with 5 g/l glucose at 30°C. Antibiotics were added as selection agents when appropriate: ampicillin 200µg/ml, erythromycin 5 µg/ml and

Table 1. Strains of bacteria used in this study.

Species	Strain	Plasmid	Protein expressed	Antibiotic selection*	Reference
<i>E. coli</i>	Rosetta 2(DE3) pLysS	pGH165	St OmpA	Amp, Cm	This study
	Rosetta 2(DE3) pLysS	pGH201	St SseB	Amp, Cm	This study
<i>Bt</i>	VPI-5482				DMSZ Collection
	GH290			Tet	This study
	GH490	pGH090		Ery	[21]
	GH484	pGH182	St OmpA	Ery	This study
	GH486	pGH183	St SseB	Ery	This study
	GH474	pGH173	Hu. KGF-2	Ery	This study
	GH503	pGH184	IAV H5F	Ery	This study
<i>S. enterica</i> ser. Typhimurim	SL1344				DMSZ collection
<i>L. lactis</i>	UKLc10				[22]

*Amp = ampicillin; Cm = chloramphenicol; Tet = tetracycline; Ery = erythromycin

Table 2. Primer sequences used in this study.

Primer	Sequence (5' → 3') ^a
f-5'ompA_SphI	ATCTGCATGCTTTCGAGGAAGAACCATGGTTGC
r-5'ompA_Sall	ATACGTCGACAATATAGCGGACTGCAATCC
f-3'ompA_BamHI	ACTTGGATCCTTCTGAATCGTGTGGTATTGG
r-3'ompA_SacI	ACTAGAGCTCATCTGTAGAGAAGAAACGGG
SPBTompA_fwd	CATGTTGCTGGCTTTTCCGGCGTTGCGTCTGCTTCTG CGCAGCAAACCGTGACTGTAAGTGAATACGAGGTTATTCATATGTGACC
SPBTompA_rev	AATTCGTCACATATGAATAACCTCGTATTACAGTTACAGTCACGG TTTGCTGCGCAGAAGCGACAGACGCAACCGCGCAAAGCCAGCAA
OmpAST_fwd	TGACCATATGGCTCCGAAAGATAACACC
OmpAST_rev	GTCAGAATTCTTAAGCCTGCGGCTGAGTTA
SseB_fwd	TGACCATATGTCTTCAGGAAACATCTT
SseB_rev	TGACGAATTCATGAGTACGTTTTCTGCG
XhoI_STOmpA_rev	ATATCTCGAGGAACTTAAGCCTGCGG
XhoI_SseB_rev	ATATCTCGAGATGAGTACGTTTTCTGCG

chloramphenicol 10 µg/ml. The *E. coli* strain J53/R751 was supplemented with trimethoprim 200 µg/ml when grown for 18 h. The *E. coli* strain GC10 and the *L. lactis* strain UKLc10 were transformed by electroporation using a Gene Pulser II (Bio-Rad). For constructs relating to pUK200, the host *L. lactis* strain UKLc10 was used. Construction of other plasmids described below was achieved using *E. coli* strain GC10 as the host. Plasmids were mobilized from the *E. coli* into the Bt following a triparental filter mating protocol [19] using the helper strain J53/R751. All primers used are detailed in Table 2.

Construction of a *BT_3852* deletion mutant

A 1018 bp chromosomal DNA fragment upstream from *BT_3852* and including the first 18 nucleotides of its 5'-end region was amplified by PCR using the primer pair f-5'ompA_SpHI, r-5'ompA_Sall. This product was then cloned into the SpHI/Sall sites of the *E. coli*-*Bacteroides* suicide shuttle vector pGH014 [20]. A 761 bp chromosomal DNA fragment downstream from *BT_3852*, including the last 46 nucleotides of the 3'-end region, was amplified by PCR using the primer pair f-3'ompA_BamHI, r-3'ompA_SacI and was cloned into the BamHI/SacI sites of the pGH014-based plasmid. The resulting plasmid containing the $\Delta BT_{3852}::tetQ$ construct, was mobilized from *E. coli* strain GC10 into Bt by triparental filter mating [19], using *E. coli* HB101(pRK2013) as the helper strain. Transconjugants were selected on BHI-haemin agar containing gentamicin (200 mg/L) and tetracycline (1 mg/L). Determination of susceptibility to either tetracycline or erythromycin was done to identify recombinants that were tetracycline resistant and erythromycin susceptible after re-streaking transconjugant bacteria on LB-agar containing tetracycline or

both antibiotics. PCR analysis and sequencing were used to confirm allelic exchange. A transconjugant, GH290, containing the $\Delta BT_{3852}::tetQ$ construct inserted into the Bt chromosome was selected for further studies.

Generation of recombinant *BT* strains

BT Salmonella OmpA/SseB

The *Bacteroides* expression vector pGH090 [21] was first digested with *NdeI* to remove this site by Klenow treatment and to create a blunt-ended fragment that was then religated. A sequence containing 90 bp of the *BT_3852* gene 5' end (encoding a major outer membrane protein, OmpA) corresponding to the signal peptide sequence (SpOmpA) of the protein obtained from the microbial genome database (<http://mbgd.genome.ad.jp/>) was used to design the complementary oligonucleotide pair SPBTompA_fwd and SPBTompA_rev. Signal peptide prediction was obtained by SignalP (<http://www.cbs.dtu.dk/services/SignalP/>). After annealing of the oligonucleotides the resulting double-strand DNA contained *EcoRI* and *SpHI* 5' overhangs at each end. This linker was cloned into the *EcoRI/SpHI* sites of the *NdeI* deleted version of pGH090, resulting in the pGH202 plasmid. The 1131 bp *Salmonella ompA* (without signal peptide) and the 591 bp *sseB* coding region were amplified by PCR from *S. enterica* ser. Typhimurium SL 1334 genomic DNA using the primer pairs OmpAST_fwd with OmpAST_rev, and SseB_fwd with SseB_rev, respectively. The resulting fragments were digested with *NdeI* and *EcoRI* and cloned into *NdeI/EcoRI*-digested pGH202, yielding plasmids pGH182 and pGH183, respectively. The latter plasmid was then transformed into *E. coli*-competent cells (GC10) by electroporation using a Gene Pulser II (Bio-Rad). Successful cloning was confirmed by sequencing. The plasmid was mobilized from *E. coli* to Bt

using a triparental mating procedure [19], together with *E. coli* J53 (pR751); the correct structure of the Bt carrying pGH182 (GH484) was confirmed by sequencing.

BT IAV

A 635bp synthetic gene construct encoding a synthetic influenza (H5F; from IAV strain H5N1 [VN/04:A/VietNam/1203/04]) pre-fusion headless HA mini-stem N-terminally fused to the OmpA signal peptide of Bt was created *in silico* and its codon usage was optimised for expression in the same species. The resulting gene cassette was obtained by gene synthesis and subsequently cloned into the *E. coli* plasmid pEX-K168 (Eurofins). The cassette contained *Bsp*HI and *Eco*RI restriction sites at its 5' and 3' ends, respectively, allowing for the translational fusion of the gene to the start codon in the *Bacteroides* expression vector pGH090 [21]. The gene was excised from pEX-K168 using *Bsp*HI and *Eco*RI and ligated into the *Nco*I/*Eco*RI-restricted pGH090 expression vector, resulting in pGH184. Finally the sequence integrity of the cloned fragment was confirmed by sequencing. The plasmid was mobilized from *E. coli* into Bt through a triparental mating procedure.

BT KGF-2

A 581bp synthetic gene construct encoding the human fibroblast growth factor-10/keratinocyte growth factor-2 (KGF-2) N-terminally fused to the OmpA signal peptide of Bt was created *in silico* and its codon usage was optimised for expression in the same species. The resulting gene cassette was obtained by gene synthesis and subsequently cloned into the *E. coli* plasmid pEX-A2 (Eurofins) as described for the IAV constructs. The cassette contained *Bsp*HI and *Eco*RI restriction sites at its 5' and 3' ends, respectively, allowing for the translational fusion of the gene to the start codon in the *Bacteroides* expression vector pGH0902. The gene was excised from pEX-A2 using *Eco*53KI and *Eco*RI and ligated into pUK200 [22], which had been restricted with *Sma*I and *Eco*RI, resulting in plasmid pUK200_KGF-2. Next the KGF-2 cassette was excised from pUK200_KGF-2 through restriction with *Bsp*HI and *Eco*RI and subsequently ligated into the *Nco*I/*Eco*RI-restricted pGH090 expression vector, resulting in pGH173. Finally the sequence integrity of the cloned fragment was confirmed by sequencing. The plasmid was mobilized from *E. coli* into Bt using a triparental mating procedure.

Expression and purification of recombinant StOmpA and StSseB

StOmpA was cloned into His6-tag expression vector pET-15b (Novagen). Briefly, PCR fragments incorporating the coding sequences of *ompA* and *sseB* genes

were cloned into the *Nde*I/*Xho*I restriction sites of pET-15b and the resulting plasmids pGH165 and pGH201 transformed into Rosetta2 (DE3) pLysS cells (Table 1). Cultures of the resulting strains were induced at an $OD_{600\text{ nm}}$ of 0.6 by adding 1mM IPTG for 5 h after which time cells were harvested by centrifugation (5500 g for 20 min). The pellet was stored at -20°C for future use. StOmpA and StSseB proteins were purified under native conditions using protocols adapted from the QIAexpress Ni-NTA Fast Start Handbook (Qiagen) with the amount of protein recovered determined using the Bio-Rad Protein Assay.

OMV isolation and characterisation

OMVs were isolated following a method adapted from Stentz et al. [20]. Briefly, cultures of Bt (500 mL) were centrifuged at 5500 g for 45 min at 4°C and the supernatants filtered through polyethersulfone (PES) membranes (0.22 μm pore-size) (Sartorius) to remove debris and cells. Supernatants were concentrated by ultrafiltration (100 kDa molecular weight cut-off, Vivaspin 50R, Sartorius), the retentate was rinsed once with 500 mL of PBS (pH 7.4) and concentrated to 1 mL (approx. 700 $\mu\text{g}/\text{mL}$ total protein). The final OMV suspensions were filter sterilized (0.22 μm pore size). The protein content of the final OMV suspensions was determined using the Bio-Rad Protein Assay.

The distribution of heterologous proteins within Bt OMVs was established in a Proteinase K accessibility/protection assay [20]. Briefly, a suspension of 250 μg (total protein) of OMVs in 0.1 M phosphate/1 mM EDTA buffer (pH 7.0) was incubated for 1 h at 37°C in the presence of 100 mg/L proteinase K (Sigma-Aldrich). Proteinase K activity was stopped by addition of 1 mM phenylmethanesulfonyl fluoride (PMSF) and samples analysed by immunoblotting. The Sseb content of Bt OMVs was determined by targeted proteomics done by the Proteomics Facility, University Bristol, UK.

Nanoparticle analysis

Size distribution of vesicles was performed on 1ml of OMV suspensions diluted 100 times with PBS. Videos were generated using a Nanosight nanoparticle instrument (NanoSight Ltd) to count the number of OMVs in each sample. A 1-min AVI file was recorded and analysed using NTA (Version 2.3 Build 0011 RC, Nanosight) software to calculate size distributions and vesicle concentrations using the following settings: calibration: 166 nm/pixel; blur: auto; detection threshold: 10, minimum track length: auto, temperature: 21.9°C , viscosity:

0.96 cP. The accuracy of the measurement was confirmed using 100 nm silver nanoparticles (Sigma-Aldrich).

Electron microscopy

The volume of OMV suspensions in PBS (1ml) was adjusted to 8.9 ml with PBS and then concentrated by ultracentrifugation; 150,000 g for 2 h at 4°C in a Ti70 rotor (Beckman Instruments). The vesicle containing pellet was resuspended in 200 µl of PBS. The OMV suspension was fixed for 1 h using 25% glutaraldehyde then centrifuged at 13,000g for 10 min. The OMV pellets were mixed 1:1 with molten 2% low gelling temperature agarose (TypeVII, Sigma), which was solidified by chilling and then cut into ~1 mm³ cubes. The sample pieces were then further fixed in 2.5 % glutaraldehyde in 0.1 M PIPES buffer for 16 h at 4°C after which time they were washed three times in 0.1 M PIPES buffer and dehydrated through a series of ethanol solutions (30, 50, 70, 80, 90%, and 3 times in 100%) after which the ethanol was replaced with a 1:1 mix of 100% ethanol:LR White medium grade resin and put on a rotator for 1 h. This was followed by a 1:2 and then a 1:3 mix of 100% ethanol:LR White resin mix and finally 100% resin, with at least 1 h between each change. The resin was changed twice more with fresh 100% resin with 8 h between changes. The sample pieces were each transferred into BEEM embedding capsules with fresh resin and polymerised for 16 h at 60°C. Sections of ~90 nm thick were cut using an ultramicrotome (Ultracut E, Reichert-Jung) with a glass knife and collected on film/carbon coated gold grids. A modified version of the Aurion Immunogold labelling (IGL) protocol (http://www.aurion.nl/the_aurion_method/Post_embedding_conv) was used with 1 h antibody incubations and detergent (0.1% TWEEN). The primary anti-Bt OmpA antisera was obtained by immunising rabbits with the peptide GGPREDGSYKQRWDYMN (Cambridge Research Biochemical), and was used at a dilution of 1/500. The secondary anti-rabbit Ig (GAR-10, Agar Scientific) was used at a dilution of 1/50. After antibody labelling, sections were stained with 2% uranyl acetate for 40 min and imaged in a FEI Tecnai G2 20 Twin transmission electron microscope at 200 kV.

Immunoblotting

Bt cell and OMV extracts were obtained by sonication and the supernatants added to SDS Page loading buffer (NuPage) containing dithiothreitol (Invitrogen). Approximately 7 µg of the total protein was loaded onto 12% precast Tris-Glycine gels (Novex) and separated by

electrophoresis at 180 volts for 40 min. The gel was then transferred onto a polyvinylidene difluoride (PVDF) membrane at 25 volts for 2 h in a solution containing Tris-Glycine Transfer Buffer (Novex). The membrane was blocked with 10% BSA in TBS-Tween (TBS [50 mM Tris-HCl; 150 mM NaCl; pH 7.5] with 0.05% Tween) by shaking for 30 min at 20°C. The blocking solution was then discarded and the membrane incubated for 16–18 h at 4°C in TBS-Tween with 5% BSA containing primary antibody (anti-*Salmonella* OmpA [Antibody Research Corporation], -KGF-2 [Peprotech] or -IAV or Anti-polyHisidine Clone HIS-1 (Sigma-Aldrich). After washing with TBS-Tween, membranes were incubated in 5% BSA in TBS-Tween containing HRP-conjugated goat anti rabbit IgG (1:1000 dilution, ThermoFisher) for 1 h at 20°C. After 3 washes with TBS-Tween, SuperSignal West Pico chemiluminescent Substrate (ThermoFisher) was used to detect bound antibody.

Mammalian cell culture

The human colonic epithelial cell line Caco-2 (ECACC 86,010,202) was cultured at 37°C and 5% CO₂ in Dulbecco's Modified Eagle Medium (DMEM) with 4.5 g/L glucose and L-glutamine (Lonza) supplemented with 5% foetal bovine serum (FBS, Lonza).

Epithelial cell scratch assay

Caco-2 cells were grown in T25 flasks until they reached 90% confluency. Cells were digested using trypsin EDTA (200 mg/L, 170,000 U Trypsin/L, Lonza) and seeded onto 8-well µ-slides (Ibidi). Cells were grown until they formed a 90% confluent monolayer and then serum-starved for 8 h. A scratch was made on the monolayer using a sterile tip and cells were washed with PBS to remove cell debris. The remaining cells were incubated for 72 h in 1% FBS medium supplemented with heparin (300 µg/mL grade I-A, >180USP units/ml; Sigma-Aldrich) in the presence of PBS, naïve OMVs, KGF-2 OMVs or recombinant KGF-2 (500 ng/mL, PeproTech). Wound healing was monitored by taking images immediately after scratching (time 0 control) and every 24 hours using an Invertoskop ID03 inverted microscope (Carl Zeiss) and a Sony Xperia Z5 compact digital camera (Sony). The measurements of the recovered scratch area (pixel²) at each time point were analysed using ImageJ software. The experiment was performed in triplicate.

Animal experiments

All animal experiments were done using 6 to 8 week old C57BL/6 male mice that were bred and maintained

in animal facilities either at the University of East Anglia (UK) or the University of Liverpool. Mice were housed in individually ventilated cages and exposed to a 12 h light/dark cycle with free access to a standard laboratory chow diet. Animal experiments were conducted in full accordance with the Animal Scientific Procedures Act 1986 under UK Home Office (HMO) approval and HMO project license 70/8232 (UEA) and 70/8599 (UoL).

OMV vaccines and vaccination: To evaluate oral *Salmonella* OMV vaccine formulations, groups of mice ($n = 5\text{--}6/\text{group}$) were gavaged with either 100 μl containing approximately 70 μg of total protein and 10^{10} vesicles of StOmpA-OMVs or naïve OMVs in PBS. Prior to each immunization food was removed for approximately 4 h to decrease stomach acidity. Booster oral immunisations were given 1 and 2 months later. An additional control group of animals were immunised with StOmpA-OMVs via the intraperitoneal route. To assess intranasal immunisation with *Salmonella* and influenza virus OMV vaccine formulations, groups of mice ($n = 5\text{--}10/\text{group}$) mice were anaesthetized then intranasally dosed with either StOmpA OMVs, StSseB OMVs, H5F OMVs, naïve OMVs (~ 70 μg of total protein) or PBS and 14 and 21 days later received booster immunizations. For infectious challenge with *Salmonella*, StOmpA-OMV orally or intraperitoneally (IP) immunised mice were orally administered 10^8 CFU of *S. enterica* ser. Typhimurium SL1344 on day 70 and 5 days later the bacterial load in different tissues was determined. For infectious challenge with IAV, H5F-OMV immunised mice were anaesthetised on day 28 with ketamine via the intra-muscular route and inoculated intranasally with 10^3 PFU A/PR/8/34 (PR8) H1N1 strain of IAV in 50 μl sterile PBS, which is equivalent to a 10-fold lethal dose. Weights of each animal were recorded from the day of challenge up until the end point at day 33 when the mice were euthanised. At necropsy, blood, serum and bronchoalveolar lavage fluid were taken for antibody and cytokine analyses and lung tissue was used to determine virus titre. For *in vivo* OMV trafficking studies, mice were intranasally administered with DiO-labelled H5F-OMVs and 1 and 5 days later OMV acquisition and uptake was determined using flow cytometry in: the macrophage and dendritic cells of the BAL; nasal associated lymphoid tissue (NALT); and cervical and mediastinal lymph nodes.

IAV quantification

Plaque assays were performed on homogenates of lung tissue from PR8-infected mice as described previously [23]. Briefly, viral samples from lungs were titrated in a 10-fold serial dilution from 10^1 to 10^6 in DMEM

supplemented with TPCK-trypsin. Each dilution was incubated with MDCK cells in individual wells of a 24 well plate for 1 hour at 37°C , 5% CO_2 . The media was aspirated and replaced with overlay media containing 2.4% Avicel. Plates were incubated at 37°C , 5% CO_2 for 72 hours. Avicel was aspirated, plates were washed and cells were fixed in acetone:methanol (60:40) for 10 min. Cells were allowed to air dry prior to staining with crystal violet for 10 minutes, washed and air dried. Plaques were counted and then multiplied by the dilution factor and the volume of virus plated to give viral titre (PFU/ml).

Acute colitis

The dextran sulphate sodium (DSS) induced mouse model of acute colitis was used to test the therapeutic potential of KGF-2-containing OMVs. Mice were divided into six groups ($n = 5/\text{grp}$) and administered with either PBS, naïve OMVs, KGF-2 OMVs, DSS + PBS, DSS + naïve OMVs or, DSS + KGF-2 OMVs for 7 days. Experimental colitis was induced in the appropriate treatment groups of mice by administration of 2.5% w/v DSS (36,000--50,000 Da, MP Biomedicals, USA) in drinking water *ad libitum* for 7 days. The other groups of mice received fresh water alone throughout the duration of the experiment. PBS and OMVs were administered by oral gavage (100 μl) on days 1, 3 and 5 and on day 7 mice were euthanized. Fresh faecal pellets were collected daily by placing individual mice in an empty cage without bedding material for 5--15 min. The extent of colitis was evaluated using a disease activity index (Table S1) comprising daily body weights, stool consistency and rectal bleeding assessments. At autopsy the colon was aseptically extracted and photographed, and the contents collected in sterile vials and stored at -80°C . The colon length was measured, and representative samples (0.5 cm length) were taken from the distal region for histology. Histological samples were fixed in 10% neutral buffered formalin and embedding in paraffin. Tissue sections (5 μm) were prepared from each block, stained with hematoxylin (Mayer's hemalum, Merck) and eosin (Y-solution 0.5% aqueous, Merck) (H&E), and with Alcian blue (Sigma-Aldrich) and Nuclear Red (Sigma-Aldrich) to visualise goblet cells. Sections were observed under a DMI 3000B microscope at 40X magnification (Leica) and assessed in a blinded fashion. The histological changes were scored (Table S2) and goblet cells were enumerated using ImageJ software.

Antibody ELISA

ELISA plates were coated with target antigens (UV inactivated IAV [PR8] virus or H5 (H5N1) (A/Vietnam/1203/2004) Recombinant Protein (P5060, 2B Scientific Ltd), *Salmonella* OmpA or SseB proteins) in

0.1M NaHCO₃ and incubated for 12–16 hours at 4° C. Plates were washed three times with PBS that had been supplemented with 0.05% Tween 20 (PT), and then incubated with blocking solution (PBS with 2% BSA) for 3 h at 20°C, and then washed six times with PT. Fecal pellets were homogenized in phosphate-buffered saline (pH, 7.2) with soybean trypsin inhibitor (0.5 mg/mL; Sigma), phenylmethylsulfonyl fluoride (0.25 mg/mL; Sigma), 0.05 M EDTA, and 0.05% Tween 20 (Sigma). The fecal homogenates and bronchoalveolar lavage (BAL) and serum samples were diluted in PBS with 1% BSA, 0.05% Tween (PBT) and added to the plate wells and incubated for 12–16 h at 4° C. Immune serum and BAL from PR8 IAV-infected mice were used as reference samples for analysing anti-IAV antibody responses in H5F-OMV-immunised animals. Plates were then washed six times with PT and incubated with PBT containing either HRP-anti-mouse IgG (1:1000, Thermo-Fisher) or HRP-anti-mouse IgA (1:1000, Life Technologies) for 20 min at 20°C. Plates were again washed six times with PT then incubated in darkness with TMB High Sensitivity substrate solution (BioLegend) for 30 min at 20°C. The reaction was stopped by the addition of 2 N H₂SO₄ and the optical density was measured at 450 nm using a TECAN infinite f50 spectrophotometer (Männedorf, Switzerland). Abcam's IgA Mouse ELISA Kit was used to determine total IgA in salivary glands and BAL

Flow cytometry

Approximately 1×10^6 tissue-derived cells were incubated in PBS supplemented with 2% FCS (PBS-FCS) for 15 min at 4°C prior to the addition of fluorochrome-conjugated monoclonal antibodies specific for CD11b (clone M1/70, eBioscience) CD11c (clone N418, eBioscience), or CD103 (clone 2E7, eBioscience) in PBS-FCS and incubated for 30 min at 4°C in darkness. Cells were then washed in PBS-FCS and fixed in PBS supplemented with 4% paraformaldehyde for 15 min at 20 °C prior to analysis on a MACSQuant Analyzer 10 (Miltenyi Biotech). Data were analysed using FlowJo.

Immunohistology

From all mice, the entire, skinned heads were fixed in 10% buffered formalin for 48 h. Subsequently, approximately 2 mm slices were prepared by sagittal sections, using a diamond saw (Exakt Band System 300 CL; EXAKT Technologies Inc.), yielding a total of six sections from the tip of the nose to the foramen occipitale magnum. Sections were gently decalcified for 7 days in RDF Mild Decalcifier (CellPath Ltd) at room

temperature. Likewise, thoracic organs (lungs, lymph nodes, heart and thymus) were removed en bloc, fixed for 24 h in 10% buffered formalin and trimmed. Head and organ specimens were then routinely paraffin wax embedded. Consecutive sections (3–5 µm) were prepared and were stained with haematoxylin eosin for histological examination, or subjected to immunohistological staining. Immunohistology (IH) was performed using the horseradish peroxidase method as previously described [24,25]. Primary antibodies used were rat anti-mouse CD45R (clone B220, BD Biosciences; B cells), rabbit anti-CD3 (clone SP7; Bioscience; T cells) and rabbit anti-Iba-1 (Wako; macrophages and dendritic cells).

Statistical analysis

Data were subjected to the D'Agostino & Pearson omnibus normality test. One-way ANOVA followed by a Tukey's multiple comparison post hoc tests were made using GraphPad Prism 5 software. Statistically significant differences between two mean values were established by a p-value < 0.05. Data are presented as the mean ± standard deviation.

Results

Characteristics and physical properties of BT OMVs

Using electron microscopy we showed that OMVs budded off from the outer membrane of Bt during its growth cycle (Figure 1(a)) and could be recovered by filtration and ultracentrifugation from early stationary growth phase cultures (see Material and Methods). Bt OMVs were identified by their characteristic double membrane of their parental cells and by immunoreactivity with anti-Bt OmpA antisera (Figure 1(b)). Bt OMVs ranged in size from approximately 100 nm to greater than 400 nm with a mean size of 237 nm (Figure 1(c)). Bt OMVs are also highly stable with minimal loss of luminal proteins (<10% of total protein or heterologous protein) detected after exposure to an elevated ambient temperature of 40 °C for up 30 days (Figure 1(d)).

Heterologous bacterial, viral and human proteins expressed in BT and incorporated into OMVs

To test whether the delivery of a wide range of heterologous antigens into Bt OMVs was possible we compared delivery of a number of selected candidate vaccine antigens. These included antigens for the important bacterial and viral pathogens *S. enterica*

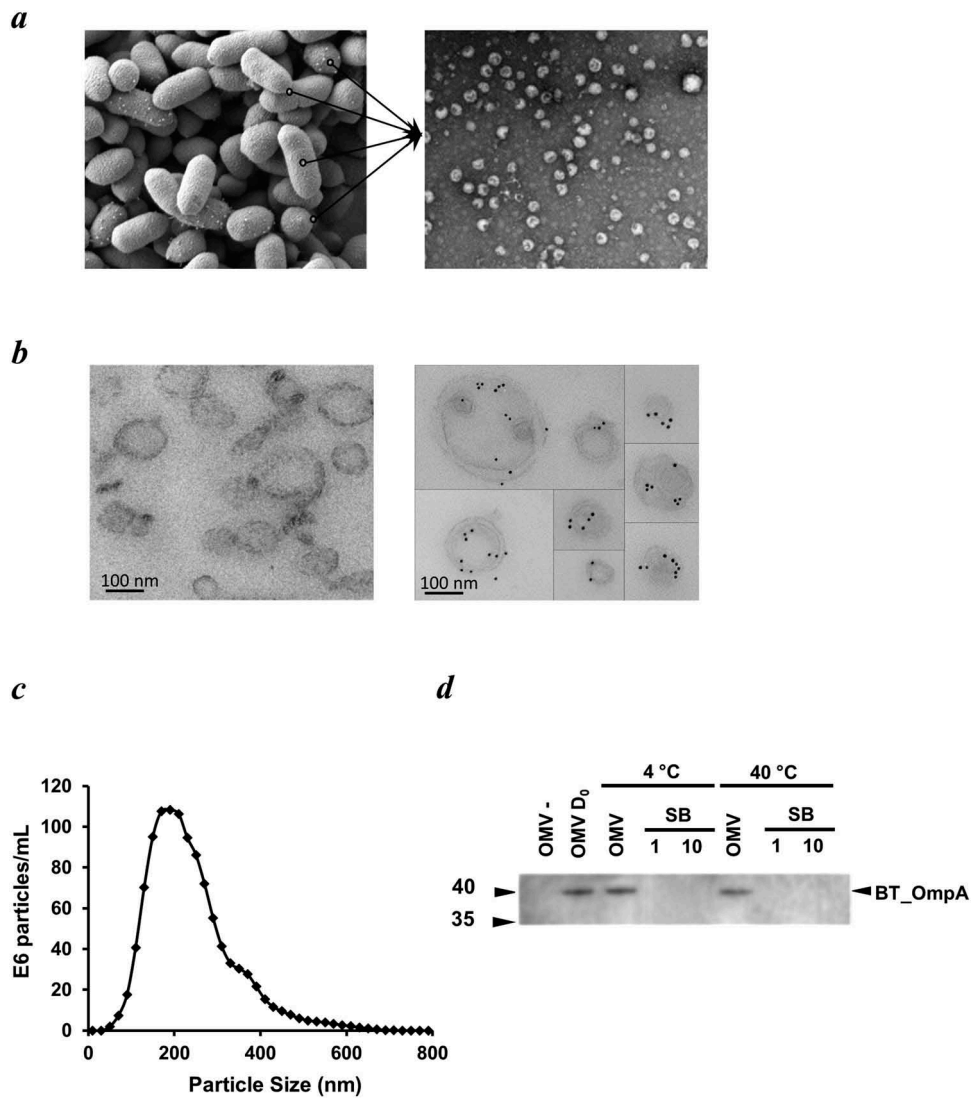


Figure 1. Appearance, size, structure and stability of Bt OMVs. (a) Electron microscopy (EM) of Bt cells showing vesicles budding from their surface before release into the milieu (lines in left panel), and EM image of OMVs extracted from cell culture supernatants (right panel). (b) Immunodetection of naïve Bt OMVs using colloidal gold anti-rabbit Ig to detect binding of rabbit anti-Bt OmpA antisera (right panel). Left panel shows absence of staining of OMVs produced by an OmpA deletion mutant of Bt. (c) Size distribution of OMVs produced by Bt determined by nanoparticle tracking analysis. (d) Thermostability of OMVs at day 0 (OMV D₀) and after storage of OMV suspensions at 4°C or 40°C for 30 days as measured using immunoblotting to detect OmpA in extracts of naïve OMVs (OMV) or OMVs of *ompA* deletion mutants (OMV-), and of neat (1) or ten-times concentrated (10) OMV storage buffer (SB) (PBS was the storage buffer).

ser. Typhimurium *enterica* and IAV, respectively. For a human protein we chose keratinocyte growth factor-2 (KGF-2). For *S. enterica* ser. Typhimurium we chose the outer membrane protein, OmpA and the SPI-2 translocon subunit (SseB) because they elicit antibody and T cell responses and confer some degree of protective immunity in mice, and because antibody responses in humans correlate with immune protection [26–34]. For IAV, the H-stalk protein H5 of the H5N1 VN/04:A/VietNam/1203/04 subtype was selected as it confers robust protection against challenge by multiple strains of IAV and can reduce lung viral titres by 3-fold

[35–37]. We also chose KGF-2 because it is essential for epithelial cell proliferation and preserving the integrity of the intestinal mucosa [37], and has therapeutic potential for the treatment of inflammatory bowel disease [38].

Mini-genes encoding the selected bacterial, viral and human proteins were cloned downstream of sequences encoding the N-terminal signal peptide of the major outer membrane protein OmpA (BT_3852), the products of which are contained within the lumen or outer membrane of OMVs (Figure 2(a)). These constructs were created in *L. lactis* (for KGF-2) or *E. coli* (for

OmpA, SseB and HF) hosts and then mobilised into Bt via a triple filter mating protocol using a helper strain. Immunoblotting of whole cell and OMV lysates of recombinant Bt strains confirmed expression of OmpA (Figure 2(b)) and KGF-2 proteins (Figure 2(c)). The luminal versus outer membrane distribution of these heterologous proteins in Bt OMVs was established using a protease protection assay which showed that *Salmonella* OmpA distribution was associated with the outer membrane (Figure 2(b)) whereas KGF-2 (Figure 2(c)) was contained within the lumen of OMVs. SseB expression was undetectable in OMV preparations using immunoblotting, but was detectable by liquid chromatography and mass spectrometry-(LC-MS) based proteomics, which also established its localization to the lumen of OMVs (Supplementary Table S3).

BT OMVs have inherent adjuvanticity

Many conventional vaccines rely on the inclusion of adjuvants to enhance their immunogenicity and to reduce the number of doses and amount of antigen

(or pathogen component) required to elicit a protective immune response, particularly in immunocompromised individuals [2,39]. To formally evaluate the adjuvant properties of Bt OMVs, mice were administered a single dose of native OMVs in PBS via the intranasal route and 5 days later head and thoracic organs were removed *en bloc* and analysed by immunohistology for the presence of organised lymphoid structures and follicles indicative of an active immune response. Large organised lymphoid follicles were present in both the nasal cavity (nasal-associated lymphoid tissue or NALT (Figure 3(a)) and the lungs (bronchus-associated lymphoid tissue or BALT) (Figure 3(b)) which contained dendritic cells, T cells and large numbers of B cells. These structures were absent in mice administered PBS alone (Figure 3(a,b)). Of note, OMVs were also effective at eliciting the formation of lymphoid clusters in mediastinal adipose tissue (fat-associated lymphoid clusters or FALC) (Figure 3(c)). Consistent with the immune response priming ability of Bt OMVs, within 24 h of intranasal administration of fluorescent labelled native OMVs it was possible to detect their uptake in the NALT and draining cervical

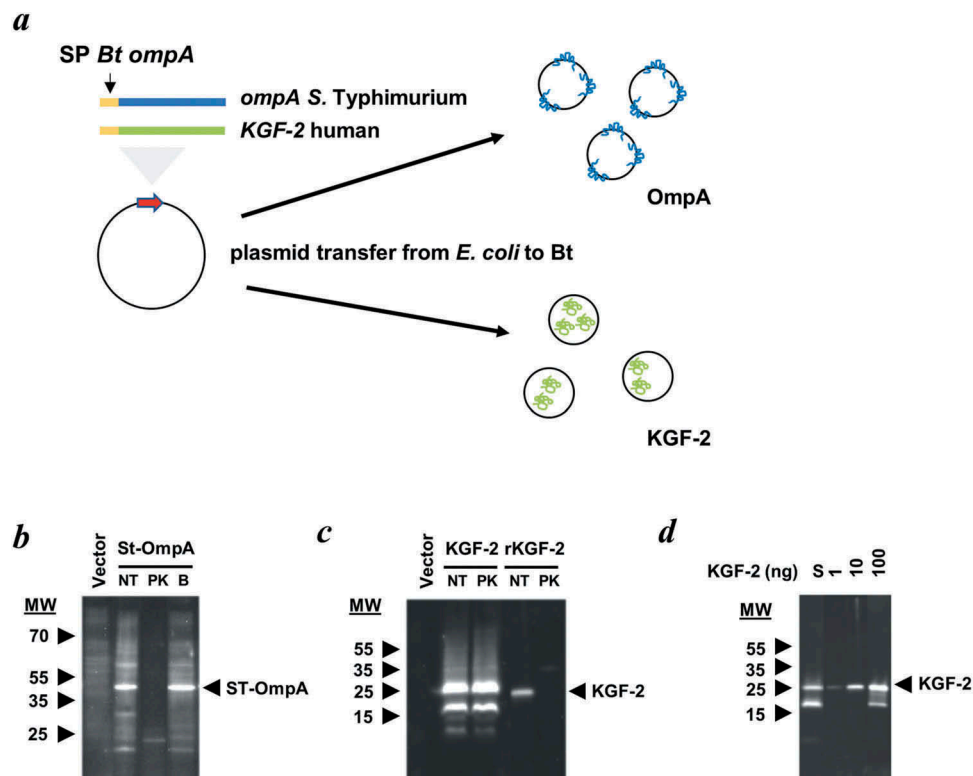


Figure 2. Expression of heterologous proteins in Bt OMVs. (a) Schematic of cloning procedure for the export of proteins of interest into the lumen or at the surface membrane of OMVs. The secretion peptide of Bt OmpA (SP BtompA) is indicated in yellow and fused at the N-terminus of the gene of interest. (b and c) Determination of protein location after treatment with proteinase K (PK). Immunoblotting of StOmpA (b) and KGF-2 (c) with and without pre-treatment of OMV suspensions with proteinase K. NT: not treated; PK: + Proteinase K; B: PK buffer alone. (d) KGF-2 quantification within OMVs. Comparison of recombinant KGF-2 (1–100 ng) with 10 μ l of 1 ml OMV suspension (S).

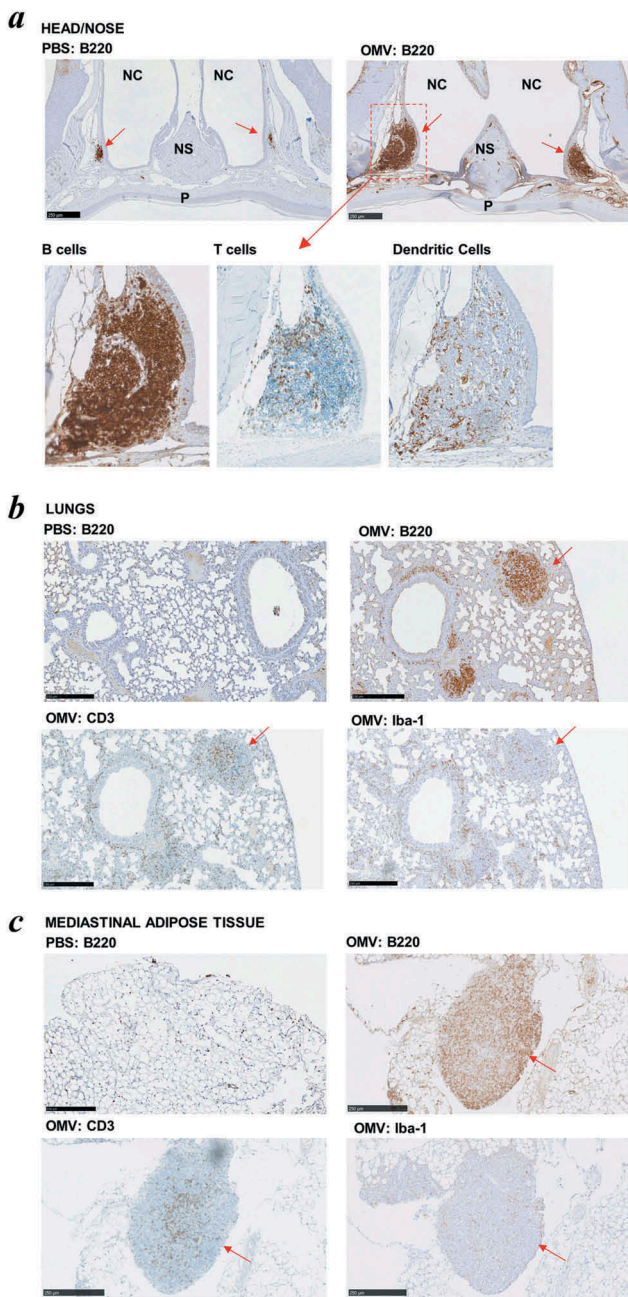


Figure 3. Intrinsic adjuvanticity of Bt OMVs. (a) Mice ($n = 5$) were intranasally administered PBS alone native Bt OMVs (OMV) in PBS and 5 days later heads and thoracic tissue was processed for immunohistology to visualise immune cell activation and formation of organised lymphoid tissue containing $CD45R^+$ B cells (B220), $CD3^+$ T cells (CD3) and macrophages/dendritic cells (Iba-1) in the nasal associated lymphoid tissue (a) the lung parenchyma (b) and mediastinal adipose tissues (c). Red arrows define nasal-associated lymphoid tissue (NALT), bronchus-associated lymphoid tissue (BALT) and fat-associated lymphoid tissue (FALC) in a, b and c respectively. NC: nasal cavity, NS: nasal septum, P: hard palate.

lymph nodes (CLN) (Supplementary Fig. S1). At day 5, there was evidence of trafficking of OMVs to both the cervical and mesenteric lymph nodes which was almost

exclusively mediated by $CD11c^+$, $CD11b^+$ $CD103^-$ dendritic cells (Supplementary Figure S1).

From a biosafety perspective, neither orally nor intranasally administered native OMVs or vaccine antigen formulated OMVs had any adverse health effects with no tissue pathology evident in treated animals at post mortem (data not shown). Orally administered OMVs also had no or a minor and/or transient effects on intestinal microbes as determined from culturing faecal samples on selective media (Supplementary Fig. S2).

Mucosal delivery of OMV vaccine formulations

We used preparations of OMVs expressing *Salmonella* vaccine antigen (St-OmpA and St-SseB) to compare and optimise the effectiveness of different formulations and routes of administration for the generation of mucosal and systemic antibody responses. St-OmpA and St-SseB expressing OMVs were administered to mice via the oral or nasal routes (Figure 4(a)) and also parenterally for comparison. At the end of the study BAL and serum samples were analysed by ELISA for antigen-specific IgA (mucosal) and IgG (serum) antibodies, respectively. For St-OmpA OMVs the intraperitoneal route of administration generated the highest levels of antigen-specific serum IgG antibodies compared with the oral or intranasal routes of delivery, for which there were comparable, but only low levels, of St-OmpA-specific IgG (Figure 4(b)). For St-SseB OMVs, the intranasal route of administration generated significantly higher levels of antigen-specific serum IgG antibodies compared with oral delivery and were equivalent to the levels of antigen-specific IgG seen after intraperitoneal immunisation (Figure 4(b)).

St-OmpA and St-SseB OMVs were equally effective at eliciting antigen specific IgA antibodies in the lower respiratory tract and BAL (Figure 4(c)). However, there was more individual variation in the IgA levels and response to St-OmpA OMVs compared with animals administered St-SseB OMVs. Intranasally-administered St-OmpA and St-SseB OMVs also increased global IgA antibody production and secretion in both the salivary glands (Figure 4(d)) and BAL (Figure 4(e)). Of note, naïve OMVs also increased global IgA levels in these sites (Figure 4(d,e)), which is consistent with the adjuvant properties of Bt OMVs and their ability to activate the immune system in both of these sites, and generate organised lymphoid follicles and tissues containing large numbers of B cells (Figure 3).

Despite the induction of *Salmonella* antigen-specific IgG antibodies, neither oral nor parenteral vaccination with StOmpA-OMVs conferred significant levels of protection to oral *Salmonella* infection as judged by the pathogen burden (CFU) in intestinal and extra-

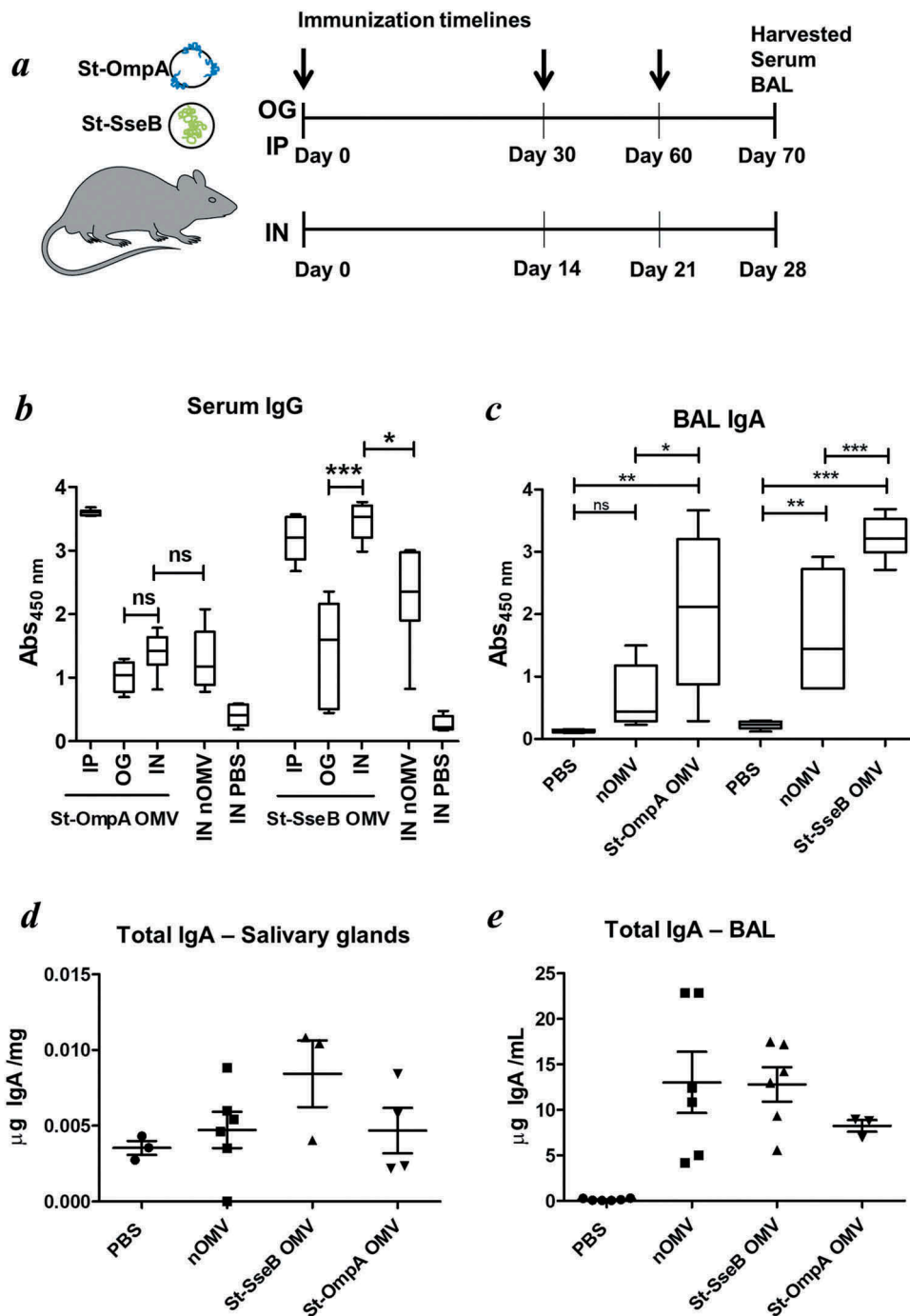


Figure 4. Bt OMV-elicited systemic and mucosal antibody responses. (a) Mice ($n = 5\text{--}6/\text{grp}$) were administered Bt OMVs expressing the *Salmonella* OmpA or SseB proteins via the oral (OG), intranasal (IN) or intraperitoneal (IP) routes according to the dosing regimen described in the Material and Methods section. Arrows indicate time of immunization. Naïve OMVs (nOMV) and PBS were administered to mice ($n = 5\text{--}6/\text{grp}$) as control groups. At autopsy, serum (b) and brochoalveolar lavage fluid (BAL) (c) were analysed for anti-OmpA and anti-SseB IgG and IgA antibody titres, respectively, by ELISA. The boxplots identify the mean and upper and lower quartile values for data sets obtained from animals within each treatment group. Analysis of variance for multiple comparisons of means between independent samples (ANOVA) was followed by a Tukey's test. * $P < 0.05$; ** $P < 0.01$; *** $P < 0.001$; ns, not significant. Total IgA levels were also determined in salivary gland tissue homogenates (d) and in BAL (e) samples from each group of animals by ELISA using IgA standards as described in the Materials and Methods section.

intestinal tissues at 5 days post infection (Supplementary Fig. S3).

Intranasal OMV viral vaccine formulations protect against pulmonary IAV infection

Based on the potent adjuvant effect of intranasally administered OMVs (Figure 3) and higher levels of antigen specific mucosal and systemic antigen specific antibodies after intranasal immunisation with OMV based vaccines (Figure 4), we used IAV vaccine formulated OMVs to investigate further the possibility that intranasal immunisation with OMV-based vaccines is a better option for mucosal vaccination and conferring protection to infectious challenge.

Serum anti-IAV IgG antibody levels were higher in H5F-OMV immunised animals than the other groups (Figure 5(a)). Animals immunized with naïve OMVs had levels of BAL anti-IAV IgG antibodies significantly higher than in non-immunized animals (Figure 5(b)). However, it should be noted that levels of specific IgG in the OMV-vaccinated groups were far lower than that seen with a positive control serum from PR8-infected mice (Figure 5(b,c); black triangles). IAV specific IgA antibody levels were significantly higher in the BAL samples from animals immunised with H5F-OMVs compared with the other groups ($p = 0.004$) (Figure 5(d)). Of note, the levels of anti-PR8 (H1N1)-specific IgA seen in OMV-inoculated mice were comparable to those seen in the positive control BAL from homologous PR8-infected mice. Also, the levels of H5 HA-specific IgA in BAL of the control PR8-infected mice were not above control, demonstrating the lack of cross-type specific HA IgA antibodies in PR8-infected mice. Thus, vaccination with OMVs and H5F-OMVs induced levels of antibodies, in particular IgA in the BAL that were able to react with homologous H5 as well as heterotypic H1 HA molecules. During infection the weight of all infected animals declined with the greatest weight loss seen in the control (PBS administered) animals that lost almost 20% of their body weight (Figure 5(f)). Animals immunised with H5F-OMVs displayed a more gradual decline in weight loss after infection, as did those immunized with naïve OMVs. Notably, the body weight of the H5F-OMV-immunised animals stabilised with no further decline between day 4 and day 5 post-infection; this is indicative of a less severe infection from which they recovered. This was confirmed by the lung viral titre data (Figure 5(g)); viral load in animals that had been immunised with H5F-OMVs was significantly lower ($p < 0.006$) than that of the other groups, reflecting an approximate 7 to 8-fold lower level of virus.

KGF-2 containing omvs protect against acute colitis

To determine whether Bt OMVs were suitable for mucosal delivery of human therapeutic proteins, the KGF-2 protein was expressed in Bt OMVs. This was achieved by cloning a mini-gene containing the coding sequence of the mature human *kgf-2* gene and the Bt *OmpA* signal peptide in Bt (Bt-KGF-2). Immunoblotting of lysates of OMVs harvested from cultures of Bt-KGF-2 (KGF-2 OMVs) established that they contained approximately 5 $\mu\text{g/ml}$ of KGF-2 (Figure 2(d)) and that the protein was contained within the lumen of the OMVs (Figure 2(c)). The biological activity of KGF-2 OMVs was confirmed in an epithelial cell wounding (scratch) assay in which the addition of intact KGF-2 OMVs to the epithelial cell cultures promoted epithelial cell proliferation and accelerated wound closure (Supplementary Fig. S4). KGF-2 OMVs were tested in the acute murine DSS colitis model (Figure 6(a)), which is a well characterised, simple and reproducible model of intestinal inflammation that is independent of lymphocyte-mediated responses and in which the clinical severity can be quantified and new therapeutic agents evaluated [40]. Since DSS primarily affects epithelial cells and inhibits their proliferation [40] this model is well suited to testing the therapeutic potential of KGF-2 OMVs. The dosing regimen was based in part on pilot experiments assessing the tolerability of OMVs (data not shown) and our previous studies using a *B. ovatus* strain engineered to express human KGF-2 *in vivo* that had a therapeutic effect in DSS-colitis [41].

KGF-2 OMVs controlled colitis both clinically and pathologically. Weight loss was significantly reduced in animals receiving KGF-2 OMVs compared with non-treated animals ($p < 0.01$) or animals that had been administered naïve OMVs ($p < 0.001$) (Figure 6(b)). KGF-2 OMVs also reduced the impact of DSS on colon shrinkage and reduction in length (Figure 6(c,e)), which is an independent measure of inflammation [42]. Consistent with the therapeutic effect of KGF-2 OMVs, disease activity index scores were significantly lower in KGF-2 OMV-treated animals compared with the other treatment groups (Figure 6(d) and Supplementary Tables 1 and 2). In addition, colon shortening caused by DSS-treatment was abated by KGF-2 OMV administration (Figure 6(e)). Histopathology showed that KGF-2 OMV treatment reduced epithelial damage and inflammatory infiltrate compared with non-treated mice and mice that had been administered naïve OMVs (Figure 7(a)). KGF-2

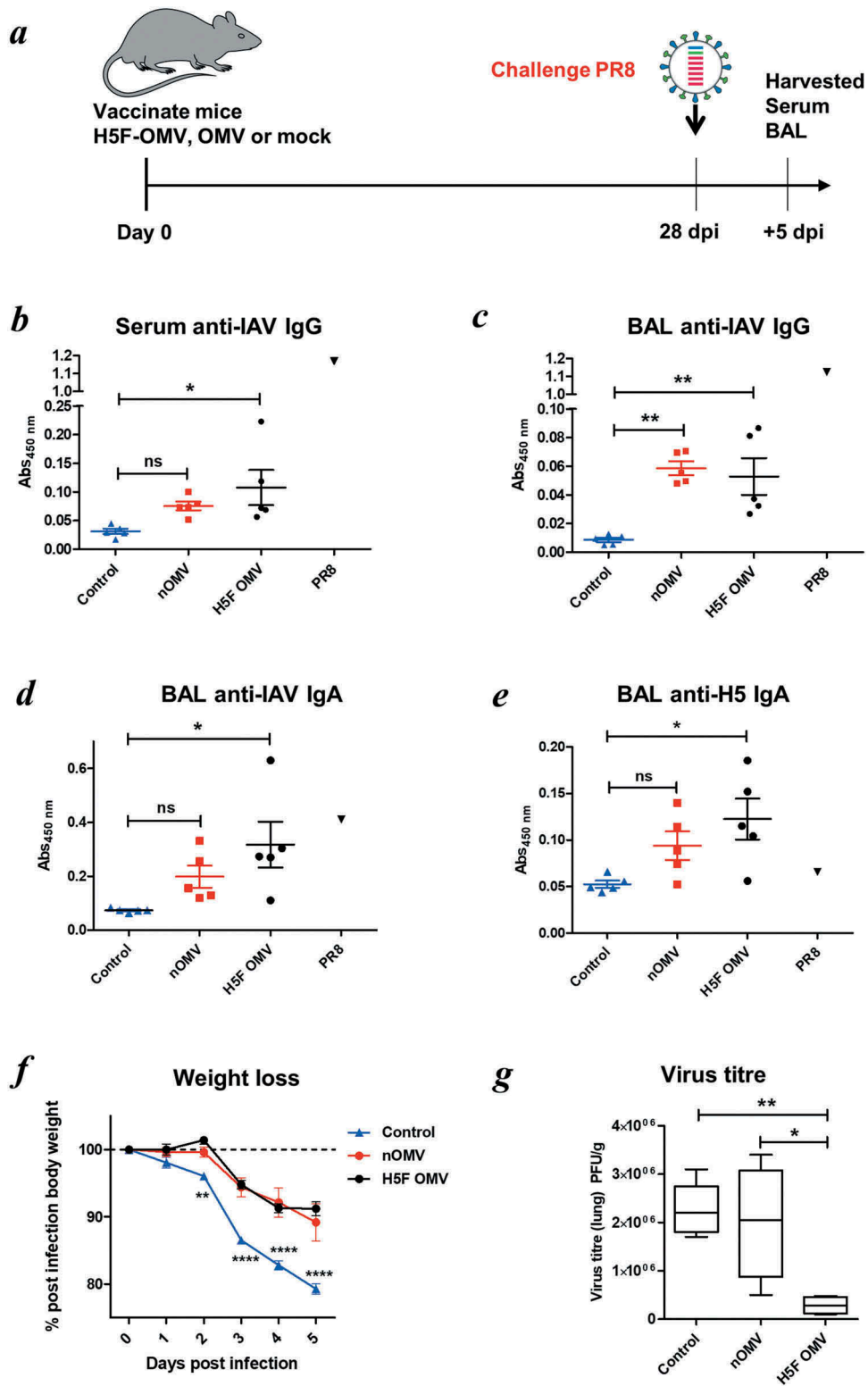


Figure 5. Bt OMVs expressing IAV H5F protein confer a level of protection to virus infection in mice. (a) Mice were immunised intranasally with H5F-OMVs in PBS; controls were administered intranasally with naïve OMVs or PBS alone (mock) at the indicated time-points; after 28 days all were challenged intranasally with a 10-fold lethal dose of IAV strain A/PR/8/34 (PR8, H1N1). At necropsy serum (b) and brochoalveolar lavage fluid (BAL) (c, d) were analysed for IAV IgG and IgA antibodies by ELISA using UV-inactivated PR8 virus. BAL samples were also analysed for H5 HA specific IgA antibodies (e) using recombinant H5 HA as the target antigen. Immune serum and BAL from PR8 IAV-infected mice (PR8) were used as reference samples. (f) The weight of individual animals in each group was assessed daily. (g) Lung homogenates were assessed for viral load (PFU/g lung tissue) at necropsy. Statistical analysis was performed using one-way ANOVA with Tukey's multiple comparison tests (panels b,c,d,e,g) or two-way ANOVA with Bonferroni post-tests. ns, not significant; *P < 0.05; **P < 0.01; ***P < 0.001.

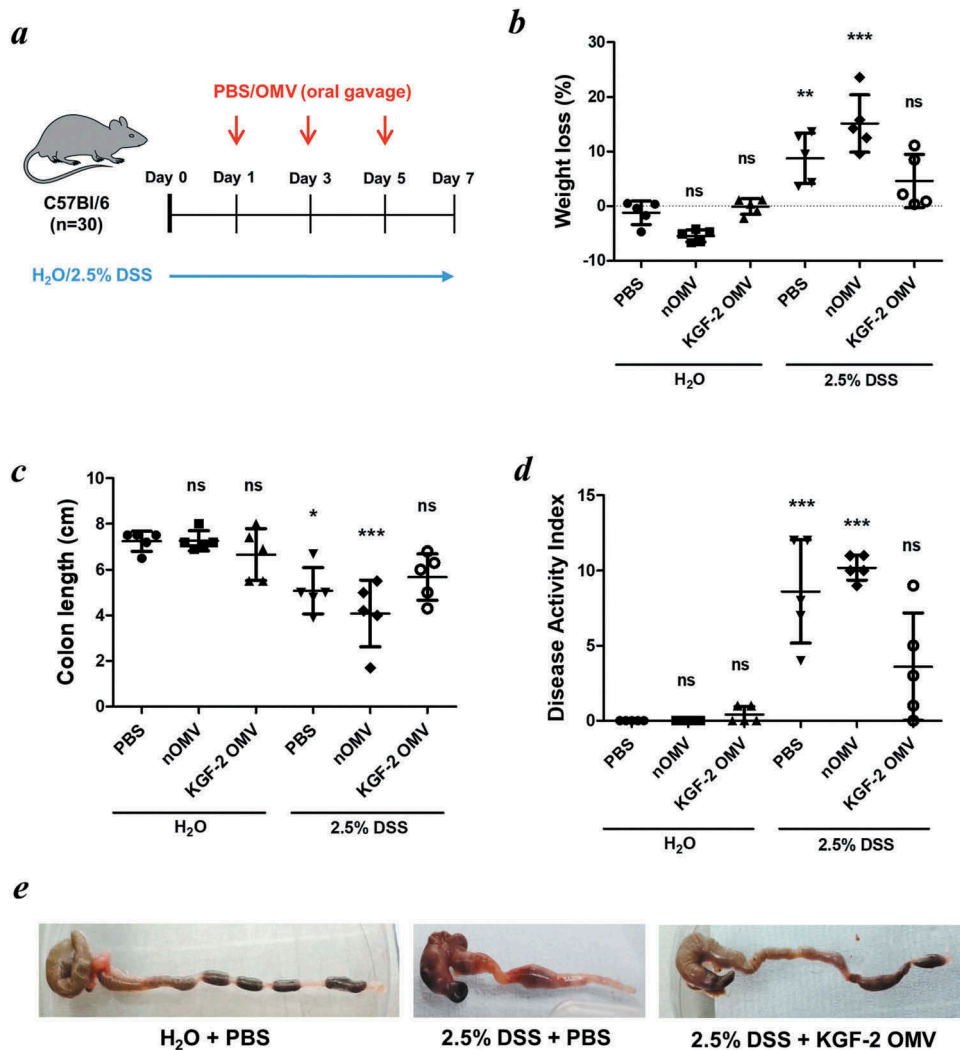


Figure 6. OMVs containing KGF-2 ameliorate DSS-induced colitis in mice. (a) Groups of mice were provided with drinking water with or without 2.5% (w/v) DSS for 7 days. On days 1, 3 and 5 mice were orally gavaged with either PBS, naïve OMVs or OMVs containing KGF-2. (b) Percent weight loss at day 7. (c) Colon length at day 7. (d) Disease Activity Index (DAI) at day 7. (e) Representative images of colons. Data expressed as mean \pm SD ($n = 5$). Statistical analysis was performed using one-way ANOVA with Tukey's multiple comparison tests. Mice gavaged with PBS and receiving regular drinking water were considered as the reference group for statistical analysis. ns, not significant; * $P < 0.05$; ** $P < 0.01$; *** $P < 0.001$.

OMVs also had a beneficial effect on mucin-producing goblet cells. Compared with non-treated animals or animals receiving naïve OMVs, there was a significant increase in the number of mucin-containing goblet cells in the colonic mucosa of KGF-OMV-treated animals (Figure 7(b)); the appearance and distribution of goblet cells resembled that of the control animals receiving water alone and no DSS (Figure 7(c)).

Discussion

In this study we have provided evidence for the suitability of using OMVs from the major human gut commensal bacterium, Bt, to deliver biologics to mucosal sites and

protect against infection and injury. The nanosize and non-replicative status of Bt OMVs together with their stability and ability to interact with mucosal and systemic host cells makes them ideally suited for drug delivery. Moreover, they possess innate adjuvant properties and the ability to activate immune cells and promote development of the organised mucosa-associated lymphoid follicles that are required for generating effective immune responses. The use of OMVs from prominent human commensal bacteria that have established a mutualistic relationship with, and are well tolerated by, their host is also desirable from a safety perspective and for minimising or preventing inappropriate host responses. This was evidenced by the absence of any change in health status and no pathology in Bt OMV-treated animals.

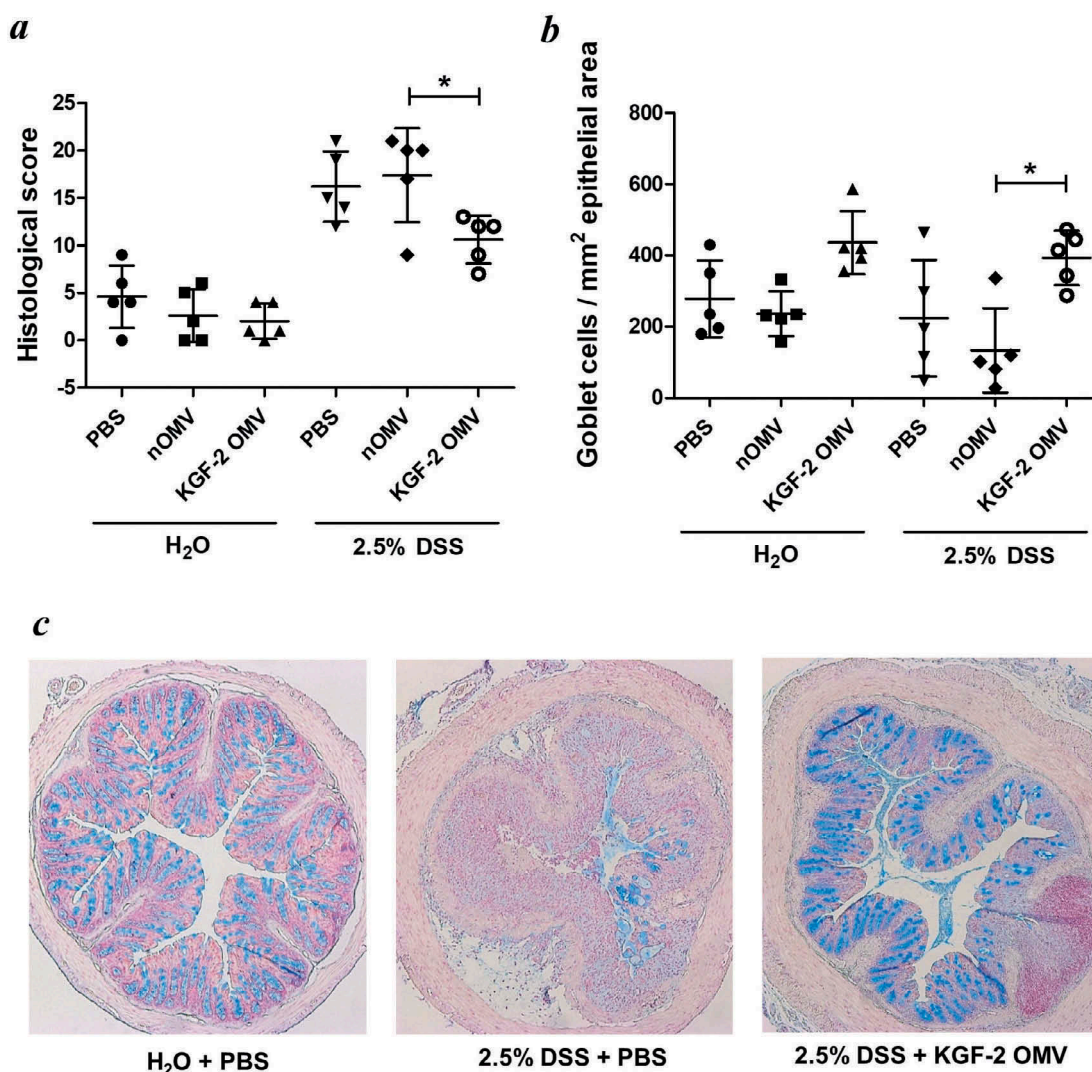


Figure 7. OMVs containing KGF-2 protect and restore goblet cells in mice with DSS-induced colitis. (a) Histological score of colon tissue as determined by microscopy of H&E stained sections obtained at necropsy. (b) Number of Alcian Blue stained goblet cells per mm² of epithelial area. (c) Microscope images of goblet cell distribution in representative colon sections stained with Alcian Blue. Data expressed as mean \pm SD (n = 5). Statistical analysis was performed using one-way ANOVA with Tukey's multiple comparison tests. *P < 0.05.

The Bt OMV technology platform is underpinned by our ability to engineer *Bacteroides* species [21,43,44] to express heterologous proteins that retain their biological activity [41,45,46]; using specific protein secretion sequences heterologous proteins can be directed to the periplasmic space for export and incorporation into the lumen or outer membrane of Bt-generated OMVs. It has not been possible to absolutely define the minimum (or optimal) level of expression of heterologous proteins necessary to elicit an appropriate host response. However, low levels of expression that are only detectable by high resolution LC-MS-based proteomics (as for *Salmonella* SseB) are sufficient to induce robust host mucosal and systemic antibody responses. For this reason there was no apparent correlation between the levels of

expression of different proteins within or at the surface of OMVs, and their ability to elicit a host response. Determining the quantity of biologically active (KGF-2) protein in OMV formulations was made difficult by their ability to resist disruption. OMV cargo does, however, become accessible after uptake by host cells and in particular, antigen presenting macrophages and dendritic cells as shown here and previously by others [8], which is most likely as a result of an OMV-intracellular membrane fusion event [12].

To date, the majority of OMV applications have focused on vaccine development [18] as they offer significant advantages over conventional vaccines; they are non-replicating, provide needle-free delivery, target mucosal sites, have an established safety record, can elicit

innate and antigen-specific adaptive immune responses, possess self-adjuvant properties (i.e. microbe-associated molecular pattern molecules [MAMPs] such as LPS), and are relatively cheap and straightforward to produce. The limitations of current non-commensal and pathogen-derived OMV vaccines are the potential for unintended toxicity due to associated toxins, low expression levels of protective antigens, variable efficacy depending on source and formulation, the need for exogenous adjuvants, and the problem of incomplete protection due to strain variation. The work we describe here demonstrates that these limitations can, to a large extent, be overcome by using bioengineered Bt OMVs. The intranasal route of administration was superior to oral administration in terms of eliciting high levels of *Salmonella* vaccine antigen-specific mucosal IgA and systemic IgG. This difference is most likely a reflection of anatomical differences and the ease of access to host immune inductive sites and effectiveness of acquisition by mucosa-associated antigen presenting-cells that occurs in the upper respiratory tract compared with the lower GI-tract. With smaller distances to travel in the less harsh environment of the lungs, OMVs are more readily accessible to host cells; within 24 h of intranasal administration Bt OMVs were acquired by CD103⁻ CD11b⁺ dendritic cells in the mucosa of the upper and lower respiratory tract, with some trafficking to draining lymph nodes. Importantly, this CD103⁻ CD11b⁺ population of tissue DC are known to traffic antigen to lymph nodes and initiate T cell responses [47].

The failure to demonstrate protection against infectious challenge in animals immunised with *Salmonella* OMV vaccine formulations may be as a consequence of various factors including sub-optimal expression of appropriate quantities of immunogenic St OmpA antigen in Bt OMVs and/or the generation of insufficient levels of functional, pathogen-neutralising, antibodies. Although St OmpA was previously identified as a potential cross-species vaccine candidate [48] our findings are in line with those of Okamura and colleagues [49] who found no protection in chickens parenterally immunised with St OmpA. However, the universal adjuvant properties of Bt OMVs suggests they may still be of value in *Salmonella* vaccine formulations as an adjuvant analogous to meningococcal OMVs that provide potent adjuvanticity to *N. meningitidis* recombinant protein-based vaccines [50,51].

We obtained more compelling evidence for the potential of Bt OMV-based vaccines in the IAV H5F-OMV system which, after intranasal administration, conferred a significant level of heterotypic protection against an unrelated subtype of IAV. There are numerous strains of IAV and the virus evolves rapidly. This presents a challenge to generating a “universal vaccine” that will protect against

multiple IAV strains. Most IAV vaccines do not afford protection against heterologous strains of virus. Recent work has shown that while the globular head of the IAV HA molecule is highly variable and does not generate cross-protective immunity, the stem/stalk is more conserved and will generate cross-protective antibodies [52]. Naïve OMVs had a positive impact on the generation of mucosal virus-specific IgA antibodies and also reduced lung viral titres. This is most likely a reflection of their potent adjuvant properties and the activation of innate and adaptive immune responses, including raised total IgA antibody levels in the upper and lower respiratory tract which would strengthen front line protection against IAV infection [53]. At 5 days post challenge with the heterologous PR8 (H1N1) virus, the mean weight of H5F-OMV-immunized animals stabilized which is indicative of recovery from virus infection; which was supported by the fact that H5F-OMV immunized animals had a 7–8-fold lower lung viral titre compared with non-vaccinated animals or animals immunized with naïve OMVs. Future refinements to the study protocol should provide a clearer picture of the efficacy of OMV-H5F vaccines in preventing IAV infection by both homotypic and heterotypic strains of influenza virus. As our study was not an end point study we cannot directly compare the level of protection against infection conferred by OMV-H5F vaccines with similar studies trialing OMV-based vaccines; these include those of Watkins and colleagues [54] who developed *E. coli* OMV-IAV vaccines and achieved 100% protection in a murine lethal infectious challenge model. Collectively, our data provides the rationale and justification for continuing the development and refinement of OMV technology to improve and optimise their vaccine capabilities and performance.

Our findings using KGF-2-containing OMVs to ameliorate experimental colitis demonstrates the potential for a broader portfolio of applications and, in particular, for the mucosal delivery of therapeutic proteins for the treatment of non-infectious, autoimmune-driven pathologies. The benefit of this form of drug delivery is exemplified by comparing the doses required to improve colonic pathology using OMV technology and a standard approach. The dose of KGF-2 OMVs (approximately 0.5 µg) used to achieve a significant reduction in colonic histopathology is 1–2 orders of magnitude lower than that required in daily injections (20–100 µg for 7 days) to achieve a comparable reduction in colonic pathology [55,56]. Also, the ability to deliver the protein directly to the target tissue using orally administered OMVs reduces the risk of side effects associated with systemic delivery.

In summary, our data adds to the growing number of new approaches being developed to express heterologous proteins in bacterial microvesicles [18] for

a variety of applications. Our work provides evidence for the utility and effectiveness of human commensal bacteria as a source of bioengineered OMVs for the mucosal delivery of different biologics.

Acknowledgments

This work was supported in part by the UK Biotechnology and Biological Sciences Research Council (BBSRC) under grant numbers BB/J004529/1, BB/R012490/1, BBS/E/F/000PR10355 and BBS/E/F/000PR10356 (SRC); a UK National Institute of Health Research grant (K-SK); British Council (Department of Business, Energy and Industrial Strategy), Newton Institutional Links award Ref: 332228521 (JPS); the Fundación Alfonso Martín Escudero (SF), and by postgraduate studentships awarded by the Universitat Rovira i Virgili (KG-C) and the University of Liverpool (EB). The authors also acknowledge the support provided by Dr Karin Overweg in the generation of Bt *OmpA* deletion mutants.

Disclosure statement

No potential conflict of interest was reported by the author.

Funding

This work was supported by the Biotechnology and Biological Sciences Research Council [BB/J004529/1]; Fundación Alfonso Martín Escudero [Fellowship]; Newton Fund [332228521]; National Institutes of Health (UK) [Fellowship]; Universitat Rovira i Virgili [studentship]; University of Liverpool [Studentship].

References

- [1] Kulp A, Kuehn MJ. Biological functions and biogenesis of secreted bacterial outer membrane vesicles. *Annu Rev Microbiol.* 2010;64:163–184. PubMed PMID: WOS:000284030600009; English.
- [2] Del Giudice G, Rappuoli R, Didierlaurent AM. Correlates of adjuvanticity: a review on adjuvants in licensed vaccines. *Semin Immunol.* 2018 May 22;39:14–21.
- [3] Ellis TN, Kuehn MJ. Virulence and immunomodulatory roles of bacterial outer membrane vesicles. *Microbiol Mol Biol Rev.* 2010 Mar;74(1):81–94. PubMed PMID: WOS:000275120100004; English.
- [4] Haurat M, Elhenawy W, Feldman M. Prokaryotic membrane vesicles: new insights on biogenesis and biological roles. *Biol Chem.* 2014;396(2):95–109.
- [5] Olsen I, Amano A. Outer membrane vesicles - offensive weapons or good Samaritans? *J Oral Microbiol.* 2015;7:27468. PubMed PMID: 25840612; PubMed Central PMCID: PMC4385126.
- [6] Elhenawy W, Debelyy MO, Feldman MF. Preferential packing of acidic glycosidases and proteases into bacteroides outer membrane vesicles. *MBio.* 2014;5(2):e00909–e00914. PubMed PMID: 24618254; PubMed Central PMCID: PMC3952158.
- [7] Rakoff-Nahoum S, Coyne MJ, Comstock LE. An ecological network of polysaccharide utilization among human intestinal symbionts. *Curr Biol.* 2014 Jan 6;24(1):40–49. PubMed PMID: 24332541; PubMed Central PMCID: PMC3924574.
- [8] Stentz R, Osborne S, Horn N, et al. A bacterial homolog of a eukaryotic inositol phosphate signaling enzyme mediates cross-kingdom dialog in the mammalian gut. *Cell Rep.* 2014 Feb 27;6(4):646–656. PubMed PMID: 24529702; PubMed Central PMCID: PMC3969271.
- [9] Bryant WA, Stentz R, Le Gall G, et al. In silico analysis of the small molecule content of outer membrane vesicles produced by *Bacteroides thetaiotaomicron* indicates an extensive metabolic link between microbe and host. *Front Microbiol.* 2017;8:2440. PubMed PMID: 29276507; PubMed Central PMCID: PMC5727896.
- [10] Shen Y, Giardino Torchia ML, Lawson GW, et al. Outer membrane vesicles of a human commensal mediate immune regulation and disease protection. *Cell Host Microbe.* 2012 Oct 18;12(4):509–520. PubMed PMID: 22999859; PubMed Central PMCID: PMC3895402.
- [11] Hickey CA, Kuhn KA, Donermeyer DL, et al. Colitogenic *Bacteroides thetaiotaomicron* antigens access host immune cells in a sulfatase-dependent manner via outer membrane vesicles. *Cell Host Microbe.* 2015 May 13;17(5):672–680. PubMed PMID: 25974305; PubMed Central PMCID: PMC4432250.
- [12] Kaparakis-Liaskos M, Ferrero RL. Immune modulation by bacterial outer membrane vesicles. *Nat Rev Immunol.* 2015 Jun;15(6):375–387. PubMed PMID: 25976515.
- [13] Stentz R, Carvalho AL, Jones EJ, et al. Fantastic Voyage: the journey of intestinal microbiota-derived microvesicles through the body. *Biochem Soc Trans.* 2018;46(5):1012–1–27.
- [14] Kesty NC, Kuehn MJ. Incorporation of heterologous outer membrane and periplasmic proteins into *Escherichia coli* outer membrane vesicles. *J Biol Chem.* 2004 Jan 16;279(3):2069–2076. PubMed PMID: WOS:000188005700062; English.
- [15] Collins BS. Gram-negative outer membrane vesicles in vaccine development. *Discov Med.* 2011 Jul;62:7–15. PubMed PMID: WOS:000208639700001; English.
- [16] de Kleijn ED, de Groot R, Labadie J, et al. Immunogenicity and safety of a hexavalent meningococcal outer-membrane-vesicle vaccine in children of 2–3 and 7–8 years of age. *Vaccine.* 2000 Feb 14;18(15):1456–1466. PubMed PMID: WOS:000085195800005; English.
- [17] Sandbu S, Feiring B, Oster P, et al. Immunogenicity and safety of a combination of two serogroup B meningococcal outer membrane vesicle vaccines. *Clin Vaccin Immunol.* 2007 Sep;14(9):1062–1069. PubMed PMID: WOS:000249488400002; English.
- [18] Gerritzen MJH, Martens DE, Wijffels RH, et al. Bioengineering bacterial outer membrane vesicles as vaccine platform. *Biotechnol Adv.* 2017 Sep;35(5):565–574. PubMed PMID: 28522212.
- [19] Shoemaker NB, Getty C, Gardner JF, et al. Tn4351 transposes in bacteroides spp and mediates the integration of plasmid R751 into the *Bacteroides* chromosome. *J Bacteriol.* 1986 Mar;165(3):929–936. PubMed PMID: WOS: A1986A276700039; English.

- [20] Stentz R, Horn N, Cross K, et al. Cephalosporinases associated with outer membrane vesicles released by bacteroides spp. protect gut pathogens and commensals against beta-lactam antibiotics. *J Antimicrob Chemother.* 2015 Mar;70(3):701–709. PubMed PMID: 25433011; PubMed Central PMCID: PMC4319488.
- [21] Wegmann U, Horn N, Carding SR. Defining the bacteroides ribosomal binding site. *Appl Environ Microbiol.* 2013 Mar;79(6):1980–1989. PubMed PMID: WOS:000315454500026; English.
- [22] Wegmann U, Klein JR, Drumm I, et al. Introduction of peptidase genes from *Lactobacillus delbrueckii* subsp. *lactis* into *Lactococcus lactis* and controlled expression. *Appl Environ Microbiol.* 1999 Nov;65(11):4729–4733. PubMed PMID: 10543778; PubMed Central PMCID: PMCPMC91636.
- [23] Matrosovich M, Matrosovich T, Garten W, et al. New low-viscosity overlay medium for viral plaque assays. *Virology.* 2006 Aug 31;363:63. PubMed PMID: 16945126; PubMed Central PMCID: PMCPMC1564390.
- [24] Stewart JP, Kipar A, Cox H, et al. Induction of tachykinin production in airway epithelia in response to viral infection. *PLoS One.* 2008;3(3):e1673. PubMed PMID: 18320026; PubMed Central PMCID: PMC2248620. eng.
- [25] Schmid AS, Hemmerle T, Pretto F, et al. Antibody-based targeted delivery of interleukin-4 synergizes with dexamethasone for the reduction of inflammation in arthritis. *Rheumatology (Oxford).* 2018 Apr 1;57(4):748–755. PubMed PMID: 29365185; PubMed Central PMCID: PMCPMC6104808.
- [26] Gil-Cruz C, Bobat S, Marshall JL, et al. The porin OmpD from nontyphoidal *Salmonella* is a key target for a protective B1b cell antibody response. *Proc Natl Acad Sci U S A.* 2009 Jun 16;106(24):9803–9808. PubMed PMID: WOS:000267045500047; English.
- [27] Kurtz JR, Petersen HE, Frederick DR, et al. Vaccination with a single CD4 T cell peptide epitope from a *Salmonella* type III-secreted effector protein provides protection against lethal infection. *Infect Immun.* 2014 Jun;82(6):2424–2433. PubMed PMID: WOS:000336378100029; English.
- [28] Barat S, Willer Y, Rizos K, et al. Immunity to intracellular *Salmonella* depends on surface-associated antigens. *PLoS Pathog.* 2012 Oct;8(10):e1002966. PubMed PMID: WOS:000310530300029; English.
- [29] Rollenhagen C, Sorensen M, Rizos K, et al. Antigen selection based on expression levels during infection facilitates vaccine development for an intracellular pathogen. *Proc Natl Acad Sci U S A.* 2004 Jun 8;101(23):8739–8744. PubMed PMID: WOS:000222037000045; English.
- [30] McSorley SJ, Cookson BT, Jenkins MK. Characterization of CD4(+) T cell responses during natural infection with *Salmonella typhimurium*. *J Immunol.* 2000 Jan 15;164(2):986–993. PubMed PMID: WOS:000084708600057; English.
- [31] Paramasivam N, Linke D. ClubSub-P: cluster-based subcellular localization prediction for Gram-negative bacteria and archaea. *Front Microbiol.* 2011;2:218. PubMed PMID: WOS:000208863500226; English.
- [32] Burton NA, Schurmann N, Casse O, et al. Disparate impact of oxidative host defenses determines the fate of *Salmonella* during systemic infection in mice. *Cell Host Microbe.* 2014 Jan 15;15(1):72–83. PubMed PMID: WOS:000330854100010; English.
- [33] Lee SJ, McLachlan JB, Kurtz JR, et al. Temporal expression of bacterial proteins instructs host cd4 t cell expansion and Th17 development. *PLoS Pathog.* 2012 Jan;8(1):e1002499. PubMed PMID: WOS:000300767100039; English.
- [34] Reynolds CJ, Jones C, Blohmke CJ, et al. The serodominant secreted effector protein of *Salmonella*, SseB, is a strong CD4 antigen containing an immunodominant epitope presented by diverse HLA class II alleles. *Immunology.* 2014 Nov;143(3):438–446. PubMed PMID: WOS:000342894300013; English.
- [35] Mallajosyula VV, Citron M, Ferrara F, et al. Influenza hemagglutinin stem-fragment immunogen elicits broadly neutralizing antibodies and confers heterologous protection. *Proc Natl Acad Sci U S A.* 2014 Jun 24;111(25):E2514–E2523. PubMed PMID: 24927560; PubMed Central PMCID: PMCPMC4078824.
- [36] Valkenburg SA, Mallajosyula VV, Li OT, et al. Stalking influenza by vaccination with pre-fusion headless HA mini-stem. *Sci Rep.* 2016 Mar 7;6:22666. PubMed PMID: 26947245; PubMed Central PMCID: PMCPMC4780079.
- [37] Werner S. Keratinocyte growth factor: a unique player in epithelial repair processes. *Cytokine Growth Factor Rev.* 1998 Jun;9(2):153–165. PubMed PMID: 9754709.
- [38] Baumgart DC, Sandborn WJ. Inflammatory bowel disease: clinical aspects and established and evolving therapies. *Lancet.* 2007 May 12;369(9573):1641–1657. PubMed PMID: 17499606.
- [39] Saroja C, Lakshmi P, Bhaskaran S. Recent trends in vaccine delivery systems: a review. *Int J Pharm Investig.* 2011 Apr;1(2):64–74. PubMed PMID: 23071924; PubMed Central PMCID: PMCPMC3465129.
- [40] Dieleman LA, Ridwan BU, Tennyson GS, et al. Dextran sulfate sodium-induced colitis occurs in severe combined immunodeficient mice. *Gastroenterology.* 1994 Dec;107(6):1643–1652. PubMed PMID: 7958674.
- [41] Hamady ZZ, Scott N, Farrar MD, et al. Xylan-regulated delivery of human keratinocyte growth factor-2 to the inflamed colon by the human anaerobic commensal bacterium *Bacteroides ovatus*. *Gut.* 2010 Apr;59(4):461–469. PubMed PMID: 19736360.
- [42] Okayasu I, Hatakeyama S, Yamada M, et al. A novel method in the induction of reliable experimental acute and chronic ulcerative colitis in mice. *Gastroenterology.* 1990;98:694–702.
- [43] Hamady ZZ, Farrar MD, Whitehead TR, et al. Identification and use of the putative *Bacteroides ovatus* xylanase promoter for the inducible production of recombinant human proteins. *Microbiology.* 2008 Oct;154(Pt 10):3165–3174. PubMed PMID: 18832322.
- [44] Wegmann U, Carvalho AL, Stocks M, et al. Use of genetically modified bacteria for drug delivery in humans: revisiting the safety aspect. *Sci Rep.* 2017 May 23;7(1):2294. PubMed PMID: 28536456; PubMed Central PMCID: PMCPMC5442108.
- [45] Farrar M, Whitehead TR, Lan J, et al. Engineering of the gut commensal bacterium *Bacteroides ovatus* to produce and secrete biologically active murine interleukin-2 in response to xylan. *J Appl Microbiol.* 2005;98:1191–1197.

- [46] Hamady ZZ, Scott N, Farrar MD, et al. Treatment of colitis with a commensal gut bacterium engineered to secrete human TGF-beta1 under the control of dietary xylan 1. *Inflamm Bowel Dis.* 2011 Sep;17(9):1925–1935. PubMed PMID: 21830271.
- [47] Ballesteros-Tato A, Leon B, Lund FE, et al. Temporal changes in dendritic cell subsets, cross-priming and costimulation via CD70 control CD8(+) T cell responses to influenza. *Nat Immunol.* 2010 Mar;11(3):216–224. PubMed PMID: 20098442; PubMed Central PMCID: PMCPMC2822886.
- [48] Brandtzaeg P. Gate-keeper function of the intestinal epithelium. *Benef Microbes.* 2013 Mar 1;4(1):67–82. PubMed PMID: 23257015.
- [49] Okamura M, Ueda M, Noda Y, et al. Immunization with outer membrane protein A from *Salmonella enterica* serovar Enteritidis induces humoral immune response but no protection against homologous challenge in chickens. *Poult Sci.* 2012 Oct;91(10):2444–2449. PubMed PMID: 22991526.
- [50] Sanders H, Feavers IM. Adjuvant properties of meningococcal outer membrane vesicles and the use of adjuvants in *Neisseria meningitidis* protein vaccines. *Expert Rev Vaccines.* 2011 Mar;10(3):323–334. PubMed PMID: 21434800.
- [51] Moshiri A, Dashtbani-Roozbehani A, Najar Peerayeh S, et al. Outer membrane vesicle: a macromolecule with multifunctional activity. *Hum Vaccin Immunother.* 2012 Jul;8(7):953–955. PubMed PMID: 22699443.
- [52] Krammer F, Palese P. Advances in the development of influenza virus vaccines. *Nat Rev Drug Discov.* 2015 Mar;14(3):167–182. PubMed PMID: 25722244.
- [53] Renegar KB, Small PA Jr., Boykins LG, et al. Role of IgA versus IgG in the control of influenza viral infection in the murine respiratory tract. *J Immunol.* 2004 Aug 1;173(3):1978–1986. PubMed PMID: 15265932.
- [54] Watkins HC, Rappazzo CG, Higgins JS, et al. Safe recombinant outer membrane vesicles that display M2e elicit heterologous influenza protection. *Mol Ther.* 2017 Apr 5;25(4):989–1002. PubMed PMID: 28215994; PubMed Central PMCID: PMCPMC5383554.
- [55] Zeeh JM, Procaccino F, Hoffmann P, et al. Keratinocyte growth factor ameliorates mucosal injury in an experimental model of colitis in rats. *Gastroenterology.* 1996 Apr;110(4):1077–1083. PubMed PMID: 8612996.
- [56] Miceli R, Hubert M, Santiago G, et al. Efficacy of keratinocyte growth factor-2 in dextran sulfate sodium-induced murine colitis. *J Pharmacol Exp Ther.* 1999 Jul;290(1):464–471. PubMed PMID: 10381813.



Chapter 11

Production, Isolation, and Characterization of Bioengineered Bacterial Extracellular Membrane Vesicles Derived from *Bacteroides thetaiotaomicron* and Their Use in Vaccine Development

Régis Stentz, Ariadna Miquel-Clopés, and Simon R. Carding

Abstract

Bacterial extracellular vesicles (BEVs) possess features that make them well suited for the delivery of therapeutics and vaccines. This chapter describes methods for engineering the commensal human intestinal bacterium *Bacteroides thetaiotaomicron* (Bt) to produce BEVs carrying vaccine antigens and accompanying methods for isolating and purifying BEVs for mucosal vaccination regimens.

Key words *Bacteroides thetaiotaomicron*, Bacterial extracellular vesicles, Crossflow ultrafiltration, Vaccines, Immunization

1 Introduction

Conventional vaccines based on the use of attenuated or inactivated forms of the target pathogen have successfully eradicated smallpox and rinderpest as well as significantly reducing the burden of many other infectious diseases throughout the past century. However, the time needed to identify vaccine targets, the high cost of vaccine development and manufacture, and the limited production capacity, make these traditional approaches less than optimal in the rapid response to epidemics and pandemics [1]. Furthermore, these vaccines are usually delivered parenterally via injection, which makes mass immunization costly particularly in resource-poor developing countries [2]. There is, therefore, a need for the development of new vaccines that are versatile, cost-effective, safe, and enable global immunization. To this end, various new vaccination technologies have emerged including the use of synthetic protein and peptide antigens [3]. Protein subunit vaccines are attractive because of their inherent safety although they can suffer from poor

immunogenicity and high manufacturing costs [4]. To address these constraints, nanoparticle-based delivery technologies have been developed which includes nanoparticle-sized extracellular vesicles naturally produced by bacteria.

Bacterial extracellular vesicles (BEVs) are spherical nanostructures composed of membrane-derived lipid bilayers with a diameter of between 20 and 400 nm. BEVs generated by gram-negative bacteria primarily consist of vesicles derived from the outer membrane containing phospholipids, outer membrane proteins, lipopolysaccharides, and capsular polysaccharides with their lumen principally filled with periplasmic content [5]. These components, which include microbe-associated molecular pattern molecules, confer inherent and potent adjuvanticity on BEVs which together with their natural temperature, chemical resistance, and straightforward isolation [6–8] makes them well suited as vaccine delivery vehicles capable of enhancing the immunogenicity of protein/peptide antigens without the need for chemical adjuvants [9]. The ability of BEVs to interact with, and be acquired by, mucosal epithelial and immune cells [10–12] further enhances their suitability for mucosal administration and the generation of local and systemic immunity [13].

We have engineered the gram-negative bacterium *Bacteroides thetaiotaomicron* (Bt), a prominent member of the intestinal microbiota of all animals [14, 15], to incorporate virus-, bacteria-, and human-derived proteins into its BEVs [8, 16]. These engineered Bt BEVs have been used to protect the gastrointestinal or respiratory tracts against infection, tissue inflammation and injury. Here, we describe the methods to implement secretion of vaccine antigens and other proteins into Bt BEVs for mucosal delivery, which are outlined in Fig. 1.

2 Materials

Unless stated otherwise, all solutions are prepared with double-distilled water (ddH₂O) with all reagents being stored at ambient (room) temperature (~20 °C). Most methods require the use of piston pipettes and sterile single-use pipette tips.

2.1 Synthetic Gene Design

1. Protein sequence (e.g., stalk of the hemagglutinin antigen of influenza A virus strain H5N1 [8, 17]).
2. Secretion sequence signal (e.g., N-terminal sequence of Bt outer membrane protein A [OmpA] (BT_3852)).
3. Optional additional sequences (e.g., His-tag or FLAG-tag sequences).
4. *Escherichia coli*/*Bacteroides* shuttle expression vector sequence (e.g., pGH90 [18]) (see Note 3).

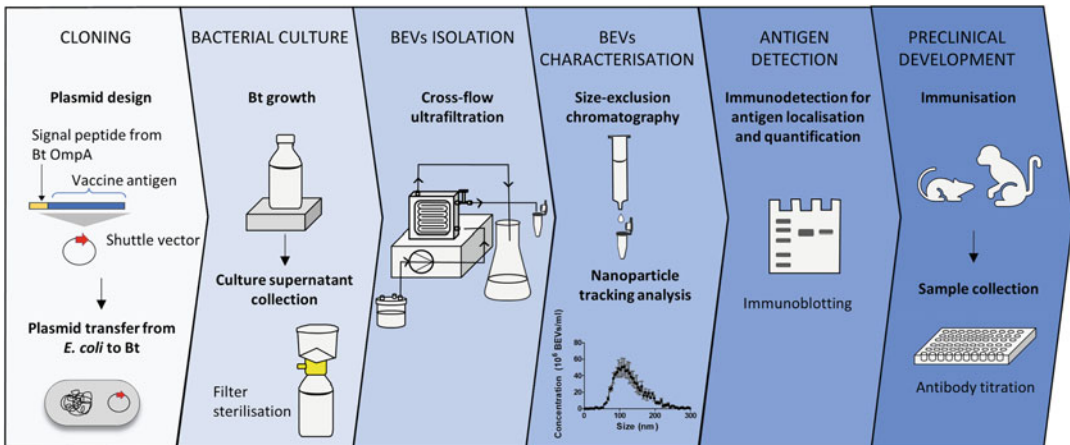


Fig. 1 Overview of the production and extraction of bioengineered bacterial extracellular vesicles (BEVs) derived from *B. thtaiotaomicron* for the development of novel vaccines. Immunization and sample collection for preclinical development and evaluation are described in **Notes 1** and **2**

2.2 Cloning of Synthetic Gene

The required materials for the cloning of the conjugative plasmid harboring the gene of interest are as follows:

2.2.1 Generation of Recombinant DNA

1. *E. coli/Bacteroides* shuttle expression vector.
2. Restriction enzymes.
3. Ligation buffer and enzyme.

2.2.2 Transformation of Competent Cells

1. Crushed ice for thawing the MAX Efficiency[®] DH10B competent cells.
2. S.O.C. medium: commercially available.
3. Luria-Bertani (LB) agar plates: prepare according to the manufacturer's instructions.
4. Shaking incubator.
5. LB broth for the dilution of the bacterial cell suspension: prepare according to the manufacturer's instructions.
6. Agar plates containing ampicillin (working concentration 100 µg/mL).
7. 1.5 mL centrifuge tubes.
8. Water bath.

2.2.3 Screening of Recombinant Bacteria

1. Shaking incubator.
2. Benchtop centrifuge.
3. Small-scale plasmid isolation kit.
4. Gel electrophoresis chamber and electrophoresis power supply.

5. Stained agarose gel: 1% (w/v) agarose, e.g., with EvaGreen[®] Dye, Biotium.
6. DNA loading buffer.
7. DNA ladder.

2.3 Conjugative Transfer of Shuttle Vector into Bt

1. *E. coli* donor strain containing shuttle vector carrying gene of interest.
2. *E. coli* helper strain, e.g., J53/R751 [19].
3. 5 mL LB bottle with ampicillin 100 µg/mL (or another suitable antibiotic).
4. 5 mL LB bottle with trimethoprim 200 µg/mL (or another suitable antibiotic)
5. Brain heart infusion (BHI) agar supplemented with hemin and antibiotics (gentamicin 200 µg/mL and/or erythromycin 5 µg/mL, or another suitable antibiotic): Dissolve 18.5 g of BHI powder and 7.5 g of agar in 0.5 liter of deionized water and add 0.75 µM of hemin (BHIIH). Autoclave the medium and leave for a minimum of 24 h in an anaerobic cabinet to fully deoxygenate.
6. Filter disc 0.45 µm pore size, 25 mm.
7. 50 mL conical centrifuge tubes.
8. Tweezers.
9. Sterile 25 mL wide neck universal glass bottle.

2.4 Assessing Protein Expression and Secretion into BEV

2.4.1 Culture of Bt Transconjugants

1. BHIIH agar plates containing gentamicin 200 µg/mL and erythromycin 5 µg/mL.
2. Sterile inoculation loop(s).
3. 20 mL BHIIH containing erythromycin 5 µg/mL in Universal bottles.
4. Anaerobic cabinet.
5. 50 mL conical centrifuge tubes.
6. Refrigerated centrifuge.
7. -20 °C freezer.

2.4.2 Cell Total Protein Extraction

1. 0.2 M Tris-HCl, pH 7.2.
2. Sonicator.
3. Refrigerated centrifuge.
4. Bradford reagent.
5. 96-well microplate.
6. Bovine serum albumin (BSA).

2.4.3 *BEV Total Protein
Extraction*

1. 20 mL syringe.
2. 0.22 μm pore-size polyethersulfone (PES) membranes (Sartorius).
3. Centrifugal concentrator, 100 kDa molecular weight cutoff.
4. Refrigerated centrifuge.
5. 0.2 M Tris-HCl, pH 7.2.
6. Sonicator.
7. Bradford reagent.
8. 96-well microplate.
9. BSA.

2.4.4 *Protein Western
Blotting/Antigen
Immunodetection*

1. Gel electrophoresis equipment.
2. Protein gel.
3. SDS sample loading buffer.
4. Reducing agent.
5. Antioxidant for protein electrophoresis.
6. Running buffer.
7. Blotting equipment.
8. Western blotting membrane.
9. Tweezers.
10. Tris-Glycine transfer buffer (25 \times): Dissolve 18.2 g Tris Base and 90.0 g of glycine in 450 mL of deionized water. Mix well and adjust the volume to 500 mL with deionized water. The pH of the buffer is 8.3. Store the buffer at 20 $^{\circ}\text{C}$. The buffer is stable for 6 months at 25 $^{\circ}\text{C}$.
11. Methanol.
12. Orbital shaker.
13. Tris-buffered saline (TBS) buffer: 50 mM Tris-HCl, 150 mM NaCl, pH 7.5.
14. TBST buffer: TBS buffer with 0.05% Tween 20.
15. Blocking buffer: TBST with 5% non-fat dry milk.
16. Chemiluminescent substrate.
17. Primary antibody (e.g., 6 \times -His Tag monoclonal antibody) used at a working concentration recommended by the manufacturer or by other providers if the antibody is not commercially available (*see Note 4*).
18. Secondary antibody labelled with horse radish peroxidase (HRP) (*see Note 5*).
19. Imaging System.

2.5 Bacteria Medium-Scale Culture

2.5.1 BHIH Bacterial Culture

1. BHIH medium.
2. Anaerobic cabinet.
3. Magnetic stirrer.
4. Sterile magnetic stirring bar.

2.5.2 BDM+ Bacterial Culture

1. *Bacteroides* defined medium Plus (BDM+): To prepare 500 ml, dissolve 2.61 g of KH_2PO_4 and 7.03 g of $\text{K}_2\text{HPO}_4 \cdot 3 \text{H}_2\text{O}$ into 481 mL of deionized water, add the following solutions to a final concentration of 15 mM NaCl and 8.5 mM $(\text{NH}_4)_2\text{SO}_4$, adjust the pH to 7.4 using 5 M NaOH, autoclave and place in the anaerobic cabinet to equilibrate for a minimum of 24 h. Add the rest of the solutions to a final concentration of 30 mM of glucose, 0.2 mM L-histidine, 100 nM vitamin B12, 6 μM vitamin K3 (menadione), 0.1 mM MgCl_2 , 50 μM CaCl_2 , 4.1 mM L-cysteine and 1.4 μM $\text{FeSO}_4 \cdot 7 \text{H}_2\text{O}$. Leave the medium for a minimum of 24 h in the anaerobic cabinet to fully deoxygenate. Add 2 μM of Protoporphyrin IX freshly made before using the media. All stock solutions in exception of Protoporphyrin IX are prepared in advance and autoclaved or filter sterilized, as below:
 - 1.5 M NaCl (autoclaved).
 - 0.85 M $(\text{NH}_4)_2\text{SO}_4$ (autoclaved).
 - 3 M Glucose (filtered).
 - 0.2 M L-histidine, store at 4 °C (filtered).
 - 1 mM vitamin B12, store at 4 °C (filtered).
 - 6 mM vitamin K3 (menadione), dissolve in ethanol and store at -20 °C (filtered).
 - 0.1 M $\text{MgCl}_2 \cdot 6 \text{H}_2\text{O}$, store in anaerobic cabinet (autoclaved).
 - 50 mM $\text{CaCl}_2 \cdot 2 \text{H}_2\text{O}$, store in anaerobic cabinet (autoclaved).
 - 0.41 M L-cysteine hydrochloride, store in anaerobic cabinet (filtered).
 - 2 mM Protoporphyrin IX.
 - 1.4 mM $\text{FeSO}_4 \cdot 7 \text{H}_2\text{O}$, store in anaerobic cabinet (filtered).
2. Anaerobic cabinet.
3. Magnetic stirrer.
4. Sterile magnetic stirring bar.

2.5.3 Supernatant Collection

1. Spectrophotometer (wavelength: 600 nm) with cuvette holder and cuvettes.

2. Refrigerated high speed floor centrifuge, including appropriate rotor with 500 mL sealable centrifuge bottles.
3. 0.2 μm PES bottle top filter unit (500 mL).
4. Membrane vacuum pump.
5. Sterile 500 mL bottles.

2.6 EV Isolation

1. Filtration cassette Vivaflow 50 R (100,000 MWCO, Hydrostat, model VF05H4, Sartorius).
2. Peristaltic pump for running the Vivaflow-unit.
3. Sterile phosphate-buffered saline (PBS), pH 7.4.
4. 0.22 μm PES syringe filters.
5. 5 mL sterile syringes.
6. 15 mL conical centrifuge tubes.
7. 1.5 mL sterile low-bind microcentrifuge tubes.
8. Deionised water.
9. 0.5 M NaOH solution.
10. 10% (v/v) ethanol.

2.7 EVs Purification

In this part of the chapter, the use of size-exclusion chromatography is described for the removal of remaining proteins. Two options are proposed: 2.7.1 and 2.7.2 for an increased resolution.

2.7.1 Routine Purification

1. qEVoriginal/35 nm SEC columns (IZON).
2. Support to maintain column in a vertical position.
3. 1.5 mL lo-bind microcentrifuge tubes.
4. Amicon Ultra 0.5 mL centrifugal filters (RC, 10 kDa MWCO).
5. Sterile PBS, pH 7.4.
6. 0.22 μm PES membrane syringe filter.
7. 1 mL sterile syringes.
8. LB and BHIH agar plates.

2.7.2 High-Resolution Fractionation

1. CL2-B Sepharose.
2. Sterile PBS, pH 7.4.
3. Chromatography column (120 cm \times 1 cm) (e.g., Econo-Column[®] Chromatography Column) in PBS.
4. Chromatography fraction collector.
5. UV spectrophotometer.
6. Vivaspin 20 centrifugal concentrator (100 kDa molecular weight cutoff).
7. 0.22 μm PES membrane syringe filter.

2.8 EVs Size and Concentration Analysis

1. Nanoparticle Analyzer (ZetaView TWIN Particle Tracking Analyzer instrument or equivalent).
2. Particle-free deionized water.
3. 1 or 10 mL sterile syringes.

2.9 Antigen Localization with Proteinase K Assay

1. Proteinase K.
2. Phenylmethanesulfonyl fluoride (PMSF).
3. Water bath.
4. Sodium Dodecyl Sulphate (SDS).
5. See also materials in Subheadings 2.4.3 and 2.4.4.

2.10 Antigen Quantification

1. Recombinant antigen.
2. See also materials in Subheadings 2.4.3 and 2.4.4.

3 Methods**3.1 Synthetic Gene Design**

The gene can be synthesized *de novo* using commercial gene synthesis services. The N-terminus of the protein of interest is fused in frame to the signal peptide of the product of BT_3852 (OmpA of Bt); MKKILMLLAFAGVASVASA. The chimeric protein sequence is tested in silico for cleavage of the OmpA signal sequence using <http://www.cbs.dtu.dk/services/SignalP/>. If unsuccessful, change or add amino acids as appropriate to the N-terminus of the gene of interest, downstream from the signal peptide sequence. To facilitate immunodetection and/or purification of the protein in downstream applications, a fusion tag can be added to the gene. It is important that the coding sequence of the desired protein incorporates codon usage optimization for expression in Bt, which is usually provided as part of gene synthesis services. The desired target sequence is then integrated into an acceptor vector.

3.2 Cloning of Gene of Interest**3.2.1 Generation of Recombinant DNA**

1. Digest the plasmid containing the synthetic gene with restriction enzymes to excise the gene from the vector carrying the synthetic gene (e.g., pEX-K168).
2. Digest the *E. coli/Bacteroides* shuttle vector pGH90 (see Subheading 2.1) (see **Note 6**).
3. Ligate the gene into the digested pGH90 expression vector to allow translational fusion (see **Note 7**).

3.2.2 Transformation of Competent Cells

1. Prepare LB agar plates containing ampicillin.
2. Thaw one vial of competent MAX Efficiency[®] DH10B on ice.
3. Gently add 1–5 μ L of ligation mixture to the MAX Efficiency[®] DH10B.

4. Place the vial with the bacteria suspension on ice for 30 min.
5. Induce a heat-shock at 42 °C for 30 s.
6. Incubate the bacteria on ice for an additional 5 min.
7. Add 950 µL S.O.C. medium.
8. Incubate at 37 °C with agitation (250 rpm).
9. Seed 100 µL of the bacterial suspension onto agar plates containing ampicillin.
10. Incubate the plates for 16–18 h at 37 °C.

**3.2.3 Screening
of Cloned
Recombinant DNA**

1. Pick individual colonies from agar plates and add each colony to a tube containing 5 mL LB medium and ampicillin.
2. Incubate the liquid cultures at 37 °C and 250 rpm for 16–18 h.
3. Isolate plasmid DNA from each culture using a small-scale isolation kit (e.g., QIAprep Spin Miniprep Kit) according to the manufacturer's instructions.
4. Digest the plasmid DNA using the appropriate restriction enzymes (*see Note 8*).
5. Resolve digested DNA on a TBE gel.
6. Confirm the identity of the plasmids containing the insert of the expected size by DNA sequencing using appropriate primers.

**3.3 Conjugative
Transfer of Shuttle
Vector into Bt**

**3.3.1 Triparental Mating
Procedure**

1. Prepare BHIH agar plates either with or without gentamycin and erythromycin.
2. Grow cultures of the *E. coli* donor strain with ampicillin (containing the plasmid with the correct inserted sequence, *see* Subheading 3.2.3) and the *E. coli* helper strain with trimethoprim in 10 mL of LB, at 37 °C, under agitation for 16–18 h. In parallel, grow culture of the Bt recipient strain in BHIH in an anaerobic cabinet at 37 °C for 16–18 h.
3. Inoculate 10 mL of LB with 100 µL of the *E. coli* donor strain and the helper strain (no antibiotics added) cultures and incubate for 2 h at 37 °C with agitation (e.g., 200 rpm). In parallel, inoculate in 30 mL BHIH contained in a 50 mL tube with 800 µL of the Bt culture and incubate for 2 h at 37 °C in an anaerobic cabinet.
4. Add donor and helper cultures to the Bt recipient in the 50 mL tube, mix by vortexing briefly and centrifuge at $2000 \times g$ for 15 min at 20 °C.
5. Remove the supernatant and resuspend cells in 100 µL of BHIH. Transfer cell suspension to the surface of a sterile 0.45 µm filter placed on a BHIH agar plate. Incubate the plate aerobically for 16–18 h at 37 °C.

6. Transfer the filter to a sterile wide-necked Universal bottle and add 1 mL of BHIH and resuspend the bacterial conjugation mixture by vortexing thoroughly.
7. Make serial dilutions and plate 100 μ L of each dilution and the non-diluted cell suspensions onto BHIH agar plates containing gentamycin (to prevent *E. coli* growth) and erythromycin (selection of Bt transconjugants).

3.4 Assessing Protein Expression and Secretion into BEVs

3.4.1 Culture of Bt Transconjugants

1. Pick 4 individual colonies and restreak each one on separate BHIH agar plates containing gentamicin and erythromycin.
2. Incubate the plates anaerobically at 37 °C for 48 h.
3. Inoculate bottles containing 20 mL of BHIH with each of the 4 isolated clones.
4. Incubate the bottles anaerobically at 37 °C for 48 h.
5. Centrifuge the 20 mL of culture in 50 mL tubes, at 6000 $\times g$ for 15 min, at 4 °C.
6. Collect the supernatant.
7. Wash cell pellets once in PBS before storing at -20 °C prior to analysis.

3.4.2 Cell Total Protein Extraction

1. Resuspend thawed cell pellets in 250 μ L of 0.2 M Tris-HCl (pH 7.2).
2. Disrupt the cells via sonication using eight 10-s pulses (amplitude, 6 μ m), with 30-s pauses on ice between each pulse.
3. Cell extracts are obtained after centrifugation at 14,000 $\times g$ for 30 min at 4 °C and harvesting the supernatant.
4. Measure total protein concentration of each supernatant/sample using the Bio-Rad protein assay according to the manufacturer's instructions using BSA to generate a standard curve.

3.4.3 BEV Total Protein Extraction

1. Filter the 20 mL supernatants through 0.22 μ m pore-size PES membranes to remove debris and cells.
2. Concentrate the supernatants by ultrafiltration (100 kDa molecular weight cutoff, Vivaspin 20) to a final volume of 250 μ L.
3. Discard the filtrate.
4. Rinse the retentate with 20 mL of 0.2 M Tris-HCl, pH 7.2 and concentrated to 250 μ L.
5. Collect the retentate and disrupt the vesicles via sonication using eight 10-s pulses (amplitude, 6 μ m), with 30-s pauses on ice between each pulse.
6. Measure the total protein content and concentration using the Bio-Rad protein assay according to the manufacturer's instructions using BSA to generate a standard curve.

3.4.4 Protein Western Blotting/Antigen Immunodetection

1. Add BEV and cell extracts obtained in Subheading 3.4.3 to loading buffer containing 0.4 M freshly prepared dithiothreitol (DTT).
2. Load 7 μg of the total protein onto a 12% precast gel and separate by electrophoresis at 180 V for 40 min.
3. Transfer the proteins from the gel onto a polyvinylidene difluoride (PVDF) membrane using the XCell II™ Blot Module or equivalent (according to the manufacturer's instructions) at 25 V for 2 h in a solution containing Tris-Glycine transfer buffer and methanol 20% (v/v).
4. Incubate the membrane with blocking buffer by gently shaking for 30 min at 20 °C using an orbital shaker.
5. Discard the blocking solution and incubate the membrane for 16–18 h at 4 °C in blocking buffer containing primary antibody (Usually 1:1000 to 1:10000).
6. After washing 3 times with TBST, membranes are incubated with HRP-conjugated secondary antibody in blocking buffer for 1 h at 20 °C.
7. After 3 washes with TBST, Enhanced Chemiluminescent substrate (ECL) is added to detect bound antibody.

3.4.5 Medium-Scale Bacterial Culture and Harvesting Conditioned mediaBHH Bacterial Culture

1. Inoculate 10 mL of BHH with a frozen stock for ~16 h.
2. Inoculate 500 mL of BHH with 0.5 mL of the preinoculum for 17 h (starting $\text{OD}_{600} \sim 0.005$) with mild stirring.

3.4.6 BDM+ Bacterial Culture

Initially BHH was used as a standard medium for generating Bt BEVs [8, 16]. However, considering the need to reduce and even exclude animal-derived products from medical/therapeutic formulations to be used in humans, we have modified a chemically defined *Bacteroides* growth media (BDM) [20] (see Subheading 2.5.2) for Bt BEV production.

1. Inoculate 10 mL of BHH with a frozen stock for ~16 h.
2. Inoculate 10 mL of BDM+ with 100 μL BHH culture from **step 1** for ~8 h.
3. Inoculate 500 mL of BDM+ with 0.5 mL of the preinoculum for 17 h (starting $\text{OD}_{600} \sim 0.005$) with gentle stirring.

3.4.7 Supernatant Collection

1. Collect bacterial cultures at final OD_{600} 1.5–2.5.
2. Precool centrifuge and canisters for 5 min at 4 °C.
3. Decant the culture into two 2 Nalgene™ PPCO centrifuge bottles and centrifuge at $6037 \times g$ for 30 min at 4 °C.

4. Filter-sterilize the supernatant with a 0.22 μm bottle-top filter unit and transfer the filtrate into a sterile 500 mL bottle (*see Note 9*).
5. Samples are stored at 4 °C prior to BEVs isolation for up to 24 h.

3.5 Isolation of BEVs

During the filtration process, the membrane will retain any molecules >100 kDa including BEVs (retentate) and concentrate them in the reservoir, whereas molecules <100 kDa will be removed in the flow-through (filtrate) directly to the waste. BEVs isolation should be performed at ambient (20–22 °C) temperature.

Three procedures are used in a step wise manner for isolating BEVs, which are illustrated in Fig. 2.

3.5.1 Module Rinsing

1. Set up the system as illustrated in Fig. 2 Option 2.
2. Place 400 mL of deionized water in the reservoir and pump the liquid through the system at an initial speed setting of 2 to remove air pockets and then increase the speed setting to 4–5 (200–300 mL/min) until 400 mL has been run through the system. Collect filtrate in waste bin. Check for any leaks.

3.5.2 Sample Concentration

1. Set up the module as illustrated in Fig. 2 Option 1.
2. Fill the reservoir with 500 mL filtrate.
3. Pump sample through the system. The initial recirculation speed setting is 2 for at least 1 cycle and then adjusted to setting 4–5 for sampling (200–300 mL/min). Maximum recirculation speed setting is 5. Reduce the speed for lower volumes to avoid foaming.
4. Concentrate the sample until there is ~5 mL left in the system.
5. Switch off the pump.
6. Pour 500 mL of PBS pH 7.4 into the reservoir and pump through the system at an initial speed setting of 2 to remove any air pockets and then increase the speed to setting 4–5.
7. Reduce the recirculation speed setting to 1–2 (20–40 mL/min) to avoid foaming.
8. Switch off the pump with 1–4 mL remaining in the system.
9. Set up the module as illustrated in Fig. 2 Option 3.
10. Start the pump at a speed setting of 1–2 and carefully collect the concentrated samples in a 15 mL tube or microcentrifuge tube (use a bigger tube than the volume to be collected to account for foam).
11. When no more concentrated sample emerges from the tubing, switch off the pump.

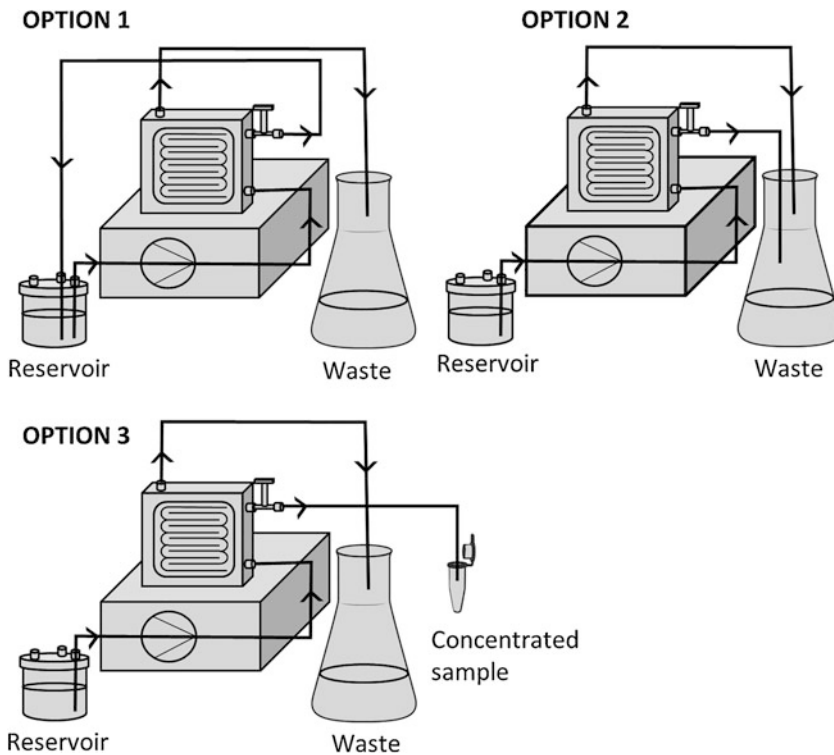


Fig. 2 BEV isolation module system. Option 1. Sample concentration. Option 2. Module rinsing/decontamination. Option 3. Collection of concentrated samples

12. Place 0.5–1 mL of PBS in the reservoir and pump through the system at speed setting 1–2 to flush out remaining BEVs. Collect in the original 15 mL tube or microcentrifuge tube. Final volume collected depends on concentration of BEVs needed.
13. Switch off the pump.
14. Centrifuge at $15,000 \times g$ for 20 min at 4°C to remove any precipitate.
15. Filter-sterilize the supernatant using a $0.22 \mu\text{m}$ syringe filter, collecting the filtrate in sterile 1.5 mL lo-bind microcentrifuge tubes or 15 mL tube.

3.5.3 Module Decontamination and Washing

1. Set up the system as illustrated in Fig. 2 Option 2.
2. Place 400 mL of deionized water in the reservoir and pump liquid through the system at an initial speed setting of 2 to remove any air pockets and increase the speed setting to 4–5 (200–400 mL/min). Collect filtrate in waste bin.
3. When all the water has been collected, switch off the pump.
4. Set up the system as illustrated in Fig. 2 Option 1.

5. Place 250 mL of decontamination solution (250 mL 0.5 M NaOH) and pump it through the system at a speed setting of 3–4 (50–100 mL/min). Allow to recirculate for a minimum of 20 min, then switch off the pump.
6. Set up the system as illustrated in Fig. 2 Option 2.
7. Place 400 mL of deionized water in the reservoir and pump liquid through the system at an initial speed setting of 2 to purge any air pockets and increase the speed setting to 4–5 (200–400 mL/min).
8. Switch off the pump.
9. Set up the system as illustrated in Fig. 2 Option 2.
10. Place 250 mL of 10% Ethanol in the reservoir and pump liquid through the system at an initial speed setting of 2 to purge any air pockets and increase the speed setting to 3–4 (50–100 mL/min).
11. When half of the 10% Ethanol has been filtered, switch off the pump and dismantle the system module.
12. Store cassette membrane in 10% Ethanol at 4 °C to avoid contamination.
13. Rinse the reservoir with water and let it air dry. Reservoir and tubing are left to dry at 20 °C.

BEV isolation waste is discarded in the sink drain.

3.6 BEVs Purification

Contaminants (e.g., proteins) of BEV preparations can be removed by size exclusion chromatography (SEC). We recommend using the method described in Subheading 3.7, **step 1** for routine preparations and in Subheading 3.7, **step 2** if increased resolution is needed, for instance, to size fractionate BEVs.

3.6.1 Routine Purification

1. Bring the BEVs preparation, column buffer (PBS pH 7.4) and qEVoriginal/35 nm SEC column(s) to ~20 °C. Do not remove the column caps until operational temperature is reached.
2. Secure the column in a vertical position using a stand.
3. Carefully remove the column top-cap.
4. Attach a column reservoir (if available) and add 1.5× column volume of buffer (PBS 1×, 15 mL).
5. Remove the bottom column cap and allow the buffer to run under gravity to waste.
6. If any buffer other than PBS is used, flush with at least 3 column volumes of the buffer (>30 mL).
7. The column will stop flowing when the buffer has entered the loading frit.
8. Load 0.5–1 mL of isolated BEVs onto the loading frit.

9. Collect the void volume (3 mL) fraction(s) into 1.5 mL lo-bind microcentrifuge tubes.
10. Allow the sample to completely run into the column.
11. Top up the reservoir with 15 mL buffer (PBS 1×) and collect 0.5–1 mL elution fractions.
12. For a loading volume of 1 mL of BEVs and collecting 0.5 mL elution fractions, BEVs will elute in fractions 7–12 with proteins eluting in fractions 10–20.
13. After the eluted fractions have been collected, flush the column with 1.5 volumes of buffer (PBS 1×, 15 mL) before loading another sample.
14. If storing the column, flush with buffer containing 20% ethanol or 0.05% sodium azide.
15. Store the column at 4 °C to avoid contamination.
16. Filter-sterilize the BEVs using a 0.22 µm syringe filter, collecting the filtrate in sterile 1.5 mL lo-bind microcentrifuge tubes or 15 mL tube.
17. Pool BEVs elution fractions and concentrate to desired volume using Amicon Ultra 0.5 mL centrifugal filters (RC, 10 kDa MWCO).

3.6.2 High-Resolution Size Fractionation

See **Note 10**.

3.7 BEVs Size and Concentration Analysis

Size and concentration of isolated BEVs suspension is determined by nanoparticle tracking analysis (NTA) using a suitable NTA instrument. The protocol described below is for the ZetaView PMX-220 TWIN instrument from Particle Metrix GmbH.

1. Prepare instrument set up according to the manufacturer's instructions.
2. Inject 10–20 mL particle-free deionized water using a 10 mL syringe to perform cell quality check; avoid injecting air bubbles.
3. Inject 5–10 mL of 1:25,000 100 nm polystyrene standard bead suspension to perform focus auto-alignment.
4. Inject 10–20 mL particle-free deionized water using a 10 mL syringe to rinse instrument; avoid injecting air bubbles.
5. Dilute aliquots of BEVs suspension in 1:1000 to 1:20,000 in particle-free deionized water.
6. Inject 1 mL sample with a syringe; avoid injecting air bubbles.

7. Acquire size distribution video data using the following settings.
 - temperature: 25 °C;
 - frames: 60;
 - duration: 2 s;
 - cycles: 2;
 - positions: 11;
 - camera sensitivity: 80; and,
 - shutter value: 100.
8. Analyse data using the ZetaView NTA software (version 8.05.12) with the following post acquisition settings:
 - minimum brightness: 20;
 - max area: 2000;
 - min area: 5; and,
 - trace length: 30.

3.8 Proteinase K Assay

To establish if heterologous proteins are expressed in the lumen or at the surface of BEVs we use broad-spectrum proteinase K. Proteinase K digests proteins exposed at the surface of BEVs but not in the lumen. Extracts of BEVs obtained in the presence or absence of Proteinase K samples and analyzed by Western blotting using antibodies specific for the heterologous protein makes it possible to distinguish between surface- and lumen-expressed antigens (*see Note 11*).

1. Add 100 mg/L of proteinase K into intact 10^{11} BEVs/mL or solubilized (in 1% SDS) and incubate for 1 h in a water bath at 37 °C.
2. The activity of proteinase K is stopped by addition of 1 mM PMSF.
3. Load samples onto a 12% polyacrylamide gel and perform a Western blot following steps described in Subheading 3.4.4.

3.9 Antigen Quantification

The amount of antigen expressed in BEVs is readily determined by Western blotting using serial dilutions of the recombinant antigen and comparing the intensity of the bands visualized on the blot to estimate the concentration of antigen in the BEVs using Image Lab Software (Bio-Rad).

1. Prepare serial dilutions of the recombinant antigen and the isolated BEVs.
2. Load samples onto a 12% polyacrylamide gel and perform a Western blot (Subheading 3.4.4).
3. Analyse the image of the blot using the quantity tool of Image Lab software (Bio Rad).

4 Notes

1. Immunization: Details of immunization protocols are provided in Carvalho et al. [8, 16]. In short, animals receive a primary immunization of filter-sterilized BEVs (*see Note 12*) via the nasal or oral route with booster immunizations carried out 7–14 days later with an infectious challenge following after a further 7–10 days. At necrosis body fluids and tissues are harvested for downstream analyses of antibody and immune cell profiles and histopathology.
2. Sample collection and antibody profiles: Serum bronchoalveolar lavage and saliva samples are routinely used in ELISAs to identify and quantify antigen-specific IgA and IgG antibodies as described in Carvalho et al. [8, 16]. In short, the ELISAs include coating the plate with recombinant protein for 16 h at 4 °C. After washing and incubating with blocking solution, serial dilutions of samples are added and incubated for 16 h at 4 °C. After washing, a secondary antibody conjugated to HRP is added for 1 h at 20 °C. A chromogenic substrate is then added and absorbance at 450 nm is recorded using a spectrophotometer. Tissue homogenates (e.g., salivary glands and lungs) can also be used in this antibody detection assay.
3. One possibility is to use the plasmid-borne inducible gene expression system developed for Bt that is based upon a Bt endogenous mannan-inducible promoter [21]. This system allows to create translational fusions and generate protein products with the possibility of adding a C-terminal polyhistidine tag.
4. A 6x-His Tag antibody should be used if the chimeric protein contains a His-tag sequence. An alternative is to use antibodies raised against epitopes of the antigenic protein either commercially available or from other sources.
5. The secondary antibody can be conjugated to with various enzyme, fluorescent proteins, biotin or to polymers. The secondary anti-Ig antibody must have specificity for the immunoglobulins present in the species in which the primary antibody was raised.
6. The digestion of the *E. coli*/*Bacteroides* shuttle vector pGH090 with NcoI and EcoRI is provided as an example. In the case of DNA sequence constraints or if the EcoRI restriction site cannot be removed from the internal sequence of the synthetic gene, other restriction sites can be used for the design of the 3'-end of the fragment (e.g., BamHI or SmaI) that are located downstream from the NcoI site of pGH090 [18].

7. If necessary, the DNA fragment containing the gene of interest can be extracted after excision of the band at the expected size from an agarose gel after electrophoresis using the QIAquick Gel Extraction Kit (Qiagen) or equivalent, following the manufacturer's instructions.
8. As an example, we describe the cloning of the gene encoding H5F the highly conserved stalk region of the hemagglutinin molecule of IAV strain H5N1 (VN/04:A/ VietNam/1203/04 [17]) into the *Bacteroides* expression vector pGH090 [8]. The synthetic gene fused at its 5'-end with a signal peptide sequence was designed to contain a BspHI restriction site at its 5'-end and an EcoRI restriction site at its 3'-end to enable DNA cloning. BspHI was chosen because a lysine residue follows the first amino acid (methionine) in the sequence of the signal peptide. Therefore, the lysine AAA/G codon which starts with an A and follows the ATG start codon is included in the BspHI (TCATGA) restriction sequence. BspHI restriction enzyme generates a cohesive end compatible with the NcoI cohesive end of the restricted pGH090 vector to allow translation fusion of the synthetic gene. As a result, the BspHI site was lost and a combination of EcoRI and a site located within the vector and outside of the gene of interest was used to digest recombinant plasmids.
9. BEV sterility is confirmed by checking for the growth of any contaminating bacterial cells. Spread 100 μ L of the filter-sterilized solution on BHIH agar plates, incubate in an anaerobic cabinet for 48 h at 37 °C and confirm the absence of colonies.
10. To increase the resolution of the SEC procedure and obtain a better separation of vesicles of different sizes, the SEC can be performed using a 120 cm \times 1 cm column (Econo-Column® Chromatography Columns, Bio-Rad) filled with 90 mL of CL2-B Sepharose (Sigma-Aldrich) [22]. The absorbance of the fractions is measured at 280 nm and the first fractions displaying an absorbance peak are pooled. Pooled fractions are concentrated to 1 mL with a Vivaspin 20 centrifugal concentrator (100 kDa molecular weight cutoff, Sartorius) and the retentate is filtered through a 0.22 μ m PES membrane (Sartorius). The concentration of the vesicles can then be determined using nanoparticle tracking analysis as described in Subheading 3.7, step 1.
11. If the protein is expressed on the surface of the BEV Proteinase K will degrade it and the band will be absent on the immunoblot. If the protein is expressed in the lumen, the band will still be evident. SDS-treatment of vesicles makes their luminal contents accessible to Proteinase K and serves as control for enzyme activity and confirmation of the protein being expressed in the lumen of BEVs.

12. The sterility of BEV suspensions stored at 4 °C is examined by checking for growth of any contaminating bacterial cells prior to immunization. Add 90 µL of sterile BHIH broth to 10 µL of BEV suspension and spread the 100 µL onto BHIH agar plates. Incubate in both aerobic and anaerobic conditions for 48 h at 37 °C and check for the absence of colony.

Acknowledgments

This work was supported in part by the UK Biotechnology and Biological Sciences Research Council (BBSRC) under grant numbers BB/J004529/1, BB/R012490/1, and BBS/E/F000PR10355. We thank Dr. Emily Jones for her contribution in setting up methods for SEC purification and the use of the Zeta-view NTA, and Dr. Rokas Juodeikis for contributing to the development of BDM+ medium.

References

1. Rauch S, Jasny E, Schmidt KE et al (2018) New vaccine technologies to combat outbreak situations. *Front Immunol* 9:1963. <https://doi.org/10.3389/fimmu.2018.01963>
2. Wallis J, Shenton DP, Carlisle RC (2019) Novel approaches for the design, delivery and administration of vaccine technologies. *Clin Exp Immunol* 196:189–204. <https://doi.org/10.1111/cei.13287>
3. Francis MJ (2018) Recent advances in vaccine technologies. *Vet Clin North Am Small Anim Pract* 48:231–241. <https://doi.org/10.1016/j.cvsm.2017.10.002>
4. Shin MD, Shukla S, Chung YH et al (2020) COVID-19 vaccine development and a potential nanomaterial path forward. *Nat Nanotechnol* 15:646–655. <https://doi.org/10.1038/s41565-020-0737-y>
5. Schwachheimer C, Kuehn MJ (2015) Outer-membrane vesicles from gram-negative bacteria: biogenesis and functions. *Nat Rev Microbiol* 13:605–619. <https://doi.org/10.1038/nrmicro3525>
6. Arigita C, Jiskoot W, Westdijk J et al (2004) Stability of mono- and trivalent meningococcal outer membrane vesicle vaccines. *Vaccine* 22:629–642. <https://doi.org/10.1016/j.vaccine.2003.08.027>
7. Kanojia G, Raeven RHM, van der Maas L et al (2018) Development of a thermostable spray dried outer membrane vesicle pertussis vaccine for pulmonary immunization. *J Control Release* 286:167–178. <https://doi.org/10.1016/j.jconrel.2018.07.035>
8. Carvalho AL, Fonseca S, Cross K et al (2019) Bioengineering commensal bacteria-derived outer membrane vesicles for delivery of biologics to the gastrointestinal and respiratory tract. *J Extracell Vesicles* 8:1632100. <https://doi.org/10.1080/20013078.2019.1632100>
9. Chen DJ, Osterrieder N, Metzger SM et al (2010) Delivery of foreign antigens by engineered outer membrane vesicles. *Proc Natl Acad Sci U S A* 107:3099–3104. <https://doi.org/10.1073/pnas.0805532107>
10. Stentz R, Carvalho AL, Jones EJ et al (2018) Fantastic voyage: the journey of intestinal microbiota-derived microvesicles through the body. *Biochem Soc Trans* 46:1021–1027. <https://doi.org/10.1042/BST20180114>
11. Cecil JD, Sirisaengtaksin N, O'Brien-Simpson NM et al (2019) Outer membrane vesicle-host cell interactions. *Microbiol Spectr* 7. <https://doi.org/10.1128/microbiolspec.PSIB-0001-2018>
12. Jones EJ, Booth C, Fonseca S et al (2020) The uptake, trafficking, and biodistribution of *Bacteroides thetaiotaomicron* generated outer membrane vesicles. *Front Microbiol* 11:57. <https://doi.org/10.3389/fmicb.2020.00057>
13. Miquel-Clopés A, Bentley EG, Stewart JP et al (2019) Mucosal vaccines and technology. *Clin Exp Immunol* 196:205–214. <https://doi.org/10.1111/cei.13285>

14. Smith CJ, Rocha ER, Paster BJ (2006) The medically important *Bacteroides* spp. in health and disease. In: Dworkin M, Falkow S, Rosenberg E, Schleifer KH, Stackebrandt E (eds) *The prokaryotes*. Springer, New York, NY. https://doi.org/10.1007/0-387-30747-8_14
15. Human Microbiome Project Consortium (2012) Structure, function and diversity of the healthy human microbiome. *Nature* 486:207–214. <https://doi.org/10.1038/nature11234>
16. Carvalho AL, Miquel-Clopés A, Wegmann U et al (2019) Use of bioengineered human commensal gut bacteria-derived microvesicles for mucosal plague vaccine delivery and immunisation. *Clin Exp Immunol* 196:287–304. <https://doi.org/10.1111/cei.13301>
17. Valkenburg SA, Mallajosyula VV, Li OT et al (2016) Stalking influenza by vaccination with pre-fusion headless HA mini-stem. *Sci Rep* 6:22666. <https://doi.org/10.1038/srep22666>
18. Wegmann U, Horn N, Carding SR (2013) Defining the *Bacteroides* ribosomal binding site. *Appl Environ Microbiol* 79:1980–1989. <https://doi.org/10.1128/AEM.03086-12>
19. Shoemaker NB, Getty C, Gardner JF et al (1986) Tn4351 transposes in *Bacteroides* spp. and mediates the integration of plasmid R751 into the *Bacteroides* chromosome. *J Bacteriol* 165:929–936. <https://doi.org/10.1128/jb.165.3.929-936.1986>
20. Bryant WA, Stentz R, Le Gall G et al (2017) *In silico* analysis of the small molecule content of outer membrane vesicles produced by *Bacteroides thetaiotaomicron* indicates an extensive metabolic link between microbe and host. *Front Microbiol* 8:2440. <https://doi.org/10.3389/fmicb.2017.02440>
21. Horn N, Carvalho AL, Overweg K et al (2016) A novel tightly regulated gene expression system for the human intestinal symbiont *Bacteroides thetaiotaomicron*. *Front Microbiol* 7:1080. <https://doi.org/10.3389/fmicb.2016.01080>
22. Durant L, Stentz R, Noble A et al (2020) *Bacteroides thetaiotaomicron*-derived outer membrane vesicles promote regulatory dendritic cell responses in health but not in inflammatory bowel disease. *Microbiome* 8:88. <https://doi.org/10.1186/s40168-020-00868-z>



OPEN ACCESS

EDITED BY

Sergio Serrano-Villar,
Ramón y Cajal University Hospital, Spain

REVIEWED BY

Elena Moreno,
Ramón y Cajal University Hospital, Spain
José Avendaño Ortiz,
University Hospital La Paz,
Spain

*CORRESPONDENCE

Simon R. Carding
simon.carding@quadram.ac.uk

SPECIALTY SECTION

This article was submitted to
Microbial Immunology,
a section of the journal
Frontiers in Microbiology

RECEIVED 21 September 2022

ACCEPTED 25 October 2022

PUBLISHED 10 November 2022

CITATION

Fonseca S, Carvalho AL, Miquel-Clopés A,
Jones EJ, Juodeikis R, Stentz R and
Carding SR (2022) Extracellular vesicles
produced by the human gut commensal
bacterium *Bacteroides thetaiotaomicron*
elicit anti-inflammatory responses from
innate immune cells.
Front. Microbiol. 13:1050271.
doi: 10.3389/fmicb.2022.1050271

COPYRIGHT

© 2022 Fonseca, Carvalho, Miquel-Clopés,
Jones, Juodeikis, Stentz and Carding. This
is an open-access article distributed under
the terms of the [Creative Commons
Attribution License \(CC BY\)](https://creativecommons.org/licenses/by/4.0/). The use,
distribution or reproduction in other
forums is permitted, provided the original
author(s) and the copyright owner(s) are
credited and that the original publication in
this journal is cited, in accordance with
accepted academic practice. No use,
distribution or reproduction is permitted
which does not comply with these terms.

Extracellular vesicles produced by the human gut commensal bacterium *Bacteroides thetaiotaomicron* elicit anti-inflammatory responses from innate immune cells

Sonia Fonseca¹, Ana L. Carvalho^{1,2}, Ariadna Miquel-Clopés¹, Emily J. Jones¹, Rokas Juodeikis¹, Régis Stentz¹ and Simon R. Carding^{1,3*}

¹Gut Microbes and Health, Quadram Institute Bioscience, Norwich, United Kingdom, ²Department of Women's and Children's Health, Institute of Life Course and Medical Sciences, University of Liverpool, Liverpool, United Kingdom, ³Norwich Medical School, University of East Anglia, Norwich, United Kingdom

Bacterial extracellular vesicles (BEVs) produced by gut commensal bacteria have been proposed to play an important role in maintaining host homeostasis *via* interactions with the immune system. Details of the mediators and pathways of BEV-immune cell interactions are however incomplete. In this study, we provide evidence for the anti-inflammatory and immunomodulatory properties of extracellular vesicles produced by the prominent human gut commensal bacterium *Bacteroides thetaiotaomicron* (Bt BEVs) and identify the molecular mechanisms underlying their interaction with innate immune cells. Administration of Bt BEVs to mice treated with colitis-inducing dextran sodium sulfate (DSS) ameliorates the symptoms of intestinal inflammation, improving survival rate and reducing weight loss and disease activity index scores, in association with upregulation of IL-10 production in colonic tissue and in splenocytes. Pre-treatment (conditioning) of murine bone marrow derived monocytes (BMDM) with Bt BEVs resulted in higher ratio of IL-10/TNF α production after an LPS challenge when compared to LPS pre-conditioned or non-conditioned BMDM. Using the THP-1 monocytic cell line the interactions between Bt BEVs and monocytes/macrophages were shown to be mediated primarily by TLR2. Histone (H3K4me1) methylation analysis showed that Bt BEVs induced epigenetic reprogramming which persisted after infectious challenge, as revealed by increased levels of H3K4me1 in Bt BEV-conditioned LPS-challenged BMDM. Collectively, our findings highlight the important role of Bt BEVs in maintaining host immune homeostasis and raise the promising possibility of considering their use in immune therapies.

KEYWORDS

extracellular vesicles, *Bacteroides*, anti-inflammatory response, innate immune tolerance, BMDM, THP-1 cells, TLR2, IL-10

Introduction

The ecosystem of the human gastrointestinal tract (GIT) is shaped by complex interactions between resident microbes (the microbiota), the epithelium and immune cells. Host–microbe interactions have traditionally been analyzed from the perspective of pathogenic relationships, but it has become evident that commensal microbes also exert important beneficial effects on the host. The ability of immune cells to discriminate between pathogens and commensal bacteria is therefore essential to maintain immune homeostasis and preserve host health, by simultaneously providing protection against pathogens and tolerance toward symbiotic microbiota (Bron et al., 2011).

Innate immunity plays an important role in intestinal protection and is the first line of host defense against infection comprising physical, chemical, and cellular barriers. Various stimuli and conserved microbe-associated molecular pattern (MAMPs) molecules can activate and modulate innate immunity and inflammatory responses with enhanced or decreased production of pro-inflammatory mediators and cytokines depending on the type and dose of the ligand recognized by individual pattern recognition receptors (PPRs; Ifrim et al., 2014). Bacterial lipopolysaccharides (LPS), one of the major triggers of inflammatory response *via* interactions with toll-like receptor 4 (TLR4), can induce a state of tolerance in macrophages and monocytes after repeated or prolonged exposure, resulting in reduced pro-inflammatory cytokine production (Novakovic et al., 2016; Seeley and Ghosh, 2017). The innate immune system can be also activated by sterile endogenous dietary substances from Western-type diets that can contribute to various chronic inflammatory diseases (Bekkering et al., 2014; Christ and Latz, 2019). Innate immune activation leads to modifications in the chromatin state of the innate immune cells, with epigenetic changes persisting even after the cells return to homeostasis, altering their long-term responsiveness to re-infection (Netea et al., 2020). Enhanced inflammatory responses in trained innate immune cells and diminished activation in tolerized innate immune cells are based on epigenetic reprogramming events, including DNA methylation and histone modifications that up- or down-regulate the transcription of inflammatory genes (Netea et al., 2020). Identifying the receptors, signaling pathways and epigenetic modifications that induce and maintain immune tolerance is therefore important for understanding how immune tolerance contributes to a state of controlled inflammation with potential benefits for autoimmune conditions and chronic inflammation diseases without contributing to immunodeficiency.

All bacteria naturally produce and release nano-sized, non-replicative extracellular vesicles (BEVs) with roles in response to stress, quorum sensing, biofilm formation, and interspecies and interkingdom communication (Schwechheimer and Kuehn, 2015). BEVs contain various cargo including enzymes, signaling molecules, and metabolites (Bryant et al., 2017). BEVs generated by Gram-negative pathogens contain toxins and virulence factors that can breach host defenses facilitating invasion and infection

by parental cells (Kaparakis-Liaskos and Ferrero, 2015). By contrast, the role of BEVs produced by commensal microbes, and in particular the vast numbers residing in the GIT, is less clear, although recent studies have identified a potential role in host-microbe communication and in maintaining immune homeostasis *via* interactions with dendritic cells (Durant et al., 2020). BEVs generated by prominent members of the microbiota such as *Bacteroides thetaiotaomicron* (Bt) can cross the epithelial barrier of the intestine and access underlying lamina propria cells and, *via* the vasculature, other organs and tissues. They mediate bacteria-host interactions which modulate the physiology of various host cells including those of the innate and adaptive immune system (Stentz et al., 2018; Jones et al., 2020; Gul et al., 2022). BEVs produced by the pathobiont *Bacteroides fragilis* have been implicated in immune homeostasis as they can mediate anti-inflammatory effects by TLR2-dependent activation of dendritic cells and the production of IL-10 by regulatory T cells (Shen et al., 2012). The inbuilt adjuvanticity and immune-potential properties of Bt-derived BEVs has also been exploited in drug delivery formulations and in mucosal vaccines for respiratory viruses (Carvalho et al., 2019a,b), supporting their ability to modulate host immune cell function.

Based upon the biophysical and immunological properties of BEVs generated by commensal bacteria, we have investigated the potential of Bt-derived BEVs to act *via* their interactions with innate immune cells as modulators of the immune tolerance and the inflammation response using well-established *in vivo* and *in vitro* models. Identifying the interactions between BEVs and host innate immune cells is an important step toward considering their use in immunotherapy.

Materials and methods

Isolation and characterization of Bt BEVs

Bacteroides thetaiotaomicron VPI-5482 was grown in 500 ml of Bacteroides Defined Medium (BDM4; Supplementary Table S1) at 37°C in an anaerobic cabinet. For BEVs preparations, cells were harvested after 16 h at an approximate OD_{600nm} of 2.5 corresponding to early stationary phase. BEVs were isolated following a method adapted from Stentz et al. (2022). Briefly, Bt cultures (500 ml) were centrifuged at 6000 g for 50 min at 4°C and the supernatants filtered through polyethersulfone (PES) membranes (0.22 µm pore-size; Sartorius) to remove debris and cells. Supernatants were concentrated by cross-flow ultrafiltration (100 kDa molecular weight cut-off, Vivaspine 50R, Sartorius), the retentate was rinsed once with 500 ml of PBS (pH 7.4) and concentrated to 1 ml. Further purification of BEVs was performed by fractionation of the suspension by size-exclusion chromatography using qEVoriginal 35 nm columns (Izon) according to manufacturer's instructions. Fractions containing BEVs were combined and filter-sterilized through a 0.22 µm PES membrane (Sartorius) and the suspensions were stored at

4°C. Absence of viable microorganisms was confirmed by plate count and absence of LPS was confirmed by Limulus Amebocyte Lysate (LAL) test.

The size and concentration of the isolated Bt BEV suspension was determined using nanoparticle tracking analysis and the ZetaView PMX-220 TWIN instrument according to manufacturer's instructions (Particle Metrix). Aliquots of BEV suspensions were diluted 1,000- to 20,000-fold in particle-free water for analysis. Size distribution video data were acquired using the following settings: temperature: 25°C; frames: 60; duration: 2 s; cycles: 2; positions: 11; camera sensitivity: 80 and shutter value: 100. The ZetaView NTA software (version 8.05.12) was used with the following post acquisition settings: minimum brightness: 20; max area: 2,000; min area: 5 and trace length: 30.

Animal studies

Specific-pathogen-free (SPF) C57BL/6 male mice were bred and maintained in the Disease Modeling Unit at the University of East Anglia (United Kingdom). Animals were housed in individually ventilated cages and exposed to a 12h light/dark cycle with free access to drinking water and standard laboratory chow diet. Animal experiments were conducted in full accordance with the Animal Scientific Procedures Act 1986 under UK Home Office (HMO) approval and HMO project license 70/8232.

Acute colitis mouse model

The dextran sulfate sodium (DSS) induced mouse model of acute colitis was used to investigate the therapeutic potential of BEVs on intestinal inflammation. SPF C57BL/6 mice, 8 weeks old, were divided into two groups and administered with either PBS ($n=8$) or BEVs ($n=6$). Experimental colitis was induced by administration of 2.25% w/v DSS (36,000–50,000 Da, MP Biomedicals) in drinking water *ad libitum* for 5 days. From day 5 until the end of the experiment, DSS was replaced by fresh water. PBS and BEVs were administered by oral gavage (100 μ l at 10^{11} BEVs/ml) on days 5, 7, and 9, and on day 11 mice were euthanized by cervical dislocation after exposure to rising concentrations of CO₂. Distal colon tissue samples (1 cm) and spleens were collected for cytokine production analysis. The extent of colitis was evaluated using survival rate and a disease activity index (Supplementary Table S2) comprising daily body weights, stool consistency, tissue and content appearance, and bleeding assessments.

Each distal colon tissue sample was cut open longitudinally and incubated in flat-bottomed 24-well plates with 0.5 ml per well of complete RPMI medium (RPMI-1640 (Sigma-Aldrich) supplemented with 10% heat-inactivated fetal bovine serum (FBS; Biosera) and 1% Pen/Strep (Sigma-Aldrich)) for 24 h in a CO₂ incubator. Spleens were macerated in a cell strainer at 70 μ m, washed with complete RPMI medium and incubated with

Ammonium-Chloride-Potassium (ACK) lysis buffer (Gibco) for 10 min to lyse red blood cells. Splenocyte count was adjusted to 5×10^6 cells/ml and incubated in flat-bottomed 96-well plates with 0.2 ml per well of complete RPMI medium, with or without restimulation with 10^9 BEVs/ml, for 72 h at 37°C and 5% CO₂ in a humidified incubator. Supernatants from colon and splenocyte cultures were then centrifuged and stored at –80°C prior to cytokine analysis.

Murine bone marrow-derived monocyte cultures

SPF C57BL/6 mice, 13–16 weeks old, were euthanized by cervical dislocation after exposure to rising concentrations of CO₂. Femurs were immediately removed and placed into cold sterile PBS. Bone marrow cell suspensions were isolated by flushing the femurs and tibias with RPMI-1640 supplemented with 10% heat-inactivated FBS and 1% Pen/Strep under sterile conditions. Debris was removed by passing the suspension through a 70 μ m cell strainer. Cells were washed with complete RPMI media and concentration was adjusted to 6×10^6 cells/ml. Cells were seeded on flat-bottomed 12-well plates (1.2 ml/well) and incubated at 37°C and 5% CO₂ in a humidified incubator.

BMDM—Bt BEVs co-culture

Bone marrow-derived monocyte (BMDM) cells (1.2 ml at 6×10^6 cells/ml) were incubated in flat-bottomed 12-well plates in complete RPMI medium for 24 h at 37°C and 5% CO₂ in a humidified incubator, in the presence of either different concentrations of Bt BEVs (3×10^9 , 3×10^7 , and 3×10^5 BEVs/ml), LPS from *E. coli* (10 ng/ml; Sigma-Aldrich) as a positive control or PBS as negative control. After 24 h, supernatants were collected and stored at –20°C prior to cytokine measurements. Cells were washed with warm PBS and maintained in complete RPMI medium for 5 days at 37°C and 5% CO₂, with fresh media added on day 3. Cells were then incubated with LPS (10 ng/ml) to mimic an infectious challenge, or PBS as negative control. After 24 h, supernatants were collected and stored at –20°C for subsequent cytokine measurement. Cells were washed with warm PBS and detached from the wells by gently scraping after 1 h incubation with ice-cold Macrophage Detachment Solution (PromoCell) at 4°C. Cells were then washed with PBS containing 0.5 mM EDTA and stored at –80°C in FBS with 10% DMSO (Sigma-Aldrich) for histone methylation analysis. All incubations were performed in triplicate in two independent experiments.

Cytokine measurements

The production of IL-10 by colon tissue and splenocytes, and TNF α , IL-6, and IL-10 produced by BMDM after 24 h of

conditioning and after 24 h of challenge was measured by ELISA (Invitrogen) according to the manufacturer's instructions. The results were recorded as pg of each cytokine per mL of supernatant.

THP1-Blue cell assay

THP1-Blue NF- κ B cells (Invivogen) were derived from the human THP-1 monocyte cell line by stable integration of an NF- κ B-inducible secreted alkaline phosphatase (SEAP) reporter construct. THP1-Blue cells were cultivated in RPMI-1640 supplemented with 10% heat-inactivated FBS, 1% Pen/Strep and 100 μ g/ml Normocin (Invivogen) at 37°C and 5% CO₂ in a humidified incubator. To maintain selection pressure during cell subculturing, 10 μ g/ml blasticidin was added to the growth medium every other passage.

To establish the threshold dose of BEVs that allows for the quantification of THP-1 cells activation, cells were seeded in flat-bottomed 96-well plates at a density of 5×10^5 cells/ml and incubated for 24 h at 37°C and 5% CO₂ in a humidified incubator in the presence of different concentrations of Bt BEVs (from 3×10^9 to 3×10^6 BEVs/ml) using LPS (10 ng/ml) as a positive control and BDM4 and PBS as negative controls.

To identify pattern recognition receptors (PRRs) involved in BEV-mediated THP1-Blue cell activation, cultures were incubated with different inhibitors of TLR2 (PAb-hTLR2 (5 μ g/ml), Invivogen), TLR4 (PAb-hTLR4 (5 μ g/ml), Invivogen), NOD1 (ML130 (5 μ g/ml), Abcam), and NOD2 (GSK717 (5 μ g/ml), Merck) prior to the addition of BEVs (3×10^8 /ml). Heat-killed *Listeria monocytogenes* (HKLM, 10^7 cells/ml, Invivogen), LPS (10 ng/ml, Sigma-Aldrich), lauroyl-g-D-glutamyl-meso-diaminopimelic acid (DAP, 1 μ g/ml, Invivogen) and N-acetylmuramyl-L-alanyl-D-isoglutamine (MDP, 10 μ g/ml, Invivogen) were used as specific ligands for each inhibitor, respectively. Subsequently, 20 μ l of the cell suspension was added to wells of 96-well plate, mixed with 180 μ l of Quanti-Blue (Invivogen) colorimetric assay reagent and incubated for 1 h at 37°C to allow color development. NF- κ B-inducible SEAP levels were quantified by absorbance reading at 620 nm. All incubations were performed in triplicate in three independent experiments.

THP1-Blue cell—Bt BEVs co-culture

To investigate phenotypic changes in THP1-Blue cells after exposure to with Bt BEVs, the cells (1.2 ml at 10^6 cells/ml) were incubated on flat-bottomed 12-well plates in complete RPMI medium for 24 h at 37°C and 5% CO₂ in a humidified incubator, in the presence of different concentrations of Bt BEVs (5×10^8 BEVs/ml, 5×10^6 BEVs/ml, and 5×10^4 BEVs/ml), using LPS from *E. coli* (10 ng/ml; Sigma-Aldrich) as a reference and positive control and PBS as a negative control. Cells were

washed with warm PBS and detached from the wells by gently scraping after 1 h incubation with ice-cold Macrophage Detachment Solution at 4°C. Cells were then washed with PBS containing 0.5 mM EDTA and collected for flow cytometry analysis.

Flow cytometry

THP1-Blue cells were stained with Zombie Aqua Fixable Viability kit (BioLegend) following the manufacturer's protocol. Cells were washed with Cell Staining Buffer (BioLegend) before blocking Fc receptors by incubation with Human TruStain FcX (BioLegend) for 10 min at 21°C. Cells were then surface stained for 20 min at 4°C in the dark using APC/Fire 750 anti-human CD14 Clone 63D3 (BioLegend) and flow cytometry performed on BD LSRFortessa Cell Analyzer (BD Biosciences) with the data analyzed using FlowJo software 10.8.1 (BD Biosciences).

Histone methylation

Histone proteins from bone marrow-derived cells were extracted using the EpiQuik Total Histone Extraction Kit (Epigentek) according to the manufacturer's instructions and quantified by measuring absorbance at 280 nm. The level of histone 3 lysine 4 mono-methylation (H3K4me1) was quantified using the ELISA-based colorimetric kit EpiQuik Global Mono Methyl Histone H3 K4 Quantification (Epigentek) and results were expressed as ng of H3K4me1 per μ g of total protein.

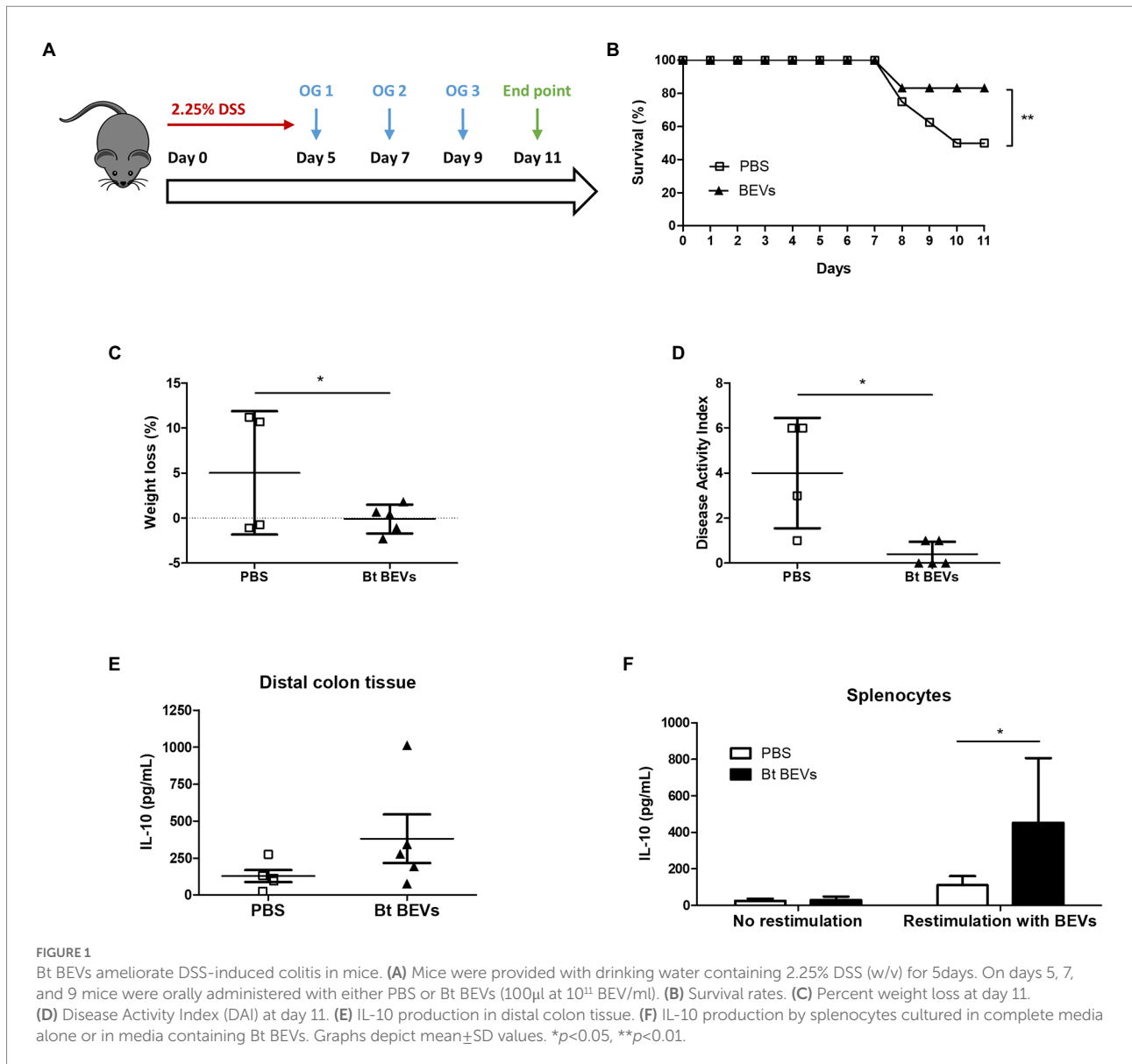
Statistical analysis

Data were subjected to One-way ANOVA or Two-way ANOVA followed by Tukey's multiple comparison *post-hoc* test or Dunnett's multiple comparison *post-hoc* test using GraphPad Prism 5 software. Statistically significant differences between two mean values were established by a $p < 0.05$. Data are presented as the mean \pm standard deviation.

Results

Anti-inflammatory effect of Bt BEVs *in vivo*

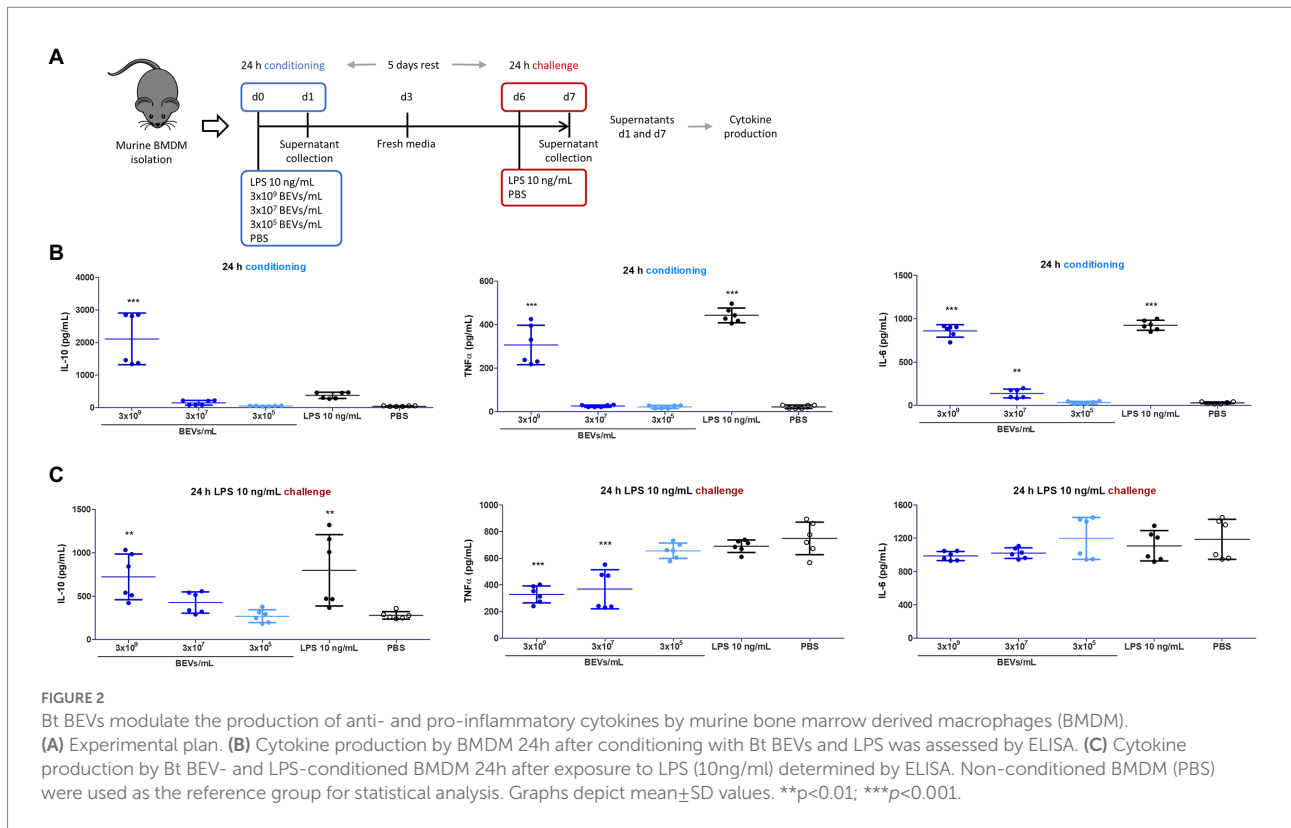
To investigate the ability of Bt BEVs to influence inflammatory responses *in vivo* we used DSS-induced murine colitis as a model of acute inflammation (Figure 1A). This is a well-established lymphocyte-independent model of intestinal inflammation in which the clinical severity can be quantified, providing a reliable method to study the contribution of the innate immune system to inflammatory responses in the host.



Mice orally administered with Bt BEVs exhibited a significantly higher ($p < 0.01$) survival rate throughout the experiment compared to mice that received vehicle (PBS) only (Figure 1B). Oral administration of Bt BEVs also contributed to a significant decrease ($p < 0.05$) in weight loss and disease activity index scores (Figures 1C,D). Analysis of cytokine production by freshly excised and cultured colonic tissue showed that production of the anti-inflammatory cytokine IL-10 was higher in distal colon tissue from mice previously administered with Bt BEVs (Figure 1E). When splenocytes from mice orally gavaged with Bt BEVs were restimulated *ex vivo* with Bt BEVs, IL-10 production was also significantly increased ($p < 0.05$). By comparison, there was no difference in IL-10 production from non-stimulated splenocytes across all experimental groups (Figure 1F).

Bt BEVs modulation of cytokine production in BMDM

Bone marrow mononuclear cells cultured under conditions that favor the growth of monocytes and macrophages were used to examine further the potential interaction of Bt BEVs with innate immune cells. Specifically, we investigated how Bt BEVs influence murine bone marrow-derived monocytes (BMDM) in response to an inflammatory stimulus. Cytokine production in BEV-conditioned BMDM was measured before and after an infection-like challenge with LPS (Figure 2A). We observed significantly increased amounts ($p < 0.001$) of IL-10 in BMDM cultures after incubation for 24h with 3×10^9 BEVs/ml. No significant changes in IL-10 production were detected in BMDM containing lower concentrations of Bt BEVs or with LPS and

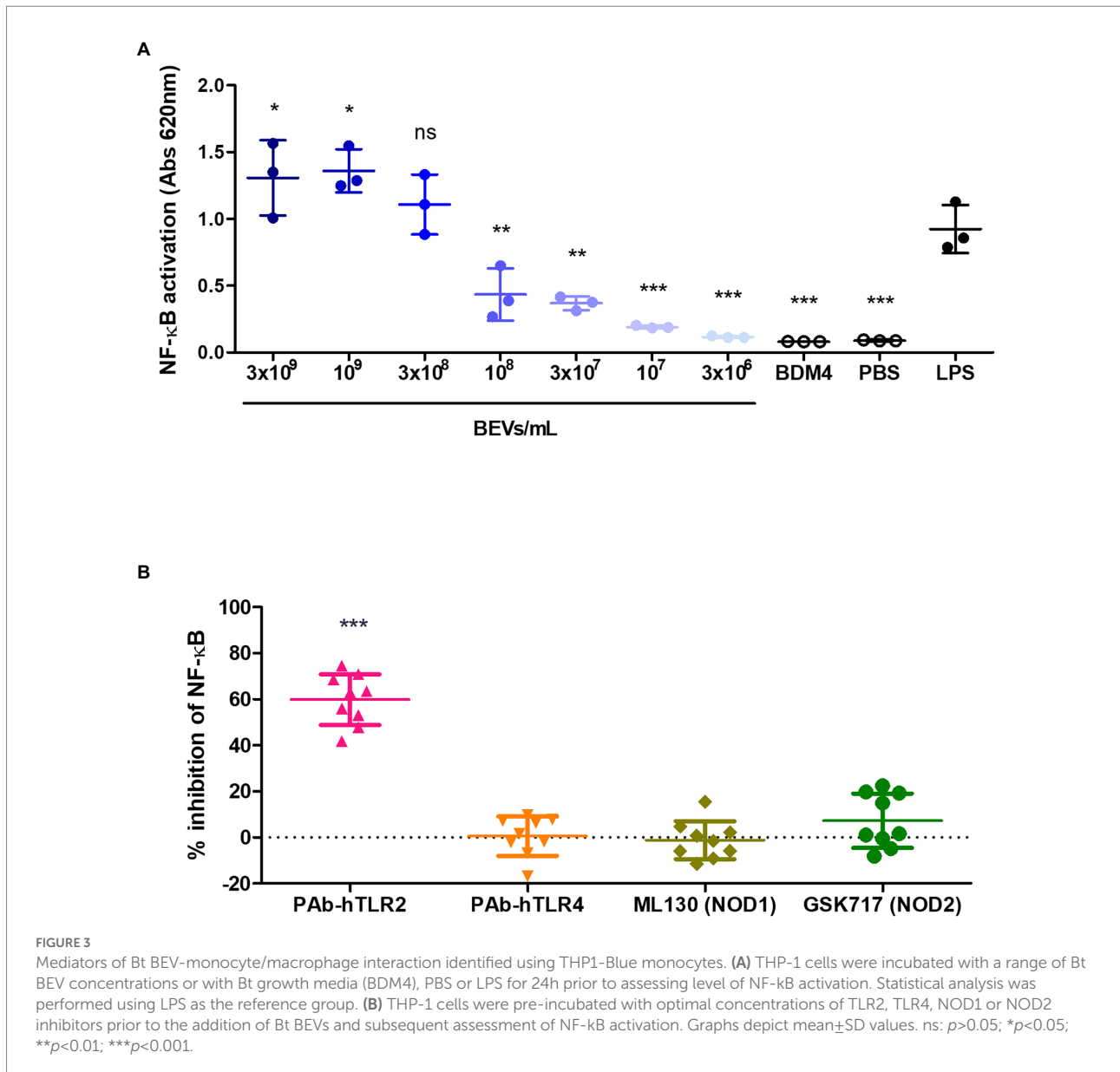


PBS. The concentrations of the pro-inflammatory cytokines TNF α and IL-6 were significantly higher ($p < 0.001$) in BMDM incubated with 3×10^9 BEVs/ml when compared to PBS alone. However, these levels were lower than in LPS-conditioned BMDM cultures (Figure 2B). Analysis of cytokine production in BEV-conditioned BMDM cultures after an LPS challenge revealed opposite trends when comparing anti- and pro-inflammatory activity. While IL-10 production was directly associated with the Bt BEVs concentration used to condition BMDM, the levels of pro-inflammatory cytokines showed an inverse relationship with the Bt BEV conditioning dose, with TNF α production significantly decreased ($p < 0.001$) when BMDM were incubated with BEVs at 3×10^7 BEVs/ml or higher concentrations (Figure 2C). Collectively, these data show that Bt BEVs exert in a dose-dependent manner anti-inflammatory responses from monocytes/macrophages, which was particularly noticeable in a re-infection (LPS challenge) scenario.

Molecular basis of BEV-monocyte interactions and the involvement of specific pattern recognition receptors

The human monocytic cell line THP-1 that expresses an NF- κ B inducible secreted alkaline phosphatase (SEAP) reporter construct (THP1-Blue) was used to identify the receptors and pathways in monocytes involved in the anti-inflammatory effect

of Bt BEVs observed in both the *in vivo* and *in vitro* model systems. To investigate if Bt BEVs can activate THP-1 cells and to establish the activation threshold, cells (5×10^5 cells/ml) were incubated with different concentrations of Bt BEVs (3×10^6 BEVs/ml to 3×10^9 BEVs/ml) using a chemically defined Bt media (BDM4) and PBS or LPS (10 ng/ml) as negative and positive controls, respectively. NF- κ B activation in THP-1 cells in response to Bt BEVs was dose-dependent (Figure 3A) with no detectable activation seen in cultures containing BDM4 or PBS alone. Based upon the level of activation induced by 3×10^8 BEVs/ml being equivalent ($p > 0.05$) to that of LPS (10 ng/ml), we established this as an optimal Bt BEVs concentration for subsequent inhibition assays. Specific inhibitors of key extracellular and intracellular PRRs were used in THP1-BEV co-cultures to identify those contributing to NF- κ B activation in THP-1 cells. In a series of optimization experiments, the optimal concentration of each inhibitor was established by titration and their specificity at that concentration was confirmed with individual PRR-specific ligands (Supplementary Figure S1). The most potent inhibition of NF- κ B activation ($\sim 60\%$) was seen in cultures containing PAb-hTLR2 (5 μ g/ml), an antibody that specifically inhibits TLR2 activation (Figure 3B; Supplementary Figure S1), consistent with TLR2 activation mediating interactions between Bt BEVs and monocyte/macrophages (Figure 3B). By contrast, no significant inhibition of NF- κ B activation was seen using inhibitors of TLR4, NOD1, or NOD2 (Figure 3B).



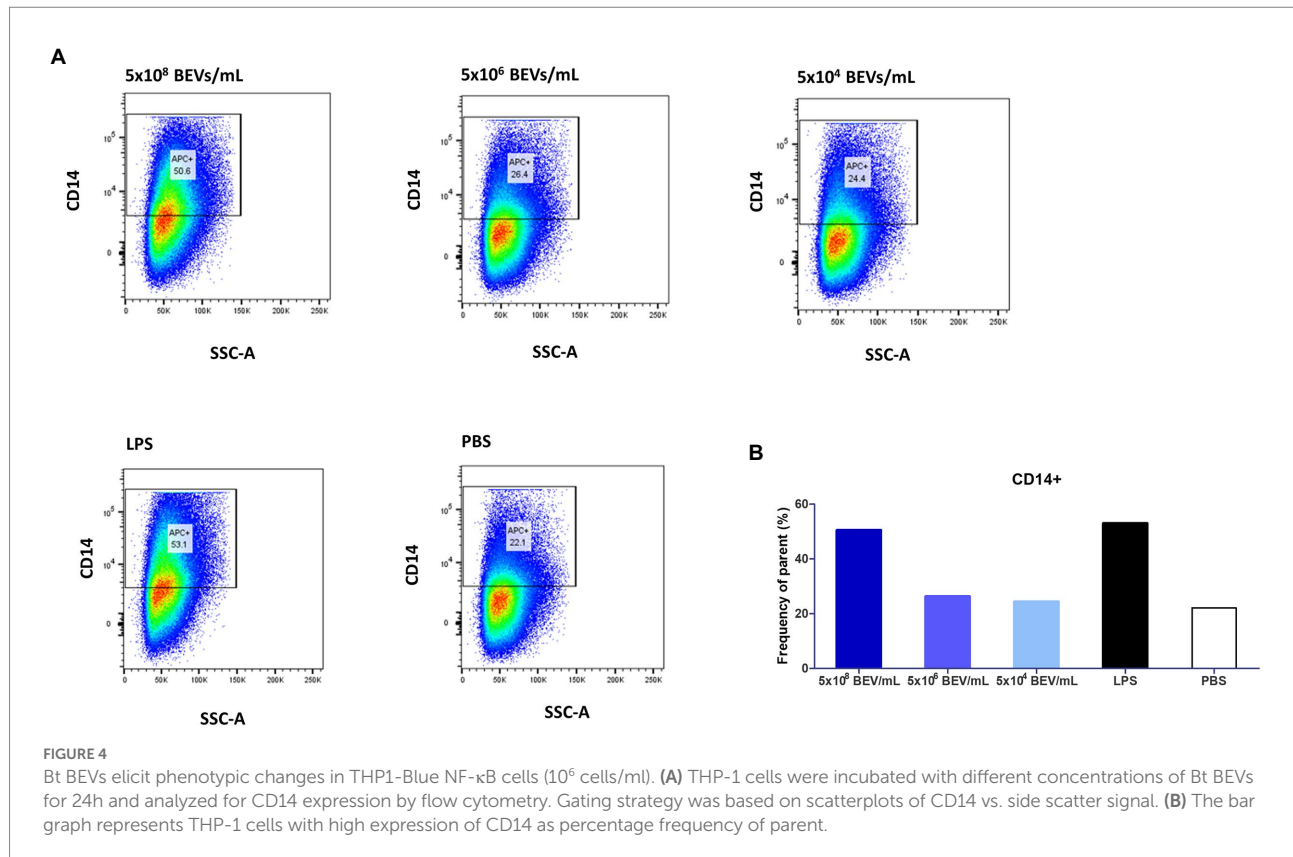
Phenotypic changes in monocytes following stimulation with Bt BEVs

We investigated the phenotypic changes in THP-1 cells after exposure to Bt BEVs by measuring levels of CD14 expression using flow cytometry. CD14⁺ cells were gated based on a fluorescence minus one (FMO) strategy. CD14 expression is a marker of activation related to pro-inflammatory monocytes, is a co-receptor for TLR4 responsivity to LPS, and contributes to the activation of other PRRs including TLR2. Among THP-1 cells cultured in media alone approximately 22% were CD14⁺ (Figure 4). In cultures containing the highest concentration of Bt BEVs (5×10^8 BEV/mL equivalent to a ratio of 500 BEVs,THP-1) the proportion of CD14⁺ cells more than doubled to approximately 51% and was equivalent to the levels seen in cultures containing

LPS (~53%; Figure 4). By contrast, THP-1 cells stimulated with lower concentrations of Bt BEVs showed no significant changes in the proportion of CD14⁺ monocytes when compared to cells incubated with PBS (Figure 4).

Effect of Bt BEVs on histone modifications in BMDM

Inflammatory processes and innate immunity are tightly regulated by epigenetic mechanisms with genomic DNA methylation and modification of histones influencing the function of innate immune cells (Saeed et al., 2014; Fraschilla et al., 2022). To determine if Bt BEVs can induce epigenetic changes, and in particular histone methylation, we measured levels of H3K4me1 in



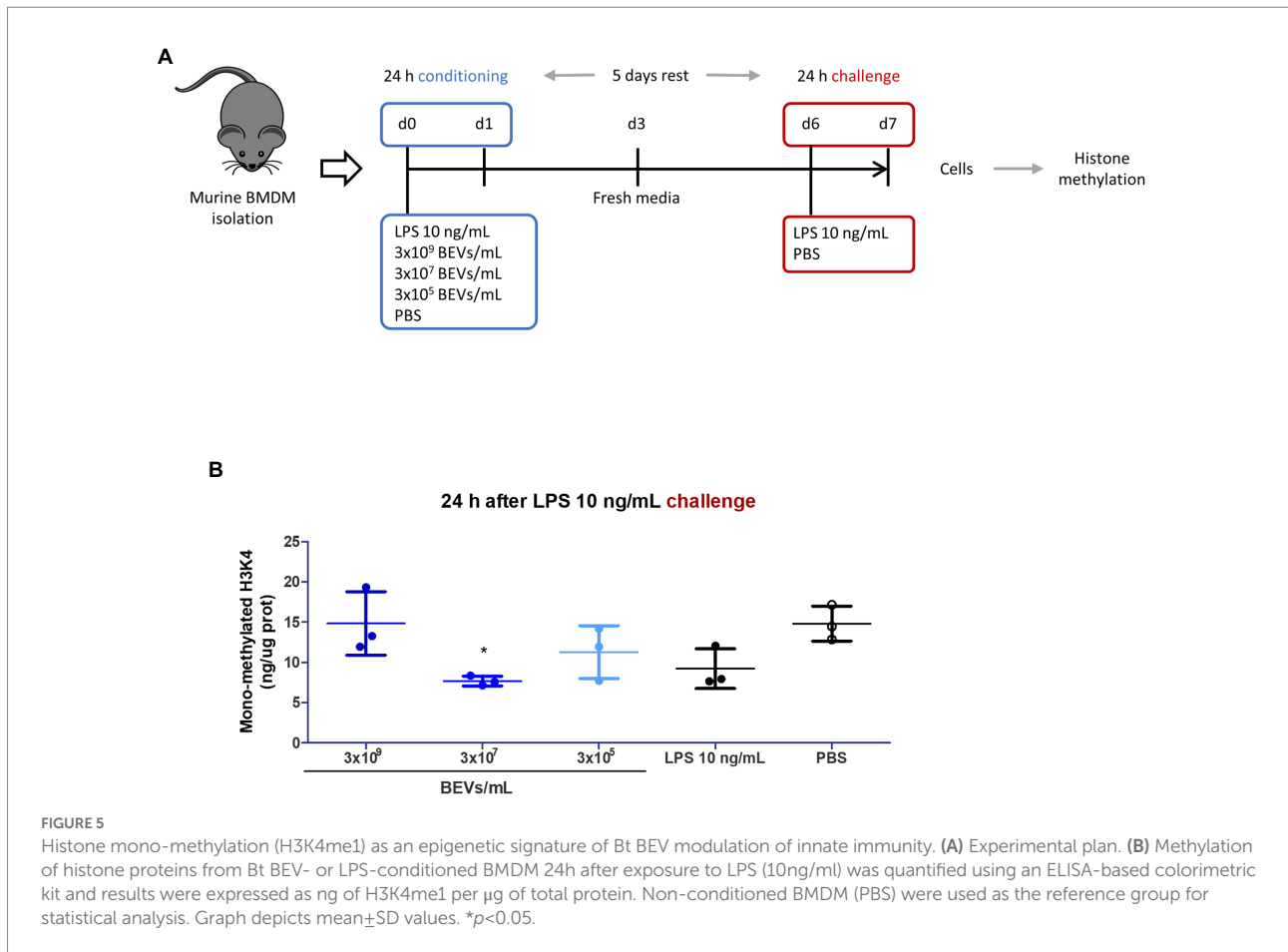
BMDM, which indicates the mono-methylation at the 4th lysine residue of histone H3 protein and is an enhancer signature (Figure 5A). Varying levels of H3K4me1 were detected in BMDM after culture with Bt BEVs, with the highest levels seen in cultures containing 3×10^9 BEV/ml, comparable to those in BMDM cultured in media alone (PBS) and higher than that in cultures containing LPS (Figure 5B). By comparison, lower levels of H3K4me1 were seen in cultures containing fewer Bt BEVs (3×10^5 and 3×10^7 BEV/ml) with the differences being significant ($p < 0.05$) for BMDM cultured with 3×10^7 BEV/ml. These data demonstrate that Bt BEVs altered the histone methylation status in innate immune cells.

Discussion

BEVs produced by gut bacteria can cross the intestinal epithelium, gaining access to host cells (Stentz et al., 2018; Jones et al., 2020) and contribute to immune homeostasis *via* interactions with innate immune cells (Maerz et al., 2018; Diaz-Garrido et al., 2019; Durant et al., 2020). However, the details and nature of this BEV-immune cell crosstalk is incomplete. In this study, we have provided *in vitro* and *in vivo* evidence for the anti-inflammatory and immunomodulatory properties of BEVs produced by the major human gut commensal bacterium Bt and identified the molecular basis of their interaction with monocytes and macrophages. We recognize that different types of particles

could be copurified with BEVs due to technical limitations but their effect is taken into consideration and appropriate controls were utilized wherever possible to aid data interpretation (Juodeikis and Carding, 2022).

Oral administration of Bt BEVs ameliorates DSS-induced colitis in mice, underlining their potential as a treatment for non-infectious autoimmune pathologies. Similar protective effects have been reported in DSS models after treatment with fresh and lyophilized cultures of Bt (Delday et al., 2019) and other *Bacteroides* species (Hudcovic et al., 2009; Chiu et al., 2014; Chang et al., 2017), although the mediators of these effects and the possibility that it includes BEVs were not investigated. The size, stability, and non-replicative status of Bt BEVs makes them good candidates for therapeutic interventions compared to whole bacteria. Conditions involving chronic inflammation of the gut are associated with dysregulation of mucosal innate immune response (Xu et al., 2014), increased NF- κ B activation (Schreiber et al., 1998) and increased levels of pro-inflammatory cytokines such as TNF- α and IL-6 (Atreya et al., 2000; Komatsu et al., 2001). In this context, the significance of BEV-elicited IL-10 from BMDM is implied from its role in the prevention of inflammatory bowel disease (Mazmanian et al., 2008; Hansen et al., 2009). Mice lacking IL-10 or IL-10 receptor genes spontaneously develop intestinal inflammation (Kuhn et al., 1993) with IL-10 acting by suppressing antigen presentation by downregulating MHC class II expression (Koppelman et al., 1997) and inhibiting pro-inflammatory cytokine synthesis by blocking the activation of the inhibitor of



NF- κ B kinase (IKK) and dysregulating NF- κ B (Schottelius et al., 1999). The beneficial effects of BEVs or Bt (Li et al., 2021) in DSS-colitis are associated with increased production of IL-10 in serum, colonic tissue and by peripheral splenocytes which can promote a non-inflammatory status by counteracting pro-inflammatory responses. The contribution of Bt BEVs to the maintenance of immune homeostasis by promoting IL-10 production by innate immune cells is also implied by our previous study in which we reported the absence of Bt BEV-elicited IL-10 production by innate immune cells isolated from patients with inflammatory bowel disease (Durant et al., 2020). It is interesting to note that lower levels of *Bacteroides* spp. are present in the gut microbiota of inflammatory bowel disease patients (Zhou and Zhi, 2016). While the present study focused on BEVs, we cannot exclude the possibility for other cell-associated or secreted constituents of Bt to contribute to immunoregulatory responses *in vivo*. Indeed, administration of live or dead (freeze dried) Bt to IL-10r-deficient mice protects the animals from developing colitis (Delday et al., 2019) which may involve different bacterial mediators and multiple interactions with host cells. Nevertheless, Bt and BEV-elicited IL-10 production by host immune cells appears to be central to their protective effects.

In BMDM cultures pre-conditioned with BEVs prior to an infection-like challenge with LPS, high doses of Bt BEVs

significantly upregulated the production of IL-10. Although Bt BEVs also increased the production of pro-inflammatory cytokine TNF α in BMDM, the levels were significantly lower than those achieved with LPS. This could be explained by the inhibitory effect of IL-10 on pro-inflammatory cytokine synthesis. This anti-inflammatory effect was more evident in a subsequent LPS-challenge. Pre-conditioning by Bt BEVs altered the cytokine profile of BMDM in a dose-dependent manner, especially in the case of the IL-10/TNF α ratio. High doses of Bt BEV pre-conditioning produced a high IL-10/TNF α ratio, indicative of a homeostatic or tolerance like status and an attenuated inflammatory response to LPS stimulation. This phenomenon resembles that of endotoxin tolerance which is characterized by upregulated IL-10 and downregulated TNF α production leading to an immune hyporesponsiveness (Biswas and Lopez-Collazo, 2009; Gu et al., 2022). Interestingly, IL-6 levels were not affected by BEV conditioning which was also noted in a related study investigating the immunomodulatory effect of different *Bacteroides* species on murine bone marrow-derived dendritic cells (BMDC; Steimle et al., 2019). In this study, IL-6 secretion was also not reduced in *Bacteroides*-primed and *E. coli*-challenged BMDC, and priming of BMDC with *Bacteroides* resulted in decreased TNF α expression after *E. coli* challenge in contrast to non-primed BMDCs. Since IL-6 is a pleiotropic cytokine capable

of acting as a defense mechanism in acute inflammation, and conversely exhibits a pro-inflammatory profile in chronic inflammation (Scheller et al., 2011), further studies are required to determine the significance of IL-6 production in BMD-innate immune cells conditioned with BEVs. It is also interesting to note the contrasting impacts of intact *Bacteroides* cells versus their BEVs on cytokine production. Whereas we have identified and confirmed IL-10 production as a signature of BEV interaction with human (Durant et al., 2020) and murine innate immune cells, this signature is not as evident using intact *Bacteroides* cells as a stimulus, suggesting that commensal gut bacteria can utilize different means including both cell-associated and secreted mediators to communicate with and influence host immune cells.

The molecular basis of Bt BEV-monocyte interactions was established using the human monocytic reporter cell line THP1-Blue NF- κ B. TLR2 activation was shown to mediate Bt BEV-elicited NF- κ B activation, whereas TLR4, NOD1, and NOD2 made no significant contribution. In a previous study (Gul et al., 2022), we reported the influence of TLR2 in Bt BEV-host communication *via* the TLR2/TLR4 adaptor protein TIRAP (toll-interleukin-1 receptor domain-containing adaptor protein), although TLR4 alone also showed some involvement. This apparent discrepancy is most likely explained by our prior use of a complex bacteria growth media (Brain-Heart Infusion, BHI) containing animal tissue and cellular lipids which may function as TLR4 ligands. This factor was excluded in this study by the use of a chemically defined media (BDM4). TLR2 recognizes several microbial products from both Gram-positive and Gram-negative bacteria, including lipoproteins and peptidoglycans, and forms heterodimers with either TLR1 or TLR6 for downstream signaling *via* NF- κ B pathway (Akira and Takeda, 2004). The polysaccharide A (PSA) antigen expressed in BEVs from the closely related commensal *Bacteroides fragilis* also interact with dendritic cells in a TLR2-dependent manner (Round et al., 2011; Shen et al., 2012). It has been recently reported the presence of serine-dipeptide lipids in Bt BEVs (Sartorio et al., 2022), which can also act as TLR2 ligands (Clark et al., 2013; Nemati et al., 2017). Further detailed biochemical characterization of BEV-associated lipoproteins is required to identify the ligands triggering TLR2 signaling pathways in innate immune cells. TLR2 signaling has been reported to have a protective role in inflammatory conditions (Lowe et al., 2010; Brun et al., 2013) and colorectal cancer (Sittipo et al., 2018), and to promote immune homeostasis by inhibiting the expression of pro-inflammatory cytokines and enhancing IL-10 production (Chang et al., 2017). These findings align with our proposal that the anti-inflammatory effect elicited by Bt BEVs is associated with modulations in the host innate immune system through the IL-10 signaling pathway, triggered by BEV-TLR2 interactions.

TLR activation depends on different co-receptors such as CD14, which is widely used as a marker of activation related to pro-inflammatory and classical monocytes (Lotz et al., 2004). Although generally characterized as a co-receptor for the TLR4

responsivity to LPS, CD14 also contributes to the activation of other PRRs including TLR2 (van Berghenhouwen et al., 2013). CD14 binds to triacylated lipopeptides, typically present in Gram-negative bacteria including *Bacteroides*, to enhance their recognition by the TLR2/TLR1 heterodimer (Jin et al., 2007). The highest proportion of CD14⁺ THP-1 cells were seen after stimulation with high concentrations of Bt BEVs, with levels equivalent to those stimulated with LPS, which suggests the functional involvement of CD14 in TLR2-mediated innate immune response induced by Bt BEVs.

The functional phenotype of immune cells is highly dependent on the establishment of unique epigenetic profiles that integrate microenvironmental cues into the genome to establish specific transcriptional programs (Calle-Fabregat et al., 2020). Among key epigenetic markers is the acquisition of histone 3 lysine 4 methylation (H3K4me1) in short lived monocytes and macrophages (van der Meer et al., 2015; Netea et al., 2016) and in long-lived myeloid bone marrow progenitors (Kaufmann et al., 2018; Mitroulis et al., 2018). The highest levels of H3K4me1 in Bt BEV-conditioned LPS-challenged BMDM, were evident in monocyte/macrophages incubated with high concentrations of Bt BEVs. Unexpectedly, these levels of H3K4me1 were higher than in LPS-conditioned BMDM and comparable to those found in non-conditioned BMDM. This seems to contradict our cytokine production results, since the repressed pro-inflammatory cytokine expression prompted by Bt BEV conditioning would be expected to correlate with close chromatin and low H3K4me1 levels. However, the IL-10 genomic locus of monocytes is poised for activation with open chromatin already at the steady state (Northrup and Zhao, 2011; Tamassia et al., 2013) and the presence of H3K4me1 is associated with IL-10 gene enhancers (Taubert, 2017), which could explain the increased levels of H3K4me1 found in BMDM conditioned with Bt BEVs. However, we cannot confirm this since our approach comprised global histone modifications. To further investigate the role of H3K4me1 and other relevant modifications involved in immune tolerance chromatin immunoprecipitation sequencing (ChIP-seq) could be used to localize these histone modifications throughout the genome.

Conclusion

We have shown that BEVs from the major gut commensal bacterium Bt elicit anti-inflammatory and immunomodulatory properties in innate immune cells, consistent with promoting and maintaining host immune homeostasis. Bt BEVs alleviated acute intestinal inflammation in DSS-treated mice, in association with increased IL-10 production. This was confirmed *in vitro* with increased IL-10 and decreased TNF α production in BEV-conditioned and LPS-challenged BMDM cultures. BEV-mediated monocyte activation and cytokine production was mediated by TLR2 interactions and resulted in stable epigenetic changes reflected by increased levels of H3K4me1. These findings

provide the rationale and basis for investigating the potential of Bt BEVs as an immune therapy.

Data availability statement

The original contributions presented in the study are included in the article/Supplementary material, further inquiries can be directed to the corresponding author.

Ethics statement

The animal study was reviewed and approved by Animal experiments were conducted in full accordance with the Animal Scientific Procedures Act 1986 under UK Home Office (HMO) approval and HMO project license 70/8232.

Author contributions

SF and SC conceived and designed the experiments and wrote the manuscript. SF carried out the experimental work with contribution from AC, AM-C, EJ, RJ, and RS. All authors contributed to the article and approved the submitted version.

Funding

This research was funded by the BBSRC Institute Strategic Programme Grant Gut Microbes and Health BB/R012490/1 and its constituent projects BBS/E/F/000PR10353 (Theme 1, Determinants of microbe-host responses in the gut across life) and BBS/E/F/000PR10355 (Theme 2, Changes in gut microbe-host

References

- Akira, S., and Takeda, K. (2004). Toll-like receptor signalling. *Nat. Rev. Immunol.* 4, 499–511. doi: 10.1038/nri1391
- Atreya, R., Mudter, J., Finotto, S., Mullberg, J., Jostock, T., Wirtz, S., et al. (2000). Blockade of interleukin 6 trans signaling suppresses T-cell resistance against apoptosis in chronic intestinal inflammation: evidence in crohn disease and experimental colitis in vivo. *Nat. Med.* 6, 583–588. doi: 10.1038/75068
- Bekkering, S., Quintin, J., Joosten, L. A., van der Meer, J. W., Netea, M. G., and Riksen, N. P. (2014). Oxidized low-density lipoprotein induces long-term proinflammatory cytokine production and foam cell formation via epigenetic reprogramming of monocytes. *Arterioscler. Thromb. Vasc. Biol.* 34, 1731–1738. doi: 10.1161/ATVBAHA.114.303887
- Biswas, S. K., and Lopez-Collazo, E. (2009). Endotoxin tolerance: new mechanisms, molecules and clinical significance. *Trends Immunol.* 30, 475–487. doi: 10.1016/j.it.2009.07.009
- Bron, P. A., van Baarlen, P., and Kleerebezem, M. (2011). Emerging molecular insights into the interaction between probiotics and the host intestinal mucosa. *Nat. Rev. Microbiol.* 10, 66–78. doi: 10.1038/nrmicro2690
- Brun, P., Giron, M. C., Qesari, M., Porzionato, A., Caputi, V., Zoppellaro, C., et al. (2013). Toll-like receptor 2 regulates intestinal inflammation by controlling integrity of the enteric nervous system. *Gastroenterology* 145, 1323–1333. doi: 10.1053/j.gastro.2013.08.047
- Bryant, W. A., Stentz, R., Le Gall, G., Sternberg, M. J. E., Carding, S. R., and Wilhelm, T. (2017). In silico analysis of the small molecule content of outer

interactions and their impact beyond the gut) and Quadram Institute Bioscience Proof-of-Concept Research Grant Fund project number 43134-000-A.

Acknowledgments

The authors gratefully acknowledge the support of the Biotechnology and Biological Sciences Research Council (BBSRC).

Conflict of interest

The authors declare that the research was conducted in the absence of any commercial or financial relationships that could be construed as a potential conflict of interest.

Publisher's note

All claims expressed in this article are solely those of the authors and do not necessarily represent those of their affiliated organizations, or those of the publisher, the editors and the reviewers. Any product that may be evaluated in this article, or claim that may be made by its manufacturer, is not guaranteed or endorsed by the publisher.

Supplementary material

The Supplementary material for this article can be found online at: <https://www.frontiersin.org/articles/10.3389/fmicb.2022.1050271/full#supplementary-material>

membrane vesicles produced by *Bacteroides thetaiotaomicron* indicates an extensive metabolic link between microbe and host. *Front. Microbiol.* 8:2440. doi: 10.3389/fmicb.2017.02440

Calle-Fabregat, C., Morante-Palacios, O., and Ballestar, E. (2020). Understanding the relevance of DNA methylation changes in immune differentiation and disease. *Genes* 11:110. doi: 10.3390/genes11010110

Carvalho, A. L., Fonseca, S., Miquel-Clopes, A., Cross, K., Kok, K. S., Wegmann, U., et al. (2019a). Bioengineering commensal bacteria-derived outer membrane vesicles for delivery of biologics to the gastrointestinal and respiratory tract. *J. Extracell. Vesicles* 8:1632100. doi: 10.1080/20013078.2019.1632100

Carvalho, A. L., Miquel-Clopes, A., Wegmann, U., Jones, E., Stentz, R., Telatin, A., et al. (2019b). Use of bioengineered human commensal gut bacteria-derived microvesicles for mucosal plague vaccine delivery and immunization. *Clin. Exp. Immunol.* 196, 287–304. doi: 10.1111/cei.13301

Chang, Y. C., Ching, Y. H., Chiu, C. C., Liu, J. Y., Hung, S. W., Huang, W. C., et al. (2017). TLR2 and interleukin-10 are involved in *Bacteroides fragilis*-mediated prevention of DSS-induced colitis in gnotobiotic mice. *PLoS One* 12:e0180025. doi: 10.1371/journal.pone.0180025

Chiu, C. C., Ching, Y. H., Wang, Y. C., Liu, J. Y., Li, Y. P., Huang, Y. T., et al. (2014). Monocolonization of germ-free mice with *Bacteroides fragilis* protects against dextran sulfate sodium-induced acute colitis. *Biomed. Res. Int.* 2014:675786. doi: 10.1155/2014/675786

- Christ, A., and Latz, E. (2019). The Western lifestyle has lasting effects on metaflammation. *Nat. Rev. Immunol.* 19, 267–268. doi: 10.1038/s41577-019-0156-1
- Clark, R. B., Cervantes, J. L., Maciejewski, M. W., Farrokhi, V., Nemati, R., Yao, X., et al. (2013). Serine lipids of *Porphyromonas gingivalis* are human and mouse toll-like receptor 2 ligands. *Infect. Immun.* 81, 3479–3489. doi: 10.1128/IAI.00803-13
- Delday, M., Mulder, I., Logan, E. T., and Grant, G. (2019). *Bacteroides thetaiotaomicron* ameliorates colon inflammation in preclinical models of Crohn's disease. *Inflamm. Bowel Dis.* 25, 85–96. doi: 10.1093/ibd/izy281
- Diaz-Garrido, N., Fábrega, M. J., Vera, R., Giménez, R., Badia, J., and Baldomà, L. (2019). Membrane vesicles from the probiotic Nissle 1917 and gut resident *Escherichia coli* strains distinctly modulate human dendritic cells and subsequent T cell responses. *J. Funct. Foods* 61:103495. doi: 10.1016/j.jff.2019.103495
- Durant, L., Stentz, R., Noble, A., Brooks, J., Gicheva, N., Reddi, D., et al. (2020). *Bacteroides thetaiotaomicron*-derived outer membrane vesicles promote regulatory dendritic cell responses in health but not in inflammatory bowel disease. *Microbiome* 8:88. doi: 10.1186/s40168-020-00868-z
- Fraschilla, I., Amatullah, H., and Jeffrey, K. L. (2022). One genome, many cell states: epigenetic control of innate immunity. *Curr. Opin. Immunol.* 75:102173. doi: 10.1016/j.coi.2022.102173
- Gu, J. Y., Fu, Z. B., Jia-Lu, C., Liu, Y. J., Cao, X. Z., and Sun, Y. (2022). Endotoxin tolerance induced by *Porphyromonas gingivalis* lipopolysaccharide alters macrophage polarization. *Microb. Pathog.* 164:105448. doi: 10.1016/j.micpath.2022.105448
- Gul, L., Modos, D., Fonseca, S., Madgwick, M., Thomas, J. P., Sudhakar, P., et al. (2022). Extracellular vesicles produced by the human commensal gut bacterium *Bacteroides thetaiotaomicron* affect host immune pathways in a cell-type specific manner that are altered in inflammatory bowel disease. *J. Extracell. Vesicles* 11:e12189. doi: 10.1002/jev.2.12189
- Hansen, J. J., Holt, L., and Sartor, R. B. (2009). Gene expression patterns in experimental colitis in IL-10-deficient mice. *Inflamm. Bowel Dis.* 15, 890–899. doi: 10.1002/ibd.20850
- Hudcovic, T., Kozakova, H., Kolinska, J., Stepankova, R., Hrnčir, T., and Tlaskalova-Hogenova, H. (2009). Monocolonization with *Bacteroides ovatus* protects immunodeficient SCID mice from mortality in chronic intestinal inflammation caused by long-lasting dextran sodium sulfate treatment. *Physiol. Res.* 58, 101–110. doi: 10.33549/physiolres.931340
- Ifrim, D. C., Quintin, J., Joosten, L. A., Jacobs, C., Jansen, T., Jacobs, L., et al. (2014). Trained immunity or tolerance: opposing functional programs induced in human monocytes after engagement of various pattern recognition receptors. *Clin. Vaccine Immunol.* 21, 534–545. doi: 10.1128/CVI.00688-13
- Jin, M. S., Kim, S. E., Heo, J. Y., Lee, M. E., Kim, H. M., Paik, S. G., et al. (2007). Crystal structure of the TLR1-TLR2 heterodimer induced by binding of a triacylated lipopeptide. *Cell* 130, 1071–1082. doi: 10.1016/j.cell.2007.09.008
- Jones, E. J., Booth, C., Fonseca, S., Parker, A., Cross, K., Miquel-Clopes, A., et al. (2020). The uptake, trafficking, and biodistribution of *Bacteroides thetaiotaomicron* generated outer membrane vesicles. *Front. Microbiol.* 11:57. doi: 10.3389/fmicb.2020.00057
- Juodeikis, R., and Carding, S. R. (2022). Outer membrane vesicles: biogenesis, functions, and issues. *Microbiol. Mol. Biol. Rev.*:e0003222. doi: 10.1128/mbr.00032-22
- Kaparakis-Liaskos, M., and Ferrero, R. L. (2015). Immune modulation by bacterial outer membrane vesicles. *Nat. Rev. Immunol.* 15, 375–387. doi: 10.1038/nri3837
- Kaufmann, E., Sanz, J., Dunn, J. L., Khan, N., Mendonca, L. E., Pacis, A., et al. (2018). BCG educates hematopoietic stem cells to generate protective innate immunity against tuberculosis. *Cell* 172, 176–190.e19. doi: 10.1016/j.cell.2017.12.031
- Komatsu, M., Kobayashi, D., Saito, K., Furuya, D., Yagihashi, A., Araake, H., et al. (2001). Tumor necrosis factor- α in serum of patients with inflammatory bowel disease as measured by a highly sensitive immuno-PCR. *Clin. Chem.* 47, 1297–1301. doi: 10.1093/clinchem/47.7.1297
- Koppelman, B., Neeftjes, J. J., de Vries, J. E., and de Waal Malefyt, R. (1997). Interleukin-10 down-regulates MHC class II alpha peptide complexes at the plasma membrane of monocytes by affecting arrival and recycling. *Immunity* 7, 861–871. doi: 10.1016/s1074-7613(00)80404-5
- Kuhn, R., Lohler, J., Rennick, D., Rajewsky, K., and Muller, W. (1993). Interleukin-10-deficient mice develop chronic enterocolitis. *Cell* 75, 263–274. doi: 10.1016/0092-8674(93)80068-p
- Li, K., Hao, Z., Du, J., Gao, Y., Yang, S., and Zhou, Y. (2021). *Bacteroides thetaiotaomicron* relieves colon inflammation by activating aryl hydrocarbon receptor and modulating CD4(+)T cell homeostasis. *Int. Immunopharmacol.* 90:107183. doi: 10.1016/j.intimp.2020.107183
- Lotz, S., Aga, E., Wilde, I., van Zandbergen, G., Hartung, T., Solbach, W., et al. (2004). Highly purified lipoteichoic acid activates neutrophil granulocytes and delays their spontaneous apoptosis via CD14 and TLR2. *J. Leukoc. Biol.* 75, 467–477. doi: 10.1189/jlb.0803360
- Lowe, E. L., Crother, T. R., Rabizadeh, S., Hu, B., Wang, H., Chen, S., et al. (2010). Toll-like receptor 2 signaling protects mice from tumor development in a mouse model of colitis-induced cancer. *PLoS One* 5:e13027. doi: 10.1371/journal.pone.0013027
- Maerz, J. K., Steimle, A., Lange, A., Bender, A., Fehrenbacher, B., and Frick, J. S. (2018). Outer membrane vesicles blebbing contributes to *B. vulgatus* mpk-mediated immune response silencing. *Gut Microbes* 9, 1–12. doi: 10.1080/19490976.2017.1344810
- Mazmanian, S. K., Round, J. L., and Kasper, D. L. (2008). A microbial symbiosis factor prevents intestinal inflammatory disease. *Nature* 453, 620–625. doi: 10.1038/nature07008
- Mitroulis, I., Ruppova, K., Wang, B., Chen, L. S., Grzybek, M., Grinenko, T., et al. (2018). Modulation of Myelopoiesis progenitors is an integral component of trained immunity. *Cell* 172, 147–161.e12. doi: 10.1016/j.cell.2017.11.034
- Nemati, R., Dietz, C., Anstadt, E. J., Cervantes, J., Liu, Y., Dewhirst, F. E., et al. (2017). Deposition and hydrolysis of serine dipeptide lipids of *Bacteroidetes* bacteria in human arteries: relationship to atherosclerosis. *J. Lipid Res.* 58, 1999–2007. doi: 10.1194/jlr.M077792
- Netea, M. G., Dominguez-Andres, J., Barreiro, L. B., Chavakis, T., Divangahi, M., Fuchs, E., et al. (2020). Defining trained immunity and its role in health and disease. *Nat. Rev. Immunol.* 20, 375–388. doi: 10.1038/s41577-020-0285-6
- Netea, M. G., Joosten, L. A., Latz, E., Mills, K. H., Natoli, G., Stunnenberg, H. G., et al. (2016). Trained immunity: a program of innate immune memory in health and disease. *Science* 352:aaf1098. doi: 10.1126/science.aaf1098
- Northrup, D. L., and Zhao, K. (2011). Application of ChIP-Seq and related techniques to the study of immune function. *Immunity* 34, 830–842. doi: 10.1016/j.immuni.2011.06.002
- Novakovic, B., Habibi, E., Wang, S. Y., Arts, R. J. W., Davar, R., Megchelenbrink, W., et al. (2016). Beta-glucan reverses the epigenetic state of LPS-induced immunological tolerance. *Cell* 167, 1354–1368.e14. doi: 10.1016/j.cell.2016.09.034
- Round, J. L., Lee, S. M., Li, J., Tran, G., Jabri, B., Chatila, T. A., et al. (2011). The toll-like receptor 2 pathway establishes colonization by a commensal of the human microbiota. *Science* 332, 974–977. doi: 10.1126/science.1206095
- Saeed, S., Quintin, J., Kerstens, H. H., Rao, N. A., Aghajani-refah, A., Matarese, F., et al. (2014). Epigenetic programming of monocyte-to-macrophage differentiation and trained innate immunity. *Science* 345:1251086. doi: 10.1126/science.1251086
- Sartorio, M. G., Valguarnera, E., Hsu, F. F., and Feldman, M. F. (2022). Lipidomics analysis of outer membrane vesicles and elucidation of the inositol Phosphoceramide biosynthetic pathway in *Bacteroides thetaiotaomicron*. *Microbiol. Spectr.* 10:e0063421. doi: 10.1128/spectrum.00634-21
- Scheller, J., Chalaris, A., Schmidt-Arras, D., and Rose-John, S. (2011). The pro- and anti-inflammatory properties of the cytokine interleukin-6. *Biochim. Biophys. Acta* 1813, 878–888. doi: 10.1016/j.bbamcr.2011.01.034
- Schottelius, A. J., Mayo, M. W., Sartor, R. B., and Baldwin, A. S. Jr. (1999). Interleukin-10 signaling blocks inhibitor of kappaB kinase activity and nuclear factor kappaB DNA binding. *J. Biol. Chem.* 274, 31868–31874. doi: 10.1074/jbc.274.45.31868
- Schreiber, S., Nikolaus, S., and Hampe, J. (1998). Activation of nuclear factor kappa B inflammatory bowel disease. *Gut* 42, 477–484. doi: 10.1136/gut.42.4.477
- Schwechheimer, C., and Kuehn, M. J. (2015). Outer-membrane vesicles from gram-negative bacteria: biogenesis and functions. *Nat. Rev. Microbiol.* 13, 605–619. doi: 10.1038/nrmicro3525
- Seeley, J. J., and Ghosh, S. (2017). Molecular mechanisms of innate memory and tolerance to LPS. *J. Leukoc. Biol.* 101, 107–119. doi: 10.1189/jlb.3MR0316-118RR
- Shen, Y., Giardino Torchia, M. L., Lawson, G. W., Karp, C. L., Ashwell, J. D., and Mazmanian, S. K. (2012). Outer membrane vesicles of a human commensal mediate immune regulation and disease protection. *Cell Host Microbe* 12, 509–520. doi: 10.1016/j.chom.2012.08.004
- Sittipo, P., Lobionda, S., Choi, K., Sari, I. N., Kwon, H. Y., and Lee, Y. K. (2018). Toll-like receptor 2-mediated suppression of colorectal cancer pathogenesis by polysaccharide A from *Bacteroides fragilis*. *Front. Microbiol.* 9:1588. doi: 10.3389/fmicb.2018.01588
- Steimle, A., Michaelis, L., Di Lorenzo, F., Kliem, T., Munzner, T., Maerz, J. K., et al. (2019). Weak agonistic LPS restores intestinal immune homeostasis. *Mol. Ther.* 27, 1974–1991. doi: 10.1016/j.ymthe.2019.07.007
- Stentz, R., Carvalho, A. L., Jones, E. J., and Carding, S. R. (2018). Fantastic voyage: the journey of intestinal microbiota-derived microvesicles through the body. *Biochem. Soc. Trans.* 46, 1021–1027. doi: 10.1042/BST20180114
- Stentz, R., Miquel-Clopes, A., and Carding, S. R. (2022). Production, isolation, and characterization of bioengineered bacterial extracellular membrane vesicles derived from *Bacteroides thetaiotaomicron* and their use in vaccine

development. *Methods Mol. Biol.* 2414, 171–190. doi: 10.1007/978-1-0716-1900-1_11

Tamassia, N., Zimmermann, M., Castellucci, M., Ostuni, R., Bruderek, K., Schilling, B., et al. (2013). Cutting edge: an inactive chromatin configuration at the IL-10 locus in human neutrophils. *J. Immunol.* 190, 1921–1925. doi: 10.4049/jimmunol.1203022

Taubert, C. M. (2017). Molecular mechanisms underlying the regulation of interleukin-10 production in macrophages. Doctoral thesis (Ph.D.), UCL (University College London).

van Bergenhenegouwen, J., Plantinga, T. S., Joosten, L. A., Netea, M. G., Folkerts, G., Kraneveld, A. D., et al. (2013). TLR2 & co: a critical analysis of the

complex interactions between TLR2 and coreceptors. *J. Leukoc. Biol.* 94, 885–902. doi: 10.1189/jlb.0113003

van der Meer, J. W., Joosten, L. A., Riksen, N., and Netea, M. G. (2015). Trained immunity: a smart way to enhance innate immune defence. *Mol. Immunol.* 68, 40–44. doi: 10.1016/j.molimm.2015.06.019

Xu, X. R., Liu, C. Q., Feng, B. S., and Liu, Z. J. (2014). Dysregulation of mucosal immune response in pathogenesis of inflammatory bowel disease. *World J. Gastroenterol.* 20, 3255–3264. doi: 10.3748/wjg.v20.i12.3255

Zhou, Y., and Zhi, F. (2016). Lower level of Bacteroides in the Gut microbiota is associated with inflammatory bowel disease: a meta-analysis. *Biomed. Res. Int.* 2016:5828959. doi: 10.1155/2016/5828959